SEMA SIMAI Springer Series 26

Luisa Beghin
Francesco Mainardi
Roberto Garrappa *Editors*

Nonlocal and Fractional Operators

SEMA
SIMAI
SOCIETÀ ITALIANA DI MATEMATICA APPLICATA E INDUSTRIALE
Springer

SEMA SIMAI Springer Series

Volume 26

As of 2013, the SIMAI Springer Series opens to SEMA in order to publish a joint series aiming to publish advanced textbooks, research-level monographs and collected works that focus on applications of mathematics to social and industrial problems, including biology, medicine, engineering, environment and finance. Mathematical and numerical modeling is playing a crucial role in the solution of the complex and interrelated problems faced nowadays not only by researchers operating in the field of basic sciences, but also in more directly applied and industrial sectors. This series is meant to host selected contributions focusing on the relevance of mathematics in real life applications and to provide useful reference material to students, academic and industrial researchers at an international level. Interdisciplinary contributions, showing a fruitful collaboration of mathematicians with researchers of other fields to address complex applications, are welcomed in this series.

THE SERIES IS INDEXED IN SCOPUS

More information about this series at http://www.springer.com/series/10532

Luisa Beghin · Francesco Mainardi ·
Roberto Garrappa
Editors

Nonlocal and Fractional Operators

Springer

Editors
Luisa Beghin
Department of Statistical Sciences
Sapienza University of Rome
Roma, Italy

Roberto Garrappa
Department of Mathematics
Università di Bari
Bari, Italy

Francesco Mainardi
Department of Physics and Astronomy
(DIFA)
Università di Bologna
Bologna, Italy

ISSN 2199-3041 ISSN 2199-305X (electronic)
SEMA SIMAI Springer Series
ISBN 978-3-030-69235-3 ISBN 978-3-030-69236-0 (eBook)
https://doi.org/10.1007/978-3-030-69236-0

This Springer imprint is published by the registered company Springer Nature Switzerland AG
The registered company address is: Gewerbestrasse 11, 6330 Cham, Switzerland

Preface

The study of nonlocal operators is an active field of research in pure and applied mathematics and has being gaining an increasing attention over the last few years. Operators of nonlocal type are used to describe complex systems in which interactions among components are not local, but extend to a neighborhood of each component (space nonlocality). Analogously, they are applied in order to model systems in which the reaction to an external excitation is not instantaneous but depends on the history of the system (time nonlocality).

Due to the large extent of their applications, nonlocal operators are employed with great success and interest in a variety of fields ranging from biology to engineering, image processing, probability theory, physics and so on.

Fractional-order operators (i.e., integrals and derivatives of non-integer order) are maybe the most famous and studied in the literature. Their origin goes back to the end of seventeenth century, but their analysis and applications have flourished only around the middle of the twentieth century.

In this book we have collected a number of invited and refereed contributions illustrating recent developments in theory and applications of Nonlocal and Fractional Operators. The chapters of this book cover different research areas, thus offering an overview of the most updated results and applications of Nonlocal and Fractional Operators.

Most of the contributions are related to talks presented during the Workshop "Nonlocal and Fractional Operators" held at La Sapienza University in Roma on April 12–13, 2019. This meeting was an occasion to bring together researchers working in different areas of mathematics and physics, and to discuss the most recent advancements and applications of Nonlocal and Fractional Operators.

The workshop "Nonlocal and Fractional Operators" was dedicated to Professor Renato Spigler (Department of Mathematics and Physics, Roma Tre University), on the occasion of his retirement, and was an opportunity to celebrate his scientific contributions in the field of applied mathematics and, in particular, of fractional calculus. A transcription of the speech delivered by Professor Michele Caputo and dedicated to the academic and research achievements of Professor Spigler is included, as an introduction to this book.

We wish to forward our special thanks to all authors and coauthors who have contributed, with their articles, to the realization of this volume and to all the anonymous referees, who allowed to select only valuable contributions, as well as to improve their quality with useful and constructive criticisms. A final special thank to the scientific and the organizing committees of the workshop "Nonlocal and Fractional Operators", which has prompted the realization of this book.

Finally, we are grateful to SIMAI, the Italian Society for Industrial and Applied Mathematics, for hosting this volume in the SIMAI-SEMA series published by Springer.

Rome, Italy — Luisa Beghin
Bari, Italy — Roberto Garrappa
Bologna, Italy — Francesco Mainardi

Presentation of the Workshop "Nonlocal and Fractional Operators" Dedicated to Prof. Renato Spigler (Rome, April 12–13, 2019)

Introductory speech by Prof. Michele Caputo (Accademia Nazionale dei Lincei)

I first want to congratulate the organizers of the meeting for celebrating Professor Renato Spigler and also for the selection of the title "Nonlocal and Fractional Operators" which has attracted many excellent mathematicians.

From the program of the workshop, we expect the presentation of many very interesting papers covering different branches of fractional calculus which also show the vitality of nonlocal operators in many fields of mathematics. Indirectly and consequently, they indicate the expansion of the applications of this branch of mathematics in an ever increasing number of different fields of science. I have seen the list of posters which, as sometime happens, seem not less interesting than the papers. Finally I like to thank the organizing committee to have given me the pleasure to open the works of the meeting and to celebrate Professor Renato Spigler.

Professor Spigler was born in Venice in 1947, so say the papers, but certainly his look does not qualify for retiring. The same seems true also when looking at the increasing rate of his current scientific production. He had his first laurea in electronic engineering at the University of Padua in 1972. He specialized in Theory and Applications of Computing Machines at the University of Bologna then he and returned to Padua where he was offered teaching positions but soon he began stages in the US first with the University of Wisconsin in 1980, later at the Courant Institute in New York as Fulbright scholar in 1983 and, after few stages at the same institute, he was there as Associate Research Scientist in 1986.

After these important experiences abroad, at a young age, he became stable in Italy where he had the chair of Analisi Matematica at the University of Roma 3 and at the Università Telematica Internazionale Uninettuno. That is not only for the registrar's office. Because his stages in different important institutions, particularly those abroad, denote a dynamic stile of life, which is reflected in his varied scientific production and collaborations with national and international Agencies. In fact professor Spigler's scientific production, besides the excellent quality, is impressive for the variety of problems treated and for his capability to give essential contributions in problems on the frontier of science.

He proved to be able also to produce first class mathematics in association with eminent colleagues, for instance, in the case of solution of hybrid problems. From existence and uniqueness of classical solutions of certain nonlinear integro-differential Fokker-Planck-type equations, professor Spigler goes to the probabilistically induced domain decomposition methods for elliptic boundary-value problems.

Concerning his recent scientific production and the variety of problems which have been attacked by him, it is worth mentioning that, in 2001, he showed the existence and uniqueness of solutions to the Kuramoto-Sakaguchi parabolic integro-differential equation. The synchronization phenomena in large populations of interacting elements are subject to intense research efforts in biological, chemical also for the study of the evolutions of different competing economies in clubs of economies, in particular of banks and also of social systems. Spigler gave, in 2005, a fundamental

contribution with a successful approach, consisting in modeling each member of the population as coupled phase oscillators.

Renato's papers generally received a large number of citations but this paper had the peak number of 2250 citations. Then in 2007 he finds L1-estimates for the higher order derivatives of solutions to parabolic equations subject to initial values of bounded total variation. In 2012 he lands on fractional calculus with a paper where he applies fractional operators for a numerical solution of two-dimensional fractional diffusion equations, by a high-order ADI method (Alternating Direction Implicit). In 2014, he studies existence, uniqueness and regularity for the Kuramoto-Sakaguchi equation with unboundedly supported frequency distribution (which later led to the Kuramoto-Sivashinsky equation) by introducing also nonlocal operators. More recently, in 2016, again in a different field, he introduces an approximation method by means of neural network operators. Finally, I like to mention that Renato ventured to land also on Earth with the most important problem of our environment, an excellent paper on mathematical models for fighting environmental pollution.

Professor Spigler had also important collaborations with NATO, CNR, EURATOM, UNESCO. He is a Member of the Editorial Board of many international scientific Journal, as well as many important scientific Societies. What at first sight appears remarkable in his splendid scientific carrier and production is the variety of different fields where he operated, not only in different topics, but also conceptually and using the modern fundamental tools of mathematics. He understood the importance of interdisciplinarity and acted at high level, contributing constructively with several eminent scientists in vanguard problems such as those concerning the synchronization in clubs of entities of different kinds, basic in the structure of our society.

As a person, I like his successful sailor behavior, in different seas at times stormy, from an important successful harbor to the next, not the nearest.

Dear Renato, thanks for being with us and congratulations for what you are and have done for all of us and, in all ways, please stay the course: *continua così*.

Rome, Italy
April 2019

Michele Caputo

Contents

On the Transient Behaviour of Fractional $M/M/\infty$ Queues

Giacomo Ascione, Nikolai Leonenko, and Enrica Pirozzi

Abstract We study some features of the transient probability distribution of a fractional $M/M/\infty$ queueing system. Such model is constructed as a suitable time-changed birth-death process. The fractional differential-difference problem is studied for the corresponding probability distribution and a fractional partial differential equation is obtained for the generating function. Finally, the interpretation of the system as an actual $M/M/\infty$ queue and as a $M/M/1$ queue with responsive server is given and some conditioned virtual waiting times are studied.

Keywords Inverse subordinator · Fractional immigration-death process · Virtual waiting time.

1 Introduction

As the link between fractional calculus and time-changed processes has been widely studied in the last years (see for instance [22, 23, 27] or also the book [25]), applications of such field to various sciences started to rise. Finance [16], biology [6, 26], population dynamics [7], and social sciences [8] are just some of such fields.
A particular field of interest, that found application also in other sciences, such as finance or information technology, is queueing theory (for the classical theory one can see [17]). Fractional queueing theory saw its birth with [10], in which the transient behaviour of a fractional $M/M/1$ queue is described.
After that, we focused on extending such results to different kind of queues such as

G. Ascione (✉) · E. Pirozzi
Dipartimento di Matematica e Applicazioni "Renato Caccioppoli", Universitá degli Studi di Napoli Federico II, 80126 Napoli, Italy
e-mail: giacomo.ascione@unina.it

E. Pirozzi
e-mail: enrica.pirozzi@unina.it

N. Leonenko
School of Mathematics, Cardiff University, Cardiff CF24 4AG, UK
e-mail: leonenkon@cardiff.ac.uk

L. Beghin et al. (eds.), *Nonlocal and Fractional Operators*, SEMA SIMAI Springer Series 26, https://doi.org/10.1007/978-3-030-69236-0_1

the $M/M/1$ queue with catastrophes [3] and the $M/E_k/1$ queue [4]. For the latter, we investigated also the behaviour of some conditioned virtual waiting time: the differences between the fractional case and the standard one arise as consequence of the lack of semigroup property of the Mittag-Leffler function [21]. In this contribution, we focus on the $M/M/\infty$ queue and the $M/M/1$ queue with responsive server (different queues with state dependent service rates are given for instance in [12] and reference therein), trying first to deduce some information in the transient behaviour and then to describe some conditioned virtual waiting times. The contribution is structured as follows:

- In Sect. 2 we recall the main properties of the classical $M/M/\infty$ queue, in particular some formulas for the state probabilities and the probability generating function;
- In Sect. 3 we define the fractional $M/M/\infty$ queue and we deduce some property of its state probabilities and its probability generating function: to do this, we also use some spectral properties that have been obtained in [5];
- In Sect. 4 we investigate the interpretation of the queueing system, studying in particular inter-arrival and inter-exit times: concerning the virtual waiting times, we underline the main differences between the $M/M/\infty$ queue and the $M/M/1$ queue with responsive server.

2 The $M/M/\infty$ Queue

An $M/M/\infty$ queue is a service system with Poisson arrivals, exponential service times and infinite servers. As it is stated in [17], it can be used to interpret both an infinite servers system than a system with one responsive server whose service time is linearly dependent of the number of customers in the service. In any case, we have arrival and service rates given by (see [17])

$$\lambda_n = \lambda > 0, \qquad \mu_n = n\mu \geq 0, \qquad n \in \mathbb{N}_0 .$$

Let us denote by $N(t)$ the number of customers in the service at time $t > 0$ and the state probabilities as

$$p_n(t) = \mathbb{P}(N(t) = n | N(0) = 0), \qquad n \in \mathbb{N}_0 .$$

It is well known that the state probabilities solve the following difference differential equations (see [30, Section 3.11.3])

$$\begin{cases} \frac{dp_0}{dt}(t) = -\lambda p_0(t) + \mu p_1(t) \\ \frac{dp_n}{dt}(t) = \lambda p_{n-1}(t) - (\lambda + n\mu) p_n(t) + (n+1)\mu p_{n+1}(t) & n \geq 1 \\ p_n(0) = \delta_{n,0} & n \geq 0 \end{cases} \tag{1}$$

where $\delta_{i,j}$ is the Kronecker symbol. Let us denote $\rho = \lambda/\mu$ and observe that the solution of such system is well known:

$$p_n(t) = \exp(-\rho(1-e^{-\mu t}))\frac{\left(\rho(1-e^{-\mu t})\right)^n}{n!}, \qquad t \geq 0. \tag{2}$$

Let us consider the probability generating function $G(t,z) = \sum_{n=0}^{+\infty} z^n p_n(t)$, which we know uniformly converges for $z \in \mathbb{R}$. By multiplying the second equation of (1) by z^n and then summing over n we have that G solves the following partial differential equation

$$\frac{\partial G}{\partial t}(z,t) = -\lambda(1-z)G(z,t) + \mu(1-z)\frac{\partial G}{\partial z}(z,t). \tag{3}$$

Moreover, the generating function can be explicitly determined. Indeed we have that

$$\sum_{n=0}^{+\infty} z^n \frac{\left(\rho(1-e^{-\mu t})\right)^n}{n!} = \exp(\rho z(1-e^{-\mu t}))$$

and then

$$G(z,t) = \exp(-\rho(1-z)(1-e^{-\mu t})), \qquad t \geq 0,\ z \in \mathbb{R}\,. \tag{4}$$

An important role will be played by the Laplace transform of the state probabilities $p_n(t)$ and the generating function $G(z,t)$. Denoting by $\pi_n(s)$ and $\mathcal{G}(z,s)$ the Laplace transforms respectively of $p_n(t)$ and $G(z,t)$, we have, for $s \geq 0$ and $z \in \mathbb{R}$,

$$\pi_n(s) = \frac{(-1)^n}{\mu}\sum_{k=n}^{+\infty}\binom{k}{n}\frac{\Gamma\left(\frac{s}{\mu}\right)}{\Gamma\left(\frac{s}{\mu}+k+1\right)}(-\rho)^k, \qquad \mathcal{G}(z,s) = \frac{1}{\mu}\sum_{k=0}^{+\infty}\frac{\Gamma\left(\frac{s}{\mu}\right)}{\Gamma\left(\frac{s}{\mu}+k+1\right)}(-\rho(1-z))^k.$$

Simple proofs of these formulas are given in Appendix 2. We are also interested in some characteristics of such queue. For instance, differentiating Eq. (3) with respect to z and then setting $z = 1$, we obtain an equation for the mean $\mathbb{E}[N(t)]$. We have

$$\begin{cases} \dfrac{d\,\mathbb{E}[N(t)]}{dt} = \lambda - \mu\,\mathbb{E}[N(t)] \\ \mathbb{E}[N(0)] = 0. \end{cases} \tag{5}$$

Another way to work with $M/M/\infty$ queues is by using their spectral decomposition. Indeed it is shown for instance in [1, 18] that considering the Charlier polynomials $C_n(m;\rho)$, defined by the generating function

$$\sum_{n=0}^{+\infty} C_n(m;\rho)\frac{t^n}{n!} = e^{-t}\left(1+\frac{t}{\rho}\right)^m, \qquad t \in \mathbb{R},\ m \in \mathbb{N}$$

and the Poisson distribution $\Pi(m;\rho) = e^{-\rho}\frac{\rho^m}{m!}$ for $m \in \mathbb{N}$, it holds

$$p_n(t) = \Pi(n;\rho)\sum_{m=0}^{+\infty}(-1)^m e^{-m\mu t}\frac{\rho^m}{m!}C_m(n;\rho), \qquad t \geq 0.$$

Moreover, for any function $h \in \ell^2(\Pi(\cdot;\rho))$ with $h(n) = \sum_{m=0}^{+\infty} h_m\sqrt{\frac{\rho^m}{m!}}C_m(n;\rho)$, defining $u(t) = \mathbb{E}[h(N(t))|N(0) = 0]$ it holds

$$u(t) = \sum_{m=0}^{+\infty}(-1)^m h_m\sqrt{\frac{\rho^m}{m!}}e^{-m\mu t}, \qquad t \geq 0.$$

If we use this formula choosing $h(n) = n$, we have $h_0 = \rho$, $h_1 = \sqrt{\rho}$, $h_n = 0$ for any $n \geq 2$ and then we obtain

$$\mathbb{E}[N(t)] = \rho(1 - e^{-\mu t}), \qquad t \geq 0.$$

If we want to use it with $h(n) = n^2$, we have $h_0 = \rho + \rho^2$, $h_1 = \sqrt{\rho}(1 + 2\rho)$, $h_2 = \rho\sqrt{2}$ and $h_n = 0$ for any $n \geq 3$. In such case we obtain

$$\mathbb{E}[N(t)^2] = \rho(1 - e^{-\mu t}) + \rho^2(1 - e^{-\mu t})^2, \qquad t \geq 0.$$

From these two relations we finally obtain the Variance

$$\mathrm{Var}(N(t)) = \rho(1 - e^{-\mu t}), \qquad t \geq 0,$$

which is coherent with the fact that for any $t > 0$ the sequence $(p_n(t))_{n\geq 0}$ constitute a Poisson distribution on $\mathbb{N}_0$.
In the next section we will introduce the fractional version of such queue.

3 The Fractional $M/M/\infty$ Queue

In this section we will construct and exploit some characteristics of the fractional $M/M/\infty$ queue.

3.1 Definition of the Queue and the Main Quantities

Let us fix $\nu \in (0, 1)$ and consider a ν-stable subordinator $\sigma_\nu(t)$ and its inverse process

$$L_\nu(t) = \inf\{y > 0 : \sigma_\nu(y) > t\}, \qquad t \geq 0$$

whose probability density function will be denoted by $f_\nu(t, y) := \mathbb{P}(L_\nu(t) \in dy)/dy$ for $t \geq 0$ and $y \geq 0$. For other information concerning the inverse stable subordinator, we refer to [24].

Let us then define the process $N_\nu(t) := N(L_\nu(t))$ where $L_\nu(t)$ is an inverse ν-stable subordinator independent of $N(t)$. We will call such process fractional $M/M/\infty$ queue. Let us denote for $n \in \mathbb{N}$

$$p_n^\nu(t) := \mathbb{P}(N_\nu(t) = n | N_\nu(0) = 0), \qquad n \in \mathbb{N}_0, t \geq 0.$$

Let us first show an easy representation formula.

Proposition 1 *For any $t > 0$ and $n \in \mathbb{N}_0$ it holds*

$$p_n^\nu(t) = \int_0^{+\infty} p_n(y) f_\nu(t, y) dy = \int_0^{+\infty} p_n\left(\left(\frac{t}{w}\right)^\nu\right) g_\nu(w) dw, \tag{6}$$

where $g_\nu(w)$ is the density of $\sigma_\nu(1)$. Moreover, the functions $p_n^\nu(t)$ are continuous.

Proof Let us observe, by the independence of L_ν by N, that

$$\begin{aligned} p_n^\nu(t) = \mathbb{P}(N(L_\nu(t)) = n | N_\nu(0) = 0) &= \int_0^{+\infty} \mathbb{P}(N(y) = n | N_\nu(0) = 0) f_\nu(t, y) dy \\ &= \int_0^{+\infty} p_n(y) f_\nu(t, y) dy. \end{aligned}$$

Moreover, let us recall [24, Formula 8]

$$f_\nu(t, y) = \frac{t}{\nu} y^{-1-\frac{1}{\nu}} g_\nu(t y^{-\frac{1}{\nu}}),$$

where $g_\nu(y)$ is the density of $\sigma_\nu(1)$. Hence Eq. (6) becomes

$$p_n^\nu(t) = \int_0^{+\infty} p_n(y) \frac{t}{\nu} y^{-1-\frac{1}{\nu}} g_\nu(t y^{-\frac{1}{\nu}}) dy = \int_0^{+\infty} p_n\left(\left(\frac{t}{w}\right)^\nu\right) g_\nu(w) dw,$$

where we used the change of variables $w = t y^{-\frac{1}{\nu}}$. Since $p_n(t) \leq 1$, we can use dominated convergence theorem to obtain continuity. □

The same can be done for the probability generating function $G_\nu(z, t) := \sum_{n=0}^{+\infty} z^n p_n^\nu(t)$ (recalling that it converges uniformly for any $z \in \mathbb{R}$). We have

Proposition 2 *For any $t > 0$ and $z \in \mathbb{R}$ it holds*

$$G_\nu(z, t) = \int_0^{+\infty} G(z, y) f_\nu(t, y) dy. \tag{7}$$

Moreover, for any fixed $z \in \mathbb{R}$ the function $t \mapsto G_\nu(z, t)$ is continuous.

Let us also recall that, being probability masses, the functions $p_n^\nu(t)$ are bounded by 1, hence in particular they are Laplace-transformable. We will denote by $\pi_n^\nu(s)$ their Laplace transform. Moreover, let us observe that for fixed z we have $G(z,t) \leq \exp(\rho|1-z|)$, hence also $G_\nu(z,t) \leq \exp(\rho|1-z|)$ and then it is Laplace-transformable in t for any $z \in \mathbb{R}$. We will denote by $\mathcal{G}_\nu(z,s)$ its Laplace transform.

3.2 Fractional Equations for the State Probabilities and the Generating Function

In this subsection we want to obtain a system of fractional difference-differential equations whose unique global solution in $\ell^2(\Pi(\cdot;\rho))$ is given by the sequence $\mathbf{p}^\nu(t) = (p_n^\nu(t))_{n\geq 0}$. In the following we will need some operators from fractional calculus. Such operators are introduced in Appendix 1.

Let us first determine a fractional PDE whose unique Laplace-transformable solution is given by the probability generating function. In the following we will use Caputo fractional derivatives as defined in Eq. (19) of Appendix 1.

Proposition 3 *The function $G_\nu(z,t)$ solves the following fractional partial differential equation:*

$$\frac{\partial^\nu G_\nu}{\partial t^\nu}(z,t) = -\lambda(1-z)G_\nu(z,t) + \mu(1-z)\frac{\partial G_\nu}{\partial z}(z,t). \tag{8}$$

Moreover, this equation admits a unique Laplace-transformable solution such that, for any $t \geq 0$, $G_\nu(0,t) = p_0^\nu(t)$ and, for any $z \in \mathbb{R}$, $G_\nu(z,0) = 1$.

Proof Let us recall (see [24]) that the Laplace transform of $f_\nu(t,y)$ is given by

$$\mathcal{L}[f_\nu(\cdot,y)](s) = s^{\nu-1}e^{-ys^\nu}, \qquad s>0,\ y\geq 0. \tag{9}$$

Let us denote by $\mathcal{G}_\nu(z,s)$ the Laplace transform of G_ν. We have

$$\mathcal{G}_\nu(z,s) = \frac{1}{s}\int_0^{+\infty} G(z,y)s^\nu e^{-ys^\nu}dy = -\frac{1}{s}\int_0^{+\infty} G(z,y)de^{-ys^\nu}.$$

Let us integrate by parts the right-hand side to obtain

$$\mathcal{G}_\nu(z,s) = \frac{1}{s} + \frac{1}{s}\int_0^{+\infty}\frac{\partial G}{\partial t}(z,y)e^{-ys^\nu}dy.$$

Now, recalling that G is solution of (3) we have

$$\begin{aligned}\mathcal{G}_\nu(z,s) &= \frac{1}{s} - \frac{\lambda(1-z)}{s}\int_0^{+\infty} G(z,y)e^{-ys^\nu}dy + \frac{\mu(1-z)}{s}\int_0^{+\infty}\frac{\partial G}{\partial z}(z,y)e^{-ys^\nu}dy\\ &= \frac{1}{s} - \frac{\lambda(1-z)}{s^\nu}\int_0^{+\infty} G(z,y)s^{\nu-1}e^{-ys^\nu}dy\\ &\quad + \frac{\mu(1-z)}{s^\nu}\int_0^{+\infty}\frac{\partial G}{\partial z}(z,y)s^{\nu-1}e^{-ys^\nu}dy\\ &= \frac{1}{s} - \frac{\lambda(1-z)}{s^\nu}\mathcal{G}_\nu(z,s) + \frac{\mu(1-z)}{s^\nu}\frac{\partial \mathcal{G}_\nu}{\partial z}(z,s).\end{aligned}$$

Multiplying everything by $s^{\nu-1}$ we achieve

$$s^{\nu-1}\left(\mathcal{G}_\nu(z,s) - \frac{1}{s}\right) = -\frac{1}{s}\lambda(1-z)\,\mathcal{G}_\nu(z,s) + \frac{1}{s}\mu(1-z)\frac{\partial\,\mathcal{G}_\nu}{\partial z}(z,s).$$

First of all, let us observe that being $t \mapsto G_\nu(z,t)$ continuous for fixed $z \in \mathbb{R}$, we have that it is fractionally integrable. Thus, taking the inverse Laplace transform, we obtain

$$\mathcal{I}_t^\nu(G_\nu(z,\cdot) - 1) = \int_0^t \left(-\lambda(1-z)G_\nu(z,s) + \mu(1-z)\frac{\partial G_\nu}{\partial z}(z,s)\right)ds.$$

Now let us observe that the integrand in the right-hand side is continuous in t (being, for each $z \in \mathbb{R}$, both $G_\nu(z,s)$ and $\frac{\partial G_\nu}{\partial z}(z,s)$ sum of normally convergent series of continuous functions in s) hence the left-hand side is in C^1 and we can differentiate both sides, obtaining

$$\frac{\partial^\nu G}{\partial t^\nu}(z,t) = -\lambda(1-z)G_\nu(z,t) + \mu(1-z)\frac{\partial G_\nu}{\partial z}(z,t).$$

Concerning the uniqueness, it follows from the invertibility of the Laplace transform together with the uniqueness of the solution of the Cauchy problem (for fixed $s > 0$):

$$\begin{cases}\frac{\partial\,\mathcal{G}_\nu}{\partial z}(z,s) = \frac{(s^\nu+\lambda(1-z))}{\mu(1-z)}\,\mathcal{G}_\nu(z,s) + \frac{s^{\nu-1}}{\mu(1-z)}\\ \mathcal{G}_\nu(0,s) = \pi_0^\nu(s)\end{cases}$$

where $\pi_0^\nu(s)$ is the Laplace transform of $p_0^\nu(t)$. □

With this in mind, we can actually show the following Proposition

Proposition 4 *The sequence* $\mathbf{p}^\nu(t) = (p_n^\nu(t))_{n\geq 0}$ *is the unique global solution belonging to* $\ell^2(\Pi(\cdot;\rho))$ *of the fractional difference-differential Cauchy problem*

$$\begin{cases}\frac{d^\nu p_0^\nu}{dt^\nu}(t) = -\lambda p_0^\nu(t) + \mu p_1^\nu(t)\\ \frac{d^\nu p_n^\nu}{dt^\nu}(t) = \lambda p_{n-1}^\nu(t) - (\lambda + n\mu)p_n^\nu(t) + (n+1)\mu p_{n+1}^\nu(t) & n \geq 1\\ p_n^\nu(0) = \delta_{n,0} & n \geq 0.\end{cases} \tag{10}$$

Moreover, $\mathbf{p}^\nu$ is locally Bochner integrable in $\ell^2(\Pi(\cdot,\rho))$, and $\frac{d^\nu \mathbf{p}^\nu}{dt^\nu}$ is well defined (as a strong $\ell^2(\Pi(\cdot,\rho))$ derivative) and locally Bochner integrable in $\ell^2(\Pi(\cdot,\rho))$.

Proof To show that $\mathbf{p}^\nu(t) = (p_n^\nu(t))_{n\geq 0}$ is solution of Eq. (10) is actually equivalent to show that the probability generating function $G_\nu(z,t)$ is solution of Eq. (8). Indeed if $\mathbf{p}^\nu(t) = (p_n^\nu(t))_{n\geq 0}$ is solution of Eq. (10), we obtain Eq. (8) by multiplying the second equation by z^n and then summing over n. Viceversa, if $G_\nu(z,t)$ is solution of Eq. (8), we obtain Eq. (10) by differentiating both sides n times (for $n \geq 0$) and taking $z = 0$. Thus, since by Proposition 3 we know that $G_\nu(z,t)$ is solution of Eq. (8) we have that $\mathbf{p}^\nu(t)$ is solution of (10). Now let us observe that $\Pi(\cdot;\rho)$ is a finite measure on $\mathbb{N}_0$, hence, since $p_n^\nu(t) \leq 1$, $\mathbf{p}^\nu(t) \in \ell^2(\Pi(\cdot;\rho))$. Moreover, one can easily show that $t \mapsto \|\mathbf{p}^\nu(t)\|_{\ell^2(\Pi(\cdot;\rho))}$ is bounded in $[0,+\infty)$. In particular this implies that, being $t \mapsto \|\mathbf{p}^\nu(t)\|_{\ell^2(\Pi(\cdot;\rho))}$ in L^1_{loc}, $\mathbf{p}^\nu$ is locally Bochner integrable (see, for instance [2, Theorem 3.14]) and, for any $t > 0$, $\tau \in [0,+\infty) \mapsto (t-\tau)^{-\nu}\mathbf{p}^\nu(\tau)\chi_{[0,t)}(\tau) \in \ell^2(\Pi(\cdot;\rho))$ is Bochner integrable. Now let us rewrite Eq. (10) as

$$\begin{cases} \frac{\partial^\nu \mathbf{p}^\nu}{\partial t^\nu} = \mathfrak{G}\,\mathbf{p}^\nu \\ \mathbf{p}^\nu(0) = (\delta_{n,0})_{n\geq 0}, \end{cases} \tag{11}$$

where $\mathfrak{G}$ is an infinite-dimensional matrix. By a simple application of Schur's test (see [14]), we know that $\mathfrak{G} : \ell^2(\Pi(\cdot,\rho)) \to \ell^2(\Pi(\cdot,\rho))$ is continuous and then $\mathfrak{G}\,\mathbf{p}^\nu$ is Bochner integrable. Thus we can write the previous equation in integral form as

$$\frac{1}{\Gamma(1-\nu)}\int_0^t \frac{1}{(t-\tau)^\nu}\mathbf{p}^\nu(\tau)d\tau = \int_0^t \mathfrak{G}\,\mathbf{p}^\nu(\tau)d\tau. \tag{12}$$

It is not difficult to show, integrating term by term in Eq. (10), that $\mathbf{p}^\nu$ is solution of (12). Moreover, let us fix $t_0 > 0$ and $\varepsilon > 0$ and observe that

$$\|\mathfrak{G}(\mathbf{p}^\nu(t) - \mathbf{p}^\nu(t_0))\|_{\ell^2(\Pi(\cdot,\rho))} \leq \|\mathfrak{G}\|\,\|\mathbf{p}^\nu(t) - \mathbf{p}^\nu(t_0)\|_{\ell^2(\Pi(\cdot,\rho))}.$$

Being, for any $n \in \mathbb{N}$, $(p_n^\nu(t) - p_n^\nu(t_0))^2 \leq 4$, the function $F : t \mapsto \|\mathbf{p}^\nu(t) - \mathbf{p}^\nu(t_0)\|^2_{\ell^2(\Pi(\cdot,\rho))}$ is continuous since it is sum of a normally convergent series of continuous functions. Moreover $F(t_0) = 0$, thus, by continuity, there exists a $\delta > 0$ such that for any $t \in (t_0-\delta, t_0+\delta)$ it holds $|F(t)| < \frac{\varepsilon^2}{\|\mathfrak{G}\|^2}$ and then

$$\|\mathfrak{G}(\mathbf{p}^\nu(t) - \mathbf{p}^\nu(t_0))\|_{\ell^2(\Pi(\cdot,\rho))} < \varepsilon,$$

concluding that $\mathfrak{G}\,\mathbf{p}^\nu$ is continuous. Thus we can differentiate both sides of (12) to obtain (11). From this relation we also obtain that $\frac{\partial^\nu \mathbf{p}^\nu}{\partial t^\nu}$ is well defined and locally Bochner integrable. Finally uniqueness follows from [3, Corollary 2]. □

Remark 1 Such result can be also achieved by spectral decomposition. Indeed the same proposition is also proved in [5], by also showing that the following spectral decomposition holds:

$$p_n^\nu(t) = \Pi(n;\rho)\sum_{m=0}^{+\infty}(-1)^m E_\nu(-m\mu t^\nu)\frac{\rho^m}{m!}C_m(n;\rho), \qquad n\in\mathbb{N},\ t\geq 0,$$

where $E_\nu(t)$ is the Mittag-Leffler function defined in Eq. (21) of Appendix 1. In particular, for any function $h\in\ell^2(\Pi(\cdot,\rho))$ with $h(n)=\sum_{m=0}^{+\infty}h_m\sqrt{\frac{\rho^m}{m!}}C_m(n;\rho)$, defining $u(t)=\mathbb{E}[h(N^\nu(t))|N^\nu(0)=0]$ it holds

$$u(t)=\sum_{m=0}^{+\infty}(-1)^m h_m\sqrt{\frac{\rho^m}{m!}}E_\nu(-m\mu t^\nu), \qquad t\geq 0. \tag{13}$$

Moreover, we can also express the probability generating function as

$$G_\nu(z,t)=\sum_{m=0}^{+\infty}(-1)^m E_\nu(-m\mu t^\nu)\frac{\rho^m}{m!}\sum_{n=0}^{+\infty}C_m(n;\rho)\Pi(n;\rho)z^n, \qquad t\geq 0,\ z\in\mathbb{R}.$$

One could check that

$$G_\nu(1,t)=\sum_{m=0}^{+\infty}(-1)^m E_\nu(-m\mu t^\nu)\frac{\rho^m}{m!}\delta_{m,0}=1, \qquad t\geq 0.$$

3.3 Laplace Transforms of $p_n^\nu(t)$ and $G_\nu(z,t)$

In this subsection we want to determine the Laplace transforms of the state probabilities $p_n^\nu(t)$ and of the probability generating function $G_\nu(z,t)$. To do this, let us first show the following easy Lemma.

Lemma 1 *Let $h:\mathbb{R}_+\to\mathbb{R}$ be a Laplace-transformable function with domain of the Laplace transform D such that $\{s\in\mathbb{C}:\ \Re(s)>0\}\subseteq D$ and define for $t>0$*

$$h_\nu(t)=\int_0^{+\infty}h(y)\,f_\nu(t,y)dy.$$

Let us denote by $\widehat{h}(s)$ and $\widehat{h}_\nu(s)$ the Laplace transform respectively of h and h_ν for $s>0$. Then

$$\widehat{h}_\nu(s)=s^{\nu-1}\widehat{h}(s^\nu). \tag{14}$$

Proof Equation (14) easily follows from Eq. (9). Indeed we have

$$\widehat{h}_\nu(s)=s^{\nu-1}\int_0^{+\infty}e^{-s^\nu y}h(y)dy=s^{\nu-1}\widehat{h}(s^\nu).$$

□

By just applying this Lemma, we have the following result.

Proposition 5 *Let $\pi_n^\nu(s)$ and $\mathcal{G}_\nu(z,s)$ be the Laplace transform respectively of $p_n^\nu(t)$ and $G_\nu(z,t)$. Then we have, for any $s>0$ and $z\in\mathbb{R}$,*

$$\pi_n^\nu(s)=\frac{(-1)^n s^{\nu-1}}{\mu}\sum_{k=n}^{+\infty}\binom{k}{n}\frac{\Gamma\left(\frac{s^\nu}{\mu}\right)}{\Gamma\left(\frac{s^\nu}{\mu}+k+1\right)}(-\rho)^k,$$

$$\mathcal{G}_\nu(z,s)=\frac{s^{\nu-1}}{\mu}\sum_{k=0}^{+\infty}\frac{\Gamma\left(\frac{s^\nu}{\mu}\right)}{\Gamma\left(\frac{s^\nu}{\mu}+k+1\right)}(-\rho(1-z))^k.$$

3.4 Mean and Variance of the Process

From Eq. (8) one can easily obtain the mean of our process.

Corollary 1 *The process $N_\nu(t)$ admits finite mean for any $t>0$, given by*

$$\mathbb{E}[N_\nu(t)]=\rho\left(1-E_\nu(-\mu t^\nu)\right),\qquad t\geq 0. \tag{15}$$

Proof Let us differentiate both sides of Eq. (8) with respect to z and then let us pose $z=1$. We have

$$\frac{\partial}{\partial z}\left(\frac{\partial^\nu G}{\partial t^\nu}\right)(1,t)=\lambda G_\nu(1,t)-\mu\frac{\partial G_\nu}{\partial z}(1,s).$$

Now let us observe that since G is defined by a power series, it is easy to check that we can exchange the order of derivatives in the left-hand side. Moreover, we have $G_\nu(1,t)=1$ and $\frac{\partial G_\nu}{\partial z}(1,s)=\mathbb{E}[N_\nu(t)]$, thus we have

$$\frac{\partial^\nu \mathbb{E}[N_\nu(t)]}{\partial t^\nu}=\lambda-\mu\,\mathbb{E}[N_\nu(t)]. \tag{16}$$

Recalling that $\mathbb{E}[N_\nu(0)]=0$, we can take the Laplace transform of Eq. (16) to achieve

$$s^\nu\,\mathcal{L}[\mathbb{E}[N_\nu(\cdot)]](s)=\frac{\lambda}{s}-\mu\,\mathcal{L}[\mathbb{E}[N_\nu(\cdot)]](s)$$

from which we have

$$\mathcal{L}[\mathbb{E}[N_\nu(\cdot)]](s)=\frac{\lambda}{s(s^\nu+\mu)}.$$

Taking the inverse Laplace transform we obtain, by using Eq. (23),

$$\mathbb{E}[N_\nu(t)] = \lambda t^\nu E_{\nu,\nu+1}(-\mu t^\nu),$$

where $E_{\nu,\nu+1}(t)$ is the two parameters Mittag-Leffler function defined in Eq. (22) in Appendix 1. Now let us write explicitly $E_{\nu,\nu+1}(-\mu t^\nu)$ to observe that we have

$$\begin{aligned}\mathbb{E}[N_\nu(t)] &= \lambda t^\nu \sum_{n=0}^{+\infty}(-1)^n \frac{\mu^n t^{\nu n}}{\Gamma(\nu(n+1)+1)} = -\rho \sum_{n=0}^{+\infty}(-1)^{n+1} \frac{(\mu t^\nu)^{n+1}}{\Gamma(\nu(n+1)+1)} \\ &= -\rho \left(\sum_{n=1}^{+\infty}(-1)^n \frac{(\mu t^\nu)^n}{\Gamma(\nu n+1)} \right) = \rho \left(1 - \sum_{n=0}^{+\infty} \frac{(-\mu t^\nu)^n}{\Gamma(\nu n+1)} \right) \\ &= \rho \left(1 - E_\nu(-\mu t^\nu)\right).\end{aligned}$$

Remark 2 One could obtain Eq. (16) starting directly from Eq. (5) and observing that

$$\mathbb{E}[N_\nu(t)] = \int_0^{+\infty} \mathbb{E}[N(y)] f_\nu(t, y) dy.$$

Thus we obtain Eq. (16) by working with the Laplace transform of $\mathbb{E}[N_\nu(t)]$. Moreover, by using relation (14), it is easy to determine directly Eq. (15) without using any fractional differential equation.

One could also use the relation (13) to determine $\mathbb{E}[N_\nu(t)]$. Indeed, by using again $h(n) = n$, we obtain Eq. (15). Moreover, by using $h(n) = n^2$, we have

$$\mathbb{E}[N_\nu^2(t)] = \rho(1 - E_\nu(-\mu t^\nu)) + \rho^2 \left(1 - 2E_\nu(-\mu t^\nu) + E_\nu(-2\mu t^\nu)\right), \ t \geq 0$$

from which we have the variance

$$\mathrm{Var}[N_\nu(t)] = \rho(1 - E_\nu(-\mu t^\nu)) + \rho^2 \left(E_\nu(-2\mu t^\nu) - E_\nu^2(-\mu t)\right), \ t \geq 0.$$

Let us observe that the lack of semigroup property due to the presence of the Mittag-Leffler function (see [21]) gives us $\mathrm{Var}[N_\nu(t)] \neq \mathbb{E}[N_\nu(t)]$ and then $N_\nu(t)$ does not admit Poisson distribution for any $t > 0$. However, it is shown in [5] that the invariant (and then the limit) distribution of $N_\nu(t)$ is still a Poisson one $\Pi(\cdot; \rho)$. This is also confirmed by the Laplace transform $\pi_n^\nu(t)$ as $n \geq 0$. The lack of semigroup property will be the main character of next section.

4 Interpretation of $N_\nu(t)$ as a Queue

In this section we will focus on the interpretation of the process $N_\nu(t)$ as a queue. In contrast of what is stated in [17], in the fractional case we will see a difference in the interpretation between the fractional $M/M/\infty$ queue and the fractional $M/M/1$

queue with responsive server. Let us first introduce some definitions, following the lines of [29].

Definition 1 We define the following quantities:

- The inter-arrival times $\{I_n, n \geq 1\}$ are the time intervals between the arrival of the $(n-1)$-th and the n-th customers, where I_1 is the arrival of the first customer;
- The arrival times $\{A_n, n \geq 1\}$ are the time instants in which the n-th customer joins the system;
- The service times $\{S_n, n \geq 1\}$ are the time intervals of service dedicated to the n-th customer;
- The inter-exit times $\{F_n, n \geq 1\}$ are the time intervals between the exit of two customers;
- The exit times $\{E_n, n \geq 1\}$ are the ordered time instants in which each customer exits the system;
- The inter-event times $\{J_n, n \geq 1\}$ are the time intervals between the $n-1$-th and the n-th events (arrival or service) in the system, while J_1 is the instant of the first event;
- The event times $\{T_n, n \geq 1\}$ are the time instants in which the n-th event happens;
- The virtual waiting time $\{W(t), t \geq 0\}$ is the time interval a customer has to wait until it exits the system if it enters the system at time t.

Let us also give the following notation:

- We say a random variable T is Mittag-Leffler distributed of parameter $\alpha > 0$ and fractional order $\beta \in (0, 1)$ if its distribution function $F_T(t) = \mathbb{P}(T \leq t)$ is given by
$$F_T(t) = (1 - E_\beta(-\alpha t^\beta))\chi_{[0,+\infty)}(t),$$
where $\chi_{[0,+\infty)}(t)$ is the indicator function of the interval $[0, +\infty)$. It will be denoted by $T \sim ML(\alpha, \beta)$;
- We say a random variable T is generalized Erlang distributed (see [22]) of shape parameter $n \in \mathbb{N}$, rate $\alpha > 0$ and fractional order $\beta \in (0, 1)$ if its probability density function $f_T(t)$ admits Laplace transform
$$\widehat{f_T}(s) = \frac{\alpha^n}{(\alpha + s^\beta)^n}, \ s > 0.$$
It will be denoted by $T \sim GE_n(\alpha, \beta)$;
- We say a random variable T is residual Mittag-Leffler distributed (see [4]) of parameter α, fractional order $\beta \in (0, 1)$ and lag interval $\Delta t \geq 0$ if its distribution function $F_T(t) = \mathbb{P}(T \leq t)$ is given by
$$F_T(t) = \left(1 - \frac{E_\beta(-\alpha(t + \Delta t)^\beta)}{E_\beta(-\alpha \Delta t^\beta)}\right) \chi_{[0,+\infty)}(t).$$
It will be denoted by $T \sim RML(\alpha, \beta, \Delta t)$.

First of all, let us recall (see [22]) that if $(T_n)_{n\geq 1}$ are independent $ML(\alpha,\beta)$ random variables then $\sum_{k=1}^{n} T_k \sim GE_n(\alpha,\beta)$. Moreover (See [4]), if $T \sim ML(\alpha,\beta)$ then

$$\mathbb{P}(T \leq t+\Delta t | T \geq \Delta t) = 1 - \frac{E_\beta(-\alpha(t+\Delta t)^\beta)}{E_\beta(-\alpha \Delta t^\beta)}.$$

4.1 Inter-arrival, Inter-event and Inter-exit Times

Given a time $t > 0$ it will be useful to define the following process

$$T(t) = \max\{T_n : \ T_n \leq t\}$$

which is the time instant of the last event before t.
Let us prove the following Proposition, which is common in both the interpretations.

Proposition 6 *It holds:*

1. *The inter-arrival times I_n are independent and distributed as $I \sim ML(\lambda, \nu)$;*
2. *The arrival times A_n are distributed as $GE_n(\lambda, \nu)$;*
3. *Let J_{k+1} be a inter-event time for $k \in \mathbb{N}$. Then*

$$\mathbb{P}(J_{k+1} \leq t | N_\nu((T_k+t)-) = n) = 1 - E_\nu(-(\lambda+n\mu)t^\nu);$$

4. *The inter-event time J_1 coincides with I_1 and A_1;*
5. *Let F_{k+1} be a inter-exit time for some $k \in \mathbb{N}$ (see Fig. 1). Then*

$$\mathbb{P}(F_{k+1} \leq t | T(E_k+t) = E_k, N_\nu((E_k+t)-) = n) = 1 - E_\nu(-n\mu t^\nu).$$

Proof Before proving the Proposition let us observe that the process $N_\nu(t)$ is a Semi-Markov process, then the set $K(\omega) = \{t > 0 : N_\nu(t-,\omega) \neq N_\nu(t,\omega)\}$ is a semi-regenerative set. Hence strong Markov property holds for any stopping time $\mathcal{T}$ such that $\mathcal{T}(\omega) \in K(\omega)$ for any $\omega \in \Omega$ (for other details see [11]).
Let us prove 1. To study arrival times, let us set $\mu = 0$ (i.e. we consider the associated pure birth process $\widetilde{N}_\nu(t)$). Now let N_n be the embedded Markov chain of the pure birth process and let us consider the Markov renewal process (N_n, I_n) (see [9]). Observe that $\mathbb{P}(N_{n+1} = i+1, I_{n+1} \leq t | N_n = i)$ is independent of n and $\mathbb{P}(N_{n+1} = i+1 | N_n = i) = 1$, hence we have

$$\begin{aligned}\mathbb{P}(I_{n+1} \leq t | N_n = i) &= \mathbb{P}(N_{n+1} = i+1, I_{n+1} \leq t | N_n = i) = \\ &= \mathbb{P}(N_1 = i+1, I_1 \leq t | N_0 = i) = \mathbb{P}(I_1 \leq t | N_0 = i).\end{aligned}$$

This means that to study the inter-arrival times between the i-th customer and the $i+1$-th customer, we can simply consider the associated pure birth process $\widetilde{N}_\nu(t)$

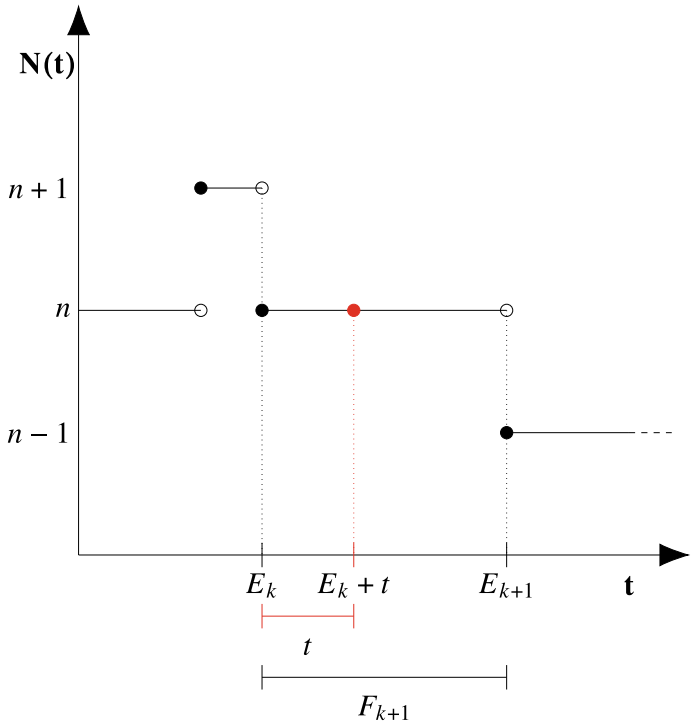

Fig. 1 Illustration of an inter-exit time as in Proposition 6, statement 5

conditioned by $\widetilde{N}_\nu(0) = i$. Moreover, since we are not interested in what happens after the $i+1$-th customer entered the queue, we can set the state $i+1$-th to be absorbent. We obtain (denoting by $\widetilde{p}_k^\nu$ the state probabilities of $\widetilde{N}_\nu(t)$)

$$\begin{cases} \frac{d^\nu \widetilde{p}_i^\nu}{dt^\nu}(t) = -\lambda \widetilde{p}_i^\nu(t) \\ \frac{d^\nu \widetilde{p}_{i+1}^\nu}{dt^\nu}(t) = \lambda \widetilde{p}_i^\nu(t) \\ \widetilde{p}_i^\nu(0) = 1 \\ \widetilde{p}_{i+1}^\nu(0) = 0. \end{cases}$$

Solving this equation we have $\mathbb{P}(I_1 > t | N_n = i) = \widetilde{p}_n^\nu(t) = E_\nu(-\lambda t^\nu)$. Independence easily follows from the independence of the inter-arrival times in the non-fractional model.
The proofs of 3 and 5 are analogous hence we omit them.
Statement 2 is consequence of the fact that $A_n = \sum_{k=1}^n I_k$. Finally in statement 4 we have $I_1 = A_1$ by definition and $I_1 = J_1$ since we are assuming $N_\nu(0) = 0$. □

Let us observe that, by the lack of semigroup property of the Mittag-Leffler function, for any inter-event time J, inter-arrival time I and service time S, given T the time instant of the last event,

$$\begin{aligned}\mathbb{P}(J > t | N(T-) = N(T) + 1, N((T+t)-) = n) \\ = \mathbb{P}(\min\{F, I\} > t | N(T-) = N(T) + 1, N((T+t)-) = n) \\ \neq \mathbb{P}(F > t | N(T-) = N(T) + 1, N((T+t)-) = n)\, \mathbb{P}(I > t),\end{aligned}$$

in contrast with what happens in the non-fractional case.

Remark 3 Let us observe that the conditioning in Statement 5 of Proposition 6 is indispensable to be sure that the process remains in the current state.

4.2 Virtual Waiting Times for the Fractional $M/M/\infty$

Let us now focus our attention on virtual waiting times. Let us recall that a $M/M/\infty$ system is a system with an infinite number of servers, hence whenever a customer enters the service, it is served. Since the service times are random variables, here we do not have a FIFO (First In First Out) service policy. Thus it will be useful to identify the customers. Let us define for the i-th customer the process

$$u_i(t) = \begin{cases} 1 & A_i \leq t < A_i + S_i \\ 0 & \text{otherwise.} \end{cases}$$

In particular $u_i(t) = 1$ if and only if the i-th customer is in the service at time $t > 0$. Moreover, we can also define the quantity $U(t_1, t_2) \in \mathbb{N}_0$ as the index of the first customer that leaves the service in the time interval $[t_1, t_2)$. Moreover, we will need to identify each exit time of each customer. Thus let us denote by $E^{(i)}$ the exit time of the i-th customer (recalling that E_i is the i-th exit time, which could not be the exit time of the i-th customer).
In the $M/M/\infty$ queue the virtual waiting time $W(t)$ coincides with the service time S of a customer if its arrival time is t. In the classical case one could consider each server to be independent of the others. This property lead to the fact that (by using then the Markov property of the process $N(t)$ and the semigroup property of the exponential) each service time was exponentially distributed of parameter μ.
Here the lack of semigroup property in the Mittag-Leffler distributions gives us a problem on determining the virtual waiting time of each customer. However, we can still express something on the minimum of the virtual waiting times of the customers that are actually in the system.

Proposition 7 *Let $A_1, \ldots, A_{n+1}$ be the arrival times of the first $n+1$ customers. Let us consider $t_1 < \cdots < t_{n+1} < s$ in $[0, +\infty)$ and let us denote by $W_i(t)$ the virtual waiting time of the i-th customer. Then, defining $X = \min_{\substack{i \leq n+1 \\ i \neq j}} \{W_i(t_i) - (s - t_i)\}$, we have*

$$\mathbb{P}\left(X \leq t | A_i = t_i \ \forall i \leq n+1,\ E^{(j)} = T(E^{(j)}+t) = s,\ U(0, s+t) = j\right) = \\ = 1 - E_\nu(-n\mu t^\nu).$$

Proof Let us just understand what the random variable X is, under our conditioning. Each user enters the system at time t_i and leaves the system at time $W_i(t_i) + t_i$. Let us sum and subtract s from this relation to obtain that the exit time is given by $W_i(t_i) - (s - t_i) + s$. The condition $E^{(j)} = T(E^{(j)} + t)$ means that the last event before t in the system was an exit hence there are no entrance in the system up to time t. In particular the state of the system is $N(t-) = n$. Moreover $W_i(t_i) - (s - t_i)$ is the time interval between the exit of the j-th customer (since $E^{(j)} = T(E^{(j)+}t)$ and $U(0, s + t) = j$) and the exit of the i-th customer. Thus the variable X is an inter-exit time. Moreover, we are conditioning with the fact that the last event is an exit and the state of the system is fixed at n, hence Statement 5 of Proposition 6 concludes the proof (see Fig. 2).

4.3 *Virtual Waiting Times for the Fractional $M/M/1$ Queue with Responsive Server*

The case of the $M/M/1$ queue with responsive server is quite different. Indeed since here we have only one server, each customer has to wait for the others to complete their service before being served. Hence the queue exhibits a FIFO service policy. For this reason we can observe that the service times S_n and the inter-exit times F_n coincide and thus are independent, while the virtual waiting times $W(t)$ are the sum of the time the customer spends in the queue and its service time. Moreover, we have $E_i = E^{(i)}$ for any $i \in \mathbb{N}$.

We need to introduce some new quantities linked with the arrival and the exit times of the customers. Let us define, for $t > 0$, $A(t) = \max\{A_n : A_n \leq t\}$ the last instant of arrival before t and $E(t) = \max\{E_n : E_n \leq t\}$ the last instant of exit before t. These quantities will play a major role in the following proposition.

Proposition 8 *Let us define the function*

$$F_W(s; t, t_0, n) = \mathbb{P}(W(t) \leq s | A(t+s) = t,\ E(t) = t_0,\ N(t) = n+1)$$

and let $f_W(s; t, t_0, n)ds$ be its distributional derivative. Let us also denote $\widehat{f_W}(z; t, t_0, n)$ the Laplace transform of $f_W(s; t, t_0, n)ds$. Then we have

$$\widehat{f_W}(z; t, t_0, n) = \left(1 - \frac{e^{\Delta t z} \sum_{k=0}^{+\infty} \frac{(-(n+1)\mu)^k}{\Gamma(k\nu+1)} z^{-k\nu} \Gamma(k\nu+1, z\Delta t)}{E_\nu(-(n+1)\mu\Delta t^\nu)}\right) \prod_{i=1}^{n} \frac{i\mu}{z^\nu + i\mu},$$

where

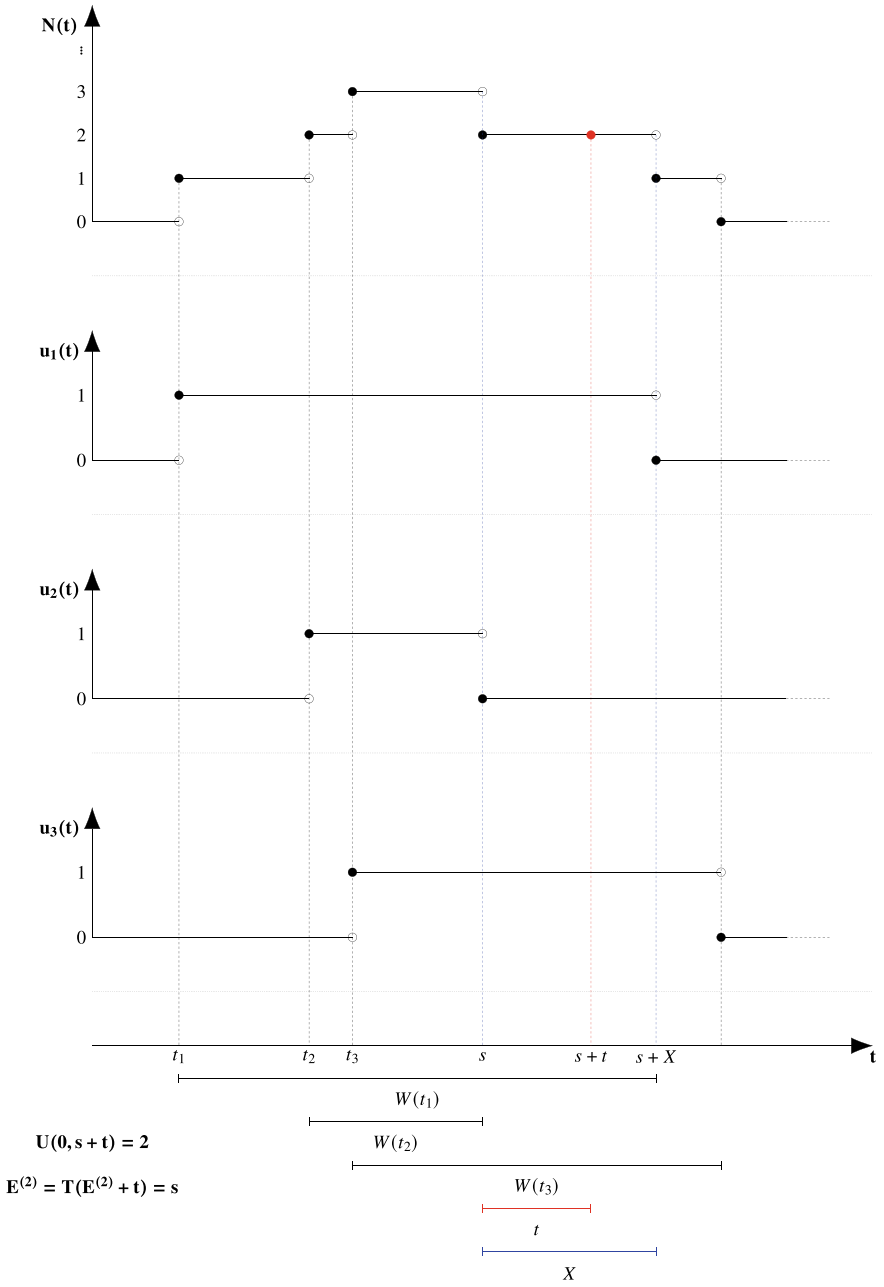

Fig. 2 Illustration of the virtual waiting times as in Proposition 7

$$\Gamma(x, y) = \int_y^{+\infty} t^{x-1} e^{-t} dt$$

is the upper incomplete Gamma function and $\Delta t = t - t_0$ *(see Fig. 3).*

Proof As we can see by the conditioning, no other customer entered the queue after t. Let us denote by S_{n+1} the service time of the customer that is being served at time t and with $S_n, \dots, S_1$ the successive service times. Thus we have

$$W(t) = \sum_{i=1}^{n} S_i + (S_{n+1} - \Delta t), \tag{17}$$

where $\Delta t = t - t_0$.
First of all, let us observe that, by Statement 5 of Proposition 6, $S_i \sim ML(i\mu, \nu)$ for any $i \leq n$. Concerning S_{n+1}, we know that the customer started its service at time t_0 hence we know that $S_{n+1} \geq \Delta t$. Thus we have that

$$\mathbb{P}(S_{n+1} - \Delta t \leq s | S_{n+1} \geq \Delta t) = 1 - \frac{E_\nu(-(n+1)\mu(s+\Delta t)^\nu)}{E_\nu(-(n+1)\mu \Delta t^\nu)}$$

and in particular, under our conditioning, $S_{n+1} - \Delta t \sim RML((n+1)\mu, \nu, \Delta t)$. Thus, taking the Laplace transform of $W(t)$ as written in Eq. (17), recalling that the random variable S_i are independent, we have

$$\widehat{f_W}(z; t, t_0, n) = z \left(\frac{1}{z} - \frac{\mathcal{L}_{s\to z}[E_\nu(-(n+1)\mu(s+\Delta t)^\nu)]}{E_\nu(-(n+1)\mu \Delta t^\nu)} \right) \prod_{i=1}^{n} \frac{i\mu}{z^\nu + i\mu}.$$

To determine the remaining Laplace transform, let us observe that

$$\begin{aligned}
\int_0^{+\infty} E_\nu(-(n+1)\mu(s+\Delta t)^\nu) e^{-sz} ds &= e^{\Delta t z} \int_{\Delta t}^{+\infty} E_\nu(-(n+1)\mu w^\nu) e^{-wz} dw \\
&= e^{\Delta t z} \sum_{k=0}^{+\infty} \frac{(-(n+1)\mu)^k}{\Gamma(k\nu+1)} \int_{\Delta t}^{+\infty} w^{k\nu} e^{-wz} dw \\
&= e^{\Delta t z} \sum_{k=0}^{+\infty} \frac{(-(n+1)\mu)^k}{\Gamma(k\nu+1)} z^{-k\nu-1} \int_{z\Delta t}^{+\infty} u^{k\nu} e^{-u} du \\
&= e^{\Delta t z} \sum_{k=0}^{+\infty} \frac{(-(n+1)\mu)^k}{\Gamma(k\nu+1)} z^{-k\nu-1} \Gamma(k\nu+1, z\Delta t),
\end{aligned}$$

concluding the proof.

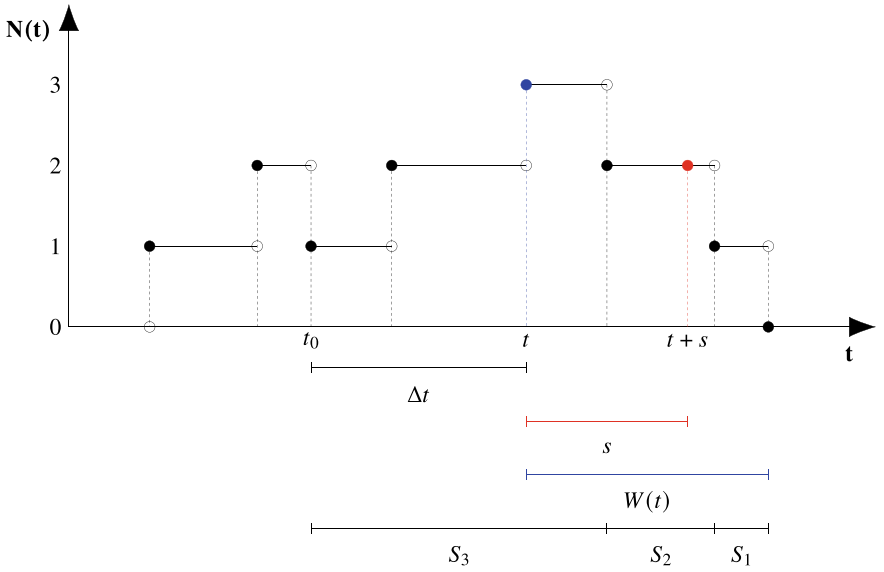

Fig. 3 Illustration of the virtual waiting times as in Proposition 8

Acknowledgements We thank the referee for its useful suggestions. Ascione and Pirozzi are partially supported by MIUR—PRIN 2017, project "Stochastic Models for Complex Systems", no. 2017JFFHSH and by INdAM Groups respectively GNAMPA and GNCS.

Appendix 1: Fractional Integrals and Derivatives

Let us recall the definition of fractional integral (see [19] for a survey). Let us fix $\nu \in (0, 1)$ and consider a function $f : \mathbb{R}_+ \to \mathbb{R}$. We define the fractional integral of f of order ν (if it exists) the function

$$\mathcal{I}_t^\nu f = \frac{1}{\Gamma(\nu)} \int_0^t (t-\tau)^{\nu-1} f(\tau) d\tau.$$

For any suitable function $f : \mathbb{R}_+ \to \mathbb{R}$, we define the fractional Riemann-Liouville derivative and the fractional Caputo derivative of order ν respectively the functions

$$\mathcal{D}_t^\nu f = \frac{d}{dt} \mathcal{I}_t^{1-\nu} f, \qquad \frac{d^\nu f}{dt^\nu} = \mathcal{I}_t^{1-\nu} \left(\frac{df}{dt} \right). \tag{18}$$

In particular any Caputo-derivable function f is also Riemann-Liouville-derivable and it holds

$$\frac{d^\nu f}{dt^\nu} = \mathcal{D}_t^\nu (f(t) - f(0)). \tag{19}$$

We can thus define the regularized Caputo derivative for Riemann-Liouville-derivable functions by relation (19).
Concerning the Laplace transform of such functions, we have, for any Laplace-transformable function f with Laplace transform $\hat{f}$:

$$\mathcal{L}_{t\to s}\left[\mathcal{I}_t^\nu f\right] = s^{\nu-1}\hat{f}(s), \quad \mathcal{L}_{t\to s}\left[\frac{d^\nu f}{dt^\nu}\right] = s^\nu \hat{f}(s) - s^{\nu-1} f(0). \tag{20}$$

Let us also recall (see [28] for instance) that fractional Cauchy problems of the form

$$\begin{cases} \frac{\partial^\nu x}{\partial t^\nu}(t) = f(x(t), t) \quad t \in (0, T] \\ x(0) = x_0 \end{cases}$$

admit a unique solution under suitable assumptions. In particular the relaxation equation

$$\begin{cases} \frac{\partial^\nu x}{\partial t^\nu}(t) = \lambda x(t) \quad t > 0 \\ x(0) = x_0 \end{cases}$$

admits as unique solution the function

$$x(t) = x_0 E_\nu(\lambda t^\nu),$$

where E_ν is the Mittag-Leffler function (see [15]), defined as

$$E_\nu(z) = \sum_{n=0}^{+\infty} \frac{z^n}{\Gamma(\nu n + 1)}, \quad \nu > 0,\ z \in \mathbb{C}. \tag{21}$$

Other functions linked to the Mittag-Leffler ones are the two parameters Mittag-Leffler functions, defined as

$$E_{\nu,\beta}(z) = \sum_{n=0}^{+\infty} \frac{z^n}{\Gamma(\nu n + \beta)}, \quad \nu, \beta > 0,\ z \in \mathbb{C}. \tag{22}$$

These functions come into play when one tries to solve a fractional differential equation via Laplace transform (see [20]). Thus, let us recall the following useful Laplace transform formula:

$$\mathcal{L}_{t\to s}[t^{\gamma-1} E_{\nu,\gamma}(\lambda t^\nu)] = \frac{s^{\nu-\gamma}}{s^\nu - \lambda}, \quad \nu, \gamma > 0,\ s \in \mathbb{C},\ |\lambda s^\nu| < 1. \tag{23}$$

Appendix 2: Laplace Transforms of $p_n(t)$ and $G(z, t)$

In this Appendix we aim to determine the Laplace transform of the state probabilities $p_n(t)$ of $N(t)$ and of the probability generating function $G(z, t)$. Let us start with the Laplace transform of $p_n(t)$.

Proposition 9 *The Laplace transform $\pi_n(s)$ of the state probabilities $p_n(t)$ of the process $N(t)$ are given by*

$$\pi_n(s) = \frac{(-1)^n}{\mu} \sum_{k=n}^{+\infty} \binom{k}{n} \frac{\Gamma\left(\frac{s}{\mu}\right)}{\Gamma\left(\frac{s}{\mu} + k + 1\right)} (-\rho)^k.$$

Proof Let us observe that

$$\pi_n(s) = \int_0^{+\infty} e^{-st} p_n(t) dt$$

and let us consider the change of variables $w = 1 - e^{-\mu t}$, recalling Eq. (2). We obtain

$$\pi_n(s) = \frac{\rho^n}{n!\mu} \int_0^1 (1-w)^{\frac{s}{\mu}-1} e^{-\rho w} w^n dw.$$

By [13, Formula 3.383.1] we conclude the proof. □

In an analogous way, one can calculate the Laplace transform of $G(z, t)$.

Proposition 10 *The Laplace transform $\mathcal{G}(z, s)$ of the probability generating function $G(z, t)$ of the process $N(t)$ is given by*

$$\mathcal{G}(z, s) = \frac{1}{\mu} \sum_{k=0}^{+\infty} \frac{\Gamma\left(\frac{s}{\mu}\right)}{\Gamma\left(\frac{s}{\mu} + k + 1\right)} (-\rho(1-z))^k.$$

References

1. Albanese, C., Kuznetsov, A.: Affine lattice models. Int. J. Theor. Appl. Financ. **8**(02), 223–238 (2005)
2. Amann, H., Escher, J.: Analysis III. Springer Basel (2009)
3. Ascione, G., Leonenko, N., Pirozzi, E.: Fractional queues with catastrophes and their transient behaviour. Math., **6.9** (2018)
4. Ascione, G., Leonenko, N., Pirozzi, E.: Fractional Erlang queues. Stoch. Proc. Appl. (2019). https://doi.org/10.1016/j.spa.2019.09.012
5. Ascione, G., Leonenko, N., Pirozzi, E.: Fractional immigration-death processes. J. Math. Anal. Appl. **495**.2, 124768 (2021)

6. Ascione, G., Toaldo, B.: A Semi-Markov leaky integrate-and-fire model. Math. **7**, 11 (2019)
7. Ascione, G., Pirozzi E.: On the construction of some fractional stochastic Gompertz models. Math. **8.1** (2020)
8. Ashton, S., Scalas, E., Georgiou, N., Kiss, I.: The mathematics of human contact: developing a model for social interaction in school children. Acta Phys. Pol. A 133.6, 1421–1432 (2018)
9. Barbu, V.S., Limnios, N.: Semi-Markov Chains and Hidden Semi-Markov Models Toward Applications: Their Use in Reliability and DNA Analysis. Springer Science & Business Media (2009)
10. Cahoy, D.O., Polito, F., Phoha, V.: Transient behavior of fractional queues and related processes. Methodol. Comput. Appl. Probab. **17**(3), 739–759 (2015)
11. Cinlar, E.: Markov additive processes and semi-regeneration. vol. 118, Northwestern University, Center for Mathematical Studies in Economics and Management Science (1974)
12. Giorno, V., Nobile, A.G., Pirozzi, E.: A state-dependent queueing system with asymptotic logarithmic distribution. J. Math. Anal. Appl. **458**(2), 949–966 (2018)
13. Gradshteyn, I.S., Ryzhik, I.M.: Table of Integrals, Series, and Products. Academic press (2014)
14. Halmos, P.R., Sunder, V.S.: Bounded Integral Operators on L^2 Spaces. Springer Science & Business Media, (2012)
15. Haubold, H.J., Mathai, A.M., Saxena, R.K.: Mittag-Leffler Functions and Their Applications. J. Appl. Math. **2011**, (2011)
16. Kerss, A., Leonenko, N.N., Sikorskii, A.: Fractional Skellam processes with applications to finance. Fract. Calc. Appl. Anal. **17**(2), 532–551 (2014)
17. Kleinrock, L.: Queueing Systems. Vol. 1, Theory. Wiley-Interscience, New York (1975)
18. Kuznetsov, A.: Solvable Markov processes. University of Toronto (2004)
19. Li, C., Qian, D., Chen, Y.: On Riemann-Liouville and Caputo derivatives. Discrete Dyn. Nat. Soc. (2011)
20. Li, K., Jigen, P.: Laplace transform and fractional differential equations. Appl. Math. Lett. **24**(12), 2019–2023 (2011)
21. Li, K., Jigen, P.: A note on property of the Mittag-Leffler function. J. Math. Anal. Appl. **370**(2), 635–638 (2010)
22. Mainardi, F., Gorenflo, R., Scalas, E.: A fractional generalization of the Poisson processes. Vietnam J. Math. **32**, 53–64 (2007)
23. Meerschaert, M.M., Nane, E., Vellaisamy, P.: The fractional Poisson process and the inverse stable subordinator. Electron. J. Prob. **16**, 1600–1620 (2011)
24. Meerschaert, M.M., Straka, P.: Inverse stable subordinators. Math. Model. Nat. Pheno. **8**(2), 1–16 (2013)
25. Meerschaert, M.M., Sikorskii, A.: Stochastic Models for Fractional Calculus. Walter de Gruyter (2011)
26. Meoli, A., Beerenwinkel, N., Lebid, M.: The fractional birth process with power-law immigration. J. Stat. Phys. 1–25 (2019)
27. Orsingher, E., Polito, F.: Fractional pure birth processes. Bernoulli **16**(3), 858–881 (2010)
28. Podlubny, I.: Fractional Differential Equations: An Introduction to Fractional Derivatives, Fractional Differential Equations, to Methods of Their Solution and Some of Their Applications. Elsevier (1998)
29. Sharma, O.P.: Markovian queues. Ellis Horwood (1990)
30. Shortle, J.F., Thompson, J.M., Gross, D., Harris, C.M.: Fundamentals of Queueing Theory. John Wiley & Sons (2018)

Sinc Methods for Lévy–Schrödinger Equations

Gerd Baumann

Abstract We shall examine the fractional generalization of the eigenvalue problem of Schrödinger's equation for one dimensional problems in connection with Lévy stable probability distributions. The corresponding Sturm–Liouville (SL) problem for the fractional Schrödinger equation is formulated and solved on $\mathbb{R}$ satisfying natural Dirichlet boundary conditions. The eigenvalues and eigenfunctions are computed in a numerical Sinc approximation applied to the Riesz–Feller representation of Schrödinger's generalized equation. We demonstrate that the eigenvalues for a fractional operator approach deliver the well known eigenvalues of the integer order Schrödinger equation and are consistent with analytic WKB estimations. We can also confirm the conjecture that only for skewness parameters $\theta = 0$ the eigenvalues are real quantities and thus relevant in quantum mechanics. However, for skewness parameters $\theta \neq 0$, the Sinc approach yields complex eigenvalues with related complex eigenfunctions, and a fortiori, real probability densities.

Keywords Lévy–Schrödinger equation · Sturm–Liouville problem · Riesz–Feller derivative · Fractional operator · Sinc approximation · Fractional Schrödinger equation · Sinc collocation · Sinc convolution · Harmonic oscillator · Quarkonium model · Finite quantum well

1 Introduction

Schrödinger's equation is one of the central equations of quantum mechanics using a probability approach for its interpretation [1]. Based on probability, Feynman and Hibbs reformulated Schrödinger's equation using the celebrated path integral approach based on the Gaussian probability distribution. Kac in his 1951 lecture pointed out that a Lévy path integral generates the functional measure in the space of left (or right) continued functions having only discontinuities of the first kind, and

G. Baumann (✉)
Mathematics Department, German University in Cairo, New Cairo City, Egypt

University of Ulm, 89069 Ulm, Germany
e-mail: Gerd.Baumann@uni-ulm.de

L. Beghin et al. (eds.), *Nonlocal and Fractional Operators*, SEMA SIMAI Springer Series 26, https://doi.org/10.1007/978-3-030-69236-0_2

thus may lead to a generalization of Feynman's path integrals to Lévy path integrals [2]. These ideas were also examined by Montroll [3] at that time using only basic concepts of quantum mechanics in order to generalize the Gaussian picture to the exotic nature of the statistical processes of Paul Lévy and the incredibly complex physical phenomena that these statistics promised to explain. A summary of the ideas was given recently by Bruce West [4] leading to a differential free formulation of a generalized Schrödinger equation based on Lévy processes in short Lévy–Schrödinger equation (LS) in the following. The assumption of scaling for the propagator directly results in the Riesz representation of Schrödinger's equation based on Lévy stable processes [4].

Laskin took up these ideas, extended Feynman's path integral to Lévy path integrals, and developed a space-fractional Schrödinger equation (SFSE) containing the Riesz–Feller fractional derivative [5, 6], as already conjectured by Kac and Montroll [2, 3]. A practical application of the fractional Schrödinger equation was proposed recently by Longhi [7]. In the framework of an optical application to the transverse modes and resonance frequencies of a resonator correspond to the eigenfunctions and energies of the stationary fractional Schrödinger equation with Lévy index α in an external potential $V(x)$.

No numerical verification has been given to date of Laskin's eigenvalues and eigenfunctions approach. The results we shall present are new in the sense that we are able to verify numerically the suggested eigenvalue relations and also, to give a general approach of eigenvalue approximations based on the Riesz–Feller operator. We note that for a special Lévy index $\alpha = 1$, Jeng et al. in [8] presented an asymptotic approach for the harmonic oscillator which is in agreement with our findings. However, we shall show numerically that the constraints introduced by Laskin in [6] for the potential $V(x) \sim |x|^{\beta}$ with $1 \leq \beta \leq 2$ are not real constraints. It turned out that for $\beta > 0$, as Laskin also mentioned in [9], we are able to determine the eigenvalues and eigenfunctions accurately and use the suggested formula given in [6] for eigenvalues for the quarkonium potentials. This allows us to compute eigenvalues for the quarkonium problem of QCD. Even more the proposed numerical approach is able to deal with a large variety of potential functions $V(x)$ to detect bound states and free quantum states as well. The access to eigenvalues and analytically defined eigenfunctions opens a broad field of applications in quantum mechanics which is no longer restricted to Gaussian processes. Introducing Lévy processes in the interpretation of quantum mechanics yields novel insights as well as novel phenomena that may be accessible for future research, especially for the application to the case of known eigenvalues and eigenfunctions for a given potential $V(x)$; see for example the recent discussion in [10, 11].

Although the $1 + 1$ dimensional formulation has in the past been applied to higher dimensional problems [12], we shall constrain our discussion to the one dimensional case

$$i\,\partial_t u(x,t) = -\frac{1}{2}\partial_{x,x} u(x,t) + V(x)u(x,t) \text{ with } -\infty < x < \infty \text{ and } t \geq 0, \quad (1)$$

where $V(x)$ is the potential of the quantum mechanical problem.

There is an ongoing discussion in the literature regarding the existence of a fractional generalization of (1) to the case of a potential with finite support [6, 8, 13, 14]. This discussion is motivated, in part, due to the lack of known methods for dealing with problems that have a potential with infinite support. Our approach does not suffer from such a restriction, and we shall thus take the classical route in this paper by assuming that the Sturm–Liouville problem satisfies Dirichlet conditions at $x = \pm\infty$. This assumption is due to the classical quantum mechanical properties that a wave function has to satisfy based on a probability interpretation.

In addition let us assume that the solution of (1) is separable as $u(x,t) = v(x)\exp(-i\lambda t)$, which allows to rewrite (1) as

$$-\frac{1}{2}\partial_{x,x}v(x) + V(x)v(x) = \lambda v(x) \text{ with } -\infty < x < \infty, \tag{2}$$

with $\lambda = E/(\hbar\omega)$, the eigenvalues measured in terms of $\hbar\omega$ and the boundary conditions for the eigenfunctions $v(\pm\infty) = 0$. The potential $V(x)$ is assumed to satisfy the minimal requirements for Sturm–Liouville boundary value problems (for details see [15, 16]). Note, we have used scaled units $x = \sqrt{\hbar/(m\omega)}\xi$ in the representation of (1) and (2) and we have adopted the original symbol for the spatial coordinate. Laskin in 2000 introduced the fractional representation of (2) using the Riesz–Feller potential to replace the Laplacian in Schrödinger's equation [5]. The corresponding Sturm–Liouville problem on $\mathbb{R}$ is given as

$$-D_\alpha \, {}_{-\infty}^{\infty}\mathscr{D}_{x;\theta}^{\alpha} v(x) + V(x)v(x) = \lambda v(x) \text{ with } -\infty < x < \infty \text{ and } v(\pm\infty) = 0, \tag{3}$$

where D_α is an appropriate constant and $\mathscr{D}_{x;\theta}^{\alpha}$ represents the Riesz–Feller pseudo-differential operator (see Appendix 5). The notation ${}_{c}^{d}\mathscr{D}_{x;\theta}^{\alpha}$ takes into account the actual interval of integration where (c,d) is either a finite, semi-infinite or infinite interval. The problems discussed in connection with (3) are how are the eigenvalues λ related to the fractional order α and how the eigenvalues are separated in terms of the quantum number n. There are only a few analytic results available, based on WKB approximations for testing these results [6, 8]. The analytic results are mainly related to the classical model of an harmonic oscillator and we extend these numerically to other types of oscillators. Another important question discussed in connection with (3) is the behavior of the eigenvalues and eigenfunctions if the potential $V(x)$ is defined on a finite support of $\mathbb{R}$. This question touches the open problem of how to define the boundary conditions for this infinite integral eigenvalue problem. The core problem is that the Riesz–Feller potential is incorporating all influences on the entire real line and that the introduction of finite boundaries will dismiss a large contribution of these interactions. We shall introduce finite boundaries and at the same time keep the influences of the Riesz–Feller potential for the rest of the space.

The separation of the finite and infinite contributions can be formally achieved by using the integral properties of the Riesz–Feller potential as follows

$$-\ D_\alpha \left({}_{-\infty}^{a}\mathscr{D}_{x;\theta}^{\alpha} v(x) + {}_{a}^{b}\mathscr{D}_{x;\theta}^{\alpha} v(x) + {}_{b}^{\infty}\mathscr{D}_{x;\theta}^{\alpha} v(x) \right) + V(x)v(x) = \lambda v(x), \tag{4}$$

with $-\infty < x < \infty$ and $v(a) = v(b) = v(\pm\infty) = 0$, where a and b are finite real values and the notation ${}_{c}^{d}\mathscr{D}_{x;\theta}^{\alpha}$ takes into account the actual interval of integration. If we rearrange in equation (4) terms as follows we are able to write

$$-\ D_\alpha {}_{a}^{b}\mathscr{D}_{x;\theta}^{\alpha} v(x) + V(x)v(x) - D_\alpha \left({}_{-\infty}^{a}\mathscr{D}_{x;\theta}^{\alpha} v(x) + {}_{b}^{\infty}\mathscr{D}_{x;\theta}^{\alpha} v(x) \right) = \lambda v(x), \tag{5}$$

which can be written as,

$$-\ D_\alpha {}_{a}^{b}\mathscr{D}_{x;\theta}^{\alpha} v(x) + V^{\text{eff}}(x)v(x) = \lambda v(x), \tag{6}$$

with $-\infty < x < \infty$ and $v(a) = v(b) = v(\pm\infty) = 0$. Here $V^{\text{eff}}(x)$ is an effective potential consisting of the "stripped" potential $V(x)$ defined on a finite support and the confining potential $W(x) = -\ D_\alpha \left({}_{-\infty}^{a}\mathscr{D}_{x;\theta}^{\alpha} \cdot + {}_{b}^{\infty}\mathscr{D}_{x;\theta}^{\alpha} \cdot \right)$ taking into account all influences outside the support $[a, b]$. So that the effective potential $V^{\text{eff}}(x) = V(x) + W(x)$ keeping the interactions of the Riesz–Feller potential on $\mathbb{R}$ with the stripped potential $V(x)$. This separation of the potentials allows also the interpretation that the Riesz–Feller derivative of the wave function evaluated at x outside the interval $[a, b]$ is determined by the values of the wave function inside the support where the stripped potential is governing the equation embedded in the confinement potential W. This fact is due to the nonlocal nature of the Riesz–Feller potential which is different from the behavior of a local Laplacian. In other words if we confine the stripped potential into the left and right sided parts of the Riesz–Feller potential, we will not loose any nonlocal information but are able to deal with the problem on a finite support. In addition such kind of division of the integral domain allows us to introduce local properties for the function which also divides the solution structure inside and outside the finite support. However, for practical applications we are only considering the finite part of the solution.

The paper is organized as follows: in Sect. 2 we present the approximation method shortly. Section 3 discusses numerical examples and in Sect. 4 we give some concluding remarks.

2 Approximation Method

The current section introduces and summarizes ideas for fractional operator approximations already available in literature [17–20]. We use the properties of Sinc functions allowing a stable and accurate approximation based on Sinc points [21]. The following subsections introduce the basic ideas and concepts for a detailed representation we refer to [22, 23].

2.1 Sinc Methods

This section introduces the basic ideas of Sinc methods [24]. We will discuss only the main ideas as a collection of recipes to set up a Sinc approximation. We omit most of the proofs of the different important theorems because these proofs are available in literature [22, 23, 25, 26]. The following subsections collect information on the basic mathematical functions used in Sinc approximation. We introduce Sinc methods to represent indefinite integrations and convolution integrals. These types of integrals are essential for representing the fractional operators of differentiation and integration [23].

To start with we first introduce some definitions and theorems allowing us to specify the space of functions, domains, and arcs for a Sinc approximation.

Definition 1 (*Domain and Conditions.*) Let $\mathscr{D}$ be a simply connected domain in the complex plane and $z \in \mathbb{C}$ having a boundary $\partial\mathscr{D}$. Let a and b denote two distinct points of $\partial\mathscr{D}$ and ϕ denote a conformal map of $\mathscr{D}$ onto $\mathscr{D}_d$, where $\mathscr{D}_d = \{z \in \mathbb{C} : |\mathscr{I}(z)| < d\}$, such that $\phi(a) = -\infty$ and $\phi(b) = \infty$. Let $\psi = \phi^{-1}$ denote the inverse conformal map, and let Γ be an arc defined by $\Gamma = \{z \in \mathbb{C} : z = \psi(x), x \in \mathbb{R}\}$. Given ϕ, ψ, and a positive number h, let us set $z_k = \psi(kh)$, $k \in \mathbb{Z}$ to be the Sinc points, let us also define $\rho(z) = e^{\phi(z)}$.

Note the Sinc points are an optimal choice of approximation points in the sense of Lebesgue measures for Sinc approximations [21].

Definition 2 (*Function Space.*) Let $d \in (0, \pi)$, and let the domains $\mathscr{D}$ and $\mathscr{D}_d$ be given as in Definition 1. If d' is a number such that $d' > d$, and if the function ϕ provides a conformal map of $\mathscr{D}'$ onto $\mathscr{D}_{d'}$, then $\mathscr{D} \subset \mathscr{D}'$. Let μ and γ denote positive numbers, and let $\boldsymbol{L}_{\mu,\gamma}(\mathscr{D})$ denote the family of analytic functions $u \in \mathbf{Hol}\,(\mathscr{D})$, for which there exists a positive constant c_1, such that, for all $z \in \mathscr{D}$

$$|u(z)| \leq c_1 \frac{|\rho(z)|^{\mu}}{(1 + |\rho(z)|)^{\mu+\gamma}}. \tag{7}$$

Now let the positive numbers μ and γ belong to $(0, 1]$, and let $\boldsymbol{M}_{\mu,\gamma}(\mathscr{D})$ denote the family of all functions $g \in \mathbf{Hol}\,(\mathscr{D})$, such that $g(a)$ and $g(b)$ are finite num-

bers, where $g(a) = \lim_{z\to a} g(z)$ and $g(b) = \lim_{z\to b} g(z)$, and such that $u \in \boldsymbol{L}_{\mu,\gamma}(\mathscr{D})$ where

$$u(z) = g(z) - \frac{g(a) + \rho(z)g(b)}{1 + \rho(z)}. \tag{8}$$

The two definitions allow us to formulate the following algorithmic steps for a Sinc approximation.

The basis of a Sinc approximation is defined as:

$$\text{Sinc}\,(z) = \frac{\sin(\pi z)}{\pi z}. \tag{9}$$

The shifted Sinc is derived from relation (9) by translating the argument by integer steps of length h and applying the conformal map to the independent variable.

$$S(j,h) \circ \phi(z) = \text{Sinc}\,([\phi(z) - jh]/h),\ \ j = -M, \ldots, N. \tag{10}$$

The discrete shifting allows us to cover the approximation interval (a, b) in a dense way while the conformal map is used to map the interval of approximation from an infinite range of values to a finite one. Using the Sinc basis we are able to represent the basis functions as a piecewise defined function $w_j(z)$ by

$$w_j = \begin{cases} \frac{1}{1+\rho(z)} - \sum_{k=-M+1}^{N} \frac{1}{1+e^{kh}} S(k,h) \circ \phi(z) & j = -M \\ S(j,h) \circ \phi(z) & j = -M+1, \ldots, N-1 \\ \frac{\rho(z)}{1+\rho(z)} - \sum_{k=-M}^{N-1} \frac{e^{kh}}{1+e^{kh}} S(k,h) \circ \phi(z) & j = N \end{cases}. \tag{11}$$

This form of the Sinc basis is chosen as to satisfy the interpolation at the boundaries. The basis functions defined in (11) suffice for purposes of uniform−norm approximation over (a, b). The error of this approximation follows from the theorem:

Theorem 1 (Sinc Approximation [25].) *Let $u \in \boldsymbol{L}_{\mu,\gamma}(\mathscr{D})$ for $\mu > 0$ and $\gamma > 0$, take $M = [\gamma\ N/\mu]$, where $[x]$ denotes the greatest integer in x, and then set $m = M + N + 1$. If $u \in \boldsymbol{M}_{\mu,\gamma}(\mathscr{D})$, and if $h = (\pi d/(\gamma N))^{1/2}$ then there exists a positive constant c_2 independent of N,such that*

$$\left\| u(z) - \sum_{k=-M}^{N} u\,(z_k)\, w_k \right\| \leq c_2 N^{1/2} e^{-(\pi d \gamma N)^{1/2}}. \tag{12}$$

with w_k the base function (see Eq. (11)).

The proof of this theorem is given in [25]. Note the choice $h = (\pi d/(\gamma N))^{1/2}$ is close to optimal for an approximation in the space $\boldsymbol{M}_{\mu,\gamma}(\mathscr{D})$ in the sense that the error bound in Theorem 1 cannot be appreciably improved regardless of the basis

[25]. It is also optimal in the sense of the Lebesgue measure achieving an optimal value less than Chebyshev approximations [21].

The above notation allows us to define a row vector $\boldsymbol{V}_m(S)$ of basis functions

$$\boldsymbol{V}_m(S) = (w_{-M}, \ldots, w_N) \ , \tag{13}$$

with w_j defined as in (11). For a given vector $\boldsymbol{V}_m(u) = (u_{-M}, \ldots, u_N)^T$ we now introduce the dot product as an approximation of the function $u(z)$ by

$$u(z) \approx \boldsymbol{V}_m(S).\boldsymbol{V}_m(u) = \sum_{k=-M}^{N} u_k w_k. \tag{14}$$

Based on this notation, we will introduce in the next few subsections the different integrals we need [23].

2.2 Discretization Formula

The errors of approximating the eigenvalues of the SL problem were introduced in [27, 28] based on conformal mappings which are also used to symmetrize the SL problem. The authors in [27, 28] derive an error estimation resulting from a Sinc collocation method delivering a dependency of order $\mathcal{O}\left(N^{3/2}\exp\left(-cN^{1/2}\right)\right)$ for some c and $N \to \infty$ where $m = 2N + 1$ is the dimension of the resulting discrete eigenvalue system. The basis of this relation is the corresponding Sturm–Liouville problem given by

$$\mathscr{L}u(x) = -v''(x) + q(x)v(x) = \lambda p(x)v(x)\,, \tag{15}$$

with $a < x < b$ and $v(a) = v(b) = 0$. Here, $q(x)$ and $p(x)$ are known functions and λ is representing the eigenvalues of the problem. The bounds (a, b) define either a finite, semi-infinite or infinite interval. Thus our aim is not only related to regular SL problems but also includes singular one, where one of the boundaries is infinity or both [29].

The SL equation can be transformed to an equivalent Schrödinger equation (SE) with a potential function defined with the functions $q(x)$, and $p(x)$ of Eq. (15). Thus a very special − but anyhow very important practical − case is $q(x) = V(x)$ and $p(x) = 1$, here (15) reduces to the Schrödinger equation (1)

$$-\frac{d^2v(x)}{dx^2} + V(x)v(x) = \lambda v(x), \tag{16}$$

with vanishing boundary conditions at $x = a$ and $x = b$. If a and/or b are infinite we call the SL problem singular. An eigenvalue of the problem is a value λ_n for

which a nontrivial solution v_n, the eigenfunction, exists which satisfies the boundary conditions. For a SE problem it is easy to show that the operator on the left-hand side of Eq. (16) is self-adjoint and hence the eigenvalues are real.

The generalization of Eq. (16) to its fractional form is discussed in literature [6, 14, 30] and stated as

$$-D_\alpha \, {}_{-\infty}\mathscr{D}^{\infty\ \alpha}_{x;\theta} v(x) + V(x)v(x) = \lambda v(x), \tag{17}$$

with ${}_{-\infty}\mathscr{D}^{\infty\ \alpha}_{x;\theta} = \mathscr{D}^{\alpha}_{x;\theta}$ the Riesz–Feller operator and $V(x)$ a potential function. For the potentials of the form $V(x) \sim |x|^\beta$ and $1 < \beta < 2$, Laskin [6] derived the eigenvalues in the representation

$$\lambda_n = \left(\frac{2\pi\hbar\, D_\alpha^{1/\alpha}}{4B(1/\beta, 1/\alpha + 1)}\right)^{\beta\alpha/(\alpha+\beta)} \left(n + \frac{1}{2}\right)^{\beta\alpha/(\alpha+\beta)} = \mathscr{A}(\beta, \alpha)\left(n + \frac{1}{2}\right)^{\beta\alpha/(\alpha+\beta)}, \tag{18}$$

where n denotes the eigenvalue order. Since (17) includes a non-local operator in the form of a convolution integral, we first have to discuss how such integrals can be represented in terms of Sinc approximations. There is a special approach to evaluate the convolution integrals by using a Laplace transform introduced by Lubich [31, 32].

For collocating an indefinite integral which is the basis to represent convolution integrals let us define the explicit approximations of the functions $(\mathscr{J}u)(x)$ defined by

$$(\mathscr{J}u)(x) = \int_a^x u(t)dt \text{ with } x \in (a, b)\,, \tag{19}$$

we use the following basic relations [25]. Let Sinc (x) be given by (9) and let e_k be defined next using the integral σ_k :

$$\sigma_k = \int_0^k \text{Sinc}\,(x)\,dx = \frac{1}{\pi}\text{Si}\,(\pi k)\,, \tag{20}$$

with Si (x) the sine integral. This sets us into position to write e_k as

$$e_k = \frac{1}{2} + \sigma_k,\ k \in \mathbb{Z}. \tag{21}$$

Let M and N be positive integers, set $m = M + N + 1$, and for a given function u defined on (a, b), define a diagonal matrix $D(u)$ by $D(u) = \text{diag}\,\left[u\,(z_{-M})\,, \ldots,\right.$ $\left. u\,(z_N)\right]$. Let $I^{(-1)}$ be a square Töplitz matrix of order m having e_{i-j}, as its $(i, j)^{\text{th}}$ entry, $i, j = -M, \ldots, N$.

$$\left(I^{(-1)}\right)_{i,j} = e_{i-j} \text{ with } i, j = -M, \ldots, N. \tag{22}$$

Define square matrices A_m and B_m by

$$\begin{aligned} A_m &= hI^{(-1)}D(1/\phi') \\ B_m &= h\left\{I^{(-1)}\right\}^T D(1/\phi'), \end{aligned} \tag{23}$$

where the superscript "T" denotes the transpose. The collocated representation of the indefinite integrals are thus given by

$$\mathscr{J}_m u = \boldsymbol{V}_m(S).A_m.\boldsymbol{V}_m(u) = h\boldsymbol{V}_m(S).I^{(-1)}.D(1/\phi').\boldsymbol{V}_m(u)\,. \tag{24}$$

These are collocated representations of the indefinite integrals defined in (19) (see details in [22]). The eigenvalues of A_m and B_m are all positive which was a 20 year old conjecture by Stenger. This conjecture was recently proved by Han and Xu [33].

In the notation introduced above we get for p

$$p = \int_a^x f(x-t)g(t)dt = F_+(\mathscr{J})g \approx F_+\left(\mathscr{J}_m\right)g\,, \tag{25}$$

and

$$q = \int_x^b f(x-t)g(t)dt = F_+(\mathscr{J}')g \approx F_+\left(\mathscr{J}'_m\right)g\,, \tag{26}$$

are accurate approximations, at least for g in a certain space [22]. Note $p+q$ is an accurate representation of a convolution integral and F_+ is the Laplace transform of $\mathscr{J}$ and $\mathscr{J}'$. The procedure to calculate the convolution integrals is now as follows. The collocated integral $\mathscr{J}_m = \boldsymbol{V}_m(S).A_m\boldsymbol{V}_m$ and $\mathscr{J}'_m = \boldsymbol{V}_m(S).B_m\boldsymbol{V}_m$, upon diagonalization of A_m and B_m in the form

$$A_m = X_m.\text{diag}\left[s_{m,-M}, \ldots, s_{m,N}\right].X_m^{-1}\,, \tag{27}$$

$$B_m = Y_m.\text{diag}\left[s_{m,-M}, \ldots, s_{m,N}\right].Y_m^{-1}\,, \tag{28}$$

with $\Sigma = \text{diag}\left[s_{-M}, \ldots, s_N\right]$ as the eigenvalues arranged in a diagonal matrix for each of the matrices A_m and B_m. Then the Laplace transform delivers the square matrices $F_+(A_m)$ and $F_+(B_m)$ defined via the equations

$$F_+(A_m) = X_m.\text{diag}\left[F_+\left(s_{m,-M}\right), \ldots, F_+\left(s_{m,N}\right)\right].X_m^{-1} = X_m F_+(\Sigma).X_m^{-1}\,, \tag{29}$$

$$F_+(B_m) = Y_m.\text{diag}\left[F_+\left(s_{m,-M}\right), \ldots, F_+\left(s_{m,N}\right)\right].Y_m^{-1} = Y_m F_+(\Sigma).Y_m^{-1}. \tag{30}$$

We can get the approximation of (25) and (26) by

$$F_+(\mathscr{J})g \approx F_+\left(\mathscr{J}_m\right) g = \boldsymbol{V}_m(S).F_+\left(A_m\right)\boldsymbol{V}_m(g) = \boldsymbol{V}_m(S).X_m F_+(\Sigma).X_m^{-1}.\boldsymbol{V}_m(g). \quad (31)$$

$$F_+(\mathscr{J}')g \approx F_+\left(\mathscr{J}'_m\right) g = \boldsymbol{V}_m(S).F_+\left(B_m\right)\boldsymbol{V}_m(g) = \boldsymbol{V}_m(S).Y_m F_+(\Sigma).Y_m^{-1}.\boldsymbol{V}_m(g). \quad (32)$$

These two formulas deliver a finite approximation of the convolution integrals p and q. The convergence of the method is exponential as was proved in [25].

2.3 Sinc Collocation of Fractional Sturm–Liouville Problems

Using the notation and expressions introduced in the previous section we are now in position to discretize equation (17). Setting the prefactor $D_\alpha = 1$, we get

$$\begin{aligned} -\left(F_+(\mathscr{J}) + F_+(\mathscr{J}')\right) v + V(x)v = \lambda v \approx \\ -c_+ F_+\left(A_m\right)\boldsymbol{V}_m(v) - c_- F_+\left(B_m\right)\boldsymbol{V}_m(v) + D\left(\boldsymbol{V}_m(V)\right)\boldsymbol{V}_m(v) = \lambda\, I\, \boldsymbol{V}_m(v). \end{aligned} \quad (33)$$

Thus the discrete version of (17) becomes

$$-c_+ F_+\left(A_m\right)\boldsymbol{V}_m(v) - c_- F_+\left(B_m\right)\boldsymbol{V}_m(v) + D\left(\boldsymbol{V}_m(V)\right)\boldsymbol{V}_m(v) = \lambda\, I\, \boldsymbol{V}_m(v)\,, \quad (34)$$

with $\mathscr{F}_+\left(A_m, B_m\right) = c_+ F_+\left(A_m\right) - c_- F_+\left(B_m\right) = \mathscr{F}_+\left(A_m, B_m\right)_{-\infty}^{\infty}$ we write the discrete eigenvalue problem as

$$-\mathscr{F}_+\left(A_m, B_m\right)_{-\infty}^{\infty} + D\left(\boldsymbol{V}_m(V)\right) = \lambda\, I. \quad (35)$$

Note, $(.,.)_a^b$ denotes the interval of the fractional operator, $D\left(\boldsymbol{V}_m(V)\right)$ represents a diagonal matrix and I a unit matrix of dimension $m \times m$.

For the finite support problems we apply the same collocation procedure by separating the different parts of the convolution integral. This results to the following representation

$$\begin{aligned} &-c_+ F_+\left(A_m\right)_a^b \boldsymbol{V}_m(v) - c_- F_+\left(B_m\right)_a^b \boldsymbol{V}_m(v) + D(V(x))\boldsymbol{V}_m(v) \\ &-c_+ F_+\left(A_m\right)_{-\infty}^a \boldsymbol{V}_m(v) - c_- F_+\left(B_m\right)_{-\infty}^a \boldsymbol{V}_m(v) \\ &-c_+ F_+\left(A_m\right)_b^\infty \boldsymbol{V}_m(v) - c_- F_+\left(B_m\right)_b^\infty \boldsymbol{V}_m(v) = \lambda\, \boldsymbol{V}_m(v). \end{aligned} \quad (36)$$

Separation of the confining part from the stripped part we get

$$
\begin{aligned}
&-c_+ F_+ \left(A_m\right)_a^b - c_- F_+ \left(B_m\right)_a^b + D(V(x)) \\
&-c_+ F_+ \left(A_m\right)_{-\infty}^a - c_- F_+ \left(B_m\right)_{-\infty}^a \\
&-c_+ F_+ \left(A_m\right)_b^\infty - c_- F_+ \left(B_m\right)_b^\infty = \lambda\, I\,,
\end{aligned} \tag{37}
$$

which finally can be written as

$$
-\mathscr{F}_+ \left(A_m, B_m\right)_a^b + D(V(x)) - \mathscr{F}_+ \left(A_m, B_m\right)_{-\infty}^a - \mathscr{F}_+ \left(A_m, B_m\right)_b^\infty = \lambda\, I\,, \tag{38}
$$

$$
-\mathscr{F}_+ \left(A_m, B_m\right)_a^b + \mathscr{D}\left(V^{\text{eff}}(x)\right) = \lambda\, I\,, \tag{39}
$$

with $\mathscr{D}\left(V^{\text{eff}}(x)\right) = D(V(x)) - \mathscr{F}_+ \left(A_m, B_m\right)_{-\infty}^a - \mathscr{F}_+ \left(A_m, B_m\right)_b^\infty$. The condition

$$
\det\left(-\mathscr{F}_+ \left(A_m, B_m\right)_a^b + \mathscr{D}\left(V^{\text{eff}}(x)\right) - \lambda\, I\right) = 0\,, \tag{40}
$$

will deliver the needed eigenvalues λ_n. To each λ_n there exists an eigenfunction v_n used in the approximations. Here, c_+ and c_- are factors independent of x related to the Riesz–Feller operators (see Appendix 5). Solving for the different eigenvalues λ_n using (40), we will also find the expansion coefficients of the eigenfunctions $\boldsymbol{V}_m^n(v)$ for each eigenvalue n allowing us to approximate the eigenfunction using the Sinc basis $\boldsymbol{V}_m(S)$ by

$$
v_n(x) \approx \boldsymbol{V}_m(S).\boldsymbol{V}_m^n(v). \tag{41}
$$

These basis functions finally can be used to approximate any function $u(x) \in L^2$ as follows

$$
u(x) \approx \sum_{k=0}^{n} a_k v_k(x)\,, \tag{42}
$$

with the expansion coefficients given as

$$
a_k = \int_a^b u(x) v_k(x) dx. \tag{43}
$$

3 Numerical Results

In this section we examine central models in quantum mechanics like the harmonic oscillator, some sort of potentials in relative coordinates useful for quarkonium models in QCD, and quantum mechanical models on a finite support. The collection of models is a selection of standard model systems with a variety of applications in quantum mechanics. We will demonstrate that for these models the eigenvalues and the eigenfunctions are accessible for Lévy governed processes and we guess that much more of the standard models can be solved with our approach of approximation.

Table 1 First four normalized eigenvalues $\lambda_n = (n + 1/2)$ for $\alpha = 1.98$. The number of Sinc points $N = 92$. Numbers are truncated to 7 digits

n	λ_n
0	0.496556
1	1.484733
2	2.467141
3	3.451038

3.1 Harmonic Oscillator

The first experiment we performed is related to the examination of the harmonic oscillator with the standard potential $V(x) = x^2/2$. We chose this classical model due to its importance in the development of quantum mechanics. We will demonstrate that the harmonic oscillator also plays a prominent role in generalized Lévy quantum mechanics. The wave function $v(x)$ is determined on $\mathbb{R}$ satisfying the boundary conditions $v(\pm\infty) = 0$. Note, in our approximation there is no need to approximate $\pm\infty$ by a large numeric value. Thus the computed eigenvalues and eigenfunctions are based on the whole real line $\mathbb{R}$. The computations were carried out for a fixed number of Sinc points $N = 96$ to reach an accurate eigenvalue for $\alpha \to 2$ (see Table 1).

We first checked the convergence of the lower eigenvalues to a stable value and observed that we need at least $N = 60$ Sinc points to get convergence to an asymptotic eigenvalue which is always positive and real if the skewness parameter $\theta = 0$. The results of these computations are collected in Fig. 1. The Figure displays the four lowest eigenvalues of these computations for different fractional orders α (α-value on top of the plots). Our observation for the first six eigenvalues (four of them are shown in the graph) is that they are reproducible and converge to a fixed value if the number of Sinc points is sufficiently large. Even more if we approach with the Lévy index $\alpha \to 2$, we are able to reproduce the classical eigenvalues $\lambda_n = E_n/\hbar\omega = n + 1/2$ for a harmonic oscillator (see Table 1).

Knowing that the eigenvalues converge to a fixed value allowed us to vary the fractional order in the LS problem to get the first six smallest real eigenvalues for the harmonic oscillator. The variation of the six smallest eigenvalues with α are shown in Fig. 3. The dependence of the eigenvalues λ_n follows a relation derived by Laskin in 2002 [6], given by the relation

$$\lambda_n = \left(\frac{2\pi\hbar\, D_\alpha^{1/\alpha}}{4B(1/2, 1/\alpha + 1)}\right)^{2\alpha/(\alpha+2)} \left(n + \frac{1}{2}\right)^{2\alpha/(\alpha+2)} = \mathscr{A}(\alpha)\left(n + \frac{1}{2}\right)^{2\alpha/(\alpha+2)} \tag{44}$$

where $B(a, b) = \int_0^1 x^{a-1}(1 - x)^{b-1}\, dx$ is Euler's Beta integral and $\mathscr{A}(\alpha)$ is the shape function of the eigenvalues depending essentially on the fractional order α. The shape function is also depending parametrically on fundamental quantities like the Bohr radius a_0, the elementary charge e, the atom number Z, and the reduced

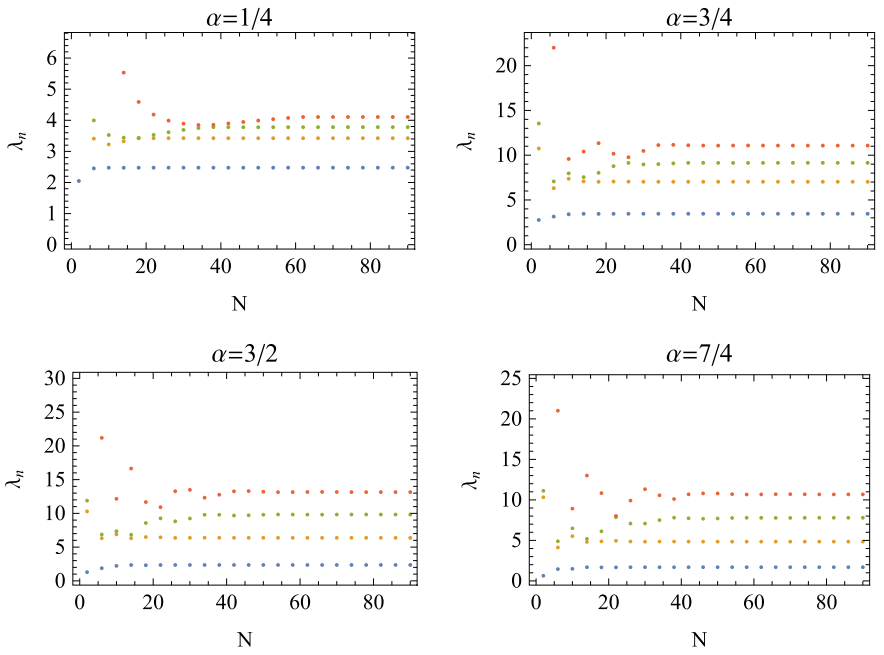

Fig. 1 Convergence to a stable value of the first four eigenvalues λ_n as function of the number of Sinc points N. The fractional orders α are given on top of the graphs. For Sinc points larger than $N = 60$ the eigenvalues are stable

Planck number $\hbar$ in the frame of the used WKB approximation. The functional relation between the fractional order α is represented as a power relation which can be derived from [6] in detail as follows

$$\mathscr{A}(\alpha) = \left(\frac{\left(a_0{}^{-1+\alpha} e^2 Z \hbar^{-\alpha}\right)^{1/\alpha}}{\alpha^{1/\alpha}\ B(1/2, 1/\alpha + 1)} \right)^{\frac{2\alpha}{2+\alpha}} . \tag{45}$$

However, for practical applications we used the distribution of eigenvalues and determined a Hermite interpolation to get the shape structure in a simplified numeric way. This allows us to predict the eigenvalues as a continuous function of α at least for the first six eigenvalues. The shape functions for the different eigenvalue orders is shown in Fig. 2. The function is unique for eigenvalue orders $n \geq 1$ while for $n = 0$ there is a deviation from this universality. This behavior is expected because the eigenvalue function for the ground state is a continuously decaying function in α while for the higher states the function is a continuously increasing function (see Fig. 2). Thus for the ground state we expect a different shape function $\mathscr{A}(\alpha)$ than for higher quantum states (see Fig. 2).

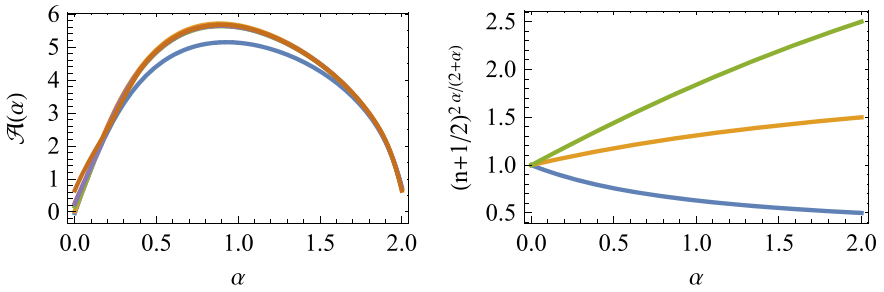

Fig. 2 Universal shape function $\mathscr{A}(\alpha)$ of the eigenvalues extracted from the numerical values of λ_n. For $n \geq 1$ the shape function is unique while for $n = 0$ the shape function is smaller than the function for higher quantum numbers. Right panel: Eigenvalue part $(n + 1/2)^{2\alpha/(2+\alpha)}$ as a function of α. The quantum number $n = 0, 1, 2$ are shown from bottom to top

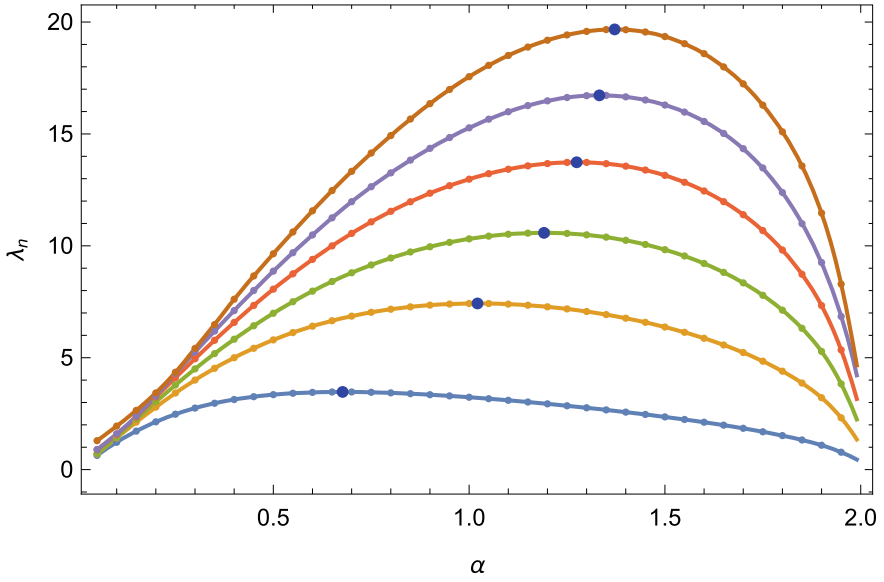

Fig. 3 Variation of eigenvalues λ_n for different fractional orders α for a harmonic oscillator. The quantum number n starts at $n = 0$ and ends at $n = 5$ from bottom to top. The small dots are the computed eigenvalues for a specific fractional order α. The solid lines are Hermite interpolation functions. The larger dots represent the maxima of the eigenvalues (see Table 2 for numeric values)

In Fig. 3 the first six eigenvalues are shown as a function of α. The numerically determined values show a maximum at a certain value of α which is moving from left to right if the eigenvalue order is increased (bottom to top in Fig. 3). For each quantum order n an α exists where the energies (eigenvalues λ_n) become maximal so that a maximal exchange in a quantum transition can be reached. The maxima of the eigenvalues are listed in Table 2 and are depicted in Fig. 3 as large dots.

Table 2 Maxima of eigenvalues. The number of Sinc points $N = 92$. Numbers are truncated to 6 digits

n	α	λ_n
0	0.6769	3.47105
1	1.0213	7.42513
2	1.1912	10.5797
3	1.2746	13.7338
4	1.3325	16.7244
5	1.3716	19.6713

To each eigenvalue $\lambda_{n,\alpha}$ there corresponds a wave function which depends beside on the quantum number also on the fractional order α. Thus the wave function depends on the quantum number n and on the fractional order α and can be written as $v(x) = v_{n,\alpha}(x)$. Samples of eigenfunctions are shown in Fig. 4 for different fractional orders. Note that the amplitude of the probability distribution decreases up to a value $\alpha \approx 1.24$ and then increases again with $\alpha \to 2$. The change of the amplitude for the ground state is shown in Fig. 5. In addition to the amplitude the width or lateral extension of the wave functions are affected by the fractional order (see Figs. 4 and 5). For small values of α the wave functions are centered around the origin with a small lateral extension; i.e. they are localized. The decay of the probability density $|u_n|^2$ is very rapidly for such small α values. If α increases in the direction to $\alpha \approx 3/2$ the extension of the wave function nearly becomes six times larger and shrinks by a factor two if we approach $\alpha \to 2$. This behavior is observed for all eigenfunctions of the harmonic oscillator. We note that the broadening of the wavefunction is also observed for other potentials of the type $V(x) \sim |x|^\beta$.

The variation of the maximal amplitude can be easily examined for the ground state displayed in Fig. 5. The minimum of the maximal amplitude occurs at $\alpha = 1.2449$ for the ground state. This decrease and increase of the amplitude means that the probability density necessarily must broaden because the total amount is a conserved quantity. The spreading and afterwards the re-localization is a characteristic behavior of the density occurring in each state and for different versions of potentials.

In the two papers by Luchko et al. [13, 14] doubts about the validity of the eigenvalue relation by Laskin [6] and Jeng [8] are acknowledged. The following Figs. 6 and 7 collect a comparison of these eigenvalue relations compared with our numerical results. Figure 6 examines the special case with $\alpha = 1$ which was solved by Jeng [8] using a WKB approximation and the asymptotic representation of the Airy function delivering the root distribution as eigenvalues for the harmonic oscillator (dashed line in Fig. 6). The solid line in Fig. 6 was gained as a least square fit to Laskin's formula (18) keeping the amplitude and the exponent factor variable. The least square fit to the eigenvalues using $\lambda_n = a(n + 1/2)^b$ with $a = 5.519$ and $b = 0.6794$ delivers numerical agreement with Jeng's result who estimated the exponent by his asymptotic approach as $b = 2/3$ in agreement with the results derived by

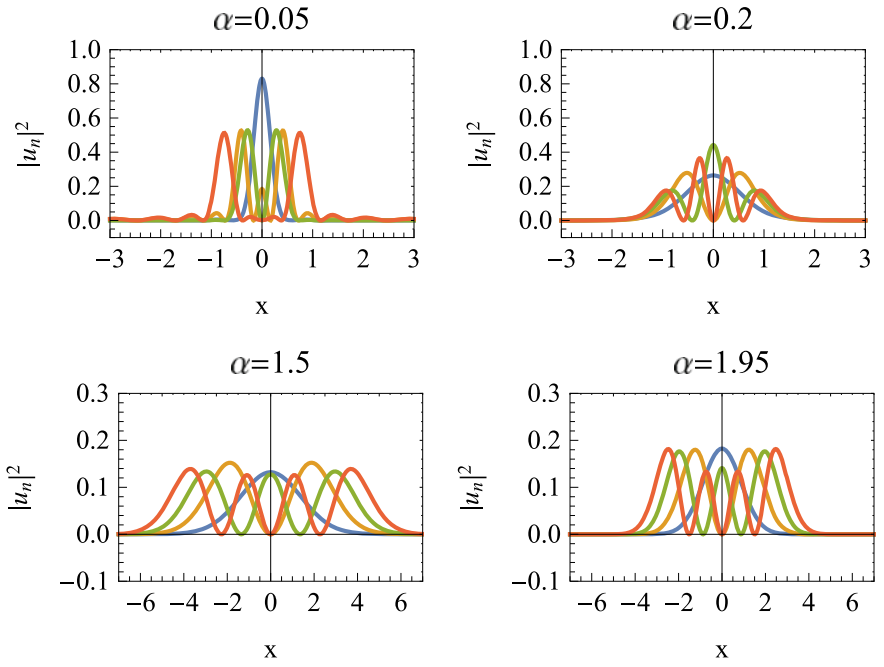

Fig. 4 Samples of probability distributions for the first four eigenvalues at different fractional orders α. The probability distributions are localized and symmetric with respect to the origin. The ground state is a single humped distribution while the higher order states show characteristic variations with minima and maxima. Note the overall amplitude decreases with increasing fractional order α in the interval $0 < \alpha \lesssim 1.24$ and increase again in the interval $1.24 \lesssim \alpha < 2$

Laskin. The absolute error of our estimation is $\epsilon = 0.012733$ corresponding to a 2% relative error which is acceptable. In Fig. 7 we show some results of the same approach for different α-values using the same dependence of the eigenvalues as given by Laskin [6] but now using instead directly $\lambda_n = a(n + 1/2)^{2\alpha/(2+\alpha)}$ which uses only one parameter the shape parameter a for a fitting. It turns out that the least square fits deliver nearly for all α-values excellent fits except for very small values $\alpha < 0.1$. The reason for this is that we did not use a sufficiently large number of Sinc points N to resolve the stable distribution of eigenvalues for this range of α. For α-values less than $1/10$ the eigenvalues of the different quantum numbers are very close to each other and cannot be resolved in a reliable way with the used number of Sinc points. This refinement remains to be resolve in an additional approach using high precession computing with a large number of Sinc points. The conclusion from these numerical examination is that the WKB approximation used by Laskin as well as by Jeng et al. [6, 8] are highly accurate in their description of the eigenvalues and are reproducible by Sinc approximations.

In another computation we examined the structural changes of the density function and the wave functions if the fractional parameter α is varied. The results are shown

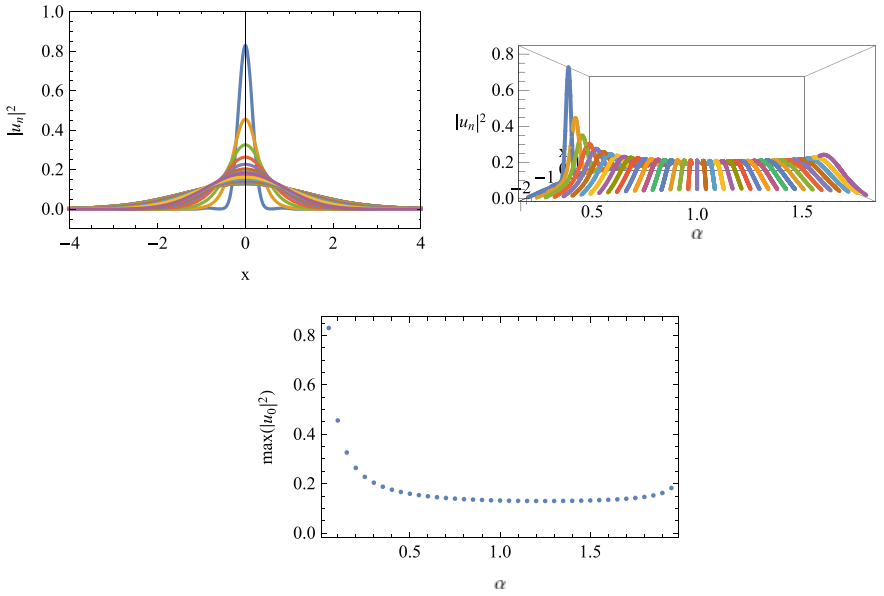

Fig. 5 Ground state of the harmonic oscillator as a function of α (top left panel). The overall amplitude decreases with increasing fractional order in the interval $0 < \alpha \lesssim 1.24$ and increase again for $1.24 \lesssim \alpha \leq 2$. Maximum value of the probability density of the ground state as a function of α (bottom panel). The minimum of the maximum value for the ground state occurs at $\alpha = 1.2449$

in Figs. 8 and 9. Our observation is that the density $|u_n|^2$ is originally localized for $\alpha \approx 0$ changing its width up to a certain value for α and again becomes narrower if α approaches the value $\alpha = 2$. The eigenfunctions on the other side show a pattern like a tiger fur. There exists a non equidistant pattern of positive and negative values occurring in a banded pattern if maxima and minima are plotted as magnitude values in a contour plot. The pattern is shown in Fig. 9 for two resolutions $\Delta\alpha$. For a physical application the sign change of the eigenfunctions does not have any impact because physically important quantities are based on the densities of the eigenfunctions. From a mathematical point of view the pattern is quite interesting due to this tiger strip pattern which shows up in an irregular way. The cumulative counting of positive and negative maxima for $n = 0$ and $n = 1$ are shown in Fig. 10. The structure of the increase of the counts resembles to a devil's staircase.

Concerning the behavior of eigenvalues λ_n with a finite skewness parameter θ, we found numerical evidence that all the eigenvalues become complex for $0 < \alpha < 2$. The real and imaginary parts of the eigenvalues are shown in Fig. 11 where on the top panel the real part and on the bottom panel the imaginary part of λ_n for different values α are shown. Although the imaginary parts are small for the first few quantum numbers this indicates that the eigenvalue problem for $\theta \neq 0$ becomes non-Hermitian and thus not in the framework of standard quantum mechanics. This behavior was con-

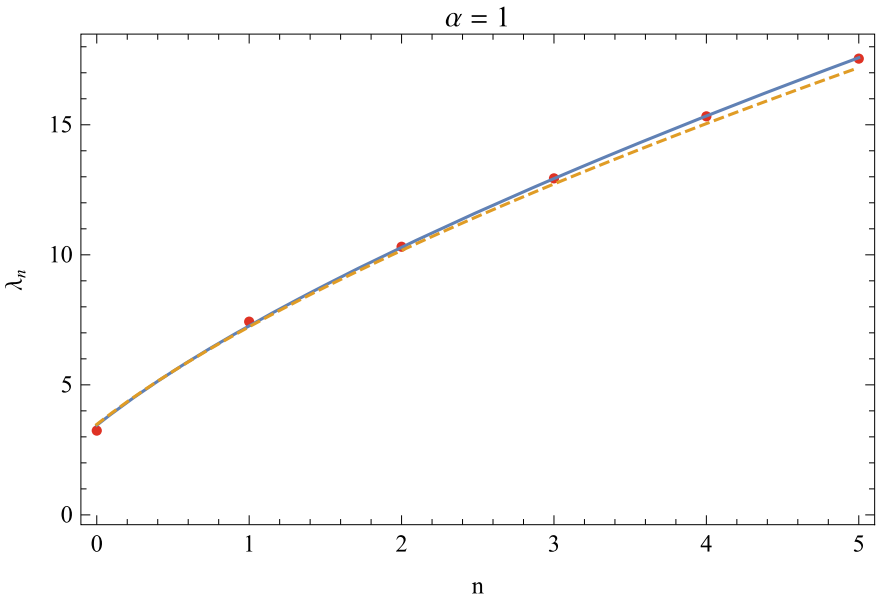

Fig. 6 The dots represent the computed eigenvalues for $\alpha = 1$. The solid line represents the least square fit to the computed eigenvalues with $\lambda_n = a(n + 1/2)^b$ with $a = 5.519$ and $b = 0.6794$. The value for b is close to the predicted WKB value by Laskin [6] and Jeng [8]. The dashed line uses $\lambda_n = a(n + 1/2)^{2/3}$ representing the root distribution of the asymptotic expansion of Airy's function [8]

jectured in [14]. However, if we examine the behavior for $\alpha \to 2$ the imaginary parts of the eigenvalues vanish. Thus it is apparent that the standard quantum mechanics is consistently incorporated in the Lévy based quantum mechanics. The conclusion at this point is that a more detailed examination is needed for nonvanishing skewness parameters to get a physical interpretation of the spectral properties.

3.2 *Quarkonium Models*

Following Laskin in his proposal for a quarkonium model [9], we assume that a quark-antiquark $\boldsymbol{q\bar{q}}$ bound system in a non-relativistic potential can be modeled by a relation of the form

$$V\left(|\boldsymbol{r}_i - \boldsymbol{r}_j|\right) = q_i q_j |\boldsymbol{r}_i - \boldsymbol{r}_j|^\beta, \tag{46}$$

where q_i and q_j are the color charges of i and j quarks respectively and the power $\beta > 0$. Using a single relative coordinate this potential reduces to the simple model $V(x) = q^2|x|^\beta$ where x denotes the distance between two quarks. To keep the system thermodynamically stable the power β should be taken from $0 < \beta < 2$ [9]. How-

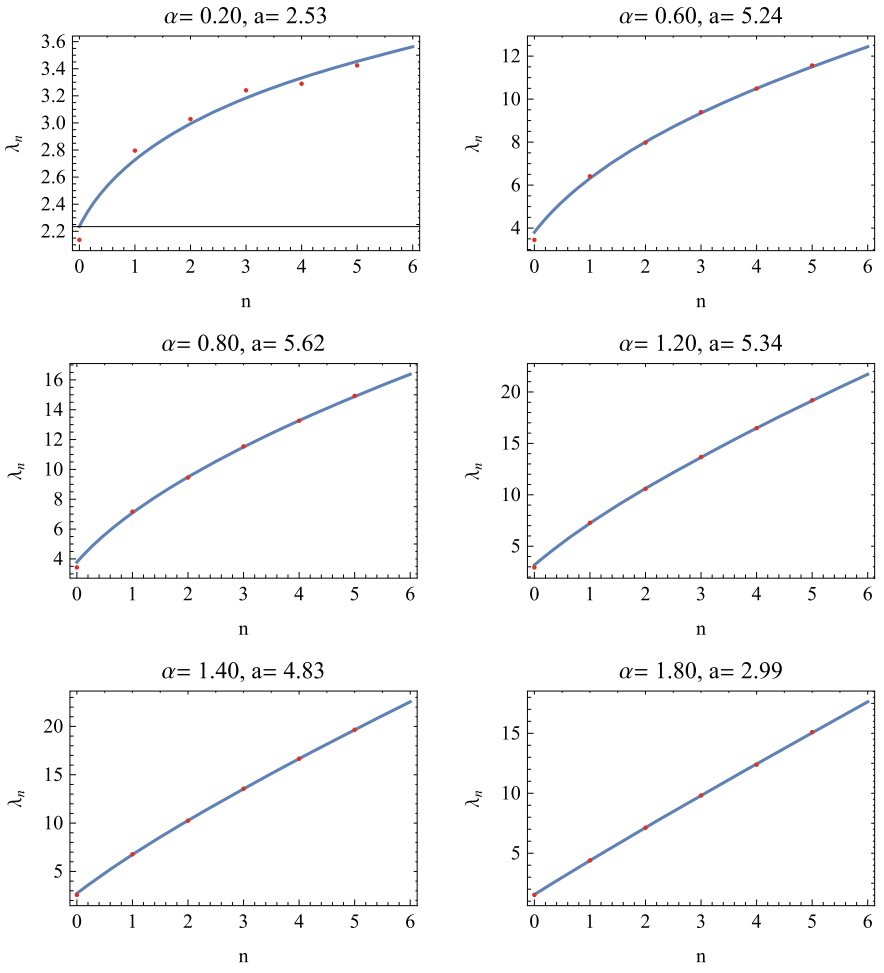

Fig. 7 Increase of the eigenvalues as a function of the quantum number n. The eigenvalues follow a relation $\lambda_n = a(n + 1/2)^{2\alpha/(2+\alpha)}$ shown as dots. The prefactor a depends on α and is shown on top of each graph. The solid line represents a least square fit where only a was estimated. The fractional eigenvalue relation for λ_n follows from a WKB approximation [6, 8]

ever, we will examine also a case where β exceeds this physical reasonable bounds. Examples of different potential versions are shown in Fig. 12, the case of panel (c) is already examine in the previous section. In Fig. 12 the horizontal lines in the graphs represent the first four energy levels (eigenvalues) of the model, respectively. Specifically we examine models with $\beta = \{1/2, 1, 2, 5\}$ denoted in the following by (a), (b), (c), and (d), respectively. The potentials for each case form a cusp, a triangular well, a parabolic one, and a deep well model (see Fig. 12). The type of potential (46) coincides with the QCD requirements: that at short distances the quarks and gluons

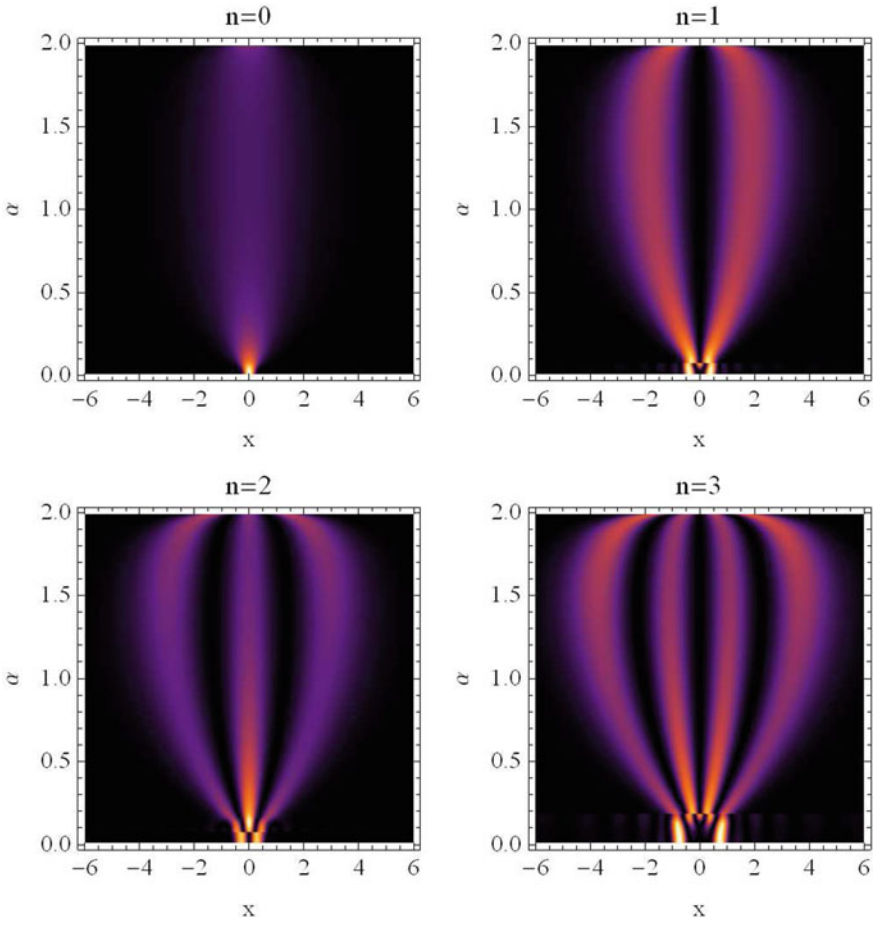

Fig. 8 Structural change of the density functions $|u_n|^2$ of the first four eigenstates varying α

appear to be weakly coupled and at large distances the effective coupling becomes strong, resulting in the phenomena of quark confinement.

The first four eigenfunctions for a specific Lévy index $\alpha = 1.499$ are shown in Fig. 13 for each of the sample models from above. The color used in the graphs for probability densities corresponds to the magnitude of the eigenvalues indicated as eigenvalue levels in Fig. 12 using the same color, respectively. The panels (a), (b), (c), and (d) of Fig. 13 are related to the eigenvalues given in Fig. 12 for each panel, respectively. We observe taking into account the scales on the x-axis that the four ground states are localized in the center of the potential. However, the localization is quite different for the different models. The largest extension is observed in model (a) while the smallest width of the density is observed in model (d). The amplitudes and the structure of the different states are similar to each other with some small

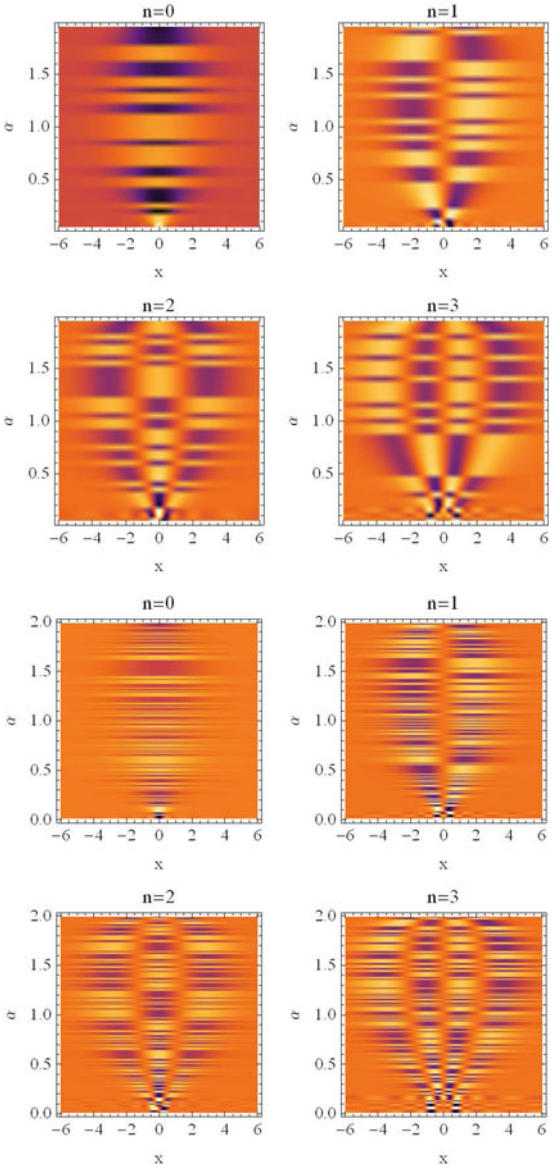

Fig. 9 Structural change of the eigenfunctions u_n of the first four eigenstates varying α. The top four graphs use a resolution $\Delta\alpha = 0.05$ while the bottom four were generated with an α step of length $\Delta\alpha = 0.01$. The increase of the resolution in α uncovers a detailed structure of amplitude switching from positive (bright) to negative (dark) values. The flipping of amplitudes seems to generate a banded self-similar pattern

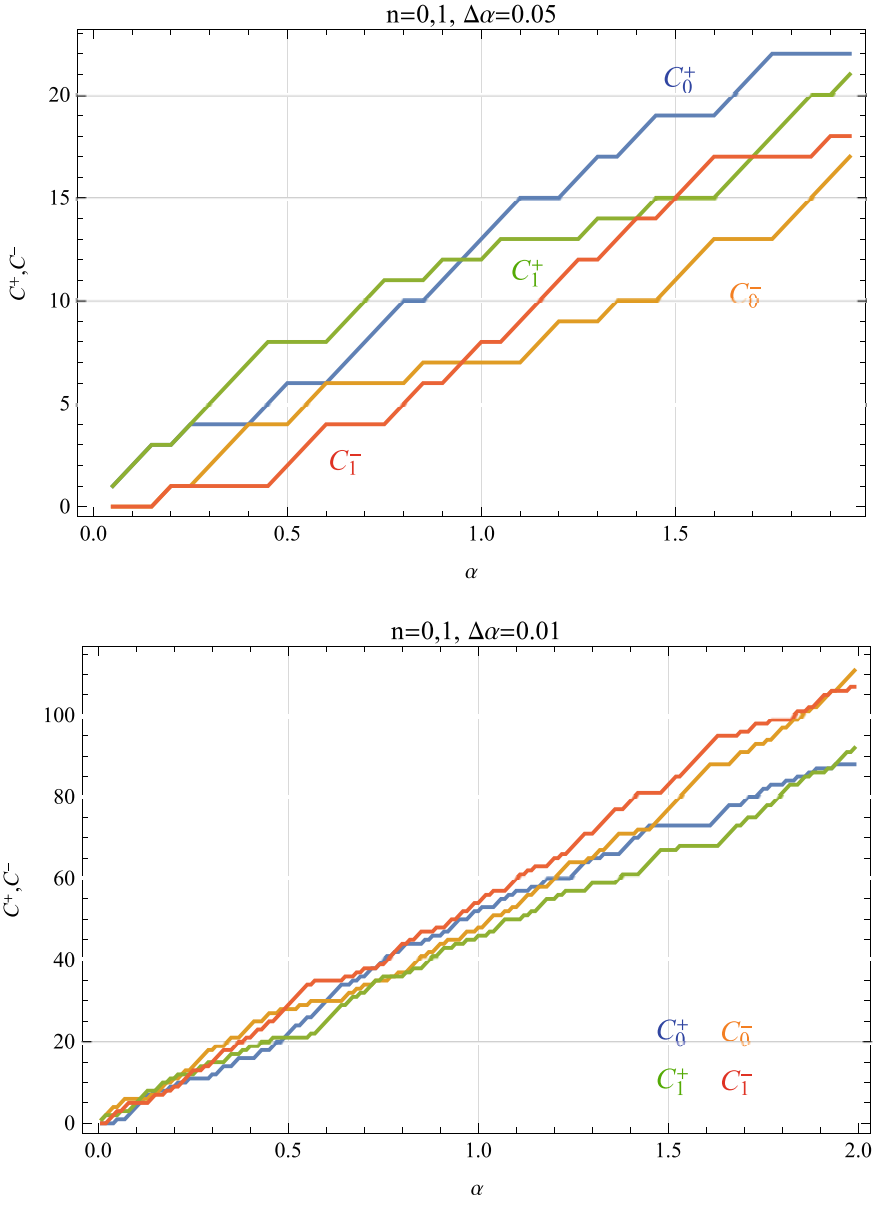

Fig. 10 Cumulative counts of positive C_i^+ and negative C_i^- maxima and minima for the first two eigenfunctions $n = 0, 1$. The steps of increase are irregular and resemble to a devil's staircase

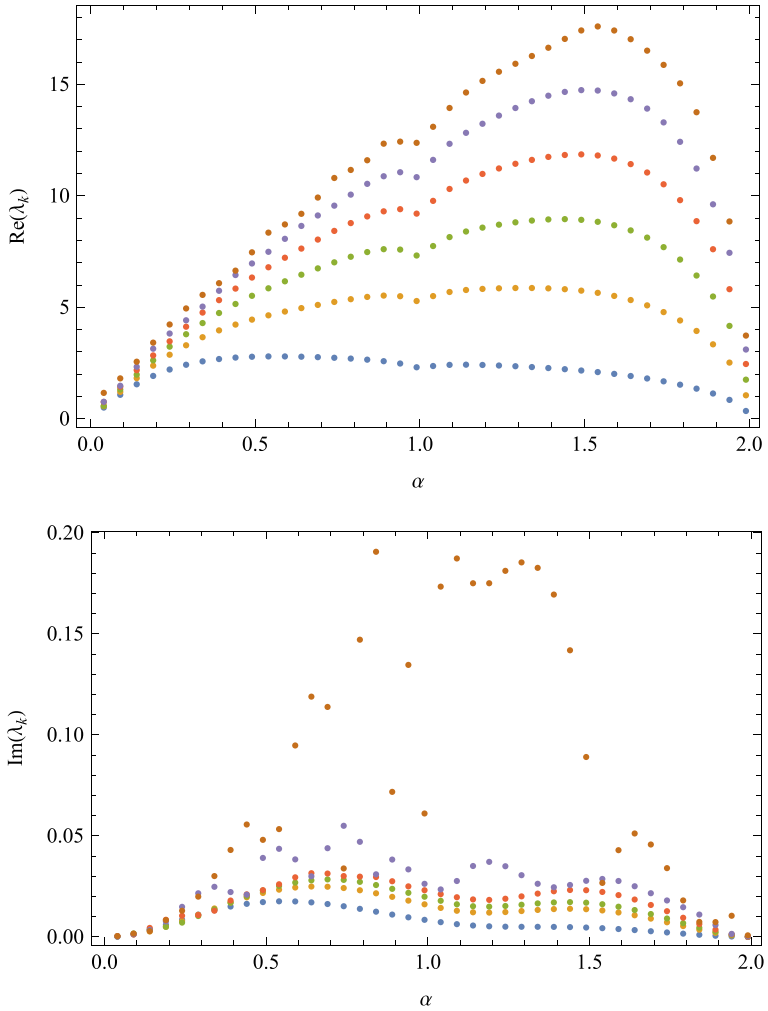

Fig. 11 Real and imaginary parts of the first six eigenvalues for the harmonic oscillator with $\theta = 0.8 \min(\alpha, 2 - \alpha)$ in the Riesz–Feller potential

variations in the amplitude. The width of the localization is the most prominent property to distinguish the models from each other. The models (*b*) and (*c*) show nearly the same width but due to the potential structure triangular (*b*) and parabolic (*c*) the ground state in (*c*) is smaller in width than in (*b*). This behavior is also true for the higher states. This property is shown for a fixed Lévy index α in Fig. 13.

We also examined the variation of the energy (eigenvalues) if the Lévy index is varied. The results are shown for each model in Fig. 14, respectively. The observation is that there exists for each of the six eigenstates a Lévy index α where the energies become maximal (dots in the graph). This is the case for all eigenstates and for all

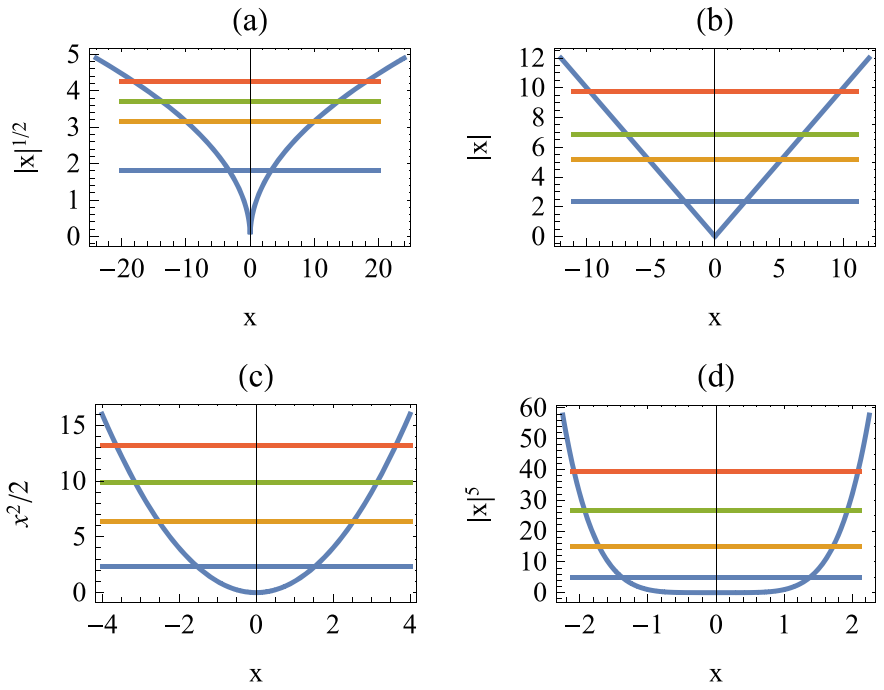

Fig. 12 Different potential versions $V(x) \sim |x|^{\beta}$ for QCD quarkonium models. The horizontal lines represent the energy levels for $\alpha = 1.499$

models. We observe that these maxima are located to the left side of the interval $0 < \alpha < 2$ if $\beta < 1$ and move to the right side if β increases ($\beta > 1$). It is also clear that the magnitude of eigenvalues in general increases if β is increased. Since the eigenvalue of a specific state increases or decreases if α is varied we expect that the width of the corresponding density also varies. Such a variation of the width of the density function is shown in Fig. 15 for model (b) where α is varied. The originally tightly localized density functions ($\alpha \approx 0$) broadens if α is increased up to a critical value for α. If this critical α is exceeded the width of the density functions start to shrink to the final level at $\alpha = 2$. This behavior is shown for model (b) in Fig. 15. However, it is a general observation in all potentials examined that such kind of critical α exists and that a broadening followed by a shrinking when α is varied from a lower to a higher value.

We also examined properties of the eigenvalues for all the models (a)–(d) and found some common behavior. Thus we select only model (b) to discuss these properties in detail. According to formula (18) the eigenvalues should satisfy a certain relation depending on the Lévy index α and the exponent β of the potentials under discussion. We examined the computed eigenvalue by using relation (18) for all models. The outcome of the calculations is that the derived formula is very accurate for all models examined and for nearly all values of α. Deviations exist for small values

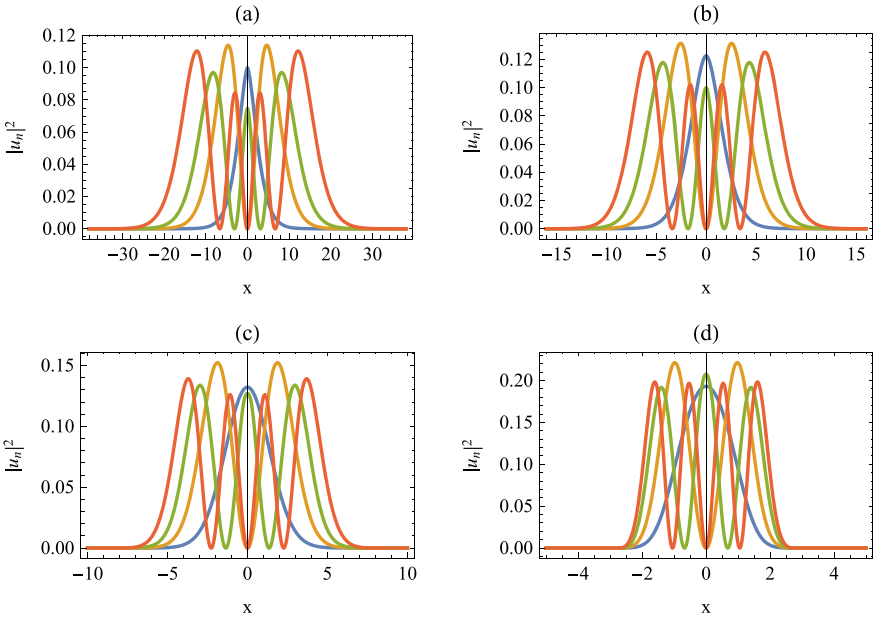

Fig. 13 The four first density functions for: **a** the potential $V(x) = |x|^{1/2}$, **b** the potential $V(x) = |x|$, **c** the potential $V(x) = x^2/2$, and **d** the potential $V(x) = |x|^5$. Th Lévy parameter was $\alpha = 1.499$. Note the x scale are different for each potential model; i.e. the localisation of the density varies from model to model. We observe again a stronger localization of the densities for smaller values of α where for $\alpha \to 2$ an concentration of the densities sets in again. While for α values approaching $\alpha \approx 1.2$ a spreading is observed

of $\alpha < 1/10$ which is a numerical problem already mentioned above. An example of the examination is the one parameter fitting of the computed eigenvalues using (18) in the determination of the screening coefficient a in the eigenvalue relation $\lambda_n = a(n + 1/2)^{\beta\alpha/(\beta+\alpha)}$. Results are shown in Fig. 16 for $\beta = 1$ demonstrating the agreement between the theoretical prediction and the numerical approximation. It is quite interesting that a single parameter least square fit for the screening parameter a delivers an accurate agreement. We note that similar results with the same accuracy were found for the three other models (not shown).

Since the screening parameter a is varying under the change of α we examined the behavior of the shape function $\mathscr{A}(\beta, \alpha)$ in (18) for the different models. The result is that for higher states there exists a unique function $\mathscr{A}(\alpha)$ for each of the models. An example for $\beta = 1$ is shown in Fig. 17 left panel. Since the function $(n + 1/2)^{\beta\alpha/(\beta+\alpha)}$ is an increasing function for $\beta > 1$ and $n \geq 1$ while for $n = 0$ the function is decreasing in α (see Fig. 17 right panel), we will find two different shape functions for the ground state and the higher quantum states, respectively. This structure is also observed in the other models.

Another common property of the models is the reduction of the amplitude of the density function in the ground state and an increase if α is increased further.

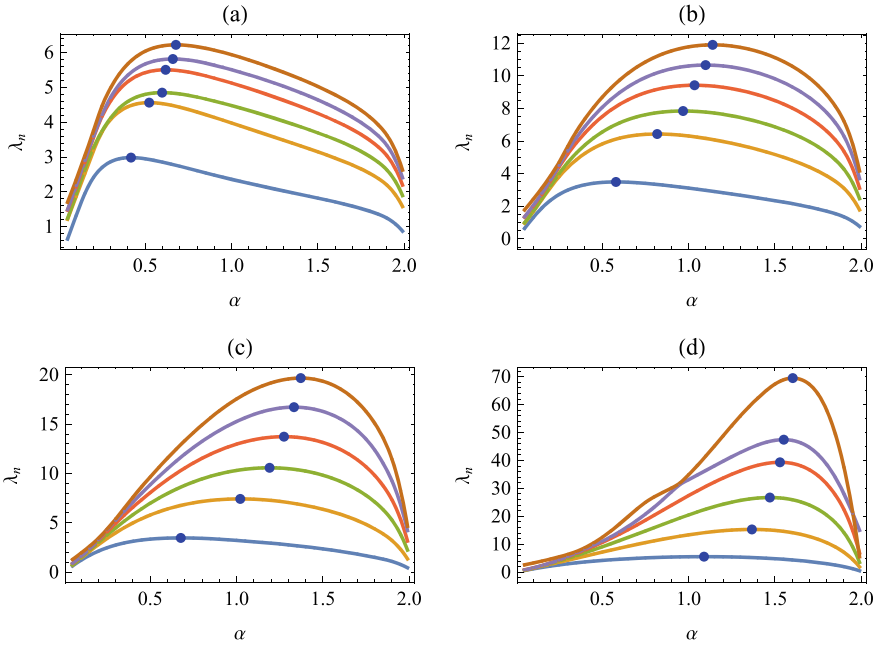

Fig. 14 Distribution of eigenvalues as a function of α for four QCD quarkonium models. **a** $\beta = 1/2$, **b** $\beta = 1$, **c** $\beta = 2$, and **d** $\beta = 5$. Shown are the first six eigenvalues depending on α

The behavior is shown for $\beta = 1$ in Fig. 18 as an example. The location where the minimum value is reached varies from model to model and is located in the interval $1 < \alpha < 3/2$. This range is a rough estimation over the four examined models. The value seems to be related to the maximal width of the ground state which occurs for the different models at different α values.

3.3 Finite Quantum Well

As a finite interval example, we examined numerically the problem where in the interval $x \in [-4, 4]$ the potential is given by

$$V(x) = \begin{cases} x^2/200 & \text{if } |x| < 4 \\ 0 & \text{if } |x| \geq 4 \end{cases}. \tag{47}$$

The potential was chosen as a flat parabola at the bottom to avoid numerical problems in the determination of eigenvalues. The eigenfunctions for the first three quantum states are shown in Fig. 19. The graphs show that the boundary values are satisfied and the structure of the density distribution delivers the expected behavior; i.e. single peak for the ground state, double peak for the first quantum state etc. In Fig. 20 we show the dependence of the real eigenvalues on α. For the eigenvalue

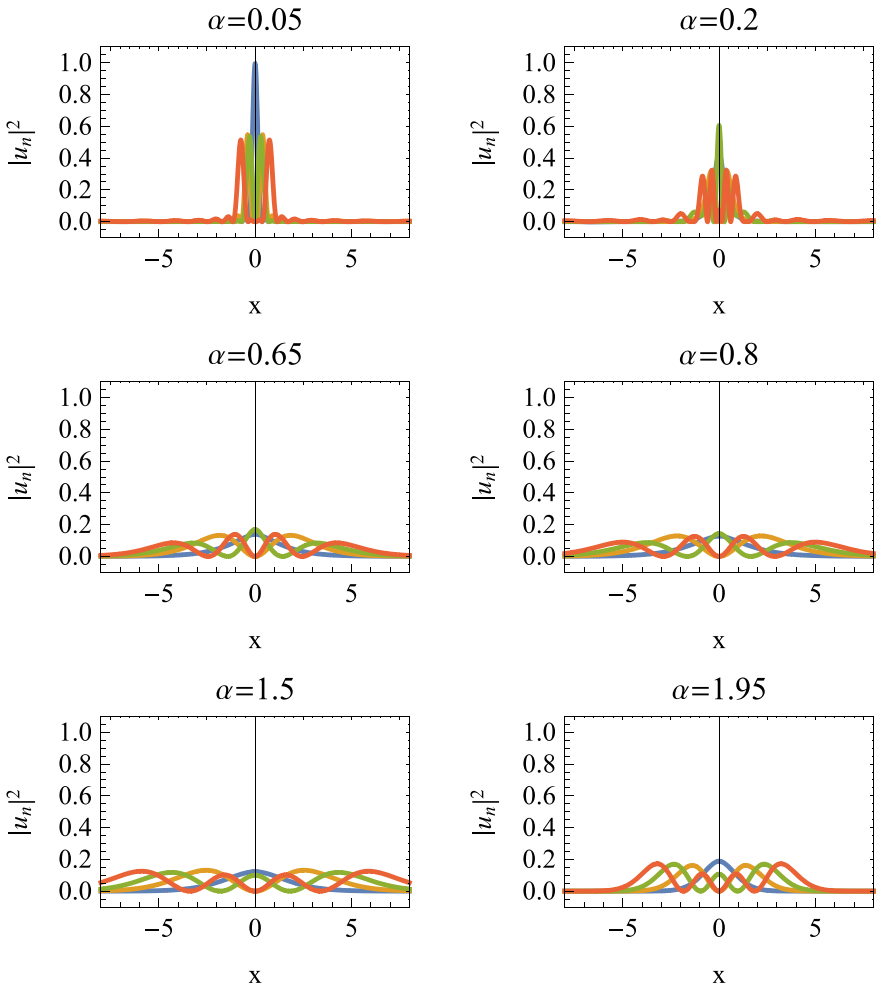

Fig. 15 The four first density functions for the potential $V(x) = |x|$ for different values of α (see top of figures). We observe again a delocalization if α is increasing but a small localization when $\alpha \to 2$

distribution as a function of α, we observe that the ground state is a single valued state while the first and second state is degenerate which separates on the α-interval. Compared with the infinite problems the distribution shows a steep increase on the right end of the interval. As for the infinite examples the distribution also shows a maximum which decreases to small values if $\alpha \to 0$. The graphs in Fig. 19 show that the boundary conditions for the wave functions at the potential limits are satisfied. It becomes also apparent that the ground state is nearly stable above a value $\alpha > 1$ while the other two states vary in their amplitude if α varies (see also Fig. 21).

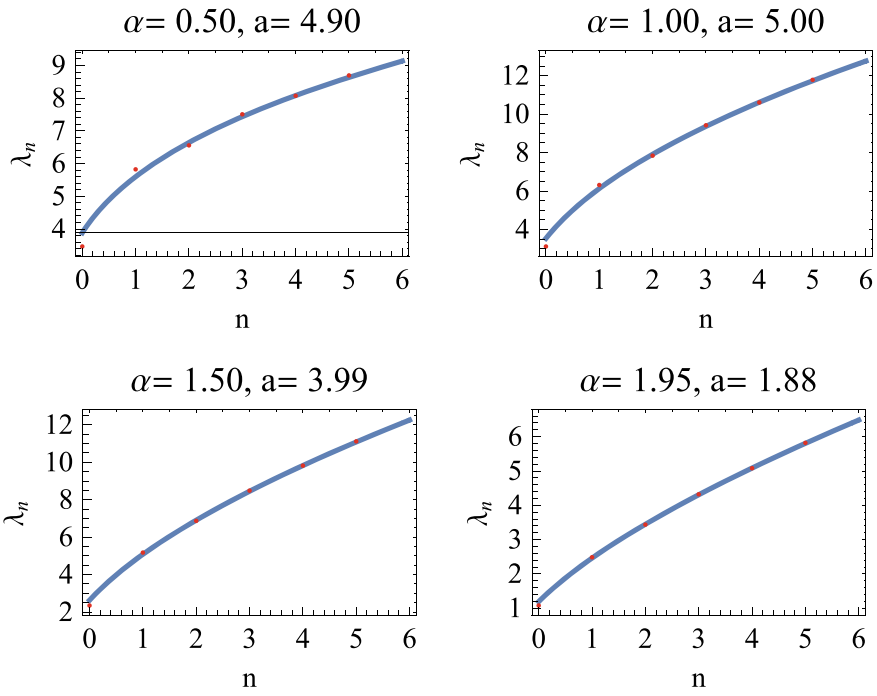

Fig. 16 Eigenvalue relation for different values of α (see top of graph). The eigenvalues are following a relation derived by Laskin [6] of the following form $\lambda_n = a(n + 1/2)^{\alpha/(1+\alpha)}$. Here a a single parameter was estimated from the numerical data using a least square fit (values are given on top of plots)

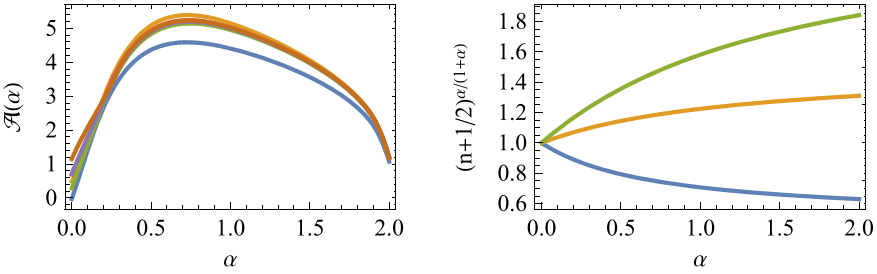

Fig. 17 The graphs (left panel) shows the shape function $\mathscr{A}(\alpha)$ of the eigenvalues extracted from the numerical values of λ_n. For $n \geq 1$ the shape function is nearly unique while for $n = 0$ the shape function is smaller than the function for higher quantum numbers. The reason is that eigenvalues according to $\lambda_n = (n + 1/2)^{\alpha/(1+\alpha)}$ is an increasing function for $n \geq 1$ and a decreasing function for $n = 0$ (right panel). This difference causes a change in the shape function

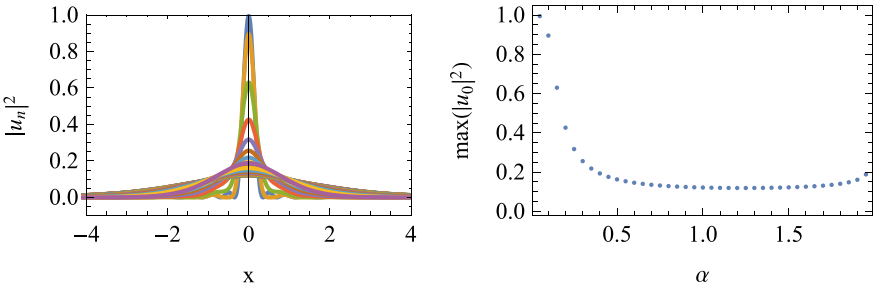

Fig. 18 Change of the maximal amplitude of the ground state density as a function of α. We observe that the maximum takes a minimum value at $\alpha = 1.23$

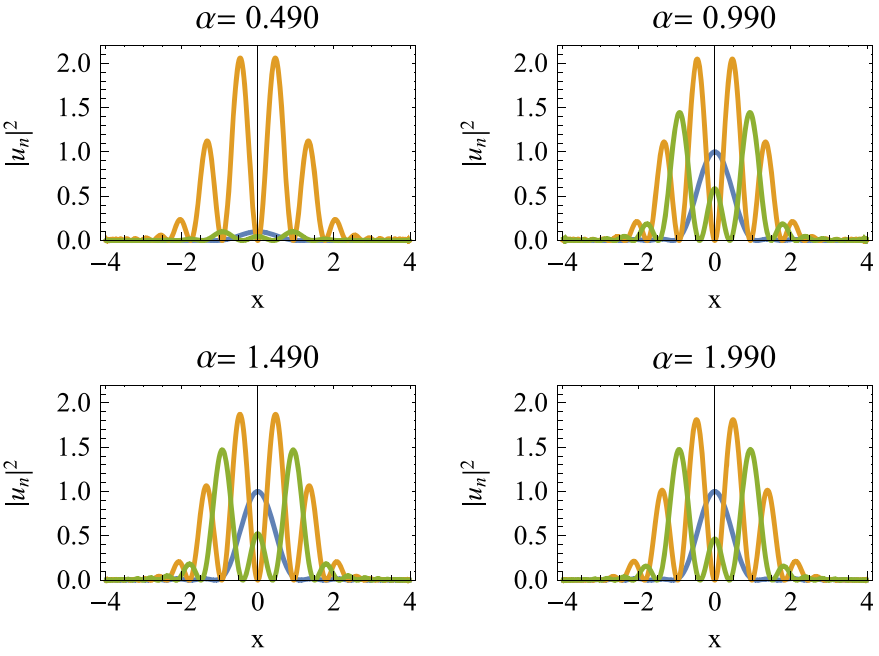

Fig. 19 Probability densities for eigenstates of the potential (47) on a finite interval $x \in [-4, 4]$

In Fig. 21 we plot the probability density as a function of α for the first three quantum states. It is apparent from the figures that for $\alpha < 1$ there is a wavy structure in the density. However, for $1 < \alpha < 2$ the probability density shows a smooth behavior. The wavy structure may indicate that the first moments of the Lévy process may not exist [9]. It is also obvious from the Figure that the even states grow in their amplitudes if $\alpha > 1/2$ while the odd state is completely present but varies in its amplitude. What is also remarkable for the finite support spectrum is that there is no broadening of the wave function on the support interval if α is changed (compare

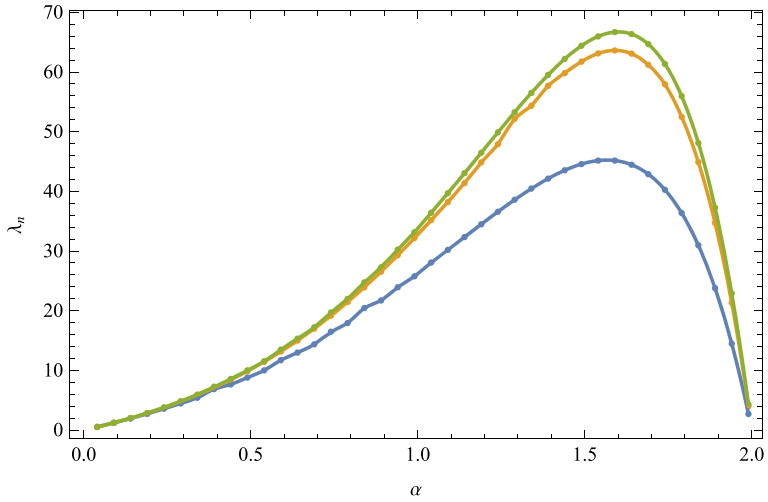

Fig. 20 The first three eigenvalues as function of α on the interval $x \in [-4, 4]$ using $N = 72$ Sinc points (colors correspond to the eigenstates in Fig. 19, respectively)

with Fig. 8). We only observe a change in the amplitude but not in the width of the probability density.

4 Conclusions

We demonstrated for the first time numerically that the conjecture by Laskin on a Lévy based quantum mechanics; i.e. a Lévy–Schrödinger description, can be numerically realized. The analytic results derived by Laskin for the harmonic potential and the quarkonium models were verified and confirmed by our Sinc approximation. The approach of approximation delivered new results and effects which are applicable to other quantum mechanical systems with known analytic potentials, too. We also demonstrated that the Riesz–Feller representation delivers real valued eigenvalues if the skewness parameter equals to zero. If the skewness parameter is different from zero the eigenvalues are complex but become real for $\alpha \to 2$, consistent with the standard quantum interpretation. At the moment it is not clear if the complex eigenvalues have any physical meaning at all. The related probability densities are real valued functions which is the basis of a quantum mechanical interpretation. However, we recall that Gamov's theory for the α-decay of atomic nuclei used complex eigenvalues which finally turned out to have a real physical meaning. We did not examine in detail so far where such kind of results may have meaningful applications. However, we definitely can state for the real valued eigenvalues, that the well known models of quantum mechanics are now accessible in a quantum mechanics based on Lévy stable probability distributions. We also presented a solution approach for

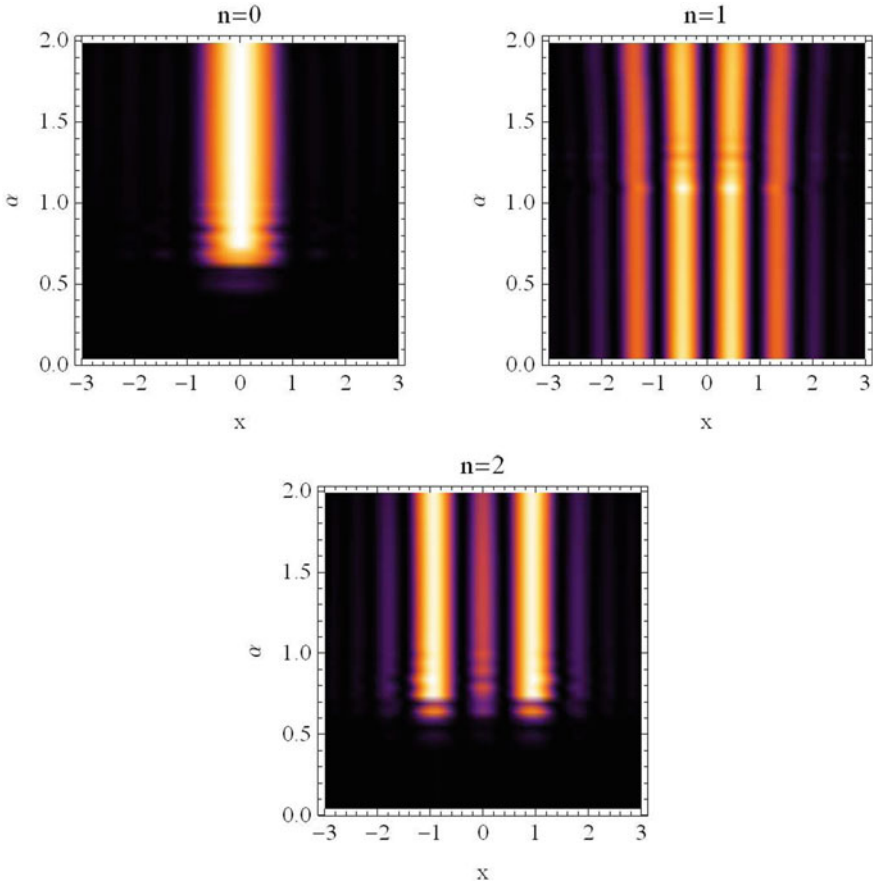

Fig. 21 Density plots for the first three probability densities $|u_n|^2$

finite boundary value problems in an environment with infinite range interactions. We approximated some eigenvalues for this finite support problem by a reinterpretation of the Riesz–Feller potential in connection with the potential term. The new results presented may open a gate of interpretation and applications in quantum mechanics which will be seen in future works.

Acknowledgements This work has been supported in part by "SAPIENZA" Universita di Roma. The author thanks Renato Spigler for the invitation to the NLFO Workshop. He is also indebted to a referee for some useful comments.

5 Appendix

This appendix collects additional relations and definitions used in the formulation and computation of fractional derivatives.

The Riesz–Feller fractional derivative is defined as follows [34, 35]

$$\mathscr{D}^{\alpha}_{x;\theta} f(x) = -\mathscr{I}^{-\alpha}_{x;\theta} f(x) = c_{-}(\alpha,\theta)\mathscr{I}^{-\alpha}_{+;x;\theta} f(x) + c_{+}(\alpha,\theta)\mathscr{I}^{-\alpha}_{-;x;\theta} f(x) \tag{48}$$

with $0 < \alpha \leq 2$, $|\theta| \leq min(\alpha, 2-\alpha)$, and the following relations

$$c_{+}(\alpha,\theta) = \frac{\sin((\alpha-\theta)\pi/2)}{\sin(\alpha\pi)} \text{ and } c_{-}(\alpha,\theta) = \frac{\sin((\alpha+\theta)\pi/2)}{\sin(\alpha\pi)} \tag{49}$$

and the corresponding fractional integral operators $\mathscr{I}^{\alpha}_{x;\theta}$ (Weyl integrals see e.g. [35]) are given as

$$\mathscr{I}^{\alpha}_{+;x;\theta} f(x) = \frac{1}{\Gamma(\alpha)} \int_{-\infty}^{x} (x-\xi)^{\alpha-1} f(\xi) d\xi \tag{50}$$

and

$$\mathscr{I}^{\alpha}_{-;x;\theta} f(x) = \frac{1}{\Gamma(\alpha)} \int_{x}^{\infty} (\xi-x)^{\alpha-1} f(\xi) d\xi. \tag{51}$$

Note the negative sign in the Riesz–Feller operator means that we are dealing with fractional derivatives which are defined in terms of integral operators as follows:

$$\mathscr{I}^{-\alpha}_{+;x;\theta} f(x) = \frac{1}{\Gamma(n-\alpha)} \int_{-\infty}^{x} (x-\xi)^{n-\alpha-1} f(\xi) d\xi \tag{52}$$

and

$$\mathscr{I}^{-\alpha}_{-;x;\theta} f(x) = \frac{1}{\Gamma(n-\alpha)} \int_{x}^{\infty} (\xi-x)^{n-\alpha-1} f(\xi) d\xi. \tag{53}$$

with $n = [\mathscr{R}e(\alpha)] + 1$ and $\mathscr{R}e(\alpha) > 0$; here $[\alpha]$ represents the integer part of α.

References

1. Schrödinger, E.: An undulatory theory of the mechanics of atoms and molecules. Phys. Rev. **28**, 1049–1070 (1926)
2. Kac, M.: Second Berkeley Symposium on Mathematical Statistics and Probability, edited by Jerzy Neyman. University of California Press, Berkeley, CA (1951)

3. Montroll, E.W.: On the quantum analogue of the Lévy distribution. In: Enz, C., Mehra, M. (eds.) Physical Reality and Mathematical Description. Reidel, Dordrecht, The Netherlands, pp. 501–508 (1974)
4. West, B.J.: Quantum Lévy propagators. J. Phys. Chem. B **104**, 3830–3832 (2000)
5. Laskin, N.: Fractional quantum mechanics. Phys. Rev. E **62**, 3135–3145 (2000)
6. Laskin, N.: Fractional Schrödinger equation. Phys. Rev. E **66**, 56108 (2002)
7. Longhi, S.: Fractional Schrödinger equation in optics. Opt. Lett. **40**, 1117–1120 (2015)
8. Jeng, M., Xu, S.-L.-Y., Hawkins, E., Schwarz, J.M.: On the nonlocality of the fractional Schrödinger equation. J. Math. Phys. **51**, 62102 (2010)
9. Laskin, N.: Fractional quantum mechanics and Lévy path integrals. Phys. Lett. A **268**, 298–305 (2000)
10. Wei, Y.: Comment on "Fractional quantum mechanics" and "Fractional Schrödinger equation". Phys. Rev. E **93**, 66103 (2016)
11. Laskin, N.: Reply to "Comment on 'Fractional quantum mechanics' and 'Fractional Schrödinger equation"'. Phys. Rev. E **93**, 66104 (2016)
12. Stenger, F., Baumann, G., Koures, V.G.: Computational methods for chemistry and physics, and Schrödinger in 3+1. In: Concepts of Mathematical Physics in Chemistry: A Tribute to Frank E. Harris - Part A, vol. 71, pp. 265–298. Elsevier (2015)
13. Al-Saqabi, B., Boyadjiev, L., Luchko, Y.: Comments on employing the Riesz-Feller derivative in the Schrödinger equation. Eur. Phys. J. Spec. Top. **222**, 1779–1794 (2013)
14. Luchko, Y.: Fractional Schrödinger equation for a particle moving in a potential well. J. Math. Phys. **54**, 12111 (2013)
15. Titchmarsh, E.C.: Eigenfunction expansions. Associated with Second-order Differential Equations. Oxford University Press, Oxford (1962)
16. Weyl, H.: Über gewöhnliche Differentialgleichungen mit Singularitäten und die zugehörigen Entwicklungen willkürlicher Funktionen. Math. Ann. **68**, 220–269 (1910)
17. Baumann, G., Stenger, F.: Fractional calculus and Sinc methods. Fract. Calc. Appl. Anal. **14**, 568–622 (2011)
18. Baumann, G., Stenger, F.: Fractional Adsorption Diffusion. Fractional Calculus and Applied Analysis **16**, 737–764 (2013)
19. Baumann, G., Stenger, F.: Fractional Fokker-Planck equation. Mathematics **5**, 1–19 (2017)
20. Baumann, G., Stenger, F.: Sinc-approximations of fractional operators: a computing approach. Mathematics **3**, 444–480 (2015)
21. Stenger, F., El-Sharkawy, H.A.M., Baumann, G.: The Lebesgue constant for sinc approximations. In: Zayed, A., Schmeisser, G. (eds.) New Perspectives on Approximation and Sampling Theory − Festschrift in the Honor of Paul Butzer's 85th birthday. Birkhaeuser, Basel (2014)
22. Stenger, F.: Handbook of Sinc Numerical Methods. CRC Press, Boca Raton (2011)
23. Stenger, F.: Numerical Methods Based on Sinc and Analytic Functions. Springer, New York (1993)
24. Stenger, F.: Summary of Sinc numerical methods. J. Comput. Appl. Math. **121**, 379–420 (2000)
25. Stenger, F.: Collocating convolutions. Math. Comput. **64**, 211–235 (1995)
26. Kowalski, M.A., Sikorski, K.A., Stenger, F.: Selected Topics in Approximation and Computation. Oxford Univ. Press, New York (1995)
27. Lund, J.R., Riley, B.V.: A sine-collocation method for the computation of the eigenvalues of the radial Schrödinger equation. IMA J. Numer. Anal. **4**, 83–98 (1984)
28. Eggert, N., Jarratt, M., Lund, J.: Sine function computation of the eigenvalues of Sturm-Liouville problems. J. Comput. Phys. **69**, 209–229 (1987)
29. Lundin, L., Stenger, F.: Cardinal-type approximations of a function and its derivatives. SIAM J. Math. Anal. **10**, 139–160 (1979)
30. Wang, S., Xu, M., Li, X.: Green' s function of time fractional diffusion equation and its applications in fractional quantum mechanics. Nonlinear Anal.: Real World Appl. **10**, 1081–1086 (2009)
31. Lubich, C.: Convolution quadrature and discretized operational calculus. I. Numer. Math. **52**, 129–145 (1988)

32. Lubich, C.: Convolution quadrature and discretized operational calculus. II. Numer. Math. **52**, 413–425 (1988)
33. Han, L., Xu, J.: Proof of Stenger's conjecture on matrix of Sinc methods. J. Comput. Appl. Math. **255**, 805–811 (2014)
34. Gorenflo, R., Mainardi, F.: Some recent advances in theory and simulation of fractional diffusion processes. Spec. Issue: Anal. Numer. Approx. Singul. Probl. **229**(2), 400–415 (2009). https://doi.org/10.1016/j.cam.2008.04.005
35. Kilbas, A.A., Srivastava, H.M., Trujillo, J.J.: Theory and Applications of Fractional Differential Equations. Elsevier, Amsterdam (2006)

Stochastic Properties of Colliding Hard Spheres in a Non-equilibrium Thermal Bath

Armando Bazzani, Silvia Vitali, Carlo E. Montanari, Matteo Monti, Sandro Rambaldi, and Gastone Castellani

Abstract We consider the problem of describing the dynamics of a test particle moving in a thermal bath using the stochastic differential equations. We briefly recall the stochastic approach to the Brownian based on the statistical properties of collision theory for a gas of elastic particles and the molecular chaos hypothesis. The mathematical formulation of the Brownian motion leads to the formulation of the Ornstein-Uhlenbeck equation that provides a stationary solution consistent with the Maxwell-Boltzmann distribution. According to the stochastic thermodynamics, we assume that the stochastic differential equations allow to describe the transient states of the test particle dynamics in a thermal bath and it extends their application to the study of the non-equilibrium statistical physics. Then we consider the problem of the dynamics of a test massive particle in a non homogeneous thermal bath where a gradient of temperature is present. We discuss as the existence of a local thermodynamics equilibrium is consistent with a Stratonovich interpretation of the stochastic differential equations with a multiplicative noise. The stochastic model applied to the test particle dynamics implies the existence of a long transient state during which the particle shows a net drift toward the cold region of the system. This effect recalls the thermophoresis phenomenon performed by large molecule in a solution in response to a macroscopic temperature gradient and it can be explained as an effect of the non-locality character of the collision interactions between the test particle and the thermal bath particles. To validate the stochastic model assumptions we analyze

A. Bazzani (✉) · C. E. Montanari · S. Rambaldi
Department DIFA, University of Bologna, INFN sezione di Bologna via Irnerio 46, 40126 Bologna, Italy
e-mail: armando.bazzani@unibo.it

S. Vitali
Basque Center for Applied Mathematics, Alameda de Mazarredo 14, 48009 Bilbao, Bizkaia, Spain

M. Monti
EPFL IC École Polytechnique Fédérale de Lausanne, Station 14, 1015 LausanneLausanne, Switzerland

G. Castellani
Department DIMES, University of Bologna, INFN sezione di Bologna, Via Giuseppe Massarenti, 1, 0138 Bologna, Italy

L. Beghin et al. (eds.), *Nonlocal and Fractional Operators*, SEMA SIMAI Springer Series 26, https://doi.org/10.1007/978-3-030-69236-0_3

the simulation results of the 2-dimensional hard sphere gas obtained by using an event-based computer code, that solves exactly the sphere dynamics. The temperature gradient is simulated by the presence of two reflecting boundary conditions at different temperature. The simulations suggest that existence of a local thermodynamic equilibrium is justified and highlight the presence of a drift in the average dynamics of an ensemble of massive particles. The results of the paper could be relevant for the applications of stochastic dynamical systems to the non-equilibrium statistical physics that is a key issue for the Complex Systems Physics.

Keywords Collisional theory · Stochastic differential equations · Non-equilibrium stationary states

1 Introduction

The understanding of the non-equilibrium statistical systems is one of the main issue of Complex Systems Physics. Modeling biological, biochemical or socio-economical complex systems usually copes with the problem of describing the evolution of a system out of equilibrium [1]. Even if one restricts the study to consider non-equilibrium stationary states (NESS) [2], the existence of universal laws cope with the peculiarities of each statistical system out of equilibrium, where some details of the interactions among elementary components play a relevant role. Despite of a great effort to find a general theoretical approach to non-equilibrium thermodynamics, the scientific community is still discussing if there exists an analogous of the Entropy Principle [3] that governs the relaxation process toward the equilibrium state. In this framework the stochastic differential equations have been recognized a powerful tool to study the dynamics of statistical systems [4]. Even if these equations cannot be derived from the fundamental physical laws, the universality of the Central Limit Theorems (CTL) and the chaotic properties of many degrees of freedom dynamical systems pointed out by Ergodic Theory, justify the applications to real systems. Some relations or assumptions that are at the base of the stochastic model approach, as the fluctuation-dissipation relations [5] or the reversibility properties of the stationary solution (Onsager relations [6]) could be extended to the NESS states. In this work we consider the problem of explaining the statistical properties of a gas of colliding elastic particles by means of the stochastic differential equations. The assumption of the molecular chaos allows to describe the dynamics of a massive particle in the gas as a Brownian motion in the vanishing mass limit for the gas particles and infinitely frequent collisions. We discuss the possible extension of this approach to consider a NESS state of a hard sphere gas between two reflecting boundary conditions at different temperatures. Assuming that the gas realizes a local pressure equilibrium, we derive some scaling laws for the relevant parameters that define the collision theory. The particle dynamics is described by a stochastic differential equation with a multiplicative noise, due to the dependence of the temperature from the position. Our result is that for a finite particle mass and a finite collision frequency,

one has to interpret the stochastic differential equation according to Stratonovich [7] to take into account the correlation among successive collisions in order to get the local equilibrium of pressure in the NESS state. Under this point of view, the collision dynamics is non-local and one has to introduce an effective force to take into account the effect of temperature gradient. We extend this result to describe the dynamics of a massive test particle in the non-uniform thermal bath and we show that the model implies a long correlation time in the evolution, that induce an average net drift of the particle toward the colder regions of the thermal bath. The effect increases as one increases the mass of the test particle and it may recall the thermophoresis phenomenon observed when real particles fluctuate in presence of a temperature gradient [8]. In order to get a validation of the proposed approach, we have performed numerical simulations for a 2-dimensional hard sphere gas. The simulation code [9] uses an event based algorithm, that allows an exact (with the round-off errors of the double precision) integration of the collision dynamics of $10^4 \div 10^5$ elastic particles. Such numbers are suitable to simulate a condition of moderate density where the particles may explore all the available space (i.e. we are simulating a gaseous state), but they relax to a local equilibrium state justified by the application of a Central Limit Theorem (CLT). The simulation results suggest that the stochastic differential equations are indeed able to explain some statistical features of the collision dynamics in presence of a temperature gradient. Our results are consistent with the Stochastic Thermodynamics approach to non-equilibrium statistical physics [10]. However a quantitative relation among the thermophoresis phenomenon in chemistry, the relaxation process we observe in the simulation of an ensemble of massive test particles and the solution of the stochastic differential equation, requires further studies.

The paper is organized as follows: in the second section we briefly present the fundamental concepts of collision theory that justify a stochastic model for the Brownian motion and its possible extension to consider the effect of a temperature gradient in the thermal bath; in the third section we discuss the results of molecular dynamics simulations and the possible validation of the stochastic model description both in a equilibrium and in a NESS state; finally some conclusions and perspective are outlined.

2 Collision Theory and Stochastic Differential Equation

To understand the mesoscopic description of statistical systems using the stochastic dynamical systems theory, we study the collisions among particles in the limit of local, instantaneous and binary interactions. When it is possible to neglect the details of the microscopic dynamics using the CLT, the statistical properties are reproduced by mesoscopic models, where one only considers the statistical effects of fluctuations. A formal approach starts from some physical assumptions on the microscopic dynamics:

1. we distinguish three different time scales: the interaction time scale $\Delta\tau$ (i.e. the time duration of a collision that we assume very small), the collision scale time τ that measures the elapsed time between successive collisions (i.e. τ is the average correlation time of microscopic dynamics and τ^{-1} the collisions frequency) and $\Delta t \gg \tau$ the evolution time scale of the dynamical variables;
2. we assume the molecular chaos: i.e. the collisions are instantaneous and successive collisions can be considered independent events (we have a discontinuous dynamics in the momentum space of a test particle);
3. the collisions are binary: we do not consider multiple collisions or collective mean field effects;
4. we have conservation laws in the collision dynamics: we consider elastic collisions where kinetic energy and momentum are preserved.

The application of the CLT to the momentum dynamics justifies a stochastic approach to model the elastic collisions effect on a test particle of mass M in a thermal bath simulated by an ensemble of particles with a mass $m \ll M$. If τ^{-1} is the collision frequency (i.e. τ is the average time interval between successive collisions), in the limit $m \to 0$ and $\tau \to 0$ with the ratio m/τ kept constant (the Brownian motion limit), the evolution of the momentum $\boldsymbol{P(t)}$ is described by the stochastic dynamical system

$$\boldsymbol{P}\,(t + \Delta t) = \boldsymbol{P(t)} - \frac{\gamma}{M}\boldsymbol{P(t)}\Delta t + \sqrt{2\gamma \Delta t T}\boldsymbol{\xi}(t) \tag{1}$$

where T is the temperature of the thermal bath according to the expectation value over the gas particles

$$E\left(\frac{\boldsymbol{p^2}}{2m}\right) = \frac{3}{2}T$$

and the parameter γ

$$\gamma = \frac{2m}{\tau}E\left(\sin^2\frac{\theta}{2}\right) \tag{2}$$

contains the statistical information of the collision dynamics through the expectation value $E(\sin^2\theta/2)$ (θ is the deflection angle due to an elastic collision and the average value is computed over all the possible collisions of the test particle with the gas particles). We observe that the Einstein fluctuation-dissipation relation is satisfied. The time step Δt is the evolution time scale for the momentum $\boldsymbol{P}(t)$ (i.e. $\boldsymbol{P}(t)$ can be considered constant during Δt with an error that vanishes in the Brownian motion limit) and $\boldsymbol{\xi}(k\Delta t)$ $k \in \mathbb{N}^0$ are independent standard Gaussian variables. The justification of the stochastic dynamics (1) requires that the collision dynamics could be described as the sum of independent events and that the gas particles colliding with the test particle are 'thermalized' so that the expectation value of the kinetic energy is $3/2T$ (the Boltzmann constant is set to one). The last requirement is a key point since it means that the test particle can be considered in a local thermal equilibrium at each time interval Δt. In the limit $\Delta t \to 0$ the random walk (1) realizes the Brownian motion for the test particle

$$
\begin{aligned}
d\boldsymbol{P} &= -\frac{\gamma}{M}\boldsymbol{P}dt + \sqrt{2\gamma T}\, d\boldsymbol{w}(t) \\
d\boldsymbol{X} &= \frac{\boldsymbol{P}}{M}dt
\end{aligned}
\tag{3}
$$

where $\boldsymbol{w}(t)$ is a vector Wiener process. To compare the analytical approach with numerical results, we consider a 2-dimensional hard spheres gas in the sequel: in such a case one explicitly evaluates $E(\sin^2\theta/2) = 1/3$ [11]. The Brownian motion limit requires that the time interval $\tau \to 0$, which is a unphysical limit when we consider an ensemble of spheres with finite dimension at a fixed average density ρ. Indeed using statistical physics results, one can estimate

$$
\tau \propto \frac{m}{d\,\|\boldsymbol{p}\|\rho} \propto \frac{m}{d\sqrt{T}\rho} \tag{4}
$$

where d is the particle diameter; it follows that τ is finite for finite temperatures. The solution $\boldsymbol{P}(t)$ of the stochastic equation is a Gaussian Ornstein-Uhlenbeck process with parameter $\alpha = \gamma/M$ and the covariance matrix of the observables reads

$$
\begin{aligned}
< \Delta P_i(t)\Delta P_j(t+\Delta t) > &= \delta_{ij} e^{-\alpha\Delta t} TM \left(1 - e^{-2\alpha t}\right) \\
< \Delta X_i(t)\Delta P_j(t+\Delta t) > &= \delta_{ij}\frac{T}{\alpha} e^{-\alpha\Delta t}\left(1 - e^{-\alpha t}\right)^2 \\
< \Delta X_i(t)\Delta X_j(t) > &= \delta_{ij}\left[\frac{2T}{\gamma}\left(t - \frac{2}{\alpha}(1 - e^{-\alpha t})\right) + \frac{1}{2\alpha}(1 - e^{-2\alpha t})\right]
\end{aligned}
\tag{5}
$$

so that for $t\alpha \gg 1$ we get

$$
< \Delta X_i^2(t) > \simeq \frac{2T}{\gamma}t
$$

whereas we have a ballistic behavior for $t\alpha \ll 1$. We remark as the correlation-relaxation time scale α^{-1} changes proportionally to the mass, so that for a test particle for $M \gg m$ we estimate a correlation time and a relaxation time much longer than for the gas particles. The stationary distribution for the momentum is Gaussian whereas for a gas confined in a finite volume, the spatial density is constant. The kinetic energy E of the particles is distributed according to the Maxwell-Boltzmann distribution $p(E) \propto \exp(-E/T)$. The equilibrium condition is consistent with the state law of gas $P = \rho T$ if one computes the pressure P on a boundary surface. The finite size effects (a finite mass and dimension for the gas particles) introduce a finite collision time scale τ so that the parameter γ (cfr. Eq. (2)) scales as τ^{-1} for a fixed mass m, which depends on the local density. Assuming a finite dimension for gas particles the average collision frequency is estimated by

$$
\tau^{-1} \propto a < \Delta v >_+ \rho
$$

where the symbol $< \Delta v >_+$ means that we take the average value only for the positive values of the relative velocity along a given direction and a is an effective surface for collisions. $< \Delta v >_+$ is estimated by $T^{1/2}$ so that, in the equilibrium condition, we expect that τ scales by $T^{1/2}$. A finite τ could prevent the application of the CLT to justify the stochastic equation for the test particle, when the condition $\Delta t \gg \tau$ is not satisfied. But, for the equilibrium state, the homogeneity of particle distribution implies that the distribution of the collision events does not depend from the position and the momentum dynamics is still described by a Gaussian process. This result is also true if the test particle is a gas particle with a finite mass, so that the probability distribution for the coordinates and momentum are representative for the density distribution of the same quantities for the whole gas.

We now consider the problem if a stochastic model could be justified in the case of a non-equilibrium stationary state (NESS): more precisely we assume that the gas particle are in contact with two thermal reservoirs at different temperature so that we have a temperature gradient along the x-direction in the system and we focus our analysis of the dynamics along this direction. We simulate the thermal reservoir T by using a reflecting boundary such that, each time a gas particle hits a barrier, it is reflected in a elastic way and the reflected velocity is distributed according to

$$\rho(v) \propto v \exp\left(-\frac{mv^2}{2T}\right) \quad v \geq 0 \tag{6}$$

which is the distribution of the particles velocity of a 2-dimensional gas at equilibrium temperature T. As a matter of fact the particle distribution relaxes to a stationary state after a certain time and the pressure equilibrium at any cross section of the system gives $P = \rho(x)T(x)$ so that

$$\rho(x) \propto T^{-1}(x) \tag{7}$$

Assuming a temperature gradient of the form

$$T(x) = T_0 + \beta(x - x_0) \qquad x \in [x_0, x_1]$$

where the parameter $\beta = (T_1 - T_0)/(x_1 - x_0)$ defines the gradient, the stationary condition implies

$$\rho(x) \propto \frac{1}{T_0 + \beta(x - x_0)} \tag{8}$$

so that the particle density increases near the cold barrier T_0. In the 2-dimensional case one can estimate the mean free path of the particles λ as the probability to collide with a particle in a given volume

$$\lambda(x) \propto \rho^{-1}(x)$$

Then if the density is small, two successive collisions of the gas particle may involve particles with different temperatures. In such a case the local thermalization of a

particle is not justified (i.e. the position x and the momentum p cannot be considered constant when one considers successive collisions) and we have to take into account a correlation effect in the collision dynamics. In such a case the stochastic differential equation (3) has to be modified and the Stratonovich interpretation has to be applied since the effect of a successive collision depends on the previous one. For a test gas particle in a NESS state we apply the following stochastic equation

$$\begin{aligned} dp_x &= -\frac{\gamma(x)}{m} p_x dt + \sqrt{2\gamma(x)T\left(x + \frac{p_x}{\gamma(x)}\right)}\, dw^*(t) \\ dx &= \frac{p_x}{m} dt \end{aligned} \tag{9}$$

where dw^* is the Wiener differential in the Stratonovich interpretation. We remark that m/γ is a characteristic correlation time for the collision dynamics of the ensemble particles and that we preserve the Einstein condition. However, the temperature of the colliding particles is not constant when one considers successive collisions since the mean free path is not small. Recalling the definition (2) and the scaling law for the collision time $\tau \propto \sqrt{T}$, we derive the functional form for the drift coefficient

$$\gamma(x) = \frac{\hat{\gamma} m}{\sqrt{T(x)}}$$

If one estimates the average momentum evolution in Eq. (9) we have two contributions: the x-dependence of the drift term gives

$$-\left\langle \frac{\gamma(x)}{m} p_x \right\rangle \simeq \frac{1}{2} \frac{\hat{\gamma}}{T^{3/2}} \frac{dT}{dx} \frac{Tm}{\gamma(x)} \simeq \frac{1}{2} \frac{dT}{dx}$$

where we compute $< p_x x >$ using the relations (5), whereas the fluctuating term according to the Stratonovich interpretation gives

$$-\frac{\gamma}{2} \frac{\partial}{\partial p} T\left(x + \frac{p}{\gamma(x)}\right) = -\frac{1}{2} \frac{dT}{dx}$$

We remark as the two terms cancel so that no effective drift can be observed for a gas test particle in the NESS state as expected from the equilibrium condition of pressure. Therefore the Stratonovich interpretation of the stochastic differential equation (9) seems physically justified to describe the evolution of the gas particle in a NESS state. This effect is the consequence of the non local character of the collision interactions when we have finite dimension gas particles and the temperature gradient introduces an effective force that is considered by the Stratonovich interpretation of the equation (9).

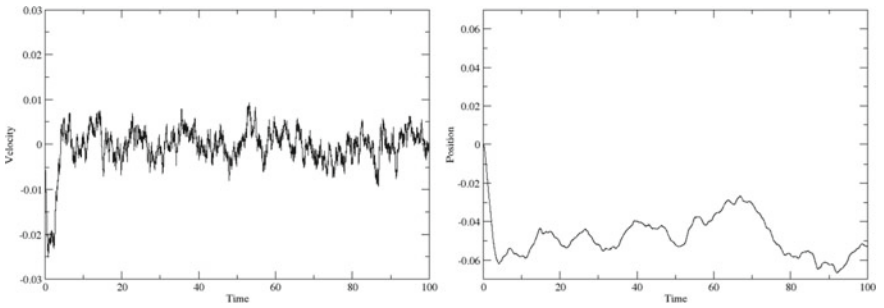

Fig. 1 Numerical solutions of Eq. (9) using the parameters $\hat{\gamma} = 1, \beta = .1, T_0 = .5$ and $T_1 = 2.5$. We have simulated 10^5 particles with $m = 1$ in a box $x \in [-10, 10]$ with initial condition $x = 0, p = 0$. The units are arbitrary. The left picture shows the evolution of the average velocity and the right picture shows the evolution of the average position

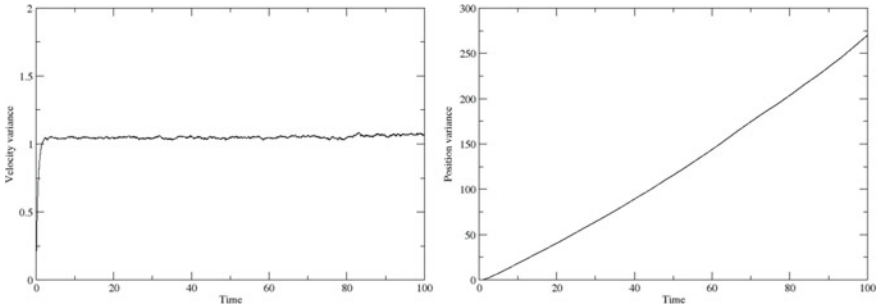

Fig. 2 Numerical solutions of Eq. (9) using the same parameters as in Fig. 1. The left picture shows the evolution of the velocity variance and the right picture shows the evolution of the position variance. We observe a normal diffusion behavior after a short transition time

In Fig. 1 we show the results of a direct integration of Eq. (9) in the Stratonovich interpretation for an ensemble of 10^5 particles (the parameters of the simulation are reported in the caption). We remark the presence of an initial transient regime where we have a drift toward the cold barrier, but then at the stationary state, we get a diffusion regime without drift as it is shown in Fig. 2, where we plot the velocity and position variances. In the case of velocity we reach a stationary value, whereas for the position we get the typical behavior of a local diffusion process: the momentum variance relaxes to the local thermal equilibrium $< \Delta v_x^2 > \to T/m = 1.05$ (according to the parameters values used in the simulations) and the position variance increases linearly with time after a short ballistic regime.

We study as the evolution changes if we consider a test particle of a larger mass $M \geq m$. From a formal point of view equation (9) is modified according to

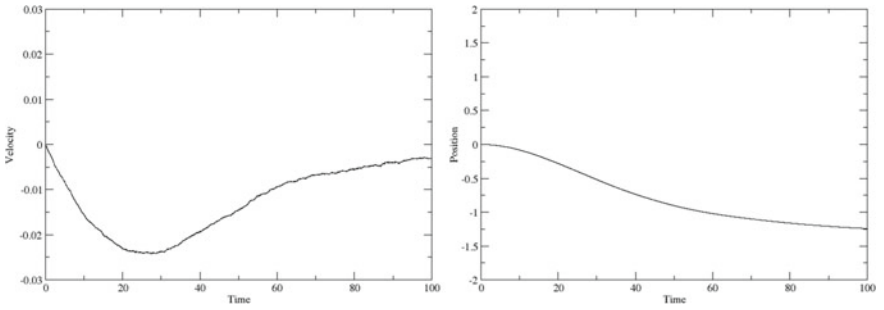

Fig. 3 Numerical solutions of Eq. (10) with $M = 25$ m, whereas the other parameters are the same as in Fig. 1. The left picture shows the evolution of the average velocity and the right picture shows the evolution of the average position. We observe as the long time correlation induces a drift of the average position toward the negative cold region

$$\begin{aligned} dP_x &= -\frac{\gamma(x)}{M} P_x dt + \sqrt{2\gamma(x)T\left(x + \frac{P_x}{\gamma(x)}\right)} dw^*(t) \\ dX &= \frac{P_x}{M} dt \end{aligned} \tag{10}$$

where the correlation time $\simeq M/\gamma$ is longer than for the gas particles. In such a case the transient regime to reach a stationary condition for the test particle M requires a much longer time and, in the Stratonovich interpretation, we expect a net average displacement toward the cold barrier in the transient regime. We have performed numerical integration of the stochastic equation (10) with $M = 25\,m$ whereas the other parameters are left constant. In Fig. 3 we report the numerical results for the average value of the velocity and the position for an ensemble of test particles. We observe that during long transition time the average velocity takes negative values and we have a net average displacement of the position toward the negative values (i.e. the colder region of the space). We have also checked the variance evolution of the velocity and the position (see Fig. 3). The velocity variance of the massive particles reaches a thermal equilibrium that corresponds to a local temperature associated to the stationary value of the average position, whereas the position variance shows a ballistic behavior for a long time. According to the previous interpretation of the collision dynamics in a thermal bath with a temperature gradient, the existence of a long relaxation time scale implies that a massive particle tends to drift in the colder region simulating the effect of a drift force, until a local equilibrium is reach and the evolution of the particle distribution recall the thermophoresis phenomenon. The overall effect of an ensemble of massive particles starting at a given position is that the distribution moves towards the cold region as shown in Figs. 3 and 4.

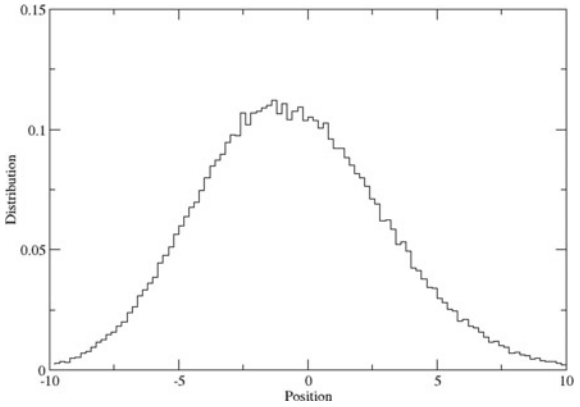

Fig. 4 Empirical distribution function computed using the numerical solution of Eq. (10) after $t = 50$ time units. We have used the same parameters as in Fig. 2. We remark that the distribution mode is shifted toward the negative values

3 Molecular Dynamics Simulations

To check the applicability of a stochastic dynamics approach to describe the collision dynamics of a test particle in a thermal bath, we developed a simulation code [9] to perform the molecular dynamics of a 2-dimensional gas composed by elastic spheres that collides between two reflecting horizontal boundary conditions, whereas we have a periodic boundary condition on the vertical axis. The numerical integration performs a event based code algorithm that computes exactly the elastic collision between two rigid spheres and moves the spheres according to a uniform rectilinear motion between two collisions. The event based algorithm [9] is quite efficient and it allows to simulate a great number of particles. The model considers an a fixed dimensional area in the simulations (i.e. a unit square) so that by varying the dimension of the spheres we change the gas particles density. In the sequel we show the simulations using 10^4 rigid spheres of radius 10^{-2} that corresponds to an average density $\rho \simeq 3\%$ defining the mean path length between successive collisions. The gas particle mass is fixed at $m = 1$ and the temperature (i.e. the kinetic energy) can be directly related to the evolution time scale so that only the ratio between the chosen values is relevant. We have first checked that in a uniform thermal bath the stochastic differential equation is suitable to describe the statistical properties of the collision dynamics: for a fixed temperature we have checked that the velocity distribution of the gas particle follows a Gaussian distribution (i.e. we get a Maxwell-Boltzmann distribution for the energy) and that the collision time scale τ, which enters in the definition of the drift parameter (see Eq. (2)) scales $\propto \sqrt{T}$. The simulation results are reported in Fig. 5 where we show as in stationary condition the gas particles relax to a thermodynamics equilibrium characterized by the Gaussian distribution: this result is consistent with the results on the dynamical properties of the hard sphere gas studied by the Ergodic Theory [12]. The probability distribution of the collision time τ is well approximated by an exponential distribution and we observe that the scaling law $\tau \propto \sqrt{T}$ is confirmed by the simulation results. The homogeneity of the

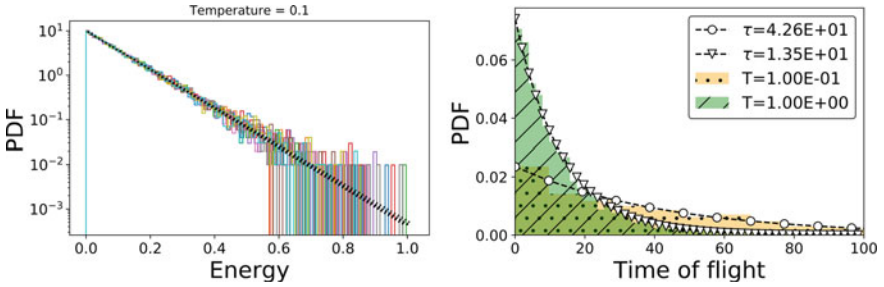

Fig. 5 Molecular dynamics simulations of a 2-dimensional hard sphere gas in the unit square $(x, y) \in [0, 1] \times [0, 1]$ using 10^4 particles with $m = 1$ and radius $r = .001$ in a thermal bath with temperature $T = 1$ (arbitrary unit). In the left picture we show the comparison of the kinetic energy distribution and the Maxwell-Boltzmann distribution (squares) in semilog scale. In the right picture we plot the distribution of the time of flight between successive collisions: the distribution is exponential with a characteristic collision time scale proportional to $T^{1/2}$ (see inset in the figure)

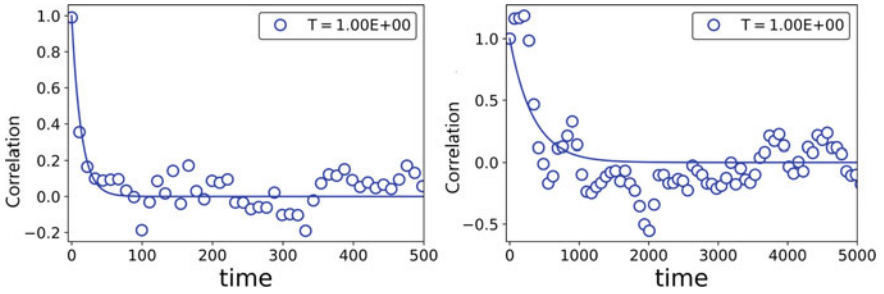

Fig. 6 Time correlation among the trajectories of the hard spheres in the molecular dynamic simulations. The left picture refers to the trajectories of the gas particles ($m = 1$), whereas the right picture refers to the trajectories of the 100 massive test particle ($M = 25$). The time unit is arbitrary

equilibrium state allows to apply the CLT even if the collision time is not negligible with respect to the evolution time scale.

We also checked that the correlation time scale depends from the inverse of the particle mass and the particles diffusion in the system is well described by the stochastic dynamics (3). In Fig. 6 we show the linear correlation in the velocity of the gas particle ($m = 1$) and an ensemble of 100 massive test particles ($M = 25$) in the thermal bath and the increase of the correlation time with the mass is observed. The computation of the time dependence of the position variance both for the gas and the test particles confirms that all the particles perform a normal diffusion with a ballistic transition time and the diffusion coefficient in the stationary regime is independent from the mass as implied by the Einstein relation (see Eq. (5)).

Then we introduced a temperature gradient in the system by mean of two reflecting boundary conditions at $x = 0$ and $x = 1$ that reproduce the velocity distribution (6) at a temperature $T_0 = .01$ and $T_1 = .1$ (the unit is arbitrary). We have checked that the density distribution of the gas particles in the NESS state is consistent with the

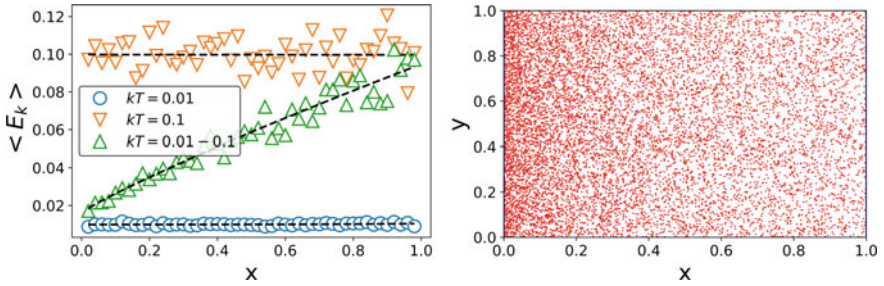

Fig. 7 Molecular dynamics simulations of a 2-dimensional hard spheres gas in the presence of a temperature gradient $T \in [.1, 1]$. The left picture shows the local temperature (i.e. the kinetic energy) computed dividing the system into 50 slices as a function of the position; the continuous line defines the linear dependence provided by the Statistical Mechanics Theory. The right picture is a snapshot of the molecular dynamic simulations that shows the particle distribution in presence of the temperature gradient

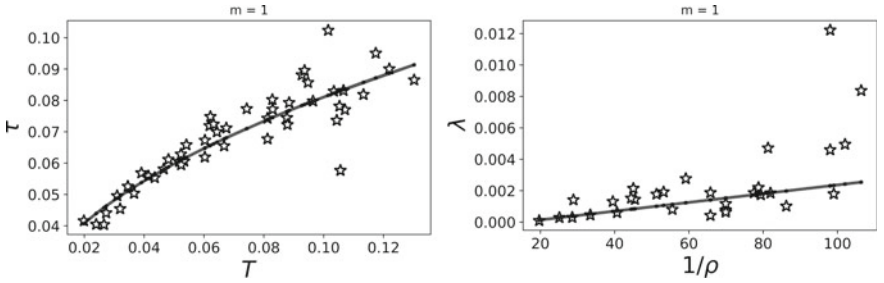

Fig. 8 (Left picture) Empirical dependence of the collision time scale from the local temperature in the hard sphere gas simulations; the continuous curve refers to the interpolation result with $\tau \propto \sqrt{T}$. (Right picture) Mean free path dependence from the inverse of the density; the continuous line is a linear interpolation as provided by the Statistical Mechanics Theory

thermodynamic equilibrium of pressure (7): this is illustrated by the numerical results shown in Fig. 7, where we have divided the system into 50 slices and computed both the local density and temperature of the gas particles. The stochastic differential equation (9) assumes a dependence of the collision time $\tau \propto \sqrt{T}$ that introduces a position dependence of the drift coefficient when a temperature gradient is present (see Fig. 8 left). We have also checked that the mean free path is proportional to the inverse of the local density so that it scales proportionally to the local temperature (see Figs. 7 and 8 right). Finally we introduced 100 test massive particles in the central position $x = .5$ and we have computed the evolution of the average position to check if there can be observed a drift toward the cold barrier during the relaxation process in the NESS state. The numerical results shown in Fig. 9 do not allow to conclude that the test particle dynamics is described by the stochastic differential equation (9) but there is a local negative drift that seems to be statistically relevant.

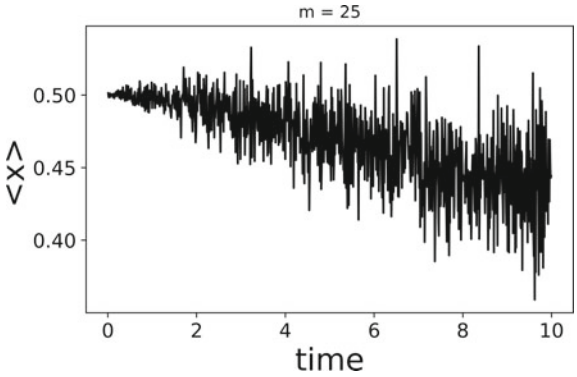

Fig. 9 Evolution of the average position for the ensemble of 100 massive test particles introduced in the hard sphere gas with a temperature gradient $T \in [.1, 1]$. The initial position is at $x = .5$. The simulations suggest the existence of an average drift toward the cold barrier

4 Conclusions

The aim of this work is to study how the stochastic dynamical systems can contribute to understand some aspects of the non-equilibrium statistical physics. We have briefly introduced simple concepts of collision theory that justify the use of stochastic differential equations in the simulation of the Brownian motion of a test particle in a thermal bath produced by a gas of elastic particles. We have proposed to extend this approach to study the dynamics of a massive test particle in the thermal bath where a temperature gradient is present. This extension is consistent with a thermodynamics description of the system assuming a local equilibrium condition, only if we interpret the stochastic differential equations according to Stratonovich. The theoretical approach points out as a massive particle has a long transient regime in which a average drift effect toward the colder region is observed. This is interpreted as the consequence of the non-local character of the collisions dynamics when one considers finite dimensional particles. In such a way, we prove that the stochastic model is able to describe a thermophoresis phenomenon. due to the long time correlation in the dynamics without the intervention of an external force. We take advantage from a simulation code able to integrate exactly the hard sphere dynamics of ensemble of 2d-particles and we have performed a first validation of the assumptions that justify the stochastic model. The simulations show that a thermodynamics approach related to the existence of a local equilibrium is realized even in presence of a temperature gradient. These results could be interesting to understand the problem connected to the NESS formation and the local Entropy production [2]. Moreover the simulations point out the existence an average drift toward the colder barrier for an ensemble of massive particles. Such a phenomenon could be interesting in biochemical reactions where large molecules move in a thermal bath (usually defined by water molecules) and the particles dimension is not negligible when a temperature gradient is present.

References

1. Schadschneider, A., Chowdhury, D., Nishinari, K.: Stochastic Transport in Complex Systems, 1st edn. Elsevier Science (2010)
2. Jiang, D.-Q., Qian, M., Qian, M.-P.: Mathematical Theory of Nonequilibrium Steady States. Lecture Notes in Mathematics, Springer, Berlin Heidelberg (2004)
3. Jaynes, E.T.: The Minimum Entropy Production Principle. Ann. Rev. Phys. Chem. **31**, 579–601 (1980)
4. Seifer, U.: Stochastic thermodynamics: principles and perspective. Eur. Phys. J. B **64**(3–4), 423 (2008)
5. Chena, L.Y.: Nonequilibrium fluctuation-dissipation theorem of Brownian dynamics. J. Chem. Phys. **129**(14), 144113 (2008)
6. Moreau, M.: On the derivation of the Onsager relations from the Master equation. Lett. Math. Phys. **1**, 715 (1975)
7. Arnold, L.: Stochastic Differential Equations Theory and Applications. Dover Publications (2013)
8. Duhr, S., Braun, D.: Why molecules move along a temperature gradient. PNAS **103**(52), 19678–19682 (2006)
9. Monti, M., Montanari, C.E.: Getting started with NOCS. https://githib.com/carlidel/pynocs (2019)
10. Seifert, U.: Stochastic thermodynamics: principles and perspectives. Eur. Phys. J. B **64**, 423431 (2008)
11. Landau, L.D., Lifshitz, E.M.: Course of Theretical Physics: Statistical Mechanics. Pergamon Press (1980)
12. Simányi, N.: Ergodicity of hard spheres in a box. Ergodic Theory Dyn. Syst. **19**(3), 741–766 (1999)

Electromagnetic Waves in Non-local Dielectric Media: Derivation of a Fractional Differential Equation Describing the Wave Dynamics

Alessandro Cardinali

Abstract The dielectric susceptibility of a wide class of dielectric materials like magnetized laboratory and astrophysical plasmas, which are non local in space, characterizes an integral relation between the polarization **P** and the electric field **E** of the propagating electromagnetic perturbation. The electromagnetic fields in such dielectric media are described by fractional differential equations with space derivatives of non-integer order. In this paper an attempt to derive the fractional differential equation from the Maxwell equation system for the quasi-longitudinal waves propagating in an unmagnetized plasma like the Lower Hybrid (LH) waves (also useful in the Thermonuclear Fusion Research domain) or the Langmuir waves is outlined. Extrapolation of the method can also been considered for magnetized plasma. A one-dimensional example of fractional wave equation is given and new family of analytical solutions has been found.

Keywords Fractional wave equation · Wave propagation in non-local media · Electromagnetic wave in anisotropic media · Plasma dielectric tensor

1 Introduction

The propagation of electromagnetic waves in laboratory, astrophysical and ionosphere plasmas has captured the attention of scientists since the fifty years of the past century (Budden [1], Stix[2]). The starting point was the differential system of equations (Maxwell equation) coupled to the Vlasov equation solved for the perturbative electric field when produce some perturbation on the plasma characterized by a Maxwellian distribution function at the equilibrium. The solution of the Maxwell-Vlasov equation system for unbounded, homogeneous and stationary plasma immersed in a static magnetic field can be obtained by Fourier analysis of the electromagnetic perturbative field, and a constitutive relation between the current density $\vec{J} = \underline{\underline{\sigma}} \cdot \vec{E}$ (or alternatively the polarization $\vec{P} = \underline{\underline{\chi}} \cdot \vec{E}$ or the displacement

A. Cardinali (✉)
ENEA FSN, C.R. Frascati, Via E. Fermi, 45, 00044 Frascati (Rome), Italy
e-mail: alessandro.cardinali@enea.it

L. Beghin et al. (eds.), *Nonlocal and Fractional Operators*, SEMA SIMAI Springer Series 26, https://doi.org/10.1007/978-3-030-69236-0_4

$\vec{D} = \vec{E} + \vec{P} = \vec{E} + \underline{\underline{\chi}} \cdot \vec{E} = \underline{\underline{\varepsilon}} \cdot \vec{E}$), can be found in the form of a tensor of rank 2. In the case of homogeneous plasma the properties of the tensors does not depend on the relative position in space and time, and space and time locality is preserved. The problem arises when the plasma must be considered inhomogeneous; in this case the tensor above is depending on the space at position **r** and **r'** (and time t, and t') separately and the non-locality of space and time must be accounted. In this paper we propose a derivation of a proper wave equation both by following the classical method i.e. by preserving the integer order of the derivatives of the wave differential operator or, alternatively, by deriving a fractional wave operator. An example based on a suitable simplification of the model is given to clarify and compare both approaches. In Sec. II the context of the physical problem and the consequent mathematical model is proposed and the solution in the "classical approach" is given and discussed. In Sec III the "fractional operator approach" is proposed for the same physical problem and a general wave equation with a "fractional Laplacian" is obtained. In Sec. IV simple 1D example is given togheter with its solution. In sec. V there are some remarks and we draw conclusions.

2 The Model "Classical Approach"

The propagation of an electromagnetic perturbation in bounded and non-homogenous plasma is described in longitudinal approximation $\left(\vec{E}||\vec{k}\right)$ by the Poisson equation,

$$\nabla \cdot \vec{E}(\vec{r}) = 4\pi\rho_{pol}(\vec{r}) \tag{1}$$

where $\vec{E}(\vec{r},\omega) = \vec{E}(\vec{r})e^{-i\omega t}$ is the electric field of a time-harmonic perturbation, the charge polarization can be written as $\rho_{pol} = -\nabla \cdot \vec{P}$, in terms of the polarization vector. If we define the displacement $\vec{D} = \vec{E} + 4\pi\vec{P}$, it is possible to write the Poisson's equation like $\nabla \cdot \vec{D}(\vec{r}) = 0$ where an integral relation relates **D** and **E**.

$$\vec{D}(\vec{r}) = \int d\vec{r}'\varepsilon\left(\vec{r},\vec{r}',\omega\right)\vec{E}\left(\vec{r}'\right) \tag{2}$$

where $\varepsilon\left(\vec{r},\vec{r}',\omega\right)$ is the electric permittivity that in an inhomogeneous medium like the plasma contains information on the non-locality of the space. Note that **D** depends on the condition away from the point **r,** i.e. **r'** (non-locality). When the plasma perturbed by the field under consideration is infinite and homogeneous the permittivity is independent on **r** and **r'** separately, This means that we can write the permittivity $\varepsilon\left(\vec{r}-\vec{r}'\right)$ depending only on $\left(\vec{r}-\vec{r}'\right)$, and therefore the relation Eq. (2) becomes

$$\vec{D}(\vec{r}) = \int d\vec{r}'\varepsilon\left(\vec{r}-\vec{r}',\omega\right)\vec{E}\left(\vec{r}'\right) \tag{3}$$

By analyzing in Fourier $\vec{E}(\vec{r}) = \int d\vec{k}\vec{E}_{\vec{k}}e^{i\vec{k}\cdot\vec{r}}$, $\vec{D}(\vec{r}) = \int d\vec{k}\vec{D}_{\vec{k}}e^{i\vec{k}\cdot\vec{r}}$ we got the following relation $\vec{D}_{\vec{k}} = \varepsilon_{\vec{k}}\vec{E}_{\vec{k}}$, where

$$\varepsilon_{\vec{k}} = \varepsilon\left(\vec{k},\omega\right) = \int d\vec{R}\varepsilon\left(\vec{R},\omega\right)e^{-i\vec{k}\cdot\vec{R}} \tag{4a}$$

and $\vec{R} = \vec{r}' - \vec{r}$. The Poisson Equation in this case reduces to an algebraic equation (the dispersion relation)

$$\varepsilon\left(\vec{k},\omega\right) = 0. \tag{4b}$$

The electric permittivity or dielectric function can be calculated by the Poisson-Vlasov system of equations for homogeneous, stationary and unbounded plasma (see for the details Ref. [3]), and it reads

$$\varepsilon(k,\omega) = 1 + \frac{2\omega_{p\alpha}^2}{k^2 v_{th\alpha}^2}\left[1 + \frac{\omega}{k v_{th\alpha}}Z\left(\frac{\omega}{k v_{th\alpha}}\right)\right] \tag{5}$$

where ω is the frequency of the electromagnetic perturbation, $\omega_{p\alpha} = \sqrt{\frac{4\pi n_\alpha Z_\alpha^2 e^2}{m_\alpha}}$ the plasma frequency, α is the species under consideration (electrons, ions) n_α the density, Z_α the charge and m_α the mass; $v_{th\alpha} = \sqrt{\frac{\kappa T_\alpha}{m_\alpha c}}$ is the thermal velocity, T_α is the temperature of the species; $Z\left(\frac{\omega}{k v_{th\alpha}}\right)$ is the plasma dispersion complex function: $Z(\zeta) = \frac{1}{\sqrt{\pi}}\int_{-\infty}^{+\infty} dt \frac{exp(-t^2)}{t-\zeta}$ [4]. In the case of weak inhomogeneity the situation is much more complicated. As suggested in Refs. [5, 6] to keep into account the space non-locality we can write

$$\vec{D}(\vec{r}) = \int d\vec{r}'\varepsilon\left(\vec{r},\vec{r}',\omega\right)\vec{E}\left(\vec{r}'\right) = \int d\vec{r}'\varepsilon\left(\vec{r}-\vec{r}',\frac{\vec{r}+\vec{r}'}{2},\omega\right)\vec{E}\left(\vec{r}'\right) \tag{6}$$

where we have considered a weak variation of the permittivity with respect to the space. If we use the Ansatz $\vec{D}(\vec{r}) = \int d\vec{k}\vec{D}_{\vec{k}}(\vec{r})e^{i\vec{k}(\vec{r})\cdot\vec{r}}$, and $\vec{E}\left(\vec{r}'\right) = \int d\vec{k}\vec{E}_{\vec{k}}\left(\vec{r}'\right)e^{i\vec{k}(\vec{r}')\cdot\vec{r}'}$, where $\vec{k}(\vec{r})$ varies on much faster radial scale with respect to the amplitude $\vec{E}_{\vec{k}}(\vec{r})$, and use it in Eq. (6) we have

$$\vec{D}_{\vec{k}}(\vec{r}) = \int d\vec{r}'\varepsilon\left(\vec{r}-\vec{r}',\frac{\vec{r}+\vec{r}'}{2}\right)\vec{E}_{\vec{k}}\left(\vec{r}'\right)e^{i\vec{k}\cdot[\vec{r}'-\vec{r}]} \tag{7}$$

This is a constitutive relation between the displacement and the electric field in the case of weekly inhomogeneous plasma in which the space non-locality is negligible. Omitting the dependence on ω in both permittivity and electric field, and putting $\vec{R} = \vec{r} - \vec{r}'$, and $\frac{\vec{r}+\vec{r}'}{2} = \vec{r} - \frac{\vec{R}}{2}$ we can expand the electric field and the permittivity as

$$\vec{E}\left(\vec{r}', \vec{k}\right) \approx \vec{E}_{\vec{k}}(\vec{r}) - \vec{R} \cdot \nabla \vec{E}_{\vec{k}}(\vec{r}) + ... \tag{8a}$$

and

$$\varepsilon\left(\vec{r} - \vec{r}', \frac{\vec{r} + \vec{r}'}{2}\right) = \varepsilon\left(\vec{R}, \vec{r} - \frac{\vec{R}}{2}\right) \approx \varepsilon\left(\vec{R}, \vec{r}\right) - \frac{\vec{R}}{2} \cdot \nabla \varepsilon\left(\vec{R}, \vec{r}\right) + ... \tag{8b}$$

substituting Eqs. (8a) and (8b) in the previous Eq. (7) and considering the following identities and definitions:

$$\frac{\vec{R}}{2} \cdot \nabla \varepsilon\left(\vec{R}, \vec{r}\right) = \frac{1}{2} \nabla \cdot \left[\vec{R} \varepsilon\left(\vec{R}, \vec{r}\right)\right] \tag{9a}$$

$$\varepsilon_{\vec{k}}(\vec{r}) = \int d\vec{R} \varepsilon\left(\vec{R}, \vec{r}\right) e^{-i\vec{k}\cdot\vec{R}} \tag{9b}$$

$$\frac{\partial \varepsilon_{\vec{k}}(\vec{r})}{\partial \vec{k}} = \frac{\partial}{\partial \vec{k}} \int d\vec{R} \varepsilon\left(\vec{R}, \vec{r}\right) e^{-i\vec{k}\cdot\vec{R}} = -i \int d\vec{R} \vec{R} \varepsilon\left(\vec{R}, \vec{r}\right) e^{-i\vec{k}\cdot\vec{R}} \tag{9c}$$

where in points arbitrarily close to $\vec{r}$, $\vec{k}(\vec{r}) \sim const$; neglecting the second order terms in the expansion we have at the lowest and first order:

$$\vec{D}_{\vec{k}}(\vec{r}) = \varepsilon_{\vec{k}}(\vec{r}) \vec{E}_{\vec{k}}(\vec{r}) - i \frac{\partial \varepsilon_{\vec{k}}(\vec{r})}{\partial \vec{k}} \cdot \nabla \vec{E}_{\vec{k}}(\vec{r}) - \frac{i}{2} \left[\nabla \cdot \frac{\partial \varepsilon_{\vec{k}}(\vec{r})}{\partial \vec{k}}\right] \vec{E}_{\vec{k}}(\vec{r}) \tag{10}$$

Inserting now $\vec{D}(\vec{r}) = \int d\vec{k} \vec{D}_{\vec{k}}(\vec{r}) e^{i\vec{k}\cdot\vec{r}}$ in the Poisson's equation and using the electrostatic potential $\vec{E}(\vec{r}) = -\nabla \Phi(\vec{r})$ instead of the electric field we have at the lowest and first order in $\mathbf{R}$

$$\varepsilon_{\vec{k}}(\vec{r}) k^2 \Phi_{\vec{k}}(\vec{r}) = 0 \tag{11}$$

and at the first order

$$\left(\frac{\partial \varepsilon_{\vec{k}}(\vec{r})}{\partial \vec{k}} \cdot \nabla \Phi_{\vec{k}}(\vec{r})\right) + \frac{1}{2} \left(\nabla \cdot \frac{\partial \varepsilon_{\vec{k}}(\vec{r})}{\partial \vec{k}}\right) \Phi_{\vec{k}}(\vec{r}) = 0 \tag{12}$$

As it is possible to see at the lowest order the wave equation reduces to a simple algebraic equation $\varepsilon_{\vec{k}}(\vec{r}) = 0$ which, at constant ω, correlates the wavevector $\vec{k}$ to the space $\vec{r}$, like in the homogeneous case Eq. (4b) this is the so-called local homogeneous dispersion relation. At the next order a partial differential equation Eq. (12) for the scalar potential is derived which takes into account the slow variation of the potential with space.

In order to illustrate the feature of these equations we can distinguish several cases. As first step the dielectric function (permittivity) of Eq. 5 can be expanded for small temperature $\zeta = \frac{\omega}{k v_{th\alpha}} >> 1$. The asymptotic expression reads like a polynomial function in $\zeta^{-1} = \frac{k v_{th\alpha}}{\omega} << 1$:

$$\begin{aligned}\varepsilon(\omega, k) \approx & 1 - \frac{\omega_{p\alpha}^2}{\omega^2}\left[1 + \frac{3}{2}\left(\frac{k v_{th\alpha}}{\omega}\right)^2 + \frac{15}{4}\left(\frac{k v_{th\alpha}}{\omega}\right)^4 + \ldots.\right] \\ & + i\frac{\omega}{k v_{th\alpha}}\frac{\omega_{p\alpha}^2}{(k v_{th\alpha})^2}\sqrt{\pi}\, e^{-\left(\frac{\omega}{k v_{th\alpha}}\right)^2}\end{aligned} \tag{13}$$

In this limit the complex susceptibility function results split in a real part which accounts for the propagation of the wave and an imaginary part for the plasma absorption of the wave (e.g. Landau damping, etc.). First of all in the case of non-dispersive plasma ($\varepsilon_{\vec{k}}(\vec{r})$ not depending on $\vec{k}$ e.g. cold plasma limit $T \to 0$), the Eq. (11) reduces to

$$\varepsilon(\omega, \vec{r}) = 1 - \frac{\omega_{p\alpha}^2(\vec{r})}{\omega^2} = 0 \tag{14}$$

which is the condition to have non-trivial solutions of Eq. (11); where the dielectric function in this limit reads: $\varepsilon(\omega) = 1 - \frac{\omega_{p\alpha}^2}{\omega^2}$ (cfr Eq. 13). Solution of Eq. (11) are the so-called plasma oscillations (or Langmuir waves) $\omega^2 = \omega_{p\alpha}^2$. At the lowest order in temperature we have:

$$\varepsilon(\omega, k, \vec{r}) \approx 1 - \frac{\omega_{p\alpha}^2}{\omega^2} - \frac{3}{2}\frac{\omega_{p\alpha}^2 k^2 v_{th\alpha}^2}{\omega^4} = 0 \tag{15}$$

whose solution is

$$\omega^2 = \omega_{p\alpha}^2(\vec{r}) + \frac{3}{2}k^2 v_{th\alpha}^2(\vec{r}) \tag{16}$$

In the case of dielectric function given by Eq. (15) it is possible to solve Eq. (12) for the slow variationof the scalar potential in one-dimensional space (1D). In this case Eq. (12) can be written as

$$\frac{d\varepsilon_{\vec{k}}(r,k)}{dk}\frac{d\Phi_{\vec{k}}(r)}{dr}+\frac{1}{2}\frac{d}{dr}\left(\frac{d\varepsilon_{\vec{k}}(r,k)}{dk}\right)\Phi_{\vec{k}}(r)=0 \tag{16bis}$$

It easy to find the solution of Eq. (16bis) by a simple analytical quadrature

$$\Phi_{\vec{k}}(r)=\Phi_{\vec{k}}(0)\sqrt{\frac{\left(d\varepsilon_{\vec{k}}(r,k)/dk\right)_0}{d\varepsilon_{\vec{k}}(r,k)/dk}}=\Phi_{\vec{k}}(0)\frac{T_{\alpha 0}}{T_\alpha(r)}\sqrt{\frac{n_{\alpha 0}}{n_\alpha(r)}\frac{k_0}{k(r)}} \tag{17}$$

where we have used Eq. (15) and the definiton of plasma frequency and thermal velocity. Equation (17) shows that a slow variation of the potential can be accounted by the theory developed before, depending on the space through density and temperature as well as the wavevector.

It is clear that when the dispersion is not included in the electric permittivity (cold plasma) the equation in both local and non-local aproach reduces to an algebraic equation which correlates the frequency to to the plasma frequency (cold Langmuir waves). When the temperature effects are included in the electric permittivity (dispersion) the effect of non-locality becomes important. At the lowest order we obtain an algebraic equation that correlates the frequency to the plasma frequency with some correction due to the temperature effect which is responible of the appearance of the wavevector. At the next order the behaviour of the scalar potential with the space can be established by solving Eq. (17).

3 Fractional Operator Approach

In this Section we try to outline a fractional differential equation approach to the problem of the propagation of the Langmuir wave in an inhomogeneous plasma by overcoming the weak inhomogeneous formulation outlined in Sec. II. To this end, combining the Poisson equation and the expression of the dielectric function Eq. (13) it is possible to obtain a wave equation by an inverse Fourier transform (which holds only in the case of homogeneous infinite plasma). It is also possible to deduce a dielectric function such that it admits solutions of type Eq. (16). The dielectric function can be written in terms of the Debye length $\lambda_{De\alpha}$, the plasma frequency and the frequency, and is written in a power-law form which results very similar to the electric permittivity studied in the paper in Ref. [7]

$$\varepsilon(\omega,k)=1-\frac{\omega^4}{3\omega_{p\alpha}^4(\lambda_0 k_0)^2\overline{\lambda}_{De\alpha}^2\overline{k}^2}\left(1-\frac{\omega_{p\alpha}^2}{\omega^2}\right)=1-\frac{f\left(\omega,\omega_{p\alpha}\right)}{\overline{\lambda}_{De\alpha}^2\overline{k}^2} \tag{18}$$

with

$$f = \frac{\omega^4}{3\omega_{p\alpha}^4 (\lambda_0 k_0)^2}\left(1 - \frac{\omega_{p\alpha}^2}{\omega^2}\right) \tag{19}$$

where λ_0 and $k_0 = \frac{\omega}{c}$ are normalization constants. As suggested in Ref. [7] this simple form of the permittivity allows us to consider non-locality by introducing a generalization of the permittivity which has a power law form. Hence we can generalize the equation by deforming the two terms in the permittivity above such as

$$\varepsilon(\omega, k) = \left|\vec{k}\right|^{\alpha-2} - \frac{f\left(\omega, \omega_{p\alpha}\right)}{\bar{\lambda}_{De\alpha}^{-2}\left|\vec{k}\right|^{2-\beta}} \tag{20}$$

The parameter α characterizes the deviation from Coulomb law due to non-local property of the medium and the parameter β the deviation from the Debye's screening. Note that in this case the plasma is characterized by zero free charge $\rho_{free} = 0$ (neutrality). And the only charge present in the Poisson's equation is the polarization charge. Using the inverse Fourier transform we have:

$$\left((-\Delta)^{\alpha/2}\Phi\right)(\vec{r}) - \frac{f\left(\omega, \omega_{p\alpha}\right)}{\bar{\lambda}_{De\alpha}^{-2}}\left((-\Delta)^{\beta/2}\Phi\right)(\vec{r}) = 0 \tag{21}$$

If $\beta = 0$ we have to solve the fractional equation:

$$\left((-\Delta)^{\alpha/2}\Phi\right)(\vec{r}) - \frac{f\left(\omega, \omega_{p\alpha}\right)}{\bar{\lambda}_{De\alpha}^{-2}}\Phi(\vec{r}) = 0 \tag{22}$$

where $(-\Delta)^{\alpha/2}$ is the Riesz fractional Laplacian Ref. [7] defined as:

$$(-\Delta)^{\alpha/2}\Phi(\vec{r}) = \Im^{-1}\left(\left|\vec{k}\right|^{\alpha}(\Im\Phi)\left(\vec{k}\right)\right) \tag{23}$$

written in terms of the Fourier transform $\Im$. For $\alpha = 2$ the classical result is obtained:

$$\Delta\Phi(\vec{r}) + \frac{f\left(\omega, \omega_{p\alpha}\right)}{\bar{\lambda}_{De\alpha}^{-2}}\Phi(\vec{r}) = 0 \tag{24}$$

which is the classical Laplace equation for the scalar potential which describes the propagation of the Langmuir waves.

4 The 1D Fractional Wave Equation

In the 1D case where the variation of the potential depends on the one single coordinate x, a fractional 1D wave equation is obtained. This is similar to the fractional linear oscillator, where the constant term $\kappa \equiv \sqrt{\frac{f(\omega,\omega_{p\alpha})}{\bar{\lambda}^2_{D e\alpha}}}$, is the inverse of an a dimensional wavelength, or more generally the normalized frequency of the mechanical oscillator. The fractional stationary wave equation can be written as

$$ {}_a^C D_x^\alpha \Phi(x) + \kappa^2 \Phi(x) = 0 \tag{25} $$

where $0 < \alpha \leq 2$ and

$$ {}_a^C D_x^\alpha \Phi(x) \equiv \frac{d^\alpha \Phi(x)}{dx^\alpha} = \frac{1}{\Gamma(n-\alpha)} \int_a^x \frac{\Phi^n(\xi)}{(x-\xi)^{\alpha+1-n}} d\xi \tag{26} $$

which is the "Caputo" formula Ref. [8] to calculate the derivative. The initial-value for Eq. (25) can be viewed as a linear initial value problem where $x > a$, $n-1 < \alpha < n$, and $\Phi^{(k)}(a) = b_k \in \Re$, $k = 0, ..., n-1$. In contrast for example to the Riemann–Liouville fractional derivative, when solving differential equations, it is not necessary to define the fractional order initial conditions. This kind of equation has been extensively studied in literature [9–11], the solution of the problem Eq. (25) is given by

$$ \Phi(x) = \sum_{k=0}^{n-1} b_k x^k E_{\alpha,k+1}\left(-\kappa^2 x^\alpha\right) \tag{27} $$

where $E_{\alpha,\beta}$ is the two parameter function Mittag–Leffler function. During the recent years the Mittag–Leffler function has caused extensive interest among physicist due to its role played in describing realistic physical systems with memory and delay. The Mittag–Leffler function is defined by the series

$$ E_{\alpha,\beta}(z) = \sum_{k=0}^{\infty} \frac{z^k}{\Gamma(\alpha k + \beta)} \tag{28} $$

Therefore the Mittag–Leffler function is a generalization of the exponential when $a = 1$ and $b = 1$. The solution of the classical second order equation coincides with the solution of the fractional IVP equation for value of $\alpha \to 2$. In the classical case the equation is

$$\frac{d^2\Phi(x)}{dx^2} + \kappa^2\Phi(x) = 0 \tag{29}$$

whose general solution can be written as

$$\Phi(x) = b_0 E_{2,1}\left(-\kappa^2 x^2\right) + b_1 E_{2,2}\left(-\kappa^2 x^2\right) = b_0 cosh\left(\sqrt{-\kappa^2 x^2}\right) + b_1 \frac{sinh\left(\sqrt{-\kappa^2 x^2}\right)}{\sqrt{-\kappa^2 x^2}} \tag{30}$$

where b_0 and b_1 are constants fixed with the initial conditions. Coming back to the solution of the fractional equation Eq. (27) being $0 < \alpha \leq 2$, we can deduce that n at most can reach the value 2. In this case

$$\Phi(x) = b_0 E_{\alpha,1}\left(-\kappa^2 x^\alpha\right) + b_1 x E_{\alpha,2}\left(-\kappa^2 x^\alpha\right) \tag{31}$$

Equation (31) represents the solution of the potential induced by an electromagnetic perturbation which propagates in a plasma medium.

5 Conclusions

In this paper a derivation of a fractional wave equation has been obtained, which is valid in an isotropic plasma when the space non-locality is taken into account. In the first part the classical approach to take into account the non-locality based on a WKB expansion of the electric field is illustrated. The second part is related to a generalization of the Laplace operator to a "fractional" one and a 1D fractional wave equation is derived which describes the propagating plasma wave valid in the non-locality case. The wave is similar in structure to the one-dimensional fractional mechanical oscillator and an analytical solution can be given in terms of the Mittag–Leffler functions.

Appendix 1. Derivation of the Integral Wave Equation for Wave Propagation in Non-Homogeneous Plasma

A valid equation describing the propagation of an electromagnetic wave in longitudinal approximation, in an isotropic and non-homogeneous plasma can be derived from the Poisson-Vlasov model, showing the non-locality of the process. The electromagnetic wave can be considered a perturbation which propagates in a Maxwellian background plasma, and for this reason the model results to be linear. The equation system under consideration is

$$\nabla \cdot \vec{E}(\vec{r}) = 4\pi q \int_{-\infty}^{+\infty} f^1(\vec{v}, \vec{r}, t) d\vec{v} \tag{1A}$$

The Poisson's equation, and f^1 is the perturbed distribution function of the particle species. The linearized distribution function satisfies the Vlasov statistical equation

$$\frac{df^1(\vec{r}, \vec{v}, t)}{dt} \equiv \frac{\partial f^1}{\partial t} + \vec{v} \cdot \frac{\partial f^1}{\partial \vec{r}} = -\frac{q}{m} \vec{E}(\vec{r}) \cdot \frac{\partial f^0(v)}{\partial \vec{v}} \tag{2A}$$

Combining Eqs. (1A) and (2A) we have the following single integral–differential equation for the electric field

$$\nabla \cdot \vec{E}(\vec{r}) = -\frac{4\pi q^2}{m} \int_{-\infty}^{+\infty} d\vec{v} \int_{-\infty}^{t} \vec{E}(\vec{r}') \cdot \frac{\partial f_0(\vec{v})}{\partial \vec{v}'} e^{-i\omega(t'-t)} dt' \tag{3A}$$

where we have considered a harmonic perturbation in time. This equation must be integrated along the characteristics lines, that in this case have a simple analytical solution

$$\begin{aligned} &\vec{r} - \vec{r}' = \vec{v}(t - t') \\ &\vec{v}' = \vec{v} = const \end{aligned} \tag{4A}$$

where $\vec{v}$ is a constant vector. Introducing the variable $T = t' - t$, and for weak non-locality we can expand the field around the position $\vec{r}' = \vec{r} + \delta\vec{r}$ with $\delta\vec{r} = \vec{v}T$. We have

$$E_i(\vec{r}') \approx E_i(\vec{r}) + \underline{\underline{g}}_i^T \cdot \delta\vec{r} + \frac{1}{2} \delta\vec{r}^T \underline{\underline{H}}_i \cdot \delta\vec{r} + \varepsilon\left(\|\delta\vec{r}\|^3\right) + ... \tag{5A}$$

where $\underline{\underline{g}}_i^T$ is the transpose of the Jacobian Matrix defined over the vector field **E**:

$$\underline{\underline{g}}^T = \begin{bmatrix} \frac{\partial E_1}{\partial x_1} & \frac{\partial E_1}{\partial x_2} & \frac{\partial E_1}{\partial x_3} \\ \frac{\partial E_2}{\partial x_1} & \frac{\partial E_2}{\partial x_2} & \frac{\partial E_2}{\partial x_3} \\ \frac{\partial E_3}{\partial x_1} & \frac{\partial E_3}{\partial x_2} & \frac{\partial E_3}{\partial x_3} \end{bmatrix} \tag{6A}$$

and H is the Hessian which is a tensor of rank 3. Note that the Hessian matrix of a single component of the field $\underline{\underline{H}}_i$ can be obtained as the Jacobian matrix of the gradient vector of $E_i(\vec{r})$.

$$\underline{\underline{H}}_i = \begin{bmatrix} \frac{\partial^2 E_i}{\partial x_1^2} & \frac{\partial^2 E_i}{\partial x_1 \partial x_2} & \frac{\partial^2 E_i}{\partial x_1 \partial x_3} \\ \frac{\partial^2 E_i}{\partial x_2 \partial x_1} & \frac{\partial^2 E_i}{\partial x_2^2} & \frac{\partial^2 E_i}{\partial x_2 \partial x_3} \\ \frac{\partial^2 E_i}{\partial x_3 \partial x_1} & \frac{\partial^2 E_i}{\partial x_3 \partial x_2} & \frac{\partial^2 E_i}{\partial x_3^2} \end{bmatrix} \tag{7A}$$

The third order term in Eq. (5A) involves a tensor of rank 4 and so on! Eq. (3A) at the lowest order becomes

$$\nabla \cdot \vec{E}(\vec{r}) = -\frac{4\pi q^2}{m} \int_{-\infty}^{+\infty} d\vec{v} \left[\vec{E}(\vec{r}) \cdot \frac{\partial f_0(\vec{v})}{\partial \vec{v}} \right] \frac{i}{\omega} \tag{8A}$$

Assuming a spherical coordinate system (isotropy) for the integral over the velocity and assuming a Maxwellian distribution function

$$f_0(\vec{v}) = \frac{n_0}{\pi^{3/2} v_{the}^3} e^{-\frac{v^2}{v_{the}^2}} \tag{9A}$$

it is easy to show that the rhs of Eq. (8A) is zero after performing the integral over the velocity space. At the next order we have

$$\nabla \cdot \vec{E}(\vec{r}) = -\frac{4\pi q^2}{m} \int_{-\infty}^{+\infty} d\vec{v} \underline{\underline{g}}_i^T \cdot \vec{v} \cdot \frac{\partial f_0(\vec{v})}{\partial \vec{v}} \int_{-\infty}^{0} T e^{-i\omega T} dT \tag{10A}$$

Evaluating the various integrals on time and velocity space (after choosing a spherical coordinate system which is coherent with isotropy), we obtain the following wave equation

$$\left(1 - \frac{\omega_{p\alpha}^2}{\omega^2}\right) \nabla \cdot \vec{E}(\vec{r}) = 0 \tag{11A}$$

This is the same result we have obtained in Section II Eqs. (11) and (14). Note that the integral on time can be easily evaluated to give $\int_{-\infty}^{0} T e^{-i\omega T} dT = \frac{1}{\omega^2}$, for imaginary $\omega^I > 0$. To the next order it is possible to show (by a heavy algebra) that there is no contribution to the wave equation. To find a further contribution to the wave equation is necessary to go to the third order in the field expansion, we obtain

$$\nabla \cdot \vec{E}(\vec{r}) = \frac{\omega_{p\alpha}^2}{\omega^2} \nabla \cdot \vec{E}(\vec{r}) + \frac{3}{2} \frac{\omega_{p\alpha}^2 v_{th\alpha}^2}{\omega^4} \nabla^2 \left(\nabla \cdot \vec{E}(\vec{r}) \right) \tag{12A}$$

The exact solution of Eq. (12A) involves a heavy algebra when performing the integral on the velocity volume. The surviving non zero terms can be collected to give

the operator $\nabla^2\left(\nabla\cdot\vec{E}(\vec{r})\right)$. Introducing the scalar potential we have the following equation to be solved:

$$\nabla^2\Phi(\vec{r}) = \frac{\omega_{p\alpha}^2}{\omega^2}\nabla^2\Phi(\vec{r}) + \frac{3}{2}\frac{\omega_{p\alpha}^2 v_{th\alpha}^2}{\omega^4}\nabla^4\Phi(\vec{r}) \tag{13A}$$

This equation in principle can be solved by setting $f := \nabla^2\Phi(\vec{r})$, and obtaining the system

$$\begin{aligned} a\nabla^2 f + bf &= 0 \\ \nabla^2\Phi &= f \end{aligned} \tag{14A}$$

where in our case $a = \frac{3}{2}\frac{\omega_{p\alpha}^2 v_{th\alpha}^2}{\omega^4}$, and $b = 1 - \frac{\omega_{p\alpha}^2}{\omega^2}$, and under prescribed boundary conditions one can solve successively for f and then for Φ. It is easy from this equation to deduce the dispersion relation when considering an infinite homogeneous plasma. In this case the scalar potential can be written as $\Phi(\vec{r}) = \Phi_{\vec{k}}e^{i\vec{k}\cdot\vec{r}}$, and the dispersion relationion is

$$\varepsilon(\omega, k) \approx 1 - \frac{\omega_{p\alpha}^2}{\omega^2} - \frac{3}{2}\frac{\omega_{p\alpha}^2 k^2 v_{th\alpha}^2}{\omega^4} = 0 \tag{15A}$$

which is similar to the Eq. (15) of Sec. II.

References

1. Budden, K.G.: Radio Waves in the Ionosphere. Cambridge University Press (1961)
2. Stix, T.H.: Waves in Plasmas. American Institute of Physics, New York (1992)
3. Swanson, D.G.: Plasma Waves. IoP Publishing, Bristol (2003)
4. Fried, B.D., Conte, S.D.: The Plasma Dispersion Function: The Hilbert Transform of the Gaussian. Academic Press, New York NY (1961)
5. Bernstein, I.B.: Phys. Fluids **18**, 320 (1975)
6. Brambilla, M., Cardinali, A.: Plasma Phys. Contr. Fusion **24**, 1187 (1982)
7. Tarasov, V.E., Trujillo, J.J.: Ann. Phys. **334**, 1 (2013)
8. Caputo, M.: Geophys. J. Int. **13**, 529 (1967)
9. Gomez Aguilar, J.F., et. al.: Proceedings of the Romanian Academy, Series A. **17** 31 (2014)
10. Gomez Aguilar, J.F.: et al. (2012) Revista Mexicana de Fisica 58 348 (2012)
11. Yepez-Martinez, H., et al.: Lat. Am. J. Phys. Educ. **8**, 155 (2014)

Some New Exact Results for Non-linear Space-Fractional Diffusivity Equations

Arrigo Caserta, Roberto Garra, and Ettore Salusti

Abstract In this paper we reconsider the classical nonlinear diffusivity equation of real gas in an heterogenous porous medium in light of the recent studies about nonlocal space-fractional generalizations of diffusion models. The obtained equation can be simply linearized into a classical space-fractional diffusion equation, widely studied in the literature. We consider the case of a power-law pressure-dependence of the permeability coefficient. In this case we provide some useful new exact analytical results. In particular, we are able to find a Barenblatt-type solution for a space-fractional Boussinesq equation, arising in this context.

Keywords Nonlinear space-fractional diffusivity equations · Fluid flow in porous medium

1 Introduction

Mathematical modelling of gas flow propagating in porous media involves a remarkable number of difficulties, due to the possible variability of permeability and the interaction of the fluid with the medium. Moreover in some cases, the heterogeneous shape of the porous medium should be taken into account. In recent papers some discussions about the limit of validity of classical conservation of mass and Darcy law have been proposed by several authors (see for example [3, 4, 20] and references therein). In particular, in various linear models of the physics of solid earth, fractional derivative operators have been considered as useful mathematical tools to consider memory effects and trapping (by means of fractional derivatives in time) and nonlocal behavior and jumps with long tails (fractional derivatives in space).

A. Caserta
Istituto Nazionale di Geofisica e Vulcanologia, Rome, Italy

R. Garra (✉)
Dipartimento di Scienze Statistiche, "Sapienza" Università di Roma, Rome, Italy
e-mail: rolinipame@yahoo.it

E. Salusti
CNR-ISMAR, Via Fosso del Cavaliere 100, Rome 00133, Italy

L. Beghin et al. (eds.), *Nonlocal and Fractional Operators*, SEMA SIMAI Springer Series 26, https://doi.org/10.1007/978-3-030-69236-0_5

In particular fractional advection-dispersion equations have been widely studied for modeling transport processes at the Earth surface, we refer to the relevant paper by Schumer et al. [17] about this topic.

From the macroscopic point of view, time-fractional models in the physics of porous media can be heuristically based on a modified Darcy law with memory that takes into account the change in time of porosity of the medium in the interaction with the fluid (see e.g. [3] and [6]). Space-fractional models can be derived by using a generalized fractional conservation of mass, according to the approach developed by Wheatcraft and Meerschaert in [20], where fractionality results from the heterogeneity of the control volume. The most of the studies on this topic regards linear models, where nonlinear terms are completely neglected, even if they play a relevant role in many realistic problems. On the other hand linear space-time fractional models are completely motivated from the probabilistic and microscopic point of view (see e.g. [17]), while physical discussions about nonlinear models involving fractional derivatives are almost missing. We observe that in the recent mathematical literature many papers have been devoted to the study of different versions of the space-fractional porous medium equation (for example [5] and many others) and relevant results have been raised out. A derivation of nonlinear fractional models from modified physically based constitutive laws can help to better understand their utility for applications. Moreover the investigation about exact solutions in this framework can play a key-role to understand some relevant features, such as finite velocity of propagation or blow-up in finite time and so on.

The main purpose of this paper is to reconsider the classical diffusivity equation of real gas in an heterogeneous porous medium in light of the recent studies on space-fractional generalizations of diffusion models. We will firstly suggest an heuristic generalization of the diffusivity equation and then show that, under suitable assumption, this equation is simply linearizable to a linear space-fractional diffusion equation, widely studied in the literature.

Then we will consider the fractional diffusivity equation in the case of pressure-dependent permeability. In particular we analyze the high pressure regimes when the permeability growth with pressure according to a power law relation. In this way an higher order nonlinear term appears and we obtain by change of variable a fractional porous-medium type equation. In this case we provide several new explicit results by using a generalized separating variable method and the invariant subspace method. In this context, we are able to find a Barenblatt's type solution for the space-fractional Boussinesq-like equation. While in the linear fractional diffusion equation, the real order of the space-fractional derivative has a clear physical meaning in the framework of CTRW models (and therefore space-fractional diffusion models have been experimentally validated in various contexts [14]), in the nonlinear case an experimental validation is still missing. We discuss, by means of the Barenblatt's type solution, the role played by the real order of the space-fractional derivative on the velocity propagation of the pressure front. Thus we suggest the way to experimentally evaluate the order of the fractional derivative starting from the measurement of the front propagation velocity.

This result for the space-fractional porous medium type equation can have relevant applications for example in the context of the studies about fluid-induced microseismicity [18, 19]. Moreover, in Appendix C, we show that the real gas space-fractional diffusivity equation can be reduced to the porous medium-type equation in the more general case of pressure dependent coefficients, under suitable mathematical assumptions. This observation stresses the utility of the obtained results in a really general unitary theory, where both pressure-dependence of the physical coefficients and nonlocality due to heterogenity are taken into account.

The main aim of this paper is finally to provide a critical revisitation of classical diffusivity models, in light of recent studies appeared in the literature about the relation between fractional derivative and mass flux in heterogeneous media. A second concrete outcome is given by the discussion of some new explicit analytical results that are related to interesting features of the generalized diffusivity equation. This study represents in our view a first step in the analysis of non-linear non-local models in physics of solid earth.

The paper is organized as follows: in Sect. 2 we briefly recall the meaning and derivation of the real gas diffusivity model and its generalization. In Sect. 3 we study the case of space-fractional diffusivity equation with pressure-dependent permeability and we show some exact analytical results, including a Barenblatt's type solution that can help to experimentally evaluate the real order of the fractional derivative. Three Appendices are also presented, about fractional derivatives, the invariant subspace method and the mathematical treatment of a more general space-fractional diffusivity equation.

2 The Real Gas Diffusivity Equation: Classical Models and Fractional Generalization

The main aim of this note is to reconsider classical models of real gas propagation through heterogeneous porous media in light of the recent studies about the applications of space-fractional operators for considering nonlocal effects in diffusion processes. We first give a simple derivation of the real gas diffusivity equation (see e.g. [2] and [21] for details). We will assume that the fluid flow is for simplicity in one dimension and in isothermal condition. Moreover the permeability of the medium is assumed to be constant. Let us consider the conservation of mass equation in the one-dimensional case, we have that

$$-\frac{\partial}{\partial t}\rho\phi = \frac{\partial}{\partial x}(v\rho). \tag{2.1}$$

The velocity flux is given by the classical Darcy law

$$v = -\frac{k}{\mu}\frac{\partial p}{\partial x}, \tag{2.2}$$

where μ is the fluid viscosity coefficient and k the permeability.

It is well-known that the Darcy law is a purely empirically-based law and it works well in many realistic models of fluid flow in porous media. Despite this, in many other physical cases, some modifications of the Darcy law have been successfully applied, such as the Forchheimer Law. Moreover space or time-fractional generalizations of the Darcy law have been recently studied, for example in [3] and [8]. The role of these more general forms of the Darcy law in the context here considered, should be object of further research.

In order to obtain a single equation governing the pressure field evolution, we should consider the relation between density and pressure field that is given by the following equation of state for real gas

$$\rho = \frac{M}{RT}\frac{p}{z}, \tag{2.3}$$

where M is the molecular weight of the gas, R is the universal gas constant, T the absolute temperature and z the so-called *gas deviation factor*. We recall that the gas deviation factor z is by definition the ratio of the volume actually occupied by the gas at a given pressure and temperature, to the volume occupied if it behaved ideally. In the more general case the gas deviation factor might depend by temperature and pressure. Typically the gas deviation factor is close to 1 (i.e. the gas behaves as an ideal gas) at low pressures and high temperatures, while for high pressure the gas is said to be *super-compressible*.

Substituting equations (2.2) and (2.3) in (2.1), we obtain

$$\frac{\partial}{\partial t}\left(\phi\frac{p}{z}\right) = \frac{\partial}{\partial x}\left(\frac{k}{2\mu z}\frac{\partial p^2}{\partial x}\right). \tag{2.4}$$

Since both the porosity and the gas deviation factor are pressure-dependent, we observe that

$$\begin{aligned}\frac{\partial}{\partial t}\left(\phi\frac{p}{z}\right) &= \left\{\left(\frac{\partial\phi}{\partial p}\right)\frac{p}{z} + \phi\frac{\partial}{\partial p}\left(\frac{p}{z}\right)\right\}\frac{\partial p}{\partial t}\\ &= \frac{\phi p}{z}(c_f + c_g)\frac{\partial p}{\partial t},\end{aligned} \tag{2.5}$$

where

$$c_g = \frac{z}{p}\frac{d}{dp}\left(\frac{p}{z}\right) \tag{2.6}$$

is the real gas compressibility and

$$c_f = \frac{1}{\phi}\frac{d\phi}{dp} \tag{2.7}$$

is the porous medium compressibility. Clearly these coefficients are constant only under specific assumptions on the pressure dependence of the porosity and gas deviation factor, in the general case they are pressure-dependent.

Therefore, according to the conservation of mass Eq. (2.1), we finally arrive to the diffusivity equation for real gas flow in porous medium

$$\frac{\phi}{z}(c_f + c_g)\frac{\partial p^2}{\partial t} = \frac{\partial}{\partial x}\left(\frac{k}{\mu z}\frac{\partial p^2}{\partial x}\right). \tag{2.8}$$

This is a nonlinear partial differential equation because to the general pressure dependence of the porosity ϕ and of the compressibility coefficients. Since in the general case it is not possible to find exact analytical solutions to (2.8), in the literature it is frequently assumed that the gas deviation factor z and the diffusivity coefficient $\alpha = k/(\mu\phi(c_f + c_g))$ are approximately constant. This is a strong physical assumption, that is generally valid only for short times, considering the physical parameters appearing in the diffusivity coefficient evaluated for the mean pressure over a time interval. In practice this diffusivity coefficient is frequently considered in correspondence to the initial reservoir pressure p_i.

Under this assumption, the non-linear Eq. (2.8) is linearizable by means of the simple change of variable $u(x, t) := p^2(x, t)$. In this case we therefore arrive to the linear diffusion equation

$$\phi(c_f + c_g)\frac{\partial u}{\partial t} = \frac{k}{\mu}\frac{\partial^2 u}{\partial x^2}. \tag{2.9}$$

In this paper, we consider the following space-fractional counterpart of the nonlinear Eq. (2.8), that is

$$\frac{\phi}{z}(c_f + c_g)\frac{\partial p^2}{\partial t} = \frac{\partial^\gamma}{\partial x^\gamma}\left(\frac{k}{\mu z}\frac{\partial p^2}{\partial x}\right), \quad x \geq 0, \gamma \in (0, 1). \tag{2.10}$$

involving fractional derivatives in the sense of Caputo (see Appendix A). Observe that, according to Eq. (2.10), we are considering in particular the space-fractional nonlinear nonlocal diffusion equation for a semi-infinite domain $x \geq 0$. Indeed, we replace the ordinary space derivative with a left-handed Caputo derivative, defined for $x \geq 0$. The corresponding initial and boundary conditions will be discussed when it is useful. We underline that in this paper we show that the model Eq. (2.10) admits some particular interesting exact solutions, but, in general, we don't start our analysis from an initial-boundary value problem. The choice to consider the evolution on the semi-infinite domain is motivated by the physical setting of the problem considered. Moreover this choice permits us to find simply meaningful exact mathematical results. This generalization is heuristically based on the idea that nonlocal effects, modelized by means of fractional derivatives, are not negligible in diffusivity models in porous media. A detailed physical derivation based on the application of the space-fractional conservation of mass will be object of further

investigations. The main aim of this note is to provide some new mathematical useful results on this equation.

First of all, we observe that this is one of the few cases of nonlinear fractional equations arising from physical models that are C-integrable, *i.e.* integrable by change of variable (see [9] and the references therein). Indeed, by means of the simple change of variable $u(x,t) := p^2(x,t)$ we obtain

$$\phi(c_f + c_g)\frac{\partial u}{\partial t} = \frac{k}{\mu}\frac{\partial^{1+\gamma} u}{\partial x^{1+\gamma}}. \tag{2.11}$$

Equation (2.11) is widely studied in the mathematical literature, we refer for example to [12] for a complete treatment.

It is well-known in the physical literature that this equation arises in the context of anomalous diffusion processes in models of particles dynamics where long jump distributions are considered (see for example [14]). Anomalous diffusions include a wide class of processes whose variance does not grow linearly in time, in contrast to normal diffusion.

Anomalous diffusion processes related to space-fractional diffusion equations, have found relevant applications in different fields of applied sciences, including particle advection-diffusion on Earth surface [17].

As already seen, in Eq. (2.10) we assume all the physical coefficients appearing in the diffusivity α as constant. In the next section we evaluate the role played by a power-law pressure dependent permeability in the pressure field diffusivity equation. In this case we are able to find exact solutions, even if the obtained equations have the form of space-fractional porous medium-type equations. In Appendix C we provide a simple mathematical scheme to reduce a more general case to the space-fractional porous-medium type equation.

3 Diffusivity Models with Permeability Variations Induced by Variations of Pressure

In realistic models of gas flow through porous media, the permeability coefficient depends by variations of pressure, and for high pressure cases an empirical power-law dependence is observed (see for example [18] and the references therein)

$$k(p) \sim k_0\, p^{\beta}, \quad \beta > 0. \tag{3.1}$$

Taking into account this dependence implies that higher order nonlinearities appear in the diffusivity equation governing the fluid flow in heterogeneous medium. Indeed, considering the governing Eq. (2.10) and the pressure-dependence of the porosity (3.1) we obtain the equation

$$\phi(c_f + c_g)\frac{\partial p^2}{\partial t} = \frac{k_0}{\mu}\frac{\partial^\gamma}{\partial x^\gamma}\left(p^\beta \frac{\partial p^2}{\partial x}\right). \tag{3.2}$$

In this case the substitution $p^2(x,t) := u(x,t)$ leads to a space-fractional porous-medium-type nonlinear equation

$$\phi(c_f + c_g)\frac{\partial u}{\partial t} = \frac{k_0}{\mu}\frac{\partial^\gamma}{\partial x^\gamma}\left(u^{\beta/2} \frac{\partial u}{\partial x}\right). \tag{3.3}$$

Fractional porous medium type equations have been widely studied in the recent mathematical literature, even if with a quite different formulation and starting from different assumptions (see e.g. [5] and references therein). As an outcome of our analysis, we have found that a fractional porous-medium type equation arises also in the treatment of diffusivity equation of gas flow in higly heterogeneous media, where the permeability variations are induced by changes of pressure. As far as we know the space-fractional Eq. (3.2) was not studied before. The second part of this paper is devoted to the analysis of some classes of explicit solutions by using generalized separating variable and invariant subspace methods. It is well known that exact solutions of nonlinear evolution equations play an important role for the study of relevant features like the aysmptotic behavior, finite velocity of propagation or blow up in finite time. Few exact results for nonlinear evolution equations involving fractional derivatives in space or time are present in the literature. In this field of research the applications of Lie symmetry methods and invariant subspace method play a central role as it is proved by many recent publications such as [1, 10, 16]. The full mathematical discussion about the properties of the Eq. (3.3) is beyond the aims of this paper. However we will show that in an interesting particular case Barenblatt–type solutions can be obtained.

3.1 Exact Analytical Results

3.1.1 Stationary Solutions

As a first simple solution that can be analitycally investigated, we study the stationary solutions of Eq. (3.3). This means that we should solve the following fractional nonlinear ordinary differential equation

$$\frac{k_0}{\mu}\frac{d^\gamma}{dx^\gamma}\left(u^{\beta/2}\frac{du}{dx}\right) = 0. \tag{3.4}$$

We can prove that an exact solution of Eq. (3.4) is given by

$$u(x) = (c_1 + c_2 x)^{\frac{2}{\beta+2}}, \tag{3.5}$$

where the real constants c_1 and c_2 depends by the boundary conditions. For the physical non-negativity constraint, we must consider suitable constants and the restriction $x > 0$.

We briefly show that (3.5) satisfies Eq. (3.4) by direct substitution. First of all, we observe that by using (3.5)

$$\left(u^{\beta/2}\frac{du}{dx}\right) = (c_1 + c_2 x)^{\frac{2}{\beta+2}\cdot\frac{\beta}{2}} \cdot \frac{2c_2}{\beta+2} \cdot (c_1 + c_2 x)^{\frac{2}{\beta+2}-1} = \frac{2c_2}{\beta+2}.$$

On the other hand, we know that the Caputo fractional derivative of a constant is null and therefore, we obtain that (3.4) admits as a solution (3.5) by direct substitution. The boundary condition, in this case, *a posteriori* is given by $u(x=0) = c_1^{\frac{2}{\beta+2}}$.

The corresponding pressure profile will be given by

$$p(x) = \sqrt{(c_1 + c_2 x)^{2/(\beta+2)}}. \tag{3.6}$$

For example, considering the steady propagation in the bounded domain $x \in [0, L]$, with $L > 0$ and taking the boundary conditions $p(0) = p_0 > 0$ and $p(L) = p_L$, we have that the constants appearing in (3.6) are given by

$$c_1 = p_0^{\beta+2},$$
$$c_2 = \frac{p_L^{\beta+2} - p_0^{\beta+2}}{L}.$$

and therefore the pressure field evolves according to the following equation

$$p(x) = \sqrt{\left(p_0^{\beta+2} + \frac{p_L^{\beta+2} - p_0^{\beta+2}}{L}\, x\right)^{2/(\beta+2)}}. \tag{3.7}$$

3.1.2 Translating Front Solution

It is simple to prove that Eq. (3.3) admits a separating variable solution (see [15]) of the form

$$u(x,t) = \mathcal{X}(x) + \mathcal{T}(t). \tag{3.8}$$

Indeed by substituting (3.8) in (3.3), we should solve the following ordinary differential equations

$$\begin{cases} \dfrac{d\mathcal{T}}{dt} = \lambda, \quad \lambda \in \mathbb{R}, \\ \alpha \dfrac{d^{\gamma}}{dx^{\gamma}} \chi^{\beta/2} \dfrac{d\chi}{dx} = \lambda, \quad \alpha = \dfrac{k_0}{\mu\phi(c_f + c_g)} \end{cases} \tag{3.9}$$

whose trivial solutions are given by

$$\mathcal{X}(x) = C_1 \, x^{\frac{2(\gamma+1)}{\beta+2}}$$
$$\mathcal{T}(t) = \lambda t + C_2,$$

where

$$C_1 = \left[\frac{\beta+2}{2(\gamma+1)} \frac{\lambda}{\alpha\Gamma(\gamma+1)} \right]^{\frac{2}{\beta+2}} \tag{3.10}$$

and the real constant C_2 depends by the initial condition. This solution corresponds to a rigid translation of the initial profile $u(x,0) \propto C_2 + x^{\frac{2(\gamma+1)}{\beta+2}}$.

Therefore, going back to the equation governing the evolution of the pressure field, assuming as initial condition

$$p(x,0) = \sqrt{p_0 + C_1 \, x^{\frac{2(\gamma+1)}{\beta+2}}}, \tag{3.11}$$

a solution to (3.3) is given by

$$p(x,t) = \sqrt{p_0 + C_1 \, x^{\frac{2(\gamma+1)}{\beta+2}} + \lambda t}. \tag{3.12}$$

This is a rigid translation without changing of shape.

We here observe again that the main aim of this paper is to consider some particular classes of exact explicit solutions admitted by the model nonlinear fractional Eq. (3.3). In the most of the cases, the corresponding initial conditions are derived *a posteriori*, we don't start from a physically based initial-boundary condition problem. This means that some of these results are mainly mathematically oriented and can find a possible physical interpretation by considering the corresponding initial conditions.

3.1.3 Separating Variable Solutions

A second interesting class of analytical solutions of porous-medium-type equations is given by separating variable solutions, i.e. (see the encyclopedic Handbook of Polyanin and Zaitsev [15])

$$u(x,t) = X(x)T(t), \tag{3.13}$$

where the functions $X(x)$ and $T(t)$ should solve the following nonlinear ordinary equations

$$\phi(c_f + c_g)\frac{dT}{dt} = \lambda T^{\frac{\beta}{2}+1}, \tag{3.14}$$

$$\frac{k_0}{\mu}\frac{d^\gamma}{dx^\gamma}X^{\beta/2}\frac{dX}{dx} = \lambda X. \tag{3.15}$$

This is a nonlinear eigenvalue probem and, as usual, this kind of solutions strongly depends by the value of λ. We consider the nonlinear eigenvalue problem (3.14) for $\lambda > 0$ that can be reduced to the more simple case $\lambda = 1$ by simple scaling of $X(x)$. The solution of the ordinary equation in $T(t)$ is rather trivial and it is given by

$$T(t) = \left[\frac{\beta}{2\phi(c_f + c_g)}(t_0 - t)\right]^{-2/\beta}, \tag{3.16}$$

with $t_0 > 0$. The solution of (3.15) clearly depends by the boundary conditions and in general is not trivial to find an explicit form. However it is simple to prove that Eq. (3.15) admits as a solution the following function

$$X(x) = \left(\frac{\mu}{k_0}\frac{\beta}{2\gamma+2}\frac{\Gamma(\frac{2\gamma+2}{\beta}+1)}{\Gamma(\frac{2\gamma+2}{\beta}+\gamma+1)}\right)^{2/\beta} x^{\frac{2\gamma+2}{\beta}}. \tag{3.17}$$

Indeed, we first recall that

$$\frac{d^\gamma}{dx^\gamma}x^\nu = \frac{\Gamma(\nu+1)}{\Gamma(\nu+1-\gamma)}x^{\nu-\gamma}, \tag{3.18}$$

for $\nu > 0$ and $\gamma \in (0, 1)$. Therefore, if we search a solution to (3.15) by taking the ansatz

$$X(x) = c_0 \cdot x^\nu, \tag{3.19}$$

where c_0 and ν are two parameters that will be specified in the next. By substitution in (3.15) we have (recalling that we are considering for simplicity the case $\lambda = 1$)

$$\frac{k_0}{\mu}\frac{d^\gamma}{dx^\gamma}X^{\beta/2}\frac{dX}{dx} = \frac{k_0}{\mu}c_0^{\frac{\beta}{2}+1}\nu\frac{\Gamma(\frac{\beta\nu}{2}+\nu)}{\Gamma(\frac{\beta\nu}{2}+\nu-\gamma)}x^{\frac{\beta\nu}{2}+\nu-\gamma-1} = c_0 x^\nu. \tag{3.20}$$

The last equation is clearly satisfied only in the case in which we take in (3.19)

$$\begin{cases} \nu = \frac{2\gamma+2}{\beta}, \\ c_0 = \left(\frac{\mu}{k_0}\frac{\beta}{2\gamma+2}\frac{\Gamma(\frac{2\gamma+2}{\beta}+1)}{\Gamma(\frac{2\gamma+2}{\beta}+\gamma+1)}\right)^{2/\beta}, \end{cases} \tag{3.21}$$

as claimed.

Therefore, substituting (3.17) and (3.16) in (3.13), we obtain a simple solution by separating variables of the form

$$u(x,t) = \left(\frac{\mu}{k_0}\frac{2\phi(c_f+c_g)}{2\gamma+2}\frac{\Gamma(\frac{2\gamma+2}{\beta}+1)}{\Gamma(\frac{2\gamma+2}{\beta}+\gamma+1)}\right)^{2/\beta}\left(\frac{x^{2\gamma+2}}{(t_0-t)^2}\right)^{1/\beta}. \tag{3.22}$$

This solution clearly leads to a blow-up in finite time for $t = t_0$ and should be carefully considered. This kind of solutions leading to an explosive behavior in finite time are interesting for the mathematical theory behind the space-fractional porous-medium Eq. (3.3).

3.1.4 Barenblatt-Type Solutions

A relevant role in the theory of porous-medium equations is played by the so-called Barenblatt solution, corresponding to the *fundamental solution* of the porous medium equation, leading to a pressure profile propagating with finite velocity. We refer to the classical book of Vázquez [22] for a complete analysis about this topic.

Here we start our analysis, by considering self-similar solutions of (3.3) of the form

$$\mathcal{U}(x,t) = t^{-k} f(xt^{-s}) = t^{-k} f(\eta), \quad \eta = xt^{-s}, \tag{3.23}$$

where k and s are similarity exponents and $f(\cdot)$ the self-similar profile. Since, by simple calculations we have that

$$\frac{\partial \mathcal{U}}{\partial t} = -t^{-k-1}\left(k\,\mathcal{U}(\eta) + s\eta\frac{\partial \mathcal{U}}{\partial \eta}\right)$$
$$\frac{\partial^\gamma}{\partial x^\gamma}\mathcal{U}^{\beta/2}\frac{\partial \mathcal{U}}{\partial x} = t^{-s(\gamma+1)-\frac{k\beta}{2}}\frac{\partial^\gamma}{\partial \eta^\gamma}\mathcal{U}^{\beta/2}\frac{\partial \mathcal{U}}{\partial \eta}.$$

We have therefore

$$-t^{-k-1}\left(k\,\mathcal{U}(\eta) + s\eta\frac{\partial \mathcal{U}}{\partial \eta}\right) = t^{-s(\gamma+1)-\frac{k\beta}{2}}\frac{\partial^\gamma}{\partial \eta^\gamma}\mathcal{U}^{\beta/2}\frac{\partial \mathcal{U}}{\partial \eta}. \tag{3.24}$$

In order to eliminate the time dependence we have the first relation between similarity coefficients

$$k\left(\frac{\beta}{2}-1\right) + (\gamma+1)s = 1. \tag{3.25}$$

We therefore should solve the nonlinear fractional '*eigenvalue*' problem

$$\left(k\,f(\eta) + s\eta\frac{\partial f}{\partial \eta}\right) + \frac{\partial^\gamma}{\partial \eta^\gamma}f^{\beta/2}\frac{\partial f}{\partial \eta} = 0. \tag{3.26}$$

The free parameter β is then fixed on the basis of the physical constraints of the conservation of mass

$$\int \mathcal{U}(x,t)dx = const. \tag{3.27}$$

which implies $\alpha = s$ and, by substitution in (3.25), we have the explicit form of the similarity exponents

$$k = s = \frac{1}{\gamma + \frac{\beta}{2} + 1}. \tag{3.28}$$

In the general case, unfortunately, we are not able to solve the nonlinear fractional differential Eq. (3.26).

We now show that, for a specific case of the model Eq. (3.3), we are able to find in explicit form a Barenblatt-type profile. For the more general case, this kind of solutions cannot be found by using the method here employed. A general analysis of the problem of finite velocity of propagation for this formulation of the fractional porous medium equation should be studied, but this is beyond the aim of this paper. In our view this is an interesting example that can be useful both for the physical meaning and the future mathematical analysis of the nonlocal porous medium Eq. (3.3). In this case we adopt the invariant subspace method [7] as a useful mathematical tool to find a Barenblatt-type solution. We refer to the monograph [7] and to the Appendix B for details about this method.

Let us consider Eq. (3.3) for $\beta = 2$, corresponding to the space-fractional Boussinesq equation. The resulting equation can be written as

$$\frac{\partial u}{\partial t} = \alpha \frac{\partial^\gamma}{\partial x^\gamma}\left(u\frac{\partial u}{\partial x}\right), \tag{3.29}$$

with $(x,t) \in \mathbb{R}^+ \times \mathbb{R}^+$ and the diffusion coefficient $\alpha = k_0/(\mu\phi(c_f + c_g))$. This is a non-local generalization of the classical Boussinesq equation that plays a key-role in hydrology. We observe that in the recent paper [13], the authors have discussed a physical derivation of the space-fractional Boussinesq equation for modelling unconfined underground flow. Let us define

$$F\left[t, u(x,t), \frac{\partial^\gamma u}{\partial x^\gamma}, \frac{\partial u}{\partial x}\right] := \frac{\partial^\gamma}{\partial x^\gamma}\left(u\frac{\partial u}{\partial x}\right), \quad x \geq 0. \tag{3.30}$$

It is simple to prove that the nonlinear operator $F[\cdot]$ defined in (3.30) admits as invariant subspace $W^2 = \langle 1, x^{\gamma+1}\rangle$.

Indeed by simple calculations (see Appendix A and B for more details), we have that

$$F(c_1 + c_2 x^{\gamma+1}) = (\gamma+1)\frac{\partial^\gamma}{\partial x^\gamma}\left(c_1 c_2 x^\gamma + c_2^2 x^{2\gamma+1}\right) = (\gamma+1)\left[c_1 c_2 \Gamma(\gamma+1) + \frac{\Gamma(2\gamma+2)}{\Gamma(\gamma+2)} c_2^2 x^{\gamma+1}\right] \tag{3.31}$$

and therefore the subspace $W^2 = \langle 1, x^{\gamma+1}\rangle$ is invariant under the operator $F[\cdot]$.

This means that we can search a solution of (3.29) in the form

$$u(x,t) = a(t)x^{\gamma+1} + b(t), \tag{3.32}$$

By substituting (3.32) into (3.29), we obtain

$$x^{\gamma+1}\frac{da}{dt} + \frac{db}{dt} = \alpha\left(\frac{(\gamma+1)\Gamma(2\gamma+2)}{\Gamma(\gamma+2)}a^2x^{\gamma+1} + \Gamma(\gamma+2)ab\right)$$

and therefore the functions $a(t)$ and $b(t)$ must solve the coupled system of nonlinear differential equations

$$\begin{cases} \dot{a} = \dfrac{\alpha(\gamma+1)\Gamma(2\gamma+2)}{\Gamma(\gamma+2)}a^2, \\ \dot{b} = \alpha\Gamma(\gamma+2)ab. \end{cases} \tag{3.33}$$

By simple calculations we finally find the following solution

$$u(x,t) = \frac{1}{t^{c_2}}\left[1 - \frac{c_1 x^{\gamma+1}}{t^{1-c_2}}\right]_+, \quad x \geq 0 \tag{3.34}$$

where $(\cdot)_+ = \max\{\cdot, 0\}$ (for the positivity physical constraint $u \geq 0$) and

$$\begin{cases} c_1 = \dfrac{\Gamma(\gamma+2)}{\alpha(\gamma+1)\Gamma(2\gamma+2)}, \\ c_2 = \dfrac{\Gamma^2(\gamma+2)}{(\gamma+1)\Gamma(2\gamma+2)}. \end{cases} \tag{3.35}$$

This solution corresponds in the classical theory, to the *source solution* that is related to a Dirac's delta function as an initial condition. In this case the pressure propagates with finite velocity, starting from a strong pulse and at fixed time the solution is always with compact support. The rigorous way to obtain this solution requests more sophisticated limit arguments and the development of the mathematical analysis of weak solutions for this kind of problems. This is beyond the aims of this paper that is devoted to find some special solutions that can have a clear motivation in our physical framework. In our case, following the seminal investigations about the fundamental solutions of the porous medium equation, we have roughly cutted off the part of the profile that is physically meaningless (corresponding to negative values of pressure). This corresponds to find a pressure front propagating at finite velocity (Fig. 1).

This solution describes a front evolving as $x(t) \sim t^{\frac{1-c_2}{1+\gamma}}$, therefore with a strong dependence of the velocity propagation by the parameter γ, parametrizing nonlocal effects in the nonlinear evolution.

We can also observe that for $\gamma = 1$, the classical Barenblatt solution for the porous medium equation is recovered (by choosing a suitable initial intensity of the source

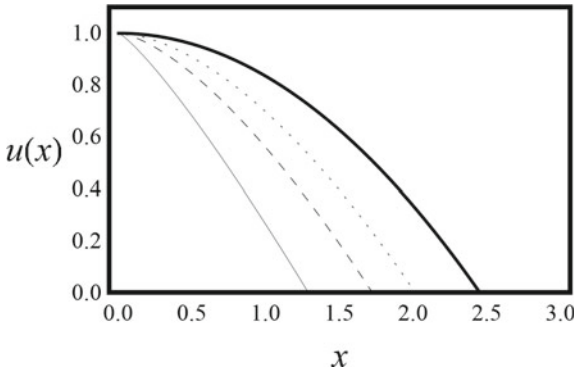

Fig. 1 We represent the solution (3.34) for $x \geq 0$, and (for simplicity) $t = \alpha = 1$. The continuous line corresponds to $\gamma = 1/2$, the dashed to $\gamma = 1/5$, the dotted to $\gamma = 1/7$ and the bold line to $\gamma = 1$. The function is zero outside the set where the pressure is positive and therefore the support is compact

pulse). Indeed in this case we obtain that

$$u(x,t) = \frac{1}{t^{1/3}} \left[1 - \frac{1}{6} \frac{|x|^2}{t^{2/3}} \right]_+, \tag{3.36}$$

that coincides with equation (1.8) of [22] up to a multiplicative constant. Observe that in our case the modulus is missing because we are considering the problem in the semiline $x \geq 0$. It is therefore clear the role played by the nonlocality that changes the shape and amplitude of the support of the evolving front, as can be seen in Fig.1. A relevant outcome of this result is related to the experimental evaluation of the fractional order of derivative and its physical meaning. Indeed, it can be found from the measured velocity of the front.

This kind of solutions can play an interesting role also in the context of the studies about fluid-induced micoseismicity [18], this will be object of further studies. We conclude this section, observing that the relevant feature of the finite velocity of propagation is therefore preserved in the space-fractional Boussinesq equation.

4 Conclusions

In this paper we have reconsidered the model of nonlinear diffusivity of real gas through a strongly heterogenous porous medium, considering nonlocal effects by means of space-fractional derivatives. A part of this paper has been devoted to the derivation of rigorous exact analytic results for the obtained equations of space-fractional diffusion and porous-medium type.

Nonlinear models involving space or time fractional derivatives should be still object of research in the physics of solid earth. This topic of research is motivated by recent discussions about the generalized Darcy law and the space-fractional conservation of mass in heterogeneous media. This paper is the first step in this direction, with the main aim to present the advantages of fractional calculus models for possible

future experimental validation and investigations. From a theoretical mathematical point of view, we suggest some issues that should be investigated, in particular regarding the existence of finite velocity propagating solutions and the more complicated multidimensional cases.

5 Appendix A: Some Details on Fractional Caputo Derivatives

Here we give some details about the fractional Caputo derivatives and some simple mathematical rules that we have applied in the text. Let $0 < \gamma \leq 1$, the Caputo fractional derivative is defined by

$$D_C^{\gamma} f(x) = \begin{cases} \int_0^x \frac{(x-x')^{-\gamma}}{\Gamma(1-\gamma)} f'(x')\,\mathrm{d}x', & \gamma \in (0,1) \\ f'(x), & \gamma = 1, \end{cases} \tag{5.1}$$

where $f'(x)$ is the ordinary first order derivative with respect to x. We can observe that $D_C^{\gamma} f(x) = J_x^{1-\gamma}\left(\frac{df}{dx}\right)$, where

$$J_x^{\gamma} f(x) = \frac{1}{\Gamma(\gamma)} \int_0^x (x-x')^{\gamma-1} f(x')dx', \tag{5.2}$$

is the Riemann-Liouville integral of order $\gamma \in (0,1)$.

It is simple to prove the following properties of Caputo fractional derivative of order $\gamma \in (0,1)$ (see e.g. [11]):

$$\begin{aligned} &D_C^{\gamma} J_x^{\gamma} f(x) = f(x), \\ &D_C^{\gamma} x^{\delta} = \frac{\Gamma(\delta+1)}{\Gamma(\delta-\gamma+1)} x^{\delta-\gamma} \qquad \delta \in (-1,0) \bigcup (0,\infty), \\ &D_C^{\gamma} const. = 0. \end{aligned}$$

6 Appendix B: The Invariant Subspace Method

The Invariant Subspace Method, introduced in the literature by Galaktionov (see the monograph [7] and [16] for details), allows to solve exactly nonlinear equations by separating variables.

We recall the main idea of this method: consider a scalar evolution equation

$$\frac{\partial u}{\partial t} = F\left[u, \frac{\partial u}{\partial x}, \ldots\right], \tag{6.1}$$

where $u = u(x,t)$ and $F[\cdot]$ is a nonlinear differential operator. Given n linearly independent functions

$$f_1(x),\ f_2(x),\ ....,\ f_n(x),$$

we call W^n the n-dimensional linear space

$$W^n = \langle f_1(x),\ ....,\ f_n(x)\rangle.$$

This space is called invariant under the given operator $F[u]$, if $F[y] \in W_n$ for any $y \in W_n$. This means that there exist n functions $\Phi_1,\ \Phi_2,\ ...,\ \Phi_n$ such that

$$F[C_1 f_1(x) + ...C_n f_n(x)] = \Phi_1(C_1,\ ....,\ C_n) f_1(x) + ... \\ + \Phi_n(C_1,\ ....,\ C_n) f_n(x),$$

where $C_1,\ C_2,\ .....,\ C_n$ are arbitrary constants.

Once the set of functions $f_i(x)$ that form the invariant subspace has been determined, we can search an exact solution of (6.1) in the invariant subspace in the form

$$u(x,t) = \sum_{i=1}^{n} g_i(t) f_i(x). \tag{6.2}$$

where $f_i(x) \in W_n$. In this way, we arrive to a system of ODEs. In many cases, this problem is simpler than the original one and allows to find exact solutions by just separating variables [7]. We refer to the monograph [7] for further details and applications of this method. The first applications of the invariant subspace method to fractional equations is due to Gazizov and Kasatkin [10].

7 Appendix C: A Mathematical Analysis of the More General Case

A strong limitation in the analysis developed in this paper is given by the assumption that the diffusivity coefficient (involving compressibility coefficients, porosity, permeability and viscosity) is constant and pressure-independent. Here we show that, under some mathematical assumptions, we are able to reduce a more general case to a fractional porous medium-type equation, similar to the one considered in the previous section. Here we provide a syntetic scheme to obtain this result:

- Assume that the coefficients appearing in (2.8) are pressure-dependent according to the following equalities

$$\frac{\phi(c_f + c_g)}{z} \sim C_1 p^{n_1} \quad \frac{k}{\mu z} \sim C_2 p^{n_2}, \tag{7.1}$$

with n_1, n_2, C_1, C_2 arbitrary real positive constants. Therefore Eq. (2.8) becomes

$$C_1 p^{n_1} \frac{\partial p^2}{\partial t} = C_2 \frac{\partial^\gamma}{\partial x^\gamma} p^{n_2} \frac{\partial p^2}{\partial x}. \tag{7.2}$$

- Define $u = p^2$, such that (7.2) becomes

$$\frac{2C_1}{n_1+2} \frac{\partial}{\partial t} u^{\frac{n_1}{2}+1} = C_2 \frac{\partial^\gamma}{\partial x^\gamma} u^{\frac{n_2}{2}} \frac{\partial u}{\partial x}. \tag{7.3}$$

- Define $s = u^{\frac{n_1}{2}+1}$ and therefore we finally obtain a space-fractional porous-medium-type equation

$$C_1 \frac{\partial s}{\partial t} = C_2 \frac{\partial^\gamma}{\partial x^\gamma} s^{\frac{n_2+2}{n_1+2}-1} \frac{\partial s}{\partial x} \tag{7.4}$$

Thus we can apply the methods used before to solve (3.3) also in this more general case.

References

1. Artale Harris, P., Garra, R.: Nonlinear time-fractional dispersive equations. *Communications in applied and industrial mathematics*. **6**(1), e-487 (2014)
2. Beygi, M.E., Rashidi, R.: Analytical solutions to gas flow problems in low permeability porous media, Transp. Porous Media **87**, 421-436 (2011)
3. Caputo, M.: Models of flux in porous media with memory. Water Resources Research **36**(3), 693–705 (2000)
4. Chang, A., Sun, H., Zhang, Y., Zheng, C., Min, F.: Spatial fractional Darcys law to quantify fluid flow in natural reservoirs. Physica A **519**, 119–126 (2019)
5. Pablo, A., Quiros, F., Rodriguez, A., Vazquez, J.L.: A fractional porous medium equation. Adv. Math. **226**(2), 1378–1409 (2011)
6. Di Giuseppe, E., Moroni, M., Caputo, M.: Flux in porous media with memory: models and experiments. Transp. Porous Media **83**(3), 479–500 (2010)
7. Galaktionov, V., Svirshchevskii, S.: Exact solutions and invariant subspaces of nonlinear partial differential equations in mechanics and physics. Chapman Hall/CRC Appl. Math. Nonlinear Sci. Ser. (2007)
8. Garra, R., Salusti, E.: Application of the nonlocal Darcy law to the propagation of nonlinear thermoelastic waves in fluid saturated porous media. Physica D **250**, 52–57 (2013)
9. Garra, R.: On the generalized Hardy-Hardy-Maurer model with memory effects. Nonlinear Dyn. **1–8**, (2016)
10. Gazizov, R., Kasatkin, A.: Construction of exact solutions for fractional order differential equations by the invariant subspace method. Comput. Math. Appl. **66**(5), 576–584 (2013)
11. Kilbas, A.A., Srivastava, H.M., Trujillo, J.J.: Theory and Applications of Fractional Differential Equations, vol. 204. Elsevier Science Limited (2006)
12. Mainardi, F., Luchko, Y., Pagnini, G.: The fundamental solution of the spacetime fractional diffusion equation. Fractional Calc. Appl. Anal. **4**(2), 153–192 (2001)
13. Mehdinejadiani, B., Jafari, H., Baleanu, D.: Derivation of a fractional Boussinesq equation for modelling unconfined groundwater. Eur. Phys. J. Spec. Top. **222**(8), 1805–1812 (2013)

14. Metzler, R., Klafter, J.: The restaurant at the end of the random walk: recent developments in the description of anomalous transport by fractional dynamics. J. Phys. A: Math. Gen. **37**(31), R161 (2004)
15. Polyanin, A.D., Zaitsev, V.F.: Handbook of nonlinear partial differential equations. CRC Press (2004)
16. Sahadevan, R., Bakkyaraj, T.: Invariant subspace method and exact solutions of certain nonlinear time fractional partial differential equations. Fractional Calc. Appl. Anal. **18**(1), 146–162 (2015)
17. Schumer, R., Meerschaert, M.M., Baeumer, B.: Fractional advection-dispersion equations for modeling transport at the Earth surface. J. Geophys. Res. Earth Surf. **114**(F4), 15 (2009)
18. Shapiro, S.A., Dinske, C.: Fluid-induced seismicity: pressure diffusion and hydraulic fracturing. Geophys. Prospect. **57**, 301–310 (2009)
19. Shapiro, S.A.: Fluid-induced seismicity. Cambridge University Press (2015)
20. Wheatcraft, S.W., Meerschaert, M.M.: Fractional conservation of mass. Adv. Water Resour. **31**, 1377–1381 (2008)
21. Wu, Y.S., Pruess, K.: Gas flow in porous media with Klinkenberg effects. Transp. porous Media **32**(1), 117–137 (1998)
22. Vázquez, J.L.: The porous medium equation: mathematical theory. Oxford University Press (2007)

A Note on Hermite-Bernoulli Polynomials

Clemente Cesarano and Alexandra Parmentier

Abstract Using the concepts and formalism of different families of Hermite polynomials, we discuss here some generalizations of polynomials belonging to the Bernoulli class, and we also show how to represent the action of the operators involving fractional derivatives. In particular, by using the method of generating function, we introduce generalized Bernoulli polynomials by operating in their generating function with the formalism of the two-variable Hermite polynomials. In addition, we extend some operational techniques in order to derive different forms of Bernoulli numbers and polynomials. Finally, we explore some general properties of generalized Bernoulli polynomials, focusing on their extension to the 2D case, and we introduce a family of polynomials strictly related to the Hermite polynomials in order to compute the effect of fractional operators on a given function.

Keywords Hermite polynomials · Bernoulli polynomials · Generating functions · Fractional calculus.

1 Introduction

Bernoulli numbers and polynomials can be introduced through their generating functions [1]:

$$\frac{t}{e^t - 1} = \sum_{n=0}^{+\infty} \frac{t^n}{n!} B_n, \tag{1}$$

C. Cesarano (✉)
Section of Mathematics, International Telematic University UNINETTUNO, C.so Vittorio Emanuele II 39, 00186 Rome, Italy
e-mail: c.cesarano@uninettunouniversity.net

A. Parmentier
INFN - Division of Rome Tor Vergata, Via della Ricerca Scientifica 1, 00133 Rome, Italy
e-mail: alexandra.parmentier@roma2.infn.it

L. Beghin et al. (eds.), *Nonlocal and Fractional Operators*, SEMA SIMAI Springer Series 26, https://doi.org/10.1007/978-3-030-69236-0_6

$$\frac{te^{xt}}{e^t-1}=\sum_{n=0}^{+\infty}\frac{t^n}{n!}B_n(x), \tag{2}$$

where t is real and nonzero.

It is also known that Bernoulli polynomials can be expressed in terms of Bernoulli numbers; indeed, exploiting the generating function of Bernoulli polynomials, we retrieve:

$$\frac{te^{xt}}{e^t-1}=e^{xt}\frac{t}{e^t-1}=\sum_{s=0}^{+\infty}\frac{x^st^s}{s!}\sum_{m=0}^{+\infty}\frac{t^m}{m!}B_m, \tag{3}$$

and then

$$\frac{te^{xt}}{e^t-1}=\sum_{s=0}^{+\infty}\sum_{m=0}^{+\infty}\frac{x^st^{s+m}}{s!m!}B_m. \tag{4}$$

If we set $s+m=n$, and equate coefficients of corresponding powers in Eq. 4, we get:

$$B_n(x)=\sum_{s=0}^{n}\binom{n}{s}B_{n-s}x^s \tag{5}$$

that is valid $\forall n\in\mathbb{N}$. A significant recurrence relation, which is satisfied by Bernoulli polynomials, can be easily derived from their generating functions. Indeed, differentiating Eq. 2 with respect to x, we obtain

$$\frac{t^2e^{xt}}{e^t-1}=\sum_{n=0}^{+\infty}\frac{t^n}{n!}\frac{d}{dx}B_n(x), \tag{6}$$

that is,

$$\sum_{n=0}^{+\infty}\frac{t^{n+1}}{n!}B_n(x)=\sum_{n=0}^{+\infty}\frac{t^n}{n!}\frac{d}{dx}B_n(x), \tag{7}$$

and, after rearranging indices and equating coefficients of corresponding powers, the following relation

$$\frac{d}{dx}B_n(x)=nB_{n-1}(x) \tag{8}$$

that holds for all value of n is straightforwardly recovered.

Equation 8 suggests us to look at Bernoulli polynomials as a particular class of orthogonal polynomials. The theory of hybrid polynomials and special functions can

be found in literature only in very particular cases [2], the only exception in this field, is the class of Hermite polynomials, which was introduced from the beginning in the general case and can be found in a classical book of P. Appell and J. Kampé de Fériet [3]. It has also been shown [4–8] that the Hermite polynomials play a fundamental role in the extension of the classical special functions. Starting from the Hermite polynomials it has already been possible to obtain some extensions of some classical special sets of functions, including the Bessel functions [9], Dickson polynomials [10], Laguerre polynomials [11], Chebyshev polynomials [12–14]. In this paper we show that, starting from two-variable Hermite polynomials, it is possible to introduce generalizations of Bernoulli polynomials.

We note, indeed, Kampé de Fériet Hermite polynomials [3]

$$He_n(x) = n! \sum_{s=0}^{\left[\frac{n}{2}\right]} \frac{(-1)^s}{(n-2s)!s!2^s} x^{n-2s} \tag{9}$$

are defined by means of the following generating function:

$$e^{xt-\frac{t^2}{2}} = \sum_{n=0}^{+\infty} \frac{t^n}{n!} He_n(x); \tag{10}$$

and, since the $He_n(x)$ polynomials solve the differential-difference equation

$$\frac{d}{dx} He_n(x) = nHe_{n-1}(x), \tag{11}$$

that holds for all value of n, we are allowed, in some specific cases, to treat Bernoulli polynomials as a particular case of Hermite polynomials. Moreover, the class of polynomials recognized as part of Hermite family could be used to derive interesting generalizations involving Bernoulli polynomials.

The reader must be reminded here that Bernoulli polynomials satisfy the following recurrence relation

$$B_n(x+1) - B_n(x) = nx^{n-1}, \tag{12}$$

which stems from the partial sum

$$\sum_{k=0}^{m} k^n = \frac{B_{n+1}(m+1) - B_{n+1}}{n+1} \tag{13}$$

for $n, m \in \mathbb{N}$, after noticing that

$$B_n = B_n(0). \tag{14}$$

2 Generalized Hermite Polynomials and Bernoulli Polynomials

In the previous section we have introduced Kampé de Fériet Hermite polynomials of one variable (Eq. 9), together with their related generating function (Eq. 10).

In order to introduce a first two-variable generalization, we can draw on the formalism and techniques of exponential operators. For an analytic function $f(x)$, the Taylor expansion, after addition of a real parameter λ, looks like

$$f(x+\lambda) = \sum_{n=0}^{+\infty} \frac{\lambda^n}{n!} f^{(n)}(x), \tag{15}$$

provided the analyticity of f at $x+\lambda$ as well.

Since the action of exponential operators on an analytic function corresponds to a translation [4]

$$e^{\lambda \frac{d}{dx}} f(x) = \sum_{n=0}^{+\infty} \frac{\lambda^n}{n!} f^{(n)}(x), \tag{16}$$

we can utilize Eq. 16 to introduce two-variable Hermite polynomials. Indeed, if we take into account the second derivative, we can write:

$$e^{\lambda \frac{d^2}{dx^2}} f(x) = \sum_{n=0}^{+\infty} \frac{\lambda^n}{n!} f^{(2n)}(x). \tag{17}$$

It must be noticed that

$$\frac{d^{2n}}{dx^{2n}}(x^m) = \frac{m!}{(m-2n)!} x^{m-2n}, \tag{18}$$

and

$$e^{\lambda \frac{d}{dx}}(x^m) = (x+\lambda)^m, \tag{19}$$

from which we can infer

$$e^{\lambda \frac{d^2}{dx^2}}(x^m) = \sum_{n=0}^{\left[\frac{m}{2}\right]} \frac{\lambda^n}{n!} \frac{m!}{(m-2n)!} x^{m-2n}. \tag{20}$$

Finally, since λ is real by definition, we can state that two-variable Hermite polynomials $H_n(x, y)$ of Kampé de Fériet form are defined by the following formula [15]:

$$H_n(x, y) = \sum_{s=0}^{\left[\frac{n}{2}\right]} \frac{n!}{s!(n-2s)!} y^s x^{n-2s}. \tag{21}$$

Two-variable Hermite polynomials are linked to ordinary Hermite polynomials $He_n(x)$ by the relation:

$$H_n\left(x, -\frac{1}{2}\right) = He_n(x). \tag{22}$$

It is also important to notice that Hermite polynomials $H_n(x, y)$ satisfy the equation [16, 17]

$$H_n(x, 0) = x^n. \tag{23}$$

The definition of a family of polynomials belonging to the Appell class [18] and, in particular, to the large class of Hermite polynomials, can be carried out in many ways [17]; we have introduced the polynomials $H_n(x, y)$ by means of the operational techniques of exponential operators, and we have outlined their nature in relation to the differential-difference Eq. 11 (see Introduction).

We can move on and state an important operational relation possibly useful to reach our goal. First, we prove the following significant result:

Theorem 1 *$H_n(x, y)$ polynomials solve the following partial differential equation:*

$$\frac{\partial^2}{\partial x^2} H_n(x, y) = \frac{\partial}{\partial y} H_n(x, y). \tag{24}$$

Proof By separate differentiation with respect to x and y, respectively, in Eq. 21, we obtain

$$\begin{aligned} \frac{\partial}{\partial x} H_n(x, y) &= n H_{n-1}(x, y) \\ \frac{\partial}{\partial y} H_n(x, y) &= n(n-1) H_{n-2}(x, y). \end{aligned} \tag{25}$$

The proof of the theorem is straightforwardly derived from Eqs. 25, differentiating the former relation with respect to x and then applying the latter one. □

The differential equation stated in Theorem 1 allows for inferring a remarkable operational rule for this class of Hermite polynomials. Indeed, Eq. 24 can be considered as ordinary in y and, thus, linear, so that we can immediately solve the following Cauchy problem:

$$\begin{aligned} \frac{\partial}{\partial y} H_n(x, y) &= \frac{\partial^2}{\partial x^2} H_n(x, y) \\ H_n(x, 0) &= x^n, \end{aligned} \tag{26}$$

leading to

$$H_n(x, y) = e^{y\frac{\partial^2}{\partial x^2}} x^n. \tag{27}$$

We have previously mentioned the natural link between Hermite polynomials and the differential-difference Eq. 11. In order to better investigate this issue, we prove here the following theorem:

Theorem 2 *The polynomials $H_n(x, y)$ satisfy the following differential-difference equation*

$$\begin{aligned} \frac{d}{dz} Y_n(z) &= anY_{n-1}(z) + bn(n-1)Y_{n-2}(z) \\ Y_n(0) &= \delta_{n,0}. \end{aligned} \tag{28}$$

where z is a real variable, and a and b are real constants.

Proof Using the generating-function method [18], and setting

$$G(z; t) = \sum_{n=0}^{+\infty} \frac{t^n}{n!} Y_n(z) \tag{29}$$

with t a real variable, we can rewrite Eqs. 28 as

$$\begin{aligned} \frac{d}{dz} G(z; t) &= (at + bt^2) G(z; t) \\ G(0; t) &= 1, \end{aligned} \tag{30}$$

that is, as a linear ordinary differential equation, whose solution reads

$$G(z; t) = e^{xt+yt^2}, \tag{31}$$

where $az = x$ and $bz = y$.

Finally, exploiting the r.h.s. of Eq. 31, the initial thesis is immediately obtained since:

$$e^{xt+yt^2} = \sum_{n=0}^{+\infty} \frac{t^n}{n!} H_n(x, y). \tag{32}$$

Theorem 2 returns the connection between Hermite polynomials of type $H_n(x, y)$ and their generating function, that is,

$$e^{xt+yt^2} = \sum_{n=0}^{+\infty} \frac{t^n}{n!} H_n(x, y). \tag{33}$$

In this paper we want to explore the relations involving Bernoulli and Hermite polynomials of type $H_n(x, y)$. More precisely, we will show how Bernoulli polynomials can be generalized, and how some significant relations, related to the wide family of polynomials recognized as Hermite polynomials, appearing in the literature, can be derived for polynomials which involve Bernoulli in terms of Hermite.

We have defined a special class of functions by using families of polynomials that belong to the Hermite family. In this context, we use Hermite polynomials of type $H_n(x, y)$ to introduce a generalization of Bernoulli polynomials.

Starting from the generating function of $H_n(x, y)$ polynomials stated in Eq. 32, we can introduce here Hermite-Bernoulli polynomials by manipulation of Eq. 2:

$$\frac{te^{xt+yt^2}}{e^t-1} = \sum_{n=0}^{+\infty} \frac{t^n}{n!}\, {}_H B_n(x, y). \tag{34}$$

Equation 34 can be considered as a sort of definition of this family of Bernoulli polynomials ${}_H B_n(x, y)$, that is, Bernoulli polynomials in the Hermite basis. In order to derive their explicit form, and, consequently, to elucidate their nature, we have to further manipulate Eq. 34. Indeed, from Eqs. 1 and 32:

$$\frac{t}{e^t-1}e^{xt+yt^2} = \sum_{m=0}^{+\infty} \frac{t^m}{m!} B_m \sum_{s=0}^{+\infty} \frac{t^s}{s!} H_s(x, y). \tag{35}$$

If we set $m + s = n$, we get

$$\frac{t}{e^t-1}e^{xt+yt^2} = \sum_{n=0}^{+\infty}\sum_{s=0}^{+\infty} \frac{t^n}{(n-s)!s!} B_{n-s} H_s(x, y), \tag{36}$$

and, equating coefficients of corresponding n-powers in Eq. 36, while taking into account the definition given in Eq. 34, we end up with

$${}_H B_n(x, y) = \sum_{s=0}^{n} \binom{n}{s} B_{n-s} H_s(x, y), \tag{37}$$

which represents the explicit form of Hermite-Bernoulli polynomials.

A first identity that can be easily retrieved for this class of polynomials occurs when $y = 0$. Indeed, from Eq. 37:

$${}_H B_n(x, 0) = \sum_{s=0}^{n} \binom{n}{s} B_{n-s} H_s(x, 0); \tag{38}$$

and, applying the analogous identity reported in Eq. 23:

$$ {}_H B_n(x,0) = \sum_{s=0}^{n} \binom{n}{s} B_{n-s} x^s. \tag{39} $$

The r.h.s. of Eq. 39 represents the ordinary Bernoulli polynomial appearing in Eq. 5, so that

$$ {}_H B_n(x,0) = B_n(x). \tag{40} $$

The structure of Hermite-Bernoulli polynomials, as well as the relations they satisfy, suggest that it is worth deriving differential operational relations similar to those presented in the case of Hermite polynomials of type $H_n(x,y)$. In particular, starting from the partial differential equation stated in Eq. 24, we can recover a comparable result for polynomials ${}_H B_n(x,y)$.

We start from proving some significant properties.

Theorem 3 *Hermite-Bernoulli polynomials satisfy the following recurrence relations:*

$$ \frac{\partial}{\partial x} {}_H B_n(x,y) = n\, {}_H B_{n-1}(x,y) \tag{41} $$

$$ \frac{\partial}{\partial y} {}_H B_n(x,y) = n(n-1)\, {}_H B_{n-2}(x,y) \tag{42} $$

Proof If we differentiate both sides of Eq. 37 with respect to x, we get

$$ \frac{\partial}{\partial x} {}_H B_n(x,y) = \sum_{s=0}^{n} \binom{n}{s} B_{n-s} \frac{\partial}{\partial x} H_s(x,y), \tag{43} $$

and, exploiting Eqs. 25, we find

$$ \frac{\partial}{\partial x} {}_H B_n(x,y) = \sum_{s=1}^{n} \binom{n}{s} B_{n-s}\, s\, H_{s-1}(x,y), \tag{44} $$

which gives Eq. 41. After an analogous differentiation of Eq. 37 with respect to y, we find

$$ \frac{\partial}{\partial y} {}_H B_n(x,y) = \sum_{s=0}^{n} \binom{n}{s} B_{n-s} \frac{\partial}{\partial y} H_s(x,y), \tag{45} $$

that is, using Eqs. 25 once again, we are left with Eq. 42. □

Theorem 4 *Hermite-Bernoulli polynomials satisfy the following Cauchy problem:*

$$\begin{aligned} \frac{\partial}{\partial y}\,{}_H B_n(x,y) &= \frac{\partial^2}{\partial x^2}\,{}_H B_n(x,y) \\ {}_H B_n(x,0) &= B_n(x). \end{aligned} \tag{46}$$

This amounts to reading the partial differential equation as ordinary (linear) in y.

Proof If Eq. 41 is differentiated with respect to x, the relation

$$\frac{\partial^2}{\partial x^2}\,{}_H B_n(x,y) = n(n-1)\,{}_H B_{n-2}(x,y) \tag{47}$$

is obtained. When compared to Eq. 42, it returns Eq. 46.

Since the partial differential equation in the Cauchy problem is intended as ordinary (that is, linear) in y, the use of the initial condition

$${}_H B_n(x,0) = B_n(x) \tag{48}$$

returns the solution

$${}_H B_n(x,y) = e^{y\frac{\partial^2}{\partial x^2}} B_n(x), \tag{49}$$

which is the proof of the theorem.

It is worth noticing here that Theorem 4 returns an operational identity for Hermite-Bernoulli polynomials, which is similar to that satisfied by two-variable Hermite polynomials (Eq. 27). This feature is expected, since Hermite-Bernoulli polynomials have been introduced by means of $H_n(x,y)$ polynomials used as a basis.

An interesting point can be the exploration of different families of Hermite polynomials in order to recover further generalizations of Bernoulli polynomials, as well as a set of significant differential relations involving the latter.

3 Further Generalizations of Hermite-Bernoulli Polynomials

A different class of generalized two-variable Hermite polynomials could be directly introduced by replacing (x,y) by $(2x,-y)$ in Eq. 21, but, in order to emphasize the link between Hermite polynomials and the differential difference equation, we prefer to follow the same procedure, so as to outline differences and analogies.

Starting from differential-difference Eqs. 28, we consider a slight modification:

$$\begin{aligned} \frac{d}{dz}Y_n(z) &= 2anY_{n-1}(z) - bn(n-1)Y_{n-2}(z) \\ Y_n(0) &= \delta_{n,0}, \end{aligned} \tag{50}$$

with z a real variable, and a, b real constants again. When implementing the usual generating-function method, the following relations are derived:

$$\begin{aligned} \frac{d}{dz}G(z;t) &= (2at - bt^2)G(z;t) \\ G(0;t) &= 1, \end{aligned} \tag{51}$$

which represents a linear differential equation, whose solution reads

$$G(z;t) = e^{2xt-yt^2}, \tag{52}$$

where $az = x$, $bz = y$.

Using the r.h.s. of Eq. 52, the following generalized two-variable Hermite polynomials can be introduced [16]:

$$e^{2xt-yt^2} = \sum_{n=0}^{+\infty} \frac{t^n}{n!} \bar{H}_n(x, y); \tag{53}$$

and, making use of the Cauchy problem stated in Eqs. 50, we get a chance to recover the explicit form of $\bar{H}_n(x, y)$ polynomials:

$$\bar{H}_n(x, y) = \sum_{s=0}^{\left[\frac{n}{2}\right]} \frac{n!}{s!(n-2s)!}(-y)^s(2x)^{n-s}. \tag{54}$$

Let us take a look now at a set of differential relations satisfied by Hermite polynomials of type $\bar{H}_n(x, y)$, in complete analogy to $H_n(x, y)$ polynomials.

Theorem 5 *Hermite polynomials of type $\bar{H}_n(x, y)$ satisfy the following recurrence relations:*

$$\frac{\partial}{\partial x}\bar{H}_n(x, y) = 2n\bar{H}_{(n-1)}(x, y), \tag{55}$$

$$\frac{\partial}{\partial y}\bar{H}_n(x, y) = -n(n-1)\bar{H}_{(n-2)}(x, y), \tag{56}$$

Proof If Eq. 53 is differentiated with respect to x, we recover

$$2te^{2xt-yt^2} = \sum_{n=0}^{+\infty} \frac{t^n}{n!}\frac{\partial}{\partial x}\bar{H}_n(x, y), \tag{57}$$

and, applying Eq. 53 once again:

$$2\sum_{n=0}^{+\infty}\frac{t^{n+1}}{n!}\bar{H}_n(x,y)=\sum_{n=0}^{+\infty}\frac{t^n}{n!}\frac{\partial}{\partial x}\bar{H}_n(x,y), \tag{58}$$

which proves Eq. 55.

Then, differentiating Eq. 53 with respect to y, the following relation is retrieved:

$$-t^2e^{2xt-yt^2}=\sum_{n=0}^{+\infty}\frac{t^n}{n!}\frac{\partial}{\partial y}\bar{H}_n(x,y), \tag{59}$$

which is a proof of Eq. 56. □

As for the case of $H_n(x,y)$ polynomials presented in Sect. 2 (Eq. 26), Theorem 5 helps us recover a differential relation for $\bar{H}_n(x,y)$ polynomials.

Theorem 6 *Hermite polynomials of type* $\bar{H}_n(x,y)$ *solve the following partial differential equation:*

$$-\frac{1}{4}\frac{\partial^2}{\partial x^2}\bar{H}_n(x,y)=\frac{\partial}{\partial y}\bar{H}_n(x,y), \tag{60}$$

Proof If Eq. 55 is differentiated with respect to x, the following equation is obtained:

$$\frac{\partial^2}{\partial x^2}\bar{H}_n(x,y)=2n\frac{\partial}{\partial x}\bar{H}_{n-1}(x,y), \tag{61}$$

from which:

$$\frac{\partial^2}{\partial x^2}\bar{H}_n(x,y)=2n[2(n-1)]\bar{H}_{n-2}(x,y). \tag{62}$$

Then, applying Eq. 56, we get

$$-\frac{1}{4}\frac{\partial^2}{\partial x^2}\bar{H}_n(x,y)=\frac{\partial}{\partial y}\bar{H}_n(x,y), \tag{63}$$

which is the proof of the theorem.

Following the same line of reasoning as the one employed for polynomials of type $H_n(x,y)$, we can recover an interesting operational identity.

Let us notice that

$$\bar{H}_n(x,0)=\sum_{s=0}^{\left[\frac{n}{2}\right]}\frac{n!}{s!(n-2s)!}(0)^s(2x)^{n-2s}, \tag{64}$$

which is not trivial for $s=0$ alone; this gives

$$\bar{H}_n(x,0) = (2x)^n. \tag{65}$$

Equation 60 can be considered as an ordinary linear differential equation in y; then, Eq. 65 being the initial condition for $y = 0$, we can straightforwardly write its solution:

$$\bar{H}_n(x,y) = e^{-\frac{1}{4}y\frac{\partial^2}{\partial x^2}}(2x)^n, \tag{66}$$

which is just a useful operational relation for $\bar{H}_n(x,y)$ polynomials.

A further interesting relation stems from Eq. 66; indeed, since

$$e^{-\frac{y}{4}\frac{\partial^2}{\partial x^2}} = \sum_{n=0}^{+\infty}(-1)^n\left(\frac{y}{4}\right)^n\frac{\partial^{2n}}{\partial x^{2n}}, \tag{67}$$

after noticing that the effect of the derivative of $(2x)^n$ is trivial for $2s > n$, we obtain

$$\bar{H}_n(x,y) = \left[\sum_{s=0}^{\left[\frac{n}{2}\right]}(-1)^s\left(\frac{y}{4}\right)^s\frac{\partial^{2s}}{\partial x^{2s}}\right](2x)^n. \tag{68}$$

This further class of Hermite polynomials can be utilized to generalize Bernoulli polynomials according to the same approach exposed in Sect. 2. We introduce here Hermite-Bernoulli polynomials of type ${}_H\bar{B}_n(x,y)$ by means of their generating function. Indeed, combining generating functions of Bernoulli numbers (Eq. 1) and Hermite polynomials of type $\bar{H}_n(x,y)$ (Eq. 53), we retrieve here

$$\frac{te^{2xt-yt^2}}{e^t-1} = \sum_{n=0}^{+\infty}\frac{t^n}{n!}\,{}_H\bar{B}_n(x,y). \tag{69}$$

Similarly to what seen in the previous section, Eq. 69 represents the definition of this class of Hermite-Bernoulli polynomials, for which the basis is now the set of Hermite polynomials of type $\bar{H}_n(x,y)$. We can explicit Eq. 69 as

$$\frac{t}{e^t-1}e^{2xt-yt^2} = \sum_{m=0}^{+\infty}\frac{t^m}{m!}B_m\sum_{s=0}^{+\infty}\frac{t^s}{s!}\bar{H}_s(x,y), \tag{70}$$

and, setting $m+s=n$, it follows:

$$\sum_{n=0}^{+\infty}\frac{t^n}{n!}\,{}_H\bar{B}_n(x,y) = \sum_{n=0}^{+\infty}\sum_{s=0}^{+\infty}\frac{t^n}{s!(n-s)!}B_{n-s}\bar{H}_s(x,y), \tag{71}$$

which returns the explicit form of Hermite-Bernoulli polynomials of type ${}_H\bar{B}_n(x,y)$, that is,

$$ {}_H\bar{B}_n(x, y) = \sum_{s=0}^{+\infty} \binom{n}{s} B_{n-s} \bar{H}_s(x, y). \tag{72} $$

When $y = 0$, it is found:

$$ {}_H\bar{B}_n(x, 0) = \sum_{s=0}^{+\infty} \binom{n}{s} B_{n-s} (2x)^s, \tag{73} $$

or, applying in cascade the identity reported in Eq. 65 and Eq. 5:

$$ {}_H\bar{B}_n(x, 0) = B_n(2x), \tag{74} $$

which represents the link between ordinary Bernoulli polynomials and their generalization in the basis of Hermite polynomials of type $\bar{H}_n(x, y)$.

Using properties, and related formalism, of Hermite polynomials of type $\bar{H}_n(x, y)$, we can derive useful differential relations for polynomials of type ${}_H\bar{B}_n(x, y)$.

Theorem 7 *Hermite-Bernoulli polynomials of type* ${}_H\bar{B}_n(x, y)$ *satisfy the following relations:*

$$ \frac{\partial}{\partial x} {}_H\bar{B}_n(x, y) = 2n \, {}_H\bar{B}_{n-1}(x, y), \tag{75} $$

$$ \frac{\partial}{\partial y} {}_H\bar{B}_n(x, y) = -n(n-1) \, {}_H\bar{B}_{n-2}(x, y), \tag{76} $$

Proof When differentiating Eq. 72 with respect to x, we obtain

$$ \frac{\partial}{\partial x} {}_H\bar{B}_n(x, y) = \sum_{s=0}^{n} \binom{n}{s} B_{n-s} \frac{\partial}{\partial x} \bar{H}_s(x, y), \tag{77} $$

after which, applying Eq. 55, it is found:

$$ \frac{\partial}{\partial x} {}_H\bar{B}_n(x, y) = \sum_{s=1}^{n} \binom{n}{s} B_{n-s} 2s \bar{H}_{s-1}(x, y), \tag{78} $$

returning Eq. 75.

Similarly, after a differentiation with respect to y

$$ \frac{\partial}{\partial y} {}_H\bar{B}_n(x, y) = \sum_{s=0}^{n} \binom{n}{s} B_{n-s} \frac{\partial}{\partial y} \bar{H}_s(x, y), \tag{79} $$

which complete the proof by direct application of Eq. 56. □

Theorem 7 allows for deriving a significant result for polynomials of type ${}_H\bar{B}_n(x, y)$.

Theorem 8 *Hermite-Bernoulli polynomials of type* ${}_H\bar{B}_n(x, y)$ *satisfy the following differential equation:*

$$\frac{\partial}{\partial y}\,{}_H\bar{B}_n(x, y) = -\frac{1}{4}\frac{\partial^2}{\partial x^2}\,{}_H\bar{B}_n(x, y), \tag{80}$$

Proof Let us differentiate Eq. 75 with respect to x, so as to retrieve

$$\frac{\partial^2}{\partial x^2}\,{}_H\bar{B}_n(x, y) = 2n[2(n-1)]\,{}_H\bar{B}_{n-2}(x, y), \tag{81}$$

i.e.,

$$\frac{1}{4}\frac{\partial^2}{\partial x^2}\,{}_H\bar{B}_n(x, y) = n(n-1)\,{}_H\bar{B}_{n-2}(x, y). \tag{82}$$

The r.s.h of Eq. 82 is similar to the r.h.s of Eq. 76, from which:

$$\frac{1}{4}\frac{\partial^2}{\partial x^2}\,{}_H\bar{B}_n(x, y) = -\frac{\partial}{\partial y}\,{}_H\bar{B}_n(x, y), \tag{83}$$

which is the thesis of the theorem.

Theorem 8 can be exploited to state an important operational identity for polynomials of type ${}_H\bar{B}_n(x, y)$. Indeed, the partial differential equation appearing in the statement of Theorem 8 (Eq. 80) can be read as ordinary linear in y, and, Eq. 74 holding true, this means that

$${}_H\bar{B}_n(x, y) = e^{-\frac{y}{4}\frac{\partial^2}{\partial x^2}} B_n(2x). \tag{84}$$

Equation 84 plays the role of operational exponential definition for polynomials ${}_H\bar{B}_n(x, y)$.

4 Application to Fractional-Order Operators and Concluding Remarks

In concluding this discussion on the properties satisfied by this special class of Bernoulli polynomials, we want to offer here a few further considerations on the topic, and present some applications for the fractional calculus using a generalized form of the Hermite polynomials.

In primis, a further extension of Bernoulli polynomials can be obtained by means of two-variable generalized Laguerre polynomials [11, 19] of the form

$$\sum_{n=0}^{+\infty} \frac{t^n}{n!} L_n(x, y) = e^{yt} C_0(xt), \tag{85}$$

where $C_0(x)$ is the 0^{th}-order Tricomi function [1]

$$C_0(x) = \sum_{n=0}^{+\infty} \frac{(-1)^n x^n}{(n!)^2}. \tag{86}$$

The explicit form of Laguerre polynomials of type $L_n(x, y)$ is easily obtained:

$$L_n(x, y) = \sum_{s=0}^{+\infty} \frac{n!(-1)^s y^{n-s} x^s}{(n-s)!(s!)^2}. \tag{87}$$

Exploiting concepts and formalism presented in the case of Hermite-Bernoulli polynomials, it is possible to introduce the following discrete convolution:

$${}_L B_n(x, y) = \sum_{n=0}^{n} \binom{n}{s} B_{n-s} L_s(x, y), \tag{88}$$

which defines Laguerre-Bernoulli polynomials, to be discussed in a forthcoming paper.

In addition, according to the same procedure implemented in this study, the previously mentioned Appell polynomials $P_n(x, y)$, which satisfy the generating function [18]

$$\sum_{n=0}^{n} \frac{t^n}{n!} P_n(x, y) = A(yt) e^{xt} \tag{89}$$

with $A(0) \neq 0$, can be employed to introduce further forms of polynomials stemming from the properties of the Bernoulli class [20]. Indeed, we can set:

$${}_P B_n(x, y) = \sum_{s=0}^{n} \binom{n}{s} B_{n-s} P_s(x, y). \tag{90}$$

The above generalizations are planned to be discussed in a forthcoming paper in order to emphasize the simplification of finite sums of the type

$$\sum_{n=1}^{N-1} n^r = \frac{1}{r+1} \left[B_{r+1}(N) - B_{r+1} \right]. \tag{91}$$

Finally, the same procedure could be exploited in the case of orthonormal Bernoulli polynomials of order n:

$$b_n(x) = \sqrt{2n+1} \sum_{s=0}^{n} (-1)^s \binom{n}{s} \binom{2n-s}{n-s} x^{n-s}, \tag{92}$$

which can be easily generalized to the 2D case:

$$b_{nm}(x, y) = b_n(x) b_m(x) \tag{93}$$

defined over $[0, 1] \times [0, 1]$.

As we have seen above, the Hermite polynomials represent a powerful tool for investigating the properties of other families of polynomials and special functions, but they also allow to simplify numerous computational aspects, such as the representation of fractional derivatives. We note that, from relations presented in Sect. 2 (Eqs. (15)–(21)), it is possible to deduce the following integral representations [21]:

$$\begin{aligned} e^{b^2} &= \frac{1}{\sqrt{\pi}} \int_{-\infty}^{+\infty} e^{-u^2+2bu} du, \quad b \text{ constant} \\ e^{\lambda \frac{d^2}{dx^2}} &= \frac{1}{\sqrt{\pi}} \int_{-\infty}^{+\infty} e^{-u^2+2\sqrt{2}\frac{d}{dx}} du, \quad \lambda \in \mathbb{R} \end{aligned} \tag{94}$$

with integral transform

$$e^{\lambda \frac{d^2}{dx^2}} f(x) = \frac{1}{\sqrt{\pi}} \int_{-\infty}^{+\infty} e^{-u^2} f(x + 2\sqrt{2}u) du. \tag{95}$$

Taking advantage of the definition of the Euler gamma function $\Gamma(x) = \int_0^{+\infty} e^{-t} t^{x-1} dt$, it is possible to exploit the integral transform in the following way:

$$\left(\frac{d}{dx}\right)! f(x) = \int_0^{+\infty} e^{-t} t^{\frac{d}{dx}} f(x) dt, \tag{96}$$

i.e.,

$$\left(\frac{d}{dx}\right)! f(x) = \int_0^{+\infty} e^{-t} f(x + log(t)) dt. \tag{97}$$

The above result allows for deducing further integral transforms for more complicated operators [22]:

$$\begin{aligned} \left(x\frac{d}{dx}\right)! f(x) &= \int_0^{+\infty} e^{-t} f(xt) dt \\ \left(\frac{d}{dx}\right)^{-\nu} f(x) &= \frac{1}{\Gamma(\nu)} \int_0^{+\infty} t^{\nu-1} f(x-t) dt. \end{aligned} \tag{98}$$

Furthermore, if one notes that:

$$a^{-\nu} = \frac{1}{\Gamma(\nu)} \int_0^{+\infty} t^{\nu-1} e^{-at} dt, \tag{99}$$

the expression

$$\left(x \frac{d}{dx}\right)^{-\nu} f(x) = \frac{1}{\Gamma(\nu)} \int_0^{+\infty} t^{\nu-1} f(e^{-t} x) dt \tag{100}$$

becomes more interesting, after noting that:

$$\left(x \frac{d}{dx}\right)^{-\nu} \left[\frac{1}{1-x} - 1\right] = \frac{1}{\Gamma(\nu)} \int_0^{+\infty} \frac{t^{\nu-1} x}{e^t - 1} dt = \sum_{n=1}^{+\infty} \frac{x^n}{n^\nu}. \tag{101}$$

Similarly, for the second-order derivative:

$$\left(\alpha - x \frac{d^2}{dx^2}\right)^{-\nu} f(x) = \frac{1}{\Gamma(\nu)} \int_0^{+\infty} e^{-\alpha t} t^{\nu-1} e^{t \frac{d^2}{dx^2}} f(x) dt, \tag{102}$$

since

$$e^{t \frac{d^2}{dx^2}} f(x) = \frac{1}{2\sqrt{\pi t}} \int_{-\infty}^{+\infty} e^{-\frac{(x-\xi)^2}{4t}} f(\xi) d\xi, \tag{103}$$

the following expression is recovered:

$$\left(\alpha - x \frac{d^2}{dx^2}\right)^{-\nu} f(x) = \frac{1}{2\Gamma(\nu)} \int_0^{+\infty} \frac{e^{-\alpha t} t^{\nu-1}}{\sqrt{\pi t}} dt \left[\int_{-\infty}^{+\infty} e^{-\frac{(x-\xi)^2}{4t}} f(\xi) d\xi\right]. \tag{104}$$

For example, when $f(x) = e^{-x^2}$, the Gauss transform can be explicitly worked out, thus returning:

$$\left(\alpha - x \frac{d^2}{dx^2}\right)^{-\nu} e^{-x^2} = \frac{1}{\Gamma(\nu)} \int_0^{+\infty} \frac{e^{-\alpha t} t^{\nu-1}}{\sqrt{1+4t}} e^{-\frac{x^2}{1+4t}} dt. \tag{105}$$

By using the Hermite polynomials in their explicit form (see Eq. 21), we can write the above Gauss transform in the form:

$$H_n(x, y) = \frac{1}{2\sqrt{\pi y}} \int_{-\infty}^{+\infty} e^{-\frac{(x-\xi)^2}{4y}} \xi^n d\xi, \tag{106}$$

and the fractional derivative acting on the monomial turns out as:

$$\left(\alpha - x\frac{\partial^2}{\partial x^2}\right)^{-\nu} x^n = \frac{1}{\Gamma(\nu)}\int_0^{+\infty} e^{-\alpha t} t^{\nu-1} H_n(x, yt)dt. \tag{107}$$

The integral transform appearing in Eq. 107 defines a new family of polynomials, strictly related to Hermite polynomials and denoted by

$${}_{\nu}H_n(x, y; \alpha). \tag{108}$$

There are many interesting relations satisfied by this family of Hermite-like polynomials, which can be derived by analogous properties of ordinary Hermite polynomials [23]. Furthermore, these polynomials allow us to state interesting operational rules involving the fractional derivative, such as the following relevant relation:

$$\left(\alpha - y\frac{\partial^2}{\partial x^2}\right)^{\nu} {}_{\nu}H_n(x, y; \alpha) = x^n. \tag{109}$$

The formalism and the polynomials proposed here may offer significant advantages in computing the effect of fractional operators on a given function: the combined use of integral transforms and special polynomials provides a powerful tool to deal with fractional derivatives and integrals, which will be investigated in a forthcoming article.

References

1. Abramowitz, M., Stegun, I.A.: Handbook of Mathematical Functions: With Formulas, Graphs, and Mathematical Tables. Courier Corporation (1965)
2. Dattoli, G., Lorenzutta, S., Cesarano, C.: Bernestein polynomials and operational methods. J. Comput. Anal. Appl. **8**, 369–377 (2006)
3. Appell, P., de Fériet, J.K.: Fonctions Hypergéométriques et Hypersphériques: Polynômes d'Hermite. Gauthier-Villars, Paris (1926)
4. Cesarano, C., Cennamo, G.M., Placidi, L.: Operational methods for Hermite polynomials with applications. WSEAS Trans. Math. **13**, 925–931 (2014)
5. Khan, S., Yasmin, G., Khan, R., Hassan, N.A.M.: Hermite-based Appell polynomials: properties and applications. J. Math. Anal. Appl. **351**, 756–764 (2009)
6. Khan, S., Razab, N., Ali, M.: Finding mixed families of special polynomials associated with Appell sequences. J. Math. Anal. Appl. **447**, 398–418 (2017)
7. Khan, S., Ali, M.: A linear algebra approach to the hybrid Sheffer-Appell polynomials. Math. Sci. **13**(2), 153–164 (2019)
8. Khan, S., Naikoo, S.A., Ali, M.: Recurrence relations and differential equations of the Hermite-Sheffer and related hybrid polynomial sequences. Iran. J. Sci. Technol. Trans. A: Sci. **43**, 1607–1618 (2019)
9. Cesarano, C., Assante, D.: A note on generalized Bessel functions. Int. J. Math. Models Methods Appl. Sciences **7**(6), 625–629 (2013)
10. Dattoli, G., Ricci, P.E., Cesarano, C.: A note on multi-index polynomials of Dickson type and their applications in quantum optics. J. Comput. Appl. Math. **145**(2), 417–424 (2002)
11. Cesarano, C., Germano, B., Ricci, P.E.: Laguerre-type Bessel functions. Integral Transform. Spec. Funct. **16**(4), 315–322 (2005)

12. Cesarano, C.: Multi-dimensional Chebyshev polynomials: a non-conventional approach. Commun. Appl. Ind. Math. **10**, 1–19 (2019)
13. Cesarano, C., Ricci, P.E.: Orthogonality properties of the pseudo-Chebyshev functions (variations on a Chebyshev's theme). Mathematics **7**, 1–11 (2019)
14. Cesarano, C., Pinelas, S., Ricci, P.E.: The third and fourth kind pseudo-Chebyshev polynomials of half-integer degree. Symmetry **11**, 1–11 (2019)
15. Gould, H.W., Hopper, A.T., et al.: Operational formulas connected with two generalizations of Hermite polynomials. Duke Math. J. **1962**, *29*(1), 51–63 (1962)
16. Cesarano, C., Fornaro, C., Vazquez, L.: A note on a special class of Hermite polynomials. Int. J. Pure Appl. Math. **98**(2), 261–273 (2015)
17. Cesarano, C.: Operational methods and new identities for Hermite polynomials. Math. Model. Nat.l Phenomena **12**(3), 44–50 (2017)
18. Srivastava, H., Manocha, H.L.: Treatise on Generating Functions. Wiley, New York (1984)
19. Cesarano, C., Ricci, P.E.: The Legendre polynomials as a basis for Bessel functions. Int. J. Pure Appl. Math. **111**(1), 129–139 (2016)
20. Bretti, G., Ricci, P.E.: Multidimensional extensions of the Bernoulli and Appell Polynomials. Taiwan. J. Math. **8**, 415–428 (2004)
21. Assante, D., Cesarano, C., Fornaro, C., Vazquez, L.: Higher order and fractional diffusive equations. J. Eng. Sci. Technol. Rev. **8**, 202–204 (2015)
22. Cesarano, C.: Generalized special functions in the description of fractional diffusive equations. Commun. Appl. Ind. Math. **10**, 31–40 (2019)
23. Cesarano, C., Cennamo, G.M., Placidi, L.: Humbert polynomials and functions in terms of Hermite polynomials towards applications to wave propagation. WSEAS Trans. Math. **13**, 595–602 (2014)

A Fractional Hawkes Process

J. Chen, A. G. Hawkes, and E. Scalas

Abstract We modify ETAS models by replacing the Pareto-like kernel proposed by Ogata with a Mittag-Leffler type kernel. Provided that the kernel decays as a power law with exponent $\beta + 1 \in (1, 2]$, this replacement has the advantage that the Laplace transform of the Mittag-Leffler function is known explicitly, leading to simpler calculation of relevant quantities.

Keywords Point processes · Stochastic processes · Hawkes processes

Mathematics Subject Classification (2000) 60G55 · 26A33

1 Introduction

In 1971, Hawkes [7, 8] introduced a class of self-exciting processes to model contagious processes. In their simpler version, these are point processes with the following conditional intensity

$$\lambda(t|\mathcal{H}_t) = \lim_{h\to 0} \frac{\mathbb{E}(N(t, t+h)|\mathcal{H}_t)}{h} = \lambda + \alpha \int_{-\infty}^{t} f(t-u)\, dN(u),$$

J. Chen
School of Mathematics, Cardiff University, Cardiff, UK
e-mail: chenj60@cardiff.ac.uk

A. G. Hawkes
School of management, Swansea University, Swansea, UK
e-mail: a.g.hawkes@swansea.ac.uk

E. Scalas (✉)
Department of Mathematics, University of Sussex, Brighton, UK
e-mail: e.scalas@sussex.ac.uk

L. Beghin et al. (eds.), *Nonlocal and Fractional Operators*, SEMA SIMAI Springer Series 26, https://doi.org/10.1007/978-3-030-69236-0_7

where $\lambda > 0$, $N(t)$ is a Hawkes self-exciting counting process, $\mathcal{H}_t$ represents the history of the process, α is a branching ratio that must be smaller than 1 for stability, and $f(t)$ is a suitable kernel ($f(t)$ must be a probability density function for a positive random variable).

In 1988, Ogata [11] proposed the use of a power-law kernel for self-exciting processes of Hawkes type in order to reproduce the empirical Omori law for earthquakes. Ogata's models are also known as *Epidemic Type Aftershock Sequence* models or ETAS models. Within this framework, it is natural to replace Ogata's power-law kernel with a Mittag-Leffler kernel and this will be the main contribution of this chapter. We will first introduce the Mittag-Leffler distribution for positive random variables, then we will define a "fractional" version of Hawkes processes. Spectral properties and intensity expectation will be discussed using the fact that the Laplace transform of the one-parameter Mittag-Leffler function of argument $-t^\beta$ with $\beta \in (0, 1]$ is known analytically. Finally, we will present a simple algorithm based on the thinning method by Ogata [10] that simulates the conditional intensity process.

2 Mittag-Leffler Distributed Positive Random Variables

Consider the one-parameter Mittag-Leffler function

$$E_\beta(z) := \sum_{n=0}^{\infty} \frac{z^n}{\Gamma(n\beta + 1)}, \tag{1}$$

with $\beta \in (0, 1]$. If computed on $z = -t^\beta$ for $t \geq 0$, the Mittag-Leffler function $E_\beta(-t^\beta)$ has the meaning of survival function for a positive random variable T with infinite mean. This function interpolates between a stretched exponential for small times and a power-law with index β for large times. Its sign-changed first derivative

$$f_\beta(t) := -\frac{dE_\beta(-t^\beta)}{dt} = t^{\beta-1} E_{\beta,\beta}(-t^\beta) \tag{2}$$

is the probability density function of T, where $E_{\alpha,\beta}(z)$ is the two-parameter Mittag-Leffler function defined as

$$E_{\gamma,\delta}(z) := \sum_{n=0}^{\infty} \frac{z^n}{\Gamma(n\gamma + \delta)}. \tag{3}$$

Notice that the one-parameter Mittag-Leffler function coincides with the two parameter one with $\gamma = \beta$ and $\delta = 1$. For a suitable function $f(t)$ defined for positive t, let us define its Laplace transform as

$$\tilde{f}(s) = \mathcal{L}(f(t), s) = \int_0^\infty f(t)\, \mathrm{e}^{-st}\, dt.$$

The functions $E_\beta(-t^\beta)$ and $f_\beta(t)$ have explicit Laplace transforms. The survival function has the following Laplace transform

$$\mathcal{L}(E_\beta(-t^\beta); s) = \frac{s^{\beta-1}}{1+s^\beta}, \tag{4}$$

and the probability density function has the following Laplace transform

$$\mathcal{L}(f_\beta(t); s) = \frac{1}{1+s^\beta}. \tag{5}$$

Moreover, they have an explicit representation as an infinite (actually continuous) sum of exponential functions [5];

$$E_\beta(-t^\beta) = \int_0^\infty \mathrm{e}^{-\theta t} K_\beta(\theta)\, d\theta, \tag{6}$$

with

$$K_\beta(\theta) = \frac{1}{\pi} \frac{\theta^{\beta-1} \sin(\beta\pi)}{\theta^{2\beta} + 2\theta^\beta \cos(\beta\pi) + 1}, \tag{7}$$

leading to

$$f_\beta(t) = \int_0^\infty \theta \mathrm{e}^{-\theta t} K_\beta(\theta)\, d\theta. \tag{8}$$

These functions play an important role in fractional calculus. For instance $E_\beta(-t^\beta)$ is the solution of the following anomalous relaxation problem

$$\frac{d^\beta g(t)}{dt^\beta} = -g(t), \tag{9}$$

where d^β/dt^β is the Caputo derivative defined as

$$\frac{d^\beta g(t)}{dt^\beta} = \frac{1}{\Gamma(1-\beta)} \frac{d}{dt} \int_0^t \frac{g(\tau)}{(t-\tau)^\beta}\, dt - \frac{t^{-\beta}}{\Gamma(1-\beta)} g(0^+), \tag{10}$$

with initial condition $g(0^+) = 1$.

3 The Fractional Hawkes Processes

It becomes natural to use $f_\beta(t)$ as kernel for a version of Hawkes processes that we can call *fractional* Hawkes processes. The conditional intensity of the process is given by

$$\lambda(t|\mathcal{H}_t) = \lim_{h\to 0} \frac{\mathbb{E}(N(t,t+h)|\mathcal{H}_t)}{h} = \lambda + \alpha \int_{-\infty}^{t} f_\beta(t-u)\, dN(u), \tag{11}$$

where $\lambda > 0$ and $N(t)$ is a Hawkes self-exciting point process, leading to

$$\lambda(t|\mathcal{H}_t) = \lambda + \alpha \sum_{t_i<t} f_\beta(t-t_i). \tag{12}$$

with the branching ratio $\alpha < 1$ for stability. Hainaut [6] gives a different definition of fractional Hawkes process. Let us use his notation in the following remark. In his paper, he considers the time-changed intensity process λ_{S_t} where, in his case, the conditional intensity λ_t of the self-exciting process is the solution of a mean-reverting stochastic differential equation

$$d\lambda_t = \kappa(\theta - \lambda_t)\, dt + \eta d P_t,$$

where κ, θ and η are suitable parameters and the driving process P_t is given by

$$P_t := \sum_{k=1}^{N_t} \xi_k,$$

where N_t is a counting process and ξ_is are independent and identically distributed marks with finite positive mean and finite variance. The time-change S_t is the inverse of a β-stable subordinator. Our definition (11) is much simpler and it is directly connected with ETAS processes given that the kernel $f_\beta(t)$ has power-law tail with index $\beta + 1$. [9]. In particular, given the explicit Laplace transform of $f_\beta(t)$ and its representation in terms of infinite sum of exponentials, we can derive some explicit formulas.

3.1 Spectral Properties

From Eq. (11) in [7], we get the following equation for the covariance density $\mu(\tau)$ for $\tau > 0$.

$$\mu(\tau) = \alpha \left[\Lambda f_\beta(\tau) + \int_0^\tau f_\beta(\tau - v)\, \mu(v)\, dv + \int_0^\infty f_\beta(\tau + v)\, \mu(v)\, dv \right], \tag{13}$$

where Λ represents the asymptotic stationary value of the conditional intensity as derived in Eq. (19) below. If we now take the Laplace transform of (13), we get

$$\tilde{\mu}(s) = \alpha \left[\Lambda \tilde{f}_\beta(s) + \tilde{f}_\beta(s)\tilde{\mu}(s) + \mathcal{L}\left(\int_0^\infty f_\beta(\tau + v)\, \mu(v)\, dv; s \right) \right]. \tag{14}$$

Now, using (8) and setting

$$h(\theta) = \theta K_\beta(\theta) = \frac{1}{\pi} \frac{\theta^\beta \sin(\beta\pi)}{\theta^{2\beta} + 2\theta^\beta \cos(\beta\pi) + 1},$$

we can write

$$f_\beta(\tau) = \int_0^\infty h(\theta) \mathrm{e}^{-\theta\tau}\, d\theta,$$

so that the last summand in (14) becomes

$$\begin{aligned} \mathcal{L}\left(\int_0^\infty f_\beta(\tau + v)\, \mu(v)\, dv; s \right) &= \int_0^\infty \mathrm{e}^{-s\tau} \left[\int_0^\infty \left[\int_0^\infty h(\theta) \mathrm{e}^{-\theta(\tau+v)}\, d\theta \right] \mu(v)\, dv \right] d\tau \\ &= \int_0^\infty h(\theta) \frac{1}{\theta + s} \tilde{\mu}(\theta)\, d\theta. \end{aligned} \tag{15}$$

In principle, a numerical approximation of the integral in Eq. (15) plugged into (14) and coupled with Eq. (5) can lead to an explicit approximate expression for the Laplace transform $\tilde{\mu}(s)$. This will be the subject of a further paper. An alternative approach is given in [8] where the Bartlett spectrum is defined for real ω as

$$f(\omega) = \frac{1}{2\pi} \int \mathrm{e}^{-i\omega\tau} \mu^{(c)}(\tau)\, d\tau, \tag{16}$$

where, because $\mathbb{E}[(dN(t))^2] = \mathbb{E}[dN(t)]$ if events cannot occur multiply, the complete covariance density contains a delta function

$$\mu^{(c)}(\tau) = \Lambda\delta(t) + \mu(t).$$

Then it is shown in [8] p. 441 that

$$f(\omega) = \frac{\Lambda}{2\pi(1 - G(\omega))(1 - G(-\omega))}, \tag{17}$$

where, in our case, we would have

$$G(\omega) = \int_0^\infty \mathrm{e}^{-i\omega\tau} \alpha f_\beta(\tau)\, d\tau = \frac{\alpha}{1 + (i\omega)^\beta}.$$

The proof of this result depended on the assumption that the exciting kernel decays exponentially asymptotically. However, this is not true for the Mittag-Leffler distribution, which decays as a power law. Bacry and Muzy [2] prove a more general result using Laplace transforms in the complex plane, more easily digested from section 2.3.1 in [1]. Then the Laplace transform of the covariance density is given by

$$\tilde{\mu}^{(c)}(s) = \frac{\Lambda}{(1 - \tilde{\Phi}(s))(1 - \tilde{\Phi}(-s))}, \tag{18}$$

where

$$\tilde{\Phi}(s) = \int_0^\infty \mathrm{e}^{-s\tau} \Phi(\tau)\, d\tau$$

is the Laplace transform of the exciting kernel. In our case for $\tau > 0$, we have

$$\Phi(\tau) = \alpha f_\beta(\tau)$$

and

$$\tilde{\Phi}(s) = \frac{\alpha}{1 + s^\beta}.$$

Equations (17) and (18) look much the same, apart from a change of notation and a factor 2π. The difference, however, is that in (17) we are dealing with real ω while, in (18), s is a general complex variable and we can choose its domain to obtain well-behaved functions.

3.2 Intensity Expectation

Let us consider the expectation $\Lambda(t) = \mathbb{E}[\lambda(t|\mathcal{H}_t)]$ for both a stationary and non-stationary fractional Hawkes process. In the stationary case (process from $t = -\infty$), from Eq. (11), we get $\Lambda = \lambda + \alpha\Lambda$, leading to

$$\Lambda = \frac{\lambda}{1 - \alpha}. \tag{19}$$

On the contrary in the non-stationary case (process from $t = 0$), we can modify Eq. (11) as follows

$$\lambda(t|\mathcal{H}_t) = \lambda + \alpha \int_0^t f_\beta(t - u)\, dN(u), \tag{20}$$

so that the time-dependent expectation obeys the equation

$$\Lambda(t) = \lambda + \alpha \int_0^t f_\beta(t - u)\, \Lambda(u)\, du. \tag{21}$$

Taking Laplace transforms, we get

$$\tilde{\Lambda}(s) = \frac{\lambda}{s} + \alpha \tilde{f}_\beta(s)\tilde{\Lambda}(s),$$

so that

$$\tilde{\Lambda}(s) = \frac{\lambda}{s}\frac{1}{1-\alpha\tilde{f}_\beta(s)}.$$

Using Eq. (5) yields

$$\tilde{\Lambda}(s) = \frac{\lambda}{s}\frac{1+s^\beta}{(1-\alpha)+s^\beta}. \tag{22}$$

Equation (22) can be inverted numerically (or analytically for $\beta = 1/2$) to give $\Lambda(t)$ as well as the expected number of events from 0 to t as

$$\mathbb{E}[N(t)] = \int_0^t \Lambda(\tau)\, d\tau.$$

Also, based on a continuous version of Hardy-Littlewood Tauberian theorem [3] we get

$$\lim_{t\to\infty} \Lambda(t) = \frac{\lambda}{1-\alpha}$$

as given by Eq. (19). This result is exemplified in Fig. 1 for $\beta = 1/2$, $\lambda = 1$ and $\alpha = 1/2$. In that case, we get, for $t > 0$

$$\Lambda(t) = 2 - \mathrm{e}^{t/4}\mathrm{erfc}(\sqrt{t}/2).$$

From Fig. 1, one can see that $\Lambda(t)$ goes up very fast at first and, then, slowly converges to its asymptotic value 2. This is presumably due to the long tail of the Mittag-Leffler kernel.

4 Simulation

In order to simulate the intensity process introduced in Eq. (11), we use the thinning algorithm introduced by Ogata [10] (see also [12] report [12]). The function `ml.m` described in [4] is needed to compute the Mittag-Leffler functions described above and can be retrieved from the Matlab file exchange. The algorithm is as follows

1. Set the initial time $t = 0$, a counter $i = 0$ and a final time T.
2. Compute $M = \lambda + \alpha \sum_{t_i<t+\varepsilon} f_\beta(t + \varepsilon - t_i)$, for some small value of ε.
3. Generate a positive exponentially distributed random variable E with the meaning of a waiting time, with rate $1/M$.

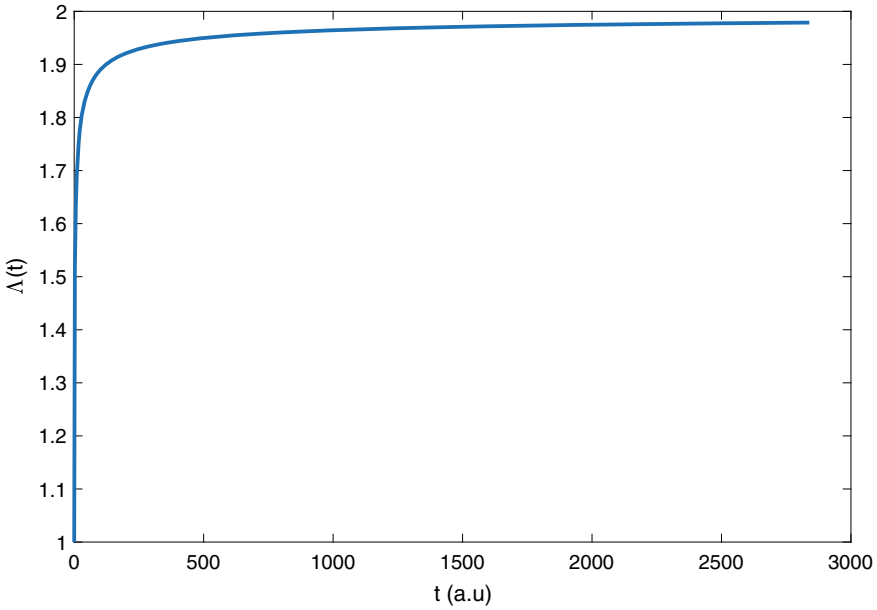

Fig. 1 $\Lambda(t)$ as a function of t for $\beta = 1/2$, $\lambda = 1$ and $\alpha = 1/2$

4. Set $\tau = t + E$.
5. Generate a uniform random variate U between 0 and 1.
6. If $U < [\lambda + \alpha \sum_{t_i < \tau} f_\beta(\tau - t_i)]/M$, set $t_{i+1} = \tau$ and update time to $t = \tau$, else, just set $t = \tau$.
7. Return to step 2 until t exceeds T.
8. Return the set of event times (or epochs) t_i.

An implementation of this algorithm in Matlab is presented below.

```
T=5;
t=0;
n=0;
alpha=0.9; % For stability
mu=1;
epsilon=1e-10;
beta=0.7;

SimPoints=[];

while t<T
t
M=mu+sum(alpha*ml(-(t+epsilon-SimPoints).^beta,beta,beta,1). …
*(t+epsilon-SimPoints).^(beta-1));
E=exprnd(1/M,1,1);
t=t+E;
```

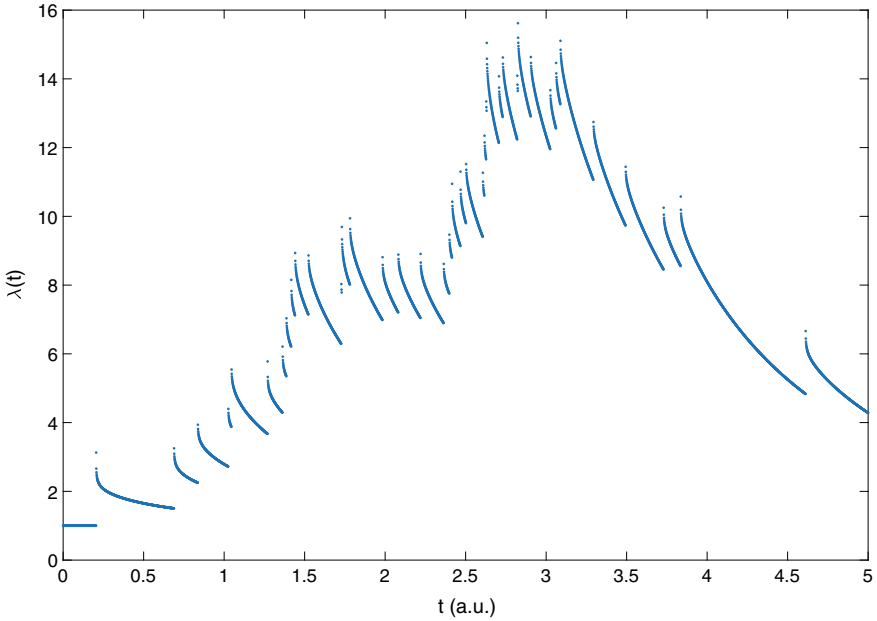

Fig. 2 $\lambda(t|\mathcal{H}_t)$ as a function of time t for $\beta = 0.9$, $\lambda = 1$ and $\alpha = 0.9$

```
U=rand;
if (U<(((mu+sum(alpha*ml(-(t-SimPoints).^beta,beta,beta,1). …
*(t-SimPoints).^(beta-1))))/M))
n=n+1;
SimPoints = [SimPoints, t];
end
end
index=find(SimPoints<10);
SimPoints=SimPoints(index);
```

Two examples of intensity process simulated up to $t = 5$ are presented in Figs. 2 and 3 for $\beta = 0.9$ and $\beta = 0.7$, respectively.

5 Outlook

In this paper, we defined a "fractional" Hawkes process and we studied its spectral properties and the expectation of its intensity. Thanks to explicit expressions for Laplace transforms, we could derive some analytical expressions that are only asymptotically available for power-law kernels of Pareto type as originally suggested

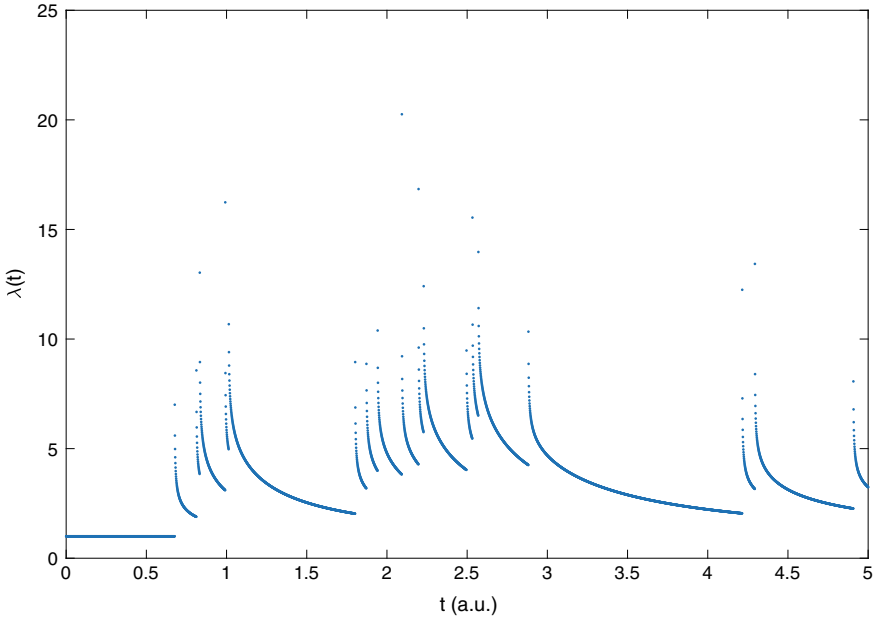

Fig. 3 $\lambda(t|\mathcal{H}_t)$ as a function of t for $\beta = 0.7$, $\lambda = 1$ and $\alpha = 0.9$

by Ogata. We also presented an explicit simulation of the intensity process based on the so-called thinning method.

Further work is needed to better characterize our process. In particular, we did not deal with parameter estimation, the multivariate version of the process, and we did not use the model to fit earthquake data (or any other data for what matters including financial data). We do hope that all this and more can become the subject of an extensive future paper on this process.

References

1. Bacry, E., Mastromatteo, I., Muzy, J.F.: Hawkes processes in finance, market microstructure and liquidity, **1**, 59 (2015). http://dx.doi.org/10.1142/S2382626615500057
2. Bacry, E., Muzy, J.F.: First- and second order statistics characterization of Hawkes processes and non-parametric estimation. IEEE Trans. Inf. Theory **62**(4), 2184–2201 (2016)
3. Feller, W.: An introduction to probability theory and its applications, vol. II, 2nd edn. John Wiley & Sons (1971)
4. Garrappa, R.: Numerical evaluation of two and three parameter Mittag-Leffler functions. SIAM J. Numer. Anal. **53**(3), 1350–1369 (2015)
5. Gorenflo, R., Mainardi, F.: Fractional calculus: integral and differential equations of fractional order in fractals and fractional calculus in continuum mechanics. In: Carpinteri, A., Mainardi, F. (eds.) pp. 223–276, Springer (1997)
6. Hainaut, D.: Fractional Hawkes processes, UCLouvain preprint, (2019)

7. Hawkes, A.G.: Spectra of some self-exciting and mutually exciting point processes. Biometrika **58**, 83–90 (1971)
8. Hawkes, A.G.: Spectra of some mutually exciting point processes. J. Roy. Stat. Soc. B **33**(3), 438–443 (1971)
9. Mainardi, F., Raberto, M., Gorenflo, R., Scalas, E.: Fractional calculus and continuous-time finance II: the waiting-time distribution. Phys. A **287**, 468–481 (2000)
10. Ogata, Y.: On Lewis' simulation method for point processes. IEEE Trans. Inf. Theory **27**, 23–31 (1981)
11. Ogata, Y.: Statistical models for earthquake occurrences and residual analysis for point processes **83**(401), 9–27 (1988)
12. Zhuang, J., Touati, S.: Stochastic simulation of earthquake catalogs, community online resource for statistical seismicity analysis, (2015). Available at http://www.corssa.org

Fractional Diffusive Waves in the Cauchy and Signalling Problems

Armando Consiglio and Francesco Mainardi

Abstract This work deals with the results and the simulations obtained for the time-fractional diffusion-wave equation, i.e. a diffusion-like linear integro partial differential equation containing a pseudo-differential operator interpreted as a fractional derivative in time. The data function (initial signal) is provided by a box-function and the solutions are so obtained by a convolution of the Green function with the initial data function. The relevance of the topic lies in the possibility of describing physical processes that interpolates between the different responses of the diffusion and waves equations, equipped with a physically realistic initial signal. Here two problems are considered where the use of the Laplace transform in the analysis of the problems has lead since 1990s to special functions of the Wright type.

Keywords Laplace transform · Wright functions · Fractional calculus

1 Introduction

Fundamental processes that find applications in different fields, spanning from physics to economy, are the diffusion and the wave propagation ones. The PDEs describing them only differ for the order of the time-derivative of the field variable, at least in the most simple formulation, and indeed we have:

$$\frac{\partial u(\mathbf{r},t)}{\partial t} = D\nabla^2 u(\mathbf{r},t) \qquad (\textit{Diffusion Equation}) \tag{1}$$

A. Consiglio (✉)
Institut für Theoretische Physik und Astrophysik, Universität Würzburg, 97074 Würzburg, Germany
e-mail: armando.consiglio@physik.uni-wuerzburg.de

F. Mainardi
Department of Physics & Astronomy, University of Bologna and INFN, Via Irnerio 46, 40126 Bologna, Italy
e-mail: francesco.mainardi@bo.infn.it

L. Beghin et al. (eds.), *Nonlocal and Fractional Operators*, SEMA SIMAI Springer Series 26, https://doi.org/10.1007/978-3-030-69236-0_8

$$\frac{\partial^2 u(\mathbf{r},t)}{\partial^2 t} = c^2 \nabla^2 u(\mathbf{r},t) \qquad (\textit{Wave Equation}) \tag{2}$$

This difference in the time-derivative results in very different processes, as respectively the disturbance spreads infinitely fast or the propagation velocity of the disturbance is a constant.

The time-fractional diffusion-wave equation is obtained from the standard diffusion (or wave) equation by replacing the first order (or second order) derivative in time with a fractional derivative in the Caputo sense. For readers convenience we refer to the Appendix A the essentials of this fractional derivative in the framework of the so-called Riemann-Liouville Fractional Calculus. As a consequence the time-fractional diffusion-wave equation, which includes Eqs. 1 and 2 as particular cases, reads as:

$$\frac{\partial^\alpha u(\mathbf{r},t)}{\partial t^\alpha} = D \nabla^2 u(\mathbf{r},t), \quad D > 0, \quad 0 < \alpha \leq 2 \tag{3}$$

where the time fractional derivative is intended in the Caputo sense, as introduced in Appendix A for readers' convenience

In this paper we limit ourselves to the one-dimensional case characterized by the space variable x. Following the analysis by Mainardi carried out in the 1990s, we must distinguish the cases $0 < \alpha \leq 1$ and $1 < \alpha \leq 2$ that correspond to time-fractional diffusion processes and to fractional transition from diffusion to to waves, respectively

$$\frac{1}{\Gamma(1-\alpha)} \int_0^t (t-\tau)^{-\alpha} \left(\frac{\partial u}{\partial \tau} \right) d\tau = D \frac{\partial^2 u}{\partial x^2}, \quad 0 < \alpha \leq 1; \tag{4}$$

$$\frac{1}{\Gamma(2-\alpha)} \int_0^t (t-\tau)^{1-\alpha} \left(\frac{\partial^2 u}{\partial \tau^2} \right) d\tau = D \frac{\partial^2 u}{\partial x^2}, \quad 1 < \alpha \leq 2; \tag{5}$$

In this paper we devote our attention to the second case, that is the evolution of the so-called fractional diffusive waves.

This work is organized as follows. In Sect. 2 we introduce the Wright functions, entire in the complex plane that we distinguish in two kinds in relation on the value-range of the two parameters on which they depend. In particular we devote our attention on two Wright functions of the second kind introduced by Mainardi with the term of auxiliary functions. One of them, known as M-Wright function generalizes the Gaussian function. It was shown to play a fundamental not only in fractional diffusion processes but also in the transition from diffusion to wave, namely to the so called fractional diffusive waves on which this work is based [19].

It is a relevant matter in dealing with fractional diffusive waves to distinguish the related space-time boundary conditions with which their equation must be equipped. For this purpose in Sect. 3 we introduce the two simplest boundary value problems referred by us to as Cauchy and Signalling problems, respectively. For both of them

we express the solutions in terms of two Green functions (depending of the order-derivative) properly convoluted with the initial data. In this Section we show the plots of the two Green function, both versus space x at fixed time t and versus t at fixed x in order to have a detailed visualization of the related processes. In Sect. 4 we plot the evolution of particular fractional diffusive waves; for the Cauchy problem we consider the evolution in space of the response to a space initial box whereas for the Signalling problem the evolution in time of the response to a time initial box. Surely the choice of a initial box is quite simple, but it corresponds to an input signal with finite energy at variance with what it occurs for the Green functions corresponding to delta-type input data. Sections 5 and 6 are focused on some basic results regarding *diffusive waves* and the *multi-dimensional time-fractional diffusion-wave equation*. In Sect. 7, finally, some concluding remarks are given.

2 The Wright Function and the Mainardi Auxiliary Functions

The *Wright function*, that we denote by $W_{\lambda,\mu}(z)$, is defined by the series representation convergent on the whole complex plane $\mathbb{C}$,

$$W_{\lambda,\mu}(z) = \sum_{n=0}^{\infty} \frac{z^n}{n!\Gamma(\lambda n + \mu)}, \lambda > -1, \ \mu \in \mathbb{C}. \tag{6}$$

One of its *integral representations* reads as:

$$W_{\lambda,\mu}(z) = \frac{1}{2\pi i} \int_{Ha} \mathrm{e}^{\sigma + z\sigma^{-\lambda}} \frac{d\sigma}{\sigma^{\mu}}, \ \lambda > -1, \ \mu \in \mathbb{C}, \tag{7}$$

where Ha denotes the Hankel path. It is a loop, which starts from $-\infty$ along the lower side of negative real axis, encircles the axes origin and ends at $-\infty$ along the upper side of the negative real axis.

$W_{\lambda,\mu}(z)$ is then an *entire function* for all $\lambda \in (-1, +\infty)$. Originally, in 1930s Wright assumed $\lambda \geq 0$ in connection with his investigations on the asymptotic theory of partitions [21, 22], and only in 1940 [23] he considered $-1 < \lambda < 0$.

We note that in the Vol 3, Chap. 18 of the handbook of the Bateman Project [4], presumably for a misprint, the parameter λ is restricted to be non-negative, whereas the Wright functions remained practically ignored in other handbooks. In 1990s Mainardi, being aware only of the Bateman handbook, proved that the Wright function is entire also for $-1 < \lambda < 0$ in his approaches to the time fractional diffusion equation, see [15–17].

In view of the asymptotic representation in the complex domain and of the Laplace transform for positive argument $z = r > 0$ (r can denote the time variable t or the positive space variable x) the Wright functions are distinguished in *first kind* ($\lambda \geq 0$)

and *second kind* ($-1 < \lambda < 0$) as outlined more recently in the Appendix F of the 2010 book by Mainardi [18]. As a matter of fact two particular Wright functions of the second kind, were introduced by Mainardi named $F_\nu(z)$ and $M_\nu(z)$ ($0 < \nu < 1$), called *auxiliary functions* in virtue of their role in the time fractional diffusion equations. These functions are indeed special cases of the Wright function of the second kind by setting, respectively, $\lambda = -\nu$ and $\mu = 0$ or $\mu = 1 - \nu$. Hence we have:

$$F_\nu(z) := W_{-\nu,0}(-z), \quad 0 < \nu < 1, \tag{8}$$

and

$$M_\nu(z) := W_{-\nu,1-\nu}(-z), \quad 0 < \nu < 1, \tag{9}$$

These functions are interrelated through the following relation:

$$F_\nu(z) = \nu z M_\nu(z). \tag{10}$$

The series and integral representations of the auxiliary functions are derived from those of the general Wright functions. Then for $z \in \mathbb{C}$ and $0 < \nu < 1$ we have:

$$F_\nu(z) = \sum_{n=1}^{\infty} \frac{(-z)^n}{n!\Gamma(-\nu n)} = -\frac{1}{\pi} \sum_{n=1}^{\infty} \frac{(-z)^n}{n!} \Gamma(\nu n + 1) \sin(\pi \nu n), \tag{11}$$

$$M_\nu(z) = \sum_{n=0}^{\infty} \frac{(-z)^n}{n!\Gamma[-\nu n + (1 - \nu)]} = \frac{1}{\pi} \sum_{n=1}^{\infty} \frac{(-z)^{n-1}}{(n-1)!} \Gamma(\nu n) \sin(\pi \nu n), \tag{12}$$

and

$$F_\nu(z) := \frac{1}{2\pi i} \int_{Ha} \mathrm{e}^{\sigma - z\sigma^\nu} d\sigma, \tag{13}$$

$$M_\nu(z) := \frac{1}{2\pi i} \int_{Ha} \mathrm{e}^{\sigma - z\sigma^\nu} \frac{d\sigma}{\sigma^{1-\nu}}. \tag{14}$$

Explicit expressions of $F_\nu(z)$ and $M_\nu(z)$ in terms of known functions are expected for some particular values of ν as shown and recalled in the cited papers by Mainardi, see [15–17], that is

$$M_{1/2}(z) = \frac{1}{\sqrt{\pi}} \mathrm{e}^{-z^2/4}, \tag{15}$$

$$M_{1/3}(z) = 3^{2/3} \mathrm{Ai}(z/3^{1/3}). \tag{16}$$

More recently Liemert and Klenie [9] have added the following expression for $\nu = 2/3$

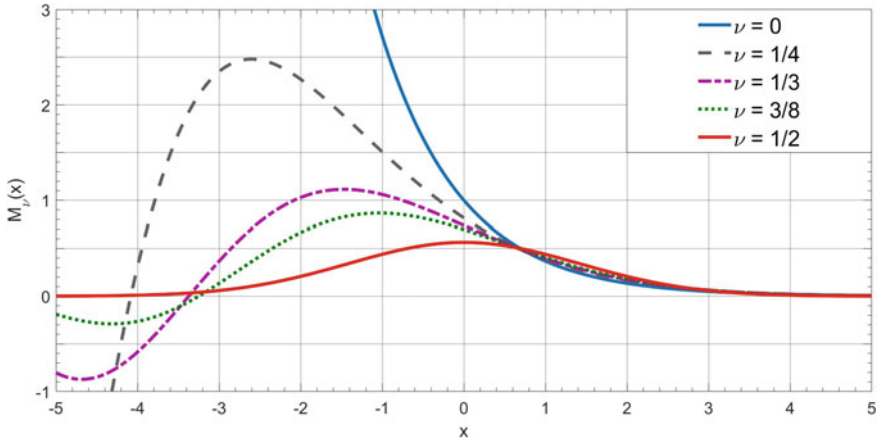

Fig. 1 Plots of the M-Wright function as a function of the x variable, for $0 \le \nu \le 1/2$

$$M_{2/3}(z) = 3^{-2/3}\, \mathrm{e}^{-2z^3/27} \left[3^{1/3}\, z\, \mathrm{Ai}\left(z^2/3^{4/3}\right) - 3\mathrm{Ai}'\left(z^2/3^{4/3}\right)\right], \qquad (17)$$

where Ai and Ai′ denote the *Airy function* and its first derivative. Furthermore they have suggested in the positive real field $\mathbb{R}^+$ and $\nu \in (0, 1)$ the following remarkably integral representation

$$M_\nu(x) = \frac{1}{\pi}\, \frac{x^{\nu/(1-\nu)}}{1-\nu} \cdot \int_0^\pi C_\nu(\phi) \exp\left(-C_\nu(\phi)\right)\, x^{1/(1-\nu)}\, d\phi, \qquad (18)$$

where

$$C_\nu(\phi) = \frac{\sin(1-\nu)}{\sin\phi} \left(\frac{\sin\nu\phi}{\sin\phi}\right)^{\nu/(1-\nu)}, \qquad (19)$$

corresponding to equation (7) of the article written by Saa and Venegeroles [20].

We find it convenient to show the plots of the M-Wright functions on a space symmetric interval of $\mathbb{R}$ in Figs. 1, 2, corresponding to the cases $0 \le \nu \le 1/2$ and $1/2 \le \nu \le 1$, respectively. We recognize the non-negativity of the M-Wright function on $\mathbb{R}$ for $1/2 \le \nu \le 1$ consistently with the analysis on distribution of zeros and asymptotics of Wright functions carried out by Luchko, see [10, 14].

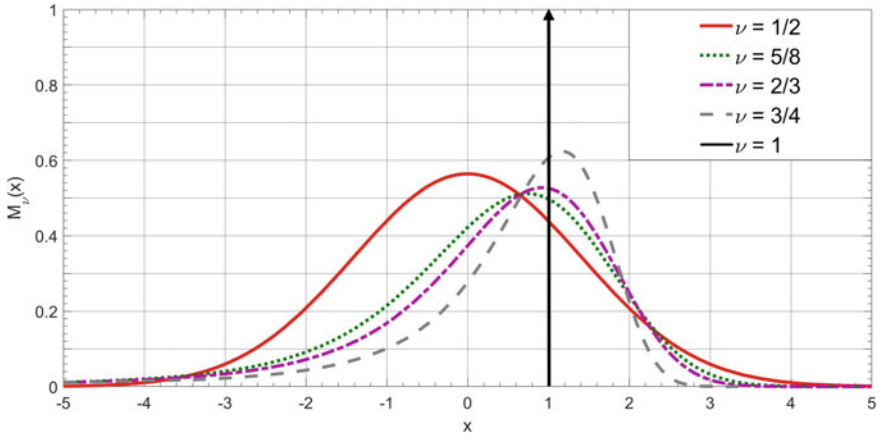

Fig. 2 Plots of the M-Wright function as a function of the x variable, for $1/2 \leq \nu \leq 1$

3 Cauchy and Signaling Problems: Green Functions for Fractional Diffusive Waves

Cauchy and Signaling problems are well-know boundary value problems (BVP) for Partial Differential Equations (PDE's) of evolution type. In this section we will extend these BVP's to the time-fractional PDE's described in Eqs. (4) and (5).

In the *Cauchy problem* the medium is supposed to be unlimited ($-\infty < x < +\infty$) and to be subjected at $t = 0$ to a known disturbance provided by the data function $f(x)$, that must admit the Fourier transform or the Fourier series expansion if the support is finite. Formally:

$$\lim_{t \to 0^+} u(x,t) = f(x), \qquad -\infty < x < +\infty; \tag{20}$$

$$\lim_{x \to \pm\infty} u(x,t) = 0, \qquad t > 0. \tag{21}$$

In the *Signalling problem* the medium is supposed to be semi-infinite ($0 \leq x < +\infty$) and initially undisturbed. At $x = 0^+$ (the accessible end) and for $t > 0$ the medium is then subjected to a known disturbance provided by the causal function $g(t)$, that must admit the Laplace Transform. Formally:

$$\lim_{t \to 0^+} u(x,t) = 0, \qquad 0 \leq x < +\infty; \tag{22}$$

$$\lim_{x \to 0^+} u(x,t) = g(t), \quad \lim_{x \to +\infty} u(x,t) = 0 \qquad t > 0. \tag{23}$$

For each problem can be defined the *Green Function* $\mathcal{G}$, i.e. the fundamental solution obtained by considering respectively initial inputs of Dirac delta type, that is of $f(x) = \delta(x)$ and $g(t) = \delta^+(t)$. As a consequence, because of the linearity of the

problems the solutions to the generic input data $f(x)$ and $g(t)$ are then expressed by a proper convolution integral between the data functions and the Green Functions, For the Cauchy problem we have:

$$u(x,t) = \int_{-\infty}^{+\infty} \mathcal{G}_C(\xi,t;\alpha)\, f(x-\xi)\, d\xi = \mathcal{G}_C(x,t;\alpha) * f(x)\,. \tag{24}$$

For the Signaling problem we have:

$$u(x,t) = \int_0^t \mathcal{G}_S(x,\tau;\alpha) g(t-\tau)\, d\tau = \mathcal{G}_S(x,t;\alpha) * g(t)\,. \tag{25}$$

In above equations we note the different nature of the convolution integrals: for the Cauchy problem a space or Fourier convolution whereas for the Signalling problem a time or Laplace convolution.

If $1 < \alpha \leq 2$, because the presence of the first derivative in the definition of the corresponding time fractional derivative, we must consider also the initial value of the first-order derivative of the field variable $u_t(x, 0^+; \alpha)$. Here we assume $u_t(x, 0^+; \alpha) = 0$ in order to ensure the continuous dependence of the solutions on the parameter α in the transition from $\alpha = 1^-$ to $\alpha = 1^+$. This in practice means to neglect the effect of a second Green function.

Through the Laplace Transform technique as show by Mainardi in his 1990s papers and the introduction of the parameter ν with the related similarity variable

$$\nu = \frac{\alpha}{2}\,, \quad z = \frac{x}{\sqrt{D}t^{\nu}}\,, \tag{26}$$

the following *reciprocity relation* can be obtained for the Green Functions for $x \geq 0$ and $t \geq 0$:

$$2\nu x \mathcal{G}_C(x,t;\nu) = t\mathcal{G}_S(x,t;\nu) = F_\nu(z) = \nu z M_\nu(z)\,. \tag{27}$$

The explicit expression for the Cauchy and Signaling Green function are, respectively:

$$G_C(x,t;\nu) = \frac{t^{-\nu}}{2\sqrt{D}} M_\nu\left(\frac{|x|}{\sqrt{D}t^{\nu}}\right), \quad -\infty < x < +\infty, \quad t \geq 0, \tag{28}$$

and

$$G_S(x,t;\nu) = \frac{\nu x t^{-\nu-1}}{\sqrt{D}} M_\nu\left(\frac{x}{\sqrt{D}t^{\nu}}\right), \qquad x \geq 0, \qquad t \geq 0. \tag{29}$$

The Green functions are so expressed in terms of only the M-Wright function the most relevant Mainardi auxiliary function.

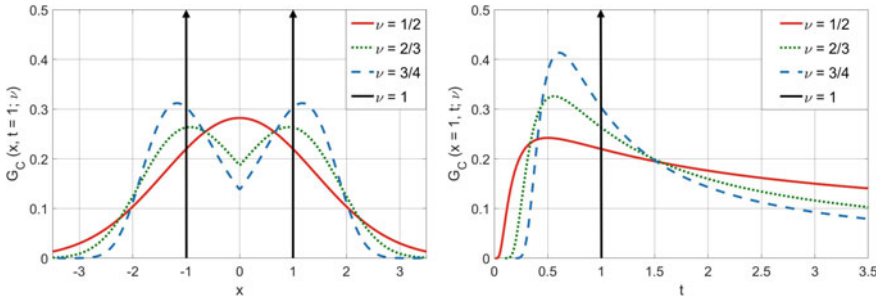

Fig. 3 Green functions for the Cauchy problem versus x and t for $\nu = 1/2$, $\nu = 2/3$, $\nu = 3/4$ and $\nu = 1$

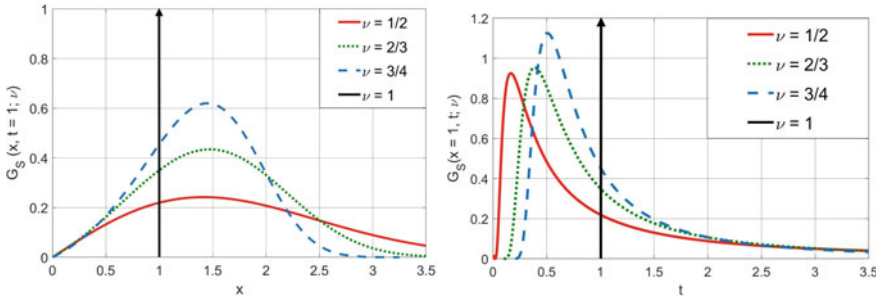

Fig. 4 Green functions for the Signaling problem versus x and t for $\nu = 1/2$, $\nu = 2/3$, $\nu = 3/4$ and $\nu = 1$

The interested reader can find on YouTube (title: *Simulation of M-Wright function*) the simulation of the fundamental solution $M_\nu(|x|, t)$, at $t = 1$ and $-5 \leq x \leq 5$, for varying values of the parameter ν ($0 \leq \nu \leq 0.85$).

In the following we exhibit at selected values ν ($\nu = 1/2, 2/3, 3/4, 1$) the spatial and temporal evolution the Cauchy and Signaling Green functions in their temporal and spatial domains. For the Cauchy Green function we will show the plots versus $x \in [-3.5, +3.5]$ at fixed time $t = 1$ and versus $t \in [0, 3.5]$ at fixed space $x = 1$. For the Signaling Green function we will show the plots versus time $t \in [0, 3.5]$ at fixed space $x = 1$ and versus $x \in [0, 3.5]$ at fixed time $t = 1$. In all computations we agree to take $D = 1$. These 2-D plots are expected to give an idea of the spatial-temporal evolution the two Green functions. Furthermore the selected values of ν are the most relevant in understanding the passage from standard diffusion to standard propagation because $\nu = 1/2$ (standard diffusion), $\nu = 2/3$ (diffusion-wave), $\nu = 3/4$ (diffusion-wave) and $\nu = 1$ (standard propagation) (Figs. 3, 4).

4 Cauchy and Signaling Problems: Box Evolution for Fractional Diffusive Waves

4.1 Solutions for the Cauchy Problem

The first graphical results that are shown regards the Cauchy problem where the time-evolution of the general solution is based on Eq. 24 with the Green function given by Eq. 28; different values of the parameter ν are considered in order to observe how the evolution changes when the process is more diffusion-like or wave-like.

In particular the initial data is given by an initially centered box-signal $f(x)$, such that $f(x) = 1$ for $x \in [-1, 1]$ and $f(x) = 0$ otherwise, represented as a blue dashed line in next Figs. 5, 6, 7 and 8.

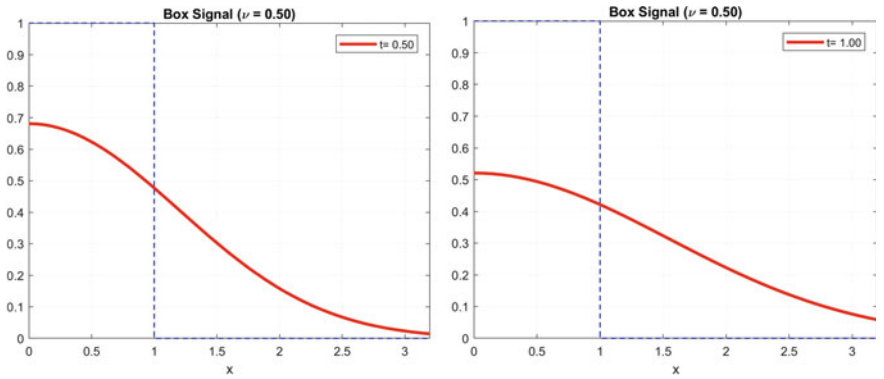

Fig. 5 Time evolution of an initial box-signal for $\nu = 0.50$, seen at $t = 0.50$ (left) and $t = 1.00$ (right). The figures are symmetric on the negative axis

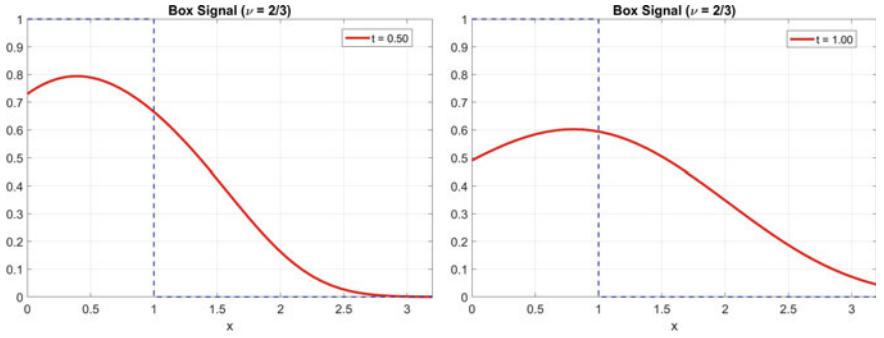

Fig. 6 Time evolution of an initial box-signal for $\nu = 2/3$, seen at $t = 0.50$ (left) and $t = 1.00$ (right). The figures are symmetric on the negative axis

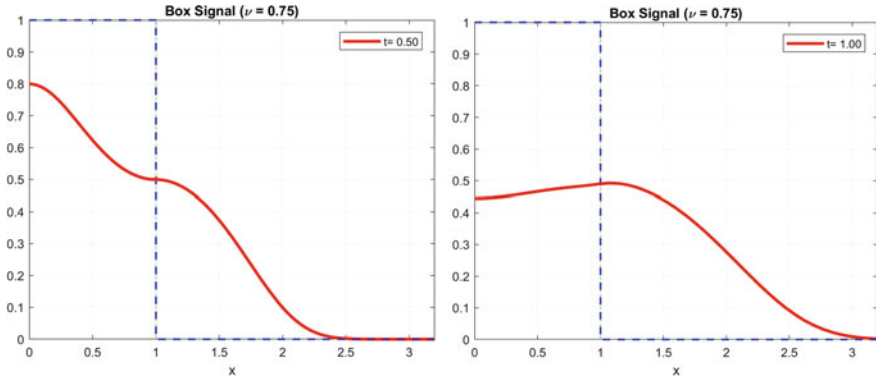

Fig. 7 Time evolution of an initial box-signal for $\nu = 0.75$, seen at $t = 0.50$ (left) and $t = 1.00$ (right). The figures are symmetric on the negative axis

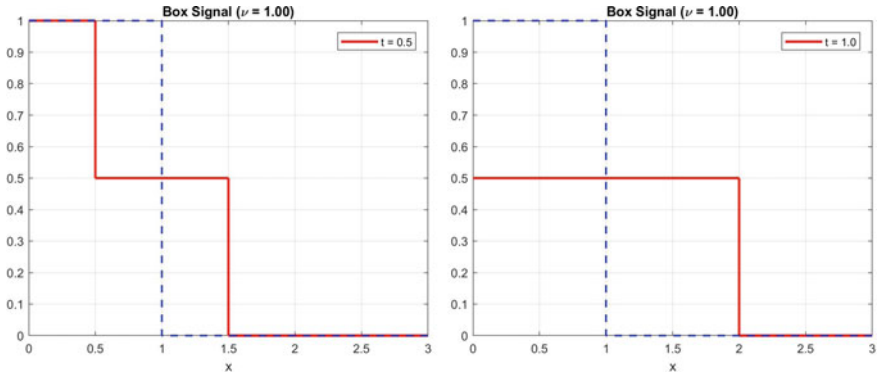

Fig. 8 Time evolution of an initial box-signal for $\nu = 1.00$, seen at $t = 0.50$ (left) and $t = 1.00$ (right). The figures are symmetric on the negative axis

4.2 Solutions for the Signaling Problem

In this subsection we show the graphical results regarding the Signaling problem; the time-evolution of the general solution is based on Eq. 25 with the Green function given by Eq. 29.

The initial data is given by a box-signal in time $g(t)$, such that $g(t) = 1$ for $t \in [0, 1]$ and $g(t) = 0$ otherwise.

Note that the initial box is represented in the following Figs. 9, 10, 11 and 12 by the dashed blue line, located in the accessible end.

Also in this case we consider the same values of the parameter ν.

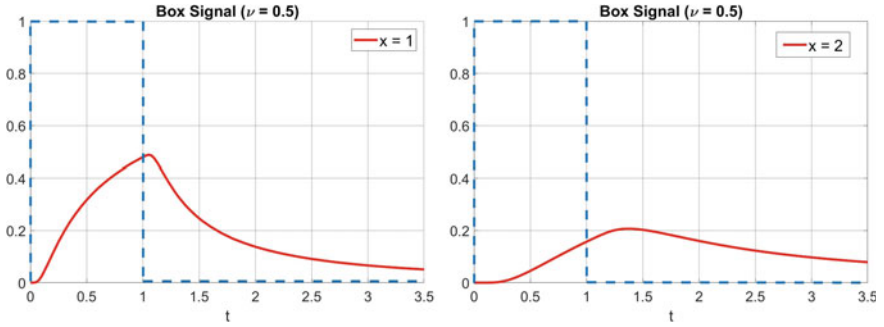

Fig. 9 Solution of the Signaling problem for $\nu = 1/2$ as a function of time ($x = 1, x = 2$)

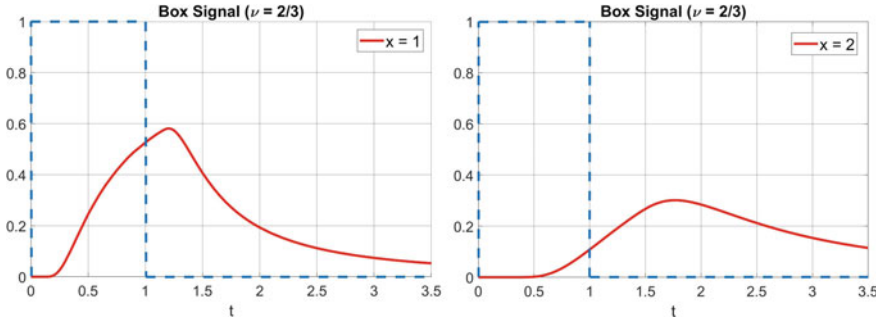

Fig. 10 Solution of the Signaling problem for $\nu = 2/3$ as a function of time ($x = 1, x = 2$)

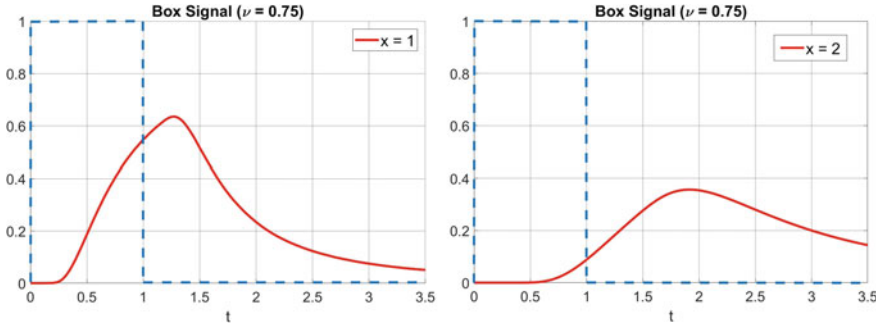

Fig. 11 Solution of the Signaling problem for $\nu = 3/4$ as a function of time ($x = 1, x = 2$)

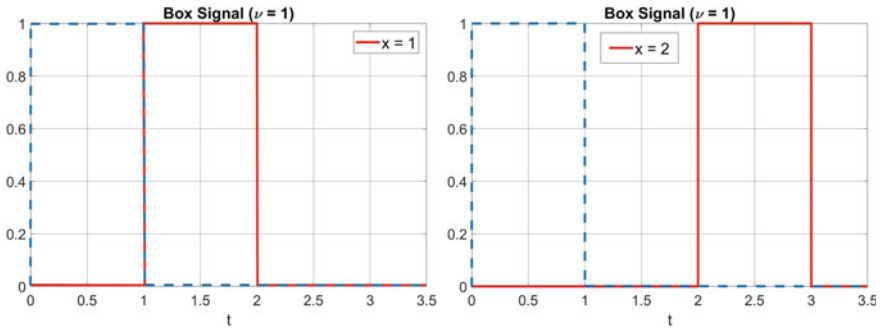

Fig. 12 Solution of the Signaling problem for $\nu = 1$ as a function of time ($x = 1, x = 2$)

5 Interpretation of the Green Functions as Diffusive Waves

In Sect. 3 we introduced the Green Functions (i.e. the fundamental solutions) for the Cauchy and Signaling problems, and we used them in Sect. 4 inside convolution integrals to find the general solutions of the time-fractional diffusion-wave equation; in particular we introduced the concept of diffusive waves when $1/2 < \nu < 1$. Here we recall some basic results concerning the Green functions and their interpretation as diffusive waves, in order to gain a deeper physical and mathematical understanding. The focus will be on the maximum locations, maximum values and propagation velocities of the maximum points of $\mathcal{G}_C$ and $\mathcal{G}_S$, and some results concerning the center of gravity and the medians of the Green functions will be given.

5.1 Cauchy Problem

It can demonstrated in a probabilistic way [5] that the maximum of the Green function $\mathcal{G}(x, t, \nu)$ for the Cauchy problem is given by the points:

$$x_*(t) = \pm c_\nu t^\nu, \ \ \nu = \beta/2 \tag{30}$$

where $t \in \mathbb{R}^+$, $1/2 < \nu < 1$ and c_ν is a constant determined by ν.
The analytical proof of the previous relation is given in [13].

It is straightforward to obtain the finite velocity of propagation $v_C(t, \nu)$ of the maximum point of the Green function for $t > 0$ as the first order derivative of Eq. 30:

$$v_C(t, \nu) := x'_*(t) = \nu c_\nu t^{\nu-1} \tag{31}$$

For $\nu = 1/2$ and $\nu = 1$ we must respectively recover the well know results for the diffusion and propagation processes. In particular the propagation velocity is zero

when $\nu = 1/2$ ($c_{1/2} = 0$) and it is a constant when $\nu = 1$ ($c_1 = 1$). For all the other cases in between, Eq. 31 tell us that the propagation velocity of the maximum point of the Green function is a decreasing function of the t variable, ranging from $+\infty$ when $t = 0^+$ to 0 when $t \to +\infty$.

The maximum value $\mathcal{G}_C^*(t, \nu)$ of $\mathcal{G}_C(x, t, \nu)$ is given by:

$$\mathcal{G}_C^*(t, \nu) = m_\nu t^{-\nu}, \; m_\nu = \frac{1}{2} M_\nu(c_\nu) = \frac{1}{\pi} \int_0^\infty E_{2\nu}(-\tau^2) \cos(c_\nu \tau) d\tau \tag{32}$$

where E_α is the Mittag-Leffler function.

From the reciprocity relation (27) we also have that

$$\mathcal{G}_C^*(t, \nu) \cdot x_*(t) = c_\nu m_\nu, \quad 0 < t < \infty \tag{33}$$

is a constant that depends only on ν, leading to certain hyperbola for fixed values of ν.

We also briefly recall that the location of the center of gravity of the Green function for the Cauchy problem is:

$$r_\nu^C(t) = \frac{\int_0^\infty r \mathcal{G}_C(x, t; \nu) dr}{\int_0^\infty \mathcal{G}_C(x, t; \nu) dr} = g_C(\nu) t^\nu, \; g_C(\nu) = \frac{1}{\Gamma(1 + \nu)} \tag{34}$$

The velocity of the center of gravity is given by:

$$v_C^g(t, \nu) = \frac{d}{dt} r_\nu^C(t) = \frac{t^{\nu-1}}{\Gamma(\nu)}, \tag{35}$$

Finally we report the location of the median

$$x_m^C = m_C(\nu) t^\nu \tag{36}$$

that shows a power function in the t variable with ν as exponent, and where the coefficient $m_C(\nu)$ represents the location of the median at $t = 1$.

The interested reader can find more details in [11].

5.2 Signaling Problem

The same concepts introduced in the previous subsection can be introduced also for the Signaling problem.

Again the reciprocity relation (27) is used to get the representation for the maximum location $x_* = x_*(t, \nu)$ of $\mathcal{G}_S(x, t; \nu)$:

$$x_*(t, \nu) = Dt^{\nu}, \quad D = x_*(1, \nu) = d_\nu \tag{37}$$

Hence the propagation velocity of the maximum point is:

$$v_S(t, \nu) = \frac{d}{dt} x_* = \nu d_\nu t^{\nu-1}. \tag{38}$$

which reminds us what we have seen for the Cauchy problem. The only difference with the Cauchy case is that, when $\nu = 1/2$ (diffusion equation), is that the velocity of the maximum location of the Green function is equal to $\frac{\sqrt{2}}{2}\frac{1}{\sqrt{t}}$.

The maximum value $\mathcal{G}^*_S(t; \nu)$ of $\mathcal{G}_S(x, t; \nu)$ is given by:

$$\mathcal{G}^*_S(t; \nu) = \frac{n_\nu}{t}, \; n_\nu = F_\nu(d_\nu) = \frac{2}{\pi} \int_0^\infty \tau E_{2\nu,2\nu}(-\tau^2) \sin(d_\nu \tau) d\tau \tag{39}$$

where $E_{\alpha,\beta}$ is the generalized Mittag-Leffler function.

Regarding the center of gravity of the Green function, its location is considered with respect to the spatial variable because the location with respect to the variable t is infinite for all $x > 0$.
We obtain the following formula:

$$r^S_\nu(t) = \frac{\int_0^\infty r \mathcal{G}_S(x, t; \nu) dr}{\int_0^\infty \mathcal{G}_S(x, t; \nu) dr} = \frac{\sqrt{\pi} 2^{1-2\nu}}{\Gamma(\nu + 1/2)} t^\nu \tag{40}$$

Consequently the velocity of the center of gravity of $\mathcal{G}_S$ can be calculated:

$$v^g_S(t; \nu) = \frac{d}{dt} r^S_\nu(t) = \frac{\sqrt{\pi} 2^{1-2\nu} \nu}{\Gamma(\nu + 1/2)} t^{\nu-1} \tag{41}$$

Finally we recall that the location $t = t^S_m$ of the median of the Green function for fixed $x > 0$ and $1/2 \le \nu \le 1$ is:

$$t^S_m = m_S(\nu) x^{1/\nu}, \quad m_S(\nu) = \frac{1}{(m_C(\nu))^{1/\nu}} \tag{42}$$

More details can be found in [11].

6 Multi-dimensional Fractional Diffusion-Wave Equation

Due to its importance in applications, we find useful to introduce some concepts regarding the multidimensional fractional diffusion-wave equation, which reads:

$$D_t^\beta u(\mathbf{x},t) = -(-\Delta)^{\alpha/2} u(\mathbf{x},t),\ \mathbf{x}\in\mathbb{R}^n,\ t>0,\ 1<\alpha\le 2,\ 0<\beta\le 2. \quad (43)$$

$(-\Delta)^{\alpha/2}$ is the fractional Laplacian, defined as a pseudo-differential operator with the symbol $|\kappa|^\alpha$:

$$(\mathcal{F}(-\Delta)^{\alpha/2} f)(\kappa) = |\kappa|^\alpha (\mathcal{F} f)(\kappa) \quad (44)$$

where $(\mathcal{F}f)(\kappa)$ is the Fourier transform of a function f at the point $\kappa\in\mathbb{R}^n$. D_t^β instead is the Caputo time-fractional derivative of order β.

Referring to the Cauchy problem and limiting ourselves to $1<\beta\le 2$, we pose two initial conditions in the form:

$$u(\mathbf{x},0) = \phi(\mathbf{x}),\ \frac{\partial u(\mathbf{x},0)}{\partial t} = 0,\ \mathbf{x}\in\mathbb{R}^n \quad (45)$$

Because of linearity, the solution is:

$$u(\mathbf{x},t) = \int_{\mathbb{R}^n} G_{\alpha,\beta,n}(\mathbf{x}-\xi,t)\phi(\xi)d\xi, \quad (46)$$

with $G_{\alpha,\beta,n}$ being the fundamental solutions to the problem with initial conditions:

$$u(\mathbf{x},0) = \prod_{i=1}^{n} \delta(x_i),\ \mathbf{x} = (x_1, x_2, ..., x_n)\in\mathbb{R}^n \quad (47)$$

and

$$\frac{\partial u}{\partial t}(\mathbf{x},0) = 0,\ \mathbf{x}\in\mathbb{R}^n \quad (48)$$

with δ being the Dirac delta function.

The following integral representation for the fundamental solution can be obtained applying the Fourier transform and its inverse [12]:

$$G_{\alpha,\beta,n}(\mathbf{x},t) = \frac{|\mathbf{x}|^{1-\frac{n}{2}}}{(2\pi)^{\frac{n}{2}}} \int_0^\infty E_\beta(-\tau^\alpha t^\beta)\tau^{\frac{n}{2}} J_{\frac{n}{2}-1}(\tau|\mathbf{x}|)d\tau, \quad (49)$$

where J_ν denotes the Bessel function.

Via the Mellin integral Transform, the previous equation can be transformed to the following Mellin-Barnes representation:

$$G_{\alpha,\beta,n}(\mathbf{x},t)=\frac{1}{\alpha}\frac{t^{-\frac{\beta n}{\alpha}}}{(4\pi)^{\frac{n}{2}}}\frac{1}{2\pi i}\int_{\gamma-i\infty}^{\gamma+i\infty}\frac{\Gamma(\frac{s}{2})\Gamma(\frac{n}{\alpha}-\frac{s}{\alpha})\Gamma(1-\frac{n}{\alpha}+\frac{s}{\alpha})}{\Gamma(1-\frac{\beta}{\alpha}n+\frac{\beta}{\alpha}s)\Gamma(\frac{n}{2}-\frac{s}{2})}\Big(\frac{|\mathbf{x}|}{2t^{\frac{\beta}{\alpha}}}\Big)^{-s}ds \tag{50}$$

that is valid for $|\mathbf{x}|\neq 0$, under the condition $\max(n-\alpha,0)<\gamma<n$.

Equation 50 is particularly useful because can be used to determine particular (and simpler) cases compared to the general one. Simpler cases corresponds to a simpler form of the quotient:

$$K_{\alpha,\beta,n}(s)=\frac{\Gamma(\frac{s}{2})\Gamma(\frac{n}{\alpha}-\frac{s}{\alpha})\Gamma(1-\frac{n}{\alpha}+\frac{s}{\alpha})}{\Gamma(1-\frac{\beta}{\alpha}n+\frac{\beta}{\alpha}s)\Gamma(\frac{n}{2}-\frac{s}{2})} \tag{51}$$

resulting from some canceled Gamma functions in the Mellin-Barnes representation. Some of these cases e.g. are:

Diffusion equation ($\beta=1,\alpha=2$):
This case results in the most simple Mellin-Barnes representation, that via the Jordan lemma and the Cauchy residue theorem leads to the well-known formula:

$$G_{2,1,n}(\mathbf{x},t)=\frac{1}{(\sqrt{4\pi t})^n}\exp\Big(-\frac{|\mathbf{x}|^2}{4t}\Big). \tag{52}$$

Space-fractional diffusion equation ($\beta=1,1<\alpha\leq 2$)

With the same procedure of the previous case, we can define the fundamental solution via the generalized Wright function, defined by:

$${}_p\Psi_q\Big[\frac{(a_1,A_1),...,(a_p,A_p)}{(b_1,B_1),...,(b_p,B_p)};z\Big]=\sum_{k=0}^{\infty}\frac{\prod_{i=1}^{p}\Gamma(a_i+A_ik)}{\prod_{i=1}^{q}\Gamma(b_i+B_ik)}\frac{z^k}{k!}. \tag{53}$$

In particular:

$$G_{\alpha,1,n}(\mathbf{x},t)=\frac{2t^{-\frac{n}{\alpha}}}{(4\pi)^{\frac{n}{2}}}{}_1\Psi_1\Big[\frac{(\frac{n}{\alpha},\frac{2}{\alpha})}{(\frac{n}{2},1)};-\frac{|x|^2}{4t^{\frac{2}{\alpha}}}\Big] \tag{54}$$

Two-dimensional α-fractional diffusion equation ($\beta=\frac{\alpha}{2},n=2$)
In this case:

$$G_{\alpha,\frac{\alpha}{2},2}(\mathbf{x},t)=\frac{1}{4\pi t}\Big(\frac{|x|}{2\sqrt{t}}\Big)^{\alpha-2}E_{\frac{\alpha}{2},\frac{\alpha}{2}}\Big(-\Big(\frac{|x|}{2\sqrt{t}}\Big)^{\alpha}\Big) \tag{55}$$

Note that this fundamental solution can be interpreted as a spatial probability density function evolving in time.

One-dimensional α*-fractional wave equation* ($\alpha = \beta, n = 1$)
Finally, for this particular case, we have:

$$G_{\alpha,\alpha,1}(\mathbf{x}, t) = \frac{1}{\pi} \frac{|x|^{\alpha-1} t^{\alpha} \sin(\pi\alpha/2)}{t^{2\alpha} + 2|x|^{\alpha} t^{\alpha} \cos(\pi\alpha/2) + |x|^{2\alpha}} \tag{56}$$

This case is usually known as *neutral-fractional diffusion-wave equation*.

We end this section recalling the the following subordination formula, valid for the fundamental solution of the multidimensional space-time-fractional diffusion-wave equation (with $0 < \beta \leq 1, 0 < \alpha \leq 2, 2\beta + \alpha < 4$):

$$G_{\alpha,\beta,n}(\mathbf{x}, t) = \int_0^{\infty} t^{-\frac{2\beta}{\alpha}} \Phi_{\alpha,\beta}(s t^{-\frac{2\beta}{\alpha}}) G_{2,1,n}(\mathbf{x}, s) ds \tag{57}$$

where the kernel function $\Phi_{\alpha,\beta}(\tau)$ is a pdf whose definition depends on the values of β/α and τ.

More details can be found in [12].

7 Conclusions

We have studied the fractional diffusive waves in the framework of fractional calculus through the so-called time-fractional diffusion-wave equation, and we observed how this equation interpolates the standard processes of diffusion and wave propagation. We have continued the work began in [3]. by considering both the Cauchy and Signaling problems. In particular, after recalling the form of the Green Functions for both problems, we analyzed and simulated the time evolution of the system for an initial data given by a box-function (in space for the Cauchy problem, and in time for the Signaling problem); the solutions are obtained by the well-known space or time convolution (depending on the chosen problem) of the Green functions with the input functions (initial data). Also already known results regarding the interpretation of the fundamental solutions as diffusive waves and concepts on the multi-dimensional time-fractional diffusion-wave equation have been added to the manuscript for a more complete and useful treatment.

In the next future we plan to study both the Cauchy and Signaling problems taking into account also the effects of the second Green function that may arise in more general fractional diffusion-wave processes.

Acknowledgements The results contained in the present paper have been partially presented at the Workshop *Non-local and Fractional Operators* (NLFO) held at the Department of Statistical Sciences, Sapienza University of Rome, Italy, April 12–13 (2019), and to the XX International Conference *Waves and Stability in Continuous Media* (WASCOM 2019) held in Maiori (Sa), Italy, June 10–14 (2019).

The research activity of both the authors has been carried out in the framework of the activities of the National Group of Mathematical Physics (GNFM, INdAM), Italy.

8 Appendix A: Fractional Calculus: An Introduction

The standard notions of integral and derivative can be generalized in the framework of Fractional Calculus to non-integer orders.
The history goes back to September 30th 1695, when L'Hopital asked to Leibniz what would be if $n = 1/2$ in his notation for the nth-order derivative $\frac{d^n}{dx^n}$; Leibniz answered: "An apparent paradox, from which one day useful consequences will be drawn.".

Herewith we describe the essentials of fractional calculus necessary to understand the time fractional derivative in the Caputo sense used in the text. For this we follow the introduction notes in the 1997 Survey by Gorenflo and Mainardi [7]. More details on Fractional Calculus ma be found in more recent treatises, see e.g. the 2006 book by Kilbas et al. [8] and the 2014 book by Gorenflo et al. [6].

The usual starting point for the topic of Fractional Calculus is the *Cauchy formula for repeated integrals*:

$$ {}_aI_t^n f(t) := \int_a^t \int_a^{\tau_{n-1}} \ldots \int_a^{\tau_1} f(\tau)\, d\tau\, d\tau_1 .. d\tau_{n-1} = \frac{1}{(n-1)!} \int_a^t (t-\tau)^{n-1} f(\tau\, d\tau\,, \tag{58} $$

where the time t is the independent variable ($t > 0$) and $f(t)$ is a sufficiently well-behaved function. In this way the n-fold primitive ($n \in \mathbb{N}$) of a function can be calculated in terms of a single integral of convolution type.

One step forward is done by replacing the factorial term $(n-1)!$ that appears in Eq. (60) with the corresponding representation given by the *Gamma Function*, defined by

$$ \Gamma(z) := \int_0^\infty u^{z-1} \mathrm{e}^{-u}\, du,\ \Re\mathfrak{e}(z) > 0\,, $$

and then replacing n with a positive real number α.

Writing $\Gamma(n) = (n-1)!$ in Eq. (60) hence it follows the definition of *fractional integral* ${}_aI_t^\alpha f(t)$ of order α ($\alpha > 0$)

$$ {}_aI_t^\alpha f(t) := \frac{1}{\Gamma(\alpha)} \int_a^t (t-\tau)^{\alpha-1} f(\tau)\, d\tau\,. \tag{59} $$

The order α of the primitive so is no longer restricted to positive, integer values. Follows the definition of the *fractional derivative* of order α defined in the *Riemann-Liouville* sense as the left-inverse operator of the corresponding fractional integral, and it reads:

$$ {}_aD_t^{\alpha} f(t) = \frac{d^n}{dt^n} {}_aI_t^{n-\alpha} f(t) \qquad (n = [\mathfrak{Re}(\alpha)] + 1)\,, \tag{60} $$

The standard notion of derivative is obtained back when $\alpha = n$.
By taking from now on $a \equiv 0$ we agree to delete the starting point in the notations for fractional integrals and derivatives.

Let us note that with the definition given by Eq. (61) unlike the standard case $\alpha = n$, the fractional derivative of a constant function is different from zero. If for example $f(t) \equiv 1$, then we have:

$$ D_t^{\alpha} 1 = \frac{t^{-\alpha}}{\Gamma(1-\alpha)}, \quad \alpha \geq 0, \quad t > 0. \tag{61} $$

If $\alpha = n \in \mathbb{N}$ in Eq. (62), then the result is equal to zero due to the poles of the Gamma function in the points $0, -1, -2, \ldots$
The fractional derivative can be also alternatively defined in the *Caputo* sense [1, 2] by swapping the order of the fractional integral and the nth-order derivative:

$$ D_C^{\alpha} f(t) := I_t^{n-\alpha} \frac{d^n}{dt^n} f(t) = \frac{1}{\Gamma(n-\alpha)} \int_0^t \frac{f^{(n)}(\tau)}{(t-\tau)^{\alpha+1-n}}\, d\tau, \qquad n-1 < \alpha \leq n, \tag{62} $$

In general we have that:

$$ D_t^{\alpha} f(t) := \frac{d^n}{dt^n} {}_aI_t^{n-\alpha} f(t) \neq I_t^{n-\alpha} \frac{d^n}{dt^n} f(t) := D_C^{\alpha} f(t), \tag{63} $$

unless the function $f(t)$ along with its first $n-1$ derivatives vanishes at $t = 0^+$. Indeed we have:

$$ D_t^{\alpha} f(t) = D_C^{\alpha} f(t) + \sum_{k=0}^{n-1} \frac{t^{k-\alpha}}{\Gamma(k-\alpha+1)} f^{(k)}(0^+). \tag{64} $$

Having in mind the following result regarding the fractional derivative of the power function,

$$ D_t^{\alpha} t^{\gamma} = \frac{\Gamma(\gamma+1)}{\Gamma(\gamma+1-\alpha)} t^{\gamma-\alpha}, \quad \alpha > 0, \quad \gamma > -1, \quad t > 0, \tag{65} $$

we finally have:

$$ D_t^{\alpha} \left(f(t) - \sum_{k=0}^{n-1} \frac{t^k}{k!} f^{(k)}(0^+) \right) = D_C^{\alpha} f(t)\,. \tag{66} $$

The Caputo definition requires the absolute integrability of the nth-order derivative but provides a regularization of the Riemann-Liouville fractional derivative at $t = 0^+$.

It comes out also that the Caputo derivative appears suitable to be treated by the Laplace Transform technique for causal systems, i.e. systems that are quiescent for $t < 0$, as the result is a natural generalization of a well-known relation of standard analysis (obtained when $\alpha = n$). Indeed we have, using the symbol $\div$ for the juxtaposition of a function with its Laplace Transform:

$$D_C^\alpha f(t) \div s^\alpha \tilde{f}(s) - \sum_{k=0}^{n-1} f^{(k)}(0^+) s^{\alpha-1-k}, \quad n-1 < \alpha \le n\,. \tag{67}$$

In Eq. (68) it is required to know the initial values of the function and of its integer derivatives, and this fact is useful in particular in physical problems.
Moreover we find another result known from standard analysis, i.e. that the derivative of a constant vanishes:

$$D_C^\alpha 1 = 0, \qquad \alpha > 0\,. \tag{68}$$

References

1. Caputo, M.: Linear models of dissipation whose Q is almost frequency independent, Part II. Geophys. J. R. Astr. Soc. **13**, 529–539 (1967) [Reprinted in Fract. Calc. Appl. Anal. **11** No 1, 4–14 (2008)]
2. Caputo, M.: Elasticità e Dissipazione. Zanichelli, Bologna (1969). [in Italian]
3. Consiglio, A., Mainardi, F.: On the Evolution of Fractional Diffusive Waves. Ricerche di Matematica, published online 06 Dec (2019) https://doi.org/10.1007/s11587-019-00476-6 [E-print: arxiv.org/abs/1910.1259]
4. Erdélyi, A., Magnus, W., Oberhettinger, F., Tricomi, F. : Higher Transcendental Functions, 3-rd Volume. McGraw-Hill, New York. [Bateman Project] (1955)
5. Fujita, Y.: Integrodifferential equation which interpolates the heat equation and the wave equation, I. II. Osaka J. Math. **27**(309–321), 797–804 (1990)
6. Gorenflo, R. , Kilbas, A.A., Mainardi, F., Rogosin, S.: Mittag-Leffler Functions. Related Topics and Applications. Springer, Berlin (2020)
7. Gorenflo, R, Mainardi, F.: .Fractional calculus: integral and differential equations of fractional order. In: Carpinteri, A. and Mainardi, F. (Eds.) Fractals and Fractional Calculus in Continuum Mechanics Springer, Wien, pp. 223-276 (1997). arXiv:0805.3823
8. Kilbas, A.A., Srivastava, H.M. Trujillo, J.J.: Theory and Applications of Fractional Differential Equations. Elsevier, Amsterdam (2006) [North-Holland Series on Mathematics Studies No 204]
9. Liemert, A., Kleniem, A.: Fundamental solution of the tempered fractional diffusion equation. J. Math. Phys **56**, 113504 (2015)
10. Luchko, Yu.: On the asymptotics of zeros of the Wright function. Zeitschrift für Analysis und ihre Anwendungen **19**, 597–622 (2000)
11. Luchko Yu., Mainardi F.: Cauchy and signaling problems for the time-fractional diffusion-wave equation, ASME J. Vib. Acoust. **136**(5) (2014), 050904/1-7, 10.1115/1.4026892
12. Luchko, Y., Mainardi F.: Fractional diffusion-wave phenomena. Chapter. In: Vasily E. Tarasov (Ed.), Handbook of Fractional Calculus with Applications. Vol.5: Applications in Physics, Part B, Walter de Gruyter, Berlin/Boston, 2019, pp. 71–98

13. Luchko, Y., Mainardi, F., Povstenko, Y.: Propagation speed of the maximum of the fundamental solution to the fractional diffusion-wave equation. Comput. Math. Appl. **66**, 774–784 (2013). E-print: arXiv:1201.5313v2 [math-ph]
14. Luchko, Y.: The Wright function and its applications. In: A. Kochubei, Y. Luchko (Eds.), Handbook of Fractional Calculus with Applications Vol. 1: Basic Theory, pp. 241– 268 (2019). De Gruyter GmbH, 2019, Berlin/Boston. Series edited by J. A. Tenreiro Machado
15. Mainardi, F.: On the initial value problem for the fractional diffusion-wave equation. In: Rionero, S., Ruggeri, T. (Eds.) Waves and Stability in Continuous Media. World Scientific, Singapore, pp. 246–251 (1994). [Proceedings of the VII-th WASCOM, International Conference "Waves and Stability in Continuous Media", Bologna, Italy, 4–7 October 1993]
16. Mainardi, F.: The fundamental solutions for the fractional diffusion-wave equation. Appl. Mathe. Lett. **9**(6), 23–28 (1996)
17. Mainardi, F.: Fractional relaxation-oscillation and fractional diffusion-wave phenomena. Chaos, Solitons Fractals **7**, 1461–1477 (1996)
18. Mainardi, F.: Fractional Calculus and Waves in Linear Viscoelasticity. Imperial College Press, London and World Scientific, Singapore (2010)
19. Mainardi, F., Consiglio, A.: The Wright functions of the second kind in Mathematical Physics. Mathematics (MDPI) **8**(6), 884/1–26 (2020). https://doi.org/10.3390/math8060884; E-print: arXiv:2007.02098 [math.GM]
20. Saa, A., Venegeroles, R.: Alternative numerical computation of one-sided Lévy and Mittag-Leffler distributions. Phys. Rev. E **84**, 026702 (2011)
21. Wright, E.M.: On the coefficients of power series having exponential singularities. J. London Math. Soc. **8**, 71–79 (1933)
22. Wright, E.M.: The asymptotic expansion of the generalized Bessel function. Proc. London Math. Soc. (Ser. II) **38**, 257–270 (1935)
23. Wright, E.M.: The generalized Bessel function of order greater than one. Quart. J. Math., Oxford Ser. **11**, 36–48 (1940)

Some Extension Results for Nonlocal Operators and Applications

Fausto Ferrari

Abstract In this paper, we deal with some recent and old results, concerning fractional operators, obtained via the extension technique. This approach is particularly fruitful for exploiting some of those well known properties, true for the local operators obtained via the extension approach, for deducing some parallel results about the underlaying nonlocal operators.

Keywords Fractional laplacian · Marchaud derivative · Weyl derivative · Extension techniques · Carnot groups · Harnack inequality.

1 Some Nonlocal Operators

We start this note by reviewing some recent and old results concerning fractional operators, putting in evidence the extension technique used in [12] for the fractional Laplace operator and successively applied to other operators, see e.g. [7, 10, 52]. This approach results particularly fruitful for exploiting some, perhaps, well known properties of the local operators obtained from the nonlocal ones, for which we would like to prove some results. The typical easier example is given in [12] where, for proving the Harnack inequality for the fractional Laplace operator, the authors reduce themselves to apply the Harnack inequality associated with a degenerate local operator in divergence form and for which there exist in literature many results, see [17]. We point out that Harnack inequality for the fractional Laplace operator was already known in literature for $s-$harmonic functions being $s \in (0, 1)$. Namely, there exists a positive constant C such that for every sufficiently smooth function $u : \mathbb{R}^n \to \mathbb{R}$, $u \geq 0$ in $\mathbb{R}^n$, such that $(-\Delta)^s u = 0$ in $\Omega \subset \mathbb{R}^n$, then for every ball $B_{2R} \subset \Omega$ of radius $2R$ we have:

F. Ferrari (✉)
Dipartimento di Matematica dell'Università di Bologna, Piazza di Porta S. Donato, 5, 40126 Bologna, Italy
e-mail: fausto.ferrari@unibo.it

L. Beghin et al. (eds.), *Nonlocal and Fractional Operators*, SEMA SIMAI Springer Series 26, https://doi.org/10.1007/978-3-030-69236-0_9

$$\sup_{B_R} u \leq C \inf_{B_R} u.$$

The classical proof can be found, for instance, in [40, 48] using potential theory techniques and, via probabilistic approach, in [6]. In the Harnack inequality, the different hypotheses that have to be done between the local and the nonlocal case are explicit. In fact, without extra assumptions on the positivity of u in all of $\mathbb{R}^n$, instead of the required positivity of u only on the set Ω as well as in the local setting, the result is false, see e.g. [38].

This approach can be adapted to different operators. In particular the case of Weyl-Marchaud derivative has been faced in [10], while the case of degenerate operators in [23]. Recently, some further generalizations and applications to Kolmogorov operators type have been obtained in [31], see also [29, 30] and [54] for a recent review of these results.

We continue this section introducing some basic nonlocal operators, while in Sect. 2 we deal with the extension technique. More precisely: In Sect. 2.1 we deal with the extension approach adapted to the case of the Marchaud derivative, in Sect. 2.2 we introduce the main tools for working in a non-commutative framework and successively, in Sect. 2.3, we describe the extension approach technique in Carnot groups. The applications are collected in Sect. 3. We conclude with Sect. 4 discussing the construction of the solutions of the extended problem associated with a periodic function, via the Fourier series approach.

The following notation concerns the difference of fractional order $\alpha \in \mathbb{R}$ for a function f. Let

$$(\Delta_h^\alpha f)(x) := \sum_{k=0}^{\infty} (-1)^k \binom{\alpha}{k} f(x - kh), \tag{1}$$

where

$$\binom{\alpha}{n} = \frac{\Gamma(\alpha + 1)}{n!\Gamma(\alpha + n - 1)}.$$

The Grünwald-Letnikov derivative, [33, 41], is:

$$\mathbb{D}^\alpha f(x) = \lim_{h \to 0^+} \frac{(\Delta_h^\alpha f)(x)}{h^\alpha},$$

whenever the pointwise limit exists.

In addition, see Theorem 20.4, [51], for $L^p(\mathbb{R})$ functions, we know that Grüwald-Letnikov-derivative exists if and only if Marchaud-derivative exists in the following sense:

$$\lim_{h \to 0^+, L^p(\mathbb{R})} \frac{(\Delta_h^\alpha f)(x)}{h^\alpha} = \lim_{\epsilon \to 0^+, L^p(\mathbb{R})} \frac{\alpha}{\Gamma(1 - \alpha)} \int_\epsilon^\infty \frac{f(x) - f(x - \tau)}{\tau^{1+\alpha}} d\tau,$$

being $\alpha \in (0, 1)$ and

$$\mathbf{D}_{+}^{\alpha} f(x) := \frac{\alpha}{\Gamma(1-\alpha)} \int_0^{\infty} \frac{f(x) - f(x-\tau)}{\tau^{1+\alpha}} d\tau$$

the Marchaud-derivative, see [45] and [10, 22, 50]. For further information about these relationships, we recall the classical handbooks [39, 46, 50] as well. We have to say that, for function defined in $[a, t]$, sometime the Caputo derivative

$$ {}_{a}D_{t}^{\alpha} f(t) := \frac{1}{\Gamma(1-\alpha)} \int_a^t \frac{f'(s)}{(t-s)^{\alpha}} ds \tag{2}$$

is used, see e.g. [14], instead of the Riemann-Lioville one, defined as:

$$ {}_{a}\mathscr{D}_{+}^{\alpha} f(t) := \frac{1}{\Gamma(1-\alpha)} \frac{d}{dt} \int_a^t \frac{f'(s)}{(t-s)^{\alpha}} ds,$$

see [51].

The Riemann-Liouville derivative is closely related to Marchaud derivative. In fact, the interested reader may check this fact one more time in [51] or e.g. in [22], but, in any case, also Caputo derivative is strictly linked to Marchaud derivative. In fact, integrating by parts (2), we obtain:

$$\Gamma(1-\alpha) {}_{a}D_{t}^{\alpha} f(t) = \frac{f(t) - f(a)}{(t-a)^{\alpha}} + \alpha \int_a^t \frac{f(t) - f(s)}{(t-s)^{1+\alpha}} ds.$$

Thus for functions f defined in $(-\infty, t]$, letting $a = -\infty$, we obtain, after a change of variable:

$$ {}_{-\infty}D_{t}^{\alpha} f(t) := \frac{1}{\Gamma(1-\alpha)} \int_{-\infty}^t \frac{f(t) - f(s)}{(t-s)^{1+\alpha}} ds = \mathbf{D}_{+}^{\alpha} f(t)$$

that is exactly the Marchaud derivative.

Keeping in mind the subject contained in Sect. 4, as well as the Weyl definition of derivative, see [55], we wish to remark how the Weyl derivative can be justified for pointing out its relationship with Marchaud derivative.

Let us consider a periodic function, let us say for simplicity a 2π-periodic function having zero average. We can associate to this function its own Fourier series, see [22]:

$$\sum_{k=-\infty}^{+\infty} c_k e^{ikx},$$

where of course $\{c_k\}_{k\in\mathbb{Z}}$ is the sequence of the Fourier coefficients. Thus, formally, the derivative may be written as:

$$\sum_{k=-\infty}^{+\infty} c_k (ik) e^{ikx}.$$

Then, defining a new function for each fixed $\alpha < 1$:

$$\sum_{k=-\infty}^{+\infty} \frac{c_k}{(ik)^\alpha} e^{ikx},$$

(morally the integral), we formally obtain, by taking its derivative:

$$D\left(\sum_{k=-\infty}^{+\infty} \frac{c_k}{(ik)^\alpha} e^{ikx}\right) = \sum_{k=-\infty}^{+\infty} \frac{c_k}{(ik)^{\alpha-1}} e^{ikx}. \tag{3}$$

Following this path, Weyl analogously introduces the parallel fractional integral, see [55]. Thus, it is natural to define the fractional derivative of f as:

$$\sum_{k=-\infty,}^{+\infty} c_k (ik)^\alpha e^{ikx}.$$

We recall that, given two periodic functions f, g, the new function

$$\frac{1}{2\pi} \int_0^{2\pi} g(t) f(x-t) dt$$

is represented by the Fourier series

$$\sum_{k=-\infty}^{\infty} g_k c_k e^{ikx},$$

where $\{g_k\}_{k\in\mathbb{Z}}$ and $\{c_k\}_{k\in\mathbb{Z}}$ are the respective Fourier coefficients. As a consequence, considering

$$\sum_{k=-\infty}^{+\infty} \frac{c_k}{(ik)^\alpha} e^{ikx}$$

as representing the Fourier series of an integral like the following one:

$$\frac{1}{2\pi} \int_0^{2\pi} g(t) f(x-t) dt,$$

we deduce that previous integral has to be written in the following form:

$$\frac{1}{2\pi}\int_0^{2\pi} f(x-t)\left(\sum_{k=-\infty,k\neq 0}^{+\infty}\frac{e^{ikt}}{(ik)^\alpha}\right)dt.$$

It can be proved that (see [51])

$$\sum_{k=-\infty,k\neq 0}^{+\infty}\frac{e^{ikt}}{(ik)^\alpha}=2\sum_{k=1}^{\infty}\frac{\cos(kt-\alpha\frac{\pi}{2})}{k^\alpha}.$$

Then, denoting the kernel

$$\psi_+^\alpha(t):=\sum_{k=-\infty,k\neq 0}^{+\infty}\frac{e^{ikt}}{(ik)^\alpha},$$

Weyl obtains the fractional integral

$$I_+^{(\alpha)}f(x)=\frac{1}{2\pi}\int_0^{2\pi} f(x-t)\psi_+^\alpha(t)dt.$$

At this point, see [51], Weyl defines the fractional derivative as

$$\mathscr{D}_+^{(\alpha)}(x):=D\left(I_+^{(1-\alpha)}f\right)(x).$$

This definition corresponds to the Weyl-Riemann-Lioville version of this derivative, see one more time [51] for the details. Then taking formally the derivative, Weyl obtains the Weyl-Marchaud derivative that is:

$$\mathbf{D}_+^{(\alpha)}f(x):=\frac{1}{2\pi}\int_0^{2\pi}(f(x)-f(x-t))\frac{d}{dt}\psi_+^{1-\alpha}(t)dt.$$

Of course, the case concerning $\mathbf{D}_-^{(\alpha)}f$ is analogous.

The Weyl derivative and the Marchaud derivative of 2π periodic functions in $L^p(0,2\pi)$ coincide a.e., whenever they exist, see Lemma 19.4 in [50]. It is worth to point out that the numerical evaluation of these derivatives is particularly important, see e.g. [32] or [19], so that it is useful to understand their properties considering their different representations.

Concerning the applications of these nonlocal operators, it would be very difficult to list all the papers published on this subject, nevertheless we like to cite [3], where Riemann-Liouville-Marchaud-Weyl-Caputo derivative as well as the fractional Laplace operator appeared in the description of a porous medium flow problem, and [43] for a description of many other problems.

We have just quoted the fractional operator, so that we formally introduce it. Let $\alpha\in(0,1)$, we recall that the fractional Laplace operator is defined, let us say for

every $f \in \mathscr{S}(\mathbb{R}^n)$, the set of rapidly decreasing set functions on $\mathbb{R}^n$, as:

$$\begin{aligned}(-\Delta)^{\alpha} f(x) &= C_{\alpha,n} \int_{\mathbb{R}^n} \frac{f(x) - f(y)}{|x-y|^{n+2\alpha}} dy \\ &:= \lim_{r \to 0^+} C_{\alpha,n} \int_{\mathbb{R}^n \setminus B_r(x)} \frac{f(x) - f(y)}{|x-y|^{n+2\alpha}} dy,\end{aligned} \tag{4}$$

where $B_r(x)$ denotes the ball centered at x pf radius r and the constant $C_{\alpha,n}$ depends only on α, n and represents a normalizing constant determined by the following condition

$$\mathscr{F}^{-1}(|\xi|^{2\alpha} \mathscr{F}(f))(x) = (-\Delta)^{\alpha} f(x).$$

Here we denote, as usual, by $\mathscr{F}$ the Fourier transform. We remark indeed that $\mathscr{F}^{-1}(|\xi|^{2\alpha} \mathscr{F}(f))$ is often taken as the definition of the fractional Laplace operator itself $(-\Delta)^{\alpha} f$, see e.g. [51] and [20].

There exists a relationship between the Marchaud derivative and the fractional Laplace operator that is given for $\alpha \in (0, 1)$ by:

$$\int_{\partial B_1(0)} \mathbf{D}_h^{\alpha} f(x) d\mathscr{H}^{n-1}(h) = (-\Delta)^{\alpha/2} f(x),$$

where

$$\mathbf{D}_h^{\alpha} f(x) = c_{\alpha} \int_0^{\infty} \frac{f(x) - f(x - th)}{t^{1+\alpha}} dt,$$

$h \in \partial B_1(0)$, $h \in \mathbb{R}^n$ and c_{α} is the suitable normalizing constant, see Lemma 26.2 in [50] and also [22] for an equivalent statement. In addition, we remark that in [50] further relationships between Marchaud derivative and hypergeometric integrals are studied.

2 Extension Approach to Nonlocal Operators

In this section we discuss few cases in which we adapt the extension approach to the Marchaud derivative and to Carnot groups, respectively introduced in Sect. 2.1 and Sect. 2.3. Moreover, for dealing with Carnot groups, we arranged the preparatory Sect. 2.2, where we introduce the main notations and definitions useful in that non-commutative field.

2.1 The Marchaud Case

In [12], the authors observed that the fractional Laplace operator can be represented as well as:

$$(-\Delta)^{\alpha} f(x) = C \lim_{y \to 0} y^{1-2\alpha} \frac{\partial V(x, y)}{\partial y},$$

where $0 < \alpha < 1$ and V is the solution to the following problem:

$$\begin{cases} \operatorname{div}(y^{1-2\alpha} \nabla_{x,y} V) = 0, & \mathbb{R}^n \times \mathbb{R}^+, \\ V(x, 0) = f, & x \in \mathbb{R}^n, \end{cases}$$

and C a suitable constant. We will come back to this point in Sect. 2.2 discussing the fractional Laplace case.

This extension approach, in defining the Weyl-Marchaud derivative, has been faced in [10]. We describe below the rough idea in case $\alpha = \frac{1}{2}$ for obtaining $\mathbf{D}^{\frac{1}{2}}$. Let $\varphi : \mathbb{R} \to \mathbb{R}$ be a given function, sufficiently smooth. Let U be a solution to the problem

$$\begin{cases} \frac{\partial U}{\partial t} = \frac{\partial^2 U}{\partial x^2}, & (x, t) \in (0, \infty) \times \mathbb{R} \\ U(0, t) = \varphi(t), & t \in \mathbb{R}. \end{cases} \tag{5}$$

We point out that (5) is not the usual Cauchy problem associated with the heat operator, but a heat conduction problem.

It is known that, without extra assumptions, we can not expect to have a unique solution of the problem (5), see e.g. [53]. Nevertheless, if we denote by $T_{1/2}$ the operator that associates to φ the partial derivative $\frac{\partial U}{\partial x}$, whenever U is sufficiently regular, we have that

$$T_{1/2} T_{1/2} \varphi = \frac{d\varphi}{dt}.$$

That is the operator $T_{1/2}$ acts like an half derivative, that is a fractional derivative of order $1/2$, indeed

$$\frac{\partial}{\partial x} \frac{\partial U}{\partial x}(x, t) = \frac{\partial U}{\partial t}(x, t) \underset{x \to 0}{\longrightarrow} \frac{d\varphi(t)}{dt}.$$

The solution of problem (5) under the reasonable assumptions that φ is bounded and Hölder continuous, is explicitly known (check e.g. [53]) to be

$$\begin{aligned} U(x, t) &= cx \int_{-\infty}^{t} e^{-\frac{x^2}{4(t-\tau)}} (t - \tau)^{-\frac{3}{2}} \varphi(\tau)\, d\tau \\ &= cx \int_{0}^{\infty} e^{-\frac{x^2}{4\tau}} \tau^{-\frac{3}{2}} \varphi(t - \tau)\, d\tau, \end{aligned} \tag{6}$$

where (6) is obtained performing a change of variable.

We get moreover that

$$\int_0^\infty x e^{-\frac{x^2}{4\tau}} \tau^{-\frac{3}{2}}\, d\tau = 2\int_0^\infty e^{-t} t^{-\frac{1}{2}}\, dt = 2\Gamma(\frac{1}{2}).$$

Hence,

$$\frac{U(x,t)-U(0,t)}{x} = c\int_0^\infty e^{-\frac{x^2}{4\tau}} \tau^{-\frac{3}{2}} \left(\varphi(t-\tau)-\varphi(t)\right) d\tau, \tag{7}$$

choosing c that takes into account the right normalization. This yields, by passing to the limit, that

$$-\lim_{x\to 0^+} \frac{U(x,t)-U(0,t)}{x} = c\int_0^\infty \frac{\varphi(t)-\varphi(t-\tau)}{\tau^{\frac{3}{2}}} d\tau, \tag{8}$$

that, possibly up to a multiplicative constant, is exactly $\mathbf{D}^{\frac{1}{2}}\varphi$.

The previous description enters as a particular case of the following results proved in [10], see also [7],

Theorem 1 *Let $s \in (0,1)$ and $\varphi\colon \mathbb{R} \to \mathbb{R}$ be a bounded, locally $C^{\bar\gamma}$ function for $s < \bar\gamma \le 1$. Let $U\colon [0,\infty)\times\mathbb{R} \to \mathbb{R}$ be a solution to the problem*

$$\begin{cases} \frac{\partial U(x,t)}{\partial t} = \frac{1-2s}{x}\frac{\partial U(x,t)}{\partial x} + \frac{\partial^2 U(x,t)}{\partial x^2}, & (x,t)\in(0,\infty)\times\mathbb{R} \\ U(0,t) = \varphi(t), & t\in\mathbb{R} \\ \lim_{x\to\infty} U(x,t) = 0, & t\in\mathbb{R}. \end{cases} \tag{9}$$

Then U defines the extension operator for ϕ, such that

$$\mathbf{D}^s\varphi(t) = -\lim_{x\to 0^+} c_s x^{-2s}(U(x,t)-\varphi(t)), \tag{10}$$

where

$$c_s = 4^s\Gamma(s).$$

Adapting the constant c_s given in Theorem 1 by fixing $c_s = \frac{4^s\Gamma(s)s}{\Gamma(1-s)}$, in

$$\mathbf{D}^s\varphi(t) = -\lim_{x\to 0^+} c_s x^{1-2s}\frac{\partial U}{\partial x}(x,t), \tag{11}$$

in analogy with formula (3.1) in [12] we straightforwardly obtain the definition

$$\mathbf{D}^s_{\pm} f(t) = \frac{s}{\Gamma(1-s)}\int_0^\infty \frac{f(t)-f(t\mp\tau)}{\tau^{1+s}} d\tau. \tag{12}$$

The advantage of this choice is that $\mathbf{D}^s_{\pm}\varphi \to \varphi$ as $s \to 0^+$ and $\mathbf{D}^s_{\pm}\varphi \to \varphi'$ as $s \to 1^-$. Eventually, for recent result about the regularity theory in this framework, see [2].

2.2 Carnot Setting

In this subsection, preparatory to the next one, we introduce the basic language for dealing with Carnot groups. We recall that fractional operators may be defined also for degenerate PDEs associated with non-negative quadratic forms on non-commutative structures. In fact, a stratified Carnot group of step m $(\mathbb{G}, \circ)$ is a set, in general endowed with a non-commutative law and a Lie algebra g with m stratifications. More precisely there exist $\{g_i\}_{1\le i\le m}$, $m \in \mathbb{N}$, $m \le N \in \mathbb{N}$, vector spaces such that:

$$g_1 \bigoplus g_2 \bigoplus \cdots \bigoplus g_m = g \equiv \mathbb{R}^N \equiv \mathbb{G},$$

$$[g_1, g_1] = g_2, \quad [g_1, g_2] = g_3, \quad \ldots, [g_1, g_{m-1}] = g_m \neq \{0\}$$

and

$$[g_1, g_m] = 0.$$

Moreover

$$x \in \mathbb{G} \equiv \mathbb{R}^N = \mathbb{R}^{k_1} \times \ldots \mathbb{R}^{k_m}, \quad \sum_{j=1}^{m} k_j = N$$

and $\sum_{j=1}^{m} jk_j = Q$ is called the homogeneous dimension. For every $\lambda > 0$ is defined the anisotropic dilation:

$$\delta_\lambda(x) = (\lambda x^{(1)}, \lambda^2 x^{(2)}, \ldots, \lambda^m x^{(m)}), \quad \text{where} \quad x^{(j)} \in \mathbb{R}^{k_j}, \quad j = 1, \ldots, m.$$

In addition if $Z_1, \ldots, Z_{k_1} \in g_1$ are left invariant vector fields such that $Z_j(0) = \frac{\partial}{\partial x_j}_{|x=0}$, $j = 1, \ldots, k_1$ then

$$\operatorname{rank}(\operatorname{Lie}\{Z_1, \ldots, Z_{k_1}\})(x) = N, \quad \text{(Hörmander condition)}$$

for every $x \in \mathbb{R}^N \equiv \mathbb{G}$. Let us consider the sublaplacian on the stratified Carnot group $\mathbb{G}$ given by

$$\mathscr{L}_{\mathbb{G}} \equiv -\Delta_{\mathbb{G}} = -\sum_{j=1}^{k_1} X_j^2, \tag{13}$$

where $\operatorname{span}\{X_1, \ldots, X_{k_1}\} = g_1$.

In particular there exists a $N \times k_1$ matrix σ such that $\sigma \cdot \sigma^T$ is a $N \times N$ matrix such that

$$\operatorname{div}(\sigma \cdot \sigma^T \nabla \cdot) = \Delta_{\mathbb{G}}.$$

Moreover

$$\sigma^T \nabla u = \sum_{j=1}^{k_1} X_j u X_j \equiv \nabla_{g_1} u,$$

is the so called horizontal gradient of u.

Hence

$$A = \sigma \cdot \sigma^T$$

The simplest example is the Heisenberg group, that is

$$\mathbb{G} = \mathbb{H}^1 \equiv \mathbb{R}^3, \quad (\mathbb{H}^1, \circ)$$

where for every $(x_1, y_1, t_1), (x_2, y_2, t_2) \in \mathbb{H}^1$

$$(x_1, y_1, t_1) \circ (x_2, y_2, t_2) = (x_1 + x_2, y_1 + y_2, t_1 + t_2 + 2(x_2 y_1 - x_1 y_2)).$$

The opposite of $\xi := (x, y, t) \in \mathbb{H}^1$ is usually denoted by ξ^{-1} and $\xi^{-1} := (-x, -y, -t)$ and the dilation by $\lambda > 0$ is: $\delta_\lambda(\xi) = (\lambda x, \lambda y, \lambda^2 t)$.

Moreover,

$$g_1 = \operatorname{span}\{X, Y\}, \quad g_2 = \operatorname{span}\{T\}$$

where $X = \frac{\partial}{\partial x} + 2y \frac{\partial}{\partial t}$, $Y = \frac{\partial}{\partial y} - 2x \frac{\partial}{\partial t}$, and $T = -4 \frac{\partial}{\partial t}$, and

$$[X, Y] = T,$$

so that $[g_1, g_1] = g_2$, $[g_1, g_2] = \{0\}$,

$$g_1 \bigoplus g_2 = \mathbb{R}^3.$$

Hence, Heisenberg group is a 2 step groups and g_1 is the first layer, namely the horizontal vector space. Moreover

$$\Delta_{\mathbb{H}^1} = X^2 + Y^2 = \frac{\partial^2}{\partial x^2} + 4y \frac{\partial^2}{\partial x \partial t} + \frac{\partial^2}{\partial y^2} - 4x \frac{\partial^2}{\partial y \partial t} + 4(x^2 + y^2) \frac{\partial^2}{\partial t^2}$$

Thus

$$\Delta_{\mathbb{H}^1} = \mathrm{Tr}\left(\begin{bmatrix} 1, & 0, & 2y \\ 0, & 1, & -2x \\ 2y, & -2x, & 4(x^2+y^2) \end{bmatrix}\right) = \mathrm{div}\left(\begin{bmatrix} 1, & 0, & 2y \\ 0, & 1, & -2x \\ 2y, & -2x, & 4(x^2+y^2) \end{bmatrix} \nabla u\right)$$
$$= \mathrm{div}\left(\begin{bmatrix} 1, & 0 \\ 0, & 1 \\ 2y, & -2x \end{bmatrix} \begin{bmatrix} 1, & 0, & 2y \\ 0, & 1, & -2x \end{bmatrix} \nabla u\right) = X^2 u + Y^2 u.$$

In our framework

$$\mathscr{L} \equiv -\Delta_{\mathbb{G}} := -\sum_{j=1}^{k_1} X_j^2,$$

and considering the example given by the Heisenberg group, we have $k_1 = 2$, $X_1 \equiv X$ and $X_2 \equiv Y$, so that $\mathscr{L} \equiv -\Delta_{\mathbb{H}^1}$.

We point out that with this presentation we include, as a very particular case, the Laplace operator on $\mathbb{R}^n$ that is a commutative structure. The main difference with the general elliptic case, usually given by the Laplace operator, for instance considering the Kohn-Laplace operator on the Heisenberg group $\mathbb{H}^n$ is that $\Delta_{\mathbb{H}^n}$ represents a degenerate operator associated with a non-negative quadratic form having the smallest eigenvalue always zero. This structure is in some way associated with the quantum description of a system of moving particles with classical position and momentum coordinates, see [26, 47]. The fundamental contribution about the analytic properties of sublaplacians (13) can be found in [36]. Thus, the properties of fractional operators in this framework is particularly interesting.

Thus, following [25], Sect. 3, see also [5, 37, 57], it results:

Theorem 2 *The operator $\mathscr{L}$, see (13), is a positive self-adjoint operator with domain $W_{\mathbb{G}}^{2,2}(\mathbb{G})$. Denote now by $\{E(\lambda)\}$ the spectral resolution of $\mathscr{L}$ in $L^2(\mathbb{G})$. If $\alpha > 0$ then*

$$\mathscr{L}^{\alpha/2} = \int_0^{+\infty} \lambda^{\alpha/2} dE(\lambda)$$

with domain

$$W_{\mathbb{G}}^{\alpha,2}(\mathbb{G}) := \{u \in L^2(\mathbb{G}) \ : \ \int_0^{+\infty} \lambda^{\alpha} d\langle E(\lambda)u, u\rangle < \infty\},$$

endowed with the graph norm.

Let us denote by $h = h(t, x)$ the fundamental solution of $\mathscr{L} + \partial/\partial t$. Recall that Q denotes the homogeneous dimension as well. Then:

Theorem 3 *([25], Proposition 3.3) Suppose $Q \geq 3$ and $0 < \beta < Q$. Then the integral*

$$R_\beta(x) = \frac{1}{\Gamma(\beta/2)} \int_0^{\infty} t^{\frac{\beta}{2}-1} h(t, x)\, dt$$

converges absolutely for $x \neq 0$. In addition, R_β is a kernel such that:

(i) R_2 *is the* $\mathscr{L}$ *fundamental solution;*
(ii) *if* $\alpha \in (0,2)$ *and* $u \in \mathscr{D}(\mathbb{G})$, *then* $\mathscr{L}^{\alpha/2}u = \mathscr{L}u * R_{2-\alpha}$.
(iii) *the kernels* R_α *admit the following convolution rule: if* $\alpha > 0$, $\beta > 0$ *and* $x \neq 0$, *then* $R_{\alpha+\beta}(x) = R_\alpha(x) * R_\beta(x)$.

In this case we cannot apply straightforwardly the Fourier transform, because the operator may have variable coefficients. We faced in [23] the problem, see also [12], by considering the following result.

Lemma 1 *If* $-\infty < \alpha < 1$, *the boundary value problem*

$$\begin{cases} -t^\alpha \phi'' + \phi = 0 \\ \phi(0) = 1 \\ \lim_{t\to+\infty} \phi(t) = 0 \end{cases} \tag{14}$$

has a solution $\phi \in \mathbf{C}^{2-\alpha}([0,\infty))$ *of the form*

$$\phi(t) = c_\alpha\, t^{1/2} K_{1/2k}(k^{-1}t^k),$$

where $c_\alpha := 2^{1-1/2k}\Gamma(1/2k)^{-1}k^{-1/2k} > 0$ *is a positive constant,* $k = \frac{2-\alpha}{2}$, *and* $K_{1/2k}$ *is the modified Bessel function of second kind (see [56]).*

In addition:

(i) $0 < \phi < 1$. Moreover $\phi'(t)$ has a finite limit as $t \to 0$ and, recursively,

$$t^{\alpha+h-2}\phi^{(h)}(t) \text{ has a finite limit as } t \to 0$$

for $h = 2, 3, \ldots$;
(ii) $\phi' \in L^2((0,\infty))$;
(iii) $\phi(t) = c\sqrt{\frac{\pi k}{2}}\, t^{\alpha/2}\, e^{-t^k/k}\big(1 + O(\frac{1}{t})\big)$ as $t \to \infty$;
(iv) $\phi^{(h)}(t) = c_h\, t^{\alpha(1-h)/2}\, e^{-t^k/k}\big(1 + o(1)\big)$ as $t \to \infty$ for $h = 1, 2, \ldots$.

The problem (14) in Lemma 1 takes the place of the problem that we obtain when we apply the Fourier transform to the Laplace operator.

We explain now why in Carnot groups we need to a new tool that takes the place of the Fourier transform and how the extension approach may be applied as it will be clear reading the subsequent explanation.

Following [12], for studying problem (14), we consider the Euclidean case for the Laplace operator Δ in $\mathbb{R}^n$. Recalling the argument that we have already described for the extension problem in the construction of the Marchaud derivative, we reduce, supposing to deal with the fractional operator associated with Δ, to consider the following PDE:

$$\Delta_x U + \frac{a}{y}\frac{\partial U}{\partial y} + \frac{\partial^2 U}{\partial y^2} = 0, \quad \text{in } \mathbb{R}^n \times (0,+\infty). \tag{15}$$

Then applying the Fourier transform to (15) with respect to x, we obtain:

$$\mathscr{F}\Delta_x U + \mathscr{F}\frac{a}{y}\frac{\partial U}{\partial y} + \mathscr{F}\frac{\partial^2 U}{\partial y^2} = 0. \tag{16}$$

Thus it results:

$$-|\xi|^2 \mathscr{F}U(\xi, y) + \frac{a}{y}\frac{\partial \mathscr{F}U(\xi, y)}{\partial y} + \frac{\partial^2 \mathscr{F}U(\xi, y)}{\partial y^2} = 0.$$

If $U(x, 0) = u$, by considering the problem,

$$\begin{cases} v'' + \frac{a}{y}v' = |\xi|^2 v \\ v(0) = 1 \\ \lim_{y\to\infty} v(y) = 0, \end{cases} \tag{17}$$

then it results, (knowing the solution v to (17)) via a scaling argument:

$$\mathscr{F}U = \mathscr{F}uv(|\xi|y).$$

If $a = 0$ then $v = e^{-|\xi|y}$ and

$$U(x, y) = u * \mathscr{F}^{-1}(e^{-|\xi|y}).$$

In general:

$$\mathscr{F}^{-1}(v(|\xi|y)) \equiv P_a(x, y) = C_{n,a}\frac{y^{1-a}}{(|x|^2 + |y|^2)^{\frac{n+1-a}{2}}}.$$

and we obtain:

$$U(x, y) = u * P_a(\cdot, y).$$

Now: with a change of variable we transform problem (17) in problem (14).

Unfortunately, in our Carnot groups framework, we can not use the classical Fourier transform having a dependence on the coefficients that is much complicate with respect to the benchmark case represented by the Laplace operator in the Euclidean setting. Thus, we start from Lemma 1 for applying the approach described in [23] in Carnot groups.

2.3 The Extension Approach in Carnot Groups

We have already pointed out in the previous Sect. 2.2 that we cannot apply the Fourier transform, so we use the solution ϕ of problem (1) to define a new operator via the spectral resolution of $\mathscr{L}$, see (13) for recalling the definition.

Hence, for every $u \in L^2(\mathbb{G})$ and $y > 0$, we set, see [23]:

$$v(\cdot, y) := \phi(\theta y^{1-a} \mathscr{L}^{(1-a)/2})u := \int_0^\infty \phi(\theta y^{1-a} \lambda^{(1-a)/2})\, dE(\lambda)u, \tag{18}$$

where $\theta := (1-a)^{a-1}$, ϕ solves (14), and $\{E(\lambda)\}$ is the spectral resolution of $\mathscr{L}$ in $L^2(\mathbb{G})$ and therefore $v \in L^2(\mathbb{G})$ for $y > 0$.

Moreover we proved in [23] the following result.

Theorem 4 (generalized subordination identity) *Let $h(t, \cdot)$ be the heat kernel associated with $\mathscr{L} + \frac{\partial}{\partial t}$. We denote by $P_{\mathbb{G}}(\cdot, y)$ the "Poisson kernel"*

$$P_{\mathbb{G}}(\cdot, y) := C_a\, y^{1-a} \int_0^\infty t^{(a-3)/2} e^{-\frac{y^2}{4t}} h(t, \cdot)\, dt, \tag{19}$$

where

$$C_a = \frac{2^{a-1}}{\Gamma((1-a)/2)}.$$

Then

$$P_{\mathbb{G}}(\cdot, y) \geq 0,$$

and

$$v(\cdot, y) = u * P_{\mathbb{G}}(\cdot, y). \tag{20}$$

The last part is a consequence of some results contained in [25, 37], Theorem 3.1. In addition, we recall that the existence of the heat kernel h is proved in [25]. As a byproduct of Theorem 4, we obtain, see [23], that

$$\mathscr{L}^{\frac{1-a}{2}} u(x) = \tilde{C}_a \int_{\mathbb{G}} (u(\xi) - u(x)) \tilde{R}_{a-1}(\xi) d\xi. \tag{21}$$

In fact, whenever u is sufficiently smooth:

$$\begin{aligned} & y^a \frac{v(x, y) - v(x, 0)}{y} = y^a \frac{u * P_{\mathbb{G}}(\cdot, y) - u(x)}{y} \\ & = \left(C_a \int_0^\infty t^{(a-3)/2} e^{-\frac{y^2}{4t}} u * h(t, \cdot)\, dt \right. \\ & \qquad \left. - C_a u(x) \int_{\mathbb{G}} \int_0^\infty t^{(a-3)/2} e^{-\frac{y^2}{4t}} h(t, \xi^{-1} x)\, dt d\xi \right) \\ & = C_a \int_{\mathbb{G}} \int_0^\infty t^{(a-3)/2} e^{-\frac{y^2}{4t}} h(t, \xi^{-1} x)\, dt (u(\xi) - u(x)) d\xi. \end{aligned} \tag{22}$$

On the other hand

$$\lim_{y\to 0^+} C_a \int_0^\infty t^{(a-3)/2} e^{-\frac{y^2}{4t}} h(t, \xi^{-1}x)\, dt = \tilde{C}_a \tilde{R}_{a-1}. \tag{23}$$

Thus

$$\lim_{y\to 0^+} y^a \frac{v(x,y)-v(x,0)}{y} = C_a \int_{\mathbb{G}} (u(\xi)-u(x))\tilde{R}_{a-1}(\xi)d\xi = \tilde{C}_a \mathscr{L}^{\frac{1-a}{2}} u(x),$$

where

$$\widetilde{R}_\beta(x) = \frac{\frac{\beta}{2}}{\Gamma(\beta/2)} \int_0^\infty t^{\frac{\beta}{2}-1} h(t,x)\, dt. \tag{24}$$

It boils down:

$$\mathscr{L}^{\frac{1-a}{2}} u(x) = \lim_{y\to 0^+} y^a \frac{v(x,y)-v(x,0)}{y} = \tilde{C}_a \int_{\mathbb{G}} (u(\xi)-u(x))\tilde{R}_{a-1}(\xi)d\xi.$$

This construction is very general, nevertheless it is not always easy to write explicitly the kernel $\tilde{R}_{a-1}$ even in the simplest non-commutative case like in the Heisenberg group $\mathbb{H}^1$. In fact, the heat kernel in the Heisenberg group $\mathbb{H}^1$ is written via an integral. More precisely, if $(z,s) \in \mathbb{C}\times\mathbb{R} \equiv \mathbb{H}^1$, then the heat kernel h of $-\Delta_{\mathbb{H}^1} + \frac{\partial}{\partial t}$ in $]0,+\infty[\times\mathbb{H}^1$ is:

$$h(t,(z,s)) = (4\pi t)^{-2} \int_{\mathbb{R}} e^{-\frac{f(z,s,\kappa)}{t}} V(\kappa)d\kappa,$$

where

$$f(z,s,\kappa) = \frac{1}{2}(-i\kappa s + \frac{\kappa|z|^2}{2\tanh(2\kappa)})$$

and

$$V(\kappa) = \frac{2\kappa}{\sinh(2\kappa)}.$$

Thus, recalling (24), we obtain in the Heisenberg case $\mathbb{H}^1$ the following kernel:

$$\widetilde{R}_\beta(z,s) = \frac{\frac{\beta}{2}}{\Gamma(\beta/2)} \int_0^\infty t^{\frac{\beta}{2}-1} \left((4\pi t)^{-2} \int_{\mathbb{R}} e^{-\frac{f(z,s,\kappa)}{t}} V(\kappa)d\kappa \right) dt. \tag{25}$$

It is clear that the double integration in the representation of $\widetilde{R}_\beta$ produces some technical difficulties that do not appear in dealing with the usual heat kernel in $\mathbb{R}^3$.

In fact, if $(\mathbb{G},\circ) = (\mathbb{R}^3,+)$, then for every $\alpha > 0$ it results

$$\widetilde{R}_\alpha(x) = -\frac{\alpha}{2\Gamma(-\alpha/2)} \frac{1}{(4\pi)^{\frac{3}{2}}} \int_0^\infty t^{-\alpha/2-3/2-1} e^{-\frac{|x|^2}{4t}} dt,$$

being $\frac{1}{(4\pi t)^{\frac{3}{2}}} e^{-\frac{|x|^2}{4t}}$ the heat kernel of $-\Delta + \frac{\partial}{\partial t}$ in $]0, +\infty[\times\mathbb{R}^3$. Thus, after a changing of variables, we obtain:

$$\begin{aligned}\widetilde{R}_\alpha(x) &= -\frac{\alpha}{2\Gamma(-\alpha/2)} \frac{4^{\frac{\alpha}{2}+\frac{3}{2}}}{(4\pi)^{\frac{3}{2}}} |x|^{-\alpha-3} \int_0^\infty y^{\frac{1+\alpha}{2}} e^{-y} dy \\ &= -\frac{\alpha}{2\Gamma(-\alpha/2)} \frac{4^{\frac{\alpha}{2}+\frac{3}{2}}}{(4\pi)^{\frac{3}{2}}} \Gamma\Big(\frac{\alpha+3}{2}\Big) |x|^{-\alpha-3}.\end{aligned} \tag{26}$$

Moreover, denoting $c := -\frac{\alpha}{2\Gamma(-\alpha/2)} \frac{4^{\frac{\alpha}{2}}}{\pi^{\frac{3}{2}}} \Gamma\Big(\frac{\alpha+3}{2}\Big)$, we get the usual kernel that appears in the representation of $(-\Delta)^{\frac{\alpha}{2}}$ that is:

$$\widetilde{R}_\alpha(x) = c \frac{1}{|x|^{3+\alpha}},$$

see (4) when $n = 3$.

As far as we are concern, we don't know if a simpler representation of the kernel (25) exists when we are in a non-commutative group.

We conclude this section pointing out that some tentatives to define the fractional operator, starting from the notion of the intrinsic translation, has been done in [21]. Moreover, it is known that in CR structures the extension can be done with a little different approach, see [28].

3 Applications

In this section we discuss some applications of the extension method to solutions of nonlocal operators. In particular in Sect. 3.1 we review the Harnack inequality for positive solutions of the equation $\mathbf{D}^\alpha u = 0$ in $I \subset \mathbb{R}$. In Sect. 3.2 we recall how to prove Harnack inequality for $\alpha-$harmonic function in Carnot groups, while in Sect. 3.3 we revisit an application of the extension approach to the notion of perimeter in Carnot groups.

3.1 Weyl-Marchaud Derivative: The Harnack Inequality

Concerning the PDE of the problem (9), in this particular case, the conductivity coefficient (i.e. the coefficient in front of the x derivative) and the specific heat (the coefficient of the t derivative) coincide. In [16], this type of equation has been studied in a more general framework. In fact a more general form of that equation is given as follows:

$$w(x)\frac{\partial u}{\partial t} = \frac{\partial}{\partial x}(a(x)\frac{\partial U}{\partial x}). \tag{27}$$

We assume that:

$$\lambda^{-1} w(x) \leq a(x) \leq \lambda w(x)$$

and that the following integrability condition (known as a Muckehoupt, or A_2 weight condition) on the weight w holds as well:

$$\sup_J (\frac{1}{|J|}\int_J w(x)\,dx)\,(\frac{1}{|J|}\int_J \frac{1}{w(x)}\,dx) = c_0 < \infty, \tag{28}$$

for every interval $J \subseteq (-R, R)$. The constant c_0 is indicated as the A_2 constant of w. In our case, of course, we are left with the condition (28). In [16] the authors also proved the following Harnack inequality.

Theorem 5 (Chiarenza-Serapioni) *Let U be a positive solution in $(-R, R) \times (0, T)$ of the equation in (9) and assume that condition (28) holds, with constant c_0. Then there exists $\gamma = \gamma(c_0) > 0$ such that*

$$\sup_{(\frac{\rho}{2},\frac{\rho}{2})\times(t_0-\frac{3\rho^2}{4},t_0-\frac{\rho^2}{4})} U \leq \gamma \inf_{(\frac{\rho}{2},\frac{\rho}{2})\times(t_0+\frac{3\rho^2}{4},t_0+\rho^2)} U \tag{29}$$

holds for $t_0 \in (0, T)$ and any ρ such that $0 < \rho < R/2$ and $[t_0 - \rho^2, t_0 + \rho^2] \subset (0, T)$.

As a consequence, in [10], has been proved the following Harnack inequality for the Marchaud derivative:

Corollary 1 *Let $s \in (0, 1)$. There exists a positive constant γ such that, if $\mathbf{D}^s\phi = 0$ in $J \subseteq \mathbb{R}$ and $\phi \geq 0$ in $\mathbb{R}$, then*

$$\sup_{[t_0-\frac{3}{4}\delta,t_0-\frac{1}{4}\delta]} \phi \leq \gamma \inf_{[t_0+\frac{3}{4}\delta,t_0+\delta]} \phi \tag{30}$$

for every $t_0 \in \mathbb{R}$ and for every $\delta > 0$ such that $[t_0 - \delta, t_0 + \delta] \subset J$.

3.2 *Fractional Operators of Sublaplacians in Carnot Groups: The Harnack Inequality*

Having in hand the characterization of the fractional operator recalled in (21) and (22), we may reduce ourselves to work with local operator (as well as we have already remarked for the Marchaud derivative), see also [23] for this part. In fact, if Y is the following vector field $\frac{\partial}{\partial y}$ and $\hat{\mathbb{G}} := \mathbb{G} \times \mathbb{R}$, then $\hat{\mathbb{G}}$ is still a Carnot group and its Lie algebra $\hat{g}$ admits the stratification

$$\hat{g} = \hat{g}_1 \bigoplus g_2 \bigoplus \cdots \bigoplus g_m,$$

where $\hat{g}_1 = \text{span}\{Y, g_1\}$.

Then the following result holds.

Theorem 6 *([23]) Let $u \in W^{1-a,2}_{\mathbb{G}}(\mathbb{G})$ be given, $u \geq 0$, and assume $\mathscr{L}^{(1-a)/2}u = 0$ in an open set Ω. Denoting by $\hat{v}$ the function on $\hat{\mathbb{G}}$ obtained by continuing v by parity across $y = 0$. Then*

(i) $\hat{v} \geq 0$;
(ii) $\hat{v} \in W^{1,2}_{\hat{\mathbb{G}},\text{loc}}(\hat{\Omega};\ y^a dx\, dy)$, *where* $\hat{\Omega} := \Omega \times (-1, 1)$;
(iii) $\hat{v}$ *is a weak solution of the equation*

$$div_{\hat{\mathbb{G}}}\left(|y|^a \nabla_{\hat{\mathbb{G}}} \hat{v}\right) = 0 \quad \text{in } \hat{\Omega}. \tag{31}$$

We recall the following well known definition in the study of operators with weights.

Definition 1 (see [17]) A function $\omega \in L^1_{\text{loc}}(\mathbb{G})$ is said to be a A_2-weight with respect to the cc-metric of $\mathbb{G}$ if

$$\sup_{x\in\mathbb{G},\, r>0} |B_c(x,r))|^{-1} \int_{B_c(x,r)} \omega(y)\, dy \cdot |B_c(x,r))|^{-1} \int_{B_c(x,r)} \omega(y)^{-1}\, dy < \infty.$$

Remark. The function $\omega(x, y) = |y|^a$ is a A_2-weight with respect to the CC-metric of $\mathbb{G} \times \mathbb{R}$ if and only if $-1 < a < 1$.

The following result is well known in literature, see: [34, 35, 42].

Theorem 7 *Let $\mathbb{G}$ be a Carnot group, and let $\Omega \subset \mathbb{G}$ be an open set. Let now $\omega \in L^1_{\text{loc}}(\mathbb{G})$ be a A_2-weight with respect to the Carnot-Carathéodory metric d_c of $\mathbb{G}$. If $u \in W^{1,2}_{\mathbb{G}}(\Omega, \omega dx)$ is a weak solution to*

$$\text{div}_{\mathbb{G}}\,(\omega\, \nabla_{\mathbb{G}} u) = 0, \tag{32}$$

then u is locally Hölder continuous in Ω. Moreover, if $u \geq 0$, then there exist $C, b > 0$ (independent of u) such that the following invariant Harnack inequality holds:

$$\sup_{B_c(x,r)} u \leq C \inf_{B_c(x,r)} u \tag{33}$$

for any metric ball $B_c(x, r)$ such that $B_c(x, br) \subset \Omega$.

In addition, if Ω satisfies the following local condition: for any $x_0 \in \partial\Omega$ there exist $r_0 > 0$ and $\alpha > 0$ such that

$$|B_c(x_0, r) \cap \Omega^c| \geq \alpha |B_c(x_0, r)| \quad \text{for } r < r_0.$$

Then u is locally Hölder continuous in $\overline{\Omega}$. Thus, applying Theorem 7 we obtain the Harnack inequality. In fact we get the following theorem.

Theorem 8 *([23]) Let $-1 < a < 1$ and let $u \in W_{\mathbb{G}}^{1-a,2}(\mathbb{G})$ be given, $u \geq 0$ on all of $\mathbb{G}$. Assume $\mathscr{L}^{(1-a)/2}u = 0$ in an open set $\Omega \subset \mathbb{G}$.*

Then there exist $C, b > 0$ (independent of u) such that the following invariant Harnack inequality holds:

$$\sup_{B_c(x,r)} u \leq C \inf_{B_c(x,r)} u$$

for any metric ball $B_c(x, r)$ such that $B_c(x, br) \subset \Omega$.

In fact, the proof of Theorem 8 is consequence of the following argument. Since the function (18), that may be written as (20) as well, after to be prolonged by parity and denoted by $\hat{v}$, is solution to the local problem (31) in an extended set obtained by parity. Then, recalling that $\hat{v}$ is positive, the Harnack inequality holds true for $\hat{v}$ applying the well known theory of the operators with weights, see Theorem 7. In this way, we straightforwardly obtain the desired inequality from (33), because $u(x) = \hat{v}(x, 0) = v(x, 0)$.

3.3 Carnot Groups: A Perimeter Notion

Having in mind the previous results described in Sect. 2.2, we would like to show some applications of them to fractional perimeter in Carnot groups. This is a first tentative of extending a research theme already explored in the Euclidean case, see e.g. [11], to the non-commutative setting, see also [8].

We start as usual recalling some remarks $\mathbb{R}^n$. Let $h_\alpha(t, z)$ be the fundamental solution of the fractional heat equation in $\mathbb{R}_+ \times \mathbb{R}^n$

$$u_t + (-\Delta)^\alpha u = 0. \tag{34}$$

Setting $\tilde{h}_\alpha(z) = h_\alpha(1, z)$, h_α satisfies

$$\int_{\mathbb{R}^n} h_\alpha(t, z)\, dz = 1 \qquad \forall\, t > 0, \qquad h_\alpha(t, z) = \frac{1}{t^{n/2\alpha}} \tilde{h}_\alpha(t^{-1/2\alpha} z) \tag{35}$$

and

$$\lim_{t \to 0} \frac{h_\alpha(t, x)}{t} = \frac{C_{n,\alpha}}{|x|^{n+2\alpha}}, \tag{36}$$

see Theorem 2.1 in [9], where the exact value of the constant is given. The fractional heat semigroup that gives the solution of (34) with initial datum f is given by

$$e^{-t(-\Delta)^\alpha} f(x) = \int_{\mathbb{R}^n} h_\alpha(t, y) f(x - y)\, dy, \qquad f \in L^1(\mathbb{R}^n),$$

and, since the kernel h_α has integral one, we have

$$e^{-t(-\Delta)^\alpha} f(x) - f(x) = \int_{\mathbb{R}^n} h_\alpha(t, y)\Big(f(x-y) - f(x)\Big)\, dy.$$

On the other hand:

$$\begin{aligned} &\|(-\Delta)^{\alpha/2} f\|^2_{L^2(\mathbb{R}^n)} \\ &= \int_{\mathbb{R}^n} f(-\Delta)^\alpha f\, dx = C(n,\alpha) \int_{\mathbb{R}^n} f(x) \int_{\mathbb{R}^n} \frac{f(x) - f(y)}{|x-y|^{n+2\alpha}}\, dydx \\ &= \frac{C(n,\alpha)}{2} \int_{\mathbb{R}^n}\int_{\mathbb{R}^n} \frac{|f(x) - f(y)|^2}{|x-y|^{n+2\alpha}}\, dydx = \frac{C(n,\alpha)}{2} [f]^2_{W^{\alpha,2}}. \end{aligned} \tag{37}$$

Thus we consider the following quantity

$$Q^\alpha_t(f) = \int_{\mathbb{R}^n\times\mathbb{R}^n} h_\alpha(t, y)\Big(f(x-y) - f(x)\Big)^2\, dx\, dy.$$

Using (36) we get

$$\lim_{t\to 0} \frac{Q^\alpha_t(f)}{t} = C_{n,\alpha}[f]^2_{W^{\alpha,2}(\mathbb{R}^n)}.$$

Hence we have that $f \in W^{\alpha,2}(\mathbb{R}^n)$ if and only if

$$\lim_{t\to 0} \frac{Q^\alpha_t(f)}{t} < \infty,$$

see [4] and [18].

The following properties have been proved in [27].

Theorem 9 *There exists a function h defined in $\hat{\mathbb{G}}$ such that:*

(i) $h \in C^\infty(\hat{\mathbb{G}} \setminus \{(0,0)\})$
(ii) $h(\lambda^2 t, \delta_\lambda(x)) = \lambda^{-Q} h(t,x)$ *for every* $t > 0$, $x \in \mathbb{G}$ *and* $\lambda > 0$;
(iii) $h(t,x) = 0$ *for every* $t < 0$ *and* $\int_{\mathbb{G}} h(t,x)dx = 1$ *for every* $t > 0$;
(iv) $h(t,x) = h(t,x^{-1})$ *for every* $t > 0$ *and* $x \in \mathbb{G}$;
(v) there exists $c > 0$ *such that for every* $x \in \mathbb{G}$ *and* $t > 0$

$$c^{-1}t^{-Q/2}\exp\Big(-\frac{\|x\|^2)}{c^{-1}t}\Big) \le h(x,t) \le ct^{-Q/2}\exp\Big(-\frac{\|x\|^2}{ct}\Big). \tag{38}$$

As well as in the Euclidean case, we introduce the heat semigroup

$$e^{-t\mathscr{L}} f(x) := \int_{\mathbb{G}} h(t, y^{-1}\circ x) f(y) dy, \quad f \in L^1(\mathbb{G}). \tag{39}$$

For every $\alpha > 0$ let

$$\tilde{R}_\alpha(x) := -\frac{\alpha}{2\Gamma(-\alpha/2)} \int_0^\infty t^{-\frac{\alpha}{2}-1} h(t,x)dt, \tag{40}$$

where

$$R_\alpha(x) = \frac{1}{\Gamma(\alpha/2)} \int_0^\infty t^{\frac{\alpha}{2}-1} h(t,x)dt.$$

Then, see [23], $\tilde{R}_\alpha$ and R_α are smooth functions in $\mathbb{G} \setminus \{0\}$ and $\mathscr{L} R_{2-\alpha} = \tilde{R}_{-\alpha}$. In addition, $\tilde{R}_\alpha$ is positive and homogeneous of degree $-\alpha - Q$.

Moreover, using (iv) and (v) of Theorem 9, we get

$$\tilde{R}_\alpha(x) = \tilde{R}_\alpha(x^{-1}), \tag{41}$$

and

$$c^{-1}\|x\|^{-\alpha-Q} \le \tilde{R}_\alpha(x) \le c\|x\|^{-\alpha-Q} \qquad \forall x \in \mathbb{G}. \tag{42}$$

Thus, defining

$$\|x\|_\alpha := \left(\tilde{R}_\alpha(x)\right)^{-\frac{1}{\alpha+Q}}, \tag{43}$$

we deduce that $\|x\|_\alpha$ is a homogeneous symmetric norm because from (42) follows that there exists a constant $c > 0$, depending only on α, such that for every $x \in \mathbb{G}$

$$c^{-1}\|x\| \le \|x\|_\alpha \le c\|x\|.$$

After a straightforward calculation we obtain the following result.

Lemma 2 *If $u \in \mathscr{S}(\mathbb{G})$ then*

$$\mathscr{L}^\alpha u(x) = -\frac{1}{2} \int_{\mathbb{G}} \frac{u(x \circ y) + u(x \circ y^{-1}) - 2u(x)}{\|y\|_\alpha^{Q+2\alpha}} dy. \tag{44}$$

Moreover for any $u \in \mathscr{S}(\mathbb{G})$:

$$\lim_{\alpha \to 1^-} (1-\alpha)\mathscr{L}^\alpha u(x) = \mathscr{L} u(x), \qquad \forall x \in \mathbb{G}.$$

For the proof see e.g. [24] and [23]. The notion of α-horizontal perimeter in Carnot groups can be introduce as follow, see [24].

Definition 2 For a Borel set $E \subset \mathbb{G}$ and $\alpha \in (0,1)$ the fractional $\alpha-$horizontal perimeter of E is

$$\mathrm{Per}_{\alpha,\mathbb{G}}(E) := \int_E \int_{E^c} \frac{1}{\|y^{-1} \circ x\|_\alpha^{Q+\alpha}} dxdy.$$

We say that $E \subset \mathbb{G}$ has finite fractional $\alpha-$horizontal perimeter if $\mathrm{Per}_{\alpha,\mathbb{G}}(E) < \infty$.

We recall here, for permitting a quick comparison, that the fractional perimeter in $\mathbb{R}^n$ of a Borel set $E \subset \mathbb{R}^n$, in $\mathbb{R}^n$, assuming that $\alpha \in (0, 1)$ is defined as follows:

$$\mathrm{Per}_{\alpha,\mathbb{R}^n}(E) := \int_E \int_{E^c} \frac{1}{|x - y|^{n+\alpha}} dxdy.$$

The interested reader may easily compare this definition keeping in mind the role of the kernel $\frac{1}{|x-y|^{n+\alpha}}$ in defining the fractional Laplace operator in $\mathbb{R}^n$, see (4). For further details about the notion of fractional perimeter of a set E in a set Ω that is not necessarily all of $\mathbb{R}^n$ see [1] and [13].

Moreover, continuing our description in Carnot groups, we remark that

$$\int_{\mathbb{G}} \int_{\mathbb{G}} \frac{|\chi_E(x) - \chi_E(y)|}{\|y^{-1} \circ x\|_\alpha^{Q+\alpha}} dxdy = \int_{E \cup E^c} \int_{E \cup E^c} \frac{|\chi_E(x) - \chi_E(y)|}{\|y^{-1} \circ x\|_\alpha^{Q+\alpha}} dxdy$$
$$= \int_E \int_{E^c} \frac{2}{\|y^{-1} \circ x\|_\alpha^{Q+\alpha}} dxdy.$$

So that, the function

$$Q_t^\alpha(\chi_E) = \int_{\mathbb{G} \times \mathbb{G}} h_\alpha(t, y) |\chi_E(y^{-1} \circ x) - \chi_E(x)| dxdy$$

establishes a relationship between the fractional heat semigroup and the fractional perimeter. In fact, see the following result whose detailed proof is given in [24].

Theorem 10 *There are constants $c_1(\alpha), c_2(\alpha) > 0$ such that for every Borel set E there holds.*

$$c_1(\alpha)\mathrm{Per}_{\alpha,\mathbb{G}}(E) \le \liminf_{t \to 0} \frac{Q_t^{\alpha/2}(\chi_E)}{t} \le \limsup_{t \to 0} \frac{Q_t^{\alpha/2}(\chi_E)}{t} \tag{45}$$
$$\le c_2(\alpha)\mathrm{Per}_{\alpha,\mathbb{G}}(E).$$

More precisely, the upper estimates follow from [15] where it is proved that:

$$c^{-1}\Big(t^{-Q/2\alpha} \wedge \frac{t}{\|z\|^{Q+2\alpha}}\Big) \le h_\alpha(t, z) \le c\Big(t^{-Q/2\alpha} \wedge \frac{t}{\|z\|^{Q+2\alpha}}\Big), \tag{46}$$

and the following lemma that has been proved in [49], see Theorems 9 and 14.

Lemma 3 *Let $u \in W^{\alpha/2,2}(\mathbb{G})$; then there exists $c_\alpha > 0$ such that for all $z \in \mathbb{G}$, denoting by $\tau_z u(x) := u(z^{-1}x)$, there holds*

$$\|\tau_z u - u\|^2_{L^2(\mathbb{G})} \leq c_\alpha \|z\|^\alpha \int_{\mathbb{G}\times\mathbb{G}} \frac{|u(x) - u(w^{-1} \circ x)|^2}{\|w\|^{Q+\alpha}} dxdw.$$

We sketch the proof of Theorem 10 for helping the reader, recalling that the detail can be found in [24]:

$$\begin{aligned}
&Q_t^{\alpha/2}(\chi_E) = \int_{\mathbb{G}\times\mathbb{G}} h_{\alpha/2}(t,z)|\chi_E(z^{-1}\circ x) - \chi_E(x)|dxdz \\
&\leq c_2 t^{-Q/\alpha} \int_{B(t^{1/\alpha})} \|z\|^\alpha [\chi_E]^2_{W^{\alpha/2,2}} dz \\
&+ c_2 t \int_{B^c(t^{1/\alpha})\times\mathbb{G}} \frac{|\chi_E(z^{-1}\circ x) - \chi_E(x)|}{\|z\|^{Q+\alpha}} dxdz \leq 2tc_2|B(1)|\mathrm{Per}_{\alpha,\mathbb{G}}(E) \\
&+ c_2 t \int_{B^c(t^{1/\alpha})\times\mathbb{G}} \frac{|\chi_E(z^{-1}\circ x) - \chi_E(x)|}{\|z\|^{Q+\alpha}} dxdz \leq c_2(\alpha) t \mathrm{Per}_{\alpha,\mathbb{G}}(E).
\end{aligned}$$

Concerning the lower bound, we start from (46), keeping in mind that on the complement of the ball $B(t^{\frac{1}{\alpha}})$ we have the estimate

$$h_{\alpha/2}(t,y) \geq c_1 \frac{t}{\|y\|^{Q+\alpha}},$$

so that we deduce

$$\begin{aligned}
&Q_t^{\alpha/2}(\chi_E) = \int_{\mathbb{G}\times\mathbb{G}} h_{\alpha/2}(t,y)|\chi_E(y^{-1}\circ x) - \chi_E(x)|dxdy \\
&\geq c_1(\alpha) t \int_{\mathbb{G}\setminus B(t^{\frac{1}{\alpha}})} \int_{\mathbb{G}} \frac{|\chi(y^{-1}\circ x) - \chi_E(x)|}{\|y\|_\alpha^{Q+\alpha}} dxdy.
\end{aligned}$$

It follows

$$\begin{aligned}
c_1(\alpha) \int_{\mathbb{G}\times\mathbb{G}} \frac{|\chi(y^{-1}\circ x) - \chi_E(x)|}{\|y\|_\alpha^{Q+\alpha}} &= \lim_{t\to 0} c_1 \int_{\mathbb{G}\setminus B(t^{\frac{1}{\alpha}})} \int_{\mathbb{G}} \frac{|\chi(y^{-1}\circ x) - \chi_E(x)|}{\|y\|_\alpha^{Q+\alpha}} \\
&\leq \liminf_{t\to 0} \frac{Q_t^{\alpha/2}(\chi_E)}{t},
\end{aligned}$$

ending the proof. Of course Theorem 10 can be generalized to every function $u \in L^2(\mathbb{G})$, see [24] , Theorem 3.5. So that $u \in W^{\alpha,2}(\mathbb{G})$ if and only if

$$\limsup_{t\to 0^+} \frac{Q_t^\alpha(u)}{t} < +\infty.$$

4 Extension Approach: The Periodic Function Case via Fourier Series Tool

In this section we test the extension approach considering a periodic function. To do this we face the problem considering Fourier series. In particular, in the case $s = \frac{1}{2}$, we obtain as a byproduct a Poincaré inequality, see (63).

In fact let $L \in (0, \infty)$ be a fixed number and $s \in (0, 1)$. Let $\varphi \in C_{2\pi}(\mathbb{R})$ be a 2π periodic, continuous given function. We want to solve the following problem

$$\begin{cases} \frac{\partial U}{\partial t}(x,t) = \frac{1-2s}{x}\frac{\partial U}{\partial x}(x,t) + \frac{\partial^2 U}{\partial x^2}(x,t), & (x,t) \in (0,L) \times (-\pi,\pi) \\ U(0,t) = \varphi(t), & t \in [-\pi,\pi] \\ U(x,-\pi) = U(x,\pi), & x \in [0,L], \end{cases} \tag{47}$$

compare with [10] and Sect. 2, Theorem 1.

We look for a solution of the previous problem in the following form:

$$U = \frac{a_0}{2} + \sum_{k=1}^{\infty} (a_k(x)\cos(kt) + b_k(x)\sin(kt)),$$

where $\{a_k\}_{k\in\mathbb{N}}$ and $\{b_k\}_{k\in\mathbb{N}}$ are functions defined in $[0, L]$ that have to be determined, but assuming that

$$a_0(0) = \frac{1}{\pi}\int_{-\pi}^{\pi} \varphi(\tau)d\tau$$

and

$$a_k(0) = \frac{1}{\pi}\int_{-\pi}^{\pi} \varphi(\tau)\cos(k\tau)d\tau, \quad b_k(0) = \frac{1}{\pi}\int_{-\pi}^{\pi} \varphi(\tau)\sin(k\tau)d\tau.$$

We can suppose without, any restriction, that $a_0(0) = 0$ simply considering $\varphi - \frac{\varphi_0}{2}$, where $\varphi_0 := \frac{1}{\pi}\int_{-\pi}^{\pi} \varphi(\tau)d\tau$. Inserting formally our formal solution U in the equation of the problem (47), we get the following sequence of ODE systems

$$a_0'' + a_0' \frac{1-2}{x} = 0, \quad x \in (0, L) \tag{48}$$

and for every $k \in \mathbb{N}$, $k \geq 1$

$$\begin{cases} b_k'' + \frac{1-2}{x}b_k' = -ka_k, & x \in (0,L) \\ a_k'' + \frac{1-2}{x}a_k' = kb_k & x \in (0,L) \end{cases} \tag{49}$$

with the initial conditions $a_0(0) = 0$, and such that for every $k \in \mathbb{N}$, $k \geq 1$,

$$a_k(0) = \frac{1}{\pi}\int_{-\pi}^{\pi} \varphi(\tau)\cos(k\tau)d\tau, \quad b_k(0) = \frac{1}{\pi}\int_{-\pi}^{\pi} \varphi(\tau)\sin(k\tau)d\tau.$$

4.1 The Case $s = \frac{1}{2}$

In case $s = \frac{1}{2}$, from (48) and (49) we get:

$$a_0'' = 0, \quad x \in (0, L)$$

and for every $k \in \mathbb{N}$, $k \geq 1$

$$\begin{cases} b_k'' = -k a_k, \ x \in (0, L) \\ a_k'' = k b_k \quad x \in (0, L) \end{cases} \tag{50}$$

with the initial conditions $a_0(0) = 0$, and for every $k \in \mathbb{N}$, $k \geq 1$,

$$a_k(0) = \varphi_{a_k}(0), \quad b_k(0) = \varphi_{b_k}(0),$$

where

$$\varphi_{a_k}(0) = \frac{1}{\pi} \int_{-\pi}^{\pi} \varphi(\tau) \cos(k\tau) d\tau \quad b_k(0) = \varphi_{b_k}(0) = \frac{1}{\pi} \int_{-\pi}^{\pi} \varphi(\tau) \sin(k\tau) d\tau$$

In this special case we get, for every $k \geq 1$, $b_k^{(iv)} + k^2 b_k = 0$ and $b_k'' = -k a_k$. As a consequence the solution of $b_k^{(iv)} + k^2 b_k = 0$, $b_k(0) = \varphi_{b_k}(0)$ takes the following form:

$$\begin{aligned} b_k &= \varphi_{b_k}(0) \cosh(\frac{\sqrt{2k}}{2}x) \cos(\frac{\sqrt{2k}}{2}x) + c_2 \cosh(\frac{\sqrt{2k}}{2}x) \sin(\frac{\sqrt{2k}}{2}x) \\ &+ c_3 \sinh(\frac{\sqrt{2k}}{2}x) \cos(\frac{\sqrt{2k}}{2}x) + c_4 \sinh(\frac{\sqrt{2k}}{2}) \sin(\frac{\sqrt{2k}}{2}x) \\ &= \cosh(\frac{\sqrt{2k}}{2}x) \left(\varphi_{b_k}(0) \cos(\frac{\sqrt{2k}}{2}x) + c_2 \sin(\frac{\sqrt{2k}}{2}x) \right) \\ &+ \sinh(\frac{\sqrt{2k}}{2}x) \left(c_3 \cos(\frac{\sqrt{2k}}{2}x) + c_4 \sin(\frac{\sqrt{2k}}{2}x) \right). \end{aligned} \tag{51}$$

From $b_k'' = -k a_k$, $a_k(0) = \varphi_{a_k}(0)$ we get

$$\begin{aligned} b_k &= \cosh(\frac{\sqrt{2k}}{2}x) \left(\varphi_{b_k}(0) \cos(\frac{\sqrt{2k}}{2}x) + c_2 \sin(\frac{\sqrt{2k}}{2}x) \right) \\ &+ \sinh(\frac{\sqrt{2k}}{2}x) \left(c_3 \cos(\frac{\sqrt{2k}}{2}x) - \varphi_{a_k}(0) \sin(\frac{\sqrt{2k}}{2}x) \right) \end{aligned} \tag{52}$$

and

$$
\begin{aligned}
a_k = \cosh(\frac{\sqrt{2k}}{2}x)\left(\varphi_{a_k}(0)\cos(\frac{\sqrt{2k}}{2}x) + c_2\sin(\frac{\sqrt{2k}}{2}x)\right) \\
+ \sinh(\frac{\sqrt{2k}}{2}x)\left(c_3\cos(\frac{\sqrt{2k}}{2}x) + \varphi_{b_k}(0)\sin(\frac{\sqrt{2k}}{2}x)\right).
\end{aligned} \tag{53}
$$

While

$$a_0(x) = c_0 x + \varphi_0,$$

for some $c_0 \in \mathbb{R}$.

Then

$$a_k'(0) = \frac{\sqrt{2k}}{2}(c_{2,k} + c_{3,k}), \quad b_k'(0) = \frac{\sqrt{2k}}{2}(c_{2,k} + c_{3,k})$$

and

$$
\begin{aligned}
\frac{\partial U}{\partial x}(0,t) &= \frac{c_0}{2} + \sum_{k=1}^{\infty}(a_k'(0)\cos(kt) + b_k'(0)\sin(kt)) \\
&= \frac{c_0}{2} + \frac{\sqrt{2}}{2}\sum_{k=1}^{\infty}\sqrt{k}(c_{2,k} + c_{3,k})\,(\cos(kt) + \sin(kt)) \\
&= \frac{c_0}{2} + \frac{\sqrt{2}}{2}\sum_{k=1}^{\infty}\sqrt{k}(c_{2,k} + c_{3,k})\left(\cos(kt) + \cos(kt - \frac{\pi}{2})\right) \\
&= \frac{c_0}{2} + \sqrt{2}\sum_{k=1}^{\infty}\sqrt{k}(c_{2,k} + c_{3,k})\cos(kt - \frac{\pi}{4})\cos\frac{\pi}{4} \\
&= \frac{c_0}{2} + \sum_{k=1}^{\infty}\sqrt{k}(c_{2,k} + c_{3,k})\cos(kt - \frac{\pi}{4}).
\end{aligned} \tag{54}
$$

In this way we do not have the convergence of the Fourier solution, in general.

Thus from the fundamental system of solutions

$$
\begin{aligned}
&\{\exp(\frac{\sqrt{2k}}{2}x)\cos(\frac{\sqrt{2k}}{2}x), \exp(\frac{\sqrt{2k}}{2}x)\sin(\frac{\sqrt{2k}}{2}x), \\
&\exp(-\frac{\sqrt{2k}}{2}x)\cos(\frac{\sqrt{2k}}{2}x), \exp(-\frac{\sqrt{2k}}{2}x)\sin(\frac{\sqrt{2k}}{2}x)\}
\end{aligned} \tag{55}
$$

we consider only the functions

$$\{\exp(-\frac{\sqrt{2k}}{2}x)\cos(\frac{\sqrt{2k}}{2}x), \exp(-\frac{\sqrt{2k}}{2}x)\sin(\frac{\sqrt{2k}}{2}x)\}.$$

Let us consider the following linear combination

$$c_1 \exp(-\frac{\sqrt{2k}}{2}x)\cos(\frac{\sqrt{2k}}{2}x) + c_2 \exp(-\frac{\sqrt{2k}}{2}x)\sin(\frac{\sqrt{2k}}{2}x).$$

We impose that $c_1 = \varphi_{b_k}$, so that

$$b_k = \varphi_{b_k} \exp(-\frac{\sqrt{2k}}{2}x)\cos(\frac{\sqrt{2k}}{2}x) + c_2 \exp(-\frac{\sqrt{2k}}{2}x)\sin(\frac{\sqrt{2k}}{2}x).$$

Moreover

$$b_k' = \frac{\sqrt{2k}}{2}\exp(-\frac{\sqrt{2k}}{2}x)\left((c_2 - \varphi_{b_k})\cos(\frac{\sqrt{2k}}{2}x) - (c_2 + \varphi_{b_k})\sin(\frac{\sqrt{2k}}{2}x)\right).$$

and

$$b_k'' = -k\exp(-\frac{\sqrt{2k}}{2}x)\left(c_2\cos(\frac{\sqrt{2k}}{2}x) - \varphi_{b_k}\sin(\frac{\sqrt{2k}}{2}x)\right).$$

so that $b_k'' = -a_k$ if $c_2 = \varphi_{a_k}$. Hence

$$a_k = \exp(-\frac{\sqrt{2k}}{2}x)\left(\varphi_{a_k}\cos(\frac{\sqrt{2k}}{2}x) - \varphi_{b_k}\sin(\frac{\sqrt{2k}}{2}x)\right)$$

and

$$b_k = \exp(-\frac{\sqrt{2k}}{2}x)\left(\varphi_{b_k}\cos(\frac{\sqrt{2k}}{2}x) + \varphi_{a_k}\sin(\frac{\sqrt{2k}}{2}x)\right)$$

satisfies the system.

In particular

$$\begin{aligned} a_k' &= -\frac{\sqrt{2k}}{2}\exp(-\frac{\sqrt{2k}}{2}x)\left(\varphi_{a_k}\cos(\frac{\sqrt{2k}}{2}x) - \varphi_{b_k}\sin(\frac{\sqrt{2k}}{2}x)\right) \\ &\quad + \exp(-\frac{\sqrt{2k}}{2}x)\left(-\frac{\sqrt{2k}}{2}\varphi_{a_k}\sin(\frac{\sqrt{2k}}{2}x) - \frac{\sqrt{2k}}{2}\varphi_{b_k}\cos(\frac{\sqrt{2k}}{2}x)\right) \\ &= -\frac{\sqrt{2k}}{2}\exp(-\frac{\sqrt{2k}}{2}x)\left((\varphi_{a_k} + \varphi_{b_k})\cos(\frac{\sqrt{2k}}{2}x) + (\varphi_{a_k} - \varphi_{b_k})\sin(\frac{\sqrt{2k}}{2}x)\right) \end{aligned} \tag{56}$$

and

$$b_k' = \frac{\sqrt{2k}}{2}\exp(-\frac{\sqrt{2k}}{2}x)\left((\varphi_{a_k} - \varphi_{b_k})\cos(\frac{\sqrt{2k}}{2}x) - (\varphi_{a_k} + \varphi_{b_k})\sin(\frac{\sqrt{2k}}{2}x)\right).$$

As a consequence

$$a_k'(0) = -\frac{\sqrt{2k}}{2}(\varphi_{a_k} + \varphi_{b_k})$$

and

$$b_k'(0) = \frac{\sqrt{2k}}{2}(\varphi_{a_k} - \varphi_{b_k}).$$

$$\begin{aligned}\frac{\partial U}{\partial x}(0,t) &= \frac{c_0}{2} + \sum_{k=1}^{\infty}(a_k'(0)\cos(kt) + b_k'(0)\sin(kt)) \\ &= \frac{c_0}{2} - \frac{\sqrt{2}}{2}\sum_{k=1}^{\infty}\sqrt{k}\left((\varphi_{a_k} + \varphi_{b_k}))\cos(kt) - (\varphi_{a_k} - \varphi_{b_k})\sin(kt)\right).\end{aligned} \tag{57}$$

Moreover now $\psi_{a_k}(0) = -\sqrt{k}\frac{\sqrt{2}}{2}(\varphi_{a_k} + \varphi_{b_k})$ and $\psi_{b_k}(0) = \sqrt{k}\frac{\sqrt{2}}{2}(\varphi_{a_k} - \varphi_{b_k})$

$$\begin{aligned}\frac{\partial}{\partial x}\frac{\partial U}{\partial x}(0,t) &= -\frac{\sqrt{2}}{2}\sum_{k=1}^{\infty}\sqrt{k}\left((\psi_{a_k} + \psi_{b_k})\cos(kt) - (\psi_{a_k} - \psi_{b_k})\sin(kt)\right) \\ &= -\frac{1}{2}\sum_{k=1}^{\infty}k\left((-(\varphi_{a_k} + \varphi_{b_k}) + (\varphi_{a_k} - \varphi_{b_k}))\cos(kt) - (\psi_{a_k} - \psi_{b_k})\sin(kt)\right) \\ &= -\frac{1}{2}\sum_{k=1}^{\infty}k\left(-2\varphi_{b_k}\cos(kt) - (-(\varphi_{a_k} + \varphi_{b_k}) - (\varphi_{a_k} - \varphi_{b_k}))\sin(kt)\right) \\ &= -\frac{1}{2}\sum_{k=1}^{\infty}k\left(-2\varphi_{b_k}\cos(kt) + 2\varphi_{a_k}\sin(kt)\right) \\ &= \sum_{k=1}^{\infty}k\left(\varphi_{b_k}\cos(kt) - \varphi_{a_k}\sin(kt)\right) = \frac{\partial U}{\partial x}(0,t).\end{aligned}$$

From (57) it follows that, fixing $c_0 = 0$, we can define

$$\frac{d^{\frac{1}{2}}\varphi}{d^{\frac{1}{2}}t}(t) = -\frac{\sqrt{2}}{2}\sum_{k=1}^{\infty}\sqrt{k}\left((\varphi_{a_k} + \varphi_{b_k}))\cos(kt) - (\varphi_{a_k} - \varphi_{b_k})\sin(kt)\right). \tag{58}$$

as the representative of a class of functions $[\frac{d^{\frac{1}{2}}\varphi}{dt^{\frac{1}{2}}}]$ such that for every $\eta \in [\frac{d^{\frac{1}{2}}\varphi}{dt^{\frac{1}{2}}}]$ then

$$\eta - \frac{d^{\frac{1}{2}}\varphi}{dt^{\frac{1}{2}}}$$

is constant.

Moreover for every $c_0 \in \mathbb{R}$, the operator U_{c_0} acts on φ as it follows

$$\frac{c_0 x+\varphi_0}{2}+\sum_{k=1}^{\infty}(a_k(x)\cos(kt)+b_k(x)\sin(kt)) \tag{59}$$

that is

$$U_{c_0}(\varphi):=U_{c_0}\equiv\frac{c_0 x+\varphi_0}{2}+\sum_{k=1}^{\infty}(a_k(x)\cos(kt)+b_k(x)\sin(kt))$$

is a solution of the extension problem and since

$$\frac{\partial U_{c_0}}{\partial x}(0,t)=\frac{c_0}{2}-\frac{\sqrt{2}}{2}\sum_{k=1}^{\infty}\sqrt{k}\left((\varphi_{a_k}+\varphi_{b_k}))\cos(kt)-(\varphi_{a_k}-\varphi_{b_k})\sin(kt)\right)$$

we define

$$T_{1/2,c_0}(\varphi)=\frac{c_0}{2}-\frac{\sqrt{2}}{2}\sum_{k=1}^{\infty}\sqrt{k}\left((\varphi_{a_k}+\varphi_{b_k}))\cos(kt)-(\varphi_{a_k}-\varphi_{b_k})\sin(kt)\right).$$

In case $c_0\neq 0$, then applying the operator $T_{1/2,c_1}$ to $T_{1/2,c_0}(\varphi)$, after a further extension where we generate a new operator U_{c_1} associated with the constant $c_1\in\mathbb{R}$, we get

$$\begin{aligned}T_{1/2,c_1}T_{1/2,c_0}(\varphi)&=\frac{c_1}{2}-\frac{\sqrt{2}}{2}\sum_{k=1}^{\infty}\sqrt{k}\left((\varphi_{a_k}+\varphi_{b_k}))\cos(kt)-(\varphi_{a_k}-\varphi_{b_k})\sin(kt)\right)\\&=\frac{c_1}{2}+\sum_{k=1}^{\infty}k\left(\varphi_{b_k}\cos(kt)-\varphi_{a_k}\sin(kt)\right)=\frac{c_1}{2}+\frac{d\varphi}{dt}(t),\end{aligned} \tag{60}$$

because

$$\begin{aligned}&-\frac{\sqrt{2}}{2}\sqrt{k}\left(-\sqrt{k}\frac{\sqrt{2}}{2}(\varphi_{a_k}+\varphi_{b_k})+\sqrt{k}\frac{\sqrt{2}}{2}(\varphi_{a_k}-\varphi_{b_k})\right)\\&=k\varphi_{b_k}\end{aligned} \tag{61}$$

and

$$\begin{aligned}&\frac{\sqrt{2}}{2}\sqrt{k}\left(-\sqrt{k}\frac{\sqrt{2}}{2}(\varphi_{a_k}+\varphi_{b_k})-\sqrt{k}\frac{\sqrt{2}}{2}(\varphi_{a_k}-\varphi_{b_k})\right)\\&=-k\varphi_{a_k}\end{aligned} \tag{62}$$

and

$$\phi'(t)=\sum_{k=1}^{\infty}(-ka_k(x)\sin(kt)+kb_k(x)\cos(kt))=\sum_{k=1}^{\infty}(kb_k(x)\cos(kt)-ka_k(x)\sin(kt))$$

We remark that if

$$f = \frac{d^{\frac{1}{2}}\varphi}{dt^{\frac{1}{2}}}(t) = -\frac{\sqrt{2}}{2}\sum_{k=1}^{\infty}\sqrt{k}\left((\varphi_{a_k}+\varphi_{b_k})\cos(kt) - (\varphi_{a_k}-\varphi_{b_k})\sin(kt)\right),$$

then

$$||f||^2_{L^2} = \frac{\pi}{2}\sum_{k=1}^{\infty}k\left((\varphi_{a_k}+\varphi_{b_k})^2 + (\varphi_{a_k}-\varphi_{b_k})^2\right) = \pi\sum_{k=1}^{\infty}k\left(\varphi^2_{a_k}+\varphi^2_{b_k}\right).$$

Thus if $\varphi_0 = 0$, then

$$||\varphi||^2_{L^2(-\pi,\pi)} \leq \pi\sum_{k=1}^{\infty}k\left(\varphi^2_{a_k}+\varphi^2_{b_k}\right) = \pi||\frac{d^{\frac{1}{2}}\varphi}{dt^{\frac{1}{2}}}||^2_{L^2(-\pi,\pi)}. \tag{63}$$

That is we have proved the following Poincaré inequality:

$$||\varphi - \frac{\varphi_0}{2}||^2_{L^2(-\pi,\pi)} \leq \pi||\frac{d^{\frac{1}{2}}\varphi}{dt^{\frac{1}{2}}}||^2_{L^2(-\pi,\pi)}. \tag{64}$$

4.2 General Case with Bessel Functions: A Short Remark

Let

$$a_0'' + a_0'\frac{1-2s}{x} = 0, \quad x \in (0, L)$$

and for every $k \in \mathbb{N}$, $k \geq 1$

$$\begin{cases} b_k'' + \frac{1-2s}{x}b_k' = -ka_k, & x \in (0, L) \\ a_k'' + \frac{1-2s}{x}a_k' = kb_k & x \in (0, L) \end{cases} \tag{65}$$

It is convenient to consider the following differential equation in $\mathbb{C}$

$$\frac{d^2w_k}{dx^2} + \frac{1-2s}{x}\frac{dw_k}{dx} + ikw = 0, \tag{66}$$

where $k \in \mathbb{N}$. Indeed $\Re w$ and $\Im w$ satisfy the following system

$$\begin{cases} \Im w_k'' + \frac{1-2s}{x}\Im w_k' = -k\Re w_k, \\ \Re w_k'' + \frac{1-2s}{x}\Re w_k' = k\Im w_k \end{cases} \tag{67}$$

Then, see [44] Sect. 3.5, p. 77, a solution of previous Eq. (66) is given by

$$w_k = x^s Z_s(\sqrt{\frac{k}{2}}(1+i)x),$$

or also

$$w_k = x^s Z_s(-\sqrt{\frac{k}{2}}(1+i)x),$$

where Z_v is an arbitrary solution of Bessel's differential equation:

$$z^2\frac{d^2w_k}{dz^2} + z\frac{dw_k}{dz} + (z^2 - v^2)w = 0. \tag{68}$$

Then solving the problem we get

$$U_k(x,t) = \phi_{a_k}\frac{(L-x)^s Z_s(\sqrt{\frac{k}{2}}(1+i)(L-x))}{L^s Z_s(\sqrt{\frac{k}{2}}(1+i)L)}e^{-ikt}.$$

Using this functions we may expect to obtain inequalities for $\alpha \in (0,1)$ analogous to (64) obtained for $\alpha = \frac{1}{2}$.

Acknowledgements The author is supported by MURST, Italy, INDAM-GNAMPA project 2018: *Costanti critiche e problemi asintotici per equazioni completamente non lineari* and INDAM-GNAMPA project 2019: *Proprietà di regolarità delle soluzioni viscose con applicazioni a problemi di frontiera libera.*

References

1. Ambrosio, L., De Philippis, G., Martinazzi, L.: Gamma-convergence of nonlocal perimeter functionals. Manuscripta Math. **134**(3–4), 377–403 (2011)
2. Abadias, L., de León-Contreras, M., Torrea, J.: Non-local fractional derivatives. Discrete and continuous. J. Math. Anal. Appl. **449**, 734–755 (2017)
3. Allen, M., Caffarelli, L., Vasseur, A.: Porous medium flow with both a fractional potential pressure and fractional time derivative. Chin. Ann. Math. Ser. B **38**(1), 45–82 (2017)
4. Angiuli, L., Miranda, Jr. M., Pallara, D., Paronetto, F.: BV functions and parabolic initial boundary value problems on domains. Ann. Mat. Pura Appl. **188**(4):297–311 (2009)
5. Balakrishnan, A.V.: Fractional powers of closed operators and the semigroups generated by them. Pac. J. Math. **10**, 419–437 (1960)
6. Bogdan, K.: The boundary Harnack principle for the fractional Laplacian. Studia Math. **123**, 43–80 (1997)
7. Bernardis, A., MartíReyes, F.J., Stinga, R.P., Torrea, J.L.: Maximum principles, extension problem and inversion for nonlocal one-sided equations. J. Diff. Eqs. **260**(7), 6333–6362 (2016)
8. Bramanti, M., Miranda Jr., M., Pallara, D.: Two characterization of BV functions on Carnot groups via the heat semigroup. Int. Math. Res. Not. **17**, 3845–3876 (2012)
9. Blumenthal, R.M., Getoor, R.K.: Some theorems on stable processes. Trans. Amer. Math. Soc. **95**, 263–273 (1960)
10. Bucur, C., Ferrari, F.: An extension problem for the fractional derivative defined by Marchaud. Fract. Calc. Appl. Anal. **19**(4), 867–887 (2016)

11. Caffarelli, L., Savin, O., Valdinoci, E.: Minimization of a fractional perimeter-Dirichlet integral functional. Annales de l'Institut Henri Poincaré C Analyse non Linéaire **32**, 901–924 (2015)
12. Caffarelli, L., Silvestre, L.: An extension problem related to the fractional Laplacian. Comm. Partial Diff. Eqs. **32**(7–9), 1245–1260 (2007)
13. Caffarelli, L., Valdinoci, E.: Uniform estimates and limiting arguments for nonlocal minimal surfaces. Calc. Var. Partial Diff. Eqs. **41**(1–2), 203–240 (2011)
14. Caputo, M.: Diffusion of fluids in porous media with memory. Geothermics **28**(1), 113–130 (1999)
15. Chen, Z.-Q., Kumagai, T.: Heat kernel estimates for jump processes of mixed types on metric measure spaces. Probab. Theory Related Fields **140**, 277–317 (2008)
16. Chiarenza, F., Serapioni, R.: A remark on a Harnack inequality for degenerate parabolic equations. Rend. Sem. Mat. Univ. Padova **73**, 179–190 (1985)
17. Fabes, E., Kenig, C., Serapioni, R.: The local regularity of solutions of degenerate elliptic equations. CPDE **7**, 77–116 (1982)
18. Cygan, W., Grzywny, T.: Heat content for convolution semigroups. J. Math. Anal. Appl. **446**, 1393–1414 (2017)
19. Diethelm, K., Ford, N.J., Freed, A.D., Luchko, Y.: Algorithms for the fractional calculus: A selection of numerical methods. Comput. Methods Appl. Mech. Eng. **194**, 743–773 (2005)
20. Di Nezza, E., Palatucci, G., Valdinoci, E.: Hitchhiker's Guide to the Fractional Sobolev Spaces. Bull. Sci. Math. **136**, 521–573 (2012)
21. Ferrari, F.: Some nonlocal operators in the first Heisenberg group. Frac. Fract. **1**, 1–17 (2017)
22. Ferrari, F.: Weyl and Marchaud derivatives: A forgotten history. Mathematics **6**(1), 2018, Article number 6
23. Ferrari, F., Franchi, B.: Harnack inequality for fractional sub-Laplacians in Carnot groups. Math. Z. **279**(1–2), 435–458 (2015)
24. Ferrari, F., Miranda Jr., M., Pallara, D., Pinamonti, A., Sire, Y.: Fractional Laplacians, perimeters and heat semigroups in Carnot groups. Discrete Contin. Dyn. Syst. Ser. S **11**(3), 477–491 (2018)
25. Folland, G.B.: Subelliptic estimates and function spaces on nilpotent Lie groups. Ark. Mat. **13**(2), 161–207 (1975)
26. Folland, G.B.: Quantum field theory. A tourist guide for mathematicians. Mathematical Surveys and Monographs, 149. American Mathematical Society, Providence, RI, 2008
27. Folland, G.B., Stein, E.: Hardy Spaces on Homogeneous Groups. Princeton University Press (1982)
28. Frank, R.L., del Mar Gonzáles, M., Monticelli, M., Tan, J.: An extension problem for the cr fractional laplacian. Adv. Math. **270**, 97–137 (2015)
29. Garofalo, N.: Fractional thoughts. Contemporary Math. **723**, 1–124 (2019). (New developments in the analysis of nonlocal operators)
30. Garofalo, N.: Some properties of sub-Laplaceans. Elec. J. Diff. Eqs., Conf. **25**, 103–131 (2018)
31. Garofalo, N., Tralli, G.: A class of nonlocal hypoelliptic operators and their extensions. To appear in Indiana Univ. Math. J
32. Garrappa, R., Kaslik, E., Popolizio, M.: Evaluation of fractional integrals and derivatives of elementary functions: Overview and tutorial Mathematics Vol. 7, Issue 5, 2019, Article number 407
33. Grünwald, A.K.: Uber "begrenzte" derivationen und deren anwen-dung. Zeit. fur Mathematik und Physik **12**, 441–480 (1867)
34. Gutiérrez, C.E., Wheeden, R.L.: Harnack's inequality for degenerate parabolic equations. Comm. Partial Diff. Eqs. **16**(4–5), 745–770 (1991)
35. Gutiérrez, C.E., Wheeden, R.L.: Mean value and Harnack inequalities for degenerate parabolic equations. Colloq. Math. **60/61**(1):157–194 (1990)
36. Hörmander, L.: Hypoelliptic second order differential equations. Acta Math. **119**, 147–171 (1967)
37. Hunt, G.A.: Semi-groups of measures on Lie groups. TAMS **81**, 264–293 (1956)

38. Kassmann, M.: A new formulation of Harnack's inequality for nonlocal operators. C. R. Math. Acad. Sci. Paris **349**(11–12), 637–640 (2011)
39. Kilbas, A.A., Srivastava, H.M., Trujillo, J.J.: Theory and Applications of Fractional Differential Equations. North-Holland Mathematics Studies, vol. 204. Elsevier Science B.V, Amsterdam (2006)
40. Landkof, N.S.: Foundations of modern potential theory. Die Grundlehren der mathematischen Wissenschaften, Band 180. Springer, New York-Heidelberg (1972)
41. Letnikov, A.V.: Theory of differentiation with an arbitrary index. Mat. Sb. **3**, 1–66 (1868)
42. Lu, G.: Weighted Poincaré and Sobolev inequalities for vector fields satisfying Hörmander's condition and applications. Rev. Mat. Iberoamericana **8**, 367–439 (1992)
43. Mainardi, F.: Fractional Calculus and Waves in Linear Viscoelasticity. An introduction to mathematical models. Imperial College Press, London (2010)
44. Magnus, W., Oberhettinger, F., Soni, R.P.: Formulas and theorems for the special functions of mathematical physics. Third enlarged edition. Die Grundlehren der mathematischen Wissenschaften, Band 52 Springer-Verlag New York, Inc., New York (1966)
45. Marchaud, A.: Sur les dérivées et sur les différences des fonctions de variables réelles. Journ. Math. Pures Appl. **9**(6), 337–425 (1927)
46. Miller, K.S., Ross, B.: An Introduction to the Fractional Calculus and Fractional Differential Equations. A Wiley-Interscience Publication. John Wiley & Sons Inc, New York (1993)
47. Montgomery, R.: A tour of subriemannian geometries, their geodesics and applications. Mathematical Surveys and Monographs, 91. American Mathematical Society, Providence, RI, 2002
48. Riesz, M.: Intégrale de Riemann-Liouville et potentiels. Acta Litt. Sci. Univ., Szeged, Sect. Sci. math. 9, 1–42. Published (1938)
49. Saka, K.: Besov spaces and Sobolev spaces on a nilpotent Lie group. Tohoku Math. Journ. **31**, 383–437 (1979)
50. Samko, S.G.: Hypersingular Integrals and Their Applications. Analytical Methods and Special Functions, vol. 5. Taylor & Francis Ltd, London (2002)
51. Samko, S.G., Kilbas, A.A., Marichev, O.I.: Fractional integrals and derivatives. Theory and applications (1993)
52. Stinga, P.R., Torrea, J.L.: Extension problem and Harnack's inequality for some fractional operators. Comm. Partial Diff. Eqs. **35**(11), 2092–2122 (2010)
53. Tichonov, A.N., Samarskij, A.A.: Problemi della fisica matematica. Mir (1982)
54. Tralli, G.: Some Global Sobolev Inequalities Related to Kolmogorov-Type Operators, Bruno Pini Mathematical Seminar Analysis 11(1) 143–156, 2020. Special issue dedicated to the workshop: Something about nonlinear problems, Bologna, June 13, 14, 2019
55. Weyl, H.: Bemerkungen zum Begriff des Differentialquotienten gebrochener Ordnung. Zürich. Naturf. Ges. **62**, 296–302 (1917)
56. Watson, G.N.: A Treatise on the Theory of Bessel Functions. Cambridge University Press, Cambridge, England (1944)
57. Yosida, K.: Functional Analysis, 6th edn. Springer, Berlin, Germany (1980)

The Pearcey Equation: From the Salpeter Relativistic Equation to Quasiparticles

A. Lattanzi

Abstract This work presents the Pearcey equation, a quasi-relativistic wave equation for spinless particles with non-zero rest mass. This equation was introduced as a mathematical tool to address the problem of nonlocality concerning the pseudo-differential operator in the Hamiltonian of the Salpeter equation. The Pearcey equation can be considered as a *way* to relativity since it embeds the peculiar features of the relativistic evolution even if it looks very similar to the Schrödinger equation. In light of the catastrophe theory, the Pearcey equation acquires a deeper physical meaning as a candidate for describing quasiparticles.

Keywords Pearcey equation · Quasiparticles · Relativistic equation · Catastrophe theory

1 The Salpeter Equation: An Historical Review from Classical to Quantum Mechanics

At the end of the 19th century, physicists believed that Newton's laws of mechanics and Maxwell's electromagnetic theory provided the necessary foundations for the understanding of almost all physical phenomena. It was well known that Newton's laws explained the dynamics of matter from heavenly bodies down to falling apples while Maxwell's four equations correctly described the character of radiation not only by the unification of electrical and magnetic phenomena but also by laying the foundations of the study of light [1–4].

Distinguished examples of the effectiveness of the "classical" interpretative model based on Newton's laws and Maxwell's equations, were the discovery of the planet Neptune, made in 1846 by the astronomer Galle using the calculations of Leverrier,

A. Lattanzi (✉)
H. Niewodniczański Institute of Nuclear Physics, Polish Academy of Sciences, ul. Eljasza-Radzikowskiego 152, 31342 Kraków, Poland
e-mail: ambra.lattanzi@ifj.edu.pl; ambra.lattanzi@gmail.com

ENEA FSN-FUSPHYS-TSM, Via E. Fermi 45, 00044 Frascati, Rome, Italy

L. Beghin et al. (eds.), *Nonlocal and Fractional Operators*, SEMA SIMAI Springer Series 26, https://doi.org/10.1007/978-3-030-69236-0_10

and the discovery of electromagnetic waves by Hertz in 1886 supporting the theoretical predictions by Maxwell in 1873. These outstanding experimental confirmations led physicists to believe that they had reached the *end of physics*.

In the wake of this *optimism*, they began to erect Newton's laws and Maxwell's equations as pillars of Hercules in order to mark the confines of Physics. In fact, they thought that the few remaining unanswered questions could be solved in the well-understood framework of that time.

The words of Albert A. Michelson [5] could summarize the optimistic spirit of the physicists at the end of the XIX century:
"*The more important fundamental laws and facts of physical science have all been discovered, and these are now so firmly established that the possibility of their ever being supplanted in consequence of new discoveries is exceedingly remote*".

The revolution, which upset Physics at the beginning of the XX century, was carried by the theory of special relativity and by quantum wave mechanics.

In 1926, Schrödinger introduced a partial differential equation [6], the so-called free-Schrödinger equation, which describes the de Broglie's "matter waves" [7] inaugurating the quantum wave mechanics.

As Felix Bloch recollected, Erwin Schrödinger claimed with satisfaction: "*My colleague Debye suggested that one should have a wave equation; well I have found one!*" [8] whose expression in $(1 + 1)$ dimensions reads

$$i\hbar\partial_t \Psi(x,t) = -\frac{\hbar^2}{2m}\partial_x^2 \Psi(x,t). \tag{1}$$

In the above equation, the initial condition is denoted with $\Psi(x,0) = \Psi_0(x)$, $\hbar = \frac{h}{2\pi}$ is the reduced Planck constant and m is the (rest) mass of the particle.

The Schrödinger equation was very successful in describing the known energy levels of the hydrogen atom. It has been highly successful in describing the absorption or emission of radiation where an atom undergoes the transition from one energy state to another. The frequency of the emitted radiation follows the Bohr radiation condition $\hbar\nu = E_f - E_i$. But contrary to what Bohr did, Schrödinger did not have to impose quantization because this flowed naturally from the boundary conditions imposed on the solutions of his equation.

In general, the solution to the Schrödinger equation describes the dynamical behaviour of the particle in quantum mechanics, in a similar way as Newton's equation describes the dynamics of a particle in classical physics. However, there is an important difference: the wave function Ψ does not give the trajectory of a particle as Newton's law does. Therefore physicists asked themselves what type of information Ψ gives. The answer was given by Max Born: the square-modulus of Ψ gives the probability to find the particle in a region of space at a given time. The probabilistic statement replaces the deterministic statement of classical physics and from then on, our concept of physical reality has changed.

Einstein was among many who objected to this vision, suggesting that quantum theory was incomplete. He explained his point of view in a letter to P. S. Epstein: "*I incline to the opinion that the wave function does not (completely) describe what is real, but only a (to us) empirically accessible maximal knowledge regarding that which really exists [...]. That is what I mean when I advance the view that quantum mechanics gives an incomplete description of the real state of affairs...*" [9].

Einstein's opposition was overcome thanks to the great power of prediction that the established theory of quantum mechanics had shown in explaining experiments conducted during the last century.

These experimental confirmations pushed scientists to accept the principles and postulates of quantum mechanics, although the question of what there is beyond the experiments, remains an open question. Bohr offered consolation stating that: "*There is no quantum world. There is only an abstract quantum physical description. It is wrong to think that the task of physics is to find out how Nature is. Physics concerns what we can say about Nature*" [10].

In the attempt to unify special relativity and quantum wave mechanics the spinless Salpeter equation was introduced to generalize the Schrödinger equation in the context of relativistic quantum mechanics [11–13].

Without loss of generality, limiting ourselves to consider the initial value problem in (1+1) dimensions, the spinless Salpeter equation is

$$\begin{aligned} i\hbar\partial_t\ \psi(x,t) &= \sqrt{m^2c^4 - c^2\hbar^2\frac{\partial^2}{\partial x^2}}\ \psi(x,t), \\ \psi(x,0) &= \psi_0(x), \end{aligned} \tag{2}$$

where $\psi(x,0) = \psi_0(x)$ denotes the initial condition, c is the speed of light in vacuum and m the mass of the particle.

As shown in [14–19], the solution of the initial value problem of the spinless Salpeter equation in coordinate space is given by

$$\begin{aligned} \psi(x,t) &= \int_{-\infty}^{+\infty} S(x-x',t)\psi_0(x')dx' \\ &= \frac{mc^2t}{\pi\hbar}\int_{-\infty}^{+\infty} \frac{K_1\left(\frac{imc}{\hbar}\sqrt{c^2t^2-(x-x')^2}\right)}{\sqrt{c^2t^2-(x-x')^2}}\psi_0(x')dx', \end{aligned} \tag{3}$$

where K_1 is the modified Bessel function of the second kind of first order, also well known as McDonald function [20].

The spinless Salpeter equation (2) is different from the Klein-Gordon [21] equation, since it is a first-order in the time derivative, which would make it more similar to the Dirac equation [22]. The difference between the two is that the spinless Salpeter equation preserves the scalar nature of the wave function and it does not present

problems of probabilistic interpretation at quantum level: it only possesses positive energy solutions.
Moreover, the spinless Salpeter equation, differently from the Dirac equation, has a well-defined classical relativistic counterpart.

Although the Salpeter equation is a relativistic version of the Schrödinger equation, it has only recently stimulated the interest of the scientific community [14–19, 23–28]. This is definitely because of the mathematical complexity concerning its non local nature carried by the pseudo-differential Hamiltonian operator in (3).
However, the non locality does not disturb the light cone structure as it was analytically and numerically proven in [14–16] but makes it difficult to obtain rigorous analytical statements about the time-dependent and stationary solutions of the equation.
Another difficulty arises from the fact that the equation is not a covariant equation as it should be according to the special relativity principles.

However, it has been proven that the Hilbert space of its solutions is invariant under the Lorentz-group of transformations [29].
To conclude, the Salpeter equation makes it possible to have a quantum relativistic description which does not conflict with the principles of the special relativity, even if it is a non-local and non-covariant equation: it is widely used in the phenomenological description of the quark-antiquark-gluon systems as a hadron model [30, 31] and it is as good as the Klein-Gordon equation in describing the experimental spectrum of mesonic atoms [32].

From the analysis of the Salpeter equation, a new wave-like equation, the Pearcey equation has been introduced in [14–19] in order to probe the onset of the relativistic features. This equation was introduced as an alternative way to deal with the problem of nonlocality in relativistic quantum mechanics.

It allowed to test the correctness of the results obtained for the Salpeter equation in the analysis of its solutions and the Lie-point symmetries establishing a link between two theories: the classical quantum wave mechanics and the relativistic quantum wave mechanics.

The aim of this work is to present the Pearcey equation in the context of quasi-relativistic physics. The parallelism with optics and with the catastrophe theory gives a deeper physical meaning to the Pearcey equation and its solutions. In particular, the Pearcey equation can be a candidate to describe quasiparticles.

The rest of the paper is organized as follows. Section 1 introduces the Pearcey equation, a new partial evolution equation first order in time.
Section 3 analyzes the behaviour of a Lorentzian wave-packet in order to add another example of evolution ruled by the Pearcey equation with respect to the ones presented in the previous papers on the subject [14–19]. Section 4 is devoted to the role of catastrophe theory in the light-cone structure of the solution of the Pearcey equation and of the Salpeter equation.

2 The Pearcey Equation

In the Introduction, we emphasized the important role played by the Schrödinger equation in non-relativistic quantum mechanics [1–3] and the corresponding remarkable role played by the Salpeter equation as a counterpart of the Schrödinger equation within the framework of the relativistic quantum mechanics.
Since the specific features of the solutions of the Schrödinger equation are definitely different from those of the Salpeter equation, as emerged from the numerical and asymptotic analysis developed in [14–16], it is within reason to ponder about the existence of a third theory that could bridge the two approaches, emerging as an asymptotic limit between the classical and the relativistic quantum mechanics.
This third possibility can be named quasi-relativistic.

In order to define the dynamic evolution of a quasi-relativistic quantum system, the first step to consider is the series expansion of the relativistic energy-momentum relation for a freely moving particle

$$E = \sqrt{m^2c^4 + p^2c^2}, \tag{4}$$

where m and p denote respectively the rest mass and the momentum of the particle and c is the speed of light in vacuo.

The first correction of the Schrödinger equation is given by stopping the series expansion of (4) with respect to $\frac{p}{mc}$ at the fourth order, namely

$$E = mc^2\Big[1 + \frac{1}{2}\Big(\frac{p}{mc}\Big)^2 - \frac{1}{8}\Big(\frac{p}{mc}\Big)^4\Big]. \tag{5}$$

By the standard quantization rules

$$E \to i\hbar\frac{\partial}{\partial t} \qquad\qquad x \to x \qquad\qquad p \to -i\hbar\frac{\partial}{\partial x}$$

consistent with the Newton-Wigner localization scheme, we get the (1+1)D Pearcey equation

$$i\hbar\frac{\partial\tilde{\psi}(p,t)}{\partial t} = mc^2\Big[1 + \frac{1}{2}\Big(\frac{p}{mc}\Big)^2 - \frac{1}{8}\Big(\frac{p}{mc}\Big)^4\Big]\tilde{\psi}(p,t), \tag{6}$$

which in coordinate representation reads

$$i\hbar\frac{\partial\psi(x,t)}{\partial t} = mc^2\Big[1 - \frac{\hbar^2}{2m^2c^2}\frac{\partial^2}{\partial x^2} - \frac{\hbar^4}{8m^4c^4}\frac{\partial^4}{\partial x^4}\Big]\psi(x,t). \tag{7}$$

The Pearcey equation (7) is an evolution equation in time and thus, it requires the knowledge of the initial condition $\psi(x,0) = \psi_0(x)$ to fix the dynamics of the system.

In order to define the solution of the Pearcey equation (7), we resort to one of the most applied techniques: the Fourier transform method.

Following the Fourier-transformed procedure, the general solution of (7) is

$$\psi(x,t) = \frac{e^{-\frac{it}{\hbar}mc^2}}{\sqrt{2\pi\hbar}} \int_{-\infty}^{+\infty} e^{\frac{i}{\hbar}mc^2\left(\frac{t}{8}p^4 - \frac{t}{2}p^2 + p\cdot x\right)} \tilde{\psi}_0(p)dp. \tag{8}$$

To simplify the analysis of the equation and to facilitate the parallelism between optics and quantum mechanics, we introduce the dimensionless variables ξ and τ, expressed in term of the reduced Compton wavelength λ_C:

$$\xi = \frac{x}{\lambda_C}, \quad \tau = \frac{ct}{\lambda_C}, \quad \kappa = \frac{p}{mc} \tag{9}$$

so that (6) becomes:

$$i\frac{\partial\tilde{\psi}(\kappa,\tau)}{\partial\tau} = \left[1 + \frac{1}{2}\kappa^2 - \frac{1}{8}\kappa^4\right]\tilde{\psi}(\kappa,\tau). \tag{10}$$

Fixing the initial condition equals to a Dirac delta function, $\psi_0(\xi) = \delta(\xi)$, the above equation yields the response of the system to an impulse, i.e.

$$S(\xi,\tau) = \frac{e^{-i\tau}}{2\pi} \int_{-\infty}^{+\infty} e^{i\left(\frac{\tau}{8}\kappa^4 - \frac{\tau}{2}\kappa^2 + \kappa\cdot\xi\right)} d\kappa. \tag{11}$$

$S(\xi,\tau)$ represents the fundamental solution of (10), and hence also the kernel of the transformation which encodes also the reason behind the choice of the name: Pearcey equation. The integral $S(\xi,\tau)$ is known in optics and in particular in catastrophe theory as the Pearcey function (see Sect. 4 and reference therein for further details). The Pearcey function is defined in [33–35] by

$$P(x,y) = \int_{-\infty}^{+\infty} e^{i(s^4 + xs^2 + ys)} ds, \tag{12}$$

where x, y may be in general complex numbers and s is the integration variable.

The analogy can be clearly appreciated by making a comparison between the contourplots of the Pearcey function in Fig. 1a and the fundamental solution of the Pearcey equation in Fig. 1b where the peculiar caustic-like structure conveyed by "isolated spots" can be still recognized.
The "isolated spots" in Fig. 1 seem to resemble the uniformly distributed *granularity*, which is also present in the contourplot of the fundamental solution of the Salpeter equation [14, 15], the distinctive pattern of the relativistic behaviour.
The symmetric distribution of the spots positioned at the intersections of the parallels to the edges of the light cone is due to the homogeneity of the spacetime and, when the first and the second order coupling interactions are involved [15], it is resembling

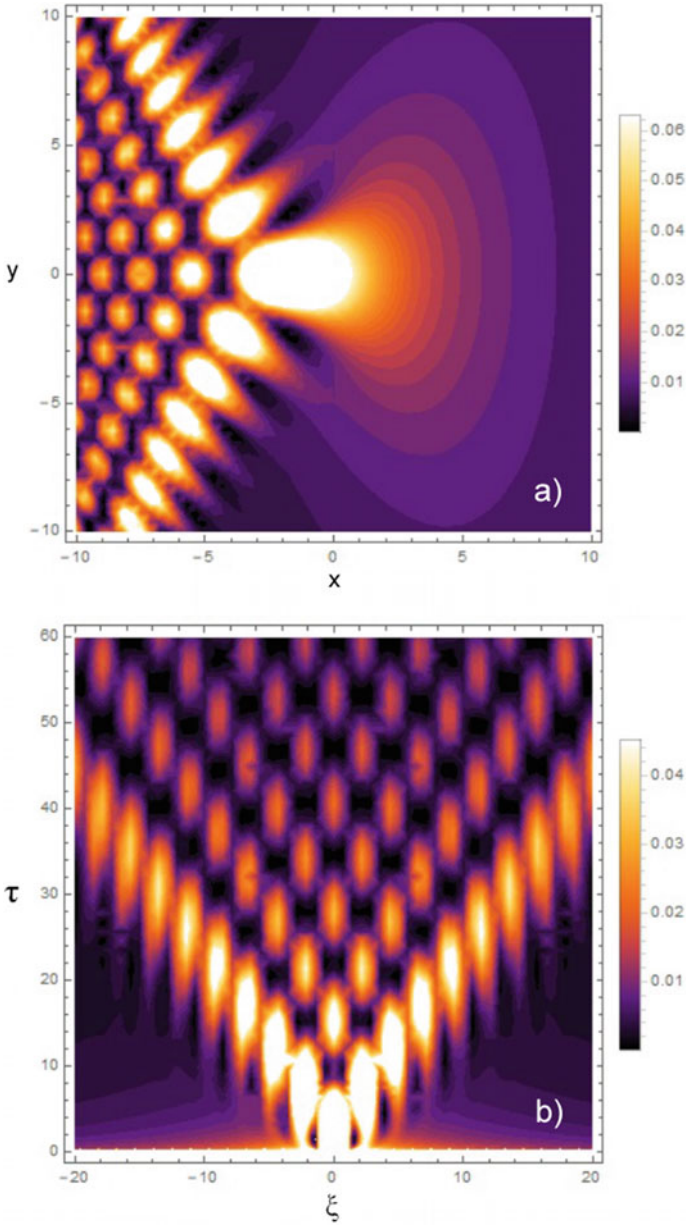

Fig. 1 A comparison between the (ξ, τ)-contourplots of the squared modulus of the Pearcey function $|P(\xi, \tau)|^2$ (**a**) and the squared modulus of the fundamental solution of the Pearcey equation $|\psi(\xi, \tau)|^2$ (**b**)

the discrete-like diffraction patterns arising from the impulse response (i.e. single state excitation) in periodic photonic lattices.

3 Evolution of the Lorentzian Wave Packet

The wave function arising from an initial Lorentzian function manifests an interesting behavior from the optical point of view, i.e. the Lorentz beams [36].
The Lorentz beam, based on experimental observations, is suitable to model the radiation emitted by single-mode diode laser [37–39].

So, as a further example in the collection of results presented for the Pearcey equation in [14–18], we can consider as initial wave function a Lorentzian defined as

$$\psi_0^L(\xi) = \frac{1}{\pi}\frac{w}{(\xi^2 + w^2)}, \qquad w > 0, \tag{13}$$

and normalized such that $\lim_{\xi\to 0}\psi_0^L(\xi) = \delta(\xi)$.
The evolution of the Lorentzian initial input (13) ruled by the Peaecey equation reads

$$\psi^L(\xi,\tau) = \frac{1}{2\pi}\int_{-\infty}^{+\infty} e^{\frac{i\tau}{8}\kappa^4 - i\frac{\tau}{2}\kappa^2 + i\kappa\xi} e^{-w|\kappa|} d\kappa = \\ = \frac{1}{2\pi}\left\{\int_0^{+\infty} e^{i\frac{\tau}{8}\kappa^4 - i\frac{\tau}{2}\kappa^2 + i\kappa(\xi+iw)} d\kappa + \int_0^{+\infty} e^{i\frac{\tau}{8}\kappa^4 - i\frac{\tau}{2}\kappa^2 - i\kappa(\xi-iw)} d\kappa\right\}.$$

Here, the parameter w determines the "height" of the curve, being $\psi_0^L(0) = \frac{1}{w\pi}$, the width at the half maximum is $\psi_0^L(\pm w) = \frac{1}{2\pi w} = \frac{1}{2}\psi_0^L(0)$, and the variances of the function in both the spaces are $\sigma_\xi^2 = w^2$ and $\sigma_\kappa^2 = \frac{1}{2w^2}$, yielding $\sigma_\xi\sigma_\kappa = \frac{1}{\sqrt{2}}$.
Just like $\psi^L(\xi,\tau)$, the integrals entering the above expression can be put in relation with the Pearcey function but with the integral extending from 0 to ∞, i.e. with what is reported in the literature as the half-Pearcey function $P_{\frac{1}{2}}(x, y)$ [40, 41].
The (ξ,τ)-contour plots of the squared modulus of ψ^L are shown in the Fig. 2 for some value of w which rules the width of the Lorentzian.

As for the Gaussian initial input, the isolated spots of the fundamental function, roughly comprised within a V-like contour, dominates the evolution for small w-values.
The wave function behaves much like the fundamental solution $S(\xi,\tau)$. With increasing w, as it is evident from Fig. 2d, the spots tend to be "absorbed" in a more compact structure, as observed in Fig. 3 for the Lorentzian input under the Salpeter evolution. As w further increases, the solutions displays a hybrid relativistic-non relativistic behaviour.

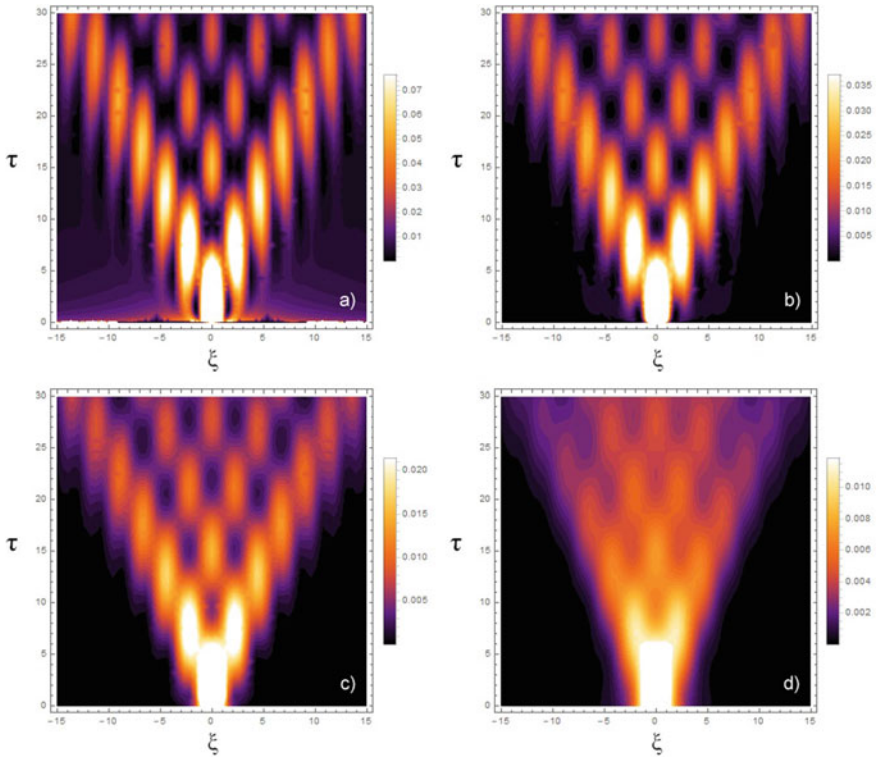

Fig. 2 (ξ, τ)-contourplot of the squared modulus of the Pearcey function $|\psi^L(\xi, \tau)|^2$ for a Lorentzian initial input with $w = 0.01$, $w = 0.5$, $w = 1$ and $w = 2$ in **a**, **b**, **c** and **d** respectively

4 Quantum Caustics and Light-Cone Structure: The Onset of Granularity in the Nature of the Light-Cone Structure

The catastrophe theory is a framework originated by the French mathematician René Thom in the 1960s [42]; it deals with the modeling of the so-called *catastrophes* which are discontinuous transitions and even sudden changes caused by smooth variations of the control parameters (or variables) involved in the system. Among all the catastrophes, there are seven types called *elementary* since they have a dependency only on a few parameters.

This classification shows a hierarchical structure where the elementary catastrophes of higher order contain the lower order ones. The lowest catastrophe is called fold and it occurs when, given one control parameter and a single state variable, the gradient of the mapping vanishes. The next higher order catastrophe is the cusp and it is originated exactly in the point where two fold lines meet [43]. Other higher order catastrophes can be generated in the same hierarchical way: the intersection of two cusp lines results in a swallowtail, and so on.

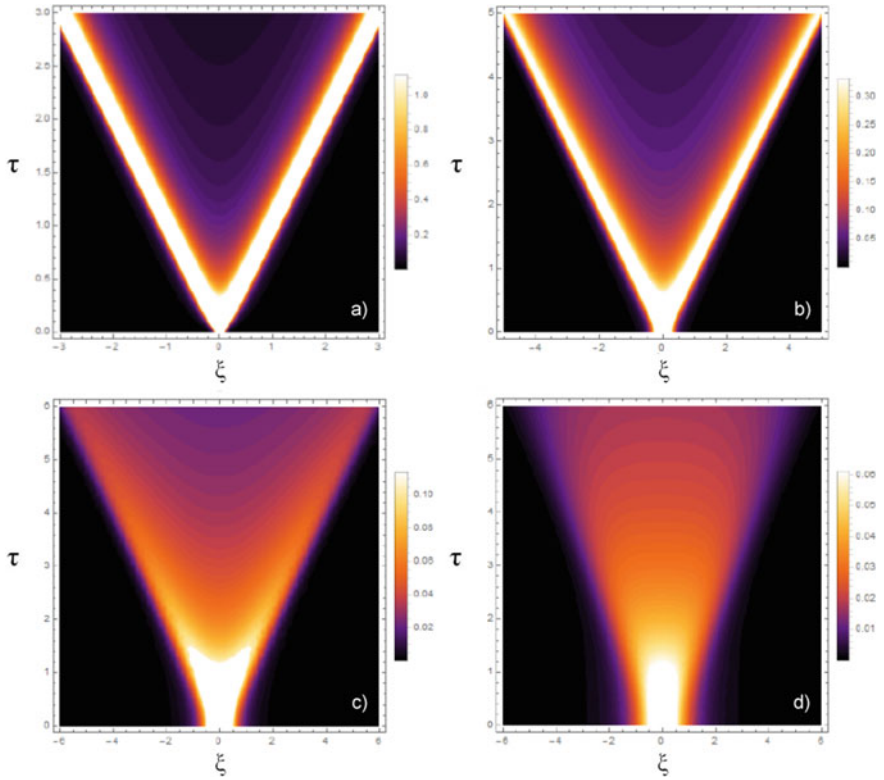

Fig. 3 (ξ, τ)-contourplot of the squared modulus of the fundamental solution of the Salpeter equation $|\psi^{L}_{Salpeter}(\xi, \tau)|^2$ for a Lorentzian initial input with $w = 0.01$, $w = 0.5$, $w = 1$ and $w = 2$ in **a**, **b**, **c** and **d** respectively

Table 1 collects the descriptions and formulas of all the seven elementary catastrophes as listed in [42].

In catastrophe theory, the wave function ϕ, also known as diffraction integral or caustic beam, is an essential tool in the description of a variety of diffraction phenomena. These seven catastrophes share the same general formula for their diffraction integrals

$$\phi(\mathbf{v}) = \int_{-\infty}^{+\infty} e^{i F(\mathbf{s},\mathbf{v})} d\mathbf{s}, \tag{14}$$

where the function F is one of the generating functions listed in Table 1 depending on the state variable vector $\mathbf{s} = (s, t)$ and on the vector $\mathbf{v} = (x, y, z, w)$ whose components are the control parameters. Each generating function defines a specific diffraction integral.

Replacing the cusp generating function (see Table 1) in (14), we get the Pearcey function (12) as defined in Sect. 2, displayed below for the reader's convenience:

Table 1 Classification of the Seven Elementary Catastrophes. The co-rank is the number of the state variables involved: s and t, whereas the control variables x, y, z and w are independent parameters that influence the state of the system. The codimension is a measure of the function's degeneracy removed by the generating functions. The generating function gives the universal unfolding of the corresponding singularity

Catastrophe	Co-rank	Control variables	Codimension	Potential functions
Fold	1	1	1	$s^3 + xs$
Cusp	1	2	2	$s^4 + xs^2 + ys$
Swallowtail	1	3	3	$s^5 + xs^3 + ys^2 + zs$
Butterfly	1	4	4	$s^6 + xs^4 + ys^3 + zs^2 + ws$
Hyperbolic umbilic	2	3	3	$s^3 + t^3 + xst + ys + zt$
Elliptic umbilic	2	3	3	$s^3 - st^2 + x(s^2 + t^2) + ys + zt$
Parabolic umbilic	2	4	4	$s^2t + t^4 + xs^2 + yt^2 + zs + wt$

$$P(x, y) = \int_{-\infty}^{+\infty} e^{i(s^4 + xs^2 + ys)} ds. \tag{15}$$

Considering the similarity between Fig. 1a, b, there should be also a mathematical correspondence between the Pearcey function and the fundamental solution of the Pearcey equation. This correspondence can be unveiled by changing the variable in the fundamental solution of the Pearcey equation (11) according to the following formula

$$\kappa = s\left(\frac{8}{\tau}\right)^{\frac{1}{4}}. \tag{16}$$

After changing the variable (16), the fundamental solution of the Pearcey equation can be written in terms of the Pearcey function:

$$\begin{aligned} S(\xi, \tau) &= \frac{1}{\pi(2\tau)^{\frac{1}{4}}} \int_{-\infty}^{+\infty} e^{i\left[s^4 - \sqrt{2\tau}s^2 + \left(\frac{8}{\tau}\right)^{\frac{1}{4}} \xi s\right]} ds \\ &= \frac{e^{-i\tau}}{\pi(2\tau)^{\frac{1}{4}}} P\big(-\sqrt{2\tau}, (\frac{8}{\tau})^{\frac{1}{4}}\xi\big), \end{aligned} \tag{17}$$

allowing to interpret the fundamental solution as a *caustic*-like beam.
Equation (17) extends the analogy between optics and classical mechanics which characterizes the solutions of the Schrödinger equation and the paraxial wave equa-

tion to a quasi-relativistic framework [18].
The term *quasi-relativistic* denotes what happens in the gray region between the classical and the relativistic quantum theories. It is an appropriate definition since the solutions of the Pearcey equation recall the relativistic ones ruled by the Salpeter, although the former contains only one more term compared to the Schrödinger equation, that is the first relativistic correction to the kinetic energy.
Among all the peculiar features, the most relevant one is the presence of a light-cone structure. The more terms are considered in the series expansion of the relativistic energy-momentum relation (4), the more the kernel of the corresponding evolution equation tends to the Salpeter one and consequently the corresponding light-cone structure starts to visibly emerge.
Adding more terms in the Hamiltonian of the Pearcey function—namely, considering higher orders of the series expansion of the Salpeter Hamiltonian—other equations can be introduced in quasi-relativistic physics as for example the butterfly equation whose partial differential equation in the momentum space reads

$$i\hbar\frac{\partial\tilde{\psi}(p,t)}{\partial t} = mc^2\Big[1+\frac{1}{2}\Big(\frac{p}{mc}\Big)^2-\frac{1}{8}\Big(\frac{p}{mc}\Big)^4+\frac{1}{16}\Big(\frac{p}{mc}\Big)^6\Big]\tilde{\psi}(p,t), \tag{18}$$

and in coordinate representation is

$$i\hbar\frac{\partial\psi(x,t)}{\partial t} = mc^2\Big[1-\frac{\hbar^2}{2m^2c^2}\frac{\partial^2}{\partial x^2}-\frac{\hbar^4}{8m^4c^4}\frac{\partial^4}{\partial x^4}-\frac{\hbar^6}{16m^6c^6}\frac{\partial^6}{\partial x^6}\Big]\psi(x,t). \tag{19}$$

This process for building up quasi-relativistic wave equations, based on the series expansion of the square root operator in the Hamiltonian of the Salpeter equation, allows to probe the relativistic onset in the solutions, overcoming the difficulties related to the presence of the square root. The Hamiltonians in the evolution equations generated by the series expansion seem to show a hierarchical structure quite similar to the one illustrated for the diffraction generating functions in the catastrophe theory [44].

Each higher order Hamiltonian embeds the previous smaller order one as it can be easily deduced comparing the Pearcey equation (7) with the butterfly equation (19). This hierarchical organization can be extended asymptotically until it naturally reaches the fundamental solution of the Salpeter equation which can be interpreted as the highest order diffraction integral function or caustic beam embedding the entire hierarchy of the light-cones structures, that can now be considered as caustics. This mathematical consideration has a relevant physical consequence: the Pearcey equation can be a candidate to describe quasiparticles.

Quasiparticle is a key concept that provides an intuitive understanding of complex phenomena in many-body physics [45]: it is a collective state of many particles, an elementary excitation or even a bound state of a pair of particles that has an energy-momentum relationship like a particle. An example borrowed from superconductors is the Cooper pair [46]. In a Cooper pair, the electrons can form a bound state with

opposite momenta and opposite spin. So, they can be defined in terms of a standard s-wave or a spin-0 object.

To support this idea, the light-cone structure should be related to an intrinsic velocity limit. The observed light-cone hides the presence of such a limit on the velocity of the particles and for this the Pearcey equation is a candidate for describing particles in quasi-relativistic framework. It is important to verify the caustic nature of the light-cone since this condition is a key notion for introducing the limit on the velocity for the particles.

Previously, it has been shown that the fundamental solution of the Pearcey equation is a caustic beam and all the probability density can be embedded by a couple of caustics forming a first attempt of a light-cone. In order to have further confirmations, let us consider the result shown in [44, 47] where the caustic nature of the light-cone can be mathematically appreciated considering the following couple of equations

$$\begin{aligned} \frac{dF}{ds} &= 0 \\ \frac{d^2F}{ds^2} &= 0, \end{aligned} \tag{20}$$

defining the necessary condition to have caustics as the edges of the light-cone.

In [44], the conditions (20) can be replaced by the so-called Lieb-Robinson (LR) maximal group velocity. The LR velocity [48] is a theoretical upper limit on the speed at which information can propagate: information cannot travel instantaneously in quantum theory, even when the relativity limits of the speed of light do not play a central role.

This velocity is finally associated with quasiparticles that were previously excited by a quench and then freely propagated in the sample [44, 49]:

$$v_{LR} = \max_k \left| \frac{d\epsilon_k}{dk} \right|, \tag{21}$$

where ϵ_k is the dispersion relation for a quasiparticle in function of the quasimomentum k.

This result confirms that the Pearcey equation can bridge the Schrödinger equation and the relativistic spinless Salpeter equation, since it shows the rising of the light-cone structure and therefore it unveils the intrinsic velocity limit. In this scenario, the connection between optics and quantum mechanics, remarked by the formal analogy between the Schrödinger equation and the paraxial wave equation, is strengthened and it is extended to the quasi-relativistic physics.

Another interesting feature emerged in the analysis of the fundamental solution of the Pearcey equation (but also in the Salpeter equation) is the granularity of the edges in the light-cone structure which is still present whereas the spot-like pattern in the central part of the light-cone tends to disappear when higher order terms in the Hamiltonian are considered.

This nests the idea that spots along the edges have a different origin from the spots inside the light-cone in the fundamental solution of the Pearcey equation. The strategy consists into focusing our attention not on the "colored" spots, i.e. where the probability to find the particle or the intensity is greater, but on the darkest regions in Fig. 1, which are usually called vortices in the optical catastrophe theory [44].

An optical vortex corresponds to a zero in the optical field, so it explains why it can be found in the darkest region between the spots in the contourplot of Fig. 1. The appearance of these vortices in the fundamental solution of the Pearcey equation can be explained considering the relation with the Pearcey caustic beam, whose complex nature is at the origin of the vortices.

As observed in [44], it is possible to distinguish the darkest regions or vortices in two "groups" forming a fine structure in the diffraction integrals. The reason behind the vortices classification is their positions in the light-cone structure. In fact there is a network of vortex-antivortex pair inside it and single rows of vortices lining the outer edges.

The procedure to find these vortices in a continuum approach, consists in covering the plane with loops around which we integrate the phase of the Pearcey function. This interpretation is intriguing and it perfectly matches the result obtained in [14–19] concerning the fundamental solution of the Pearcey and the Salpeter equations. The singularity on the edges of the light-cone structure shows a discontinuity by $e^{i\pi}$ which generates the peculiar granularity in the relativistic behaviour.

In conclusion, the Pearcey equation, introduced from the series expansion of the Hamiltonian in the spinless Salpeter equation, seems to be a perfect candidate for describing spinless quasiparticles in the quasi-relativistic framework.

Acknowledgements A.L. was supported by the Polish National Agency for Academic Exchange NAWA project: Program im. Iwanowskiej PPN/IWA/2018/1/00098 and supported by the NCN research project OPUS 12 no. UMO-2016/23/B/ST3/01714. I would like to thank the anonymous referee for giving valuable suggestions and constructive comments.

References

1. Purrington, R.D.: Physics in the Nineteenth century, NJ. Rutgers University Press, New Brunswick (1997)
2. Messiah, A.: Quantum Mechanics, vol. II. Dover Publications Inc, New York (2014)
3. Sakurai, J.J., Napolitano, J.J.: Modern Quantum Mechanics, 2nd ed. Addison-Wesley, San Francisco, (2010)
4. Feyman, R.P., Bleighton, R., Sands, M.: The Feyman lectures of Physics - Vol. III: Quantum Mechanics, first ed. Addison-Wesley, Massachusetts (1965)
5. Michelson, A.A.: Light Waves and Their Uses. University of Chicago, 1903, pp. 23–24
6. Schrödinger, E.: An undulatory theory of the mechanics of atoms and molecules. Phys. Rev. **28**(6), 10491070 (1926)
7. De Broglie, L.: Recherches sur la théorie des quanta (Researches on the quantum theory), Thesis, Paris, 1924, Ann. de Physique (10) **3**, 22 (1925)
8. Bloch, F.: Phys. Today **29**(12), 23–24 (1976)
9. A. Einstein, Letter to P. S. Epstein, 10 November 1945, extract from D. Howard [1990] p. 103

10. Petersen, A.: The philosophy of Niels Bohr. Bulletin of the Atomic Scientists **19**, 7 (1963)
11. Salpeter, E.E., Bethe, H.A.: A relativistic equation for bound-state problems. Phys. Rev. **84**, 1232–1242 (1951)
12. Salpeter, E.E.: Mass corrections to the fine structure of hydrogen-like atoms. Phys. Rev. **87**, 328–343 (1952)
13. Greiner, W., Reinhardt, J.: Quant. Electrodyn. Springer-Verlag, Berlin (1994)
14. Lattanzi, A.: Thesis, University of Rome Three (I), 2016
15. Torre, A., Lattanzi, A., Levi, D.: Time-Dependent Free-Particle Salpeter Equation: Numerical and Asymptotic Analysis in the Light of the Fundamental Solution. Annalen der Physik (2017)
16. A. Torre, A. Lattanzi and D. Levi, Time-Dependent Free-Particle Salpeter Equation: Features of the Solutions, in: Dobrev V. (eds) Quantum Theory and Symmetries with Lie Theory and Its Applications in Physics Volume 2. LT-XII/QTS-X: Springer Proceedings in Mathematics & Statistics, vol. 255. Springer, Singapore (2017)
17. Lattanzi, A., Levi, D., Torre, A.: The missing piece: a new relativistic wave equation, the Pearcey equation. Journal of Physics: Conference Series. Vol. 1194. No. 1. IOP Publishing, (2019)
18. Lattanzi, A., Levi, D., Torre, A.: Evolution Equations in a Nutshell, Proceeding of the conference organized by Society of Physicist of Macedonia and Institute of Physics PMF Ss. Cyril and Methodius University Skopje, Macedonia. Published in Conference Proceedings CSPM 2018 (2019)
19. Lattanzi, A.: How to deal with nonlocality and pseudodifferential operators. An example: the Salpeter equation, Accepted to be published in the proceeding of Quantum Theory and Symmetry-XI Conference in Montréal edited by Springer (2020)
20. Gradshteyn, I.S., Ryzhik, I.M.: Table of Integrals, Series, and Products, Zwillinger, D., Moll, V. (Eds.), Eighth Edition. Academic Press (2014)
21. Klein, O.: Quantentheorie und fünfdimensionale Relativitätstheorie. Zeitschrift für Physik **37**, 895–906 (1926)
22. Dirac, P.A.M.: The quantum theory of the electron. Proc. R. Soc. Lond. A **117**, 610–624 (1928)
23. Frederico, T., Pace, E., Pasquini, B., Salmè, G.: Generalized parton distributions of the pion in a covariant Bethe-Salpeter model and light-front models. Nucl. Phys. Proc. Suppl. **199**, 264–269 (2010)
24. Frederico, T., Salmè, G.: Projecting the Bethe-Salpeter equation onto the light-front and back: A short review. Few Body Syst. **49**, 163–175 (2011)
25. Frederico, T., Salmè, G., Viviani, M.: Quantitative studies of the homogeneous Bethe-Salpeter equation in Minkowski space. Phys. Rev. D **89**, 016010 (2014)
26. Salmè, G., Frederico, T., Viviani, M.: Quantitative studies of the homogeneous Bethe-Salpeter equation in Minkowski space. Few Body Syst. **55**, 693–696 (2014)
27. Kowalski, K., Rembieliński, J.: The Salpeter equation and probability current in the relativistic Hamiltonian quantum mechanics. Phys. Rev. A **84**, 012108 (2011)
28. Dattoli, G., Sabia, E., Górska, K., Horzela, A., Penson, K.A.: Relativistic wave equations: An operational approach. J. Phys. A: Math. Theor. **48**, 125203 (2015)
29. Foldy, L.L.: Synthesis of covariant particle equations. Phys. Rev. **102**, 568–581 (1956)
30. Nickisch, L.J., Durand, L.J., Durand, B.: Salpeter equation in position space: numerical solutions for arbitrary confining potentials, Phys. Rev. D **30**, 660-70 (1984) Erratum Phys. Rev. **30** (3), (1984)
31. Basdevant, J.L., Boukraa, S.: Success and difficulties of unified quark-antiquark potential models, Z. Phys. C - Part. & Fields **28**, 413–426 (1985)
32. Friar, J.L., Tomusiak, E.L.: Relativstically corrected Schrödinger equation with Coulomb interaction. Phys. Rev. C **29**, 1537–1539 (1984)
33. Pearcey, T.: The structure of an electromagnetic field in the neighborhood of a cusp of a caustic. Phil. Mag. S. **737**, 311317 (1946)
34. Poston, T., Stewart, I.: Catastrophe Theory and its Applications. Dover Publications Inc. (1997)
35. Berry, M.V., Upstill, C.: Catastrophe optics: morphologies of caustics and their diffraction patterns. Prog. Opt. **18**, 257346 (1980)

36. El Gawhary, O., Severini, S.: Lorentz beams and symmetries properties in paraxial optics. J. Opt. A: Pure Appl. Opt. **8**, 409–414 (2006)
37. Dumke, W.P.: The angular beam divergence in double-heterojunctiojn lasers with very thin active regions. IEEE J. Quant. Electron. **11**, 400–402 (1975)
38. Naqwi, A., Durst, F.: Focus of diode laser beams: A simple mathematical model. Appl. Opt. **29**, 17801785 (1990)
39. Yang, J., Chen, T., Ding, G., Yuan, X.: Focusing of diode laser beams: a partially coherent Lorentz model. Proc. SPIE **6824**, 68240A (2008)
40. Borghi, R.: On the numerical evaluation of cuspoid diffraction catastrophes. J. Opt. Soc. Am. **25**, 1682–1690 (2008)
41. Kovalev, A.A., Kotlyar, V.V., Zaskanov, S.G., Porfirev, A.P.: Half Pearcey Laser beams. J. Opt. **17**, 035604 (2015)
42. Thom, R.: Structural Stability and Morphogenesis. Benjamin, Reading MA (1975)
43. Kravtsov, Y.A., Orlov, Y.I.: Caustics, catastrophes, and wave fields. Soviet Physics Uspekhi **26**(12), 1038 (1983)
44. Kirkby, W., Mumford, J., O'Dell, D.H.J.: Quantum caustics and the hierarchy of light cones in quenched spin chains. Physical Review Research **1**(3), 033135 (2019)
45. Jurcevic, P., Lanyon, B.P., Hauke, P., Hempel, C., Zoller, P., Blatt, R., Roos, C.F.: Quasiparticle engineering and entanglement propagation in a quantum many-body system, Nature (London) 511, 202 (2014)
46. Tinkham, M.: Introduction to Superconductivity. Courier Corporation (2004)
47. Berry, M.V.: Singularities in waves and rays. Physics of Defects **35**, 453–543 (1981)
48. Lieb, E.H., Robinson, D.W.: The finite group velocity of quantum spin systems. Commun. Math. Phys. **28**, 251 (1972)
49. Calabrese, P., Cardy, J.: Time dependence of correlation functions following a quantum quench. Phys. Rev. Lett. **96**(13), 136801 (2006)

Recent Developments on Fractional Point Processes

Aditya Maheshwari and Reetendra Singh

Abstract In the last two decades, the theoretical advancement of the point processes witnessed an important and deep interconnection with the fractional calculus. It was also found that the stable subordinator plays a vital role in this connection. The survey intends to present recent results on the fractional versions of point processes. We will also discuss generalization attempted by several authors in this direction. Finally, we present some plots and simulations of the well-known fractional Poisson process of Laskin (2003).

Keywords Poisson process · Levy subordinator · Fractional point processes

1 Introduction

The classical integer-ordered calculus is the most famous tool to model physical phenomena since last 400 years. Their applications, meaning, usefulness and simplicity led to its widespread acceptability in the scientific and the technological domains. Although the fractional order calculus, which have equally old origins, does not find a place for acceptability of the scientific community at large. It is only from the last four decades, the ideas of fractional calculus started to get some attention of researchers. The usefulness and applications of the fractional calculus in the science and technology are now started to gain attention. Sun et al. [70] presented an excellent modern review of applications for the fractional calculus in science and engineering. It provides a case for interested audience to 'try out' models based on non-integer ordered calculus.

The fractional calculus has also found its way in connection to stochastic processes. The stochastic models like fractional Brownian motion and anomalous dif-

A. Maheshwari (✉) · R. Singh
Operations Management and Quantitative Techniques Area, Indian Institute of Management Indore, Indore 453556, India
e-mail: adityam@iimidr.ac.in

R. Singh
e-mail: reetendras@iimidr.ac.in

L. Beghin et al. (eds.), *Nonlocal and Fractional Operators*, SEMA SIMAI Springer Series 26, https://doi.org/10.1007/978-3-030-69236-0_11

fusions are some important examples for the same. In this review, we will explore the interconnection of fractional calculus and point processes. The interlinking of the fractional calculus and the Poisson process was first established by Laskin [44]. Later on, a rich development in this field has taken place. We first try to collect a (non-exhaustive) list of the advantages of fractional-ordered calculus based stochastic models.

(a) **Power-law decay**: The classical stochastic models are based on exponential decay of density functions, however in applications (see [31, 32, 64, 66]) power law based distribution are useful.
(b) **Long memory**: The observations in nature, for example errors in astronomical observations, water level of rivers, yearly tree ring measurements (see [12]), exhibits dependence over long time scale. The popular assumption of independence may not be the best way to study the dependence or memory in some cases. The fractional calculus based stochastic process helps in modelling phenomenon with long memory (see [29, 76]).
(c) **Heavy-tailed distributions**: The standard diffusion models are light-tailed distribution while some application are more suited for heavy-tailed distributions (see [13, 43, 45]). The fractional stochastic models allow us to study heavy tailed distributions.
(d) **Fractional-order controls**: The classical models do not have flexibility to adjust the order of differentiation or integration while fractional-order derivatives or integrals allow great flexibility to adjust the model to tune it with the data (see [23, 40, 53, 54]).
(e) **Self-similarity**: It is known that the fractional Brownian motion has the self similar property. This property is widely applied for studying fractals and have a connection with fractional calculus and special functions. The real-life applications self similarity are found in studying the properties of signal transmission (see [59, 60]).

With these advantages and applications in real-life, the study of fractional calculus inspired stochastic processes becomes an interesting exercise for both theoretical and applied researchers. Last two decades witnessed considerable advancement in theoretical research about fractional point processes. We here survey some important result chalking out the journey of evolution of the fractional stochastic processes. The article aims to provide a big picture of the field and authors tried to discuss the developments to the best of their knowledge.

In this review, we will survey results about the fractional point processes. In Sect. 2, we provide introduction to the fractional Poisson processes. In Sect. 3, we collect the results which interconnect the fractional derivatives with the Lévy processes. Section 4 contains some more results about fractional point processes. In Sect. 5, we provide plots and sample paths of the fractional Poisson process.

2 Fractional Poisson Process

In this section, we focus our attention to the relation between the fractional calculus and the Poisson process. The fractional Poisson process (FPP) was first introduced and studied by Laskin [44], he defined it by generalizing the governing difference-differential equation of the Poisson process. We summarize his approach below.

Define $\{N(t)\}_{t\geq 0}$ to be the Poisson process with rate parameter $\lambda > 0$. It is known that the probability mass function (*pmf*) $p(n,t) = \mathbb{P}[N(t) = n]$ of the Poisson process solves the following difference-differential equation

$$\frac{d}{dt}p(n,t) = -\lambda\left[p(n,t) - p(n-1,t)\right],$$

with $p(n,0) = 1$ if $n = 0$ and is zero if $n \geq 1$. Laskin [44] proposed a fractional generalization of Poisson process by replacing the derivative on the left-hand side with the fractional derivative and called it as the fractional Poisson process, denoted by $\{N_\beta(t)\}_{t\geq 0}$. Its *pmf*

$$p_\beta(n,t) = \mathbb{P}[N_\beta(t) = n]$$

happens to solve the following difference-differential equation

$$\mathcal{D}_t^\beta p_\beta(n,t) = -\lambda\left[p_\beta(n,t) - p_\beta(n-1,t)\right], 0 < \beta \leq 1,$$

with $p_\beta(n,0) = 0$ if $n = 0$ and is zero if $n \geq 1$. Here $\mathcal{D}_t^\beta$ denotes the Dzhrbashyan-Caputo fractional derivative which is defined below.

Let $f(t)$ be absolutely continuous function on $[0,T]$, then the (left-hand) Dzhrbashyan-Caputo fractional derivative of f (see [37, Theorem 2.1]) is defined by (with $\mathcal{D}_t^0 f = f$)

$$\mathcal{D}_t^\beta f(t) := \begin{cases} \dfrac{1}{\Gamma(1-\beta)}\displaystyle\int_0^t \frac{f'(s)}{(t-s)^\beta}ds, & 0 < \beta < 1, \\ \dfrac{d}{dt}f(t), & \beta = 1. \end{cases} \tag{1}$$

Note that

$$\mathcal{D}_t^\beta u = \partial_t^\beta u - u(0^+)\frac{t^{-\beta}}{\Gamma(1-\beta)}$$

is the Dzhrbashyan-Caputo fractional derivative and

$$\partial_z^\alpha u = \frac{\partial^\alpha u}{\partial z^\alpha} = \frac{1}{\Gamma(1-\alpha)}\frac{\partial}{\partial z}\int_0^z \frac{u(s)\,ds}{(z-s)^\alpha}$$

is the Riemann-Liouville fractional derivative.

The idea of fractional Poisson distribution was first conceived by Repin and Saichev [65]. In their work, they have considered a Poisson process with random intensity for which the distribution of intervals between jumps was described by an equation with fractional derivatives. Similar ideas can also be attributed to Jumarie [33].

Mainardi et al. [52] used renewal process approach to define the fractional Poisson process and it turns out the both this approach also leads to the same process defined above. The renewal process approach is explained as follows.

It is known that the Poisson process is a renewal process with independent and identically distributed (*iid*) inter-arrival times $J_1, J_2, \ldots, J_n$ with $J_i \sim \text{Exp}(\lambda)$, $\lambda > 0$, $1 \leq i \leq n$. Then

$$N(t) = \max\{n \geq 0 : S_n \leq t\}, t \geq 0,$$

where $S_n = J_1 + J_2 + \cdots + J_n$, is the Poisson process with rate parameter $\lambda > 0$. Consider now θ_i, $1 \leq i \leq n$, follows *iid* Mittag-Leffler distribution, that is, $\mathbb{P}[\theta_i > t] = L_\beta(-\lambda t^\beta)$, $0 < \beta < 1$, where $L_\beta(z)$ is the Mittag-Leffler function defined as (see [22])

$$L_\alpha(z) = \sum_{k=0}^{\infty} \frac{z^k}{\Gamma(1+\alpha k)}, \quad \alpha, z \in \mathbb{C} \text{ and } \text{Re}(\alpha) > 0. \tag{2}$$

Then the Mittag-Leffler renewal process (see[52])

$$N_\beta(t) = \max\{n \geq 0 : \widetilde{S}_n \leq t\}, \ t \geq 0, \ 0 < \beta < 1,$$

where $\widetilde{S}_n = \theta_1 + \cdots + \theta_n$, is the FPP with fractional index β. The *pmf* $p_\beta(n,t) = \mathbb{P}[N_\beta(t) = n]$ of the FPP is given by (see [44])

$$p_\beta(n,t) = \frac{(\lambda t^\beta)^n}{n!} \sum_{k=0}^{\infty} \frac{(n+k)!}{k!} \frac{(-\lambda t^\beta)^k}{\Gamma(\beta(k+n)+1)}.$$

The mean and the variance of the FPP are given by (see [44])

$$\begin{aligned} \mathbb{E}[N_\beta(t)] &= qt^\beta, \\ \text{Var}[N_\beta(t)] &= qt^\beta \left[1 + qt^\beta \left(\frac{\beta B(\beta, 1/2)}{2^{2\beta-1}} - 1\right)\right], \end{aligned}$$

where $q = \lambda/\Gamma(1+\beta)$ and $B(a,b)$ denotes the beta function. An alternative form for $\text{Var}[N_\beta(t)]$ is given in [9, Eq. (2.8)] as

$$\text{Var}[N_\beta(t)] = qt^\beta + \frac{(\lambda t^\beta)^2}{\beta} \left(\frac{1}{\Gamma(2\beta)} - \frac{1}{\beta\Gamma^2(\beta)}\right).$$

The equivalence for above two forms of variances can be proved using the Legendre's duplication formula (see [3, p. 22])

$$\Gamma(2a)\Gamma(1/2) = 2^{2a-1}\Gamma(a)\Gamma(a+1/2),\ a > 0.$$

The covariance function of the FPP is given by (see [47, p. 9])

$$\text{Cov}\left[N_\beta(s), N_\beta(t)\right] = qs^\beta + q^2\left[\beta s^{2\beta} B(\beta, 1+\beta) + F(\beta; s, t)\right], \tag{3}$$

where $F(\beta; s, t) = \beta t^{2\beta} B(\beta, 1+\beta; s/t) - (st)^\beta$ and $B(a, b; x) = \int_0^x u^{a-1}(1-u)^{b-1}du$ for $a > 0,\ b > 0$, is the incomplete beta function. It was proved by Vellaisamy and Maheshwari (2018) ([72]) that the one-dimensional distributions of the FPP are not infinite divisible.

Long Memory

The importance, relevance and the applicability of the long memory or the long-range dependence (LRD) is known in the literature. Various applications to several areas can be found in scientific literature such as on Internet data-traffic modelling [35], finance [20], econometrics [63], hydrology [21], climate studies [71] and etc. The definition of the LRD property differs from author to author, for example, Heyde (see [27, 28]) defined long-range dependence for non-stationary stochastic processes. The long-range dependence property of the FPP was proved by Leonenko et al. [47]. Biard and Saussereau [15] showed that the increments of the fractional Poisson process $\{Z^1_\beta(n-1)\}_{n\geq 1}$, defined by

$$Z^\delta_\beta(t) = N_\beta(t+\delta) - N_\beta(t),\ 0 < \beta < 1,\ \delta > 0,\ t \geq 0, \tag{4}$$

has the LRD property, using Heyde and Yang's [28] definition of long-range dependence for non-stationary processes. Later on, Maheshwari and Vellaisamy [49] also proved the long-range dependence of the increments of the FPP $\{Z^\delta_\beta(t)\}_{t\geq 0}$.

3 Interlinking the Fractional Operators, the Lévy Process and the Poisson Process

The increasing Lévy process (also called as Lévy subordinator) have a special connection with the fractional derivatives. We first have an introduction to the Lévy subordinator.

3.1 Lévy Subordinator

A Lévy subordinator (hereafter referred to as the subordinator) is a one-dimensional Lévy process with non-decreasing sample paths (*a.s.*) with Laplace transform (see [4, Sect. 1.3.2])

$$\mathbb{E}[e^{-sD_f(t)}] = e^{-tf(s)},$$

where

$$f(s) = bs + \int_0^\infty (1 - e^{-sx})\nu(dx), \ b \geq 0,$$

is the Bernstein function. Here b is the drift coefficient and ν is a non-negative Lévy measure on positive half-line such that $\int_0^\infty (x \wedge 1)\nu(dx) < \infty$. The assumption $\nu(0, \infty) = \infty$ guarantees that the sample paths of $D_f(t)$ non-decreasing *a.s.* Some well known examples of subordinators are such as gamma process, inverse Gaussian process, stable process and tempered stable process. A subordinated process is obtained by a random time-change with a subordinator, see e.g. [4, 18, 67].

The first-exit time of the subordinator $\{D_f(t)\}_{t\geq 0}$ is its right-continuous inverse, defined by

$$E_f(t) = \inf\{r \geq 0 : D_f(r) > t\}, \quad t \geq 0,$$

and is called an *inverse subordinator* (see [14]). Note that for any $\rho > 0, \mathbb{E}[E_f^\rho(t)] < \infty$ (see [1, Sect. 2.1]).

We next present some details about the stable subordinator which is a special case of a Lévy subordinator. We also discuss about the right-continuous inverse of stable subordinator which is called as inverse stable subordinator.

Stable Subordinator

Let $0 < \beta < 1$ be the β-stable subordinator (see [4, p. 53]) with LT

$$\mathbb{E}[e^{-sD_\beta(t)}] = e^{-ts^\beta}.$$

Here, the drift coefficient b is zero, the corresponding Lévy measure is

$$\nu(dx) = \frac{\beta dx}{\Gamma(1-\beta)x^{1+\beta}},$$

and the associated Bernstein function $f(s) = s^\beta$. The density of $D_\beta(t)$ is (see [26, Eq. (4.7)])

$$g_\beta(x, t) = \beta t x^{-(\beta+1)} M_\beta(tx^{-\beta}), \quad x > 0,$$

where $M_\beta(z), 0 < \beta < 1$ is the M-Wright function (see [26, 51]) is defined as

$$M_\beta(z) = \sum_{n=0}^{\infty} \frac{(-z)^n}{n!\Gamma(-\beta n + (1-\beta))} = \frac{1}{\pi} \sum_{n=1}^{\infty} \frac{(-z)^{n-1}}{(n-1)!} \Gamma(\beta n) \sin(\pi \beta n), \ z \in \mathbb{C}.$$

A stochastic process $\{X(t)\}_{t \geq 0}$ is self-similar (see [4]) with Hurst index $H > 0$ if

$$X(ct) \stackrel{d}{=} c^H X(t),$$

in the sense of all finite dimensional distributions for all $c \geq 0$. It is well known that the β-stable subordinator is self-similar with Hurst index $1/\beta$, that is,

$$D_\beta(ct) \stackrel{d}{=} c^{1/\beta} D_\beta(t), \ c > 0.$$

Inverse Stable Subordinator

The inverse β-stable subordinator (see [16, 58]) is defined as the right-continuous inverse of the β-stable subordinator

$$E_\beta(t) = \inf\{r > 0 : D_\beta(r) > t\}, \ \ 0 < \beta < 1, t \geq 0.$$

The density of $E_\beta(t)$ is (see [26, Eq. (5.7)])

$$h_\beta(x, t) = t^{-\beta} M_\beta(t^{-\beta} x), \quad x > 0.$$

It can be seen that (see e.g. [57, 72]) the inverse β-stable subordinator is self-similar with Hurst index β, that is

$$E_\beta(ct) \stackrel{d}{=} c^\beta E_\beta(t), \ c > 0.$$

We now explore the connection between the fractional derivatives and the Poisson process via a Lévy subordinator.

3.2 Fractional Poisson Process and Lévy Subordinator

The first connection between the FPP and the stochastic time-change (or subordination) was obtained by Beghin and Orsingher [9]. They obtained an interesting probabilistic representation in terms of a composition of the Poisson process with a random time-change which is related to the solution $f(y, t)$ of the fractional diffusion equation

$$\frac{\partial^{2\nu} f}{\partial t^{2\nu}} = \frac{\partial^2 f}{\partial y^2}, t > 0, y \in \mathbb{R},$$

with $f(y,0) = \delta(y)$ and $0 < \nu < 1$. Some extensions on the FPP are also worked out in [10]. It is proved in [56] that the FPP can be seen as the subordination of the Poisson process by an independent inverse β-stable subordinator, that is,

$$N_\beta(t) = N(E_\beta(t)),\ t \geq 0,\ 0 < \beta < 1, \tag{5}$$

where $N(t)$ is the Poisson process with rate $\lambda > 0$. This result unifies the two main approaches towards the definition of the FPP, namely, the stochastic subordination method and governing fractional difference-differential equation method. They also studied the Poisson process time-changed by inverse subordinator $\{E_f(t)\}_{t\geq 0}$ and proved that it is a renewal process with the *iid* inter-arrival times T_n with distribution

$$\mathbb{P}[T_n > t] = \mathbb{E}[e^{-\lambda E_f(t)}].$$

Space Fractional Poisson Process

Orsingher and Polito [61] introduced the space fractional Poisson process whose one-dimensional distributions are governed by difference-differential equation where the fractional non-local operator acts on the "space" variable n. We elaborate their approach below.

Define the *backward shift operator* as $B_n x(n) = x(n-1)$, then the governing equation of the Poisson process can be re-written as

$$\frac{d}{dt}p(n,t) = -\lambda(1 - B_n)p(n,t).$$

Let $0 < \alpha \leq 1$. The space fractional Poisson process (SFPP), which is a generalization of the Poisson process $\{N(t)\}_{t\geq 0}$, is defined to be a stochastic process for which $\bar{p}_\alpha(n,t) = \mathbb{P}[\bar{N}_\alpha(t) = n]$ satisfies

$$\frac{d}{dt}\bar{p}_\alpha(n,t) = -\lambda^\alpha(1 - B_n)^\alpha \bar{p}_\alpha(n,t), \tag{6}$$

with $\bar{p}_\alpha(n,0) = 1$ if $n = 0$ and is zero if $n \geq 1$ and $(1-B)^\alpha$ is the fractional difference operator. The *pmf* $\bar{p}_\alpha(n,t)$ of the SFPP is given by (see [61, Eq. (1.2)])

$$\bar{p}_\alpha(n,t) = \frac{(-1)^n}{n!}\sum_{k=0}^{\infty}\frac{(-\lambda^\alpha t)^k}{k!}\frac{\Gamma(\alpha k + 1)}{\Gamma(\alpha k + 1 - n)}. \tag{7}$$

An alternative characterization of the SFPP is to subordinate the Poisson process $\{N(t)\}_{t\geq 0}$ by an independent α-stable subordinator $\{D_\alpha(t)\}_{t\geq 0}$ (see [61, Remark 2.3]), that is,

$$\bar{N}_\alpha(t) = N(D_\alpha(t)),\ t \geq 0. \tag{8}$$

The SFPP turns out be a Lévy process with infinite mean. After the above characterisation of the SFPP, the authors have defined the space-time fractional Poisson process where the one fractional index is over the time derivative and the other over the difference operator. In [8], multivariate space-time fractional Poisson processes are studied by considering common random time-changes of a (finite-dimensional) vector of independent Poisson processes.

4 More Results on Fractional Point Processes

In the previous section, we have seen that the fractional derivative and stochastic subordination are interconnected. Taking a cue from this interconnection, several authors have studied new "fractional" versions of point processes by using the subordination approach. In this section, we will survey results related to the same. We first begin with a brief survey about the negative binomial process.

Stochastic processes with marginal negative binomial distributions were studied in [42, 55, 69] which is defined by stopping the Poisson process at gamma distributed random variable. Hougaard et al. (see [30]) followed the subordination approach to construct negative binomial process by using an independent gamma subordinator to time-change the Poisson process. The equivalent representation of the negative binomial process is also found in [24, pp. 155–157], [25, pp. 348–349] and [19, 77]. Kozubowski and Podgórski (see [38, 39]) presented a definitive study on negative binomial Lévy process. A fractional generalization of the negative binomial process is given by Beghin and Claudio [7]. They have used the compound Poisson representation of the negative binomial process to define the fractional negative binomial process. Vellaisamy and Maheshwari [72] defined fractional negative binomial process by time-changing the FPP $\{N_\beta(t)\}_{t\geq 0}$ by a gamma subordinator $\{Y(t)\}_{t\geq 0}$ as

$$\mathrm{NB}_\beta(t) = N_\beta(Y(t)), t \geq 0.$$

They have studied their distributional properties and long-range dependence of the increments of the fractional negative binomial process in [49].

Several authors have studied other time-changed Poisson processes and we survey some results on it. Kumar et al. [41] studied the Poisson process subordinated with the inverse Gaussian, the first-exit time of the inverse Gaussian, the stable and the tempered stable subordinator. They derived governing equation for various forms of the time-changed Poisson process. For instance, the following governing equation

$$\frac{d^{2^k}}{dt^{2^k}} p(n,t) = -\lambda[p(n,t) - p(n-1,t)],$$

has the solution as the one-dimensional distribution of the Poisson process iteratively time-changed by $\frac{1}{2}$-stable subordinator, that is,

$$p(n,t) = \mathbb{P}[N(D^1_{\frac{1}{2}}(D^2_{\frac{1}{2}}(\ldots(D^k_{\frac{1}{2}})(t)))) = n].$$

In [62], Orsingher and Toaldo (2015) studied the Poisson process subordinated with independent Lévy subordinator $\{D_f(t)\}_{t\geq 0}$, that is

$$N_f(t) = N(D_f(t)), t \geq 0.$$

They have shown that the probabilities $p_f(n,t) = \mathbb{P}[N_f(t) = n]$, $n \geq 0$, are solutions to the equation

$$\frac{d}{dt}p_f(n,t) = -f(\lambda)p_f(n,t) + \sum_{m=1}^{n}\frac{\lambda^m}{m!}p_f(n-m,t)\int_0^\infty e^{-s\lambda}s^m\nu(ds), k \geq 0, t > 0,$$

with initial condition

$$p_f(n,0) = \begin{cases} 1, & n = 0 \\ 0, & n \geq 1. \end{cases}$$

They have also studied the hitting-times

$$T_k^f = \inf\left\{t \geq 0 : N_f(t) \geq k\right\},$$

of the subordinated Poisson processes and obtained

$$\Pr\left\{T_k^f \in ds\right\}/ds = \sum_{l=0}^{k-1}\frac{(-\lambda)^l}{l!}\left(\frac{d^l}{d\lambda^l}e^{-sf(\lambda)}\right)\int_0^\infty\left(1 - \sum_{r=0}^{k-l-1}\frac{(\lambda u)^r}{r!}e^{-\lambda u}\right)\nu(du).$$

It is noteworthy that the Lévy subordinator covers most of the special subordinators (see [4, Theorem 1.3.15]) considered in the literature. The following are some special cases for the Lévy subordinators.

Example 1 (*Gamma subordinator*) The gamma subordinator $\{Y(t)\}_{t\geq 0}$, $Y(t) \sim G(\alpha, pt)$, has the one-dimensional density

$$f(x|\alpha, pt) = \frac{\alpha^{pt}}{\Gamma(pt)}e^{-\alpha x}x^{pt-1}, \ x > 0,$$

where both α and p are positive. It is known that (see [4, p. 54])

$$\mathbb{E}[e^{-sY(t)}] = \left(1 + \frac{s}{\alpha}\right)^{-pt} = \exp\left(-pt\log\left(1 + s/\alpha\right)\right).$$

Example 2 (*Tempered α-stable subordinator*) The tempered α-stable subordinator $\{D^\mu_\alpha(t)\}_{t\geq 0}$, $\mu > 0, 0 < \alpha < 1$ is defined by the Laplace transform as

$$\mathbb{E}[e^{-s D_\alpha^\mu(t)}] = e^{-t((\mu+s)^\alpha - \mu^\alpha)}.$$

The *pdf* of the tempered α-stable subordinator is given by (see [2, Eq. (2.2)])

$$g_\mu(x,t) = e^{-\mu x + \mu^\beta t} g(x,t),\ x > 0,$$

where $g(x,t)$ is the *pdf* of the α-stable subordinator $\{D_\alpha(t)\}_{t\geq 0}$.

Example 3 (*Inverse Gaussian subordinator*) The inverse Gaussian subordinator $\{G(t)\}_{t\geq 0}$ is defined using the Laplace transform as (see [4, Example 1.3.21])

$$\mathbb{E}[e^{-sG(t)}] = e^{-t\left(\delta(\sqrt{2s+\gamma^2}-\gamma)\right)},\quad \delta, \gamma > 0.$$

Some extensions of the FPP are also considered in the literature by adding the drift term to the FPP. For example, the FPP with the additive random drift component defined below was studied in [6]. The drifted process

$$N(D_\gamma(E_\beta(t))) + aD_\alpha(E_\beta(t)),\ t > 0,\ a \geq 0,\ \alpha, \gamma, \beta \in (0,1],$$

where $D_\gamma(E_\beta(t))$ and $D_\alpha(E_\beta(t))$ are independent from $N(t)$. It has probability law

$$\begin{aligned}\mathbb{P}\left[N(D_\gamma(E_\beta(t))) + aD_\alpha(E_\beta(t)) \in dx\right]/dx &= \sum_{k=0}^{\infty} \frac{(-\lambda\partial_\lambda)^k}{k!} \int_0^\infty e^{-s\lambda^\gamma} h_\alpha(x-k, a^\alpha s) l_\beta(s,t) ds \\ &= \sum_{k=0}^{\infty} \frac{(-\lambda\partial_\lambda)^k}{k!} \mathbb{E}\left[\exp(-\lambda^\gamma E_\beta(t))\, h_\alpha(x-k, a^\alpha E_\beta(t))\right]\end{aligned}$$

which is the solution to the equation

$$\left(\mathcal{D}_t^\beta + a^\alpha \partial_x^\alpha + \lambda^\gamma (I-K)^\gamma\right) u(x,t) = 0,\quad x \in \mathbb{R}_0^+,\ t > 0$$

with initial condition $u(x,0) = \delta(x)$, where

$$(I-K)^\gamma = \sum_{j=0}^{\infty} (-1)^j \binom{\gamma}{j} K^j$$

and

$$K^j = \begin{cases} e^{-j\partial_x}, & \text{if } a > 0 \\ B^j, & \text{if } a = 0. \end{cases}$$

Beghin [5] formulated the fractional gamma process and gamma-subordinated processes. The fundamental aspects of the inverse stable subordinator is studied in detail by Meerschaert and Straka in [58].

Table 1 Examples for intensity and rate functions

Name	Intensity function $\lambda(s)$	Rate function $\Lambda(t)$
Weibull	$\frac{a}{b}\left(\frac{s}{b}\right)^{a-1}, a, b > 0$	$\left(\frac{t}{b}\right)^{a}$
Gompertz-Makeham's	$ae^{bs} + \mu, a, b, \mu > 0$	$\frac{a}{b}\left(e^{bt} - 1\right) + \mu t$
Musa-Okumoto	$\frac{ab}{1+bs}, a, b, \mu > 0$	$a \ln(1 + bt)$

Non-homogeneous Poisson Process

The non-homogeneous Poisson process (NPP) is defined as the Poisson process where the time variable is replaced by rate function $\Lambda(t) = \int_0^t \lambda(u)du$ is the rate function with intensity function $\lambda(u)$, $u \geq 0$, that is, $\widetilde{N}(t) = N(\Lambda(t))$ with rate parameter as one. A fractional version of the NPP was recently studied by Leonenko et al. [46] defined by time-changing the NPP by an inverse β-stable subordinator. They also pointed out an another way of defining the fractional version of the NPP (see [46, Sect. 6]) which can be obtained by replacing the time variable of the FPP by the rate function $\Lambda(t)$, $t \geq 0$. Maheshwari and Vellaisamy [50] recently used an alternative approach to define non-homogeneous space-time fractional Poisson process as

$$W_\beta^\alpha(t) = N_\beta^\alpha(\Lambda(t)), \ t \geq 0,$$

where $\{N_\beta^\alpha(t)\}_{t\geq 0}$ is the space-time fractional Poisson process (space fractional index $= \alpha$ and time fractional index $= \beta$) with rate parameter as one and $\Lambda(t) = \int_0^t \lambda(u)du$ is the rate function with intensity function $\lambda(u), u \geq 0$. The following table lists some of the important intensity and rate function Table 1.

They have also obtained the limit theorems and long-range dependence property for the non-homogeneous space-time fractional Poisson process. An alternative non-homogeneous extension of the FPP is studied by Beghin and Ricciuti (see [11]).

A different approach for fractional generalization of the Poisson process was discussed in [73–75]. They followed the integral representation method used for defining the fractional Brownian motion and then replacing the Brownian motion by the Poisson process. Kataria and Vellaisamy [36] used Saigo fractional derivatives to define another version of the fractional Poisson process using the difference-differential equation approach. The time-changed Poisson process of order k is studied by Sengar et al. [68] and its first hitting time probabilities are studied in [48].

5 Plots and Simulations of Fractional Poisson Process

In this section, we present plots of the *pmf* and simulation of the sample paths for the FPP.

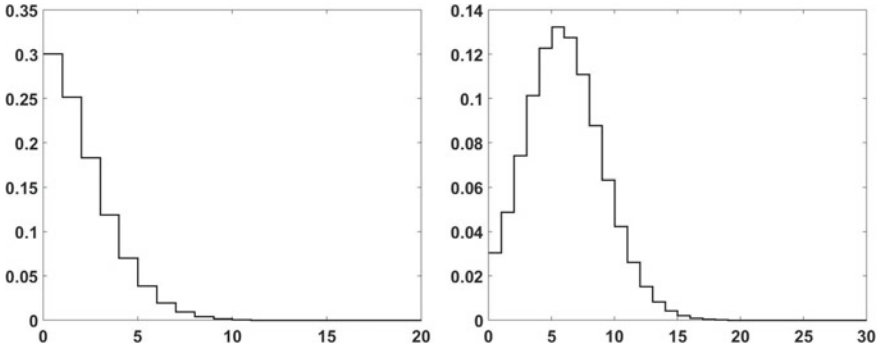

Fig. 1 Plots for the *pmf* of the FPP

Plots for the FPP

For certain chosen values of β, t and λ, two plots of the *pmf* of the FPP process, computed using Mathematica 10 to the order of 10^{-6}, are given below (Fig. 1).

Cahoy et al. [17] proposed a formal estimation procedure for parameters of the FPP to make the FPP model usable in applied situations. They established the asymptotic normality of the estimators for the two parameters appearing in FPP model and tested the estimators using simulated data. The following results are reproduced which is used in simulating the sample paths of the FPP.

Lemma 1 ([17]) *The inter arrival times T_i of the FPP $\{N_\beta(t)\}_{t\geq 0}$ has the representation*

$$T_i \stackrel{d}{=} T \stackrel{d}{=} \frac{|\ln(U)|^{1/\beta}}{\lambda^{1/\beta}} D_\beta(1), \tag{9}$$

where $U \sim U[0,1]$ and is independent of $D_\beta(t)$, $0 < \beta < 1$, the β-stable subordinator.

Remark 1 From (9),

$$T \stackrel{d}{=} \frac{|\ln(U_1)|^{1/\beta}}{\lambda^{1/\beta}} D_\beta(1), \tag{10}$$

where $U_1 \sim U(0,1)$, and $D_\beta(1)$ are independent. From [34, Corollary 4.1],

$$D_\beta(1) \stackrel{d}{=} \frac{(\sin \beta U)(\sin(1-\beta)U)^{(1-\beta)/\beta}}{(\sin U)^{1/\beta} W^{(1-\beta)/\beta}}, \tag{11}$$

where $U \perp W$, $U \sim (0, \pi)$, $W \sim \text{Exp}(1)$. Let now U_2 and U_3 be independent $U(0,1)$ variables so that $U \stackrel{d}{=} \pi U_2$, and $W = |\ln U_3|$. Hence, from (11),

$$D_\beta(1) \stackrel{d}{=} \frac{\sin(\beta \pi U_2)[\sin(1-\beta)\pi U_2]^{1/\beta - 1}}{[\sin(\pi U_2)]^{1/\beta} |\ln U_3|^{1/\beta - 1}}$$

and from (10), we have

$$T \stackrel{d}{=} \frac{|\ln U_1|^{1/\beta}}{\lambda^{1/\beta}} \frac{\sin(\beta\pi U_2)[\sin(1-\beta)\pi U_2]^{1/\beta-1}}{[\sin(\pi U_2)]^{1/\beta}|\ln U_3|^{1/\beta-1}}. \tag{12}$$

We now present the algorithm to generate the simulated sample paths of the FPP using the above mentioned results. The simulated sample paths are shown in Fig. 2.

Algorithm **(Simulation of fractional Poisson process)**
This algorithm gives the number of events $N_\beta(t)$, $0 < \beta < 1$ of the FPP upto a fixed time T.

(a) Fix the parameters $\lambda > 0$ and $0 < \beta < 1$ for the FPP. Set $n = 0$ and $t = 0$;
(b) Repeat while $t < T$

(i) Generate three independent uniform random variables $U_i \sim U(0, 1)$, $i = 1, 2, 3$.
(ii) Compute

(a) Simulation for the FPP process for $\beta = 0.4$, $n = 60$ and $\lambda = 1.5$.

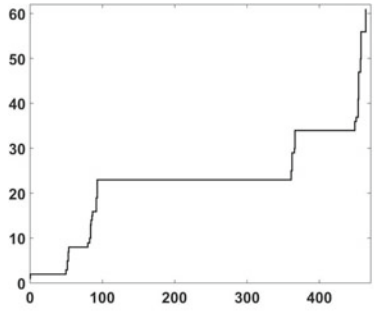

(b) Simulation for the FPP process for $\beta = 0.6$, $n = 60$ and $\lambda = 1.5$.

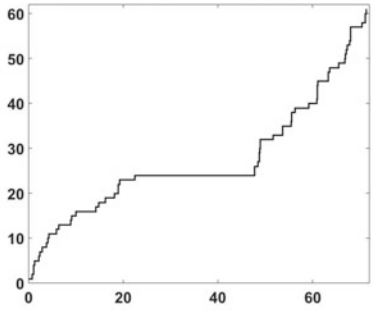

(c) Simulation for the FPP process for $\beta = 0.8$, $n = 60$ and $\lambda = 1.5$.

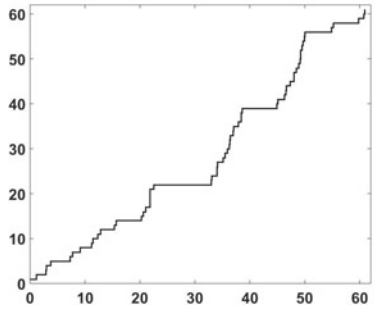

(d) Simulation for the FPP process for $\beta = 1.0$, $n = 60$ and $\lambda = 1.5$.

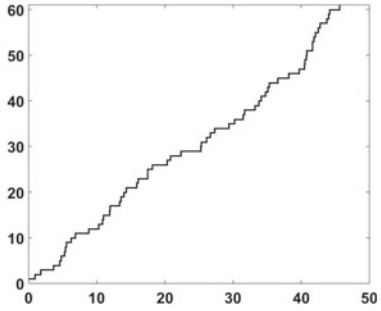

Fig. 2 Simulations for the FPP

$$dt = \frac{|\ln U_1|^{1/\beta}}{\lambda^{1/\beta}} \frac{\sin(\beta\pi U_2)[\sin(1-\beta)\pi U_2]^{1/\beta-1}}{[\sin(\pi U_2)]^{1/\beta}|\ln U_3|^{1/\beta-1}}.$$

(iii) $t = t + dt$ and $n = n + 1$.

Next t;
Then n denotes the number of events $N_\beta(t)$ occurred upto time T. □

Interpretation of Simulated Paths

It is clear from the graphs below that the sample paths of the FPP displays larger variation in waiting time of occurrence of events as the fractional index β decreases given the fixed value for the arrival rate λ. The fractional index β can be used to adjust the model with the data where the waiting times of events have larger variation given the same arrival rate.

References

1. Aletti, G., Leonenko, N., Merzbach, E.: Fractional Poisson fields and martingales. J. Stat. Phys. **170**(4), 700–730 (2018)
2. Alrawashdeh, M.S., Kelly, J.F., Meerschaert, M.M., Scheffler, H.-P.: Applications of inverse tempered stable subordinators. Comput. Math. Appl. (2016)
3. Andrews, G.E., Askey, R., Roy, R.: Special functions. Encyclopedia of Mathematics and its Applications, vol. 71. Cambridge University Press, Cambridge (1999)
4. Applebaum D.: Lévy Processes and Stochastic Calculus, Cambridge Studies in Advanced Mathematics, vol. 116, 2nd edn. Cambridge University Press, Cambridge (2009)
5. Beghin, L.: Fractional gamma and gamma-subordinated processes. Stoch. Anal. Appl. **33**(5), 903–926 (2015)
6. Beghin, L., D'Ovidio, M.: Fractional Poisson process with random drift. Electron. J. Probab. **19**(122), 26 (2014)
7. Beghin, L., Macci, C.: Fractional discrete processes: compound and mixed poisson representations. J. Appl. Probab. **51**(1), 9–36 (2014)
8. Beghin, L., Macci, C.: Multivariate fractional Poisson processes and compound sums. Adv. Appl. Probab. **48**(3), 691–711 (2016)
9. Beghin, L., Orsingher, E.: Fractional Poisson processes and related planar random motions. Electron. J. Probab. **14**(61), 1790–1827 (2009)
10. Beghin, L., Orsingher, E.: Poisson-type processes governed by fractional and higher-order recursive differential equations. Electron. J. Probab. **15**(22), 684–709 (2010)
11. Beghin, L., Ricciuti, C.: Time-inhomogeneous fractional Poisson processes defined by the multistable subordinator. Stoch. Anal. Appl. (2019)
12. Beran, J., Feng, Y., Ghosh, S., Kulik, R.: Long-Memory Processes: Probabilistic Properties and Statistical Methods (2013)
13. Berezinsky, V., Gazizov, A.Z.: Diffusion of cosmic rays in the expanding universe. I. Astrophys. J. (2006)
14. Bertoin, J.: Lévy processes. Cambridge Tracts in Mathematics, vol. 121. Cambridge University Press, Cambridge (1996)
15. Biard, R., Saussereau, B.: Fractional Poisson process: long-range dependence and applications in ruin theory. J. Appl. Probab. **51**(3), 727–740 (2014)
16. Bingham, N.H.: Limit theorems for occupation times of Markov processes. Z. Wahrscheinlichkeitstheorie Und Verw. Geb. **17**, 1–22 (1971)

17. Cahoy, D.O., Uchaikin, V.V., Woyczynski, W.A.: Parameter estimation for fractional Poisson processes. J. Stat. Plan. Inference **140**(11), 3106–3120 (2010)
18. Cont, R., Tankov, P.: Financial Modelling with Jump Processes. Financial Mathematics Series. Chapman & Hall, Boca Raton (2004)
19. Diggle, P.J., Milne, R.K.: Negative binomial quadrat counts and point processes. Scand. J. Stat. **10**(4), 257–267 (1983)
20. Ding, Z., Granger, C.W., Engle, R.F.: A long memory property of stock market returns and a new model. J. Empir. Financ. **1**(1), 83–106 (1993)
21. Doukhan, P., Oppenheim, G., Taqqu, M.S. (eds.): Theory and Applications of Long-Range Dependence. Birkhäuser Boston Inc., Boston (2003)
22. Erdélyi, A., Magnus, W., Oberhettinger, F., Tricomi, F.G.: Higher Transcendental Functions, vol. III. McGraw-Hill Book Company Inc., New York-Toronto-London (1955). Based, in part, on notes left by Harry Bateman
23. Feliu-Talegon, D., San-Millan, A., Feliu-Batlle, V.: Fractional-order integral resonant control of collocated smart structures. Control Eng. Pract. (2016)
24. Feller, W.: An Introduction to Probability Theory and its Applications, vol. I, 3rd edn. Wiley, New York (1968)
25. Feller, W.: An Introduction to Probability Theory and its Applications, vol. II, 2nd edn. Wiley, New York (1971)
26. Gorenflo, R., Mainardi, F: On the fractional Poisson process and the discretized stable subordinator (2013). arXiv:1305.3074 [math.PR]
27. Heyde, C.C.: On modes of long-range dependence. J. Appl. Probab. **39**(4), 882–888 (2002)
28. Heyde, C.C., Yang, Y.: On defining long-range dependence. J. Appl. Probab. **34**(4), 939–944 (1997)
29. Hilfer, R.: Applications of Fractional Calculus in Physics (2000)
30. Hougaard, P., Lee, M.-L.T., Whitmore, G.A.: Analysis of overdispersed count data by mixtures of Poisson variables and Poisson processes. Biometrics **53**(4), 1225–1238 (1997)
31. Jeon, J.H., Monne, H.M.S., Javanainen, M., Metzler, R.: Anomalous diffusion of phospholipids and cholesterols in a lipid bilayer and its origins. Phys. Rev. Lett. (2012)
32. Jeon, J.H., Tejedor, V., Burov, S., Barkai, E., Selhuber-Unkel, C., Berg-Sørensen, K., Oddershede, L., Metzler, R.: In vivo anomalous diffusion and weak ergodicity breaking of lipid granules. Phys. Rev. Lett. (2011)
33. Jumarie, G.: Fractional master equation: non-standard analysis and Liouville-Riemann derivative. Chaos Solitons Fractals **12**(13), 2577–2587 (2001)
34. Kanter, M.: Stable densities under change of scale and total variation inequalities. Ann. Probab. **3**(4), 697–707 (1975)
35. Karagiannis, T., Molle, M., Faloutsos, M.: Long-range dependence ten years of internet traffic modeling. Internet Comput., IEEE **8**(5), 57–64 (2004)
36. Kataria, K., Vellaisamy, P.: Saigo space time fractional Poisson process via adomian decomposition method. Stat. Probab. Lett. **129**, 69–80 (2017)
37. Kilbas, A.A., Srivastava, H.M., Trujillo, J.J.: Theory and Applications of Fractional Differential Equations. North-Holland Mathematics Studies. Elsevier Science B.V, Amsterdam (2006)
38. Kozubowski, T., Podgorski, K.: Invariance properties of the negative binomial levy process and stochastic self-similarity. **2**(30), 1457–1468 (2007)
39. Kozubowski, T.J., Podgórski, K.: Distributional properties of the negative binomial Lévy process. Probab. Math. Stat. **29**(1), 43–71 (2009)
40. Krijnen, M.E., Van Ostayen, R.A., HosseinNia, H.: The application of fractional order control for an air-based contactless actuation system. ISA Trans. (2018)
41. Kumar, A., Nane, E., Vellaisamy, P.: Time-changed Poisson processes. Stat. Probab. Lett. **81**(12), 1899–1910 (2011)
42. Lampard, D.G.: A stochastic process whose successive intervals between events form a first order markov chain. J. Appl. Probab. **5**(3), 648–668, 12 (1968)
43. Landman, K.A., Pettet, G.J., Newgreen, D.F.: Mathematical models of cell colonization of uniformly growing domains. Bull. Math. Biol. (2003)

44. Laskin, N.: Fractional Poisson process. Commun. Nonlinear Sci. Numer. Simul. **8**(3–4), 201–213 (2003). Chaotic transport and complexity in classical and quantum dynamics
45. Le Vot, F., Abad, E., Yuste, S.B.: Continuous-time random-walk model for anomalous diffusion in expanding media. Phys. Rev. E (2017)
46. Leonenko, N., Scalas, E., Trinh, M.: The fractional non-homogeneous Poisson process. Stat. Probab. Lett. **120**, 147–156 (2017)
47. Leonenko, N.N., Meerschaert, M.M., Schilling, R.L., Sikorskii, A.: Correlation structure of time-changed lévy processes. Commun. Appl. Ind. Math. (2014)
48. Maheshwari, A., Orsingher, E., Sengar, A.S.: Superposition of time-changed poisson processes and their hitting times (2019)
49. Maheshwari, A., Vellaisamy, P.: On the long-range dependence of fractional Poisson and negative binomial processes. J. Appl. Probab. **53**, 989–1000 (2016)
50. Maheshwari, A., Vellaisamy, P.: Non-homogeneous space-time fractional Poisson processes. Stoch. Anal. Appl. **37**(2), 137–154 (2019)
51. Mainardi, F.: Fractional Calculus and Waves in Linear Viscoelasticity. Imperial College Press, London (2010). An introduction to mathematical models
52. Mainardi, F., Gorenflo, R., Scalas, E.: A fractional generalization of the Poisson processes. Vietnam J. Math. **32**, 53–64 (2004)
53. Mandić, P.D., Lazarević, M.P., Šekara, T.B.: D-decomposition technique for stabilization of Furuta pendulum: fractional approach. Bull. Pol. Acad. Sci.: Tech. (2016)
54. Marinangeli, L., Alijani, F., HosseinNia, S.H.: A fractional-order positive position feedback compensator for active vibration control. IFAC-PapersOnLine (2017)
55. McKenzie, E.: Autoregressive moving-average processes with negative-binomial and geometric marginal distributions. Adv. Appl. Probab. **18**(3), 679–705 (1986)
56. Meerschaert, M.M., Nane, E., Vellaisamy, P.: The fractional Poisson process and the inverse stable subordinator. Electron. J. Probab. **16**(59), 1600–1620 (2011)
57. Meerschaert, M.M., Scheffler, H.-P.: Limit theorems for continuous-time random walks with infinite mean waiting times. J. Appl. Probab. **41**(3), 623–638 (2004)
58. Meerschaert, M.M., Straka, P.: Inverse stable subordinators. Math. Model. Nat. Phenom. **8**(2), 1–16 (2013)
59. Nigmatullin, R.R., Ceglie, C., Maione, G., Striccoli, D.: Reduced fractional modeling of 3D video streams: the FERMA approach. Nonlinear Dyn. (2015)
60. Nigmatullin, R.R., Giniatullin, R.A., Skorinkin, A.I.: Membrane current series monitoring: essential reduction of data points to finite number of stable parameters. Front. Comput. Neurosci. (2014)
61. Orsingher, E., Polito, F.: The space-fractional Poisson process. Stat. Probab. Lett. **82**(4), 852–858 (2012)
62. Orsingher, E., Toaldo, B.: Counting processes with Bernstein intertimes and random jumps. J. Appl. Probab. **52**(4), 1028–1044 (2015)
63. Pagan, A.: The econometrics of financial markets. J. Empir. Financ. **3**(1), 15–102 (1996)
64. Pandey, V., Holm, S.: Connecting the grain-shearing mechanism of wave propagation in marine sediments to fractional order wave equations. J. Acoust. Soc. Am. **140**(6), 4225–4236 (2016)
65. Repin , O.N., Saichev, A.I.: Fractional Poisson law. Radiophys. Quantum Electron. **43**(9), 738–741 (2001), 2000
66. Reverey, J.F., Jeon, J.H., Bao, H., Leippe, M., Metzler, R., Selhuber-Unkel, C.: Superdiffusion dominates intracellular particle motion in the supercrowded cytoplasm of pathogenic Acanthamoeba castellanii. Sci. Rep. (2015)
67. Sato, K.: Lévy Processes and Infinitely Divisible Distributions, vol. 68, Cambridge Studies in Advanced Mathematics. Cambridge University Press, Cambridge (1999). Translated from the 1990 Japanese original, Revised by the author
68. Sengar, A.S., Maheshwari, A., Upadhye, N.S.: Time-changed Poisson processes of order k. Stoch. Anal. Appl. **38**(1), 124–148 (2020)
69. Sim, C.H., Lee, P.A.: Simulation of negative binomial processes. J. Stat. Comput. Simul. **34**(1), 29–42 (1989)

70. Sun, H., Zhang, Y., Baleanu, D., Chen, W., Chen, Y.: A new collection of real world applications of fractional calculus in science and engineering. Commun. Nonlinear Sci. Numer. Simul. **64**, 213–231 (2018)
71. Varotsos, C., Kirk-Davidoff, D.: Long-memory processes in ozone and temperature variations at the region 60 °s-60 °n. Atmos. Chem. Phys. **6**(12), 4093–4100 (2006)
72. Vellaisamy, P., Maheshwari, A.: Fractional negative binomial and Polya processes. Probab. Math. Stat. **38**(1), 77–101 (2018)
73. Wang, X.-T., Wen, Z.-X.: Poisson fractional processes. Chaos Solitons Fractals **18**(1), 169–177 (2003)
74. Wang, X.-T., Wen, Z.-X., Zhang, S.-Y.: Fractional Poisson process II. Chaos Solitons Fractals **28**(1), 143–147 (2006)
75. Wang, X.-T., Zhang, S.-Y., Fan, S.: Nonhomogeneous fractional Poisson processes. Chaos Solitons Fractals **31**(1), 236–241 (2007)
76. West, B.J.: Fractional Calculus View of Complexity: Tomorrow's Science (2016)
77. Wolpert, R.L., Ickstadt, K.: Biometrika **85**(2), 251–267 (1998)

Some Results on Generalized Accelerated Motions Driven by the Telegraph Process

Alessandra Meoli

Abstract We investigate a generalization of the randomly accelerated motion obtained by iterated integration of the telegraph signal. We give the exact and explicit expression for the cumulative distribution function, conditionally on the number n of Poisson events, when n is sufficiently small. The unconditional mean value and variance are also obtained.

Keyword Telegraph process · Riemann-Liouville fractional integral · Conditional distributions

1 Introduction

Kelbert and Orsingher [9] introduced a model of a one-dimensional uniformly accelerated motion where the time intervals between changes in the sign of the acceleration are Poisson-paced. Specifically, if $N(t)$ is the number of events of a homogeneous Poisson process (with rate $\lambda > 0$) occurred in the time interval $[0, t]$, the two-fold integration of a random telegraph signal is considered as follows:

$$\begin{aligned} A(t) &= A_0 (-1)^{N(t)}, \\ V(t) &= \int_0^t A(s)\,\mathrm{d}s = A_0 \int_0^t (-1)^{N(s)}\,\mathrm{d}s, \\ X(t) &= \int_0^t V(s)\,\mathrm{d}s = A_0 \int_0^t (t-s)(-1)^{N(s)}\,\mathrm{d}s, \end{aligned}$$

where A_0 is a random variable independent of $N(t)$ taking values $\pm a$ with equal probability. Therefore, $X(t)$ represents the position of a particle with acceleration $A(t)$ and velocity $V(t)$. A probabilistic derivation of the Euler-Poisson-Darboux equation

A. Meoli (✉)
Dipartimento di Matematica, Università degli Studi di Salerno, Via Giovanni Paolo II, 132, 84084 Fisciano, SA, Italy
e-mail: ameoli@unisa.it

L. Beghin et al. (eds.), *Nonlocal and Fractional Operators*, SEMA SIMAI Springer Series 26, https://doi.org/10.1007/978-3-030-69236-0_12

based on a motion with random acceleration is given in Glushak and Orsingher [5]. We recall that some of the fundamental papers on the (integrated) telegrapher random process are due to Goldstein [6], Kac [8], Orsingher [12], Foong and Kanno [4].

Although the partial differential equation governing the joint distribution of $(X(t), V(t), t > 0)$ has been derived in [9], it has not been possible to obtain the equation for the marginal distribution of $(X(t), t > 0)$. Conti and Orsingher [2] proved recurrence relationships for the conditional distribution of $X(t)$ given the number of Poisson events and the initial acceleration. The same authors in [3] established suitable approximations both for the conditional and the unconditional distribution of the displacement of the particle. Iterated integration of the telegraph signal has been considered in [13] as a generalization of the randomly accelerated telegraph process. This paper aims at further extending the outlined procedure into a Riemann-Liouville fractional integral of the telegraph signal.

2 Explicit Conditional Distribution for Small n

We consider the conditional distributions

$$\mathrm{P}\left(X^{\alpha}(t) \leq y \mid N(t) = n\right), \qquad n \in \mathbb{N},$$

of the process

$$\begin{aligned} X^{\alpha}(t) &:= \left[X^{\alpha}\left(t; \tau_1, \ldots, \tau_{N(t)}\right)\right] \\ &= \frac{1}{\Gamma(\alpha)} \int_0^t (t-s)^{\alpha-1} (-1)^{N(s)} \, \mathrm{d}s, \qquad \alpha > 0, \ t \geq 0, \end{aligned}$$

where $N(t)$ is the number of events of a homogeneous Poisson process occurred in the time interval $[0, t]$ and $\tau_j s$ are the random times of the Poisson events, $j = 1, \ldots, N(t)$. It is assumed that at time $t = 0$ the particle is at the origin and moves with positive unitary acceleration. We recall here the definition of the Riemann-Liouville fractional integral, so that the connection with fractional calculus is obvious. Let $\Omega = [a, b]$ $(-\infty < a < b < +\infty)$ be a finite interval on the real axis $\mathbb{R}$. The Riemann-Liouville fractional integral $I_{a^+}^{\alpha} f$ of order $\alpha > 0$ is defined by

$$\left(I_{a^+}^{\alpha} f\right)(x) := \frac{1}{\Gamma(\alpha)} \int_a^x \frac{f(t)}{(x-t)^{1-\alpha}} \mathrm{d}t, \quad x > a,$$

where $\Gamma(\alpha)$ is the Gamma function. In view of the above, the considered process can be regarded as the Riemann-Liouville fractional integral of the telegraph signal. Moreover, if $N(t) = n$, and $0 = \tau_0 < \tau_1 < \tau_2 < \cdots < \tau_n < \tau_{n+1} = t$ are the random instants at which the Poisson events occur, then the conditional fractional inte-

grated telegraph process $X_n^\alpha(t) := \left[X^\alpha\left(t;\tau_1,\ldots,\tau_{N(t)}\right)|N(t)=n\right]$ can be written down as follows:

$$\begin{aligned} X_n^\alpha(t) &= \frac{1}{\Gamma(\alpha)}\left(\int_0^{\tau_1}(t-s)^{\alpha-1}\,\mathrm{d}s - \int_{\tau_1}^{\tau_2}(t-s)^{\alpha-1}\,\mathrm{d}s + \ldots\right. \\ &\quad \left. + (-1)^n\int_{\tau_n}^{t}(t-s)^{\alpha-1}\,\mathrm{d}s\right) \\ &= \frac{1}{\Gamma(\alpha+1)}\sum_{j=1}^{n+1}(-1)^j\left[\left(t-\tau_j\right)^\alpha - \left(t-\tau_{j-1}\right)^\alpha\right]. \end{aligned} \tag{1}$$

Figure 1 shows simulated sample paths of $X_n^\alpha(t)$ stopped after 6 changes of velocity.

Proposition 1 *For any fixed $t>0$, $\alpha>0$ and $n\in\mathbb{N}$, one has $\left|X_n^\alpha(t)\right| < \frac{t^\alpha}{\Gamma(\alpha+1)}$ almost surely (a.s.).*

Proof Fix $t>0$, $\alpha>0$ and $n\in\mathbb{N}$. When $N(t)=n$, the displacement at time t given in (1) can be alternatively rewritten as

$$X_n^\alpha(t) = \frac{1}{\Gamma(\alpha+1)}\left[t^\alpha - 2(t-\tau_1)^\alpha + 2(t-\tau_2)^\alpha + \cdots + (-1)^n 2(t-\tau_n)^\alpha\right]. \tag{2}$$

Since

$$-2(t-\tau_1)^\alpha + 2(t-\tau_2)^\alpha + \cdots + (-1)^n 2(t-\tau_n)^\alpha < 0,$$

from (2) we have

$$X_n^\alpha(t) < \frac{t^\alpha}{\Gamma(\alpha+1)} \quad a.s.$$

Moreover, since

$$t^\alpha - (t-\tau_1)^\alpha + (t-\tau_2)^\alpha + \cdots + (-1)^n(t-\tau_n)^\alpha > 0,$$

Equation (2) implies

$$X_n^\alpha(t) + \frac{t^\alpha}{\Gamma(\alpha+1)} > 0 \quad a.s.,$$

and this finishes the proof.

□

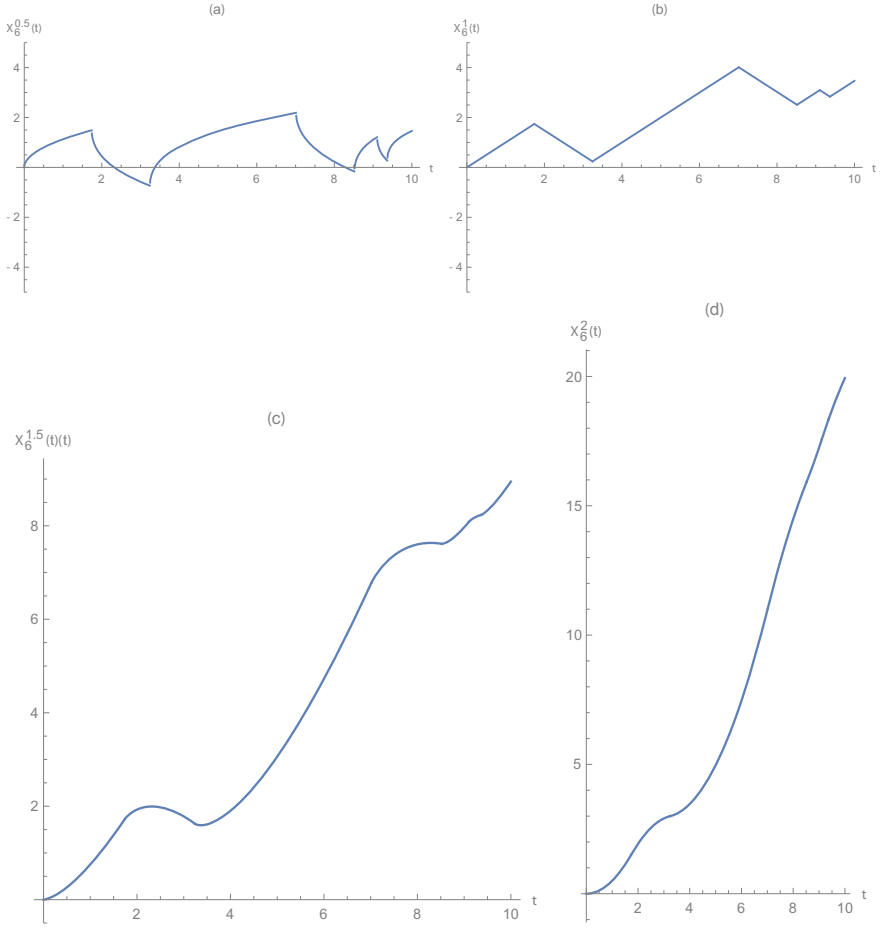

Fig. 1 Sample paths of $X_6^{\alpha}(t)$ with $\lambda = 1$ and **a** $\alpha = 0.5$, **b** $\alpha = 1$, **c** $\alpha = 1.5$, **d** $\alpha = 2$

We restrict the analysis of the probability distribution function of (1) to the cases $n = 1$ and $n = 2$, because of an excessively large quantity of entangled calculations. This is clearly of interest when the intensity λ of $N(t)$ is sufficiently small.

Proposition 2 *Let $t > 0$, $\alpha > 0$ and $n = 1$. The conditional probability distribution of $X^{\alpha}(t)$ is*

$$\mathrm{P}\left(X_1^{\alpha}(t) \leq y\right) = \begin{cases} 0 & \text{if } y < -\frac{t^{\alpha}}{\Gamma(\alpha+1)} \\ 1 - \left(\frac{t^{\alpha} - \Gamma(\alpha+1)y}{2t^{\alpha}}\right)^{\frac{1}{\alpha}} & \text{if } -\frac{t^{\alpha}}{\Gamma(\alpha+1)} \leq y < \frac{t^{\alpha}}{\Gamma(\alpha+1)} \\ 1 & \text{if } y \geq \frac{t^{\alpha}}{\Gamma(\alpha+1)}. \end{cases}$$

Proof Due to Proposition 1, we focus on the interval $-\frac{t^\alpha}{\Gamma(\alpha+1)} \leq y < \frac{t^\alpha}{\Gamma(\alpha+1)}$. It is well known that if $N(t) = k$, the joint distribution of the random times $(\tau_1, ..., \tau_k)$ where the Poisson events occur is given by

$$\mathrm{P}\{\tau_1 \in \mathrm{d}s_1, \ldots, \tau_n \in \mathrm{d}s_n\} = \frac{n!}{t^n}, \quad 0 < s_1 < s_2 < \cdots < s_n < t.$$

Hence, taking into account (1), we get the following result:

$$\begin{aligned}
\mathrm{P}\left(X_1^\alpha(t) \leq y\right) &= \mathrm{P}\left(\tau_1 \leq t - \left(\frac{t^\alpha - \Gamma(\alpha+1)\, y}{2}\right)^{1/\alpha}\right) \\
&= \int_0^{t-\left(\frac{t^\alpha-\Gamma(\alpha+1)y}{2}\right)^{1/\alpha}} \mathrm{P}\{\tau_1 \in \mathrm{d}s_1\} \\
&= \int_0^{t-\left(\frac{t^\alpha-\Gamma(\alpha+1)y}{2}\right)^{1/\alpha}} \frac{1}{t}\,\mathrm{d}s_1 \\
&= \frac{1}{t}\left[t - \left(\frac{t^\alpha - \Gamma(\alpha+1)\, y}{2}\right)^{\frac{1}{\alpha}}\right] \\
&= 1 - \left(\frac{t^\alpha - \Gamma(\alpha+1)\, y}{2t^\alpha}\right)^{\frac{1}{\alpha}}.
\end{aligned}$$

The claimed result is then obtained.

□

Before stating Proposition 3, we recall the Euler integral representation of the Gauss hypergeometric function:

$${}_2F_1(a, b; c; z) = \frac{\Gamma(c)}{\Gamma(b)\,\Gamma(c-b)} \int_0^1 t^{b-1}(1-t)^{c-b-1}(1-zt)^{-a}\,\mathrm{d}t, \qquad (3)$$

for $0 < \mathrm{Re}\, b < \mathrm{Re}\, c$ and $|\arg(1-z)| < \pi$.

Proposition 3 *Let $t > 0$, $\alpha > 0$ and $n = 2$. The conditional probability distribution of $X^\alpha(t)$ is*

$$\mathrm{P}\left(X_2^\alpha(t) \leq y\right) = \begin{cases} 0 & \text{if } y < -\frac{t^\alpha}{\Gamma(\alpha+1)} \\ \frac{2!}{t^2}\left(\frac{t^\alpha+\Gamma(\alpha+1)y}{2}\right)^{\frac{1}{\alpha}}\left[t - \left(\frac{t^\alpha-\Gamma(\alpha+1)y}{2}\right)^{\frac{1}{\alpha}}\right. & \\ \quad \left.\times {}_2F_1\left(-\frac{1}{\alpha}, \frac{1}{\alpha}; \frac{1}{\alpha}+1; -\frac{t^\alpha+\Gamma(\alpha+1)y}{t^\alpha-\Gamma(\alpha+1)y}\right)\right] & \\ \qquad \text{if } -\frac{t^\alpha}{\Gamma(\alpha+1)} \leq y < \frac{t^\alpha}{\Gamma(\alpha+1)} \\ 1 \qquad \text{if } y \geq \frac{t^\alpha}{\Gamma(\alpha+1)}. \end{cases}$$

Proof Let $y \in \left[-\frac{t^\alpha}{\Gamma(\alpha+1)}, \frac{t^\alpha}{\Gamma(\alpha+1)}\right)$. We evaluate the conditional probability distribution as follows:

$$\begin{aligned}\mathrm{P}\left(X_2^\alpha(t) \le y\right) &= \mathrm{P}\left(\frac{1}{\Gamma(\alpha+1)}\left(t^\alpha - 2(t-\tau_1)^\alpha + 2(t-\tau_2)^\alpha\right) \le y\right) \\ &= \int_D \mathrm{P}\left\{\tau_1 \in \mathrm{d}s_1, \tau_2 \in \mathrm{d}s_2\right\},\end{aligned}$$

where the region of integration is

$$D = \left\{(s_1, s_2) \in \mathbb{R}^2 : 0 < s_1 < s_2 < t,\ \frac{\left(t^\alpha - 2(t-s_1)^\alpha + 2(t-s_2)^\alpha\right)}{\Gamma(\alpha+1)} \le y\right\}.$$

In the light of this, we have

$$\begin{aligned}\mathrm{P}\left(X_2^\alpha(t) \le y\right) &= \int_{t-\left(\frac{t^\alpha+\Gamma(\alpha+1)y}{2}\right)^{1/\alpha}}^{t} \int_0^{t-\left(\frac{t^\alpha-\Gamma(\alpha+1)y+2(t-s_2)^\alpha}{2}\right)^{1/\alpha}} \mathrm{P}\left\{\tau_1 \in \mathrm{d}s_1, \tau_2 \in \mathrm{d}s_2\right\} \\ &= \frac{2!}{t^2}\int_{t-\left(\frac{t^\alpha+\Gamma(\alpha+1)y}{2}\right)^{1/\alpha}}^{t} \mathrm{d}s_2 \int_0^{t-\left(\frac{t^\alpha-\Gamma(\alpha+1)y+2(t-s_2)^\alpha}{2}\right)^{1/\alpha}} \mathrm{d}s_1 \\ &= \frac{2!}{t^2}\int_{t-\left(\frac{t^\alpha+\Gamma(\alpha+1)y}{2}\right)^{1/\alpha}}^{t} t - \left(\frac{t^\alpha - \Gamma(\alpha+1)y + 2(t-s_2)^\alpha}{2}\right)^{1/\alpha} \mathrm{d}s_2 \\ &= \frac{2!}{t^2}\left[I_1 - \frac{1}{2^{1/\alpha}} I_2\right], \qquad (4)\end{aligned}$$

where

$$\begin{aligned}I_1 &:= \int_{t-\left(\frac{t^\alpha+\Gamma(\alpha+1)y}{2}\right)^{1/\alpha}}^{t} t\,\mathrm{d}s_2, \\ I_2 &:= \int_{t-\left(\frac{t^\alpha+\Gamma(\alpha+1)y}{2}\right)^{1/\alpha}}^{t} \left(t^\alpha - \Gamma(\alpha+1)y + 2(t-s_2)^\alpha\right)^{1/\alpha} \mathrm{d}s_2.\end{aligned}$$

It turns out that

$$I_1 = t\left(\frac{t^\alpha + \Gamma(\alpha+1)y}{2}\right)^{1/\alpha}, \qquad (5)$$

while the computation of I_2 is more laborious. Indeed, by setting

$$s_2 = \left(\frac{t^\alpha + \Gamma(\alpha+1)\, y}{2}\right)^{1/\alpha} (u-1) + t,$$

we get

$$I_2 = \left(\frac{t^\alpha + \Gamma(\alpha+1)\, y}{2}\right)^{1/\alpha} \int_0^1 \left(t^\alpha - \Gamma(\alpha+1)\, y + \left(t^\alpha + \Gamma(\alpha+1)\, y\right)(1-u)^\alpha\right)^{1/\alpha} \mathrm{d}u.$$

We perform the change of variable $u = 1 - z^{1/\alpha}$ so to obtain

$$\begin{aligned} I_2 &= \left(\frac{t^\alpha + \Gamma(\alpha+1)\, y}{2}\right)^{1/\alpha} \frac{1}{\alpha} \\ &\quad \times \int_0^1 \left(t^\alpha - \Gamma(\alpha+1)\, y + \left(t^\alpha + \Gamma(\alpha+1)\, y\right) z\right)^{1/\alpha} z^{1/\alpha - 1} \mathrm{d}z \\ &= \left(\frac{t^\alpha + \Gamma(\alpha+1)\, y}{2}\right)^{1/\alpha} \frac{\left(t^\alpha - \Gamma(\alpha+1)\, y\right)^{1/\alpha}}{\alpha} \\ &\quad \times \int_0^1 \left(1 + \frac{t^\alpha + \Gamma(\alpha+1)\, y}{t^\alpha - \Gamma(\alpha+1)\, y} z\right)^{1/\alpha} z^{1/\alpha - 1} \mathrm{d}z. \end{aligned} \tag{6}$$

If $a = -1/\alpha,\ b = 1/\alpha,\ c = 1/\alpha + 1$ in Eq. (3), then Eq. (6) becomes

$$\begin{aligned} I_2 &= \left(\frac{t^\alpha + \Gamma(\alpha+1)\, y}{2}\right)^{1/\alpha} \frac{\left(t^\alpha - \Gamma(\alpha+1)\, y\right)^{1/\alpha}}{\alpha} \frac{\Gamma\left(\frac{1}{\alpha}\right)\Gamma(1)}{\Gamma\left(\frac{1}{\alpha}+1\right)} \\ &\quad \times {}_2F_1\left(-\frac{1}{\alpha}, 1; \frac{1}{\alpha}+1; -\frac{t^\alpha + \Gamma(\alpha+1)\, y}{t^\alpha - \Gamma(\alpha+1)\, y}\right) \\ &= \left(\frac{t^\alpha + \Gamma(\alpha+1)\, y}{2}\right)^{1/\alpha} \left(t^\alpha - \Gamma(\alpha+1)\, y\right)^{1/\alpha} \\ &\quad \times {}_2F_1\left(-\frac{1}{\alpha}, 1; \frac{1}{\alpha}+1; -\frac{t^\alpha + \Gamma(\alpha+1)\, y}{t^\alpha - \Gamma(\alpha+1)\, y}\right). \end{aligned} \tag{7}$$

Finally, by putting together (5) and (7) in Equation (4), we get

$$\begin{aligned} \mathrm{P}\left(X_2^\alpha(t) \le y\right) = \frac{2!}{t^2} \left(\frac{t^\alpha + \Gamma(\alpha+1)\, y}{2}\right)^{1/\alpha} \Bigg[t - \left(\frac{t^\alpha - \Gamma(\alpha+1)\, y}{2}\right)^{1/\alpha} \\ \times {}_2F_1\left(-\frac{1}{\alpha}, 1; \frac{1}{\alpha}+1; -\frac{t^\alpha + \Gamma(\alpha+1)\, y}{t^\alpha - \Gamma(\alpha+1)\, y}\right)\Bigg], \end{aligned}$$

as desired.

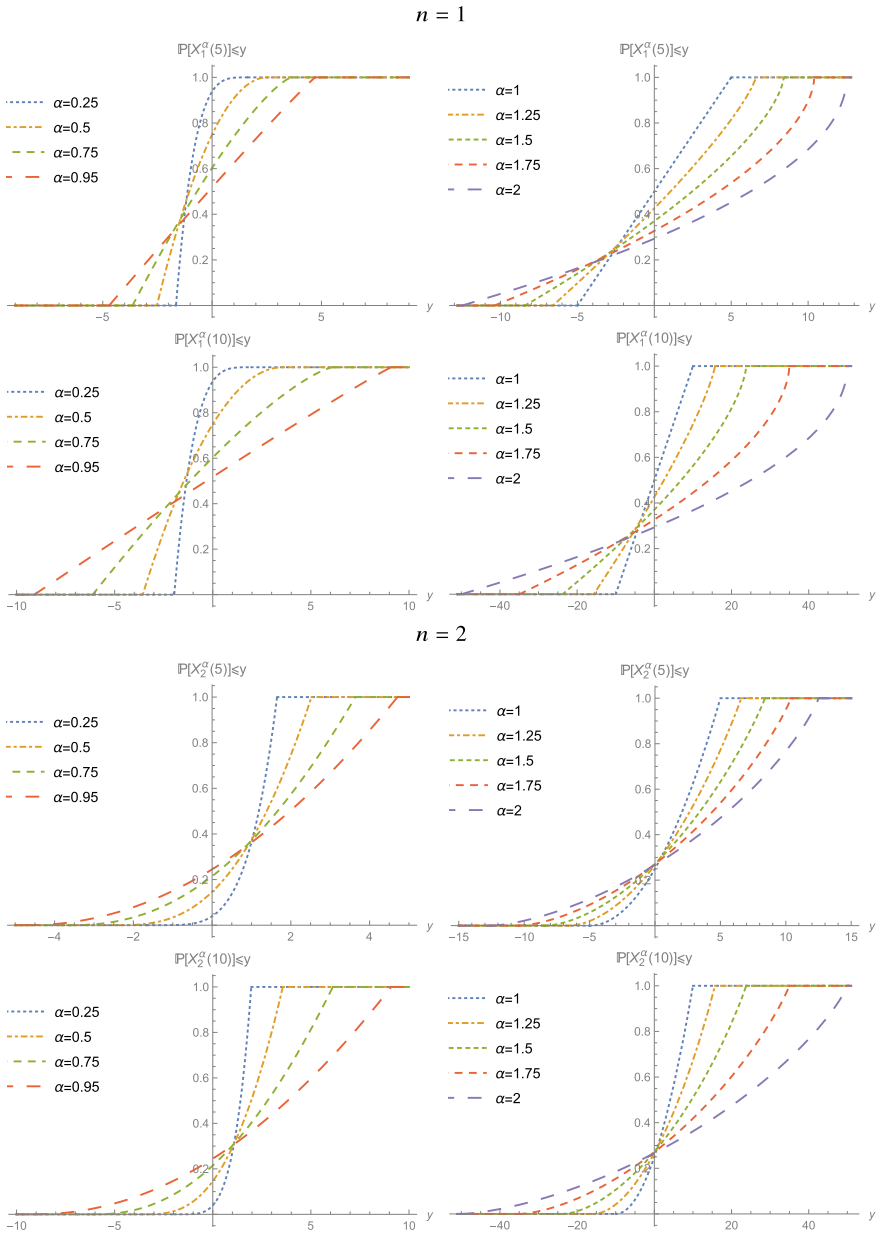

Fig. 2 Conditional probability distribution function of $X_n^\alpha(t)$ for $n = 1, 2$ and various choices of α

Plots of the conditional probability distribution of $X^{\alpha}(t)$ are given in Fig. 2. It is straightforward to derive, from Proposition 1 and from Proposition 2, the analytical expression of the probability density function of the conditional process. Indeed, if $t > 0$,

$$ {}_t f_1^{\alpha}(y) := \frac{\mathrm{dP}\left(X_1^{\alpha}(t) \leq y\right)}{\mathrm{d}y} = \begin{cases} \frac{\Gamma(\alpha+1)}{\alpha 2t^{\alpha}} \left(\frac{t^{\alpha}-\Gamma(\alpha+1)y}{2t^{\alpha}}\right)^{\frac{1}{\alpha}-1} \\ \quad \text{if } -\frac{t^{\alpha}}{\Gamma(\alpha+1)} \leq y < \frac{t^{\alpha}}{\Gamma(\alpha+1)} \\ 0 \qquad\qquad \text{otherwise} \end{cases} $$

and

$$ {}_t f_2^{\alpha}(y) := \frac{\mathrm{dP}\left(X_2^{\alpha}(t) \leq y\right)}{\mathrm{d}y} $$

$$ \begin{cases} \frac{2!}{t^2} \left\{ \frac{1}{\alpha} \left(\frac{t^{\alpha}+\Gamma(\alpha+1)y}{2}\right)^{\frac{1}{\alpha}-1} \frac{\Gamma(\alpha+1)}{2} \right. \\ \quad \left[t - \left(\frac{t^{\alpha}-\Gamma(\alpha+1)y}{2}\right)^{\frac{1}{\alpha}} {}_2F_1\left(-\frac{1}{\alpha}, \frac{1}{\alpha}; \frac{1}{\alpha}+1; -\frac{t^{\alpha}+\Gamma(\alpha+1)y}{t^{\alpha}-\Gamma(\alpha+1)y}\right) \right] \\ \quad + \frac{1}{\alpha} \left(\frac{t^{\alpha}+\Gamma(\alpha+1)y}{2}\right)^{\frac{1}{\alpha}} \frac{\Gamma(\alpha+1)}{2} \left(\frac{t^{\alpha}-\Gamma(\alpha+1)y}{2}\right)^{\frac{1}{\alpha}-1} \\ \quad \times {}_2F_1\left(-\frac{1}{\alpha}, \frac{1}{\alpha}; \frac{1}{\alpha}+1; -\frac{t^{\alpha}+\Gamma(\alpha+1)y}{t^{\alpha}-\Gamma(\alpha+1)y}\right) \\ \quad - \left(\frac{t^{\alpha}+\Gamma(\alpha+1)y}{2}\right)^{\frac{1}{\alpha}} \left(\frac{t^{\alpha}-\Gamma(\alpha+1)y}{2}\right)^{\frac{1}{\alpha}} \frac{2t^{\alpha}\Gamma(\alpha+1)}{\alpha(\alpha+1)(t^{\alpha}-\Gamma(\alpha+1)y)^2} \\ \quad \left. \times {}_2F_1\left(-\frac{1}{\alpha}+1, \frac{1}{\alpha}+1; \frac{1}{\alpha}+2; -\frac{t^{\alpha}+\Gamma(\alpha+1)y}{t^{\alpha}-\Gamma(\alpha+1)y}\right) \right\} \\ \qquad\qquad \text{if } -\frac{t^{\alpha}}{\Gamma(\alpha+1)} \leq y < \frac{t^{\alpha}}{\Gamma(\alpha+1)} \\ 0 \qquad\qquad\qquad\qquad\qquad\qquad \text{otherwise.} \end{cases} $$

Plots of the conditional probability density function are shown in Fig. 3.

3 Unconditional Mean and Variance

Hereafter, we shall obtain the explicit expressions of $\mathrm{E}[X^{\alpha}(t)]$ and $\mathrm{Var}[X^{\alpha}(t)]$.

Proposition 4 *Let $t > 0$ and $\alpha > 0$. Then the unconditional mean of $X^{\alpha}(t)$ is*

$$ \mathrm{E}\left[X^{\alpha}(t)\right] = \frac{1}{\Gamma(\alpha+1)} t^{\alpha} e^{-2\lambda t} {}_1F_1(\alpha; 1+\alpha; 2\lambda t). \tag{8} $$

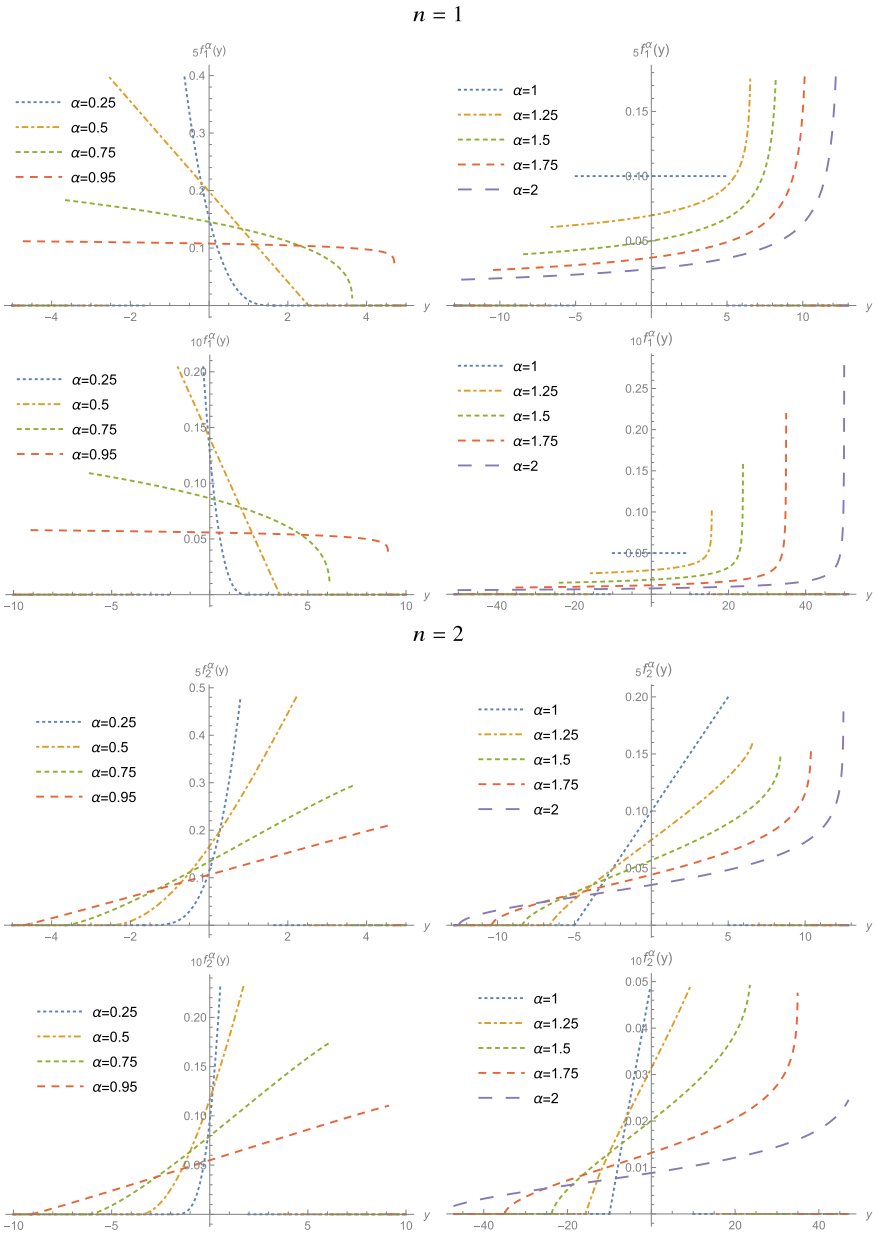

Fig. 3 Conditional probability density function of $X_n^{\alpha}(t)$ for $n = 1, 2$ for various choices of α

Proof Since

$$\mathrm{E}\left[(-1)^{N(s)}\right] = e^{-2\lambda s}, \qquad s > 0,$$

it results

$$\begin{aligned}
\mathrm{E}\left[X^{\alpha}(t)\right] &= \mathrm{E}\left[\frac{1}{\Gamma(\alpha)}\int_0^t (t-s)^{\alpha-1}(-1)^{N(s)}\,\mathrm{d}s\right] \\
&= \frac{1}{\Gamma(\alpha)}\int_0^t (t-s)^{\alpha-1}\,\mathrm{E}\left[(-1)^{N(s)}\right]\mathrm{d}s \\
&= \frac{1}{\Gamma(\alpha)}\int_0^t (t-s)^{\alpha-1}e^{-2\lambda s}\mathrm{d}s \\
&= \frac{1}{\Gamma(\alpha)}e^{-2\lambda t}\int_0^t s^{\alpha-1}e^{2\lambda s}\mathrm{d}s.
\end{aligned}$$

A useful integration formula is Eq. 3.383.1 of [7], valid for $Re(\mu) > 0,\ Re(\nu) > 0$:

$$\int_0^u x^{\nu-1}(u-x)^{\mu-1}e^{\beta x}\mathrm{d}x = B(\mu,\nu)\,u^{\mu+\nu-1}{}_1F_1(\nu;\mu+\nu;\beta u). \tag{9}$$

From this,

$$\begin{aligned}
\mathrm{E}\left[X^{\alpha}(t)\right] &= \frac{B(1,\alpha)}{\Gamma(\alpha)}t^{\alpha}e^{-2\lambda t}{}_1F_1(\alpha;1+\alpha;2\lambda t) \\
&= \frac{1}{\Gamma(\alpha+1)}t^{\alpha}e^{-2\lambda t}{}_1F_1(\alpha;1+\alpha;2\lambda t),
\end{aligned}$$

so that formula (8) easily follows.

In Fig. 4 we show some plots of $\mathrm{E}[X^{\alpha}(t)]$.
Due to the fact that (cf. Formula 7.6.(4) of Luke [10])

$${}_1F_1(a;c;z) \sim \frac{\Gamma(c)}{\Gamma(a)}e^{z}z^{a-c} \quad \text{as } Re(z) \to +\infty,$$

at large times the unconditional mean value (8) displays the following behaviour:

$$\mathrm{E}\left[X^{\alpha}(t)\right] \sim \frac{t^{\alpha-1}}{2\lambda\Gamma(\alpha)} \overset{t\to+\infty}{\to} \begin{cases} 0 & \text{if } 0 < \alpha < 1 \\ \frac{1}{2\lambda} & \text{if } \alpha = 1 \\ +\infty & \text{if } \alpha > 1. \end{cases}$$

Proposition 5 *Let $t > 0$ and $\alpha > 0$. Then the second-order unconditional moment of $X^{\alpha}(t)$ is*

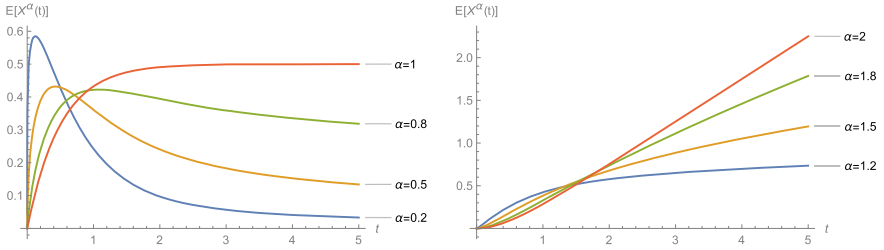

Fig. 4 Mean value of $X^{\alpha}(t)$ with $\lambda = 1$ and various choices of α

$$\begin{aligned}\mathrm{E}\left[\left(X^{\alpha}(t)\right)^2\right] = \frac{2(2\lambda)^{-\alpha}}{\Gamma(\alpha)^2}\Big[&t^{\alpha}\Gamma(\alpha)\,B(\alpha,1)\,{}_1F_1(\alpha;\alpha+1;2\lambda t)\\ &-\frac{t^{2\alpha}(2\lambda)^{\alpha}}{\alpha}B(1,2\alpha)\,{}_2F_2(2\alpha,1;\alpha+1,2\alpha+1;2\lambda t)\\ &-e^{2\lambda t}\Gamma(\alpha;2\lambda t)\,B(\alpha,1)\,t^{\alpha}\,{}_1F_1(1;\alpha+1;-2\lambda t)\Big].\end{aligned}$$

Proof It is well-known that

$$\mathrm{E}\left[(-1)^{N(s)+N(t)}\right] = e^{-2\lambda(t-s)}, \qquad t > s.$$

Therefore,

$$\begin{aligned}\mathrm{E}\left[\left(X^{\alpha}(t)\right)^2\right] &= \frac{1}{\Gamma(\alpha)^2}\int_0^t\int_0^t (t-w)^{\alpha-1}(t-s)^{\alpha-1}\,\mathrm{E}\left[(-1)^{N(w)+N(s)}\right]\mathrm{d}w\,\mathrm{d}s\\ &= \frac{1}{\Gamma(\alpha)^2}\int_0^t\int_0^t (t-w)^{\alpha-1}(t-s)^{\alpha-1}\,e^{-2\lambda|w-s|}\mathrm{d}w\,\mathrm{d}s\\ &= \frac{2}{\Gamma(\alpha)^2}\int_0^t\int_0^s (t-w)^{\alpha-1}(t-s)^{\alpha-1}\,e^{-2\lambda(s-w)}\mathrm{d}w\,\mathrm{d}s.\end{aligned}$$

We first evaluate the inner integral by performing the change of variable $2\lambda(t-w) = z$

$$\begin{aligned}\int_0^s (t-w)^{\alpha-1}e^{2\lambda w}\mathrm{d}w &= e^{2\lambda t}(2\lambda)^{-\alpha}\int_{2\lambda(t-s)}^{2\lambda t} z^{\alpha-1}e^{-z}\mathrm{d}z\\ &= e^{2\lambda t}(2\lambda)^{-\alpha}\left[\Gamma(\alpha;2\lambda(t-s)) - \Gamma(\alpha;2\lambda t)\right],\end{aligned}$$

where $\Gamma(a,x) = \int_x^{+\infty} e^{-t}t^{a-1}\mathrm{d}t$ is the incomplete gamma function. Then, we plug this solution into the outer integral and get

$$\mathrm{E}\left[\left(X^{\alpha}(t)\right)^{2}\right]=\frac{2\,(2\lambda)^{-\alpha}}{\Gamma(\alpha)^{2}}e^{2\lambda t}\left[J_{1}-\Gamma(\alpha;2\lambda t)\,J_{2}\right]. \tag{10}$$

where

$$\begin{aligned}J_{1}:&=\int_{0}^{t}(t-s)^{\alpha-1}\,e^{-2\lambda s}\Gamma(\alpha;2\lambda(t-s))\,\mathrm{d}s\\&=e^{-2\lambda t}\int_{0}^{t}y^{\alpha-1}e^{2\lambda y}\Gamma(\alpha;2\lambda y)\,\mathrm{d}y\end{aligned}$$

and

$$J_{2}:=\int_{0}^{t}(t-s)^{\alpha-1}\,e^{-2\lambda s}\mathrm{d}s.$$

A useful integration formula is Eq. 2.10.3.5 of [14], valid for a, $Re(\alpha)$, $Re(\beta)$, $Re\,(\alpha+\nu)>0$, $|\arg c|<\pi$:

$$\begin{aligned}\int_{0}^{a}x^{\alpha-1}\,(a-x)^{\beta-1}\,e^{cx}\Gamma(\nu,cx)\,\mathrm{d}x&=a^{\alpha+\beta-1}\Gamma(\nu)\,B(\alpha,\beta)\,{}_{1}F_{1}(\alpha;\alpha+\beta;ac)\\&-\frac{a^{\alpha+\beta+\nu-1}c^{\nu}}{\nu}B(\beta,\alpha+\nu)\,{}_{2}F_{2}(\alpha+\nu,1;\nu+1,\alpha+\beta+\nu;ac).\end{aligned} \tag{11}$$

A straightforward application of (11) yields

$$\begin{aligned}J_{1}=e^{-2\lambda t}\Big[&t^{\alpha}\Gamma(\alpha)\,B(\alpha,1)\,{}_{1}F_{1}(\alpha;\alpha+1;2\lambda t)\\&-\frac{t^{2\alpha}\,(2\lambda)^{\alpha}}{\alpha}B(1,2\alpha)\,{}_{2}F_{2}(2\alpha,1;\alpha+1,2\alpha+1;2\lambda t)\Big],\end{aligned} \tag{12}$$

while to compute J_2 we resort to (9) and get

$$J_{2}=B(\alpha,1)\,t^{\alpha}\,{}_{1}F_{1}(1;\alpha+1;-2\lambda t). \tag{13}$$

By substituting (12) and (13) in Eq. (10), the desired result is then proved.

□

In Fig. 5 we show some plots of the second-order unconditional moment of $X^{\alpha}(t)$. It grows faster and faster as the order of fractionality increases.

We conclude this section by presenting the expression of the unconditional variance of $X^{\alpha}(t)$, some plots of which are given in Fig. 6.

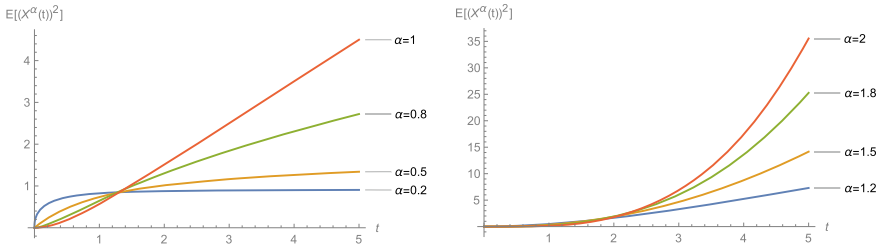

Fig. 5 Moment of order two of $X^{\alpha}(t)$ with $\lambda = 1$ and various choices of α

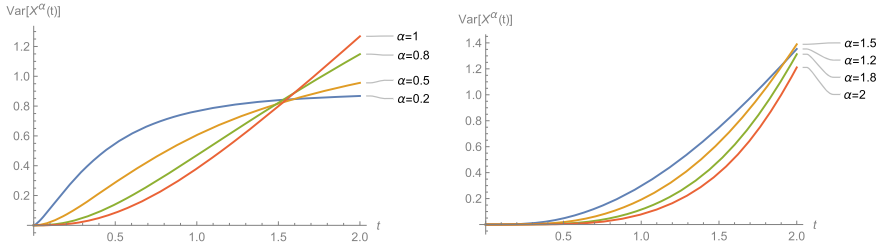

Fig. 6 Variance of $X^{\alpha}(t)$ with $\lambda = 1$ and various choices of α

Corollary 1 *Let $t > 0$ and $\alpha > 0$. Then the unconditional variance of $X^{\alpha}(t)$ is*

$$\begin{aligned}
\mathrm{Var}\left[X^{\alpha}(t)\right] &= \mathrm{E}\left[(X^{\alpha}(t))^2\right] - \left(\mathrm{E}\left[X^{\alpha}(t)\right]\right)^2 \\
&= \frac{2(2\lambda)^{-\alpha}}{\Gamma(\alpha)^2}\left[t^{\alpha}\Gamma(\alpha)\, B(\alpha,1)\, {}_1F_1(\alpha;\alpha+1;2\lambda t)\right. \\
&- \frac{t^{2\alpha}(2\lambda)^{\alpha}}{\alpha} B(1,2\alpha)\, {}_2F_2(2\alpha,1;\alpha+1,2\alpha+1;2\lambda t) \\
&\left. - e^{2\lambda t}\Gamma(\alpha;2\lambda t)\, B(\alpha,1)\, t^{\alpha}\, {}_1F_1(1;\alpha+1;-2\lambda t)\right] \\
&- \left(\frac{1}{\Gamma(\alpha+1)} t^{\alpha} e^{-2\lambda t}\, {}_1F_1(\alpha;1+\alpha;2\lambda t)\right)^2.
\end{aligned}$$

Conclusions

In this paper, a stochastic process describing a motion on the real line has been introduced, that generalizes a uniformly accelerated motion with Poisson-paced changes of its acceleration. Various results on the conditional probability distribution and on the unconditional mean and variance have been given. The case of random initial acceleration is worthy of further investigation. The study of such process is motivated by the recent interest in Monte Carlo methods based upon piecewise deterministic

Markov processes, since they offer a non-reversible alternative to traditional MCMC methods. See, for example, Monmarché [11] and Bierkens et al. [1]. Therefore, future work will also include the use of the proposed process as an alternative to standard MCMC algorithms.

Acknowledgements This paper has been performed under partial support by MIUR (PRIN 2017, project "Stochastic Models for Complex Systems" no. 2017JFFHSH). Thanks are due to Antonio Di Crescenzo for helpful comments. A.M. is member of the Research group GNCS of INdAM.

References

1. Bierkens, J., Fearnhead, P., Roberts, G.: The Zig-Zag process and super-efficient sampling for Bayesian analysis of big data. Ann. Statist. **47**(3), 1288–1320 (2019)
2. Conti, P.L., Orsingher, E.: Limiting distributions of randomly accelerated motions. Lith. Math. J. **37**(3), 219–229 (1997)
3. Conti, P.L., Orsingher, E.: On the distribution of the position of a randomly accelerated particle. Theory Probab. Math. Statist. **56**, 167–174 (1998)
4. Foong, S.K., Kanno, S.: Properties of the telegrapher's random process with or without a trap. Stochastic Process. Appl. **53**(1), 147–173 (1994)
5. Glushak, A.V., Orsingher, E.: General solution of a hyperbolic equation that arises in the study of a motion with random acceleration. Theory Probab. Math. Statist. **55**, 50–54 (1996)
6. Goldstein, S.: On diffusion by discontinuous movements, and on the telegraph equation. Quart. J. Mech. Appl. Math. **4**(2), 129–156 (1951)
7. Gradshteyn, I.S., Ryzhik, I.M.: Tables of Integrals, Series, and Products, 7th edn. Academic Press, Amsterdam (2007)
8. Kac, M.: A stochastic model related to the telegrapher's equation. Rocky Mountain J. Math. **4**(3), 497–509 (1974)
9. Kelbert, M., Orsingher, E.: On a telegraph-type equation with non-constant coefficients emerging in randomly accelerated motions. Problemy Peredachi Informatsii **30**(2), 99–103 (1994)
10. Luke, Y.L.: Mathematical Functions and Their Approximations. Academic Press (2014)
11. Monmarché, P.: Piecewise deterministic simulated annealing. ALEA **13**(1), 357–398 (2016)
12. Orsingher, E.: Probability law, flow function, maximum distribution of wave-governed random motions and their connections with Kirchoff's laws. Stochastic Process. Appl. **34**(1), 49–66 (1990)
13. Orsingher, E.: On the vector process obtained by iterated integration of the telegraph signal. Georgian Math. J. **6**(2), 169–178 (1999)
14. Prudnikov, A.P., Brychkov, Y.A., Marichev, O.I.: Integrals and Series: Special functions. CRC Press (1986)

The PDD Method for Solving Linear, Nonlinear, and Fractional PDEs Problems

Ángel Rodríguez-Rozas, Juan A. Acebrón, and Renato Spigler

Abstract We review the Probabilistic Domain Decomposition (PDD) method for the numerical solution of linear and nonlinear Partial Differential Equation (PDE) problems. This Domain Decomposition (DD) method is based on a suitable probabilistic representation of the solution given in the form of an expectation which, in turns, involves the solution of a Stochastic Differential Equation (SDE). While the structure of the SDE depends only upon the corresponding PDE, the expectation also depends upon the boundary data of the problem. The method consists of three stages: (i) only few values of the sought solution are solved by Monte Carlo or Quasi-Monte Carlo at some interfaces; (ii) a continuous approximation of the solution over these interfaces is obtained via interpolation; and (iii) prescribing the previous (partial) solutions as additional Dirichlet boundary conditions, a fully decoupled set of subproblems is finally solved in parallel. For linear parabolic problems, this is based on the celebrated Feynman-Kac formula, while for semilinear parabolic equations requires a suitable generalization based on branching diffusion processes. In case of semilinear transport equations and the Vlasov-Poisson system, a generalization of the probabilistic representation was also obtained in terms of the Method of Characteristics (characteristic curves). Finally, we present the latest progress towards the extension of the PDD method for nonlocal fractional operators. The algorithm notably improves the scalability of classical algorithms and is suited to massively parallel implementation, enjoying arbitrary scalability and fault tolerance properties. Numerical examples conducted in 1D and 2D, including some for the KPP equation and Plasma Physics, are given.

Á. Rodríguez-Rozas (✉)
Risk Division, Banco Santander, S.A., Boadilla del Monte, Spain
e-mail: angel.rodriguez.rozas@gmail.com

J. A. Acebrón
ISCTE – Instituto Universitário de Lisboa, Lisbon, Portugal
e-mail: juan.acebron@iscte-iul.pt

R. Spigler
Universitá degli Studi Roma Tre, Rome, Italy
e-mail: spigler@mat.uniroma3.it

L. Beghin et al. (eds.), *Nonlocal and Fractional Operators*, SEMA SIMAI Springer Series 26, https://doi.org/10.1007/978-3-030-69236-0_13

Keywords Probabilistic domain decomposition · Domain decomposition methods · Partial differential equations · Monte Carlo · Quasi-Monte Carlo · Elliptic operators · Transport equations · Vlasov-Poisson system · Nonlocal and fractional operators

1 Introduction

Since its introduction in 2005 for numerically solving boundary-value elliptic problems [1], the *PDD (Probabilistic Domain Decomposition) method* has been successfully extended by the authors of this article for solving a wide range of problems described through partial differential equations (PDEs) (see [2–8, 14]).

In this article, we review the PDD method highlighting its main developments [8, 14] and its latest investigations regarding fractional operators. The class of equations for which method has been applied include linear elliptic and parabolic equations, the KPP-equation, general semilinear parabolic equations, linear purely advection-dominated equations, the non-linear Vlasov-Poison system of equations governing plasma physics, and the Telegraph equation. Applications include all kind of diffusion and advection problems, finance (Black-Scholes and similar equations), plasma physics, and electrical transmission lines (see [2–8]).

For linear parabolic and elliptic problems defined in $\Omega \subseteq \mathbb{R}^d$, this method is based on the celebrated Feynman-Kac formula, that establishes a connection between the solution of a PDE and a suitable expectation over a corresponding stochastic process driven by Brownian motion, referred to as the stochastic solution. It exploits such solution to be approximated by the Monte Carlo method only at a few points along certain $\mathbb{R}^{d-1}$ interfaces, such that the original domain problem Ω is decomposed into as many independent subdomain problems as convenient. The result is a domain decomposition technique based on a probabilistic method that is suited for massively parallel computers, enjoying full scalability and fault tolerance.

For semilinear problems, the Feynman-Kac formula is generalized to solutions by means of branching stochastic processes in the real space. For linear and semilinear hyperbolic problems, the extension of the Feynam-Kac formula is based on the *method of characteristics*, where the characteristic curves play a similar role in the corresponding solution as the stochastic process does for the parabolic problems. In the case of the Vlasov-Poison system, the stochastic solution is found in the Fourier domain after coupling the equations. Finally, for fractional PDEs, the method is extended to deal with space-fractional diffusion equations.

The structure of the article is as follows: First, we give a general introduction of the method when applied to linear parabolic problems; second, we describe an important extension of the method for solving general semi-linear parabolic problems; then, we present the extension of the method for transport problems and the Vlasov-Poisson system of equations; subsequently, we present the latest progress towards the extension of the PDD method for non-local fractional operators; finally, we conclude the paper with some remarks and future work.

2 Linear Parabolic Problems

2.1 Introduction

The purpose of this section is to introduce the PDD method (see [8]) to solve initial- as well as initial-boundary value problems for linear parabolic differential equations. The linear case is merely considered here to illustrate in the simplest way the essencial features of the PDD method. Rather unexpectedly, however, it turned out that even in such case important computational advantages were observed with respect to some existing more traditional parallel schemes. To assess the computational feasibility of our algorithm, we compare our results with those obtained using competitive (freely available) parallel numerical codes, which are widely used by the high-performance scientific community.

The plan of the section is as follows. First, some necessary mathematical generalities are provided. Then, the algorithm is described and different sources of parallelization are discussed. Later, numerical examples considering one-dimensional problems are given, where the efficiency of the PDD algorithm is illustrated. In a short final section, we summarize the salient points of the method.

2.2 Mathematical Preliminaries

A variety of phenomena pertaining to Engineering, Physics, and other Sciences, are governed by diffusion equations. The relations between macroscopic diffusion and the mean statistical effect of the microscopic random (Brownian) motion of molecules goes back, among the others, to A. Einstein and M. Smoluchowski. A connection between "stochastic differential equations", that can be thought of ordinary differential equations driven by a certain kind of random noise (Langevin equations), and partial differential equations, was established.

Inspired by the work of R. Feynman on "path integrals" in quantum physics, M. Kac realized that a similar formulation could be applied to obtain a representation of the solution to the heat equation and to other diffusive (parabolic) linear partial differential equations. This lead to the so-called Feynman-Kac formula. Let $u(\mathbf{x}, t)$ be a bounded function satisfying the Cauchy problem for the linear parabolic partial differential equation,

$$\frac{\partial u}{\partial t} = Lu - c(\mathbf{x}, t)u, \quad u(\mathbf{x}, 0) = f(\mathbf{x}), \tag{1}$$

where $\mathbf{x} \in \mathbf{R}^n$, L is a linear elliptic operator, say $L := a_{ij}(\mathbf{x}, t)\partial_i\partial_j + b_i(\mathbf{x}, t)\partial_i$ (using the summation convention), with continuous bounded coefficients, $c(\mathbf{x}, t) \geq 0$ and continuous bounded initial condition, $f(\mathbf{x})$. The probabilistic representation of the solution u to Eq. (1) is given through the Feynman-Kac formula

$$u(\mathbf{x}, t) = E\left[f(\beta(t))\, e^{-\int_0^t c(\beta(s), t-s)} ds \right], \tag{2}$$

see [25, 29], e.g., where $\beta(\cdot)$ is the n-dimensional stochastic process starting at $(\mathbf{x}, 0)$, associated to the operator L, and the expected values are taken with respect to the corresponding measure. When L is the n-dimensional Laplace operator, $\beta(\cdot)$ reduces to the standard n-dimensional Brownian motion, and the measure reduces to the Gaussian measure. In general, the stochastic process $\beta(\cdot)$ is the solution of a system of stochastic differential equations (SDEs) of the Itô type, related to the elliptic operator in (1),

$$d\beta = \mathbf{b}(\mathbf{x}, t)\, dt + \sigma(\mathbf{x}, t)\, d\mathbf{W}(t). \tag{3}$$

Here $\mathbf{W}(t)$ represents the n-dimensional standard Brownian motion (or Wiener process); see [10, 29], e.g., for generalities, and [32] for related numerical treatments. As is known, the solution to (3) is a n-dimensional stochastic process, $\beta(t, \omega)$, where ω, usually not indicated explicitly in probability theory, denotes the "chance variable", which ranges on an underlying abstract probability space. The drift vector, $\mathbf{b}$, and the diffusion matrix, σ, in (3), are related to the coefficients of the elliptic operator in (1) by $\mathbf{b} = (b_1, \ldots, b_n)^T$, and $\sigma\sigma^T = \mathbf{a}$, with $\sigma = \{\sigma_{ij}\}_{i,j=1,\ldots,n}$, $\mathbf{a} = \{a_{ij}\}_{i,j=1,\ldots,n}$.

The representation in Eq. (2) can be generalized to deal with problems on *bounded* domains, say $\Omega \subset \mathbf{R}^n$, where given boundary data $u(\mathbf{x}, t)|_{\mathbf{x}\in\partial\Omega} = g(\mathbf{x}, t)$ of the Dirichlet type are prescribed. Thus, the following representation holds, for the solution of the problem, being now continuous and bounded on $\overline{\Omega} \times [0, T]$,

$$\begin{aligned} u(\mathbf{x}, t) &= E\left[f(\beta(t))\, e^{-\int_0^t c(\beta(s), t-s)} ds\, \mathbf{1}_{[\tau_{\partial\Omega} > t]} \right] \\ &+ E\left[g(\beta(\tau_{\partial\Omega}), \tau_{\partial\Omega})\, e^{-\int_0^{\tau_{\partial\Omega}} c(\beta(s), t-s)} ds\, \mathbf{1}_{[\tau_{\partial\Omega} < t]} \right]. \end{aligned} \tag{4}$$

Here $\tau_{\partial\Omega}$ denotes the first exit (or hitting) time of the path $\beta(\cdot)$, started at $(\mathbf{x}, t)$, when $\partial\Omega$ is crossed, and $\mathbf{1}_{[\tau > t]}$ is the characteristic function, which takes the value 1 or 0, depending whether $\tau_{\partial\Omega}$ is or is not greater than t.

The solution to the linear inhomogeneous problem

$$\frac{\partial u}{\partial t} = Lu - c(\mathbf{x}, t)u + F(\mathbf{x}, t), \tag{5}$$

where $F(\mathbf{x}, t)$ is a bounded continuous function of $\mathbf{x}$ and t, can also be represented probabilistically, using the related Green function, which, in turn, can be represented as above, being the solution to the associated homogeneous problem (e.g., see [3, 4]).

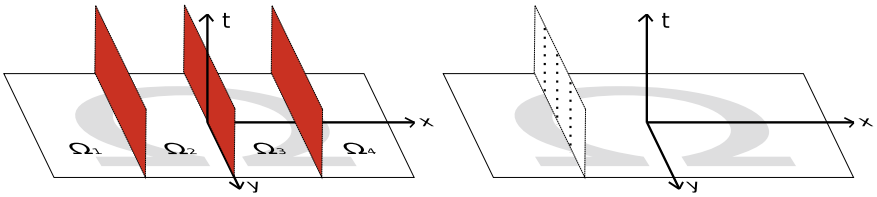

Fig. 1 A sketchy diagram illustrating the main steps of the algorithm in 2D: The figure on the left shows how the domain decomposition is done in practice. The figure on the right shows the points where the solution is computed probabilistically; these are used afterwards as nodal points for interpolation

2.3 The Numerical Method

The algorithm consists of three steps. To illustrate how it works, in Fig. 1 a sketchy diagram is plotted where such steps are shown for a two-dimensional problem. The first step consist in computing the solution at a few points by a probabilistic Monte Carlo-type method, based on averaging over certain random paths. This is done on some chosen *interfaces*, located inside the space-time domain $D := \Omega \times [0, T]$, where $\Omega \subset \mathbf{R}^n$. In the following, such interfaces are obtained, for simplicity, partitioning the domain into subdomains as $D_i := [x_{i-1}, x_i] \times \Omega_0 \times [0, T]$, being $\Omega_0 \subset \mathbf{R}^{n-1}$. For instance, in $\mathbf{R}^2$ this corresponds to divide the domain in slices where the interfaces are parallel to y-axis. For complex domains, a proper partitioning algorithm may be employed to define such interfaces. Once the solution has been computed, the second step is interpolating on such points, considered as interpolation nodes, thus obtaining continuous approximations of interfacial values of the solution. The third step, finally, consists in computing the solution inside each subdomain, which task can be assigned to separate processors. This can be realized resorting to local solvers, which may use classical numerical methods, such as finite differences or finite elements methods.

2.3.1 Probabilistic Part

The purpose of this step is to compute the sought solution at a few single points, inside the space-time domain. Computing the solution at a high number of points so as to cover a full computational domain is also possible but is exceedingly expensive, even though this approach could be pursued when the number of the available processors is extremely high. This can be done assigning the task of computing the solution at a set of points to different processors. The Monte Carlo method is, in fact, capable of fully exploiting massively parallel architectures. Moreover, it is scalable to an arbitrary number of processors as well as naturally fault tolerant.

When the parabolic equations are linear, a given number of random paths have to be generated, which obey the SDE in (3), tracking them until they either touch the

boundary for the first time or else reach a prescribed final time, t. The former case occurs in initial-boundary value problems (e.g., with Dirichlet boundary conditions), while the latter case occurs in both a purely initial value problem, and a initial-boundary value problems. The solution to the equation at a given point, $(\mathbf{x}, t)$, can then be obtained by means of the Feymann-Kac formula in (4) or (2). In practice, the expected value is replaced by an arithmetic mean, since we must deal with a finite sample size, N. An alternative strategy to evaluate the solution was proposed in [37] for initial-boundary problems, which requires generating a random exponential time, S, obeying the probability density $P(S) = c \exp(-cS)$ for every random path. Then, depending on whether $S < t$ or not, the given path $\beta(t)$, contributes or not to the solution. Therefore, the solution is computed as

$$u(\mathbf{x}, t) = E[f(\beta(t))]. \tag{6}$$

In practice, the expected value above must be replaced necessarily by a finite sum, and moreover the stochastic paths are actually simulated resorting to suitable numerical schemes. Thus, approximately,

$$u(\mathbf{x}, t) = \frac{1}{N} \sum_{j=1}^{N} f(\beta_j^*(t)), \tag{7}$$

where N is the sample size, and β^* is the stochastic path with discretized time. Such a discretization procedure unavoidably introduces two sources of numerical error. The first one is the pure Monte Carlo statistical error, which it is known to be of order $O(1/\sqrt{N})$ when N goes to infinity. The second error is due to the fact that the ideal stochastic path, $\beta_j(\cdot)$, has to be approximated, discretizing time, by some numerical scheme yielding the paths $\beta_j^*(\cdot)$. The truncation error made in solving numerically the stochastic differential equation (3), obviously depends on the specific scheme chosen, see [32], e.g. Among these are the Euler scheme, which was used here to simulate numerically Eq. (3). Such scheme is well known to have a truncation error of order $O(\Delta t^\alpha)$, where $\alpha = 1/2$ or $\alpha = 1$, understood in the "strong" or "weak" sense, respectively [32].

For the case of a boundary-value problems, a new source of numerical error should be taken into account. In fact, for the purpose of illustration let us consider the Dirichlet problem for the one-dimensional heat equation, in presence of a constant sink term, $c > 0$,

$$\begin{aligned} &\frac{\partial u}{\partial t} = \frac{\partial^2 u}{\partial x^2} - cu, \quad a < x < b,\ t > 0 \\ &u(a, t) = 0,\ u(b, t) = 0 \\ &u(x, 0) = f(x). \end{aligned} \tag{8}$$

The solution can be computed as

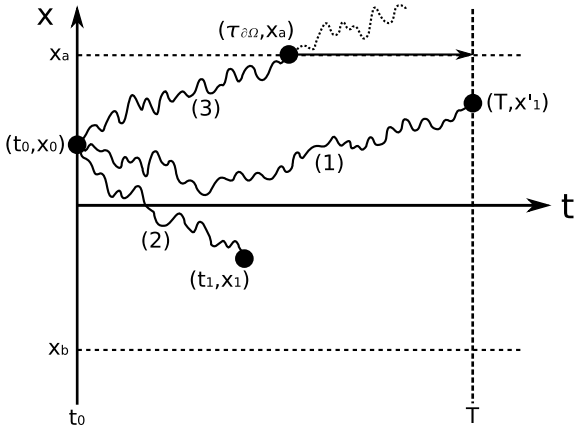

Fig. 2 The three possible scenarios for a random path, for the one-dimensional problem in (8). In (1), the random time is greater than the final time, T; in (2), the random time turns out to be smaller than T; in (3), the first exit time is smaller than both the random and the final time

$$u(\mathbf{x}, t) = \frac{1}{N} \sum_{j=1}^{N} f(\beta_j^*(t)) \mathbf{1}_{[S_j > \tau_\Omega]}. \tag{9}$$

In Fig. 2, we sketched the three possible scenarios the random paths $\beta_j^*(t)$ can undergo. Note that for the random paths of the type labelled with (3) in Fig. 2, it is required to evaluate precisely the first exit time out of the boundary. Such a task is however by far nontrivial, since $\tau_{\partial\Omega}$, in general, will be estimated numerically, and hence will be affected by numerical errors. Indeed, numerical experiments show that the error in estimating it may dominate over the other sources of numerical errors, and is therefore of paramount importance to assess accurately such a quantity.

In practice, the probability that a given approximate path exits the boundary between two consecutive time steps, is nonzero, and then it is possible that the true exit time might be systematically overestimated. This circumstance has been pointed out in several occasions, see, e.g., [12, 36, 41].

In [26], it was estimated that, due to the presence of boundaries, the weak convergence of the naive Euler scheme in evaluating (9) is reduced to $O(\Delta t^{1/2})$, being Δt the time step used in solving numerically the SDE (3). To reduce such an error (ideally, to recover the convergence order achieved in the absence of boundaries), it becomes crucial to evaluate accurately the first exit time, adopting suitable numerical strategies.

Among the various possibilities considered in the literature, we chose to implement that proposed in [34] for one-dimensional problems, which is based on a theoretical approximation of the exit probability. To solve two-dimensional problems on the square, the value of the exit probability on Ω has been taken as the maximum among the four hitting probabilities that a trajectory first exits the four possible boundary-sides. This consists on an approximation of the true two-dimensional exit probability, but it suffices in order to achieve a numerical error now well below the statistical error.

In fact, for general $n-$dimensional diffusion processes, there exist other interesting alternatives to approximate the first exit time. In [16, 36], Buchmann and Petersen presented an algorithm to simulate stopping diffusion processes to obtain again weak order one using the Euler scheme. More recently, Gobet and Menozzi proposed in [27] a new simpler and computationally more efficient approach, of weak order $o(\Delta t^{1/2})$. The idea consists of stopping the simulation of discrete paths generated by means of the Euler scheme, when such paths exit through a conveniently modified domain, shrinking (or shifting) the boundary of Ω in the direction of the inward normal. The amplitude of such shrinking (or shifting) depends on, among other values, the diffusion coefficient of the process and the square root of the time step used in the numerical scheme. Given the general applicability and simplicity of this approach, it is specially convenient when dealing with more complex geometries.

As mentioned before, for the linear case, in order to evaluate the probabilistic representation we resort to numerical simulations of the Monte Carlo type, considering a finite size sample, N. In practice, we replace the expected value with an arithmetic mean, which is known to provide the best unbiased estimator [28]. The error made in doing so is statistical in nature and of the order of $N^{-1/2}$.

Finally, a carefully analysis of the computational cost associated to this part of the algorithm is provided in the next section, when dealing with general semilinear problems.

2.3.2 Interpolation in Space-Time

Let assume that we have already computed the values of the sought solution at some points on the interfaces $x = x_i$, by the previous Monte Carlo approach. These are the points $(x_i, \mathbf{y}_j, t_k)$, where $\mathbf{y}_j \in \Omega_0 \subset \mathbf{R}^{n-1}$, for every fixed i, and very few j's and k's. A number of numerical schemes can be adopted to interpolate in the $n-1$ dimensional space Ω_0. The simplest method of obtaining multivariate interpolation is to consider a univariate method and derive from it a multivariate method by tensor product. In practice, given $n-1$ set of points, the tensor product interpolation finds the corresponding interpolation coefficients solving repeatedly univariate interpolation problems as described in [20]. For the one-dimensional examples given in this section we used the Chebyshev polynomials, while for two-dimensional examples, a tensor product interpolation based on cubic splines was adopted [9]. Here the nodal points are uniformly distributed on Ω_0, and a not-a-knot condition has been imposed, which means imposing continuity of the third derivative at the boundary. When the number of nodal points, n, is the same along each dimension, interpolating at a single point (y_j, t_k) requires $n+1$ spline calculations to obtain the spline coefficients, and then evaluating the spline value at $n+1$ points. The computational cost for calculating the spline coefficients is known to be of order $O(n)$, while for evaluating the spline value it is $O(\log n)$. The interpolation error when the interpolating function is sufficiently smooth (C^8 at least) is of order of $O(h^4 + l^4)$ [40], where h and l are the widths of the interpolating grid in the y and t axes, respectively.

2.3.3 Local Solver

Once that continuous interfacial approximations of the solution have been obtained upon interpolation on the previously computed nodes (by Monte Carlo), we can solve the original problem *on each* subdomain, D_i, *independently* of each other, since a full decoupling has been realized. Hence, the numerical treatment on each subdomain can be accomplished by a local solver, which can also be different from all the others. In the numerical examples below, we used a solver based on the LU factorization.

2.3.4 Sources of Parallelization

We stress that in practice there are three sources of parallelization, namely (1) the Monte Carlo generation of internal node functional values (even each single sample can be ran on independent processors), (2) the interpolation part (the interpolation on each interface can be accomplished independently), and (3) the domain decomposition solution (that can be assigned to independent local solver). Moreover, each of such three stages enjoyed a natural fault tolerant property: (1) if a number of processors fail in the Monte Carlo simulations, it will be enough to ignore the result from them using the remaining samples. Hence, at a price of a small additional errors, the algorithm will still provide meaningful results. (2) Failure of processors computing interpolated values of the solution on some interfaces may only imply to neglect, temporarily, the solution on those subdomains having such interfaces as part of their boundary. (3) Failure of processors responsible for the numerical solution on some sub-domains can also be temporarily neglected, while the solution computed by the local solvers on the remaining sub-domains will be computed correctly. Note that on the interfaces and on the sub-domains where the processors failed, the solution can be computed restarting again the algorithm.

For numerical examples, see [3].

2.4 Summary

We have described the PDD algorithm for solving linear parabolic partial differential equations in any space dimension, where a domain decomposition approach is used to split the given space-time domain into as many subdomains as the number of available processors. The solution at the interfaces that separates the subdomains are computed after interpolating on the nodal points for which the solution is previously obtained probabilistically via Monte Carlo. Such probabilistic computation consists of evaluating averages on suitably generated random paths, without the need of deploying a computational mesh. Moreover, every available processor is devoted to compute the solution at one of such interfaces, without introducing communication nor synchronization among other processors. This fact is of paramount importance, because once the solution on the interfaces has been independently computed, fully

in parallel, the remaining task of evaluating the solution inside each subdomain turns out to be totally independent as well, resulting in a complete, communication- and synchronization-free, fully scalable algorithm.

3 Semilinear Parabolic Problems

3.1 Introduction

Probabilistic representations do exist for some elementary *semilinear* parabolic equations. Indeed, in [33] H.P. McKean derived the representation formula

$$u(x,t) = E[\prod_{i=1}^{k_t(\omega)} f(x_i(\omega,t))] \tag{10}$$

for the KPP equation

$$u_t = u_{xx} + u(u-1), \quad x \in \mathbf{R},\ t > 0, \tag{11}$$

subject to the initial value $u(x,0) = f(x)$ (see also [25, 35, 38]), where $k_t(\omega)$ represents a time-dependent random variable that accounts for the number of branches of the underlying branching diffusion process. Later, we have found a similar representation (see also [3, 4]) for the solution of a more general semilinear parabolic problem, given by

$$\frac{\partial u}{\partial t} = Lu - cu + \sum_{j=2}^{m} \alpha_j u^j, \tag{12}$$

where L is a general linear elliptic operator, say $L := a_{ij}(\mathbf{x},t)\partial_i\partial_j + b_i(\mathbf{x},t)\partial_i$, with continuous bounded coefficients, $m \geq 2$ is an integer, $\alpha_j \geq 0$, $\sum_{j=2}^{m} \alpha_j = 1$, and c is a positive constant. Such a representation is based on generating *branching* diffusion processes, associated with the elliptic operator in Eq. (12), and governed by an exponential random time, S, with probability density $p(S) = c\ \exp(-cS)$.

In this section, we explain how the probabilistic representation was extended to deal with a wider class of semilinear parabolic problems (see also [5]), whose general form is given by

$$\frac{\partial u}{\partial t} = Lu + f(u,x,t),\ x \in \mathbf{R}^n,\ t > 0$$
$$u(x,0) = g(x), \tag{13}$$

where

$$f(u,x,t)=\sum_{j=2}^{m} c_j(x,t)u^j,$$

where the $c_j(x,t)$ are continuous given functions. It is worth to observe that this generalizes further the previous representation in (12), explained in [3, 4], since it accounts for the following aspects: A constant potential term such as $-cu$ is not required anymore; the coefficients multiplying the nonlinear terms, $c_j(x,t)$, can be chosen arbitrarily, hence overcoming the constraint imposed in the previous representation consisting in $\sum_{j=2}^{m} c_j(x,t)=1$, and finally the initial data $g(x)$ may now be chosen negative, or greater than 1.

Here it is the outline of the section. First, the generalized probabilistic representation is presented. Then, a qualitative study of the numerical errors is accomplished analyzing a few relevant test examples. Later, some numerical examples are shown, where the high efficiency of the PDD method comparing with classical methods is illustrated. Finally, we summarize the more relevant findings to close the applicability of the PDD method to parabolic problems.

3.2 A Generalized Probabilistic Representation for Semilinear Parabolic Problems

In order to generalize the class of parabolic problems amenable to a probabilistic representation in terms of branching diffusion processes, it becomes more convenient to rewrite Eq. (13) in an integral form. This can be done readily resorting to the Duhamel principle [21] for inhomogeneous initial-value parabolic problems, and yields

$$u(x,t)=\int_{\mathbf{R}^n} dy\, g(y)\, p(x,t,y,0)+\int_0^t\int_{\mathbf{R}^n} ds\, dy\, f(u(y,s),y,s)\, p(x,t,y,s), \tag{14}$$

where $p(x,t,y,\tau)$ is the associated Green's function, satisfying the equation

$$\begin{aligned}\frac{\partial p}{\partial t}&=Lp,\quad x\in\mathbf{R}^n,\quad t>\tau\\ p(x,\tau,y,\tau)&=\delta(x-y).\end{aligned} \tag{15}$$

The main difference with the previous representation obtained in (12) rests on the absence of the constant potential term $-cu(x,t)$. Such a term was crucial, since it allowed to obtain a probabilistic representation based on generating *branching* diffusion processes governed by an exponential random time, S, with density probability $p(S)=c\,\exp(-cS)$ (see previous sections, and [3, 4]). In the following we describe the main strategy derived in [5] (referred to as *Strategy B*), capable to overcome such a constraint generalizing further the aforementioned representation.

3.2.1 Probabilistic Representation

A way to obtaining a probabilistic representation for the problem in Eq. (13) consists in sampling both terms of the integral equation (14), by introducing a two-point discrete random variable ξ taking the values 0, and 1 with probability $P(0) = q,\ P(1) = 1 - q$. Therefore, the integral equation (14) can be rewritten as follows,

$$u(x,t) = q \int_\Omega dy\, \tilde{g}(y)\, p(x,t,y,0) + (1-q) \int_0^t \int_\Omega ds\, dy \sum_{j=2}^{m} \tilde{c}_j(y, t-s) u^j(y, t-s)\, p(x,s,y,0), \quad (16)$$

where $\tilde{g}(x) = g(x)/q$, and $\tilde{c}_j(x,t) = c_j(x,t)/(1-q)$. The probabilistic representation can be readily found and has the form

$$u(x,t) = E\left[\tilde{g}(\beta(t))\delta(\xi)\right] + E\left[\eta(t)\tilde{c}'_\alpha(\beta(tS), t(1-S))\, u^\alpha(\beta(tS), t(1-S))\delta(\xi-1)\right], \quad (17)$$

where the expectation is given by the measure generated by the following random variables: the diffusion processes $\beta_i(\cdot)$, the time S, a random time uniformly distributed; and α, a discrete random variable taking on the values between 2 and m with equal probability $p = 1/(m-1)$, $\tilde{c}'_\alpha = (m-1)\tilde{c}_\alpha$, and $\eta(t) = t$. The equation above is not in a closed-form but it can be recursively expanded, to yield

$$\begin{aligned} u(x,t) &= E\left[\tilde{g}(x_0(t))\,\delta(\xi_0)\right] \\ &+ E\left[\eta(t)\tilde{c}'_{\alpha_1}(y_1(tS_0), t(1-S_0)) \prod_{i=1}^{\alpha_1} \tilde{g}(x_i(t(1-S_0)))\,\delta(\xi_i)\delta(\xi_0-1)\right] \\ &+ E\left[\eta(t)\eta(t(1-S_0))\tilde{c}'_{\alpha_1}(y_1(tS_0), t(1-S_0))\right. \\ &\times \tilde{c}'_{\alpha_2}(y_2(t(1-S_0)S_1), t(1-S_0)(1-S_1)) \prod_{i=2}^{\alpha_1} g(x_i(t(1-S_0))))\,\delta(\xi_i) \\ &\left.\times \prod_{j=\alpha_1+1}^{\alpha_1+\alpha_2+1} g(x_j(t(1-S_0)(1-S_1)))\delta(\xi_j)\delta(\xi_1-1)\delta(\xi_0-1)\right] + \cdots, \end{aligned} \quad (18)$$

where x_i and y_j corresponds to the position of the i-th branch at the final time t and the position of the j-th splitting event, respectively.

While in Eq. (17) the expectation is taken with respect to the measures generated by β, ξ and α (which would be enough if consisted of a closed-form), the expectation in Eq. (18) is rather taken from the underlying measure corresponding to β (i.e., by x_i

and y_i), again, and the infinite sequence of random variables $\xi_0, \xi_1, ...$, and $\alpha_1, \alpha_2, ...$, that the determine the final configuration of every random tree generated.

Therefore, as we illustrate next, this solution can be obtained as the expectation over suitable random trees of a given multiplicative functional of the initial condition, being given now as follows:

$$u(x,t) = E\left[\prod_{i=1}^{Ne(\omega)} \eta(t\bar{S}_i(\omega))c_{\alpha_i(\omega)}(y_i(\omega), t\bar{S}_i(\omega)) \prod_{l=1}^{k(\omega)} g(x_l)\right]. \tag{19}$$

Here $k(\omega)$ and $Ne(\omega)$ are random variables that represents the number of branches at final time t, and the number of splitting events obtained when generating a particular random tree, respectively. Note that $P\{Ne(w) = i\} = (1/2)^i$. In [4], it is shown that $P(k,m)$, the probability of finding a random tree with k branches, being m the number of children, is given by

$$P(k,m) = q^k(1-q)^{Ne}\frac{1}{m\,Ne+1}\binom{m\,Ne+1}{Ne}. \tag{20}$$

By $\bar{S}$ we denote the corresponding global random time obtained by summing conveniently the random times S_i according to the specific structure of the generated random tree. It is worth to observe that such trees are used as a tool to construct the structure representing a given partial contribution to the solution, allowing afterward to follow easily how the arguments of the functions are exchanged when solving recursively Eq. (17).

To illustrate how this representation can be implemented in practice for solving a particular problem, let consider the following equation,

$$\frac{\partial u}{\partial t} = \frac{\partial^2 u}{\partial x^2} + u^2, \quad x \in \mathbf{R}, t > 0 \tag{21}$$

$$u(x,0) = f(x). \tag{22}$$

From Eq. (17), the probabilistic representation is given by

$$u(x,t) = E\left[\tilde{g}(\beta(t))\delta(\xi)\right] + E\left[\eta(t)\,u^2(\beta(tS), t(1-S))\delta(\xi-1)\right], \tag{23}$$

or in a more compact format, using Eq. (19) for the expectation value over random trees of a given multiplicative functional in Eq. (23), by

$$u(x,t) = E\left[\prod_{i=1}^{Ne(\omega)} \eta(t\bar{S}_i(\omega)) \prod_{l=1}^{k(\omega)} g(x_l)\right]. \tag{24}$$

Every random tree is built generating a sequence of interconnected binary random variables, ξ_i, branching off from the previous one as follows: Let ξ_1 the random

variable associated to the root of the tree. Only when ξ_1 takes value 1 with probability $P(1) = 1 - q$, two new random variables denoted by $\xi_{2,3}$ (child nodes of the root), are created. These new variables proceed further creating other nodes governed by the same rule, until no random number ξ_i takes anymore the value 1. At this point the procedure is concluded, giving rise to a random tree characterized by k branches or leaves, and Ne splitting events.

The nodes of the tree are labeled in binary format according to their ancestors as follows: A given node with label $[a_0 a_1 a_2 ... a_N]$, where $a_i = 0, 1$, is connected to the set of nodes $\{[a_0], [a_0 a_1], [a_0 a_1 a_2], \ldots, [a_0 a_1 a_2 \cdots a_{N-1}]\}$. The global time random variable $\bar{S}$ associated to a given tree with k branches is given by

$$\bar{S} = \prod_{i=1}^{2^{k-1}-1} S_j^{\gamma_j}, \quad \gamma_l = \sum_{j=l+1}^{2^{k-1}-1} \nu_j \langle j|l \rangle, \; l = 1, \ldots, 2^{k-1} - 1 \tag{25}$$

where ν_l is 0, or 1 depending on whether the tree contains or not the node l. The function $\langle \cdot | \cdot \rangle$ is defined as follows,

$$\langle j|l \rangle := \begin{cases} 1 \text{ if} T_j^{[l]} = l \\ 0 \text{ otherwise.} \end{cases}, \tag{26}$$

where both, j and l are numbers written in binary format, and $T_j^{[l]}$ is an operator that truncates the number j to their most significant $[l]$ digits, where $[l]$ is the number of digits of l. By example, let $j = [a_0 a_1 a_2 ... a_N]$, then $T_j^{[l]} = [a_0 a_1 ... a_{[l]-1}]$.

Figure 3 shows the different random trees obtained with $k = 4$, and $Ne = 3$, and their corresponding labels according to the rule defined above.

Finally, note that in practice, a series arises when evaluating the solution of Eq. (18) by Monte Carlo, when attempting to summing up the partial contribution of trees of different branches. This series is infinite but in practice, we always end up with a finite series because the probability of obtaining trees with an increasing number of branches is increasingly smaller and therefore, their contribution is negligible up to defining a tolerance for the numerical error. In the case of asymptotic divergent series that may appear, we resort to approximation techniques such as the Padé approach [11, 13], to approximate conveniently the sum of the aymptotic series. In this method, called Padé approximation, the idea is to replace the asymptotic divergent power series by a sequence of rational functions converging towards the solution u, as follows: Each rational function, P_M^N, given as a ratio of two polynomials of degree N and M, is constructed such that the first $N + M + 1$ terms of its series expansion match the first $M + N + 1$ terms of the divergent power series. The hope is that $P_M^N \to u$ as $N, M \to \infty$.

For the computational complexity and numerical results, we refer to the reader to [4].

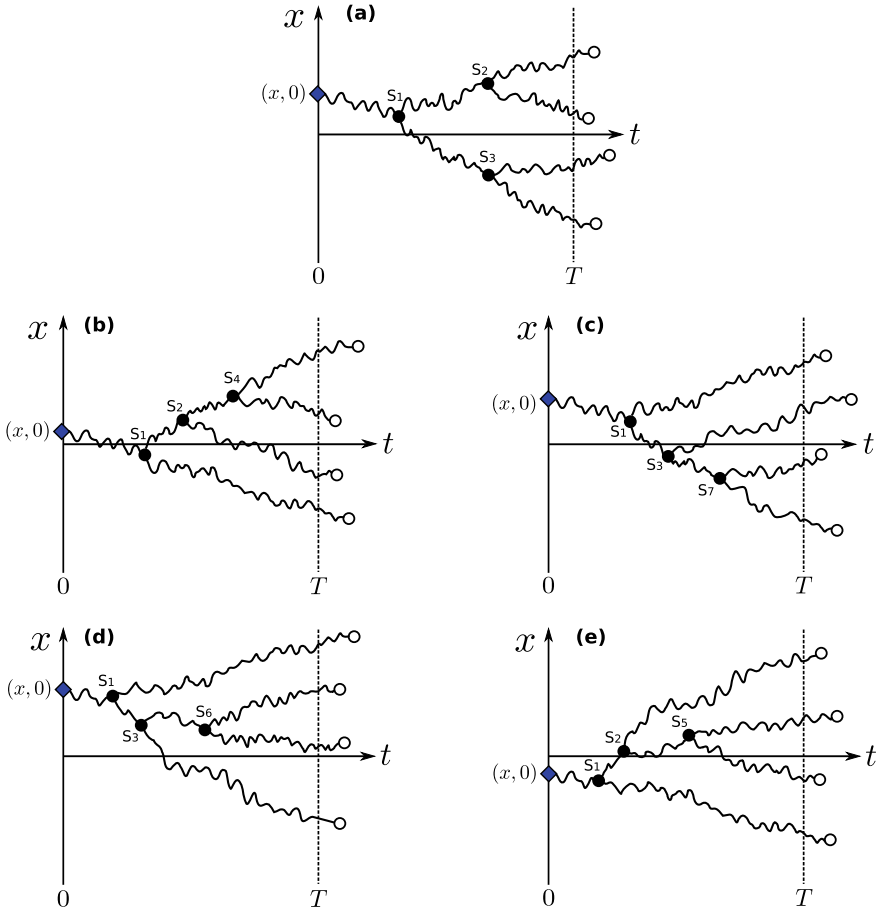

Fig. 3 Configuration diagram for the case of 4 branches and 3 splitting events. Here S_i is a random time uniformly distributed between the previous generated time, and the final time, T. The corresponding labels i of the random time S_i are defined according to the rule explained in the text

3.3 Summary

The class of semilinear parabolic problems amenable to a probabilistic solution was expanded by introducing suitable generalized random trees. The probabilistic computation consists of evaluating averages on the generated random tree, which plays a role similar to that of a random path in linear problems. The new representation allows treatment of semilinear problems without a potential term, with arbitrary coefficients multiplying the nonlinear term, and arbitrary initial data, including negative definite and greater than one. The implementation requires computing the solution through a series where the coefficients represent the partial contribution to the solution coming from generated random trees with any number of branches. Summation of divergent

asymptotic series expansions cannot be summed simply by a sequence of partial sums. Nevertheless, numerical experiments show that (see [4], in many cases, the asymptotic series can be approximated quite accurately by the Padé approximant [11, 13].

The new probabilistic representation has been used successfully as a crucial element for implementing a suitable probabilistic domain decomposition method. In fact, at the time when these simulations were conducted, numerical examples showed the excellent scalability properties of the PDD algorithm in large-scale simulations, where up to 512 processors were used on a high performance supercomputer.

4 The Vlasov-Poisson System for Plasma Physics

4.1 Introduction

To illustrate the potentiality behind these probabilistic techniques for solving numerically transport equations, in this section the method is particularized to the Vlasov-Poisson system of equations. We have considered merely periodic boundary conditions in space. This has been done for simplifying as much as possible the probabilistic representation of the solution, and thus to help the reader to understand easily such a representation. It is theoretically well-known [29, 35], that dealing with general boundary conditions requires estimating various stochastic quantities, which in turn introduces new sources of numerical errors, that we tried to avoid at this stage. The ultimate goal of this section is to show the feasibility of this method as a complementary method capable to speed up the Vlasov-Poisson simulations in a parallel environment, and this was done simplifying the nature of the boundary data as much as possible. The generalization of the method to situations where more complicated geometries and boundary conditions are imposed, is left for a future work.

Being the boundary conditions periodic in space, it becomes natural to solve numerically the problem in Fourier space for the spatial coordinates. Moreover, it turns out that for dealing accurately with the filamentation phenomenon, it is convenient to analyze also the problem in Fourier space for velocities [23]. That is why in practice the numerical method to be presented in this section is fully analyzed in Fourier space. Apart from such a mathematical reason, in some practical experimental situations one could be interested not to know the distribution function, but rather the spectrum energy or any other related quantities, being therefore natural to investigate the problem in Fourier space. Furthermore, while the probabilistic representation introduced in this section was obtained in Fourier space, there already exists representations in configuration space [43], which may potentially be used to generalize further what has been done in this section.

This section is organized as follows. Section 4.2 concerns the probabilistic representation for the Vlasov-Poisson system of equations. Here such a representation is derived in the Fourier space for arbitrary dimensions, and the validation of the

representation is done analyzing the classical linear Landau damping. In Sect. 4.3, it is explained how the probabilistic representation can be used in practice, and which are the associated numerical errors. First the algorithm is described, and analyzed the numerical error, then the computational cost is estimated, and finally several numerical tests consisting in typical problems considered often in the literature are given, focusing in both, the accuracy and performance of the method. To conclude we summarize the main results and discuss potential directions for future research.

4.2 *Probabilistic Representation for the Vlasov-Poisson System*

The Vlasov-Poisson system describes the temporal evolution of charged particles subject to the self-generated electric field created by the charged particles inside the plasma. It is actually a system of equations, consisting of a kinetic equation, the Vlasov equation which describes the transport of charged particles, along with the classical Poisson equation for electrostatic potential. The solution of the equation is the distribution function of particles in the phase space, where the independent variables are space, x, velocity, v, and time t. Consider the two-species Vlasov-Poisson equation in d dimensions conveniently adimensionalized,

$$\begin{aligned} \frac{\partial f^{(1)}}{\partial t} + \bar{v} \cdot \nabla_{\bar{x}} f^{(1)} - \nabla\phi \cdot \nabla_{\bar{v}} f^{(1)} = 0, \\ \frac{\partial f^{(2)}}{\partial t} + \bar{v} \cdot \nabla_{\bar{x}} f^{(2)} + \frac{1}{m_2} \nabla\phi \cdot \nabla_{\bar{v}} f^{(2)} = 0, \\ \triangle_{\bar{x}} \phi = -\left[\int f^{(1)} d\bar{v} - \int f^{(2)} d\bar{v} \right], \end{aligned} \tag{27}$$

along with a 2π-periodic boundary condition for the space variables, $f^{(i)}(\bar{x}, \bar{v}, t) = f^{(i)}(\bar{x} + 2\pi, \bar{v}, t)$, decay to zero as $|\bar{v}| \to \infty$ with sufficiently high rate for velocity variables, and suitable initial conditions for both, $f^{(i)}$, and the space average over a period of the electric field $\bar{E} = -\nabla\phi$. In [31] it has been proved that in order the Vlasov-Poisson equations provide a complete description of the plasma, such a quantity should be kept fixed to zero for all time. Finally, being $f^{(i)}$ a density probability, it holds that $\int_0^{2\pi} \int_{-\infty}^{\infty} d\bar{x}\, d\bar{v}\, f^{(i)} = 1$.

Since the prescribed boundary condition for space variables are periodic, it is more natural to analyze the problem in Fourier space. Moreover, it turns out to be more convenient to transform as well to the Fourier space for velocities, in order to mitigate the well known filamentation effect in velocity space observed in the solution for sufficiently long times [23]. Because of the periodicity in the space variables, the transformation in space is discrete, while for velocities is continuous. Then, transforming Eq. (27), yields

$$\frac{\partial F_{\bar{k}}^{(1)}}{\partial t} - \bar{k} \cdot \nabla_{\bar{\xi}} F_{\bar{k}}^{(1)} - \bar{k} \cdot \bar{\xi}\, \hat{\phi}_{\bar{k}} * F_{\bar{k}}^{(1)} = 0,$$
$$\frac{\partial F_{\bar{k}}^{(2)}}{\partial t} - \bar{k} \cdot \nabla_{\bar{\xi}} F_{\bar{k}}^{(2)} + \frac{1}{m_2} \bar{k} \cdot \bar{\xi} \hat{\phi}_{\bar{k}} * F_{\bar{k}}^{(2)} = 0,$$
$$-|\bar{k}|^2 \hat{\phi} = -\left[F_{\bar{k}}^{(1)}(0,t) - F_{\bar{k}}^{(2)}(0,t) \right], \quad |\bar{k}| \neq 0, \tag{28}$$

where

$$F_{\bar{k}}^{(i)}(\bar{\xi}, t) = \int_{\mathbb{R}^d} d\bar{v} \int_0^{2\pi} d\bar{x}\, e^{-i\bar{\xi}\cdot\bar{v}} e^{-i\bar{k}\cdot\bar{x}} f^{(i)}(\bar{x}, \bar{v}, t), \quad i = 1, 2, \tag{29}$$

$$\hat{\phi}_{\bar{k}}(t) = \int_0^{2\pi} d\bar{x}\, e^{-i\bar{k}\cdot\bar{x}} \phi(\bar{x}, t). \tag{30}$$

Here $\bar{k}$, and ξ corresponds to the conjugate variables of $\bar{x}$, and $\bar{v}$, respectively, being $\bar{k}$ a discrete variable, while ξ is continuous, and $*$ denotes the convolution operator for $\bar{k}$. Note that passing to the Fourier space becomes crucial to be able to reduce the system of equations into a single one. Moreover, this is mandatory for the purpose of finding a probabilistic representation for the solution of Eqs. (27), applying directly the strategy described in [6] for the semilinear transport equation. The first step towards the probabilistic representation requires rewriting the system of equations (28) in integral form, and is given by

$$F_{\bar{k}}^{(i)}(\bar{\xi}, t) = F_{\bar{k}}^{(i)}(\bar{\xi} + t\bar{k}, 0) + \rho_i \int_0^t ds \sum_{\substack{\bar{k}'=-\infty \\ \bar{k}'\neq 0}}^{\infty} \frac{\bar{k}' \cdot (\bar{\xi} + s\bar{k})}{|\bar{k}'|^2}$$
$$\times [F_{\bar{k}'}^{(1)}(0, t-s) - F_{\bar{k}'}^{(2)}(0, t-s)] F_{\bar{k}-\bar{k}'}^{(i)}(\bar{\xi} + s\bar{k}, t-s), \tag{31}$$

where $\rho_1 = 1$, and $\rho_2 = -1/m_2$. Both, the static and dynamic probabilistic representation can be derived similarly to the case of the semilinear transport equation. Here we describe the dynamic representation, since the static one is straightforward. Equation (31) can be written probabilistically as follows,

$$F_{\bar{k}}^{(i)}(\bar{\xi}, t) = E\left[\tilde{F}_{\bar{k}}^{(i)}(\bar{\xi} + t\bar{k}, 0) \delta(\zeta) \right]$$
$$+ E\left[\eta(t)\, g^{(i)}(\bar{k}, \bar{k}', \bar{\xi}, S)\, F_{\bar{k}'}^{(1)}(0, t-S)\, F_{\bar{k}-\bar{k}'}^{(i)}(\bar{\xi} + S\bar{k}, t-S) \delta(\rho - 1) \delta(\zeta - 1) \right]$$
$$+ E\left[\eta(t) g^{(i)}(\bar{k}, \bar{k}', \bar{\xi}, S)\, F_{\bar{k}'}^{(2)}(0, t-S)\, F_{\bar{k}-\bar{k}'}^{(i)}(\bar{\xi} + S\bar{k}, t-S) \delta(\rho - 2) \delta(\zeta - 1) \right], \tag{32}$$

where

$$g^{(1)}(\bar{k},\bar{k}',\bar{\xi},S)=2\rho_1\frac{\bar{k}'\cdot(\bar{\xi}+S\bar{k})}{(1-q)p(\bar{k})|\bar{k}'|^2},$$
$$g^{(2)}(\bar{k},\bar{k}',\bar{\xi},S)=-2\rho_1\frac{\bar{k}'\cdot(\bar{\xi}+S\bar{k})}{(1-q)p(\bar{k})|\bar{k}'|^2}, \tag{33}$$

and $\tilde{F}^{(i)}_{\bar{k}}=F^{(i)}_{\bar{k}}/q$. Here four random variables have been introduced, those are: ρ is a two-point, $\rho=1,2$, discrete random variable equally distributed with probability $1/2$; S a continuous random variable uniformly distributed between 0 and t, and therefore $\eta(t)=t$; $\bar{k}'$ is a discrete random variable with density probability $p(\bar{k}')$, and finally ζ, which takes the values 0, and 1, with probability $P(0)=q$, $P(1)=1-q$, respectively. E denotes the expected value taken with respect to the density probabilities corresponding to all those four random variables.

In [24], the authors proposed a probabilistic representation of the solution of the system in (27). However, such a representation is rather stringent for practical purposes, since it requires to fulfill strong constraints in terms of the allowed initial data and time. Moreover, the density probability $p(\bar{k}')$ should be carefully chosen, hindering the task of finding a valid density for any dimension. This is related to the problem of finding admissible majorizing kernels, see [15]. Indeed, it can be readily proved that the majorizing kernel chosen in [24] is no longer valid in one dimensional problems. However, this does not mean that no solution can be found for the system of equations (27), but rather that the numerical method based on such a probabilistic representation gives rise to a divergent series, which requires further numerical treatment. In fact, in this section we show that relaxing the requirements concerning the initial condition and time, the solution is still smooth, and as explained in the previous section, we resort to Padé approximant [11, 13] for approximating the asymptotic expansion of the solution given as divergent series. Since the density probability $p(\bar{k}')$ can now be chosen freely among a suitable class of functions, this can be used to reduce the statistical error done computing numerically the solution. Typically, this corresponds to the well known variance reduction techniques often used in Monte Carlo simulations.

Note that Eq. (32) is indeed a probabilistic representation of the Vlasov-Poisson system of equations (in the sense defined previously for the transport equations), and therefore, it can be used for computing the solution at a single point $(\bar{k},\bar{\xi},t)$, without the need of any computational mesh. This can be done generating suitable random trees governed by the densities probabilities mentioned above, and taking the expected value of a corresponding multiplicative functional. For a numerical purpose, the associated numerical algorithm turns out to be specially costly for computing the solution in the whole computational domain, since a large sample size is typically required to avoid a large statistical error. However, an alternative does exist, and this will be addressed in Sect. 4.3.

4.2.1 Validation of the Representation for the Linear Theory

In order to validate analytically the probabilistic representation derived above, we consider the classical linear Landau damping. This will be done linearizing conveniently the system (27) around the equilibrium solution. Let look for a density function according to the Ansatz

$$\begin{aligned} f^{(i)}(\bar{x},\bar{v},t) &= f_0^{(i)}(\bar{v}) + \varepsilon\, f_1^{(i)}(\bar{x},\bar{v},t) + O(\varepsilon^2), \\ \phi(\bar{x},t) &= \phi_0 + \varepsilon\,\phi_1(\bar{x},t) + O(\varepsilon^2), \end{aligned} \tag{34}$$

where $\varepsilon \ll 1$. Note that ϕ_0 is intentionally set to be constant to satisfy the constraint mentioned above concerning the space average over a period of the electric field. Inserting (34) into (27), we obtain to order ε

$$\begin{aligned} \frac{\partial f_1^{(1)}}{\partial t} + \bar{v}\cdot\nabla_{\bar{x}} f_1^{(1)} - \nabla\phi_1\cdot\nabla_{\bar{v}} f_0^{(1)} &= 0, \\ \frac{\partial f_1^{(2)}}{\partial t} + \bar{v}\cdot\nabla_{\bar{x}} f_1^{(2)} + \frac{1}{m_2}\nabla\phi_1\cdot\nabla_{\bar{v}} f_0^{(2)} &= 0, \\ \triangle_{\bar{x}}\phi_1 = -\left[\int f_1^{(1)} d\bar{v} - \int f_1^{(2)} d\bar{v}\right], & \end{aligned} \tag{35}$$

with initial data $f_1^{(i)}(\bar{x},\bar{v},0) = A\, g_i(\bar{v})\cos(k_1 x)$, $i = 1, 2$, 2π-periodic boundary conditions in $\bar{x}$, and $g_i(v)$ decaying to zero as $|\bar{v}| \to \infty$ with sufficiently high rate. Applying identical mathematical treatment as done previously for the fully Vlasov-Poisson system of equations, the following integral equation for the Fourier transform $F_{\bar{k}}^{(i)}(\bar{\xi},t)$ of $f_1^{(i)}$ is obtained,

$$\begin{aligned} F_{\bar{k}}^{(i)}(\bar{\xi},t) &= F_{\bar{k}}^{(i)}(\bar{\xi} - t\bar{k},0) \\ +\rho_i \int_0^t ds\, \frac{\bar{k}\cdot(\bar{\xi} - s\bar{k})}{|\bar{k}|^2}&[F_{\bar{k}}^{(1)}(0,t-s) - F_{\bar{k}}^{(2)}(0,t-s)]\hat{g}_i(\bar{\xi}_2 - s\bar{k}). \end{aligned} \tag{36}$$

Here $\hat{g}_i$ is the corresponding Fourier transform of $g_i(\bar{v})$. In the following let consider $\bar{\xi} = 0$, and for simplicity we assume $\bar{k} = (k_1, 0, 0)$. The Fourier transform of the x-component of the electric field is given by, $\hat{E}_x(k_1,t) = -\frac{i}{k_1}[F_{k_1}^{(1)}(0,t) - F_{k_1}^{(2)}(0,t)]$. A recursive solution can be obtained for $\hat{E}_x(k_1,t)$ using Eq. (36), and yields,

$$\hat{E}_x(k_1,t) = -i\frac{1}{k_1}\Phi(k_1,t) + \sum_{j=1}^{\infty}(-1)^j\,\eta_j(\bar{k},t). \tag{37}$$

Here η_j is given by

$$\eta_j(k_1,t) = \frac{(-i)^j}{k_1^j}\int_0^t ds_1\, s_1 \int_0^{t-s_1} ds_2\, s_2 \cdots \int_0^{t-\sum_{l=1}^{j} s_l} ds_j\, s_j$$
$$\times \Phi(k_1, t-\sum_{l=1}^{j} s_l)\hat{h}(-s_1\, k_1)\hat{h}(-s_2\bar{k})\cdots\hat{h}(-s_j\bar{k}), \tag{38}$$

where $\Phi(k_1,t) = F^{(1)}_{k_1}(-t\,k_1,0) - F^{(2)}_{k_1}(-t\,k_1,0)$, and $\hat{h}(-t\,k_1) = [\hat{g}_1(-t\,k_1) + \frac{1}{m_2}\hat{g}_2(-t\,k_1)]$. Note that η_j can be obtained recursively from η_{j-1} as follows

$$\eta_j(k_1,t) = \int_0^t ds\, s\, \eta_{j-1}(k_1,t-s)\hat{h}(-s\,k_1) \tag{39}$$

Multiplying Eq. (37) by $\hat{h}(-s\,k_1)$, and integrating with respect to s, it holds that

$$\int_0^t ds\, s\, \hat{E}_x(k_1,t-s)\hat{h}(-s\,k_1) = -\hat{E}_x(k_1,t) - i\frac{1}{k_1}\Phi(k_1,t), \tag{40}$$

The integral equation above turns out to be a Volterra equation of the second kind, whose solution can be obtained readily by means of the Laplace transform. In fact, Laplace transforming Eq. (40), we obtain

$$\tilde{\hat{E}}_x(k_1,\,p) = -i\frac{1}{k_1}\frac{\tilde{\Phi}(k_1,\,p)}{D(k_1,\,p)}, \tag{41}$$

where $D(k_1,\,p)$ is given by

$$D(k_1,\,p) = 1 - \frac{1}{k_1}\frac{d\tilde{\hat{h}}}{dp} \tag{42}$$

The solution can be obtained taking the inverse Laplace transform, and is given formally by

$$\hat{E}_x(k_1,t) = \frac{1}{2\pi i}\int_{\sigma-i\infty}^{\sigma+i\infty} \tilde{\hat{E}}_x(k_1,\,p)e^{p\,t}\,dp, \tag{43}$$

where integration is taken along a line parallel to the imaginary p-axis and to the right of all singularities of the integral. Then, it holds

$$\hat{E}_x(k_1,t) = \sum_j R_j e^{p_j\,t}, \tag{44}$$

where p_j are simple poles where the function $D(k_1,\,p)$ vanishes, and R_j is the residue of $\tilde{\hat{E}}_x$ at p_j. Since the poles are in general complex, Eq. (44) can be rewritten as

$$\hat{E}_x(k_1, t) = \sum_j R_j e^{\gamma_j t + i\omega_j t}, \tag{45}$$

being $p_j = \gamma_j + i\omega_j$. Note that if $\gamma_j < 0$, all terms are exponentially damped, and the electric field behaves as a damped oscillator, where γ_j, and ω_j denote the damping rate, and the frequency of the oscillation, respectively. In the following some specific examples are given:

(a) *Landau damping with homogeneous background*. Let consider only electron motion, assuming that the ions form a static, homogeneous, neutralizing background, that is $m_2 = \infty$, and the initial condition $f_1^{(2)}$ does not depend on $\bar{x}$. Suppose that the initial condition for the electrons is the maxwellian distribution, $g_1(\bar{v}) = (\alpha/\pi)^{d/2} \exp(-\alpha \bar{v}^2)$, that is

$$f_1^{(1)}(\bar{x}, \bar{v}, 0) = A\, g_1(\bar{v}) \cos(k_1 x). \tag{46}$$

Then, the function $D(k_1, p)$ takes the form

$$D(k_1, p) = 1 - \frac{\alpha}{k_1^2} Z'(\zeta), \tag{47}$$

where $\zeta = i\sqrt{\alpha} p/k_1$, and $Z(\zeta)$ the plasma dispersion function. Note that this reproduces exactly the classical result for the dispersion relation using the well-known linear Landau theory [19].

(b) *Landau damping with heterogeneous background*. Now we take into account also the ion dynamics. For simplicity, let assume that both initial conditions for ions and electrons are maxwellian distributions for velocities, given by

$$f_1^{(i)}(\bar{x}, \bar{v}, 0) = A \left(\frac{\alpha_i}{\pi}\right)^{d/2} e^{-\alpha_1 \bar{v}^2} \cos(k_1 x), \quad i = 1, 2 \tag{48}$$

The function $D(k_1, p)$ reduces to

$$D(k_1, p) = 1 - \frac{\alpha_1}{k_1^2} Z'(\zeta_1) - \frac{1}{m_2} \frac{\alpha_2}{k_1^2} Z'(\zeta_2), \tag{49}$$

where $\zeta_i = i\sqrt{\alpha_i} p/k_1$ $i = 1, 2$. Again, this coincides exactly with the results obtained using the classical linear Landau theory [19].

4.3 Evaluating Numerically the Probabilistic Representation of Vlasov-Poisson

Here we explain in detail how the probabilistic representation (32) can be used in practice to compute numerically the solution of the Fourier-transformed Vlasov-Poisson system, and which are the numerical errors done. For simplicity, in the following only the 1-dimensional case and one specie of charged particles (electrons) moving in a neutralizing homogeneous background charge (ions), has been considered. Equation (31) can then further simplified by setting $i = 1$ and $P(\rho = 1) = 1$. Note that the probabilistic representation for the Vlasov-Poisson system in (32) is not given in a closed-form. Following the same strategy as explained previously for the case of the transport equations, such an implicit equation can be solved recursively resorting to the aforementioned hybrid probabilistic representation approach, which in practice requires generating prescribed random trees governed by two random variables S, and k'.

Regarding numerical errors, recall that in general the convergence of the Padé approximant can be affected by artificial poles present in the denominator of the approximant, but not being own by the function to be approximated, see e.g. [11, 13].

Concerning the apparent robustness of the Padé approximant against the statistical error affecting the coefficients of the series expansion, a main reason could be that the solution of the test examples seems to be apparently locally Lipschitz. Thus, the error made in computing the coefficients of the Padé approximant should be bounded. In fact, in [44] it has been proved the following related theorem

$$\| P_f - P_{f'} \| \leq K \| c - c' \|, \tag{50}$$

provided that $\| c - c' \| \leq d$. Here P_f, and $P_{f'}$ are the Padé approximants of order (m, n) in $[a, b]$ of a given power series f and f' with coefficients c_j, and c'_j respectively, being $\| c \| = max_{i \leq i \leq n+m} |c_i|$, f locally Lipschitz, and K and d constants depending only on c_i and $[a, b]$.

In closing, it is worth to observe that all errors described above may be alleviated in any case by increasing conveniently the sample size N, and considering more coefficients in the expansion in order to compute the Padé approximant.

4.3.1 Numerical Test Examples

Before analyzing the performance of our algorithm when ran in parallel, we give in the following some numerical examples. These are chosen from the classical repertoire of possible initial conditions traditionally used for testing numerical methods developed for Vlasov-Poisson system, and which describe certain phenomena well known in Plasma Physics. The ultimate goal is to characterize the accuracy of the algorithm in realistic cases.

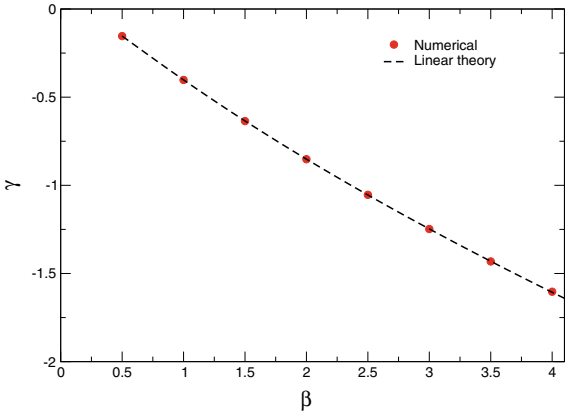

Fig. 4 Weak Landau damping: damping rate for different values of β. Parameters are: $A = 0.01$ and $M = 10^3$

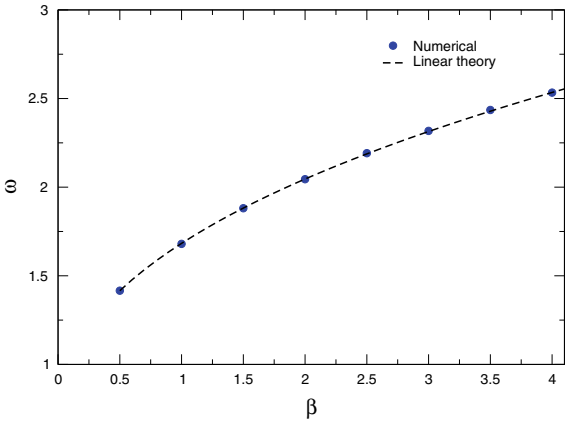

Fig. 5 Weak Landau damping: oscillation frequency for different values of β. Parameters are: $A = 0.01$ and $M = 10^3$

Landau damping. Let consider the following initial condition

$$f(x, v, 0) = \left(\frac{\alpha}{\pi}\right)^{d/2} e^{-\alpha v^2} \left[1 + A \cos(k_1 x)\right], \tag{51}$$

which in Fourier space, reads,

$$F_k(\xi, 0) = e^{-\frac{\xi^2}{4\alpha}} \left[A/2\, \delta(|k| - k_1) + \delta(k)\right] \tag{52}$$

The first numerical test deals with the so-called *weak* Landau damping, being the perturbation parameter A chosen sufficiently small. Here the damping rate and the oscillation frequency obtained numerically with our algorithm has been compared with the results obtained by the linear theory theoretically derived in Sect. 4.2.1. In Figs. 4 and 5, the damping rate and the oscillation frequency are shown for different values of α, which is related so far to different values of the plasma temperature

β, being $\beta = 1/4\alpha$. Here A has been kept fixed to 0.01. The remarkable agreement between the analytical linear theory and the numerical results allows us to safely analyze more complicated situations such as the *strong* Landau damping, where the aforementioned filamentation phenomenon is significantly more severe. Let consider the same initial condition, but now choosing larger values of A, that is $A = 0.5$ for exploring the strong Landau damping regime. The numerical solution obtained by the PDD method has been compared with the solution obtained when using an implicit upwind finite-difference scheme with a very fine mesh. The initial evolution of the mode $k = 1$ is shown in Fig. 6, showing the well-known filamentation phenomenon: an initial profile smooth in velocities, and peaked around $\xi = 0$ in Fourier space, evolves in time along the corresponding characteristics at constant velocity given by k, that is $F_k(\xi, t) = F_k(\xi - kt, 0)$. Thus, the solution propagates toward higher values of $|\xi|$, proportionally fast to the value of $|k|$, therefore faster for shorter wavelengths. Eventually this give rise to the development of small structures in the velocity distribution. So it is observed that the filamentation and mixing of modes appears strongly for long times in the nonlinear regime, and in the Fourier space, specifically for large values of ξ. Therefore, for this case, it has been considered a computational domain large enough in the $\xi-$dimension, despite in the figure it is only shown a part of it. To see more clearly that the solution is closely in agreement with the results obtained using other classical methods, the time evolution of the first harmonic of the electric field obtained by the PDD method is shown in Fig. 7, being qualitatively similar to the typical plots found in the literature [17, 30]. The solution obtained by the PDD method was satisfactorily compared in [6] with that obtained with an upwind implicit scheme with a very fine mesh. Here, $\Delta\xi$ has been kept fixed to 10^{-2} for the local solver. Note again the perfect agreement between the solution obtained by an upwind implicit scheme with a very fine mesh and our PDD method. The absolute numerical error has been numerically computed and it turns out to be or order of 10^{-2} in all simulations done.

Two streaming instability. Let consider the following initial condition, chosen for analyzing the two streaming instability phenomenon,

$$f(x, v, 0) = \left(\frac{\alpha}{\pi}\right)^{d/2} 2\alpha\, v^2 e^{-\alpha v^2} \left[1 + A\cos\left(k_1 \cdot x\right)\right], \tag{53}$$

which in Fourier space reads

$$F_k(\xi, 0) = (1 - \frac{\xi^2}{2\alpha}) e^{-\frac{\xi^2}{4\alpha}} [A/2\, \delta(|k| - k_1) + \delta(k)] \tag{54}$$

In Fig. 8 it is shown the time evolution of the predominant modes, where an initial, small perturbation leads to a final state characterized by a rapid modes grow and saturation, approximately at the time $t = 20$. As already reported in literature by other authors (e.g., see [30]), the mode-one is the dominant due to its initial excitation and reaches its maximum amplitude at $t = 18$. Once again, the numerical solution has been compared with the solution obtained with an implicit upwind scheme with

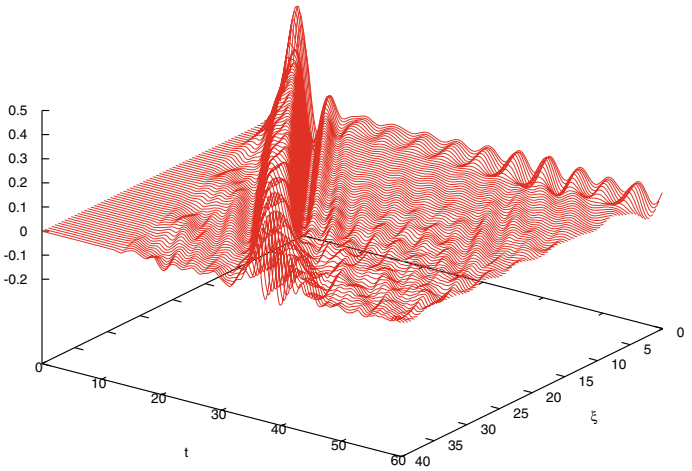

Fig. 6 Strong Landau damping: Time evolution of the numerical solution for $k = 1$. The contour lines correspond to $F_1(\xi, t) = 0$. Parameters are: $A = 0.5$, $\alpha = 2$ and $M = 10^3$

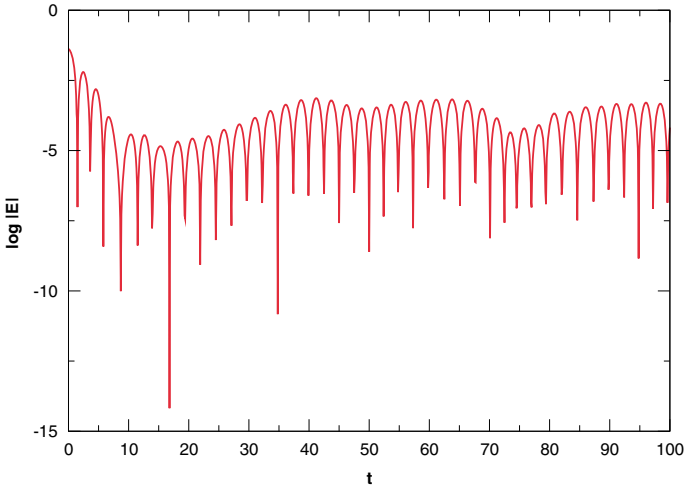

Fig. 7 Strong Landau damping: Logarithm of the absolute value of the first harmonic of the electric field. Parameters are: $A = 0.5$, and $\alpha = 2$

a very fine mesh, and the numerical error computed as in the previous example, obtaining a similar result.

For performance results of the PDD method for large scale simulations, see [6].

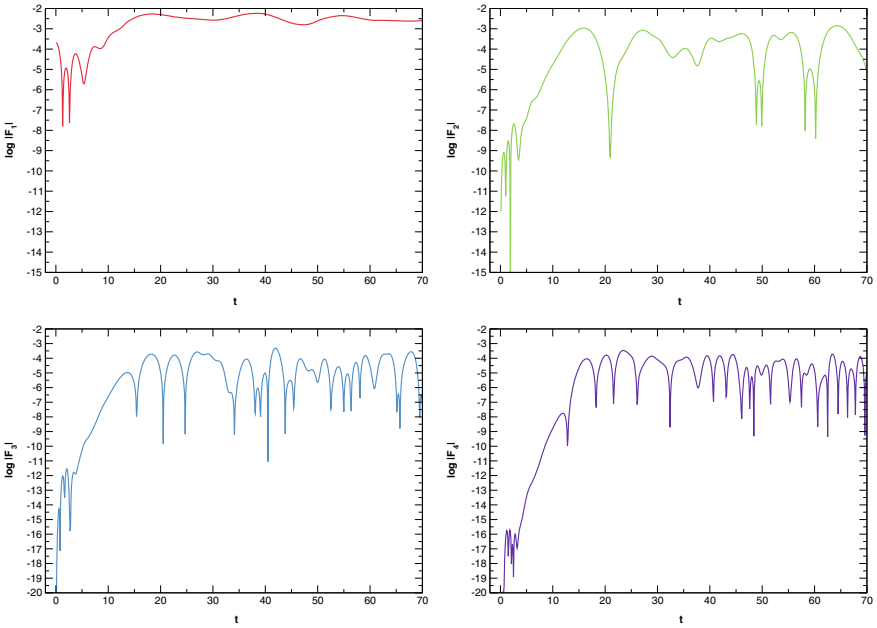

Fig. 8 Two streaming instability: Logarithm of the absolute values of the first four Fourier modes

4.4 Summary

The PDD method presented shows that, when combined with classical methods, is capable of accelerating the Vlasov-Poisson simulations, thus improving dramatically the overall scalability of classical algorithms. Such method is based on the probabilistic representation of the Vlasov-Poisson system of equations, obtained in Fourier space and generalized to deal with any realistic initial condition. The probabilistic representation allows to compute the solution at single points within the computational domain, and is obtained as the expected value of a multiplicative functional over suitable random trees. Such a feature can be exploited to decouple the original problem into independent subproblems, previously obtaining the required boundary conditions at given interfaces dividing the domain. The probabilistic method was used to compute the solution at a few points, to be used as interpolation nodes to obtain the sought boundary conditions at the interfaces. It consists therefore of a straightforward application of the Probabilistic Domain Decomposition(PDD) method for the numerical solution of the Vlasov-Poisson system.

Moreover, the probabilistic representation was validated successfully in the linear regime comparing with the classical results of the linear Landau damping theory. Regarding the numerical implementation of such representation, this requires evaluating in practice some series with terms including definite integrals, corresponding to the partial contribution to the solution of random trees with a given number of

branches. Typically, the higher terms are high dimensional, and were calculated by quasi-Monte Carlo methods. Rather than classical Monte Carlo method, the quasi-Monte Carlo offers a better convergence rate, of order of $O(1/N)$ compared with $O(N^{-1/2})$, speeding up notably the simulations. When dealing with arbitrary initial conditions, such a series might be divergent, and was approximated by the Padé approximant. To study the error made, several test problems were analyzed so far, and it was shown that considering a few coefficients of the series suffices to obtain a reasonable accuracy for sufficiently small times. Since the approximation degrades fast when the time grows, and to avoid including higher terms in the series expansion with the computational cost that this entails, a restarting procedure in time has been proposed. The solution is computed globally in the full domain from time to time, and it is reused as the new initial condition restarting the numerical procedure again. Being now the new initial condition numerically obtained, a suitable interpolation procedure was implemented, which in practice degrades the theoretical expected performance of the algorithm. However, some theoretical considerations were given and applied to the algorithm to improve its overall performance, reducing the computational cost associated to such a global interpolation.

To conclude, several examples were run in parallel and the results compared with those obtained with classical algorithms. The examples were chosen from the typical repertoire of initial conditions traditionally used for testing numerical methods developed for solving the Vlasov-Poisson system of equations. The results shows the excellent scalability properties of the algorithm proposed when run in large-scale simulations.

It is worth to remark that the method can be further generalized to deal with the Vlasov-Poisson system in configuration space, since the needed probabilistic representation does already exist [43]. Moreover, the probabilistic representation can be combined with any classical existing numerical method according to the procedure described in this section, improving notably the performance of the resulting algorithm when run in parallel supercomputers.

5 Fractional Partial Differential Boundary-Value Problems

In these days, there is a renewed interest in Fractional partial differential equations (fPDEs). Relevant aaplications in Science and Engineering include, for instance, control, biological tissues, materials for civil engineering, neurosciences, complex (heterogeneous and random) media, plasma physics, seismology and earthquakes modeling.

While solving purely initial-value problems seems to be to some extent tractable, the case of boundary-value problems on a smooth bounded domain $\Omega \subset \mathbb{R}^n$ is quite different, and it was observed that the results depends strongly on the definition of the fractional derivative used so far [22, 42]. One of the most important differences among these variety of fractional derivatives are in the type of boundary data. Essentially there are of two types: Those nonlocal boundary conditions (also called

extended boundary conditions) which are imposed on the complement Ω^c of the domain, and the local boundary conditions which are given only on $\partial\Omega$. The latter coincides with the type of boundary conditions typically imposed for classical partial differential equations, and moreover, under computational point of view, it has been found to be the more advantageous for dealing with large scale problems. In fact, note that the nonlocal boundary conditions require in practice to be able to tackle the unbounded region Ω^c, which can be computationally very costly for solving numerically those large scale problems. Therefore, in the following we focus exclusively on the case of local boundary conditions.

A promising numerical method for solving fPDEs in bounded domains was recently proposed in [18] by using the so-called spectral fractional derivative. The spectral fractional derivative is a nonlocal operator, which is defined mathematically as the spectral decomposition of the standard Laplace operator, and is given by

$$(-\Delta)^{\beta/2} v(x) = -\frac{1}{\Gamma(-\beta/2)} \int_0^\infty (e^{t\Delta} v(x) - v(x)) \frac{dt}{t^{1+\beta/2}}. \tag{55}$$

Here Δ denotes the classical Laplacian operator, and the exponential operator e^{Δ} is formally defined, as usual, through its expansion in Taylor series,

$$e^{\Delta} = \sum_{k=1}^{\infty} \frac{(\Delta)^k}{k!}. \tag{56}$$

The main idea of the numerical method consists in exploiting the integral formulation of the fractional operator using the classical heat-semigroup formalism. One of the main advantage of this formalism rests on the fact that classical methods, such as the well-known finite element method, could be adopted to solve as well fPDEs by adapting it conveniently to this different mathematical framework. This in practice will allow to potentially solve fPDEs in arbitrary complex geometries and boundary conditions, which is of paramount importance in order to be able to analyze natural phenomena modeled by fPDEs in realistic environments.

An important problem, however, remains open, which is the possibility of using this numerical method for solving large scale problems. Since the numerical method is based on the finite element method, and therefore it requires a computational mesh to be solved, it inherits all of its disadvantages. In fact an important disadvantage of the method is the strong intercommunication overhead of the algorithm for solving large scale problems in distributed memory parallel computers. The major problem is the routine use of computational meshes when solving numerically a given problem. Since the mesh is a numerical tool connecting globally the discretized domain, any classical domain decomposition techniques induce an unavoidable communication among the processors involved when the numerical method is parallelized. It is worth pointing out that such a communication overhead acts always negatively degrading the performance of the algorithms, being even worse when using a large number of

cores. Note that for the case of fPDEs this may be even more dramatic since the fractional operators are by definition nonlocal.

An alternative to the aforementioned domain decomposition method does exist, and consists in probabilistic methods based on Monte Carlo simulations. The main advantage of the probabilistic methods are mainly due to its special computational features, such as simplicity to code and parallelization. This in practice allows to develop parallel codes with extremely low communication overhead among processors, having a positive impact in parallel features such as scalability and fault-tolerance. Furthermore, there is also another distinguishing aspect of the method, which is the capability of computing the solution of the problem at specific chosen points, without the need of solving the entire problem. This remarkable feature has been explored for efficiently solving continuous problems such as boundary-value problems for classical PDEs offering important advantages in dealing with some specific applications found in Science and Engineering.

A feasible alternative, therefore, consists in generalizing the PDD method for solving now fPDE boundary-value problems. In principle, the PDD method could be applied to any problem, provided a probabilistic representation of the solution can be found. For the specific case of the spectral fractional Laplacian, it is known that the spectral operator in Eq. (55) with Dirichlet boundary conditions is the generator of a suitable subordinate stopped Brownian motion, i.e., stopped Brownian motion that is then *subordinated* by the standard *stable subordinator*. Therefore, it can be derived an analogous Feynman-Kac formula, where the corresponding Brownian motion is replaced now by a subordinate stopped Brownian motion [42]. Thus, the solution of the homogeneous Dirichlet boundary-value problem

$$\begin{aligned} \frac{\partial u}{\partial t} = \Delta^{\beta/2} u, \quad a < x < b,\ t > 0 \\ u(x,0) = f(x). \\ u(a,t) = f(a) = 0,\ u(b,t) = f(b) = 0, \end{aligned} \tag{57}$$

can be represented probabilistically as follows

$$u(x,t) = E\left[f(X_{S_t})\, \mathbf{1}_{[\tau_{\partial\Omega} > S_t]} \right] \tag{58}$$

where S_t is the subordinate process, that is an increasing *stable Lévy process* with index β, and X_t the corresponding Brownian motion. Here $\tau_{\partial\Omega}$ denotes the first exit time of the path X_t, started at $X_0 = x$, when $\partial\Omega$ is crossed, and $\mathbf{1}_{[\tau_{\partial\Omega} > t]}$ is the indicator (or characteristic) function. Note that in practice the subordination process consists merely of replacing the time t by the operational time given by the subordinator S_t.

Generating the stopped Brownian motion can be done simply by using the standard numerical techniques already available for solving probabilistically classical partial differential equations. A special care should be paid, however, when computing the first exit time and point out of the domain, as it was already mentioned in previous sections. Concerning the subordinated process, there are already several procedures

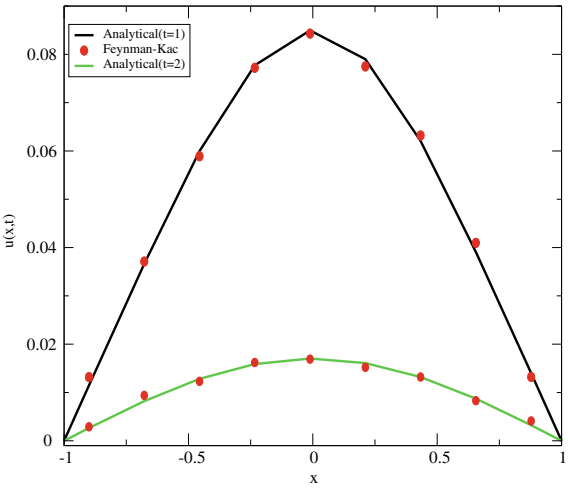

Fig. 9 Comparison between the probabilistic solution and the analytical solution of a Dirichlet fPDE boundary value problem. The fractional index has been kept fixed to $\beta = 1.5$, the sample size $N = 10^4$, and the time step $\Delta t = 10^{-2}$

available in the literature to generate numerically such a process, see [39] e.g. Since the solution is computed through an expected value of a given finite sample N, whose elements are independent from each other, it becomes straightforward to be parallelized.

In the following, to illustrate the probabilistic method we solved a simple example consisting in a Dirichlet boundary value problem for a 1D space-fractional diffusion equation in Eq. (57) using the probabilistic representation of the solution as described above. For this simple example, there exists an analytical solution [22] and is given by

$$u(x,t) = \frac{2}{\pi}\sum_{k=1}^{\infty} \frac{\cos(2k\pi/5) - \cos(3k\pi/5)}{k} e^{-(k\pi/2)^{\beta t}} \sin(k\pi/2(1+x)). \quad (59)$$

for the problem in the domain $x \in [-1, 1]$, and initial condition

$$f(x) = \begin{cases} 1 & \text{if} x \in (-0.2, 0.2) \\ 0 & \text{otherwise} \end{cases} \quad (60)$$

In Fig. 9 we compare the results corresponding to the numerical solution obtained using the probabilistic representation at different spatial points inside the domain, and the analytical solution plotted in solid line. The results correspond to two different times, $t = 1$, and $t = 2$. Note the excellent agreement between both solutions.

6 Conclusions

We have reviewed the PDD (probabilistic domain decomposition) method for numerically solving a wide range of linear and nonlinear partial differential equations of parabolic and hyperbolic type, as well as for fractional equations. This method was originally introduced for solving linear elliptic problems. It is based on a novel hybrid approach where an efficient Domain Decomposition is effectively accomplished by means of the probabilistic representation of the solution of the problem.

After an introduction detailing how this method works for linear parabolic problems, we have first showed the probabilistic representation for certain nonlinear parabolic problems, generalizing the results derived by McKean for the KPP equation. Later, a further extension of the method for dealing with semilinear parabolic partial differential equations has been presented. It is important to emphasize the major drawback faced in the attempt of such generalization, consisting in the numerical evaluation of a truncated, alternating divergent series. This issue was sorted out by relying on Padé-type approximants to obtain numerically asymptotic approximations, always proven to be robust and reliable.

On the other hand, for semilinear transport equations, a probabilistic representations has been proposed in terms of the characteristic curves. It is important to remark that for hyperbolic problems in general, the characteristic curves play a similar role in such a representation as the stochastic process does for the parabolic problems. As an important application, the PDD method has been extended to deal with the Vlasov-Poisson system of equations in Fourier Space, which represents a very important and challenging problem in the field of Plasma Physics. Here, an existing probabilistic representation in Fourier space has been conveniently reformulated for computational purposes, validated successfully in the linear regime comparing with the classical results of the linear Landau damping theory. This theory has also been used to validate the probabilistic method numerically, which has had particular importance given the lack of exact analytical solutions.

In practice, for semi-linear problems a series with terms composed of definite integrals have to be evaluated, corresponding to the partial contribution to the solution of random trees with a given number of branches. Typically, the higher terms are of high dimensionality, and are calculated by the quasi-Monte Carlo method. Rather than classical Monte Carlo method, the quasi-Monte Carlo offers a better convergence rate, speeding up notably the simulations. When dealing with arbitrary initial conditions, such a series might be divergent, and was again approximated by the Padé approximant. The PDD method has shown theoretically and in practice to accelerate the numerical simulations, improving dramatically the overall scalability of classical algorithms.

Finally, we have shown the latest progress of the PDD method for dealing with fractional PDEs. We have provided a case example for the 1D space-fractional diffusion equation, showing promising results. As future work, the PDD method should be generalize further to deal with different kind of fractional operators (in time as well), an also for high dimensions.

As a final remark, when applicable, the PDD method enables for sustained high performance computing when solving challenging scientific problems formulated via partial differential equations. As observed through several test examples when compared with classical domain decomposition techniques, the method achieves superior performance and scalability results on supercomputing environments. Based on the fact that it is naturally fault-tolerant, the method also provides robustness and reliability by construction. Given that the subproblems are fully decoupled, a system failure is no longer dramatic, as it is simply required to run the simulation again, possibly asynchronously, only for the set of subproblems that have not finished successfully.

References

1. Acebrón, J.A., Busico, M.P., Lanucara, P., Spigler, R.: Domain decomposition solution of elliptic boundary-value problems via Monte Carlo and Quasi-Monte Carlo methods. SIAM J. Sci. Comput. **27**(2), 440–457 (2005)
2. Acebrón, J.A., Busico, M.P., Lanucara, P., Spigler, R.: Probabilistically induced domain decomposition methods for elliptic boundary-value problems. J. Comput. Phys. **210**(2), 421–438 (2005)
3. Acebrón, J.A., Rodríguez-Rozas, A., Spigler, R.: Domain decomposition solution of nonlinear two-dimensional parabolic problems by random trees. J. Comput. Phys. **228**(15), 5574–5591 (2009)
4. Acebrón, J.A., Rodríguez-Rozas, A., Spigler, R.: Efficient Parallel Solution of Nonlinear Parabolic Partial Differential Equations by a Probabilistic Domain Decomposition. J. Sci. Comput. **43**(2), 135–157 (2010)
5. Acebrón, J.A., Rodríguez-Rozas, A.: A new parallel solver suited for arbitrary semilinear parabolic partial differential equations based on generalized random trees. J. Comput. Phys. **230**(21), 7891–7909 (2011)
6. Acebrón, J.A., Rodríguez-Rozas, A.: Highly efficient numerical algorithm based on random trees for accelerating parallel Vlasov-Poisson simulations. J. Comput. Phys. **250**, 224–245 (2013)
7. Acebrón, J.A., Ribeiro, M.A.: A Monte Carlo method for solving the one-dimensional telegraph equations with boundary conditions. J. Comput. Phys. **305**, 29–43 (2016)
8. Rodríguez-Rozas, A.: Highly Efficient Probabilistic-Based Numerical Algorithms for Solving Partial Differential Equations on Massively Parallel Computers. PhD Thesis in Computational Engineering, Instituto Superior Tècnico, Universidade Tècnica de Lisboa (2012)
9. Antia, H.M.: Numerical Methods for Scientists and Engineers. Tata McGraw-Hill, New Delhi (1995)
10. Arnold, L.: Stochastic Differential Equations: Theory and Applications. Wiley, New York (1974)
11. Baker, G.A., Graves-Morris, P.: Padé Approximants. Cambridge University Press, New York (1996)
12. Baldi, P.: Exact asymptotics for the probability of exit from a domain and applications to simulation. Ann. Prob. **23**, 1644–1670 (1995)
13. Bender, C., Orszag, S.A.: Advanced Mathematical Methods for Scientists and Engineers. McGraw Hill, New York (1978)
14. Bernal, F., dos Reis, G., Smith, G.: Hybrid PDE solver for data-driven problems and modern branching. European J. Appl. Math. **28**, 949–972 (2017)

15. Bhattacharya, R., Chen, L., Dobson, S., Guenther, R.B., Orum, C.: Majorizing Kernels and Stochastic Cascades with Applications to Incompressible Navier-Stokes Equations. Ossiander, M., Thomann, E., Waymire, E.C. Reviewed work (s): Source : Transactions of the American Mathematical Society , Vol . 355 , No. Transactions of the American Mathematical Society, 355:5003–5040, 2003
16. Buchmann, F.M.: Computing exit times with the Euler scheme, Research report no. 2003-02, ETH (2003)
17. Crouseilles, N., Mehrenberger, M., Sonnendrücker, E.: Conservative semi-Lagrangian schemes for Vlasov equations. J. Comput. Phys. **229**(6), 1927–1953 (2010)
18. Cusimano, N., del Teso, F., Gerardo-Giorda, L., Pagnini, G.: Discretizations of the spectral fractional Laplacian on general domains with Dirichlet, Neumann, and Robin boundary conditions. SIAM J. Numer. Anal. **56**, 1243–1272 (2018)
19. Davidson, R.C.: Kinetic Waves and Instabilities in Uniform Plasma. In: Galeev, A.A., Sudan, R.N., Handbook of Plasma Physics, Vol. 1, pp. 521–585. North-Holland Publishing Company (1983)
20. DeBoor, C.: A Practical Guide to Splines. Springer (1994)
21. DuChateau, P., Zachmann, D.: Applied Partial Differential Equations. Dover Publications (2002)
22. Duo, S., Wang, H., Zhang, Y.: A comparative study on nonlocal diffusion operators related to the fractional Laplacian. Discrete Contin. Dyn. Syst. B **24**, 231–256 (2019)
23. Eliasson, B.: Outflow Boundary Conditions for the Fourier Transformed One-Dimensional Vlasov Poisson System. J. Sci. Comput. **16**(1), 1–28 (2001)
24. Floriani, E., Lima, R., Vilela Mendes, R.: Poisson-Vlasov: stochastic representation and numerical codes. Eur. Phys. J. D **46**(2):295–302 (2007)
25. Freidlin, M.: Functional Integration and Partial Differential Equations. Annals of Mathematics Studies no. 109, Princeton Univ. Press, Princeton (1985)
26. Gobet, E.: Weak approximation of killed diffusion using Euler schemes. Stoch. Process. Appl. **87**, 167–197 (2000)
27. Gobet, E., Menozzi, S.: Stopped diffusion processes: boundary corrections and overshoot. Stoch. Process. Appl. **120**, 130–162 (2010)
28. Kalos, M.H., and Withlock, P.A.: Monte Carlo Methods, Vol. I: Basics. Wiley, New York (1986)
29. Karatzas, I., Shreve, S.E.: Brownian Motion and Stochastic Calculus, 2nd edn. Springer, Berlin (1991)
30. Klimas, A.J.: A numerical method based on the Fourier-Fourier transform approach for modeling 1-D electron plasma evolution. J. Comput. Math. **50**, 270–306 (1983)
31. Klimas, A.J.: Vlasov-Maxwell and Vlasov-Poisson equations as models of a one-dimensional electron plasma. Phys. Fluids **26**(2), 478 (1983)
32. Kloeden, P.E., Platen, E.: Numerical Solution of Stochastic Differential Equations. Springer, Berlin (1992)
33. McKean, H.P.: Application of brownian motion to the equation of Kolmogorov-Petrovskii-Piskunov. Commun. Pure Appl. Math. **28**, 323–331 (1975)
34. Mannella, R.: Absorbing boundaries and optimal stopping in a stochastic differential equation. Phys. Lett. A **254**, 257–262 (1999)
35. Milstein, G.N., Tretyakov, M.V.: Stochastic Numerics for Mathematical Physics. Springer (2004)
36. Buchmann, F.M., Petersen, W.P.: An Exit Probability Approach to Solving High Dimensional Dirichlet Problems, SIAM J. Scient. Comput. **28**(3), 1153–1166 (2006)
37. Ramirez, J.M.: (two numerical examples). J. Comput. Phys. **214**, 122–136 (2006)
38. Regnier, H., Talay, D.: Special Edition of the Proceedings of the Royal Society on Stochastic Analysis A(460), 199–220 (2004)
39. Fulger, D., Scalas, E., Germano, G.: Monte Carlo simulation of uncoupled continuous-time random walks yielding a stochastic solution of the space-time fractional diffusion equation. Phys. Rev. E **77**, 1–7 (2008)
40. Shikin, E.V., Plis, A.I.: Handbook on Splines for the User. CRC-Press (1995)

41. Strittmatter, W.: Numerical Simulation of The Mean First Passage Time. University Freiburg Report No. THEP 87/12 (unpublished)
42. Lischke, A., Pang, G., Gulian, M., Song, F., Glusa, C., Zheng, X., Mao, Z., Cai, W., Meerschaert, M., Ainsworth, M., Karniadakis, G.: What Is the Fractional Laplacian? A comparative review with new results. J. Comput. Phys. **404**, (2020)
43. R. Vilela Mendes. Poisson-Vlasov in a strong magnetic field: A stochastic solution approach. J. Mathe. Phys. **51**(4), 043101 (2010)
44. Wuytack, L.: On the conditioning of the Pade approximant problem. Lect. Notes Math. **888**, 78–89 (1981)

Fractional Diffusion and Medium Heterogeneity: The Case of the Continuous Time Random Walk

Vittoria Sposini, Silvia Vitali, Paolo Paradisi, and Gianni Pagnini

Abstract In this contribution we show that fractional diffusion emerges from a simple Markovian Gaussian random walk when the medium displays a power-law heterogeneity. Within the framework of the continuous time random walk, the heterogeneity of the medium is represented by the selection, at any jump, of a different time-scale for an exponential survival probability. The resulting process is a non-Markovian non-Gaussian random walk. In particular, for a power-law distribution of the time-scales, the resulting random walk corresponds to a time-fractional diffusion process. We relates the power-law of the medium heterogeneity to the fractional order of the diffusion. This relation provides an interpretation and an estimation of the fractional order of derivation in terms of environment heterogeneity. The results are supported by simulations.

Keywords Continuous time random walk · Medium heterogeneity · Anomalous diffusion · Time-fractional diffusion

V. Sposini
UPotsdam, Germany, and BCAM, Bilbao, Spain

Present Address:
Faculty of Physics, University of Vienna, Vienna, Austria
e-mail: vittoria.sposini@univie.ac.at

S. Vitali
BCAM, Bilbao, Spain
e-mail: svitali@bcamath.org

P. Paradisi
ISTI-CNR, Pisa, Italy
e-mail: paolo.paradisi@isti.cnr.it

G. Pagnini (✉)
BCAM and Ikerbasque, Bilbao, Spain
e-mail: gpagnini@bcamath.org

L. Beghin et al. (eds.), *Nonlocal and Fractional Operators*, SEMA SIMAI Springer Series 26, https://doi.org/10.1007/978-3-030-69236-0_14

1 Introduction and Motivation

Fractional diffusion is characterized by non-Gaussian statistics and nonlinear scaling in time of the mean-squared displacement [20–22, 28]. Many different approaches have been implemented and extensively analyzed to reproduce this type of diffusion, see, e.g., [2, 9, 10]. In particular, we recall the continuous time random walk (CTRW) [11], where a power-law tailed distribution of the waiting times can be introduced to generate fractional diffusion processes. This model was proposed to describe dispersive transport of chargers in amorphous semiconductors [25]. In general, the CTRW approach can be used to model diffusion in disordered media, which are characterized by a complex trapping mechanism. Indeed, the main ingredient of CTRW models is a power-law tailed distribution for the waiting times. A direct connection between the CTRW and fractional diffusion is provided by a waiting time probability stated accordingly to the Mittag–Leffler function (ML) [7], which displays power-law tails.

Systems coming from very different fields have been studied within this framework, from geophysics to biology [17], included neurosciences where the idea of a distribution of sojourn times has been developed to describe anomalous ions diffusion in spiny dendrites [16, 26].

From a physical point of view, each waiting time can be related to a different probability of escaping from a trap. In this contribution, we show explicitly how complex escaping probabilities that generate fractional diffusion emerge from the combination of space heterogeneity and Markovian exponential escaping probability. The main mathematical hint behind this work is the interpretation of the ML as a weighted superposition of exponential functions [19]. In particular, we can map different trap depths into different time-scales of the exponential probability. In this way, if classical diffusion is characterised by a homogeneous landscape of traps, i.e., a constant value for the time-scale, anomalous diffusion emerges when a strong heterogeneity appears in the trap landscape, that is when a population of time-scales is introduced.

This interpretation is advantageous and more suitable for real applications, because it does not introduce complex trapping mechanism, instead it considers a large heterogeneity of simple and standard mechanisms of trapping [1]. Moreover, with the approach presented in this work, medium properties can be inferred by the statistics of the diffusing particles.

Hence, this contribution aims to provide a new and more physical interpretation of the heterogeneity described by CTRW with power-law distributed waiting times. The work is structured as follows. First, we show how the memory kernel characteristic of the CTRW model can be related to the space heterogeneity. Then we present the emergence of fractional diffusion and finally we check our results against numerical simulations.

2 Markovian Random Walk in a Heterogeneous Medium

The CTRW is a successful approach to study stochastic processes [3, 5, 7, 8, 11, 15, 18, 24]. The corresponding random walk goes on according to the following iteration procedure

$$x_n = x_{n-1} + \delta x_n\,, \quad t_n = t_0 + \sum_{j=1}^{n} \tau_j\,, \tag{1}$$

where x_n and x_{n-1} are the walker positions at the instants t_n and t_{n-1}, respectively, such that the n-generated random jump δx_n is driven by the pdf $\lambda(\delta x)$, and the corresponding random waiting-time $\tau_n = t_n - t_{n-1}$ is generated by the pdf $\psi(\tau)$. Since the probability that at least one jump is made in the temporal interval $(0, \tau)$ is given by the integral $\int_0^\tau \psi(\xi)\,d\xi$, then the probability that the duration of a given waiting-interval between two successive steps is strictly greater than τ, i.e., the survival probability, is $\Psi(\tau) = 1 - \int_0^\tau \psi(\xi)\,d\xi$ and it holds [15, 23, 27]

$$\psi(\tau) = -\frac{d\Psi}{d\tau}\,. \tag{2}$$

The simplest case of CTRW is the uncoupled one, i.e., the case when the jumps and the waiting times are statistically independent, and the governing equation of the process is [15]

$$\int_0^t \Phi(t-\tau)\frac{\partial p}{\partial \tau}\,d\tau = -p(x,t) + \sum_{x'} \lambda(x-x')p(x',t)\,, \tag{3}$$

with

$$\widetilde{\Phi}(s) = \frac{1-\widetilde{\psi}(s)}{s\,\widetilde{\psi}(s)} = \frac{\widetilde{\Psi}(s)}{\widetilde{\psi}(s)} = \frac{\widetilde{\Psi}(s)}{1 - s\,\widetilde{\Psi}(s)}\,, \tag{4}$$

where the symbol $\widetilde{\cdot}$ marks the Laplace transformed function and s is the corresponding variable. As it follows from (3), the auxiliary function $\Phi(\tau)$ is a memory kernel. Hence, a Markovian model is obtained when $\Phi(\tau) = \delta(\tau)$, which implies that $\widetilde{\Phi}(s) = 1$ and then from (4) it results $\widetilde{\Psi}(s) = \widetilde{\psi}(s)$ and also $\Psi(\tau) = \psi(\tau)$. Functions $\Psi(\tau)$ and $\psi(\tau)$ are related by formula (2), then a CTRW model is Markovian if $\Psi(\tau) = \mathrm{e}^{-\tau}$. On the contrary, when $\Psi(\tau)$ is different from an exponential function the resulting CTRW model is non-Markovian.

For the following porpuses, let us write the survival probability and waiting-time pdf in the Markovian case as

$$\Psi_{\mathrm{M}}(\tau^{\mathrm{M}}) = \mathrm{e}^{-\tau^{\mathrm{M}}/T^0}\,, \quad \psi_{\mathrm{M}}(\tau^{\mathrm{M}}) = \frac{1}{T^0}\,\mathrm{e}^{-\tau^{\mathrm{M}}/T^0}\,, \tag{5}$$

where the index M reminds the Markovian setting and the time-scale T^0 is constant if the medium is homogeneous.

Consider now a complex heterogeneous medium, such that in any position x_n the walkers stay for a waiting time τ_n characterized by the medium heterogeneity. Hence, at any iteration n the waiting-time τ_n is characterized by a local time-scale T_n. Since T_n is the time-scale locally experienced by the particle in position x_n, the distribution of T_n describes the spatial heterogeneity of the medium. However, if the walker lands twice in the same point then the two values of T_n are different because independently generated. This means that the partitioning of the heterogeneity of the medium is not constant.

In this case the random walk still goes on according to the iteration procedure (1) with the same meaning for the symbols, but the probability of the waiting-time τ_n at the iteration n is affected by the local time-scale T_n. If the motion of the walker is again assumed to be Markovian, the conditioned survival probability is

$$\Psi(\tau_n|T_n) = \mathrm{e}^{-\tau_n/T_n} . \tag{6}$$

Comparing (5) and (6) we observe that τ^{M}/T^0 and τ_n/T_n have the same probability. By setting

$$\frac{\tau^{\mathrm{M}}}{T^0} = \frac{\tau_n}{T_n} = \chi , \tag{7}$$

then in formulae,

$$\mathcal{P}\left(\frac{\tau^{\mathrm{M}}}{T^0}\right) = \mathcal{P}\left(\frac{\tau_n}{T_n}\right) = \mathcal{P}(\chi) = \mathrm{e}^{-\chi} , \tag{8}$$

and the waiting-time τ_n at the iteration n is given by the product

$$\tau_n = \frac{\tau^{\mathrm{M}}}{T^0} T_n . \tag{9}$$

By remembering the formulae for computing the pdf of the quotient and product of independent variables, i.e.,

$$\int_0^\infty b\, p_A(zb)\, p_B(b)\, db , \quad Z = A/B , \tag{10}$$

$$\int_0^\infty p_A\left(\frac{z}{b}\right) p_B(b)\, \frac{db}{b} , \quad Z = AB , \tag{11}$$

and by reminding that T^0 is constant and then distributed as $f(T_0) = \delta(T^0 - T_*)$, the marginal pdf of τ is

$$\psi(\tau) = \int_0^\infty \mathrm{e}^{-\tau/T} f(T) \frac{dT}{T} , \tag{12}$$

and the corresponding survival probability is

$$\Psi(\tau) = \int_0^\infty \mathrm{e}^{-\tau/T} f(T)\, dT\,. \tag{13}$$

The memory kernel $\Phi(t)$ in the governing equation (3) is determined by the heterogeneity and, from formula (4), its Laplace transform is

$$\widetilde{\Phi}(s) = \frac{\displaystyle\int_0^\infty \frac{f(T)}{1+sT}\, dT}{\displaystyle\int_0^\infty \frac{f(T)}{1+sT}\, T\, dT}\,. \tag{14}$$

For a proper choice of the memory kernel $\Phi(t)$, the governing equation (3) results in a time-fractional diffusion equation.

3 The Emerging of Fractional Diffusion

In 1995 Hilfer and Anton [7] showed that CTRW is driven by the following fractional non-Markovian master equation

$$\frac{\partial^\beta p}{\partial t^\beta} = -p(x,t) + \sum_{x'} \lambda(x-x')p(x',t)\,, \quad 0 < \beta < 1\,, \tag{15}$$

where $\dfrac{\partial^\beta}{\partial t^\beta}$ can be the fractional derivative both in the Riemann–Liouville and in the Caputo sense [4], if the survival probability $\Psi(\tau)$ is a Mittag–Leffler function [6, 12, Appendix E], i.e.,

$$\Psi(\tau) = E_\beta(-\tau^\beta)\,, \quad E_\beta(z) = \sum_{n=0}^\infty \frac{z^n}{\Gamma(\beta n+1)}\,, \quad z \in C\,, \quad 0 < \beta < 1\,. \tag{16}$$

It is well-known that a survival probability of the Mittag–Leffler type (16), when $0 < \beta < 1$, decreases asymptotically for $\tau \to \infty$ with the power-law $\tau^{-\beta}$ [13]. The Markovian case is recovered from the special case $E_1(-z) = \mathrm{e}^{-z}$. With reference to formula (13), the survival probability of Mittag–Leffler type (16) is obtained when it holds

$$\int_0^\infty \mathrm{e}^{-ty} K_\beta(y)\, dy = E_\beta(-t^\beta)\,, \quad 0 < \beta < 1\,, \tag{17}$$

with [4, 12]

$$K_\beta(y) = \frac{1}{\pi} \frac{y^{\beta-1} \sin(\beta\pi)}{1 + 2y^\beta \cos(\beta\pi) + y^{2\beta}} \,. \tag{18}$$

Hence, by comparing (13) and (17), the distribution of time-scales T_n is

$$f(T) = \frac{1}{T^2} K_\beta \left(\frac{1}{T} \right) \,. \tag{19}$$

The asymptotic behaviour of $f(T)$ can be estimated by formula (18). Actually, it results that when $T \to \infty$ then $f(T) \sim T^{-(1+\beta)}$, and we have the following:

If the medium heterogeneity follows a distribution displaying a power-law behaviour $T^{-(1+\beta)}$, for $T \to \infty$ and $0 < \beta < 1$, then the random walk results in a time-fractional diffusion process of order β. This relation provides an interpretation and an estimation of the fractional order of derivation.

In the limit $\beta \to 1$, it holds $K_\beta(y) = \sin \pi / [\pi \, (y-1)^2] \to \delta(y-1)$ and a single time-scale follows and the Markovian case is recovered. When the distribution of the time-scales is non-stationary, i.e., $f(T) = f(T, t)$, such distribution is non-unique [19].

To conclude, when the fractional derivative in Eq. (15) is in the Caputo sense, the initial condition is $p(x, 0) = \delta(x)$, and it holds $\widehat{\lambda}(\kappa) \sim 1 - \kappa^2$, where the symbol $\widehat{\cdot}$ marks the Fourier transformed function and κ the corresponding variable, then the pdf of the particle displacement is

$$p(x, t) = \frac{1}{2t^{\beta/2}} M_{\beta/2} \left(\frac{|x|}{t^{\beta/2}} \right) \,, \quad 0 < \beta < 1 \,, \tag{20}$$

where $M_\nu(y)$, $0 < \nu < 1$, is the M-Wright/Mainardi function defined as [12, Appendix F]

$$M_\nu(y) = \sum_{n=1}^{\infty} \frac{(-y)^n}{n! \Gamma[-\nu n + (1-\nu)]} \,. \tag{21}$$

For completeness, the asymptotic behaviour of the pdf of the particle displacement (20) is here reported. In particular, the M-Wright/Mainardi function displays stretched exponential tails in space [14]:

$$M_\nu(y) \sim A_0 \, Y^{\nu - 1/2} \, \mathrm{e}^{-Y} \,, \quad y \to \infty \,, \tag{22}$$

with $A_0 = \left[\sqrt{2\pi} (1-\nu)^\nu \nu^{2\nu-1} \right]^{-1}$ and $Y = (1-\nu)(\nu^\nu y)^{1/(1-\nu)}$, and power-law decay in time:

$$\frac{1}{r^\nu} M_\nu \left(\frac{c}{r^\nu} \right) \sim \frac{1}{r^\nu} \,, \quad r \to \infty \,. \tag{23}$$

This last scaling law follows from the relation between the M-Wright/Mainardi function and the extremal Lévy density [14], i.e.,

$$\frac{1}{r^{\nu}} M_{\nu}\left(\frac{c}{r^{\nu}}\right) = \frac{r}{\nu c^{(1+\nu)/\nu}} L_{\nu}^{-\nu}\left(\frac{r}{c^{1/\nu}}\right) . \tag{24}$$

4 Numerical Simulations and Discussion

We provide numerical results as additional proof of the result obtained in the previous section. The numerical simulations are performed in C++ according to the scheme in (1).

For numerical purposes the waiting times τ_n are not extracted directly from the *pdf* defined in (12), instead we make use of the identity in (9), where it is shown that each τ_n can be defined as a product of two random variables. Namely, we have

$$\tau_n = \xi \cdot T_n , \tag{25}$$

where ξ is an exponentially distributed random variable and T_n is the random time-scale drawn from (19). For the random generation of ξ and T_n, we used the cumulative function method. That is, starting from T_n, we define $F(T)$ as the cumulative function of (19) and we obtain

$$F(T) = \int_0^T f(t)\, dt = \frac{1}{\beta\pi} \arctan\left[\frac{T^{\beta} - 1}{T^{\beta} + 1} \tan\left(\frac{\beta\pi}{2}\right)\right] + \frac{1}{2} . \tag{26}$$

Then, we consider $F(T)$ to be a function of uniform random variable between 0 and 1, i.e., $F(T) = u$, where $u \overset{d}{=} U(0, 1)$. Finally, after substituting u in (26), we get

$$T = \left[\frac{1 + A(u)}{1 - A(u)}\right]^{1/\beta} , \quad A(u) = \frac{1}{\tan(\beta\pi/2)} \tan\left(\beta\pi\left(u - \frac{1}{2}\right)\right) . \tag{27}$$

For exponentially distributed random variables, with the same procedure we can obtain the well known result

$$\xi = -\log(u) , \quad u \overset{d}{=} U(0, 1). \tag{28}$$

Concerning the jump length, we consider a walker that, after each waiting time τ_n, performs a jump of fixed length j_0 either to the left or to the right with equal probability, namely the Binomial random walk. In terms of CTRW notations this corresponds to a jump length *pdf*

$$\lambda(\delta x) = \frac{1}{2} \left[\delta\left(\delta x - j_0\right) + \delta\left(\delta x + j_0\right)\right] , \tag{29}$$

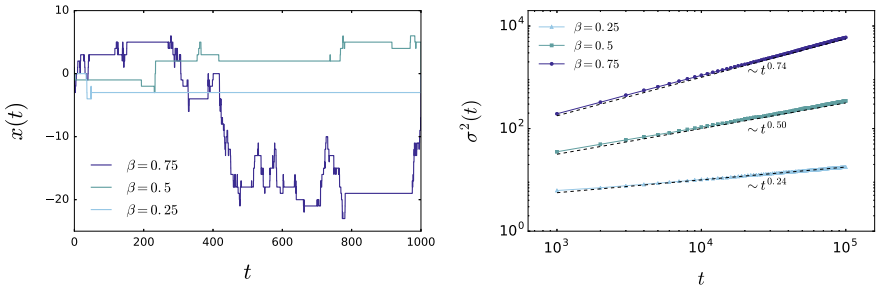

Fig. 1 Left: example of trajectories for each value of β. Right: variance for three values of $\beta = 0.25,\ 0.5,\ 0.75$. The black dashed lines represent the expected behaviour, the exponents obtained from the best fit analysis are also reported for comparison

where $\delta(x)$ is the Dirac delta function, and it is straightforward to check that

$$\hat{\lambda}(\kappa) = \frac{1}{2}\left(\mathrm{e}^{i\kappa j_0} + \mathrm{e}^{-i\kappa j_0}\right) \sim 1 - \frac{j_0^2}{2}\kappa^2\,, \quad \kappa j_0 \ll 1\,. \tag{30}$$

We simulated 10^4 trajectories with initial condition $x_0 = 0$, jump length $j_0 = 1$ and three different values of $\beta = 0.25,\ 0.5,\ 0.75$. Few trajectories were stored at 10^4 observation times, distributed linearly in the interval $[0, 10^3]$. In order to perform histograms and study the *pdf*s, the positions of all trajectories were stored at 10 moments within the time interval $[10^4, 10^5]$. The variance was computed for 10^2 points, distributed linearly in the time interval $[0, 10^5]$.

In Fig. 1 we report single trajectories and the variance for three values of β. Starting from the former, we can directly observe that when β gets closer to 1, the waiting times become smaller and smaller. For the study of the variance we performed linear fits using the logarithm of the data. The results reported in the figure show that the subdiffussive trend of the variance is properly recovered:

$$\langle x^2 \rangle = \sigma^2(t) = \frac{j_0^2}{\Gamma(1+\beta)}\, t^\beta\,. \tag{31}$$

In Fig. 2 the particle displacement *pdf*s are shown. For the comparison with the analytical results we refer to the asymptotic behaviour of the *pdf* in (20), that results in a stretched exponential, i.e.,

$$p(x,t) \sim \frac{1}{\sqrt{4\pi t^\beta (2-\beta)}} \left(\frac{2}{\beta}\right)^{(1-\beta)/(2-\beta)} \left(\frac{|x|}{\sqrt{t^\beta}}\right)^{-(1-\beta)/(2-\beta)} \times \exp\left[-\frac{2-\beta}{2}\left(\frac{\beta}{2}\right)^{\beta/(2-\beta)} \left(\frac{|x|}{\sqrt{t^\beta}}\right)^{-1/(1-\beta/2)}\right], \tag{32}$$

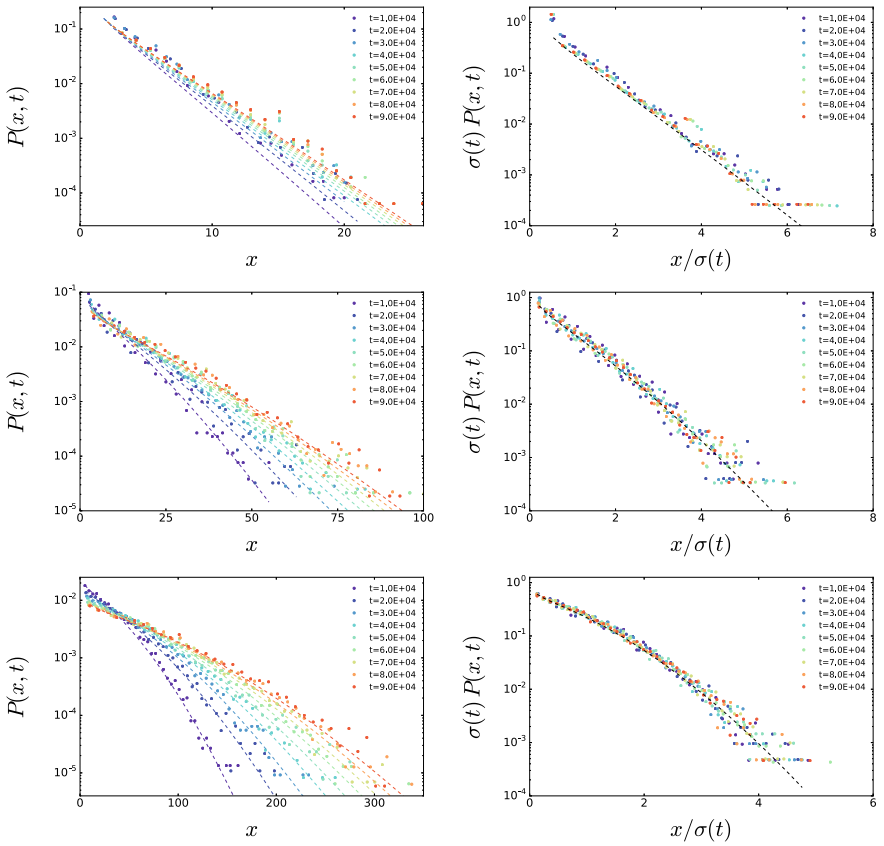

Fig. 2 Numerical results for $\beta = 0.25$ (upper panel), $\beta = 0.5$ (central panel) and $\beta = 0.75$ (lower panel). The dashed lines on the left panels indicate the analytical result in (32); each color refers to the time in the legend, respectively. On the right panels the same quantities, rescaled by the corresponding variance at each time, are shown. The analytical behaviour in (32) rescaled by the variance is reported in black

for $|x| \gg \sqrt{t^\beta}$.

We observe a good agreement between numerical and analytical results. Differences are due to the fact that the jumps are performed by using the Binomial random walk, such that the convergence occurs in the diffusive limit.

Thus, we can claim that our analysis provides a simple and explicit interpretation of the CTRW with power-law distributed waiting times as a model for diffusion in heterogeneous media. Moreover, we introduced a general and operative way to directly include the heterogeneity in the diffusive model, clarifying the emergence of non-Markovian behaviour.

5 Conclusions

In this contribution we show through a simple Markovian Gaussian random walk how anomalous diffusion emerges from medium heterogeneity. In particular, within the CTRW framework, the heterogeneity is represented by a random time-scale that affects the waiting-time interval at any jump. Since in any position a different time-scale is considered, the distribution of the time-scales is intended as a characterisation of the spatial heterogeneity of the medium.

Actually, this time-scale is always independently generated, which means that in the same position, but at different instants, different time-scales may be experienced by the walkers. That is to say that the heterogeneity of the medium is not constant.

For a proper distribution of the time-scales with a power-law behaviour for large values, the evolution equation of the density of the walkers' displacement emerges to be a time-fractional diffusion equation.

The present derivation of a time-fractional diffusion process, in terms of medium heterogeneity through a population of time-scales (19), complements the results derived in Ref. [19]. The study is supported by numerical simulations of the process. In this respect it is reported that, unlike other algorithms for fractional processes from the CTRW, the waiting-time distribution is not chosen a priori but generated through the proposed mechanism based on random time-scales applied to a Markovian Gaussian random walk. This mechanism defines a framework which is able to reproduce a large class of diffusion processes, that comes from any possible medium heterogeneity without changing the algorithm behind the single trap mechanisms, which remains a Markovian process. The fractional process emerges as a particular case in which strong heterogeneity, characterized by power law tail in the time scales distribution, is considered.

To conclude, we report that through Eq. (17) we define a relation between the medium heterogeneity and the fractional order of the diffusion equation, by the introduction of a population of timescales. Within this approach, the power law tail of the distribution of the timescales can be estimated from the fractional order of the diffusion process. This relation establishes an interpretation of the fractional order that goes beyond the one given in the standard CTRW, providing a physical interpretation of the variability of the waiting times in terms of environment heterogeneity without modifying the physical mechanism behind the single trapping event.

Acknowledgements This research was supported by the Basque Government through the BERC 2018–2021 program, and by the Spanish Ministry of Economy and Competitiveness MINECO through BCAM Severo Ochoa excellence accreditation SEV-2017-0718.

References

1. Camboni, F., Sokolov, I.M.: Normal and anomalous diffusion in random potential landscapes. Phys. Rev. E **85**, 050104(R) (2012)
2. Di Tullio, F., Paradisi, P., Spigler, R., Pagnini, G.: Gaussian processes in complex media: new vistas on anomalous diffusion. Front. Phys. **7**, 123 (2019)
3. Fulger, D., Scalas, E., Germano, G.: Monte Carlo simulation of uncoupled continuous-time random walks yielding a stochastic solution of the space-time fractional diffusion equation. Phys. Rev. E **77**, 021122 (2008)
4. Gorenflo, R., Mainardi, F.: Fractional calculus: integral and differential equations of fractional order. In: Carpinteri, A., Mainardi, F. (eds.) Fractals and Fractional Calculus in Continuum Mechanics, pp. 223–276. Springer, Wien and New York (1997)
5. Gorenflo, R., Mainardi, F.: Some recent advances in theory and simulation of fractional diffusion processes. J. Comput. Appl. Math. **229**(2), 400–415 (2009)
6. Haubold, H.J., Mathai, A.M., Saxena, R.K.: Mittag–Leffler functions and their applications. J. Appl. Math. **2011**, 298,628 (2011)
7. Hilfer, R., Anton, L.: Fractional master equations and fractal time random walks. Phys. Rev. E **51**(2), R848–R851 (1995)
8. Klafter, J., Blumen, A., Shlesinger, M.F.: Stochastic pathway to anomalous diffusion. Phys. Rev. A **35**(7), 3081–3085 (1987)
9. Klafter, J., Lim, S.C., Metzler, R.: Fractional Dynamics: Recent Advances. World Scientific, Singapore (2011)
10. Klages, R., Radons, G., Sokolov, I.M. (eds.): Anomalous Transport: Foundations and Applications. Wiley-VCH Verlag GmbH & Co. KGaA, Weinheim (2008)
11. Kutner, R., Masoliver, J.: The continuous time random walk, still trendy: fifty-year history, state of art and outlook. Eur. Phys. J. B **90**, 50 (2017)
12. Mainardi, F.: Fractional Calculus and Waves in Linear Viscoelasticity. Imperial College Press (2010)
13. Mainardi, F., Gorenflo, R.: On Mittag-Leffler-type functions in fractional evolution processes. J. Comput. Appl. Math. **118**(1–2), 283–299 (2000)
14. Mainardi, F., Luchko, Y., Pagnini, G.: The fundamental solution of the space-time fractional diffusion equation. Fract. Calc. Appl. Anal. **4**(2), 153–192 (2001)
15. Mainardi, F., Raberto, M., Gorenflo, R., Scalas, E.: Fractional calculus and continuous-time finance II: the waiting-time distribution. Phys. A **287**(3–4), 468–481 (2000)
16. Méndez, V., Iomin, A.: Comb-like models for transport along spiny dendrites. Chaos Solitons Fract. **53**(Supplement C), 46–51 (2013)
17. Metzler, R., Klafter, J.: The restaurant at the end of the random walk: recent developments in fractional dynamics descriptions of anomalous dynamical processes. J. Phys. A: Math. Theor. **37**(31), R161–R208 (2004)
18. Montroll, E.W., Weiss, G.H.: Random walks on lattices. II. J. Math. Phys. **6**(2), 167–181 (1965)
19. Pagnini, G.: Short note on the emergence of fractional kinetics. Phys. A **409**, 29–34 (2014)
20. Reynolds, A.: Liberating Lévy walk research from the shackles of optimal foraging. Phys. Life Rev. **14**, 59–83 (2015)
21. Sahimi, M.: Heterogeneous Materials I. Linear Transport and Optical Properties, 1 edn. Interdisciplinary Applied Mathematics. Springer, Berlin (2003)
22. Santamaria, F., Wils, S., Schutter, E.D., Augustine, G.J.: Anomalous diffusion in Purkinje cell dendrites caused by spines. Neuron **52**(4), 635–648 (2006)
23. Scalas, E., Gorenflo, R., Mainardi, F.: Fractional calculus and continuous-time finance. Phys. A **284**, 376–384 (2000)
24. Scalas, E., Gorenflo, R., Mainardi, F.: Uncoupled continuous-time random walks: solution and limiting behavior of the master equation. Phys. Rev. E **69**, 011107 (2004)
25. Scher, H., Montroll, E.W.: Anomalous transit-time dispersion in amorphous solids. Phys. Rev. B **12**, 2455–2477 (1975)

26. Vitali, S., Mainardi, F., Castellani, G.: Emergence of fractional kinetics in spiny dendrites. Fractal Fract. **2**(1), 6 (2018)
27. Weiss, G.H.: Aspects and Applications of the Random Walk. North-Holland, Amsterdam (1994)
28. Witzel, P., Götz, M., Lanoiselée, Y., Franosch, T., Grebenkov, D.S., Heinrich, D.: Heterogeneities shape passive intracellular transport. Biophys. J. **117**(2), 203–213 (2019)

On Time Fractional Derivatives in Fractional Sobolev Spaces and Applications to Fractional Ordinary Differential Equations

Masahiro Yamamoto

Abstract In this article, we formulate two kinds of time fractional derivatives of the Caputo type with order α in fractional Sobolev spaces and prove that they are isomorphisms between the corresponding Sobolev space of order α and the L^2-space. On the basis of such fractional derivatives, we formulate initial value problems for time fractional ordinary differential equations and prove the well-posedness.

Keywords Time fractional ordinary differential equation · Fractional Sobolev space · Initial value problem · Well-posedness

1 Introduction and Main Results

Let $m \in \mathbb{N}$ and $m - 1 < \alpha < m$. We consider the Caputo derivative

$$ {}_0^C D_t^\alpha v(t) := \frac{1}{\Gamma(m-\alpha)} \int_0^t (t-s)^{m-\alpha-1} \frac{d^m v}{ds^m}(s) ds, \tag{1} $$

which can be defined for $v \in W^{1,1}(0,T) := \left\{ v \in L^1(0,T);\ \frac{dv}{dt} \in L^1(0,T) \right\}$. For $0 < \alpha < 1$, in Gorenflo, Luchko and Yamamoto [7], in Sobolev spaces we formulate ${}_0^C D_t^\alpha$. See also Kubica, Ryszewska and Yamamoto [14]. On fractional calculus and differential equations, we can refer for example, to Gorenflo and Mainardi [6], Kilbas, Srivastava and Trujillo [10], Podlubny [20] as convenient and fundamental literature.

M. Yamamoto (✉)
Graduate School of Mathematical Scsiences, The University of Tokyo, Komaba, Meguro Tokyo 153-8914, Japan
e-mail: myama@ms.u-tokyo.ac.jp

Honorary Member of Academy of Romanian Scientists, Ilfov, nr. 3, Bucureşti, Romania

Peoples' Friendship University of Russia (RUDN University), 6 Miklukho-Maklaya St, Moscow 117198, Russian Federation

L. Beghin et al. (eds.), *Nonlocal and Fractional Operators*, SEMA SIMAI Springer Series 26, https://doi.org/10.1007/978-3-030-69236-0_15

In this article, we discuss two kinds of fractional derivatives in Sobolev spaces within the framework by [7]. The first kind of fractional derivative is a generalized fractional derivative of (1) defined by

$$\partial_{t,k}^{\alpha} v(t) = \frac{1}{\Gamma(1-\alpha)} \int_0^t (t-s)^{-\alpha} k(t-s) \frac{dv}{ds}(s) ds, \quad 0 < \alpha < 1 \tag{2}$$

for $v \in C^1[0, T]$ if $k \in L^1(0, T)$ for example. Here $k = k(\eta)$ satisfies the conditions stated later, and we know $\partial_{t,1}^{\alpha} = {}_0^C D_t^{\alpha}$.

Similarly to [7], we mainly discuss a suitable extension of the operator $\partial_{t,k}^{\alpha}$ because the domain $W^{1,1}(0, T)$ or $C^1[0, T]$ of the operator is not convenient for theoretical researches on initial value problems for fractional ordinary differential equations which we will discuss in this article. Such an adequate extension is justified in Theorem 1 stated below.

The second kind of fractional derivative is the extension of ${}_0^C D_t^{\alpha}$ in the case of $1 < \alpha < 2$ within Sobolev spaces.

Moreover, based on our formulations of these fractional derivatives, we discuss the well-posedness for initial value problems for fractional ordinary differential equations.

Here we intend to provide introductory descriptions by taking into consideration the limited page numbers, and we postpone the detailed comprehensive studies to forthcoming works.

We make operator-theoretical treatments of the two kinds of time fractional derivatives and formulate them in fractional Sobolev spaces (e.g., Adams [1]). It looks that our formulation is indirect, but as is understood by our arguments on fractional differential equations in Sects. 4 and 5, our approach greatly facilitates treatments of fractional differential equations such as the unique existence of solution to initial value problems.

For later descriptions, we introduce function spaces and operators. For $\alpha > 0$, we define the Riemann–Liouville fractional integral operator:

$$J^{\alpha} f(t) = \frac{1}{\Gamma(\alpha)} \int_0^t (t-s)^{\alpha-1} f(s) ds, \quad f \in L^2(0, T). \tag{3}$$

By $L^2(0, T)$, $H^{\alpha}(0, T)$, $W^{1,\kappa}(0, T)$ with $\alpha > 0$ and $\kappa > 1$, we mean the usual L^2-space and Sobolev space on the interval $(0, T)$ (see e.g., Adams [1], Chapter VII and Lions and Magenes [15]) and we define the norm in $H^{\alpha}(0, T)$ by

$$\|u\|_{H^{\alpha}(0,T)} := \left(\|u\|_{L^2(0,T)}^2 + \int_0^T \int_0^T \frac{|u(t) - u(s)|^2}{|t-s|^{1+2\alpha}} dt ds \right)^{\frac{1}{2}}, \quad 0 < \alpha < 1. \tag{4}$$

The L^2-norm and the scalar product in L^2 are denoted by $\| \cdot \|_{L^2(0,T)}$ and $(\cdot, \cdot)$, respectively. Since J^{α} defined by (3), is injective in $L^2(0, T)$, by $J^{-\alpha}$ we denote the algebraic inverse to J^{α}: $J^{-\alpha} = (J^{\alpha})^{-1}$.

We set

$$ {}_0C^1[0,T] = \{v \in C^1[0,T];\ v(0) = 0\}. \tag{5} $$

We further define the Banach spaces:

$$ H_\alpha(0,T) := \begin{cases} {}_0H^\alpha(0,T), & \frac{1}{2} < \alpha \le 1, \\ \left\{ v \in H^{\frac{1}{2}}(0,T);\ \int_0^T \frac{|v(t)|^2}{t} dt < \infty \right\}, & \alpha = \frac{1}{2}, \\ H^\alpha(0,T), & 0 < \alpha < \frac{1}{2} \end{cases} \tag{6} $$

with the following norm

$$ \|v\|_{H_\alpha(0,T)} = \begin{cases} \|v\|_{H^\alpha(0,T)},\ 0 < \alpha \le 1,\ \alpha \ne \frac{1}{2}, \\ \left(\|v\|^2_{H^{\frac{1}{2}}(0,T)} + \int_0^T \frac{|v(t)|^2}{t} dt \right)^{\frac{1}{2}},\ \alpha = \frac{1}{2}. \end{cases} \tag{7} $$

Here $\|v\|_{H^\alpha(0,T)}$ is defined by (4). Throughout this article, $C > 0$, $C_1 > 0$. etc. denote generic constants which are independent of solutions and functions u, etc. to be estimated.

1.1 Generalized Time-Fractional Derivative

Let $0 < \alpha < 1$. We assume

$$ \begin{cases} k \in W^{1,\kappa}(0,T) \quad k(0) \ne 0, \\ \sup_{0<\xi<T} \left| \xi^\beta \frac{\partial k}{\partial \xi}(\xi) \right| < \infty \quad \text{with some } \kappa > 1 \text{ and } \beta \in (0,1). \end{cases} \tag{8} $$

Under assumption (8), $\partial^\alpha_{t,k} v$ is well-defined for example for $v \in C^1[0,T]$ an $\partial^\alpha_{t,k} v \in L^2(0,T)$. Indeed the Sobolev embedding yields $k \in W^{1,1}(0,T) \subset L^2(0,T)$ and so $k\frac{dv}{dt} \in L^2(0,T)$. Therefore the Young inequality on the convolution implies

$$ \begin{aligned} \|\partial^\alpha_{t,k} v\|_{L^2(0,T)} &= \left\| \left(\frac{1}{\Gamma(1-\alpha)} t^{-\alpha} * k\frac{dv}{dt} \right) \right\|_{L^2(0,T)} \\ &\le \left\| \frac{1}{\Gamma(1-\alpha)} t^{-\alpha} \right\|_{L^1(0,T)} \left\| k\frac{dv}{dt} \right\|_{L^2(0,T)} < \infty. \end{aligned} $$

For the formulation and the applications of fractional differential equations in Sect. 4, it is desirable and natural to extend the domain of $\partial^\alpha_{t,k}$ larger than $C^1[0,T]$.

Now we are ready to state our first main result on the formulation of $\partial^\alpha_{t,k}$.

Theorem 1 *There exists a unique extended operator* $\overline{\partial^\alpha_{t,k}}$ *defined over* $H_\alpha(0,T)$ *of the operator* $\partial^\alpha_{t,k}$ *such that*

$$\overline{\partial^\alpha_{t,k}} v = \partial^\alpha_{t,k} v, \quad v \in {}_0C^1[0,T]$$

and there exists a constant $C > 0$ *such that*

$$C^{-1} \|\overline{\partial^\alpha_{t,k}} v\|_{L^2(0,T)} \le \|v\|_{H_\alpha(0,T)} \le C \|\overline{\partial^\alpha_{t,k}} v\|_{L^2(0,T)} \tag{9}$$

for each $v \in H_\alpha(0,T)$.

Here ${}_0C^1[0,T]$, $H_\alpha(0,T)$ and $\|v\|_{H_\alpha(0,T)}$ are defined by (5)–(7). In Sect. 2, we prove Theorem 3 and gives a representation (27) of $\overline{\partial^\alpha_{t,k}}$ by means of the inversion $J^{-\alpha}$ of J^α. Henceforth, by $\partial^\alpha_{t,k}$ we denote $\overline{\partial^\alpha_{t,k}}$ if not specified.

Concerning the generalized fractional derivatives, we refer to Kochubei [11], Luchko and Yamamoto [18, 19], Zacher [23]. Also see related articles in the handbook Kochubei, Luchko and Machado [12]. In [11], it is assumed that the Laplace transform $\int_0^\infty e^{-\xi s} k(s) ds$ of k exists for all $\xi > 0$ and satisfies some properties including the asymptotics as $\xi \to 0$ and $\xi \to \infty$. The article by [18] develops applications to initial-boundary value problems for time fractional partial differential equations. The article [23] assumes that $k \in L^1_{loc}[0,\infty)$, ≥ 0, is nondecreasing and there exists $k_{-1} \in L^1_{loc}[0,\infty)$ satisfying $\int_0^t k(t-s) k_{-1}(s) ds = 1$ for $t > 0$ and discusses initial-boundary value problems for time fractional partial differential equations. In these works the conditions on $k(t)$ are concerned with $0 < t < \infty$ even when we consider the derivative in a finite interval $(0,T)$, and the derivatives are discussed mainly pointwise. On the other hand, our condition (8) is localized to $t \in (0,T)$, and falls within a different category.

Theorem 1 provides a convenient characterization of the general fractional derivative for applications to fractional differential equations.

1.2 Caputo Derivative of the Order $1 < \alpha < 2$ in Sobolev Spaces

In [7, 14], we formulate the Caputo derivative ${}^C_0 D^\alpha_t$ in fractional Sobolev spaces for the case of $0 < \alpha < 1$ and apply to the fractional differential equations. The formulation and the applications can be naturally extended to the case of $\alpha > 1$. Here we discuss only the case of $1 < \alpha < 2$.

Let

$$\alpha = 1 + \gamma, \quad 0 < \gamma < 1.$$

We define

$$H_\alpha(0,T) := \left\{ v \in H_1(0,T);\ \frac{dv}{dt} \in H_\gamma(0,T) \right\} \tag{10}$$

and

$$\|v\|_{H_\alpha(0,T)} = \begin{cases} \|v\|_{H^\alpha(0,T)},\ 1 \le \alpha < 2, \quad \alpha \ne \frac{3}{2}, \\ \left(\|v\|^2_{H^{\frac{3}{2}}(0,T)} + \int_0^T \left| \frac{dv}{dt} \right|^2 \frac{1}{t} dt \right)^{\frac{1}{2}},\ \alpha = \frac{3}{2}. \end{cases} \tag{11}$$

Here we set

$$\|v\|_{H^\alpha(0,T)} := \left(\|v\|^2_{L^2(0,T)} + \left\| \frac{dv}{dt} \right\|^2_{L^2(0,T)} + \int_0^T \int_0^T |t-s|^{-1-2\gamma} \left| \frac{dv}{dt}(t) - \frac{dv}{dt}(s) \right|^2 dtds \right)^{\frac{1}{2}}$$

(e.g., [1]). By (10) we have

$$H_\alpha(0,T) = \begin{cases} H^\alpha(0,T) & \text{if } 0 < \alpha < \frac{1}{2}, \\ \{v \in H^\alpha(0,T);\ v(0) = 0\} & \text{if } \frac{1}{2} < \alpha < \frac{3}{2}, \\ \left\{v \in H^\alpha(0,T);\ v(0) = \frac{dv}{dt}(0) = 0\right\} & \text{if } \frac{3}{2} < \alpha < 2. \end{cases}$$

Since for $0 < \gamma < 1$, it is proved in [7] that J^γ is injective and writing $J^{-\gamma} = (J^\gamma)^{-1}$, we define

$$\partial_t^\gamma v = J^{-\gamma} v, \quad v \in H_\gamma(0,T).$$

Then the following is proved in [7].

Theorem 2 *Let* $0 < \gamma \le 1$.

(i) $J^\gamma : L^2(0,T) \longrightarrow H_\gamma(0,T)$ *is injective and surjective.*
(ii) There exists a constant $C > 0$ *such that*

$$C^{-1} \|J^\gamma v\|_{H_\gamma(0,T)} \le \|v\|_{L^2(0,T)} \le C \|J^\gamma v\|_{H_\gamma(0,T)}$$

for all $v \in L^2(0,T)$.
(iii) There exists a constant $C > 0$ *such that*

$$C^{-1} \|\partial_t^\gamma u\|_{L^2(0,T)} \le \|u\|_{H_\gamma(0,T)} \le C \|\partial_t^\gamma u\|_{L^2(0,T)} \tag{12}$$

for all $u \in H_\gamma(0,T)$.
(iv) ${}_0^C D_t^\gamma u = \partial_t^\gamma u$ *for* $u \in {}_0C^1[0,T]$.

We remark that $\partial_t^\alpha H_\alpha(0,T) = L^2(0,T)$ for $0 < \alpha < 1$. Moreover we know that $\frac{du}{dt} = J^{-1}u$ for $u \in H_1(0,T)$.

For $\alpha = 1 + \gamma$ with $\gamma \in (0,1)$, we define

$$\partial_t^\alpha u := \partial_t^\gamma \frac{du}{dt} = J^{-\gamma} J^{-1} u, \quad u \in H^{1+\gamma}(0, T).$$

As is directly verified by definition (3), we have $J^\alpha J^\beta = J^{\alpha+\beta}$ with $\alpha, \beta > 0$, and so

$$J^{-\gamma} J^{-1} = J^{-1-\gamma} = J^{-\alpha}.$$

Therefore

$$\partial_t^\alpha u = J^{-\alpha} u, \quad u \in H_\alpha(0, T), \quad 1 < \alpha < 2. \tag{13}$$

The following theorem is directly derived from Theorem 2, and is important for applications to fractional differential equations.

Theorem 3 *Let $\alpha = 1 + \gamma$ with $0 < \gamma < 1$.*

(i) $\partial_t^\alpha : H_\alpha(0, T) \longrightarrow L^2(0, T)$ is surjective and injective.
(ii) There exists a constant $C > 0$ such that

$$C^{-1} \|u\|_{H_\alpha(0,T)} \le \|\partial_t^\alpha u\|_{L^2(0,T)} \le C \|u\|_{H_\alpha(0,T)} \tag{14}$$

for each $u \in H_\alpha(0, T)$.

Theorem 3 asserts that ∂_t^α is an isomorphism between $H_\alpha(0, T)$ and $L^2(0, T)$ also for $1 < \alpha < 2$, which has been established in [7] for $0 < \alpha < 1$. Similarly to the case of $0 < \alpha < 1$, Theorem 3 is useful for discussions of fractional differential equations and in Sect. 5, we apply it to initial value problems for fractional ordinary differential equations.

The article is composed of six sections. In Sects. 2 and 3, we prove Theorems 1 and 3 respectively. In Sects. 4 and sec:5, we show how to apply Theorems 1 and 3 for proving the well-posedness of initial value problems for some fractional ordinary differential equations. Section 6 gives concluding remarks on future research topics.

2 Proof of Theorem 1

We set

$$p(t, \xi) := \int_\xi^t (t - s)^{\alpha-1} (s - \xi)^{-\alpha} k(s - \xi) ds$$

and

$$q(\xi) := \int_0^1 (1 - \eta)^{\alpha-1} \eta^{-\alpha} k(\eta\xi) d\eta, \quad 0 < \xi < T.$$

Then the change of variables $\eta := \frac{s-\xi}{t-\xi}$ yields

$$p(t,\xi) = q(t-\xi), \quad 0 < \xi < t < T. \tag{15}$$

Therefore

$$\frac{\partial(q(t-\xi))}{\partial\xi} = -\int_0^1 (1-\eta)^{\alpha-1}\eta^{1-\alpha}\frac{dk}{ds}(\eta(t-\xi))d\eta, \quad 0 < \xi < t < T. \tag{16}$$

We set

$$(Ku)(t) := \int_0^t \frac{\partial(q(t-\xi))}{\partial\xi}u(\xi)d\xi. \tag{17}$$

Now we can prove

Lemma 1 *Under assumption (8), the operators* $K : H_1(0,T) \longrightarrow H_1(0,T)$ *and* $K : L^2(0,T) \longrightarrow L^2(0,T)$ *are both compact.*

Proof By (8), we see

$$k_0(\xi) := \xi^\beta \frac{dk}{d\xi}(\xi) \in L^\infty(0,T),$$

and so

$$\frac{\partial(q(t-\xi))}{\partial\xi} = -\int_0^1 (1-\eta)^{\alpha-1}\eta^{1-\alpha}k_0(\eta(t-\xi))(\eta(t-\xi))^{-\beta}d\eta$$
$$= -(t-\xi)^{-\beta}\int_0^1 (1-\eta)^{\alpha-1}\eta^{1-\alpha-\beta}k_0(\eta(t-\xi))d\eta$$

by (16) and

$$\left|\frac{\partial(q(t-\xi))}{\partial\xi}\right| \le \|k_0\|_{L^\infty(0,T)}(t-\xi)^{-\beta}\int_0^1 (1-\eta)^{\alpha-1}\eta^{1-\alpha-\beta}d\eta$$

$$\le \|k_0\|_{L^\infty(0,T)}\frac{\Gamma(\alpha)\Gamma(2-\alpha-\beta)}{\Gamma(2-\beta)}(t-\xi)^{-\beta} \le C(t-\xi)^{-\beta}, \quad 0 < \xi < t < T. \tag{18}$$

Moreover we set

$$p_1(t-\xi) = \begin{cases} \frac{\partial(q(t-\xi))}{\partial\xi}, & 0 < \xi < t < T, \\ 0, & 0 < t < \xi < T. \end{cases}$$

Therefore, by (18) we see that

$$|p_1(t-\xi)| \le \frac{C}{|t-\xi|^\beta}, \quad 0 < \xi < t < T. \tag{19}$$

By (15), we notice that

$$\frac{\partial(q(t-\xi))}{\partial\xi} = -\frac{\partial p}{\partial\xi}(t,\xi), \quad 0 < \xi < t < T. \tag{20}$$

Here we show

Lemma 2 *Let ℓ satisfy*

$$|\ell(\xi)| \le \frac{C}{|\xi|^\beta}, \quad 0 < \xi < T$$

with some $\beta \in (0,1)$. Then the operator

$$(Lu)(t) = \int_0^t \ell(t-s)u(s)ds, \quad 0 < t < T$$

is compact from $L^2(0,T)$ to $L^2(0,T)$.

For completeness, we prove the lemma in Appendix.

Therefore, by (19) and the compactness of integral operator with weakly singular kernel p_1 with $0 < \beta < 1$ in Yosida [22], we see that $K : L^2(0,T) \longrightarrow L^2(0,T)$ defined by (17) is compact.

Next we have to prove the compactness of K in $H_1(0,T)$. We notice

$$(Ku)(t) = \int_0^t \frac{\partial(q(t-\xi))}{\partial\xi} u(\xi)d\xi$$
$$= -\int_0^t \frac{dq}{d\xi}(t-\xi)u(\xi)d\xi = -\int_0^t \frac{dq}{d\eta}(\eta)u(t-\eta)d\eta$$

by the change of the variables: $\eta = t - \xi$.

Let $u \in H_1(0,T)$. Then $u \in L^\infty(0,T)$ by the Sobolev embedding. Since $\frac{dq}{d\xi}(\cdot)u(t-\cdot) \in L^1(0,T)$ by (19) and (20), we obtain

$$(Ku)(0) = 0 \tag{21}$$

and we can obtain that

$$\frac{d(Ku)}{dt}(t) = -\int_0^t \frac{dq}{d\xi}(\xi)\frac{du}{dt}(t-\xi)d\xi, \quad 0 < t < T.$$

Again the same change of the variables yields

$$\frac{d(Ku)}{dt}(t) = -\int_0^t \frac{dq}{d\theta}(t-\xi)\frac{du}{d\xi}(\xi)d\xi$$

$$= \int_0^t p_1(t-\xi)\frac{du}{d\xi}(\xi)d\xi, \quad 0 < t < T. \tag{22}$$

Therefore, by the Young inequality, $\frac{dq}{dt} \in L^1(0,T)$ and $\frac{du}{dt} \in L^2(0,T)$ yield $\frac{d(Ku)}{dt} \in L^2(0,T)$ for each $u \in H_1(0,T)$.

Hence $KH_1(0,T) \subset H^1(0,T)$. Moreover by (21) we see that $KH_1(0,T) \subset H_1(0,T)$.

Finally we have to prove that $K : H_1(0,T) \longrightarrow H_1(0,T)$ is compact. Let $\sup_{n\in\mathbb{N}} \|u_n\|_{H_1(0,T)} < \infty$. Then $\sup_{n\in\mathbb{N}} \left\| \frac{du_n}{d\xi} \right\|_{L^2(0,T)} < \infty$. Noting (19) and (22), we again apply Lemma 2, so that we can extract a subsequence, denoted again by n, such that $\frac{d(Ku_n)}{dt}$ converges in $L^2(0,T)$. By $(Ku_n)(0) = 0$, we see that Ku_n converges in $H^1(0,T)$. Hence $K : H_1(0,T) \longrightarrow H_1(0,T)$ is compact. Thus the proof of Lemma 1 is completed.

By (8), we have

$$q(0) = k(0)\int_0^1 (1-\eta)^{\alpha-1}\eta^{-\alpha}d\eta = \Gamma(\alpha)\Gamma(1-\alpha)k(0) \neq 0. \tag{23}$$

Next we show

Lemma 3 *If $q(0)u + Ku = 0$ for $u \in L^2(0,T)$, then $u = 0$ in $(0,T)$.*

Proof Let

$$q(0)u(t) = -\int_0^t \frac{\partial(q(t-\xi))}{\partial\xi}u(\xi)d\xi, \quad 0 < t < T.$$

Then, by (23) and (19), we obtain

$$|u(t)| \leq C\int_0^t (t-\xi)^{-\beta}|u(\xi)|d\xi, \quad 0 < t < T.$$

Therefore a generalized Gronwall inequality (e.g., pp. 188–189 in Henry [8]) yields $u = 0$ in $(0,T)$. Thus the proof of Lemma 3 is completed.

By Lemmata 1 and 3, applying the Fredholm alternative, we see that $(q(0) - K)^{-1} : H_1(0,T) \longrightarrow H_1(0,T)$ and $(q(0) - K)^{-1} : L^2(0,T) \longrightarrow L^2(0,T)$ are bounded linear operators. We apply the interpolation result.

Since $[H_1(0,T), L^2(0,T)]_{1-\alpha} = H_\alpha(0,T)$, $0 < \alpha < 1$ (e.g., Sect. 11.5 (Theorem 11.6 and Remark 11.5) of Chap. 1 in Lions and Magenes [15]), we apply Theorem 5.1 in Sect. 5.1 of Chap. 1 in [15]), so that by (23) we can conclude that

$$\left(k(0) - \frac{1}{\Gamma(\alpha)\Gamma(1-\alpha)}K\right)^{-1} : H_\alpha(0,T) \longrightarrow H_\alpha(0,T)$$

is surjective and isomorphism. Thus there exists a constant $C > 0$ such that

$$C^{-1}\|u\|_{H_\alpha(0,T)} \le \left\| \left(k(0) - \frac{1}{\Gamma(\alpha)\Gamma(1-\alpha)} K \right) u \right\|_{H_\alpha(0,T)} \le C\|u\|_{H_\alpha(0,T)}, \quad u \in H_\alpha(0,T). \tag{24}$$

Now we prove

Lemma 4

$$J^\alpha \partial_{t,k}^\alpha u = \left(k(0) - \frac{1}{\Gamma(\alpha)\Gamma(1-\alpha)} K \right) u \quad in (0,T)$$

for $u \in {}_0C^1[0,T]$.

Proof Exchanging the order of integration, we obtain

$$\Gamma(1-\alpha)\Gamma(\alpha) J^\alpha \partial_{t,k}^\alpha u(t) = \int_0^t (t-s)^{\alpha-1} \left(\int_0^s (s-\xi)^{-\alpha} k(s-\xi) \frac{du(\xi)}{d\xi} d\xi \right) ds$$
$$= \int_0^t \left(\int_\xi^t (t-s)^{\alpha-1} (s-\xi)^{-\alpha} k(s-\xi) ds \right) \frac{du(\xi)}{d\xi} d\xi = \int_0^t q(t-\xi) \frac{du(\xi)}{d\xi} d\xi.$$

By (16), (17) and $u(0) = 0$, the integration by parts yields

$$\Gamma(1-\alpha)\Gamma(\alpha) J^\alpha \partial_{t,k}^\alpha u(t)$$
$$= q(0)u(t) - \int_0^t \frac{\partial (q(t-\xi))}{\partial \xi} u(\xi) d\xi = (q(0) - K)u(t).$$

Thus, in view of (23), the proof of Lemma 4 is completed.

Definition of $\overline{\partial_{t,k}^\alpha}$.
We define the extension of $\partial_{t,k}^\alpha$ by

$$\overline{\partial_{t,k}^\alpha} u = J^{-\alpha} \left(k(0) - \frac{1}{\Gamma(\alpha)\Gamma(1-\alpha)} K \right) u, \quad u \in H_\alpha(0,T). \tag{25}$$

By (25) and Theorem 2 shown in Sect. 1, we see that $\overline{\partial_{t,k}^\alpha} u \in L^2(0,T)$ is well-defined for each $u \in H_\alpha(0,T)$ and estimate (9) holds.

Finally we have to prove the uniqueness in determining the extension of $\partial_{t,k}^\alpha$ in ${}_0C^1[0,T]$. Let $\widetilde{D} : H_\alpha(0,T) \longrightarrow L^2(0,T)$ satisfy (9) and $\widetilde{D}u = \partial_{t,k}^\alpha u$ for all $u \in {}_0C^1[0,T]$.

Henceforth $\overline{Y}^X$ denotes the closure of a subset Y of a Banach space X in the topology of X. We can prove

$$\overline{{}_0C^1[0,T]}^{H_\alpha(0,T)} = H_\alpha(0,T). \tag{26}$$

Proof of (26).
For $\frac{1}{2} < \alpha \le 1$, we see that $H_\alpha(0,T) = \{u \in H^\alpha(0,T);\ u(0) = 0\}$, so that the mol-

lifier (e.g., [1]) yields the conclusion. Let $0 \le \alpha \le \frac{1}{2}$. By [15], we have

$$H_\alpha(0,T) = [H_1(0,T),\ L^2(0,T)]_{1-\alpha}$$

which is the interpolation space. Applying Proposition 6.1 (p. 28) in [15], for $\frac{1}{2} < \gamma < 1$ we see that

$$\overline{H_\gamma(0,T)}^{H_\alpha(0,T)} = H_\alpha(0,T).$$

As is already proved, we see that

$$\overline{{}_0C^1[0,T]}^{H_\gamma(0,T)} = H_\gamma(0,T).$$

Both density properties yield

$$\overline{{}_0C^1[0,T]}^{H_\alpha(0,T)} = H_\alpha(0,T)$$

for $0 \le \alpha \le \frac{1}{2}$. Thus the proof of (26) is completed.

Let $u \in H_\alpha(0,T)$ be arbitrarily given. By (26) we choose $u_n \in {}_0C^1[0,T], n \in \mathbb{N}$, such that $u_n \longrightarrow u$ in $H_\alpha(0,T)$. Then $\widetilde{D}u_n = \partial^\alpha_{t,k}u_n, n \in \mathbb{N}$. By (9) $\widetilde{D}u_n$ are convergent in $L^2(0,T)$ and $\partial^\alpha_{t,k}u_n \longrightarrow \overline{\partial^\alpha_{t,k}}u$ in $L^2(0,T)$. Therefore $\overline{\partial^\alpha_{t,k}}u = \widetilde{D}u$. Thus the uniqueness of the extension is seen and the proof of Theorem 1 is complete.

Henceforth we write $\overline{\partial^\alpha_{t,k}}$ simply by $\partial^\alpha_{t,k}$. Theorem 1 and Lemma 4 allow us to represent

$$\partial^\alpha_{t,k}u = J^{-\alpha}\left(k(0) - \frac{1}{\Gamma(\alpha)\Gamma(1-\alpha)}K\right)u, \quad u \in H_\alpha(0,T). \tag{27}$$

In the case of the Caputo derivative, i.e., $k \equiv 1$, we see that $k(0) = 1$ and $K = 0$, and so $\partial^\alpha_{t,k}$ coincides with $\partial^\alpha_t = J^{-\alpha}$, which is justified by Theorem 2 in Sect. 1.

3 Proof of Theorem 3

Let $\alpha = 1 + \gamma$ with $0 < \gamma < 1$.

(i) Proof of the injectivity.

We assume that $u \in H_\alpha(0,T)$ satisfies $\partial^\gamma_t\left(\frac{du}{dt}\right) = 0$ in $(0,T)$. By Theorem 2, ∂^γ_t is injective, and so $\frac{du}{dt} = 0$ in $(0,T)$. Sinc $u \in H_1(0,T)$ by $u \in H_\alpha(0,T) \subset H_1(0,T)$, we have $u(0) = 0$. Hence $u = 0$ in $(0,T)$. Thus ∂^α_t is injective in $H_\alpha(0,T)$.

(ii) Proof of the surjectivity.

First we see

$$JH_\gamma(0,T) \subset H_{1+\gamma}(0,T). \tag{28}$$

Indeed let $v = J\widetilde{v}$ with $\widetilde{v} \in H_\gamma(0,T)$. Then $\frac{dv}{dt} = \frac{d}{dt}(J\widetilde{v}) = \widetilde{v} \in H_\gamma(0,T)$. By the definition (10), we see that $v \in H_{1+\gamma}(0,T)$, and (28) is verified.

Let $w \in L^2(0,T)$ be arbitrarily given. We set $u := JJ^\gamma w$. By Theorem 2, we have $J^\gamma w \in H_\gamma(0,T)$ and definition (10) directly yields $u = J(J^\gamma w) \in H_{1+\gamma}(0,T)$. Moreover, since $\frac{d}{dt}Jv = v$ for $v \in L^2(0,T)$, we see that

$$\partial_t^\alpha u = \partial_t^\gamma \frac{d}{dt}(JJ^\gamma w) = \partial_t^\gamma \left(\frac{d}{dt}J\right)(J^\gamma w) = \partial_t^\gamma J^\gamma w.$$

Applying Theorem 2 again, we obtain $\partial_t^\gamma J^\gamma w = w$. Therefore $w = \partial_t^\alpha u$ with $u \in H_\alpha(0,T)$. Thus the surjectivity is proved.

(iii) Proof of (14).

By Theorem 2, we have

$$C^{-1}\left\|\frac{du}{dt}\right\|_{H_\gamma(0,T)} \le \left\|\partial_t^\gamma \frac{du}{dt}\right\|_{L^2(0,T)} \le C\left\|\frac{du}{dt}\right\|_{H_\gamma(0,T)}. \tag{29}$$

By definition (11), we easily verify

$$C^{-1}\|u\|_{H_{1+\gamma}(0,T)} \le \left\|\frac{du}{dt}\right\|_{H_\gamma(0,T)} \le C\|u\|_{H_{1+\gamma}(0,T)}, \quad u \in H_{1+\gamma}(0,T), \tag{30}$$

because $\|u\|_{L^2(0,T)} \le C_1\left\|\frac{du}{dt}\right\|_{L^2(0,T)}$ by using $u(0) = 0$ which follows from $u \in H_1(0,T)$. By (29) and (30), we reach (14). Thus the proof of Theorem 3 is complete.

4 Application to Generalized Caputo Fractional Ordinary Differential Equations

We assume (8) and $0 < \alpha < 1$. On the basis of $\partial_{t,k}^\alpha$ defined in Sect. 1, we discuss initial value problems for fractional ordinary differential equations with generalized Caputo derivative $\partial_{t,k}^\alpha$:

$$\begin{cases} \partial_{t,k}^\alpha(u-a) = G(u) + f, & 0 < t < T, \\ u - a \in H_\alpha(0,T), \end{cases} \tag{31}$$

where G is an operator acting a function u. We remark that G can be quite general including nonlinear terms, but in this section, we consider only a linear case:

$$G(u) := r(t)u, \quad r \in L^\infty(0, T).$$

More precisely,

$$\begin{cases} \partial_{t,k}^\alpha (u - a) = r(t)u(t) + f(t), \quad 0 < t < T, \\ u - a \in H_\alpha(0, T), \end{cases} \tag{32}$$

where $f \in L^2(0, T)$ and $a \in \mathbb{R}$. When we want to consider $\partial_{t,k}^\alpha u$ in the pointwise sense, we have to consider $\frac{du}{dt}$ but this derivative may not exist for the solution u to the initial value problem for not very smooth f, for example, $f \in L^2(0, T)$. In other words, by the naive understanding of $\partial_{t,k}^\alpha$, the initial condition $u(0) = a$ cannot be necessarily understood well if u is not continuous at $t = 0$. We see that $u - a \in H_\alpha(0, T)$ where $\frac{1}{2} < \alpha < 1$ implies $u - a \in C[0, T]$ by the Sobolev embedding, and so the condition $u - a \in H_\alpha(0, T)$ can be a replacement for the initial condition.

We can prove

Theorem 4 *Let $r \in L^\infty(0, T)$. For given $f \in L^2(0, T)$ and $a \in \mathbb{R}$, there exists a unique solution u to (32) and there exists a constant $C > 0$ depending on r, such that*

$$\|u - a\|_{H_\alpha(0,T)} \le C(|a| + \|f\|_{L^2(0,T)}) \tag{33}$$

and

$$\|u\|_{H^\alpha(0,T)} \le C(|a| + \|f\|_{L^2(0,T)}). \tag{34}$$

for each $f \in L^2(0, T)$ and $a \in \mathbb{R}$.

Similarly to Chap. 3 in [14], we can prove improved regularity according to smoother f and r, but we omit the details.

Proof By the definition (27), we know that (32) is equivalent to

$$\begin{cases} J^{-\alpha} \left(k(0) - \frac{1}{\Gamma(\alpha)\Gamma(1-\alpha)} K \right) (u - a) = r(t)u(t) + f(t), \quad 0 < t < T, \\ u - a \in H_\alpha(0, T). \end{cases} \tag{35}$$

Here the operator K is defined by (17), and we set

$$\widetilde{K} = k(0) - \frac{1}{\Gamma(\alpha)\Gamma(1 - \alpha)} K.$$

Then we recall that by (24) both $\widetilde{K} : L^2(0,T) \longrightarrow L^2(0,T)$ and $\widetilde{K} : H_\alpha(0,T) \longrightarrow H_\alpha(0,T)$ are surjective and injective, and

$$\|\widetilde{K}^{-1}v\|_{L^2(0,T)} \le C\|v\|_{L^2(0,T)}, \quad v \in L^2(0,T) \tag{36}$$

and

$$\|\widetilde{K}^{-1}v\|_{H_\alpha(0,T)} \le C\|v\|_{H_\alpha(0,T)}, \quad v \in H_\alpha(0,T). \tag{37}$$

Therefore (35) is equivalent to

$$\begin{cases} u - a = \widetilde{K}^{-1}J^\alpha(r(u-a)) + \widetilde{K}^{-1}J^\alpha f + \widetilde{K}^{-1}J^\alpha(r(t)a), \quad 0 < t < T, \\ u \in L^2(0,T). \end{cases} \tag{38}$$

We see that (38) implies that $u - a \in \widetilde{K}^{-1}J^\alpha L^2(0,T)$ if $u \in L^2(0,T)$, and so (38) and $u \in L^2(0,T)$ yield $u - a \in H_\alpha(0,T)$.

It is sufficient to prove that there exists a unique $u \in L^2(0,T)$ to (38). First

$$\widetilde{K}^{-1}J^\alpha(r\cdot) : L^2(0,T) \longrightarrow L^2(0,T) \text{is a compact operator.} \tag{39}$$

Indeed by (37), $r \in L^\infty(0,T)$ and Theorem 2, we obtain

$$\|\widetilde{K}^{-1}J^\alpha(rv)\|_{H_\alpha(0,T)} \le C\|J^\alpha(rv)\|_{H_\alpha(0,T)} \le C\|rv\|_{L^2(0,T)} \le C\|v\|_{L^2(0,T)}.$$

Therefore $\widetilde{K}^{-1}J^\alpha(r\cdot) : L^2(0,T) \longrightarrow H_\alpha(0,T) \subset H^\alpha(0,T)$ is bounded and by the compactness of the embedding $H^\alpha(0,T) \longrightarrow L^2(0,T)$, we see (39).

Next let $v = \widetilde{K}^{-1}J^\alpha(rv)$ in $(0,T)$. Then

$$k(0)v = \frac{1}{\Gamma(\alpha)\Gamma(1-\alpha)}Kv + J^\alpha(rv),$$

that is, using (17) we have

$$v(t) = \frac{1}{k(0)\Gamma(\alpha)\Gamma(1-\alpha)}\int_0^t \frac{\partial(q(t-\xi))}{\partial\xi}v(\xi)d\xi + \frac{1}{k(0)\Gamma(\alpha)}\int_0^t (t-s)^{\alpha-1}(rv)(s)ds.$$

By (19) and $r \in L^\infty(0,T)$, we have

$$|v(t)| \le C\int_0^t (t-\xi)^{-\beta}|v(\xi)|d\xi + C\int_0^t (t-s)^{\alpha-1}|v(s)|ds, \quad 0 < t < T.$$

Setting $\gamma = \max\{\beta, 1-\alpha\} < 1$, we reach

$$|v(t)| \le C\int_0^t (t-s)^{-\gamma}|v(s)|ds, \quad 0 < t < T.$$

The generalized Gronwall inequality (e.g., Henry [8], pp. 188–189) yields $v = 0$ in $(0, T)$. In terms of (39), applying the Fredholm alternative, we conclude that (38) possesses a unique solution $u - a \in L^2(0, T)$.

Moreover (38) and (36) imply

$$\begin{aligned}\|u-a\|_{L^2(0,T)} &\le C\|\widetilde{K}^{-1}J^{\alpha}f\|_{L^2(0,T)} + C\|\widetilde{K}^{-1}J^{\alpha}(ra)\|_{L^2(0,T)}\\ &\le C\|J^{\alpha}f\|_{L^2(0,T)} + C\|J^{\alpha}(ra)\|_{L^2(0,T)} \le C(\|f\|_{L^2(0,T)} + |a|).\end{aligned}$$

Hence, by (35), we have

$$\begin{aligned}&\|J^{-\alpha}\widetilde{K}(u-a)\|_{L^2(0,T)} \le \|ru+f\|_{L^2(0,T)} = \|r(u-a)+(ra+f)\|_{L^2(0,T)}\\ &\le C(\|f\|_{L^2(0,T)} + |a|)\end{aligned}$$

and

$$\|u-a\|_{H_\alpha(0,T)} \le C\|\widetilde{K}(u-a)\|_{H_\alpha(0,T)} \le C\|J^{-\alpha}\widetilde{K}(u-a)\|_{L^2(0,T)}$$

by Theorem 2 and (37). Therefore, since

$$\|u\|_{H^\alpha(0,T)} - \|a\|_{H^\alpha(0,t)} \le \|u-a\|_{H^\alpha(0,T)} \le \|u-a\|_{H_\alpha(0,T)},$$

we prove (33) and (34), so that the proof of Theorem 4 is complete.

5 Applications to Caputo Fractional Ordinary Differential Equations of Order $1 < \alpha < 2$

Let $\alpha = 1 + \gamma$ with $0 < \gamma < 1$. In view of our defined $\partial_t^\alpha = \partial_t^\gamma \frac{d}{dt}$, we consider two simple linear fractional ordinary differential equations. First we consider

$$\begin{cases} \partial_t^\alpha(u - bt - a) = r(t)u + f(t), \\ u - bt - a \in H_1(0,T), \\ \frac{du}{dt} - b \in H_\gamma(0,T), \end{cases} \tag{40}$$

We first show

Lemma 5 *Let $u \in C^2[0,T]$ satisfy $\frac{du}{dt} - b \in {}_0C^1[0,T]$ and (40). Then u satisfies*

$$\begin{cases} {}_0^C D_t^\alpha u(t) = r(t)u + f(t), \\ u(0) = a, \quad \frac{du}{dt}(0) = b. \end{cases} \tag{41}$$

Here we recall that the Caputo derivative ${}_0^C D_t^\alpha$ for $\alpha = 1 + \gamma$ with $0 < \gamma < 1$ is defined by

$$ {}_0^C D_t^\alpha u(t) = \frac{1}{\Gamma(1-\gamma)} \int_0^t (t-s)^{-\gamma} \frac{d^2}{ds^2} u(s) ds, \quad u \in C^2[0,T]. $$

Proof of Lemma 5
We readily see that $\lim_{t \to 0} \frac{du}{dt}(t) = b$ and $\lim_{t \to 0} u(t) = a$ by the assumption of the smoothness of u. By Theorem 2 (iv), we have

$$ \partial_t^\gamma v(t) = \frac{1}{\Gamma(1-\gamma)} \int_0^t (t-s)^{-\gamma} \frac{dv}{ds}(s) ds, \quad v \in {}_0C^1[0,T]. $$

Therefore $\frac{du}{dt} - b \in {}_0C^1[0,T]$ yields

$$ \partial_t^\gamma \left(\frac{du}{dt} - b \right) = \frac{1}{\Gamma(1-\gamma)} \int_0^t (t-s)^{-\gamma} \frac{d}{ds} \left(\frac{du}{ds} - b \right) ds $$
$$ = \frac{1}{\Gamma(1-\gamma)} \int_0^t (t-s)^{-\gamma} \frac{d^2 u}{ds^2}(s) ds = {}_0^C D_t^\alpha u(t). $$

Therefore the proof of Lemma 5 is complete.

Thus by Lemma 5, we can regard (40) as a natural formulation of an initial value problem although it looks different from the conventional way (e.g., Diethelm [3], Kilbas, Srivastava and Trujillo [10], Podlubny [20]). Since our definition of ∂_t^α is not restricted to smooth u, we can assert that (40) is more general formulation for non-smooth f. Indeed we can easily prove

Theorem 5 *Let $1 < \alpha < 2$ and $r \in L^\infty(0,T)$. For $f \in L^2(0,T)$ and $a, b \in \mathbb{R}$, there exists a unique solution $u \in H_\alpha(0,T)$ to (40). Moreover we can find a constant $C > 0$ such that*

$$ \|u\|_{H^\alpha(0,T)} \le C(|a| + |b| + \|f\|_{L^2(0,T)}) $$

for each $f \in L^2(0,T)$ and $a, b \in \mathbb{R}$.

Proof We can prove similarly to Theorem 4. Setting $v := u - bt - a$, we see that (40) is equivalent to

$$ \partial_t^\gamma \frac{du}{dt} = r(t)v + r(t)(bt + a) + f, $$

that is, since $\partial_t^\gamma w = J^{-\gamma} w$ for $w \in H_\gamma(0,T)$, we obtain

$$ \frac{dv}{dt} = J^\gamma(rv) + J^\gamma(r(bt+a)) + J^\gamma f. $$

By $v \in H_1(0,T)$, we obtain

$$ v(t) = \int_0^t \frac{dv}{ds}(s) ds = J \frac{dv}{dt}(t) $$

and so

$$v = JJ^{\gamma}(rv) + JJ^{\gamma}(r(bt+a)+f) \quad \text{in}(0,T). \tag{42}$$

As is directly proved, we see that $JJ^{\gamma}w = J^{1+\gamma}w$ for $w \in L^2(0,T)$.

Moreover we can readily prove that the operator $K_0 : L^2(0,T) \longrightarrow L^2(0,T)$ defined by $K_0 v := J^{1+\gamma}(rv)$, is compact. Indeed

$$K_0 v(t) = J^{1+\gamma}(rv)(t) = \frac{1}{\Gamma(1+\gamma)} \int_0^t (t-s)^{\gamma} r(s)v(s)ds$$

is a Hilbert-Schmidt integral operator (e.g., Yosida [22]), and so is a compact operator.

Therefore, if we prove that $v = K_0 v$ in $(0,T)$ yields $v = 0$, then the Fredholm alternative implies the unique existence v to (42). Let $v = K_0 v$ in $(0,T)$. Then

$$|v(t)| = \left| \frac{1}{\Gamma(1+\gamma)} \int_0^t (t-s)^{\gamma} r(s)v(s)ds \right| \le C \int_0^t |v(s)|ds, \quad 0 < t < T.$$

The Gronwall inequality implies $v = 0$ in $(0,T)$

Finally we have to estimate u and the proof is very similar to Theorem 4, so that we omit the details. Thus the proof of Theorem 5 is complete.

We can prove a similar result for multi-term fractional ordinary differential equation.

Theorem 6 *Let* $0 < \alpha_1 < \cdots < \alpha_m \le 1 < \alpha_{m+1} < \cdots < \alpha_{N-1} < \alpha_N < 2$, $p_N = 1$, $p_n, r \in L^{\infty}(0,T)$ *for* $1 \le n \le N-1$. *For* $f \in L^2(0,T)$ *and* $a, b \in \mathbb{R}$, *there exists a unique solution* $u \in H_{\alpha}(0,T)$ *to*

$$\sum_{n=1}^{m} p_n(t)\partial_t^{\alpha_n}(u-a) + \sum_{n=m+1}^{N} p_n(t)\partial_t^{\alpha_n}(u-bt-a)$$

$$= r(t)u(t) + f(t), \quad 0 < t < T, \tag{43}$$

and

$$u - bt - a \in H_1(0,T), \quad \frac{du}{dt} - b \in H_{\alpha_N - 1}(0,T). \tag{44}$$

Moreover we can find a constant $C > 0$ *such that*

$$\|u\|_{H^{\alpha_N}(0,T)} \le C(|a| + |b| + \|f\|_{L^2(0,T)}) \tag{45}$$

for each $f \in L^2(0,T)$ *and* $a, b \in \mathbb{R}$.

Similarly to Lemma 5, for $u \in C^2[0,T]$ satisfying $\frac{du}{dt} - b \in {}_0C^1[0,T]$, the formulation (43) and (44) is the same as

$$\begin{cases} \sum_{n=1}^{N} p_n(t) {}_0^C D_t^{\alpha_n} u = r(t)u(t) + f(t), \quad 0 < t < T, \\ u(0) = a, \quad \frac{du}{dt}(0) = b, \end{cases}$$

and so our formulation (43) and (44) is reasonable.

Proof We set $v = J^{-\alpha_N}(u - bt - a)$ and $\widetilde{r}_0(t) = -\sum_{n=1}^{m} p_n(t) \partial_t^{\alpha_n} t \in L^\infty(0,T)$. Then we see that (43) is equivalent to

$$v + \sum_{n=1}^{N-1} p_n(t) J^{-\alpha_n} J^{\alpha_N} v = r J^{\alpha_N} v + r(bt + a) + \widetilde{r}_0 b + f \quad \text{in}(0,T).$$

Since $\alpha_n, \alpha_N - \alpha_n \geq 0$, we can directly see $J^{\alpha_N} v = J^{\alpha_n} J^{\alpha_N - \alpha_n} v$ for $v \in L^2(0,T)$ and

$$J^{-\alpha_n} J^{\alpha_N} v = J^{-\alpha_n}(J^{\alpha_n} J^{\alpha_N - \alpha_n} v) = J^{-\alpha_n} J^{\alpha_n}(J^{\alpha_N - \alpha_n} v) = J^{\alpha_N - \alpha_n} v.$$

Hence (43) is equivalent to

$$v = -\sum_{n=1}^{N-1} p_n J^{\alpha_N - \alpha_n} v + r J^{\alpha_N} v + (r(bt + a) + \widetilde{r}_0 b + f) \quad \text{in}(0,T). \tag{46}$$

Similarly to Theorem 5, we can prove by Theorem 2 that the operator $J^{\alpha_N - \alpha_n} : L^2(0,T) \longrightarrow L^2(0,T)$ is compact by $\alpha_N - \alpha_n > 0$ for $1 \leq n \leq N-1$, because $J^{\alpha_N - \alpha_n} : L^2(0,T) \longrightarrow H_{\alpha_N - \alpha_n}(0,T)$ is a bounded operator.

Moreover by the generalized Gronwall inequality we know that if

$$v = -\sum_{n=1}^{N-1} p_n J^{\alpha_N - \alpha_n} v + r J^{\alpha_N} v \quad \text{in}(0,T)$$

then $v = 0$ in $(0,T)$. Therefore the Fredholm alternative implies that (46) possesses a unique solution $v \in L^2(0,T)$ for each $f \in L^2(0,T)$ and $a, b \in \mathbb{R}$, and

$$\|v\|_{L^2(0,T)} \leq C(|a| + |b| + \|f\|_{L^2(0,T)}).$$

Since $v = J^{-\alpha_N}(u - bt - a)$, we can see

$$\|u - bt - a\|_{H^{\alpha_N}(0,T)} \leq C(|a| + |b| + \|f\|_{L^2(0,T)}).$$

Since

$$\|u - bt - a\|_{H^{\alpha_N}(0,T)} \le \|u - bt - a\|_{H_{\alpha_N}(0,T)}$$

and

$$\begin{aligned}\|u - bt - a\|_{H^{\alpha_N}(0,T)} &\ge \|u\|_{H^{\alpha_N}(0,T)} - \|bt + a\|_{H^{\alpha_N}(0,T)} \\ &\ge \|u\|_{H^{\alpha_N}(0,T)} - C(|a| + |b|),\end{aligned}$$

we see estimate (45). Thus the proof of Theorem 6 is complete.

6 Concluding Remarks on Future Topics

In this article, we establish convenient formulations for two kinds of time fractional derivatives. It is very natural to apply them to initial value problems of wide classes of fractional differential equations. However we intend this article as introductory accounts, and we do not provide comprehensive expositions. In this section, we list up some of important future topics.

I. More properties of solutions:

We should study t-analyticity, asymptotics as $t \to \infty$, improved regularity with more smooth f, etc. for solutions to initial value problems. Moreover the backward problem in time is an interesting topic, and as for ∂_t^α, see Floridia, Li and Yamamoto [4], Floridia and Yamamoto [5], Sakamoto and Yamamoto [21], and the references therein.

II. Nonlinear theory:

Well-posedness and properties for solutions to

$$\partial_{t,k}^\alpha u = G(u) + f(t), \quad u - a \in H_\alpha(0, T),$$

where $G(u)$ is a nonlinear term which can include other fractional terms of u: as just one example, we can propose

$$G(u) = G(\partial_{t,k_1}^{\alpha_1} u, \dots, \partial_{t,k_N}^{\alpha_N} u),$$

where $G(\eta_1, \dots, \eta_N)$ is some function, $0 < \alpha_1 < \cdots < \alpha_N < \alpha < 1$ and the functions $k, k_1, \dots, k_N$ satisfy certain conditions similar to (8).

III. Initial-boundary value problems for fractional partial differential equations:

For a bounded domain $\Omega \subset \mathbb{R}^d$, we should consider

$$\left\{\begin{array}{l} \partial_{t,k}^{\alpha}(u(x,t)-a(x))+A(t)u(x,t)=F(x,t), \quad x\in\Omega,\ 0<t\le T,\\ u(\cdot,t)\in H_0^1(\Omega), \quad 0<t<T,\\ u(x,\cdot)-a(x)\in H_{\alpha}(0,T), \quad x\in\Omega, \end{array}\right.$$

and

$$\left\{\begin{array}{l} \partial_{t}^{\alpha}(u(x,t)-b(x)t-a(x))+A(t)u(x,t)=F(x,t),\\ \qquad\qquad x\in\Omega,\ 0<t\le T, \quad 1<\alpha<2,\\ u(\cdot,t)\in H_0^1(\Omega), \quad 0<t<T,\\ u(x,\cdot)-a(x)\in H_{\alpha}(0,T), \quad u(x,\cdot)-b(x)t-a(x)\in H_1(0,T), \quad x\in\Omega. \end{array}\right.$$

For the case of the fractional derivative ∂_t^{α} with $0<\alpha<1$, we can refer to Bazhlekova [2], Gorenflo, Luchko and Yamamoto [7], Kubica, Ryszewska and Yamamoto [14], Kubica and Yamamoto [13], Luchko [16, 17], Luchko and Yamamoto [18], Sakamoto and Yamamoto [21], Zacher [23, 24], and Kian and Yamamoto [9]. It is natural to develop the well-posedness similarly to [13, 14] based on the fractional derivatives in fractional Sobolev spaces, which we carry out in this article for fractional ordinary differential equations.

Acknowledgements The author was supported by Grant-in-Aid for Scientific Research (S) 15H05740 of Japan Society for the Promotion of Science and by The National Natural Science Foundation of China (no. 11771270, 91730303). This work was supported by the RUDN University Strategic Academic Leadership Program.

Additional Remark

The author thanks the anonymous referee for valuable comments. In particular, the referee suggests another proof of Theorem 2 in [7] within the general theoretical framework based on

[1] G. Dore and A. Venni, On the closedness of the sum of two closed operators, Math. Z. **196** (1987) 189–201.

[2] H. Triebel, Interpolation Theory, Function Spaces, Differential Operators, VEB Deutscher Verlag, Berlin, 1978.

Appendix. Proof of Lemma 2

We set $\widetilde{\ell}(\eta)=\left\{\begin{array}{l} \ell(\eta),\ 0<\eta<T,\\ 0,\ -T<\eta\le 0. \end{array}\right.$. Then we have

$$(Lu)(t)=\int_0^T \widetilde{\ell}(t-s)u(s)ds, \quad 0<t<T.$$

For $0 < \beta < \frac{1}{2}$, we see

$$\int_0^T \int_0^T |\widetilde{\ell}(t-s)|^2 ds dt < \infty$$

and $L : L^2(0,T) \longrightarrow L^2(0,T)$ is a Hilbert-Schmidt integral operator and so is compact (e.g., [22]). Let $\frac{1}{2} \leq \beta < 1$. For $\varepsilon > 0$, we set

$$\widetilde{\ell}_\varepsilon(\eta) = \begin{cases} \widetilde{\ell}(\eta), \ \varepsilon \leq \eta < T, \\ 0, \ \eta < \varepsilon \end{cases}$$

and

$$L_\varepsilon u(t) = \int_0^{t-\varepsilon} \ell(t-s)u(s)ds = \int_0^T \widetilde{\ell}_\varepsilon(t-s)u(s)ds, \quad u \in L^2(0,T).$$

Since

$$\int_0^T \int_0^T |\widetilde{\ell}_\varepsilon(t-s)|^2 ds dt < \infty,$$

we see that the operator $L_\varepsilon : L^2(0,T) \longrightarrow L^2(0,T)$ is a Hilbert-Schmidt operator and so is compact.

Next we can estimate

$$\begin{aligned} |(L_\varepsilon u - Lu)(t)|^2 &= \left| \int_0^T (\widetilde{\ell}_\varepsilon(t-s) - \widetilde{\ell}(t-s))u(s)ds \right|^2 \\ &= \left| \int_{\max\{0,t-\varepsilon\}}^t \widetilde{\ell}(t-s)u(s)ds \right|^2 \leq C \left| \int_{\max\{0,t-\varepsilon\}}^t |t-s|^{-\frac{\beta}{2}} (|t-s|^{-\frac{\beta}{2}} u(s))ds \right|^2 \\ &\leq C \int_{\max\{0,t-\varepsilon\}}^t \frac{1}{|t-s|^\beta} ds \int_{\max\{0,t-\varepsilon\}}^t \frac{|u(s)|^2}{|t-s|^\beta} ds \leq C\varepsilon^{1-\beta} \int_0^T \frac{|u(s)|^2}{|t-s|^\beta} ds \end{aligned}$$

by $0 < \beta < 1$. Therefore

$$\begin{aligned} \int_0^T |(L_\varepsilon u - Lu)(t)|^2 dt &\leq C\varepsilon^{1-\varepsilon} \int_0^T \int_0^T \frac{|u(s)|^2}{|t-s|^\beta} ds dt \\ &= C\varepsilon^{1-\varepsilon} \int_0^T |u(s)|^2 \left(\int_0^T |t-s|^{-\beta} dt \right) ds \leq C\varepsilon^{1-\beta} \|u\|^2_{L^2(0,T)}. \end{aligned}$$

Therefore $L_\varepsilon \longrightarrow L$ as $\varepsilon \to 0$ in the norm of the operators from $L^2(0,T)$ to itself. Since L_ε is compact, the limit of the compact operators by the operator norms is still compact. Thus the proof of Lemma 2 is complete.

References

1. Adams, R.A.: Sobolev Spaces. Academic Press, New York (1999)
2. Bazhlekova, E.G.: Fractional Evolution Equations in Banach Spaces. Doctoral thesis, Eindhoven University of Technology (2001)
3. Diethelm, K.: The Analysis of Fractional Differential Equations. Lecture Note in Mathematics 2004, Springer, Berlin (2010)
4. Floridia, G., Li, Z., Yamamoto, M.: Well-posedness for the backward problems in time for general time-fractional diffusion equation. Atti Accad. Naz. Lincei Rend. Lincei Mat. Appl. **31**, 593–610 (2020)
5. Floridia, G., Yamamoto, M.: Backward problems in time for fractional diffusion-wave equation. Inverse Problems **36**, 125016 (2020)
6. Gorenflo, R., Mainardi, F.: Fractional calculus: integral and differential equations of fractional order. In: Carpinteri, A., Mainardi, F. (eds.) Fractals and Fractional Calculus in Continuum Mechanics, pp. 223–276. Springer, New York (1997)
7. Gorenflo, R., Luchko, Y., Yamamoto, M.: Time-fractional diffusion equation in the fractional Sobolev spaces. Fract. Calc. Appl. Anal. **18**, 799–820 (2015)
8. Henry, D.: Geometric Theory of Semilinear Parabolic Equations. Springer, Berlin (1981)
9. Kian, Y., Yamamoto, M.: On existence and uniqueness of solutions for semilinear fractional wave equations. Fract. Calc. Appl. Anal. **20**, 117–138 (2017)
10. Kilbas, A.A., Srivastava, H.M., Trujillo, J.J.: Theory and Applications of Fractional Differential Equations. Elsevier, Amsterdam (2006)
11. Kochubei, A.N.: General fractional calculus, evolution equations, and renewal processes. Integr. Equ. Oper. Theory **71**, 583–600 (2011)
12. Kochubei, A.N., Luchko, Y., Tenreiro Machado, J.A.: Handbook of Fractional Calculus with Applications, vol. 2. De Gruyter, Berlin (2019)
13. Kubica, A., Yamamoto, M.: Initial-boundary value problems for fractional diffusion equations with time-dependent coefficients. Fract. Calc. Appl. Anal. **21**, 276–311 (2018)
14. Kubica, A., Ryszewska, K., Yamamoto, M.: Time-fractional Differential Equations: A Theoretical Introduction. Springer, Tokyo (2020)
15. Lions, J.L., Magenes, E.: Non-homogeneous Boundary Value Problems and Applications, vol. I. II. Springer, Berlin (1972)
16. Luchko, Y.: Some uniqueness and existence results for the initial-boundary value problems for the generalized time-fractional diffusion equation. Comput. Math. Appl. **59**, 1766–1772 (2010)
17. Luchko, Y.: Initial-boundary-value problems for the generalized multi-term time-fractional diffusion equation. J. Math. Anal. Appl. **374**, 538–548 (2011)
18. Luchko, Y., Yamamoto, M.: General time-fractional diffusion equation: some uniqueness and existence results for the initial-boundary-value problems. Fract. Calc. Appl. Anal. **19**, 676–695 (2016)
19. Luchko, Y., Yamamoto, M.: The general fractional derivative and related fractional differential equations. Mathematics **8**(12), 2115 (2020). https://doi.org/10.3390/math8122115
20. Podlubny, I.: Fractional Differential Equations. Academic Press, San Diego (1999)
21. Sakamoto, K., Yamamoto, M.: Initial value/boundary value problems for fractional diffusion-wave equations and applications to some inverse problems. J. Math. Anal. Appl. **382**, 426–447 (2011)
22. Yosida, K.: Functional Analysis. Springer, Berlin (1971)
23. Zacher, R.: Boundedness of weak solutions to evolutionary partial integro-differential equations with discontinuous coefficients. J. Math. Anal. Appl. **348**, 137–149 (2008)
24. Zacher, R.: Weak solutions of abstract evolutionary integro-differential equations in Hilbert spaces. Funkcialaj Ekvacioj **52**, 1–18 (2009)